DROSOPHILA MENIN PROTEIN INTERACTIONS

CHARACTERIZATION OF *DROSOPHILA* MENIN PROTEIN INTERACTIONS AND A POTENTIAL ROLE FOR MENIN IN THE INSULIN SIGNALLING PATHWAY

By
ALICIA N. PEPPER, B.Sc.

A Thesis Submitted to the School of Graduate Studies
in Partial Fulfilment of the Requirements for
the Degree Doctor of Philosophy

McMaster University

Descriptive Note

DOCTOR OF PHILOSOPHY (2013) McMaster University

(Biology) Hamilton, Ontario

TITLE: Characterization of *Drosophila* menin protein interactions and a potential role for menin in the insulin signalling pathway

AUTHOR: Alicia N. Pepper, B.Sc. (Wilfrid Laurier University)

SUPERVISOR: Dr. André Bédard

NUMBER OF PAGES: xx, 440

ABSTRACT

Menin is a tumour suppressor protein associated with the MEN1 hereditary cancer syndrome. Numerous protein interactions have been identified for menin but its specific function in tumour suppression remains enigmatic. Since the protein is well conserved, the *Drosophila* model system was used to study menin protein interactions in hopes of further elucidating menin function. In this study, two menin protein interactions were examined; the first was a novel interaction with *Drosophila* fas-associated death domain (dFADD), an important protein in innate immune signalling and the second was a conserved interaction with Trithorax (Trx), a histone methyltransferase important for activation of gene expression. Both these interactions were confirmed through co-immunoprecipitation in *Drosophila* S2 cells. Unlike *dFADD* mutants that are highly susceptible to bacterial infection, *Mnn1* mutants display normal resistance, suggesting that menin does not play an essential role in innate immune signalling. Moreover, *dFADD* mutants do not display a heat shock sensitivity phenotype, as previously reported for *Mnn1* mutants. The importance of the menin-Trx interaction in the regulation of heat shock gene expression was examined since both proteins were independently shown to be necessary for proper expression of *hsp70*. Chromatin immunoprecipitation analyses demonstrate that menin and Trx co-localize in the coding region of *hsp70*. Heat shock results in a loss of menin and an increase in Trx localization at *hsp70* and the proteins fail to co-immunoprecipitate with prolonged heat stress, suggesting a complex regulation of the interaction. Due to the recently identified interactions between mammalian menin and proteins of the insulin signalling pathway, a potential role for *Drosophila* menin in this pathway was examined. *Mnn1* mutants display increased desiccation and starvation resistance, similar to other positive regulators of insulin signalling. Overall, this thesis describes a novel interaction between menin and dFADD and a conserved interaction with Trx and also proposes a potential role for menin in the *Drosophila* insulin signalling pathway.

ACKNOWLEDGEMENTS

First and foremost I would like to thank my supervisor, Dr. André Bédard for giving me the opportunity to work in his lab. Thank you for your constant guidance and support over the years. I have learned a tremendous amount from you and appreciate the devotion you have to your research and your students. I would next like to thank my committee members Dr. Ana Campos and Dr. Roger Jacobs for being a part of my studies from the beginning. Thank you especially for your unwavering support during the difficult times of my research. A special thank you to Ana for sharing her lab with me and making me feel like I was a true Campos "fly pusher". A sincere thank you must also be extended to Dr. Alexander Mazo and members of his lab at Thomas Jefferson University for welcoming me into their lab family during the summer of 2009. Thank you for sharing your expertise and providing the technical support needed to complete some of my experiments. I would also like to acknowledge NSERC for financial support.

Next I would like to thank the former technicians of the Bédard and Campos labs, Ying Wu and Xiao Li Zhao for all of your help, especially when I was a new graduate student. You were both deeply missed in these past few years since you left the labs. To all the members of the Bédard and Campos labs, especially the wiser ones that have gone before me, thank you for your companionship over the years and for assisting me in countless ways.

I can't imagine what my grad school experience would have been like without the wonderful grad students that I met and shared this experience with at McMaster. Thank you to the once strong and genuinely missed "Phoenix Friday Crew" for sharing in the lighter side of grad student life and providing some balance to the otherwise all consuming lab work. A special thanks to MM, who was there with me to the bitter end and who was always available for commiserating over coffee. I would also like to thank my Laurier friends for your continued support over the years, even if you were on the other side of the country. Thanks for listening to my many "lab rants".

Finally I would like to thank my family for encouraging me to pursue my doctorate degree and for supporting me throughout this journey. Thank for you for being so patient and understanding when I did not have much time for you. Knowing that your love and support were always just a phone call away meant the world to me. A trip home always provided the necessary respite and recharge. And last but not least, thank you to Dejan for encouraging me to become Dr. Pepper and for being with me every step of the way. Thank for being so understanding, especially when I ruined countless weekends by being in the lab. I could not have done this without your love and support.

TABLE OF CONTENTS

Title Page....i
Descriptive Note....ii
Abstract....iii
Acknowledgements....iv
List of Figures and Tables....xiii
List of Abbreviations....xvi

CHAPTER 1. INTRODUCTION....1
1. MEN1 SYNDROME....3
2. CHARACTERIZATION OF THE *MEN1* GENE AND DISEASE-ASSOCIATED MUTATIONS....5
   2.1 The MEN1 gene....5
   2.2 MEN1 disease-associated mutations....5
3. MENIN PROTEIN STRUCTURE....6
   3.1 Overview of menin protein sequence....6
   3.2 Protein interaction domains of menin....7
   3.3 Menin crystal structure....9
4. *MEN1* IS A TUMOUR SUPPRESSOR GENE....10
5. MOUSE MODELS OF MEN1 SYNDROME....11
   5.1 Men1 knockout is embryonic lethal in mice....11
   5.2 Heterozygous Men1 mice develop tumours similar to MEN1 patients....12
   5.3 Men1 mutant pancreatic β-cell and α-cell specific mouse models....12
6. REGULATION OF *MEN1* GENE EXPRESSION AND PROTEIN FUNCTION....14
   6.1 Glucose and insulin inhibit Men1 expression through inhibition of Foxo1....15
   6.2 Post-translational regulation of menin....17
   6.3 Subcellular localization of menin....18
7. MENIN PROTEIN INTERACTIONS....19
   7.1 Menin interacts with several transcription factors....21
   7.2 Menin interacts with proteins involved in chromatin modification....24
   7.3 Menin interacts with DNA damage response and DNA repair proteins....25
   7.4 Menin interacts with ASK to repress cell cycle progression....26
   7.5 Menin interacts with cytoskeleton and motor proteins....27
   7.6 Menin interacts with proteins in the Wnt/β-catenin pathway....27
   7.7 Menin interacts with Akt and FOXO1 of the insulin signalling pathway....28
   7.8 Menin interacts with nm23 and is associated with GTPase activity....31
   7.9 Summary of menin protein-protein interactions....32
8. MENIN INTERACTS WITH MIXED LINEAGE LEUKEMIA (MLL)....32
   8.1 Menin associates with MLL histone methyltransferase complexes....32
   8.2 Menin interacts with the N-terminus of MLL....34
   8.3 Menin is required for MLL-associated leukemogenesis....35
   8.4 Menin and MLL regulate expression of Hox genes and CDK inhibitors....36
   8.5 Menin recruitment of LEDGF is required for MLL-associated leukemogenesis....38
   8.6 Menin interacts with c-Myb and GATA-3 which contributes to MLL-associated leukemogenesis and T-cell differentiation....40

8.7 Menin as a potential target for leukemia cancer therapy 41
9. MENIN IS AN IMPORTANT REGULATOR OF GENE EXPRESSION 42
9.1 Menin inhibits IGF signalling and cell cycle progression 42
9.2 Menin represses the expression of hTERT 44
9.3 Menin activates the expression of caspase 8 and regulates apoptosis 45
9.4 Examination of menin involvement in gene expression on a genome-wide scale 46
10. MENIN IS IMPORTANT FOR DNA DAMAGE RESPONSES, DNA REPAIR AND GENOME STABILITY 48
11. A LINK BETWEEN MENIN, INSULIN REGULATION AND DIABETES MELLITUS 50
12. DROSOPHILA MENIN 53
12.1 Drosophila Mnn1 gene and protein 53
12.2 Generation of Mnn1 mutants to study menin function in Drosophila 54
12.3 Drosophila menin regulates stress responses 56
12.4 Drosophila menin plays a role in DNA repair and the maintenance of genome integrity 57
12.5 Mnn1 genetic interaction studies in Drosophila 58
13. THESIS OBJECTIVES 60
CHAPTER 2. MATERIALS AND METHODS 63
1. BACTERIAL CULTURE 63
2. CELL CULTURE 63
2.1 Drosophila S2 cells 63
2.2 293T cells 64
3. HEAT SHOCK TREATMENT OF S2 CELLS 64
4. CELL TRANSFECTION 64
4.1 Calcium phosphate transfection method for 293T cells 64
4.2 Cellfectin® transfection of S2 cells 66
5. PREPARATION OF CELL LYSATES 66
5.1 Cell collection and lysis 66
5.2 Protein concentration determination using the Bradford assay 68
6. SDS-PAGE AND IMMUNOBLOTTING 68
6.1 SDS-PAGE 68
6.2 Protein transfer 69
6.3 Membrane blocking and antibody incubation 70
6.4 Primary antibodies 71
7. IMMUNOPRECIPITATION (IP) AND CO-IMMUNOPRECIPITATION (Co-IP) 71
7.1 Cell collection and lysis for IP experiments 71
7.2 Co-Immunoprecipitation 72
8. DNA GEL ELECTROPHORESIS 74
9. HA-TAGGING AND CLONING OF *dFADD* 76
9.1 PCR amplification of HA-tagged dFADD constructs 76
9.2 Cloning of HA-tagged constructs into pCR®4-TOPO 77
9.3 Subcloning of HA-tagged dFADD constructs into pIRES-GFP expression vector 78
9.4 Purification of pIRES-GFP:HA-dFADD and pIRES-GFP:dFADD-HA for transfection 79
9.5 Subcloning of HA-tagged dFADD constructs into pPACB expression vector 80
10. FLY HUSBANDRY 80

10.1 Fly food ... 80
10.2 Fly stock maintenance and crosses ... 81
10.3 Fly houses ... 81
11. FLY STOCKS ... 82
12. INFECTION ASSAYS ... 85
12.1 Preparation of bacterial cultures for infection ... 85
12.2 Pricking method for adult fly infection ... 86
12.3 Feeding method for natural infection of larvae ... 86
12.4 Induction of HSP70 after natural Infection of larvae ... 88
12.5 Feeding method for adult natural infection ... 89
13. HEAT SHOCK EXPERIMENTS ... 89
13.1 Heat shock of embryos for protein expression studies ... 89
13.2 Heat shock of larvae for protein expression studies ... 90
13.3 Heat shock of adults for protein expression studies ... 90
13.4 Heat shock of embryos for acute lethality experiments ... 91
14. LOSS OF HETEROZYGOSITY ASSAY ... 91
15. CHROMATIN IMMUNOPRECIPITATION (ChIP) ... 92
15.1 Embryo collection and dechorionation ... 92
15.2 Heat shock of embryos for ChIP ... 93
15.3 Fixation of embryos for ChIP ... 93
15.4 Lysis and sonication ... 94
15.5 Immunoprecipitation ... 94
15.6 Washes and elution ... 95
15.7 Reverse cross-linking and Proteinase K treatment ... 96
15.8 Phenol/chloroform extraction and ethanol precipitation of DNA ... 97
15.9 RNase A treatment to check sonication ... 97
15.10 Real-time PCR for ChIP ... 98
15.11 Summary of ChIP experiments conducted in Dr. Mazo's Lab ... 99
16. GENOTYPE VERIFICATION OF *Mnn1* STOCKS BY PCR ... 100
16.1 Simple fly DNA preparations ... 100
16.2 Mnn1 exon specific primers ... 101
16.3 Diagnostic primers spanning Mnn1 deletions ... 101
16.4 Primers for checking Mnn1-RNAi stocks ... 102
16.5 Polymerase Chain Reaction (PCR) ... 102
17. RESCUE OF THE $Mnn1^{e173}$ ALLELE ... 103
18. EXPERIMENTS ATTEMPTING TO RE-ESTABLISH THE *Mnn1* PHENOTYPE ... 105
18.1 Changing genetic background of $Mnn1^{e30}$ ... 105
18.2 Treatment for potential parasites ... 105
18.3 Pure fly food ... 106
18.4 Trichostatin A (TSA) treatment ... 106
18.5 Propionic acid – free food ... 108
18.6 Homologous recombination to clean-up the second chromosome ... 108
19. CHANGE TO w^{1118} GENETIC BACKGROUND ... 111
19.1 Sterility check for $Mnn1^{e173}$ ... 111
20. CONTROL FOR LARVAL DENSITY ... 114

21. STARVATION AND DESICCATION ASSAYS 114
21.1 Starvation assay 114
21.2 Desiccation assay 115
21.3 Statistical analyses of survival curves 115
CHAPTER 3. MENIN INTERACTS WITH DFADD 117
INTRODUCTION 117
1. Drosophila innate immunity 117
1.1 Pathogen recognition 118
1.2 Antimicrobial peptide (AMP) genes 121
1.3 Toll pathway overview 122
1.4 Immune deficiency (Imd) pathway overview 126
2. Further examination of dFADD and Dredd function 128
2.1 dFADD is an important adaptor in the Imd pathway 128
2.2 Dredd, a Drosophila caspase, functions at multiple locations in the Imd pathway . 132
3. Mammalian FADD 134
3.1 Role of mammalian FADD in immunity and apoptosis 135
3.2 Nuclear localization of FADD 137
3.3 FADD acts as a tumour suppressor 139
4. Objectives and hypotheses 140
RESULTS 141
1. Menin and dFADD proteins interact 141
1.1 Yeast two-hybrid identification of dFADD as a menin-binding protein 141
1.2 Drosophila menin and dFADD interact in 293T cells 141
1.3 Endogenous menin interacts with HA-dFADD in S2 cells 144
2. Menin is not required for the Drosophila immune response 146
2.1 Overview of pricking/infection assay for adult flies 146
2.2 Mnn1 mutants survive bacterial infection as well as wild-type controls 148
2.3 Natural infection of Ecc15 does not induce larval lethality 155
2.4 Natural infection of Ecc15 does not induce noticeable HSP70 protein expression .. 156
2.5 E. coli or M. luteus infection do not induce HSP70 expression 157
3. dFADD mutants are not sensitive to heat stress 160
4. Summary of menin-dFADD interaction studies 162
DISCUSSION 163
1. Confirmation of the Menin and dFADD interaction 163
2. Menin is not required for the Drosophila immune response 165
3. dFADD is not required for heat shock survival 168
4. Future Directions 169
4.1 Establish interaction in Drosophila embryos/larvae 169
4.2 Study the role of the menin-FADD interaction in genome surveillance and apoptosis 170
5. Conclusions 171
CHAPTER 4. MENIN INTERACTS WITH TRITHORAX 173
INTRODUCTION 173
1. Mixed Lineage Leukemia 173
1.1 MLL1 discovery 173

1.2 MLL1 translocations and fusion proteins 174
1.3 MLL1 and Hox gene regulation in normal development and leukemogenesis 176
1.4 MLL1 is a histone methyltransferase 179
2. MLL and Trithorax protein structure 181
2.1 Protein domains 181
2.2 Cleavage by Taspase1 185
3. Menin interacts with Mixed Lineage Leukemia (MLL) 187
4. Drosophila Trithorax 187
4.1 Characterization of the Trx gene and protein 187
4.2 Trithorax and Drosophila development 188
4.3 Trithorax mutants 190
4.4 Trithorax protein-protein interactions 190
4.5 The TAC1 complex and the heat shock response 192
5. Objectives and Hypotheses 194
RESULTS 195
1. Trx and MLL1 sequence alignment 195
2. Menin and Trithorax interact in S2 cells 196
2.1 The menin-Trithorax interaction is regulated by heat stress 197
3. Examination of menin and Trx localization at the hsp70 gene 201
3.1 Characterization of menin and Trx localization at hsp70 in Oregon R embryos 202
4. Summary 208
DISCUSSION 209
1. Menin and Trithorax represent a conserved interaction 209
2. Comparison of menin and Trx ChIP results with previously published findings 212
3. Control of the heat shock response by the menin-Trx interaction 216
4. Discussion of the various Drosophila histone methyltransferase complexes 218
5. Future Directions 225
6. Conclusions 226
CHAPTER 5. ANALYSIS OF *MNN1* STOCKS AND ATTEMPTS TO REPRODUCE THE *MNN1* HEAT SHOCK PHENOTYPE 227
INTRODUCTION 227
1. Review of previously described Mnn1 phenotype 227
2. Objectives 229
RESULTS 230
1. PCR-based genotyping of Mnn1 stocks 230
1.1 PCR testing of the Mnn1 deletion stock collection 230
1.2 Testing RNAi stocks for the presence of the dsRNA construct 237
1.3 PCR testing for the hsp70 deletion 239
2. Re-examination of the heat shock phenotype of Mnn1 mutants 241
2.1 Mnn1 deletion mutants have normal expression of HSP70 241
2.2 Mnn1-RNAi stocks have normal HSP70 expression 244
3. Genetic background change and rescue of the $Mnn1^{e173}$ allele 247
4. Examination of HS and LOH phenotypes after background change 248
4.1 Mnn1 mutants have normal HSP expression after background change 248
4.2 $Mnn1^{e30}$ mutants still show a mild heat shock lethality phenotype 250

4.3 Mnn1 mutants show no increase in loss of heterozygosity with heat shock 251
5. Testing variables that could be affecting the phenotype 254
5.1 Impurities in fly food as a source of toxin contamination 254
5.2 Potential parasite infection 255
5.3 Trichostatin A treatment 256
5.4 Removal of propionic acid from food 261
6. Homologous recombination of the second chromosome to eliminate sterility 264
6.1 Discovery of sterility in Mnn1^{e173} stock 264
6.2 Homologous recombination of second chromosome 264
7. Summary of the current status of Mnn1 mutants 267
DISCUSSION 268
1. Stock contamination issues 268
2. Mnn1 mutants no longer have a heat shock phenotype 270
3. Possible explanations for altered Mnn1 phenotype 273
3.1 Other factors that could have contributed to the altered phenotype 273
3.2 Epigenetic changes could possibly explain the altered phenotype 275
4. Conclusions 281
CHAPTER 6. INVESTIGATING A POTENTIAL ROLE FOR MENIN IN INSULIN SIGNALLING 283
INTRODUCTION 283
1. Menin regulation of pancreatic beta cells and insulin in humans and mouse models 283
1.1 Insulinomas in MEN1 syndrome and mouse models 283
1.2 Regulation of insulin and menin's interaction with insulin signalling proteins 284
2. Insulin signalling in Drosophila 285
2.1 Conservation of the insulin signalling pathway 285
2.2 Overview of insulin signalling pathway in Drosophila 287
2.3 Role of insulin signalling components in development, cell growth and proliferation 290
2.4 Insulin signalling mutants have altered longevity and stress survival phenotypes 291
2.5 Examination of the mutant phenotype of dFOXO and its target d4E-BP 295
3. Objectives and predictions 298
RESULTS 299
1. Concerns from preliminary desiccation and starvation experiments 299
2. Desiccation survival of Mnn1 mutants 301
2.1 Male desiccation survival analysis 301
2.2 Female desiccation survival analysis 306
3. Starvation survival of Mnn1 mutants 308
3.1 Male starvation survival analysis 308
3.2 Female starvation survival analysis 312
DISCUSSION 315
1. The Mnn1 mutant phenotype 315
1.1 Mnn1 mutant desiccation phenotype 315
1.2 Mnn1 mutant starvation phenotype 318
2. Important variables in desiccation and starvation survival analyses 322
3. Discussion of the Mnn1 phenotype and potential role for menin in insulin signalling 323
3.1 Role for menin in Drosophila insulin signalling 323

3.2 dFOXO-mediated transcription and enhanced starvation survival 324
3.3 Further discussion of results in relation to menin's interactions with Akt and FOXO1 325
4. Future directions 330
4.1 Testing of other Mnn1 alleles is necessary 331
4.2 Testing of other Df(2L) lines is required 331
4.3 Investigate if menin's interactions with Akt and FOXO1 are conserved 333
4.4 Additional approaches for investigating the role of menin in insulin signalling 333
5. Concluding Remarks 335
CHAPTER 7: DISCUSSION 337
1. Overview of key findings 337
2. Menin protein interactions in Drosophila 339
2.1 Menin associates with Trx in a conserved interaction 340
2.2 A novel interaction between menin and dFADD 341
3. A potential link between dFADD, menin and Trx for the regulation of apoptosis 342
4. Potential role for menin in the insulin signalling pathway 349
4.1 Proposed interaction between menin and dFOXO in response to insulin signalling 349
4.2. Prediction that menin may be important for integrating immune and insulin signalling pathways 353
5. Menin acts as a scaffold to coordinate gene expression 354
6. Future Directions 356
7. Contributions, significance and concluding remarks 358
REFERENCES 359
APPENDIX A: Generation and preliminary testing of dFADD polyclonal antibodies 389
APPENDIX B: Immunofluorescence to detect menin and dFADD localization 392
MATERIALS AND METHODS 392
RESULTS 393
APPENDIX C: Additional data and statistical analyses for infection assays 398
APPENDIX D: Sequence alignment for Trx and MLL1 403
APPENDIX E: Statistical analyses for ChIP assays 408
APPENDIX F: Preliminary results for immunostaining of polytene chromosomes 409
MATERIALS AND METHODS 409
RESULTS 409
APPENDIX G: Development of tools for studying *trx* function in *Drosophila* 412
APPENDIX H: Preliminary starvation and desiccation experiments 417
1. Initial desiccation and starvation experiments 417
1.1 Initial desiccation experiment 417
1.2 Initial starvation experiment 418
APPENDIX I: Additional data and statistical analyses for desiccation assays 422
APPENDIX J: Additional data and statistical analyses for starvation assays 432
APPENDIX K: Final genotype verification of flies used in starvation and desiccation assays .. 439

LIST OF FIGURES AND TABLES

CHAPTER 1

Table 1.1. Menin interacting proteins and domains of menin involved in the interactions 8
Figure 1.1. Summary of menin interacting proteins and associated functions. 20

CHAPTER 2

Table 2.1. Antibodies used in IB, IF, IP and ChIP experiments. 73
Table 2.2. Primers used for cloning, ChIP and genotyping. 75
Table 2.3. Fly Stocks. 83
Figure 2.1. Genetic scheme for background change of *Mnn1*^{e30} and rescue of *Mnn1*^{e173} 104
Figure 2.2. Genetic scheme using homologous recombination to attempt to clean up the second chromosome background. 110
Figure 2.3. Genetic schemes used to change *Mnn1* mutants to the *w*^{1118} background. 112
Figure 2.4. Genetic schemes used to change *Mnn1* precise excision lines to the *w*^{1118} background. 113

CHAPTER 3

Figure 3.1. Overview of *Drosophila* immune deficiency (Imd) pathway. 125
Figure 3.2. Co-immunoprecipitation of *Drosophila* menin and dFADD in 293T cells. 143
Figure 3.3. Co-immunoprecipitation of menin and dFADD in S2 cells 145
Table 3.1. Sample size for infection assays (number of flies and trials) 149
Figure 3.4. Survival of adult flies with mock ddH_2O infection. 150
Figure 3.5. Survival of adult flies infected with *E. coli* MG1655 152
Figure 3.6. Survival of adult flies infected with *M. luteus* 153
Figure 3.7. HSP70 induction in OR larvae or adults after natural infection with *Ecc15-GFP*. 158
Figure 3.8. HSP70 expression after infection through the pricking method. 159
Figure 3.9. *dFADD* mutants do not have a HS lethality phenotype. 161

CHAPTER 4

Figure 4.1. Menin and Trithorax interact in S2 cells. 199
Figure 4.2. Regulation of the menin-Trithorax interaction with heat stress. 200
Figure 4.3. Schematic representation of the location of primers used for qPCR for ChIP. 203
Figure 4.4. Chromatin Immunoprecipitation (ChIP) results from Oregon R embryos. 204
Figure 4.5. Chromatin immunoprecipitation (ChIP) results from Oregon R embryos using an H3K4me2 antibody. 207

CHAPTER 5

Figure 5.1. Screening of *Mnn1* mutants for expected deletions. 232
Figure 5.2. Screening of *Mnn1* stock collection for expected deletions. 233
Table 5.1. Genotypes and corresponding ID# used for PCR screening of *Mnn1* stocks. 234
Figure 5.3. Screening of the *Mnn1* stocks for *e173* and *e30* alleles using diagnostic primers. .. 236
Figure 5.4. Screening of *Mnn1-RNAi* lines for the dsRNA construct. 238
Figure 5.5. PCR with *hsp70* primers. 240
Figure 5.6. Expression of HSP70 in $Mnn1^{e30}$ and *Mnn1-RNAi* embryos. 242
Figure 5.7. Testing of the HSP70 antibody using $hsp70A^{-}B^{-}$ mutants. 243
Figure 5.8. HSP70 and HSP23 expression in *Mnn1-RNAi* lines with different GAL4 drivers. 245
Figure 5.9. HSP70 and HSP23 expression in *Mnn1* mutants after background change/recovery. 249
Figure 5.10. Repeat of HS lethality and LOH assays with *Mnn1* mutants after background change. 253
Figure 5.11. HSP70 expression in OR, yw and $Mnn1^{e30}$ after treatment for potential parasites followed by maintenance on pure food. 257
Figure 5.12. Treatment with the histone deacetylase inhibitor Trichostatin A (TSA). 260
Figure 5.13. HSP70 expression in larvae, adults, and progeny of flies that developed with or without propionic acid. 263
Table 5.2. Fertility Summary for $Mnn1^{e173}$ flies. 265

CHAPTER 6

Figure 6.1. Overview of the *Drosophila* insulin signalling pathway. 286
Table 6.1. Summary of insulin signalling mutant phenotypes. 293
Table 6.2. Median survival* and sample size for desiccation assay. 302
Figure 6.2. Desiccation survival of male flies. 304
Figure 6.3. Desiccation survival of female flies. 307
Table 6.3. Median survival* and sample size for the starvation assay. 309
Figure 6.4. Starvation survival of male flies. 310
Figure 6.5. Starvation survival of female flies. 314

CHAPTER 7

Figure 7.1. Proposed model for dFADD-menin-Trx interaction in stress-induced apoptosis. 346
Figure 7.2. Schematic for proposed interaction between menin and dFOXO for the regulation of insulin signalling in *Drosophila*. 352

APPENDICES

Figure A.1. Testing of full-length dFADD polyclonal antibodies. 391
Figure B.1. Immunofluorescence with menin 9561 and 5073 antibodies in S2 cells. 395
Figure B.2. Immunofluorescence with rat α-menin antibodies in S2 cells. 396

Figure B.3. Immunofluorescence with dFADD antibodies in S2 cells. 397
Figure C.1. Survival of adult flies infected with different concentrations of *M. luteus*. 399
Table C.1. Statistical summary for ddH_2O infection survival curves. 400
Table C.2. Statistical summary for *E. coli* infection survival curves. 401
Table C.3. Statistical summary for *M. luteus* infection survival curves. 402
Figure D.1. Sequence Alignment for Trx and MLL1 403
Table E.1. Statistical summary for ChIPs in OR embryos. 408
Figure F.1. Immunostaining of polytene chromosomes from OR larvae. 410
Figure F.2. Immunostaining of polytene chromosomes from heat shocked OR larvae. 411
Figure G.1. Temperature sensitive knock-down using trx^{RNAi};*tub-GAL80*^{ts}/*tub-GAL4* 414
Table G.1. Survival of trx^{RNAi};*tub-GAL80*^{ts}/*GAL4* following temperature shifts beginning at different developmental stages 415
Table G.2. Survival of trx^{RNAi};*tub-GAL80*^{ts}/*tub-GAL4* following temporary temperature shifts during different developmental stages 416
Figure H.1. Desiccation survival of male and female flies in initial experiments. 420
Figure H.2. Starvation survival of male and female flies in initial experiments. 421
Figure I.1. Male desiccation survival for all genotypes. 425
Table I.1. Statistical summary for male desiccation survival curves. 426
Figure I.2. Female desiccation survival for all genotypes. 427
Table I.2. Statistical summary for female desiccation survival curves. 428
Figure I.3. Desiccation survival of male and female flies at various time points 429
Table I.3. Statistical summary for male desiccation survival at 18 hrs and 20 hrs. 430
Table I.4. Statistical summary for female desiccation survival at 22 hrs and 26 hrs. 431
Figure J.1. Male starvation survival for all genotypes 433
Table J.1. Statistical summary for male starvation survival curves. 434
Figure J.2. Female starvation survival for all genotypes 435
Table J.2. Statistical summary for female starvation survival curves. 436
Figure J.3. Male and female starvation survival after 2 days 437
Table J.3. Statistical summary for male and female starvation survival after 2 days. 438
Figure K.1. Final genotype verification by PCR. 440

LIST OF ABBREVIATIONS

4E-BP	eIF4E-binding protein
AEL	after egg laying
Akt/PKB	v-Akt homologue (from Ak mouse strain thymoma)/protein kinase B
ALL	acute lymphoblastic leukemia
AML	acute myelogenous leukemia
AMP	antimicrobial peptide
ANT-C	Antennapedia homeotic gene cluster
AP-1	activator protein 1
ASH2L	absent, small, homeotic 2L
ASK	activator of S-phase kinase
ATF-2	activating transcription factor 2
ATM	ataxia telangiectasia mutated
ATR	ATM and Rad3-related
Att	Attacin (AMP gene)
BIR	Baculovirus IAP (inhibitor of apoptosis) repeat domain
BM	bone marrow
BMP-2	bone morphogenetic protein 2
BM-TNE	Bart's Modified Tris, Nonidet-P40, EDTA buffer
BRCA1	Breast Cancer 1
BrdU	5-bromo-2'-deoxyuridine
BSA	Bovine serum albumin
BX-C	Bithorax homeotic gene cluster
CBP	CREB (cAMP response element-binding) binding protein
CDK	cyclin-dependent kinase
Cec	*Cecropin* (AMP gene)
CGBP	CpG binding protein
CHES1	checkpoint suppressor 1
ChIP	chromatin immunoprecipitation
Chk1	checkpoint kinase 1
c-Myb	cellular myeloblastosis
c-Myc	cellular homologue of viral myelocytomatosis
Co-IP	co-immunoprecipitation
COMPASS	complex proteins associated with Set1
Cre-LoxP	cyclization recombination gene – locus of X-over of P1
CS1/2	Taspase1 cleavage site 1/2 of MLL (or Trithorax)
CTD	C-terminal repeat domain (of RNA polymerase II)
CUE	coupling of ubiquitin to ER degradation domain
DAP	diaminopimelic acid
DBD	DNA binding domain
DD	death domain
DED	death effector domain
DEDAF	death effector domain associated factor
DEDD	death effector domain-containing DNA-binding protein

Def	*Defensin* (AMP gene)
DIAP	*Drosophila* inhibitor of apoptosis
Dif	Dorsal-related immunity factor
DILP	*Drosophila* insulin-like peptide
Dl	*Dorsal* gene
DMEM	Dulbecco's Modified Eagle Medium
DmIKK	*Drosophila melanogaster* inhibitor of kappa B kinase
DMSO	dimethyl sulfoxide
DNMT	DNA methyltransferase
DOT1L	disruptor of telomeric silencing 1-like
Dpt	*Diptericin* (AMP gene)
DPY-30	DumPY protein 30
Dredd	death related ced-3/Nedd2-like protein
Dro	*Drosocin* (AMP gene)
Drs	*Drosomycin* (AMP gene)
DSB	double strand break
ECL	enhanced chemiluminescent
EGFP	enhanced green fluorescent protein
eIF4E	eukaryotic translation initiation factor 4E
ERα	estrogen receptor alpha
EZH2	enhancer of zeste homologue 2
FADD	Fas-associated death domain
FANCD2	Fanconi anemia complementation group D2
FBS	fetal bovine serum
Fkh	fork head transcription factor
FLICE	FADD-like interleukin 1β converting enzyme (later called caspase 8)
FLIP	FLICE inhibitor protein
FOXO	Forkhead box class O
FYRC	phenylalanine and tyrosine rich C-terminal region (of MLL/Trx)
FYRN	phenylalanine and tyrosine rich N-terminal region (of MLL/Trx)
G6Pase	Glucose-6-phosphatase
GAP	GTPase-activating protein
GATA-3	transcription factor binding to GATA DNA sequence
GFAP	glial fibrillary acidic protein
GNBP	Gram-negative binding protein
H3ac	acetylated Histone H3
H3K4me2	dimethylated Histone H3, Lysine 4
H3K4me3	trimethylated Histone H3, Lysine 4
HA	Hemagglutinin tag
HAT	histone acetyltransferase
HCF1/2	host cell factor 1/2
HDAC	histone deacetylase
HEK 293	Human embryonic kidney cell line 293
HeLa	Henrietta Lacks cervical cancer cell line
HepG2	human hepatocellular liver carcinoma cell line

Hid	head involution defective
hMBM	high-affinity menin-binding motif
HMT	histone methyltransferase
Hox	homeobox (or homeotic in *Drosophila*)
HS	heat shock or heat stress
HSP	Heat shock protein
hTERT	human telomerase reverse transcriptase
IAP	inhibitor of apoptosis
IBD	HIV-1 integrase binding domain (of LEDGF)
IFN	interferon
IGF	insulin-like growth factor
IGFBP	insulin-like growth factor binding protein
IIS	insulin/insulin-like growth factor signalling
IκB	inhibitor of kappa B
IKK	inhibitor of kappa B kinase
IL-1	interleukin 1
Imd	Immune deficiency
INI1	integrase interactor 1 (also called hSNF5)
InR	insulin-like receptor
INS1	rat insulinoma cell line 1
IP	Immunoprecipitation
IQGAP1	IQ motif containing GTPase activating protein 1
IRAK	interleukin-1 receptor associated kinase
Ird5	immune response deficient 5
IRS	insulin receptor substrate
JNK	Jun N-terminal kinase
Key	Kenny (DmIKKγ)
LB	Luria-Bertani broth (or Lysogeny broth)
LBD	LEDGF binding domain (of MLL)
LEDGF	lens epithelium-derived growth factor
LEF	lymphoid enhancer factor
LOH	loss of heterozygosity
LPS	lipopolysaccharide
MAPK	mitogen-activated protein kinase
MBD4	methyl-CpG binding domain protein 4
MBM	menin binding motif
MCMV	murine cytomegalovirus
MEF	mouse embryonic fibroblast cells
MEIS1	myeloid ecotrophic integration site 1
MEN1	multiple endocrine neoplasia type 1
MLL	mixed lineage leukemia
Mnn1	*Drosophila* menin gene
mSin3A	mammalian homologue of yeast Sin3 (Swi independent 3) protein A
Mtk	*Metchnikowin* (AMP gene)
mwh	*multiple wing hair*

MyD88	myeloid differentiation factor 88
NER	nucleotide excision repair
NES	nuclear export signal
NF-κB	nuclear factor kappa B
NLS	nuclear localization signal
nm23	non-metastatic gene 23
NMHC IIA	non-muscle myosin type IIA heavy chain
NSC (IPC)	neurosecretory cell (also called insulin-producing cell)
PA	propionic acid
PAFc	polymerase associated factor complex
PAMP	pathogen-associated molecular pattern
PcG	Polycomb group
PDK1	phosphoinositide-dependent kinase 1
Pem	placenta and embryonic expression gene
PEPCK	phosphoenolpyruvate carboxykinase
PGN	peptidoglycan
PGRP	peptidoglycan recognition protein
PH	pleckstrin homology domain
PHD	plant homeodomain
PI3K	phosphoinositide 3-kinase
PIP_2	phosphatidylinositol 4,5-bisphosphate
PIP_3	phosphatidylinositol 3,4,5-triphosphate
PPARγ	peroxisome proliferator-activated receptor gamma
PRE	Polycomb response element
P-TEFb	positive transcription elongation factor b (cyclin T1/2 and CDK9)
PTEN	phosphatase and tensin homology
qPCR	quantitative (or real-time) polymerase chain reaction
RBBP5	retinoblastoma binding protein 5
RING	really interesting new gene domain
RIP	receptor-interacting protein
RNAi	RNA interference
RNAP II	RNA polymerase II
RPA2	replication protein A subunit 2
Rpb1/2	RNA polymerase II subunit 1/2
Runx2	runt-related transcription factor 2
RXR	retinoid X receptor
RYBP	Ring1 and YY1 binding protein
S6K	ribosomal S6 kinase
SB	squishing buffer for DNA preparations
Sbf1	SET binding factor 1
SDS-PAGE	sodium dodecyl sulfate polyacrylamide gel electrophoresis
SDS-SB	sodium dodecyl sulfate sample buffer
seml	*semmelweis* gene for PGRP-SA
SET	su(var)3-9, enhancer of zeste, trithorax
siRNA	short interfering RNA

SKIP	Ski (Sloan-Kettering Institute) interacting protein
Smad	Sma (small body) and mothers against decapentaplegic homologue
SNR1	SNF5-related 1
spz	*spätzle* gene
SWI/SNF	switch/sucrose non-fermentable
Tab2	Tak1-binding protein 2
TAC1	Trithorax acetylation complex 1
TAD	transactivation domain
Tak1	transforming growth factor β activated kinase 1
Tat	transactivator of transcription
TCF	T-cell factor
TGF-β	transforming growth factor beta
TIF-IA	Transcriptional intermediary factor IA
TIR	Toll/interleukin-1 receptor homology domain
Tl	*Toll* gene
TLR	Toll-like receptor
TNF-α	tumour necrosis factor alpha
TNF-R1	tumour necrosis factor receptor 1
TOR	target of rapamycin
tp53	tumour protein 53
TRE	trithorax response element
Trr	Trithorax-related
Trx	Trithorax
TrxG	Trithorax group
TSA	trichostatin A
TSC	tuberous sclerosis complex
UAS	upstream activation sequence
Ubx	*Ultrabithorax* (homeotic gene in BX-C)
UTR	untranslated region
VDR	vitamin D receptor
WDR5	WD40 repeat containing protein 5
Win	WDR5 interacting domain
Wnt	wingless and Integration 1
WT1	Wilm's tumour suppressor 1
Y2H	yeast two-hybrid

CHAPTER 1. INTRODUCTION

In recent times, cancer has been in the spotlight more than any other human health issue. Everyone in their lifetime will know someone diagnosed with cancer and will in some way be personally affected by this disease. Because of its far reaching impact, the scientific community has placed tremendous emphasis on researching the causes, treatments and cures for this variable and prolific disease.

Early cancer research was conducted with the anticipation of finding a cure to eliminate all cancer, a so-called "magic bullet". As human genetics and molecular biology were essentially unknowns in the early days of cancer research, scientists were forced to search for ways to remove or kill cancer cells with minimal understanding of what was causing these tumours to develop in the first place. These early efforts consisted primarily of identifying drugs that could kill cancer cells more efficiently than their normal counterparts but this was often accompanied by terrible side effects and treatments were usually followed shortly by relapse.

As our understanding of cell biology progressed, and with the advent of molecular biology, our understanding of cancer and our ability to treat it also radically improved. The large list of diverse human cancer types was met with a vastly larger list of potential genes implicated in tumour initiation, development, progression and metastasis. Eventually some specific cancer types were cured through surgery, radiation, chemotherapy or a combination of such treatments; however, a much larger number of cancers still defy our current treatment options.

Although scientists widely accept that there will be no “magic bullet” cure for all types of cancer, there is still hope that we can improve cancer therapy, improve life expectancy and quality of life for those afflicted with cancer, as well as continue to find targeted cures for specific types of human cancer. Currently, to this end, much of the scientific research for a particular type of cancer follows a similar general trajectory; that is, identify a target gene implicated in the cancer, determine the function of that gene and the signalling pathways involved in tumourigenesis and hopefully identify mechanisms to target this gene to prevent or revert the effects of its alteration in cancer development. Due to the diversity of cancer and the ever growing list of genes contributing to tumourigenesis, including both tumour suppressors and oncogenes, this research requires the concerted effort of labs worldwide. An important part of this research relies on the extensive use of model systems long before treatments are developed for clinical trials.

Even though dramatic discoveries are occasionally made, much of cancer research progresses in small steps, with each finding contributing one small way or another to the constantly expanding pool of knowledge regarding human cancers. The research presented in this thesis represents such an effort, to contribute to the understanding of the function of a single protein, menin, that is implicated in a type of hereditary cancer, multiple endocrine neoplasia type I. This research utilizes the *Drosophila melanogaster* model system and the approach of studying protein-protein interactions to gain insight into the function of menin and how its loss of function contributes to tumourigenesis in endocrine tissues.

1. MEN1 SYNDROME

Multiple endocrine neoplasia type 1 (MEN1) is a hereditary autosomal dominant cancer syndrome characterized by tumours in numerous tissues of the endocrine system including the parathyroid, pancreatic islets and anterior pituitary (reviewed in Agarwal et al., 2004; Marx, 2005; Thakker, 2010). The *MEN1* gene contributing to this syndrome was mapped to chromosome 11q13 (Larsson et al., 1988) and cloned in 1997 (Chandrasekharappa et al., 1997). MEN1 patients inherit a mutant allele for the *MEN1* gene and tumour formation occurs following the loss of the wild-type allele, a scenario which follows Knudson's two-hit tumour suppressor model (Knudson, 1971). Thus, individuals with a recessive germline mutation are predisposed to the cancer syndrome where tumour development in endocrine tissues ensues following a loss of the remaining wild-type allele; that is, a loss of heterozygosity (LOH) at the *MEN1* locus (Larsson et al., 1988). So even though tumourigenesis occurs in a recessive manner, the inheritance pattern for the disease is dominant in nature. Since the cloning of *MEN1* in 1997, many different disease-related mutations have been characterized and the protein has been studied extensively in hopes of understanding its function and how loss of function contributes to tumourigenesis in endocrine organs (Chandrasekharappa et al., 1997).

MEN1 patients typically present with tumours in three main endocrine organs: parathyroid glands (90 % of patients), enteropancreatic tissue/islets of Langerhans (60 %), anterior pituitary gland (30 %). In addition, tumours appear less frequently in other endocrine tissues, including foregut neuroendocrine tissue, adrenal glands and thyroid glands and sometimes non-endocrine tissues are also affected (Chandrasekharappa and

Teh, 2003). Most commonly, parathyroid tumours are the first manifestation of the disease (Agarwal et al., 2004). In addition to the hereditary *MEN1* mutations, sporadic *MEN1* mutations have also been identified in a range of tumours similar to those observed in MEN1 patients. For example, approximately 10-30 % of sporadic gastrinomas, insulinomas and parathyroid adenomas have *MEN1* mutations (Chandrasekharappa and Teh, 2003).

MEN1 is a rare disease, affecting about 1 in 30000 people, with no sex or race specific prevalence (Agarwal et al., 2004). The first clinical presentation of disease symptoms occurs most frequently by age 25 to 35 (Agarwal et al., 2004). However, the reported age for onset of the disease has ranged from 5-81 years, with 80 % of individuals having clinical symptoms by age 40. MEN1 patients have a 50 % probability of death by the age of 50 (Thakker, 2010).

Since MEN1 syndrome manifests in multiple tissues it is often harder to treat than individual localized tumours. The most frequent treatment is the attempted surgical removal of affected tissues (most often parathyroidectomy) as well as preventative surgical removal of tissues that will likely become affected (*e.g.* removal of distal pancreatic tissue). There is however a high rate of reoccurrence following surgery for endocrine tumours (Agarwal et al., 2004). Another problem associated with MEN1 tumours is that since they affect endocrine tissues they are frequently associated with excessive hormone production and secretion which imparts additional negative consequences.

2. CHARACTERIZATION OF THE *MEN1* GENE AND DISEASE-ASSOCIATED MUTATIONS

2.1 The MEN1 gene

Cloning of the *MEN1* gene at 11q13 revealed that the gene is composed of 10 exons and spans a region of 9 kb. The first exon and part of the second exon are non-coding. A 2.8 kb mRNA transcript is expressed ubiquitously from the *MEN1* gene (Chandrasekharappa et al., 1997). The protein product of the *MEN1* gene, named menin, is 610 amino acids with a molecular weight of 67 kDa. The initial characterization of the menin protein sequence did not identify the presence of any known functional domains so no clues to the function of this novel protein were revealed (Chandrasekharappa et al., 1997; Guru et al., 1998). Orthologues of *MEN1* were identified in many other species and the gene is well conserved; the percent identity of the human protein with that of mouse and zebrafish is 97 % and 67 %, respectively (Guru et al., 1999; Manickam et al., 2000).

2.2 MEN1 disease-associated mutations

Identified mutations spread across the entire *MEN1* gene with no mutational hot spots existing (Tsukada et al., 2009). This insinuates that there is likely not a single important functional domain (*e.g.* enzymatic domain) in menin but that multiple regions throughout the entire protein are likely essential to proper function. Many different mutations have been identified in *MEN1* with 565 different mutations documented so far (for germline and somatic mutations combined) (Lemos and Thakker, 2008). The germline mutations were categorized as follows: 41 % frameshift deletions/insertions, 23 % nonsense mutations, 9 % splice site mutations, 20 % missense mutations, 6 % in-frame deletions/insertions and 1 % whole/partial gene deletion (Lemos and Thakker, 2008). The vast majority of mutations, about 70 %, result in truncation of the protein,

hinting at the importance of the C-terminal region to menin function. The remaining mutations, such as the missense mutations, are predicted to result in the disruption of important protein-protein interactions (see Sections 3.2 and 7) (Tsukada et al., 2009). An alternative hypothesis, for which there is some experimental evidence, is that these missense mutant proteins are unstable and are rapidly ubiquitinated and targeted for degradation by the proteasome (Yaguchi et al., 2004).

3. MENIN PROTEIN STRUCTURE

3.1 Overview of menin protein sequence

Menin shares no significant sequence similarity with known proteins and consequently its biochemical function could not be easily predicted. Nuclear localizations signals (NLS) have been identified and menin was shown to be a primarily nuclear protein. Two nuclear localization signals (NLS) were identified and functionally validated, NLS1 (479-497) and NLS2 (588-608), as well as an accessory NLSa (546-572) (Guru et al., 1998; La et al., 2006). NLS1 or NLS2, but not NLSa, fused to GFP are capable of nuclear translocation; however, mutation of NLS1, NLS2 or NLSa is not sufficient to abolish nuclear translocation, suggesting that the NLSs play redundant roles (La et al., 2006; La et al., 2004b). Although menin lacks canonical DNA binding motifs, NLS1 and NLS2 are essential for the direct binding of menin to double-stranded DNA (dsDNA) in a sequence-independent manner, as demonstrated through *in vitro gel* shift assays (La et al., 2004b). These domains are also important for the regulation of gene expression (*e.g.* repression of *IGFBP-2* and activation of *caspase 8*; see also Sections 9.1 and 9.3) (La et al., 2006).

Later, two leucine-rich domains of menin, that resemble leucine-zipper interacting domains, were shown to act as nuclear export signals (NES), NES1 (36-41) and NES2 (258-267), and were also shown to play a role in the shuttling of β-catenin from the nucleus (see Section 7.6) (Cao et al., 2009). Interestingly, NES2 encompasses a conserved LXXLL motif (LLWLL 263-267) that mediates the interaction with nuclear receptors (*e.g.* ERα, VDR, PPARγ, RXR) for transcriptional activation (see Section 7.1) (Dreijerink et al., 2006). Also of note, this domain is highly conserved from *Drosophila* to human (for an alignment see Papaconstantinou et al., 2009). Menin also contains five GTPase-like motifs, all located in the N-terminal half of the protein. These motifs are not conserved in *Drosophila* or zebrafish and the precise function of these domains has not been identified. However, menin was shown to have GTP hydrolysis activity through an interaction with nm23 (see Section 7.8) (Yaguchi et al., 2002).

3.2 Protein interaction domains of menin

Menin interacts with numerous proteins (see Section 7) and although fine-scale mapping of the residues of menin involved in all of its various protein interactions has not been completed, most interaction studies have mapped the interaction to a specific region(s) on the protein (see Table 1.1). Perhaps, as suggested by the fact that there is no mutational hotspot in the *MEN1* gene, there is also no particular region of menin that is important for all its protein-protein interactions. In fact, the regions identified for protein-protein interactions map throughout the entire protein (for a schematic please see Papaconstantinou et al., 2009). Table 1.1 summarizes the interacting proteins and the domains of menin implicated in the interactions.

Table 1.1. Menin interacting proteins and domains of menin involved in the interactions

Interaction	Important domain/aa of menin	Reference
Transcription Factors		
JunD	1-40, 139-242, 323-448	(Agarwal et al., 1999)
NF-κB (p50, p52, p65)	305-381	(Heppner et al., 2001)
Smads (1,3,5)/Runx2	40-278,477-610 (shown for Smad3)	(Kaji et al., 2001; Sowa et al., 2004)
Pem	278-476	(Lemmens et al., 2001)
CHES1	428-610	(Busygina et al., 2006)
β-catenin	1-193, 258-475	(Cao et al., 2009)
TCF/LEF (3,4/1)	N.D.	(Chen et al., 2008; Inoue et al., 2011)
Estrogen Receptor α	263-267 (LLWLL)	(Dreijerink et al., 2006)
Vitamin D Receptor	263-267 (LLWLL)	(Dreijerink et al., 2009b)
PPARγ	263-267 + unknown aa	(Dreijerink et al., 2009a)
RXR	263-267(LLWLL)	(Dreijerink et al., 2006)
FOXO1	N.D.	(Wuescher et al., 2011)
c-Myb and GATA-3	N.D.	(Jin et al., 2010; Nakata et al., 2010)
c-Myc and Tat	N.D.	(Brès et al., 2009)
tp53	N.D.	(Bazzi et al., 2008)
Chromatin Modification		
MLL1/MLL2 complexes	1-386 (N-term, thumb, palm domains)^	(Huang et al., 2012; Hughes et al., 2004; Yokoyama et al., 2004)
mSin3A	371-378	(Kim et al., 2003)
HDACs (1,2,3)	145-450 (shown for HDAC1)	(Kim et al., 2003; La et al., 2006)
Other role in transcription regulation		
RNA Pol II (p-Ser5 CTD)	N.D.	(Hughes et al., 2004)
LEDGF	1-101 (N-term domain)^	(Huang et al., 2012; Yokoyama and Cleary, 2008)
WT1	N.D.	(Xu et al., 2011)
CGBP*	N.D.	(Ansari et al., 2008)
SKIP	N.D.	(Brès et al., 2009)
DNA Repair Proteins		
FANCD2	219-395	(Jin et al., 2003)
RPA2	1-40, 286-448	(Sukhodolets et al., 2003)
Chk1	1-228	(Gallo et al., 2010)
Structural Proteins		
GFAP	N.D.	(Lopez-Egido et al., 2002)
Vimentin	N.D.	(Lopez-Egido et al., 2002)
NMHC IIA	154-306	(Obungu et al., 2003)
Other		
ASK	396-610	(Schnepp et al., 2004a)
nm23	1-486	(Yaguchi et al., 2002)
Akt	212-610	(Wang et al., 2011)
IQGAP1	N.D.	(Yan et al., 2008)

Most menin protein interactions were discovered in human or mouse cells and demonstrated by co-immunoprecipitation, *in vitro* binding assays or affinity purification followed by mass spectrometry. ^ the domains were predicted from the crystal structure; * interaction could be indirect; N.D. = domain of menin not determined; aa=amino acid. Please see text for details regarding the interactions.

3.3 Menin crystal structure

The crystal structure of menin was only recently resolved. The first menin crystal structure was reported for *Nematostella vectensis* (starlet sea anemone) as initial attempts to crystallize the human protein were unsuccessful, presumably due to the existence of unstructured regions (Murai et al., 2011). Shortly after this crystal structure was published, Huang *et al.* (2012) successfully crystallized human menin, both in its free form and also when complexed with JunD or MLL1 (mixed lineage leukemia 1) (see Sections 7.1 and 8). The structure is described as resembling a curved left hand, having an N-terminal domain preceding the "thumb", "palm" and "fingers" regions. The N-terminal domain consists of two long β-sheets forming a hairpin. The "thumb" and "palm" form a deep pocket, with the palm consisting of three TPR (tetratricopeptide repeats) motifs that are believed to be important for protein-protein interactions (Huang et al., 2012). The high-affinity menin-binding motif (hMBM) of MLL (see Section 8.2) fits into the deep pocket formed by the "thumb" and "palm" domains, with residues 6-13 of MLL contributing most to the interaction with menin. The MLL N-terminal domain has many basic residues making its positive charge complementary to the surface of the menin pocket that contains many negatively charged acidic residues (Huang et al., 2012). Several identified *MEN1* disease-related mutations (H139D, C241F, A242V, G281R) were shown to disrupt this interaction (Huang et al., 2012). The structure of menin in complex with MLL and LEDGF (lens epithelium-derived growth factor), another important protein in the menin-MLL complex (see Section 8.5), was crystallized. The N-terminal domain of menin (α-helix 4) interacts with MLL (α-helix 2) in such a way as to form a V-shaped groove for the IBD (HIV-1 integrase binding domain) of

LEDGF, demonstrating how menin and MLL both interact with LEDGF for binding (Huang et al., 2012). Similar to MLL, JunD also binds in the deep pocket of menin. Residues 27-47 of JunD represent the menin-binding motif, and show sequence similarity with the MBM of MLL. Competition assays revealed that JunD and MLL compete for menin binding (Huang et al., 2012).

4. *MEN1* IS A TUMOUR SUPPRESSOR GENE

Several lines of evidence support the notion that *MEN1* is an important tumour suppressor gene. The first is that MEN1 syndrome develops following Knudson's two hit model for tumour suppressor genes (Knudson, 1971). Patients inherit a germline mutation in *MEN1* as the first hit and the ensuing LOH at chromosome 11q13 accounts for the second hit observed in tumours (Larsson et al., 1988; Marx, 2005). The second line of evidence for menin acting as a tumour suppressor protein comes from cell culture studies demonstrating that overexpression of menin is able to partially suppress transformation and tumourigenicity associated with oncogenic ras (G12V) expression (Kim et al., 1999). Menin overexpression reverts the morphology of ras-transformed NIH-3T3 cells to that of normal fibroblasts, reduces the proliferation rate and reduces clonogenicity in soft agar assays. Furthermore, tumour formation after injection of ras-transformed NIH-3T3 cells into nude mice is reduced when menin is overexpressed. These results provide evidence that menin is able to suppress cell transformation and tumourigenesis. The third line of evidence comes from mouse models of MEN1 syndrome (Section 5) where heterozygous *Men1*$^{+/-}$ mice develop tumours in a similar spectrum of tissues as MEN1 patients, with loss of the wild-type menin observed in

tumours. In all, these experiments provide proof that *MEN1* is a bona fide tumour suppressor gene.

5. MOUSE MODELS OF MEN1 SYNDROME

5.1 Men1 knockout is embryonic lethal in mice

A *MEN1* mouse model was generated by Dr. Francis Collins' group in order to study tumourigenesis following loss of menin function. Knock-out of the *Men1* gene was established using the Cre-*loxP* system which resulted in the deletion of exons 3-8 of *Men1.* When $Men1^{+/-}$ mice are mated, the $Men1^{-/-}$ progeny are not viable. Embryonic lethality occurs between days E11.5-12.5. $Men1^{-/-}$ embryos are developmentally delayed and smaller than wild-type, with some showing cranial or facial defects, suggesting that menin could play a role in bone morphogenesis (Crabtree et al., 2001). Dr. Chang-Xian Zhang's group also developed a mouse knock-out of *Men1* but their model only deleted the third exon of *Men1* (Bertolino et al., 2003a). They also observed embryonic lethality between days E11.5-13.5. They more fully examined the cause of embryonic lethality and found defects in multiple organs. $Men1^{-/-}$ embryonic lethality is associated with an overall reduced size, defects in neural tube closure, haemorrhages, defects in nervous system, heart and liver development (Bertolino et al., 2003a). A closer examination of the embryonic liver showed abnormal tissue organization and increased apoptosis in $Men1^{-/-}$ livers. Furthermore, chimeric mice generated from injection of $Men1^{-/-}$ embryonic stem cells into wild-type blastocysts, suggest that $Men1^{-/-}$ cells contribute to all tissue types early on (E12.5); however, there are very few $Men1^{-/-}$ cells in the liver at later embryonic stages (E18), suggesting that menin function may be

required for differentiation of some cell types, such as in the liver (Bertolino et al., 2003a).

5.2 Heterozygous Men1 mice develop tumours similar to MEN1 patients

Men1$^{+/-}$ mice are viable and develop a variety of endocrine tumours similar to human MEN1 patients, with tumours observed starting at 9 months of age (Crabtree et al., 2001). Common tumours in MEN1 patients, including pancreatic insulinomas, pituitary adenomas, parathyroid adenomas and adrenal cortical tumours, were also observed in the mouse models (Bertolino et al., 2003b; Crabtree et al., 2001). Furthermore, pancreatic glucagonomas and gastrinomas were also observed in the study by Bertolino *et al.* (2003b). Almost all mice examined had multiple endocrine tumours after 13 months (Bertolino et al., 2003b). As with human patients, the tumours in mice had a loss of heterozygosity at the *Men1* locus (Bertolino et al., 2003b; Crabtree et al., 2001). Thus, the heterozygous mouse models nicely mimic what occurs in human MEN1 patients.

5.3 Men1 mutant pancreatic β-cell and α-cell specific mouse models

Since conventional homozygous *Men1* knock-out mice are embryonic lethal, conditional mouse models were developed to specifically knock-out *Men1* in various endocrine tissues. Using the Cre-*loxP* system with the expression of Cre recombinase under the control of the rat insulin promoter, a pancreatic beta cell specific *Men1* knock-out was generated (Crabtree et al., 2003). β-cell specific deletion of *Men1* results in increased proliferation of pancreatic islets. Abnormalities in pancreatic cell proliferation were observed as early as 4 weeks with adenomas appearing as early as 23 weeks. By 60 weeks more than 80 % of mice with *Men1*$^{-/-}$ β-cells had developed multiple pancreatic

islet adenomas. These pancreatic islet adenomas were accompanied by increased fasting serum insulin levels and decreased fasting blood glucose levels, assumed to be due to increase in the number of insulin secreting cells and not in insulin expression per cell (Crabtree et al., 2003). Similarly, Bertolino *et al.* (2003c) also created β-cell specific *Men1* knock-out mice and observed that insulinoma development occurred much earlier than in the heterozygous *Men1*$^{+/-}$ mice with 100 % of mice displaying tumours by 10 months (Bertolino et al., 2003c). The delay in development of insulinomas in heterozygous mice may represent the time needed for inactivation of the wild-type *Men1* allele, while these β-cells already have both copies deleted. Since there is still a delay before tumour formation in the *Men1*-ablated β-cell mice, this suggests that the accumulation of other mutational events precedes tumourigenesis.

Conditional mouse models were also developed to specifically knock-out *Men1* in the glucagon-producing alpha cells of the pancreas by expressing Cre under the control of a glucagon promoter (*Glu-Cre*) (Shen et al., 2010). Surprisingly, ablation of the α-cells results in β-cell insulinomas. There was only a slight increase in the number of α-cells in these mice and they were found to be scarce and randomly distributed in the tumours. In addition, tumours in these mice were not as numerous as in the *Men1*$^{-/-}$ β-cell model (Shen et al., 2010). The occurrence of β-cell insulinomas in mice with *Men1*-ablated α-cells could suggest that α-cells may regulate β-cell proliferation in a paracrine manner or that *Men1*$^{-/-}$ α-cells are able to transdifferentiate into insulin secreting β-cells. Another research group also generated α-cell specific *Men1* knock-out mice and observed the same surprising result that β-cell insulinomas developed along with the expected glucagonomas and some mixed islet tumours (Lu et al., 2010). They observed that there

was an initial hyperproliferation of α-cells followed by an increase in the prevalence of β-cells as tumours progressed and concluded that transdifferentiation of the α-cells was responsible for these β-cell tumours (Lu et al., 2010).

In addition to the α-cell and β-cell specific mouse models for *Men1* tumourigenesis, other tissue-specific conditional knock-outs have been generated. For example, conditional knock-out in the parathyroid (using *PTH-Cre*), results in parathyroid adenomas and the development of hypercalcemia, similar to the hyperparathyroidism observed in MEN1 patients (Libutti et al., 2003). Another conditional mouse model was generated to knock-out *Men1* in the pancreatic progenitor cells (using *Pdx1-Cre*) that develop into both the endocrine and exocrine pancreas (Shen et al., 2009). In this model pancreatic development occurred normally; however, as in human MEN1 patients, endocrine hyperproliferation occurred while the exocrine pancreas was not affected by inactivation of *Men1*. Mice with pancreatic *Men1*$^{-/-}$ ablation showed hyperplasia of islet cells by 5-6 months and insulinomas developed by 10-12 months (Shen et al., 2009). This model nicely demonstrated that only endocrine tissues appear to be sensitive to the loss of menin function. In agreement with this notion, knock-out of *Men1* in the liver, a non-endocrine tissue, is well tolerated and does not result in tumourigenesis (Scacheri et al., 2004). Overall, studies in mouse models have demonstrated that menin negatively regulates proliferation in endocrine tissues.

6. REGULATION OF *MEN1* GENE EXPRESSION AND PROTEIN FUNCTION

Although the regulation of gene expression by menin has been highly studied (see Sections 7-9), the regulation of menin itself is a rather neglected topic in comparison.

The *Men1* transcript is ubiquitously expressed (Chandrasekharappa et al., 1997) and analysis of the endogenous protein in numerous cell lines and tissue samples from humans and primates also revealed a broad expression pattern (Wautot et al., 2000). In addition, in HeLa cells menin protein level was not altered at different stages of the cell cycle (Wautot et al., 2000).

Very few transcription factors that bind to the menin promoter to activate transcription have been described, although a putative NF-κB binding site was identified (Zablewska et al., 2003). Intriguingly, there is some evidence to suggest that menin is capable of repressing its own promoter, in a negative feedback loop, though the mechanism has not been well defined (Fromaget et al., 2003). In an inducible cell culture system, overexpression of menin results in down-regulation of expression from a *Men1* promoter-luciferase construct, while knock-down of *Men1* with RNAi has the reverse effect, suggesting that the protein product regulates its own expression in a manner that aims to maintain a steady state of expression (Zablewska et al., 2003). Additional regulation of *Men1* expression seems to be cell type specific, with only a few other factors being identified so far.

6.1 Glucose and insulin inhibit Men1 expression through inhibition of Foxo1

Conditions where increased β-cell proliferation is desirable, such as hyperglycemia, also require *Men1* down-regulation since menin negatively regulates β-cell proliferation. Exposure of the rat insulinoma cell line INS1 or rat primary islets to high glucose (16.7 mM) results in decreased *Men1* mRNA and protein (Zhang et al., 2012). Islets from glucose-infused rats were isolated and showed a marked decrease in *Men1* and *p27* mRNA and protein and this corresponded to an increase in cell proliferation. On the

other hand, overexpression of *Men1* in INS1 or primary rat islets is able to repress glucose-induced proliferation (Zhang et al., 2012).

Glucose-mediated down-regulation of menin is dependent on PI3K-Akt signalling as the presence of inhibitors of PI3K (Ly294002) or Akt (Akt inhibitor IV) leads to reduced menin down-regulation. Additional proof for down-regulation of menin through this pathway is that expression of a constitutively active Akt results in reduced *Men1* expression (Zhang et al., 2012). In agreement with glucose repression of *Men1* expression, insulin stimulation also leads to down-regulation of menin at both the transcript and protein level and this is dependent on the PI3K-Akt signalling pathway (Wuescher et al., 2011).

Since FOXO1 is an important transcription factor downstream of Akt, Zhang *et al.* (2012) investigated whether it controlled *Men1* expression. Since Akt phosphorylation of FOXO1 represses FOXO1 transcriptional activity, if *Men1* was transcriptionally regulated by FOXO1, then activation of Akt would result in reduced expression of *Men1*, which agrees with the observation that PI3K-Akt signal results in *Men1* down-regulation. Indeed, *Men1* was determined to be a transcriptional target of FOXO1 through a luciferase reporter assay and chromatin immunoprecipitation (ChIP) analysis. Overexpression of *FOXO1* results in increased activity of a *Men1*-luciferase reporter and *FOXO1* overexpression in INS1 cells is associated with increased expression of *Men1* and *p27*, while siRNA-mediated knock-down of *FOXO1* markedly reduces their expression (Zhang et al., 2012). FOXO1 was able to bind directly to the promoter of *Men1* as shown by ChIP experiments and conserved FOXO1 consensus sites were identified in the

promoter of rat, mouse and human *Men1* (Zhang et al., 2012). Thus, FOXO1 was identified as an important transcription factor for the regulation of *Men1* expression.

6.2 Post-translational regulation of menin

Very little was known about post-translational modifications of menin until a paper published in 2006 revealed that menin is phosphorylated on two serine residues, S543 and S583, with S543 being the most prevalently phosphorylated site (MacConaill et al., 2006). This phosphorylation was observed in 293T cells as well as in *Men1*$^{-/-}$ mouse embryonic fibroblasts (MEFs) re-expressing *Men1*. The significance of the phosphorylation status of the menin protein is not obvious as it does not affect menin's ability to interact with MLL or other complex components, Ash2L and Rbbp5, or with RNA Polymerase II phosphorylated on Ser5 of the CTD (RNAP II p-S5) (see Section 8.1). In addition, mutation of S543 and/or S583 does not affect menin localization to *Hoxc6* or *Hoxc8* target gene loci (see Section 8.4). Menin protein degradation and sub-cellular localization are also not influenced by phosphorylation nor is the phosphorylation of S543 or S583 cell cycle regulated or affected by DNA damage (MacConaill et al., 2006).

MacConaill *et al.* (2006) suggested that other serine residues are likely phosphorylated since they observed residual phosphorylation levels in S543/S583 double mutants. Another site, S394, was later identified in 293T cells as a site of menin post-translational modification; however, this site was found to be phosphorylated in response to DNA damage (Francis et al., 2011). In agreement with this, two previous papers identifying ATM and ATR substrates on a genome-wide scale (in 293T and M059K glioblastoma cells) that are phosphorylated in response to DNA damaged induced by ionizing radiation (γ-IR) or ultraviolet light (UV), isolated menin as a potential target,

with the S394 site identified (Matsuoka et al., 2007; Stokes et al., 2007). Furthermore, S543 phosphorylation was confirmed and S487 was identified as an additional site by Francis *et al.* (2011), with both of these sites being constitutively phosphorylated.

Very recently, it was also published that menin is modified by SUMOylation on K591 (Feng et al., 2013). Other SUMOylation sites were also predicted but not identified, as K591A mutated proteins were still SUMOylated. Like the phosphorylation of S543 and S583 (MacConaill et al., 2006), the significance of SUMOylation of K591 is not apparent as mutation of this residue does not alter the expression of menin target genes in MEFs and does not affect menin's ability to regulate cell proliferation (Feng et al., 2013).

6.3 Subcellular localization of menin

EGFP-tagged menin was shown to localize primarily to the nucleus, as demonstrated by immunofluorescence and cell-fractionation (Guru et al., 1998), which is consistent with the presence of nuclear localization signals (see Section 3.1) (Guru et al., 1998; La et al., 2007). The localization of endogenous menin in various human and primate cell types and tissues is also primarily nuclear with some protein also present in the cytoplasm (Wautot et al., 2000). In agreement with the primarily nuclear localization, menin interacts with many other nuclear proteins such as transcription factors and chromatin modifying enzymes; however, some cytoplasmic binding partners have also been identified (see Section 7). Furthermore, nuclear export signals were identified in menin and shown to function in the nuclear export of β-catenin (Cao et al., 2009). Menin was also shown to localize near the plasma membrane with IQGAP1, which is involved in cell adhesion junctions with β-catenin and E-cadherin in β-islet cells, suggesting a

cytoplasmic localization and function for menin; although nuclear localization was also observed in these same cells (Yan et al., 2008).

There is some evidence that the subcellular localization of menin can be regulated. Overexpressed tagged menin, and endogenous menin, are present in the soluble, chromatin and nuclear matrix fractions, with most of the protein in the chromatin fraction under standard conditions. With γ-IR treatment, the interaction with the nuclear matrix is enhanced, which corresponds with a decrease in the amount of menin in the soluble fraction (Jin et al., 2003). In another study, insulin exposure was shown to result in menin export from the nucleus and localization in cytoplasm with FOXO1 and 14-3-3 (Wuescher et al., 2011). Thus, under some conditions the subcellular localization of menin can be altered.

7. MENIN PROTEIN INTERACTIONS

The cloning of *MEN1* and determination of the protein sequence unfortunately did not shed much light on its function and why loss of function leads to tumourigenesis. Due to the nearly complete absence of domains with known function, much of what has been learned with regards to menin function has arisen from protein interaction studies. Over the years, such research has amassed a large list of menin-interacting proteins with diverse functions (see Table 1.1 and Figure 1.1). Many of these interacting proteins can be divided into a few important categories: 1) transcription factors 2) chromatin modifying proteins 3) DNA damage response/DNA repair proteins and 4) structural/ cytoskeleton proteins.

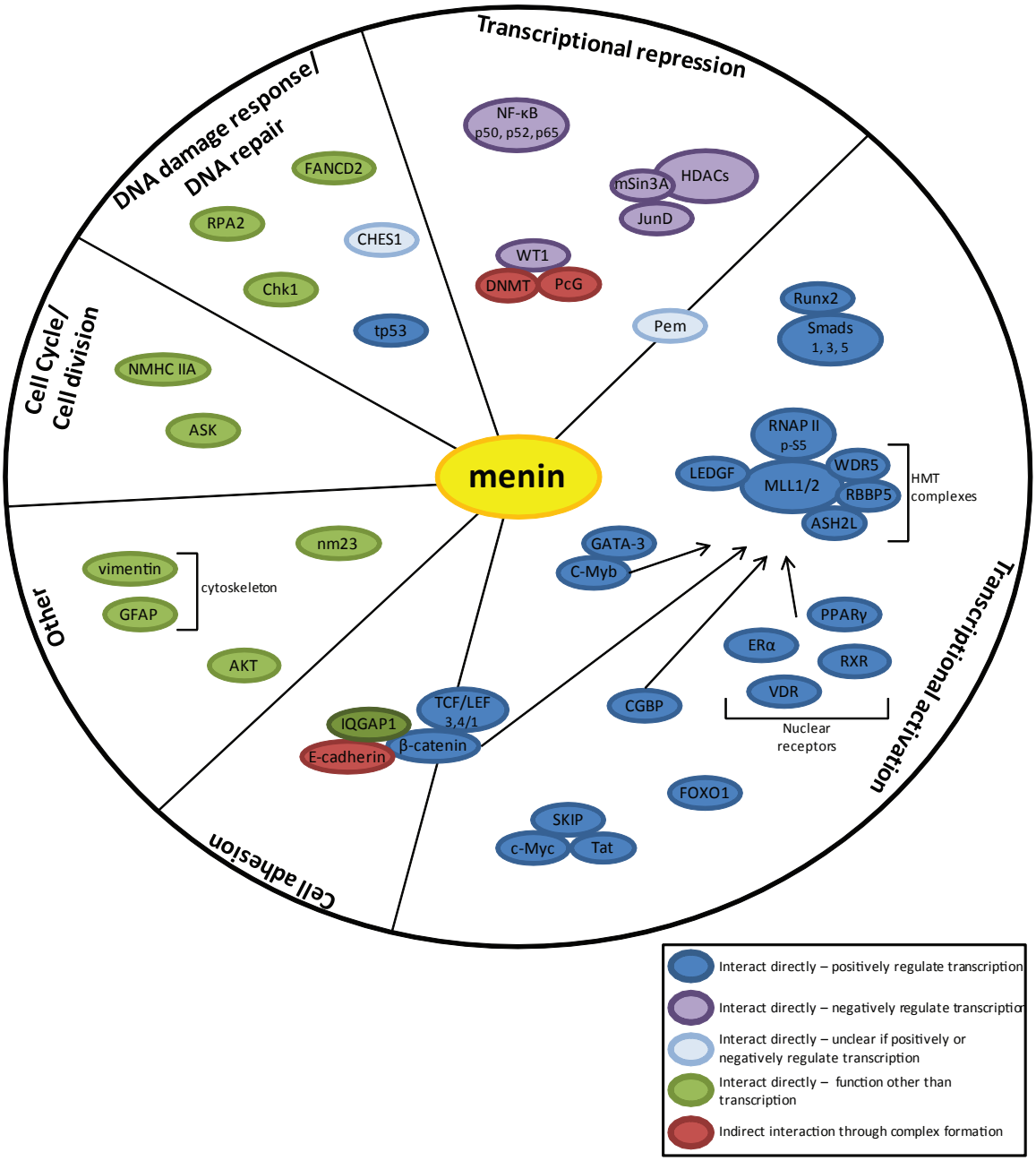

Figure 1.1. Summary of menin interacting proteins and associated functions.
Menin has been shown to interact with many different proteins with diverse functions. Most of these interactions were established in mouse or human cells using co-IP, *in vitro* binding or affinity purification followed by mass spectrometry. It is possible that not all the interactions are direct but occur through other members in the complex. The arrows show proteins/complexes believed to also interact with the MLL complex. Note that many of the interactions involved in positive/negative regulation of transcription also affect other cell processes (*e.g.* apoptosis, proliferation). Please see the text for more details on the interactions and for the associated references.

The various interactions suggest a role for menin in processes such as the regulation of gene expression, cell proliferation, apoptosis and genome stability. The primary menin protein interactions will be summarized below although many of these interactions will not be reviewed in detail. Numerous reviews dedicated to this task provide comprehensive summaries of menin protein interactions (reviewed in Agarwal et al., 2005; Balogh et al., 2010; Balogh et al., 2006; Yang and Hua, 2007). More recent interactions, as well as those that provide the framework for this thesis, will be reviewed in more detail. The menin-MLL interaction will be examined extensively in Section 8. Figure 1.1 provides a schematic summarizing all the interactions and their associated functions and Table 1.1 provides the domains of menin involved in the interactions.

7.1 Menin interacts with several transcription factors

Menin has been shown to interact with several families of transcription factors. Such interactions can either result in the negative or positive regulation of gene expression. One of the first identified menin-interacting partners, JunD, a member of the AP-1 (activator protein 1) family of transcription factors, was identified in a yeast two-hybrid screen. Interaction of menin with JunD leads to the repression of JunD-mediated transcriptional activation (Agarwal et al., 1999). Binding of menin to the N-terminus of JunD leads to the recruitment of the co-repressor mSin3A and associated histone deacetylase (HDAC) complexes resulting in inhibition of transcription (Section 7.2) (Gobl et al., 1999; Kim et al., 2003). Similarly, interaction of menin with members of the NF-κB (nuclear factor kappa B) family of transcription factors, such as p50, p52 and p65 (RelA), results in transcriptional inhibition (Heppner et al., 2001).

On the other hand, menin interaction with Smad3 of the transforming growth factor β (TGF-β) signalling pathway, enhances Smad3 DNA binding ability and thus positively regulates transcription (Kaji et al., 2001). In addition, in ST2 cells (bone marrow stromal cells) menin interacts with Smad1 and Smad5, which act downstream of the bone morphogenetic protein receptors (BMP; also part of TGF-β superfamily), and with Runx2, which is another important transcription factor that co-operates with Smads for BMP-2 and TGF-β signalling (Sowa et al., 2003; Sowa et al., 2004). The interaction of menin with Smad1/5 or Runx2 positively regulates their transcriptional activity in response to BMP-2 signalling (Sowa et al., 2004). Thus, depending on the interacting partner, menin can either function as a transcriptional repressor (JunD, NF-κB) or activator (Smads).

Menin has also been shown to interact with several nuclear receptor proteins, which are a special family of transcription factors that are activated by ligand binding. Those shown to interact with menin include estrogen receptor alpha (ERα), vitamin D receptor (VDR), peroxisome proliferator-activated receptor gamma (PPARγ) and retinoid X receptor (RXR), that forms heterodimers with many of the other nuclear receptors (Dreijerink et al., 2006; Dreijerink et al., 2009a; Dreijerink et al., 2009b). Menin functions as co-activator for each of these nuclear receptors through its recruitment of MLL1/2 histone methyltransferase complexes (see Section 8) for the trimethylation of histone H3 lysine 4 (H3K4me3) and activation of hormone-responsive genes.

The forkhead family transcription factor CHES1 (Checkpoint suppressor 1/FOXN3) was also identified as a menin interacting protein. A genetic interaction was first identified in *Drosophila* (Section 12.5) but the physical interaction was confirmed with

the human homologues (Busygina et al., 2006). Like menin, CHES1 interacts with mSin3A HDAC complexes (Section 7.2), although CHES1 is believed to antagonize HDAC function, unlike menin. This interaction was predicted to be important for the DNA damage response but how the interaction regulated transcription was not established, nor were specific target genes for this interaction identified (Busygina et al., 2006). Another yeast two-hybrid screen identified Pem (placenta and embryonic expression gene), a homeobox transcription factor, as a menin interacting protein. Apart from suggesting a potential role in spermatogenesis due to the co-localization of menin and Pem, the details or functional significance of this interaction were not established (Lemmens et al., 2001).

Menin also interacts directly with c-Myc and HIV Tat (transactivator of transcription) along with SKIP (Ski interacting protein), a transcriptional co-regulator that is also an essential component of the spliceosome (Brès et al., 2009). These interactions were determined through co-immunoprecipitation and GST pull-down assays. Menin, as well as c-Myc, SKIP and the MLL1 complex (including ASH2L and RBBP5; see Section 8.1) localized to an integrated HIV promoter in HeLa cells. Menin, c-Myc and SKIP were required for Tat-induced expression, as determined through siRNA-mediated knock-down, but MLL1 was not required (Brès et al., 2009).

In addition, menin interacts with several other transcription factors. It interacts with c-Myb and GATA-3 and forms a complex with MLL which is important in T lymphocyte development and leukemogenesis; this interaction will be discussed in relation to MLL in Section 8.6 (Jin et al., 2010; Kozuka et al., 2011; Nakata et al., 2010). The interaction with β-catenin and TCF/LEFs will be discussed in Section 7.6 (Cao et al.,

2009; Chen et al., 2008; Inoue et al., 2011; Yan et al., 2008) and that with FOXO1 in Section 7.7. Overall, menin has been shown to interact with an impressive list of transcription factors and can play a role in both transcriptional activation and repression. Whether menin regulation involves activation or repression depends on the associated transcription factors and recruited histone modifying complexes.

7.2 Menin interacts with proteins involved in chromatin modification

In addition to interacting with transcription factors, menin also influences gene expression through its association with histone modifying proteins including histone methyltransferases (HMTs) and histone deacetylases (HDACs), which modify histones in a manner that activates or represses transcription, respectively. HMTs that have been shown to interact with menin include mixed lineage leukemia homologues 1 and 2 (MLL1 and MLL2) (Section 8.1) (Hughes et al., 2004; Yokoyama et al., 2004). As mentioned above, menin also interacts with mSin3A, a co-repressor that recruits HDAC complexes that are responsible for gene repression. For example, menin was shown to co-immunoprecipitate with HDAC1/2 in HEK 293 cells (Kim et al., 2003) and La *et al.* (2006) also mention an interaction with HDAC3.

Recently menin was found to co-immunoprecipitate with Wilm's tumour suppressor protein (WT1), which is a DNA-binding protein that contains zinc finger domains (Xu et al., 2011). WT1 interacts with polycomb group (PcG) proteins and DNA methyltransferases (DNMTs), for H3K27 methylation and promoter CpG methylation, respectively, both marks associated with repression. However, unlike menin's localization with HMT and HDAC complexes directly at chromatin, menin was not localized to target genes (*i.e. Pax2*, *Paired box transcription factor 2*) repressed by the

WT1/PcG/DNMT complex. In this case menin represses gene expression in a more indirect and currently unknown manner (Xu et al., 2011). A similar role for menin in gene repression associated with H3K27me3 was found for the *pleiotropin* growth factor gene; however, unlike *Pax2*, menin was localized to the promoter of the *pleiotropin* gene along with enhancer of zeste homolog 2 (EZH2; PcG), which is responsible for the repressive H3K27me3 mark (Gao et al., 2009). Interestingly, this repression implicated menin in the suppression of lung cancer in mice.

7.3 Menin interacts with DNA damage response and DNA repair proteins

In addition to menin's association with a variety transcription factors and histone modifying complexes, it has also been shown to interact directly with proteins important for DNA repair, namely RPA2 and FANCD2 (Jin et al., 2003; Sukhodolets et al., 2003). RPA2 is the 32 kDa subunit of the heterotrimeric replication protein A (RPA) which is a single-stranded DNA binding protein important for DNA replication, recombination and repair. The menin-RPA2 interaction was identified through yeast two-hybrid screening and confirmed by co-immunoprecipitation and nuclear co-localization observed by immunofluorescence (Sukhodolets et al., 2003). The significance of this interaction is not clear since menin does not affect the localization or ssDNA binding ability of RPA. Moreover, menin is not observed in RPA2-containing DNA repair foci induced by UV light (activates nucleotide excision repair (NER) pathway) or camptothecin (inhibits topoisomerase I and activates double-strand DNA break (DSB) repair pathway) suggesting that menin does not have a direct role in the induced DNA repair pathways (Sukhodolets et al., 2003). FANCD2 (Fanconi anemia complementation group D2), which is important to the BRCA1-mediated DNA repair pathway, was also shown to interact

directly with menin (Jin et al., 2003). This interaction was identified by immunoprecipitation of FLAG-menin from 293 cells followed by mass spectrometry to identify interacting proteins. The interaction of menin with FANCD2 is enhanced following exposure of cells to γ-irradiation and thus appears to increase in response to DNA damage (Jin et al., 2003).

As well as interacting with DNA repair proteins menin associates with key proteins of the DNA damage response pathway, Chk1 and tp53 (Bazzi et al., 2008; Gallo et al., 2010). Co-immunoprecipitation experiments in HEK 293 cells show that Chk1 (checkpoint kinase 1) and menin interact and surprisingly this interaction is not enhanced by treatment with the DNA damaging agent etoposide (Gallo et al., 2010). Similarly, menin was found in immunoprecipitations performed with a total tp53 (tumour protein 53) or activated tp53 (anti K318ac tp53) antibody. This interaction is observed with or without γ-irradiation (Bazzi et al., 2008). It should be noted that both of these interactions (Chk1 and tp53) were observed in conditions of menin overexpression and direct binding assays were not performed therefore these interactions may be indirect (see Section 10 for more details on menin in the DNA damage response).

7.4 Menin interacts with ASK to repress cell cycle progression

A more direct link between menin and cell proliferation was recognized when researchers identified an interaction with activator of S-phase kinase (ASK) (Schnepp et al., 2004a). As its name implies, ASK is important for S phase entry and DNA replication; it is a required subunit for activation of the Cdc7 kinase. Menin represses ASK-induced

cell proliferation through a direct interaction although the exact mechanism for this cell cycle regulation has not been demonstrated (Schnepp et al., 2004a).

7.5 Menin interacts with cytoskeleton and motor proteins

Some other menin interactions have been published suggesting that menin interacts with cytoskeleton and motor proteins, suggesting a role in the cytoplasm, where menin is not predominantly localized. Menin interacts with the intermediate filaments vimentin and glial fibrillary acidic protein (GFAP), with the interaction more pronounced during S and G2 phases. The authors suggested that the interaction could be important for the cytoplasmic sequestration of menin in a cell cycle dependent manner (Lopez-Egido et al., 2002). Menin also interacts with the motor protein non-muscle myosin type IIA heavy chain (NMHC IIA). This interaction is predicted to be important for cell division since menin and NMHC IIA co-localize at the cleavage furrow (Obungu et al., 2003). Besides the papers describing these initial observations, no additional publications on these interactions exist, suggesting that the importance of these interactions to menin function and/or tumourigenesis is still unknown.

7.6 Menin interacts with proteins in the Wnt/β-catenin pathway

Recently, menin was shown to interact with proteins of the Wnt/β-catenin pathway, including β-catenin, TCF3/4 and LEF1 (T-cell specific transcription factor/lymphoid enhancer binding factor) (Cao et al., 2009; Chen et al., 2008; Inoue et al., 2011). These interactions result in promoter H3K4me3, presumably through MLL recruitment, and activation of Wnt/β-catenin target genes (*e.g. Axin2*) (Chen et al., 2008). Another study seems to contradict this finding and suggests that menin is important for down-regulation of Wnt signalling. Menin is important for the shuttling of β-catenin from the

nucleus and *Men1*$^{-/-}$ MEFs or insulinoma tissues display an accumulation of nuclear β-catenin (Cao et al., 2009). Furthermore, menin also interacts with the scaffold protein IQGAP1 (IQ motif containing GTPase activating protein 1) that is important for controlling cell motility and adhesion. The interaction of menin with IQGAP1 leads to further association with E-cadherin and β-catenin at the cell membrane (Yan et al., 2008). This interaction suggests that menin plays a role in cell adhesion. Additional evidence to support this is the observation that expression of menin in pre-tumour β-cells results in increased cell adhesion and reduced cell migration while *Men1*$^{-/-}$ islets have reduced E-cadherin and β-catenin co-localization at adhesion junctions (Yan et al., 2008). In addition, insulinomas isolated from *Men1*-ablated mouse pancreases are associated with reduced E-cadherin localization at the membrane and reduced β-catenin levels (Bertolino et al., 2003c). This loss of E-cadherin and β-catenin is associated with a loss of cell-cell adhesion and increased migration, therefore menin may play a role in maintaining cell adhesion and preventing migration of endocrine cells, thus, potentially playing an anti-metastatic role (Bertolino et al., 2003c; Yan et al., 2008).

7.7 Menin interacts with Akt and FOXO1 of the insulin signalling pathway

A role for menin in insulin signalling through the PI3K/Akt pathway was recently established by Wang *et al.* (2011). Menin interacts with both inactive and active Akt (phospho-Akt, S473). This interaction was established through co-immunoprecipitation of FLAG-menin and HA-Akt1 proteins overexpressed in HEK-293 cells and through co-immunoprecipitation of endogenous proteins from mouse pancreatic cells. Pull-down assays with *in vitro* expressed proteins showed that the interaction between menin and

Akt is direct, with the C-terminal domain of menin required (amino acids 212-610 were sufficient) (Wang et al., 2011).

The researchers suggested that menin negatively regulates the activation of Akt kinase activity. After serum stimulation, the level of p-Akt in *Men1*$^{-/-}$ MEFs is high in comparison to knock-out MEFs re-expressing *Men1*. Also, downstream targets of Akt (*e.g.* GSK-3β, S6K, 4E-BP) have reduced levels of phosphorylation in the cells re-expressing *Men1* compared to *Men1*$^{-/-}$ cells. *In vitro* kinase assays also confirm that menin inhibits Akt kinase activity (Wang et al., 2011). Menin inhibition of Akt also correlates with a reduction of Akt-induced proliferation and Akt-dependent anti-apoptotic effects. Furthermore, menin is believed to inhibit activation of Akt by cytoplasmic sequestration and blocking of its translocation to the plasma membrane after stimulation. This was demonstrated in HEK-293 cells by comparing localization of Akt in cells overexpressing a full-length *MEN1* to cells expressing a mutated *MEN1* (W396R) that fails to interact with and inhibit Akt; Akt localized to the cytoplasm versus at the plasma membrane, respectively. Finally, Wang *et al.* (2011) show a negative correlation between menin and p-Akt levels in wild-type mouse islet cells (*Men1*$^{+/+}$) compared to islet adenomas (*Men1*$^{+/-}$). The normal islet cells have high menin and low p-Akt levels, and islet adenomas show the opposite expression pattern (*i.e.* low menin, high p-Akt). Overall, this research shows that menin negatively regulates Akt and this could be one mechanism by which menin prevents hyperproliferation and exerts its tumour suppressor function in endocrine cells.

In another recent study, menin was found to interact with the transcription factor FOXO1 in liver cells (Wuescher et al., 2011). Through co-immunoprecipitation

experiments, these proteins were shown to interact following insulin stimulation, with the interaction being most prominent in the cytoplasmic fraction. The localization of the interaction was confirmed by immunofluorescence; both menin and FOXO1 move from the nucleus to the cytoplasm following insulin stimulation of HepG2 cells (Wuescher et al., 2011). The investigators hypothesized that menin contributes to the export of FOXO1 from the nucleus and its sequestration in the cytoplasm in order to down-regulate insulin signalling. It should be noted that the protein 14-3-3, involved in protein sequestration, was also found to co-immunoprecipitate with menin and FOXO1.

Through liver-specific down-regulation of menin, using the Cre-*loxP* system to generate heterozygous (*Men1*$^{+/-}$) mice, Wuescher *et al.* (2011) observed that decreased menin leads to increased expression of FOXO1 target genes such as the *insulin receptor* (*InR*), *Akt*, *insulin-like growth factor binding protein 1* (*Igfbp-1*) and genes involved in glucose metabolism, namely *glucose-6-phosphatase* (*G6Pase*) and *peroxisome proliferator-activated receptor gamma coactivator-1-alpha (PGC-1α)*. Interestingly, these authors noted that there was no increase in *FOXO1* transcript levels in *Men1*$^{+/-}$ livers, suggesting that menin only regulates FOXO1 at the post-translational level, likely through sequestration in the cytoplasm.

These investigators only looked at the interaction in primary mouse hepatocytes, and in the HepG2 cell line (derived from human hepatocellular carcinoma) (Wuescher et al., 2011) so it is unclear if the interaction between menin and FOXO1 occurs in other cell types. It is presumed that since the interaction was regulated by insulin signalling this interaction would likely occur in other cells where insulin receptors are expressed and insulin signalling is important. It is also unclear whether the interaction is solely

dependent on insulin signalling, or if other growth factors signalling through receptor tyrosine kinases could also stimulate the interaction in other cells types.

Although Wuescher *et al.* (2011) referred to the previous study of Wang and co-workers (2011) showing that menin negatively regulates Akt, they did not sufficiently discuss how the interaction between menin and FOXO1 fits into this picture. The story is complicated due to the fact that a negative feedback loop exists between FOXO1 and Akt, as Akt is a FOXO1 target gene and Akt inhibits FOXO1 transcriptional activity through phosphorylation and cytoplasmic sequestration. Since menin was found to inhibit Akt (Wang et al., 2011), and Akt inhibits FOXO1 transcriptional activation, then menin inhibition of Akt is expected to relieve inhibition of FOXO1. This contradicts what was discovered by Wuescher *et al.* (2011) who showed that menin actually helps to sequester FOXO1 in the cytoplasm, thus inhibiting FOXO1-mediated transcription. Accordingly, menin could be at the center of a complex series of interactions and regulations that control insulin signalling and glucose homeostasis, but many details still need to be worked out.

7.8 Menin interacts with nm23 and is associated with GTPase activity

The only putative enzymatic function assigned to menin is that of being an atypical GTPase when stimulated through an interaction with nm23 (non-metastatic gene 23), a multifunctional protein with nucleoside diphosphate kinase, protein kinase and GTPase activating (GAP) activities. In the presence of nm23, menin was shown to hydrolyze GTP to GDP, while neither protein could do this independently. This observation agrees well with the presence of five GTPase-like motifs in menin (Yaguchi et al., 2002). However,

this GTPase activity was only demonstrated *in vitro* and no additional studies have confirmed it.

7.9 Summary of menin protein-protein interactions

Overall, there has been a great deal of research effort put into identifying and characterizing menin protein-protein interactions (see Table 1.1). The diversity of these interactions is evident and suggests that menin is somewhat indiscriminate in its associations. Although such research was aimed at identifying the function of menin, in particular its tumour suppressor function, the vast number of interacting partners, and an ever growing list, make it difficult to pin-point the crucial function of menin. It is important to know that many of these novel interactions were identified by yeast two-hybrid screens or overexpression systems and many were studied in immortalized cell lines (*e.g.* 293, HeLa) and consequently some of these interactions may not be essential to the function of menin in endocrine cells. The vast number of different protein interactions suggests that there is likely cell specificity to some of these protein-protein interactions. The most numerous interactions are clearly with transcription factors, and many of these interactions also result in menin-dependent recruitment of histone modifying complexes, such as MLL, suggesting that this function is likely central to menin's tumour suppressor function in endocrine cells.

8. MENIN INTERACTS WITH MIXED LINEAGE LEUKEMIA (MLL)

8.1 Menin associates with MLL histone methyltransferase complexes

In order to identify proteins that interacted with menin under normal physiological conditions, large scale menin purification followed by mass spectrometry to identify

associated proteins was undertaken by a few labs. Using such methods, menin was found to interact with proteins of the Trithorax group (TrxG) family, including MLL2 (mixed lineage leukemia 2) and ASH2L (absent, small or homeotic 2-like) (Hughes et al., 2004). Other components isolated in this large menin-containing complex included WDR5 (WD40 repeat containing protein 5), RBBP5 (retinoblastoma binding protein 5) and hDPY-30, suggesting that menin interacts with a complex similar in composition to that of the yeast Set1 COMPASS (complex proteins associated with Set1) (Hughes et al., 2004). Similarly, around the same time, another group independently identified menin as a component of a COMPASS-like complex by purification of MLL1 (homologue of MLL2 and *Drosophila* Trithorax) and its interacting proteins (Yokoyama et al., 2004). Like the complex identified by Hughes *et al.* (2004), this menin-MLL1 complex also contained ASH2L, WDR5 and RBBP5; but, Yokoyama *et al.* (2004) found HCF1/HCF2 (Host cell factor 1 and 2) and not hDPY-30 in their complex.

Another protein that was pulled-down with menin and identified by mass spectrometry was Rpb2, the small subunit of RNAP II (Hughes et al., 2004). Further analysis showed that menin interacts with the larger subunit (Rpb1) of RNAP II when the C-terminal repeat domain (CTD) is phosphorylated on serine 5, but not when phosphorylated on serine 2 or unphosphorylated (Hughes et al., 2004). Menin was also shown to associate with CGBP (CpG binding protein), although this interaction could be indirect, as menin was observed in CGBP immunoprecipitations with the MLL complex (Ansari et al., 2008).

The menin-MLL complex has histone methyltransferase (HMT) activity that is specific to lysine 4 of histone H3 (H3K4me) (Hughes et al., 2004). This activity is

conveyed by the presence the SET1 (*su(var)3-9, enhancer of zeste, trithorax*) domain of MLL, which is a conserved histone methyltransferase domain. This H3K4 methylation is an epigenetic mark associated with transcriptional gene activation (Milne et al., 2002). Interestingly, some MEN1 disease-related missense mutations (*i.e.* H139D, A242V, T344R), are not associated with HMT activity (Hughes et al., 2004). This suggests that menin's interaction with MLL and the associated HMT activity could be important for menin's tumour suppressor function; however, since other missense mutants (*i.e.* P12L, L22R, A309P, W436R) are still associated with H3K4me, loss of MLL interaction alone cannot account for tumourigenesis in all MEN1 patients.

8.2 Menin interacts with the N-terminus of MLL

MLL is a large protein of 3969 amino acids that is cleaved by Taspase1 at conserved sites to generate two protein fragments, MLL^N and MLL^C, that remain associated (see Chapter 4 Introduction for more details on MLL structure) (Hsieh et al., 2003a; Hsieh et al., 2003b). MLL^N interacts with menin and HCF1/2, while the other components of the MLL complex (ASH2L, RBBP5 and WDR5) interact with MLL^C through the SET1 domain (Yokoyama et al., 2004). Since menin interacts with the N-terminus of MLL1 it is able to interact with MLL fusion proteins (see Section 8.3) as efficiently as with the wild-type MLL1 protein. The domain of interaction for menin was originally mapped the very N-terminus of MLL, more specifically, amino acids 6-10 (RWRFP) were identified as a high-affinity menin-binding motif (hMBM) since their deletion was sufficient to abrogate interaction of menin with MLL (Yokoyama et al., 2005). Biochemical analysis of the interaction suggested that there are two regions of MLL^N that contribute to the interaction with menin, named menin-binding motif 1 (MBM1, residues 4-15) and

MBM2 (residues 23-40), with MBM1 binding menin with significantly higher affinity (about 20 times higher). Within MBM1, mutational analyses indicate that three hydrophobic residues contribute most to the interaction with menin, F9, P10 and P13 (Grembecka et al., 2010). The recent crystallization of human menin revealed that residues 6-25 of MLL1 are necessary and sufficient for menin binding (see Section 3.3) (Huang et al., 2012). MLL2, a close homologue to MLL1, also interacts with menin (Hughes et al., 2004) and has a nearly identical N-terminal domain (MLL2 16-35) that also binds menin with high affinity (Huang et al., 2012).

8.3 Menin is required for MLL-associated leukemogenesis

Although menin is well established as a tumour suppressor (Sections 4 and 5), paradoxically, it also plays a role as an essential oncogenic co-factor in MLL-associated leukemias (Yokoyama et al., 2005). MLL1 is associated with a variety of human tumours, including acute lymphoblastic leukemia (ALL), acute myelogenous leukemia (AML) and biophenotypic/mixed lineage leukemia (MLL). In MLL-associated leukemias, chromosomal translocations result in the formation of MLL fusion proteins. Greater than 50 different translocation partners have been identified so far and the fusion partner often carries a DNA binding domain or oligomerization domain. All MLL fusions retain at least the first eight exons of MLL and thus retain the menin-interacting domain, but lose the C-terminal SET1 domain (See Chapter 4 Introduction for additional details) (reviewed in Krivtsov and Armstrong, 2007).

MLL fusion proteins retain the ability to interact with menin but not with any of the other proteins identified in the multi-protein MLL complex. Common MLL fusions (*e.g.* MLL-AF6, MLL-ENL and MLL-p300) co-immunoprecipitate with menin and co-

localize to *HoxA* target genes in ChIP analyses (see Section 8.4) (Yokoyama et al., 2005; Yokoyama et al., 2004). The interaction with menin is essential for both the initiation and the maintenance of MLL-mediated leukemia (Yokoyama et al., 2005). Deletion of the menin-binding domain of MLL-AF9 impairs the ability of the MLL fusion to transform bone marrow cells (Caslini et al., 2007). Thus, menin is required as an oncogenic co-factor in MLL-associated leukemogenesis.

8.4 Menin and MLL regulate expression of Hox genes and CDK inhibitors

Menin interaction with MLL is important for expression of *Hox* genes; this has been demonstrated for *Hoxc8, Hoxc6* (Hughes et al., 2004), *Hoxa9* (Yokoyama et al., 2004), *Hoxa7, Hoxa10* (Yokoyama et al., 2005) and the *Hox* co-factor *Meis1* (Chen et al., 2006). Knock-down of menin or MLL by RNAi, but not other components of the complex (ASH2L, WDR5 or HCF-1/2), results in decreased expression MLL target genes (*e.g. Hoxa9*), suggesting that menin is essential for MLL-regulated gene expression (Yokoyama et al., 2004). Menin appears to be required for normal haematopoiesis which is linked to its requirement for expression of *Hox* genes. Therefore, in the haematopoietic system, menin is needed for normal proliferation and/or differentiation (Chen et al., 2006). Conditional knock-out of *Men1* using the Cre-*loxP* system results in reduced white blood cell counts and reduced colony formation by bone marrow (BM) progenitor cells compared to $Men1^{+/+}$ mice (Chen et al., 2006).

Menin and MLL also coordinate to regulate expression of cyclin-dependent kinase (CDK) inhibitors $p27^{Kip1}$ and $p18^{INK4c}$. Loss-of-function of either MLL or menin results in reduced expression of these CDK inhibitors and increased cell proliferation (Milne et al., 2005). Furthermore, menin appears to be essential for recruitment of MLL

to target loci as *Men1*$^{-/-}$ MEFs do not show binding of MLL within the coding region of *p27* or *p18*; however, *MLL*$^{-/-}$ MEFs retained menin binding at these loci, as observed through ChIP assays (Milne et al., 2005).

Menin's ability to inhibit pancreatic cell proliferation was demonstrated in mouse models (Section 5) and this ability seems to rely on activation of expression of *p27* and *p18*. Additional cell culture and mouse model studies provide support to this idea. MIN6 cells, derived from mouse pancreatic β-cell tumours have severely reduced *Men1* expression levels (Karnik et al., 2005). Transfection of MIN6 cells with *Men1* results in decreased proliferation and increased expression of *p27* and *p18*, which is also associated with menin localization and H3K4me3 at these genes (Karnik et al., 2005). Likewise, as previously mentioned, *Men1*$^{+/-}$ heterozygous mice or β-cell specific knock-out mice develop insulinomas and this is associated with a loss of the wild-type *Men1,* as well as *p18* and *p27*, expression (Fontanière et al., 2006a; Karnik et al., 2005; Schnepp et al., 2006). Overall these studies suggest that control of pancreatic cell proliferation by menin occurs through the regulation of *p27* and *p18* expression, coordinated through regulation of histone methylation at the promoter, which results in the inhibition of CDK2 and/or CDK4 and thus inhibition of the transition from G1 to S phase.

The specificity of target genes in different cell types may dictate whether the menin-MLL interaction results in proliferation or growth inhibition. In the haematopoietic lineage, *Hox* genes are important target genes and their overexpression, as occurs with MLL fusions, results in proliferation and can lead to leukemogenesis. On the other hand, in endocrine cells, CDK inhibitors *p27* and *p18* are important targets and

loss of expression in the absence of menin results in increased proliferation and MEN1 syndrome (Milne et al., 2005).

8.5 Menin recruitment of LEDGF is required for MLL-associated leukemogenesis

There is clear evidence that menin is essential for MLL-mediated leukemogenesis; however, the contribution of menin to leukemogenesis and its biochemical function remained poorly understood for several years. The findings of Yokoyama and Cleary (2008) suggest that the sole function of menin in the MLL interaction is to recruit and tether another protein, lens epithelium-derived growth factor (LEDGF, also called PSIP1 or p75). LEDGF is a PWWP domain containing protein, and this domain is known to bind to modified chromatin (H3K36me3 associated with active genes) (Pradeepa et al., 2012). LEDGF was identified by co-immunoprecipitation following overexpression of menin and MLL-ENL; in this case overexpression was desirable in order to identify proteins that may interact more weakly with the MLL complex and were thus missed in the initial characterization of the complex. The interaction between the three endogenous proteins was confirmed in REH cells (human leukemia cell line) (Yokoyama and Cleary, 2008). A mutation in MLL that prevents menin interaction (deletion of hMBM, Δ6-10), also results in loss of LEDGF in co-immunoprecipitations, suggesting that menin is required for the interaction between LEDGF and MLL. Deletion of a distinct region of MLL (112-153), named the LEDGF binding domain (LBD), abolished LEDGF interaction without affecting menin binding. The MLL/menin-binding domain of LEDGF was localized to residues 335-460, which includes its IBD (HIV-1 integrase binding domain) (Yokoyama and Cleary, 2008).

LEDGF co-localizes with MLL and menin on *Hox* gene loci (*HOXA7*, *HOXA9*) as observed in ChIP assays. This is consistent for wild-type MLL (in U937 myeloid lineage cells) and the MLL fusion MLL-AF6 (expressed in ML-2 cells that have the translocation t(6;11)(q27;q23)). Additionally, knock-down of LEDGF through RNAi results in decreased expression of *HOXA9* (Yokoyama and Cleary, 2008). Like menin, LEDGF is required for MLL-mediated leukemogenesis. Deletion of or mutation (F129A) within the LBD of MLL-ENL prevents transformation of myeloid cells and results in the loss of *HOXA9* expression (Yokoyama and Cleary, 2008). This LBD is missing in the closely related MLL2 and this is believed to be the reason why MLL2 is not implicated in leukemia as a result of chromosomal translocations (Huang et al., 2012).

Interestingly, substituting the hMBM of MLL-ENL with the PWWP domain of LEDGF is sufficient for transformation of myeloid progenitors and transcriptional activation of *HOXA9*, which were previously shown to be inhibited by the loss of the hMBM (Yokoyama and Cleary, 2008; Yokoyama et al., 2005). Furthermore, PWWP-MLL-ENL is able to induce transformation in cells from conditional *Men1*$^{-/-}$ mice, while MLL-ENL cannot, suggesting that the role of menin is to recruit LEDGF whose molecular action requires only the PWWP domain (Yokoyama and Cleary, 2008). This interaction is important for both the function of wild-type MLL complexes as well as MLL-mediated leukemogenesis. Moreover, LEDGF interaction with menin also seems to be important for menin function and tumour suppression in endocrine cells. Several identified *MEN1* missense (H138D, T344R) mutations that fail to interact with MLL, also fail to interact with LEDGF and other mutants (P12L, L22R) fail to associate with LEDGF even though they retain the ability to interact with MLL (Yokoyama and Cleary, 2008).

8.6 Menin interacts with c-Myb and GATA-3 which contributes to MLL-associated leukemogenesis and T-cell differentiation

The function of menin in the MLL complex and MLL-associated leukemogenesis was expanded with the discovery that in addition to recruitment of LEDGF, menin can also bridge c-Myb to MLL (Jin et al., 2010). FLAG-tagged c-Myb was purified and found to associate with MLL and other complex proteins including menin, WDR5, ASH2L and RBBP5. Direct binding assays show that c-Myb fails to bind directly to MLL, WDR5, ASH2L, but associates directly with menin. Menin is required for interaction of c-Myb and MLL, as deletion of the hMBM of MLL that prevents menin binding, results in loss of c-Myb association (Jin et al., 2010). The authors demonstrated that c-Myb's DNA binding domain is important for recruitment of menin and MLL to *HOXA9*, presumably by binding directly to c-Myb binding sites in exons 1 and 2 of *HOXA9*. Knockdown of *c-Myb* by siRNA results in decreased expression of *HOXA9* and *MEIS1* in myeloid leukemia cell lines (K562 and ML-2), suggesting that c-Myb contributes to the expression of MLL target genes that are implicated in leukemogenesis (Jin et al., 2010). Research has not yet demonstrated how the interactions of menin with c-Myb and LEDGF are related and whether both interactions are simultaneously necessary for targeting of MLL complexes.

The interaction between menin and c-Myb was further explored and an additional menin-interacting protein was identified. Menin was found to co-immunoprecipitate with both c-Myb and GATA-3 in human primary $CD4^+$ T helper cells. *In vitro* binding assays show that although c-Myb and GATA-3 do not interact directly, menin interacts with each of these proteins and can bridge the interaction between them (Nakata et al., 2010). ChIP assays revealed that c-Myb, GATA-3, menin and MLL all

bind to the *GATA-3* promoter (gene is auto-regulated); this is also associated with H3K4me2 and H3K4me3 (Nakata et al., 2010). Therefore, menin bridges the interaction between c-Myb and GATA-3 as well as between c-Myb and MLL, establishing large complexes important for regulation of gene expression. Similarly, this complex of c-Myb, GATA-3, menin and MLL regulates the expression of *interleukin 13* (*IL-13*) in $CD4^+$ T (effector/memory) cells through binding to a conserved GATA-3 response element, implicating menin in T cell differentiation (Kozuka et al., 2011).

8.7 Menin as a potential target for leukemia cancer therapy

Since menin was the first identified essential co-factor for MLL-mediated transformation, the idea to target this interaction for cancer therapy seemed promising. In early experiments, expression of small peptides corresponding to the N-terminus of MLL, successfully reduced expression of target genes (*e.g. MEIS1*) and inhibited cell proliferation of MLL-AF9 transformed bone marrow cells (Caslini et al., 2007). This suggested that targeting the interaction between menin and MLL fusion proteins could be an effective therapeutic strategy.

Determination of the crystal structure of menin was important for the development of potential therapeutic inhibitors for MLL-associated leukemia aimed at disrupting the menin-MLL interaction (see Section 3.3) (Huang et al., 2012; Murai et al., 2011). Small molecule inhibitors (MI-2 and MI-3) were designed that are capable of binding in the menin pocket and preventing MLL binding, thus disrupting the interaction and consequently the oncogenic potential of MLL fusions (Grembecka et al., 2012). Similar results were observed in various human leukemia cell lines with different MLL fusion proteins and in all cases the inhibitor treatment resulted in inhibition of

proliferation, G0-G1 cell cycle arrest and induction of apoptosis and differentiation (Grembecka et al., 2012). This group crystallized menin in complex with MI-2, and used this information to develop the next generation of inhibitor, MI-2-2, that could bind menin with even higher affinity (Shi et al., 2012). Overall these experiments demonstrated the effectiveness of small molecule inhibitors at blocking the menin-MLL interaction and the feasibility of using such compounds to reverse the leukemogenic effects of the MLL fusions that rely on menin interaction. Thus, the outlook for generating similar compounds that can used for targeting aggressive leukemia associated with MLL translocations seems promising.

9. MENIN IS AN IMPORTANT REGULATOR OF GENE EXPRESSION

As mentioned above (Section 8.4), important genes regulated by menin include the *Hox* genes and the CDK inhibitors *p27* and *p18*. Menin positively regulates the expression of these genes through interaction with MLL complexes and H3K4me3 and this implicates menin in the regulation of differentiation and cell proliferation (Hughes et al., 2004; Milne et al., 2005; Yokoyama et al., 2004). Several other target genes that are either repressed or activated by menin have been reported and implicate menin in the regulation of processes such as proliferation and apoptosis. It is important to note that many of these targets are likely cell type specific and menin regulation of gene expression is likely dependent on its interaction with cell specific transcription factors. Some of the menin targets that may be particular important to its tumour suppressor function will be summarized.

9.1 Menin inhibits IGF signalling and cell cycle progression

A microarray analysis of the insulinomas that arise after deletion of *Men1* from β-cells revealed an overall disregulation in the expression of genes involved in signal transduction, particularly in the insulin-like growth factor (IGF) pathway, cell cycle regulation, metabolism, transcription and cell differentiation (Fontanière et al., 2006b). As expected, several *Hox* genes were down-regulated in the insulinomas. Components of the IGF pathway, including *Igf2* (*insulin-like growth factor 2*) and *Igfbp-3* (*insulin-like growth factor binding protein 3*) were found to be up-regulated. Cell cycle regulators were also up-regulated in early and late stage tumours; these include *cyclin A2*, *cyclin B2* and *cyclin D2* (Fontanière et al., 2006b). These findings suggested that loss of menin function in pancreatic β-cells leads to increased IGF signalling, increased cell cycle progression and decreased differentiation which could all contribute to the observed tumourigenesis.

In agreement with this microarray study, menin was previously shown to mediate the repression of *Igfbp-2* (La et al., 2004a). Menin-mediated repression of *Igfbp-2* may relate to its anti-proliferative function since *Igfbp-2* is important for the regulation of cell proliferation. NLS1, NLS2 and NLSa of menin were found play a crucial role in binding to the *Igfbp-2* promoter for gene repression (La et al., 2006; La et al., 2004a). Interestingly, trichostatin A (TSA), an HDAC inhibitor, failed to cause an increase in *Igfbp-2* expression in *Men1*$^{-/-}$ MEFs complemented with *Men1* despite an increase observed in *Men1*$^{-/-}$ MEFs, suggesting that menin-mediated repression is not solely mediated by HDACs but that other factors are essential (La et al., 2006). Instead, it appears that menin is important for chromatin remodelling at the promoter of *Igfbp*-2,

and prevents the formation of an open chromatin state as demonstrated by a DNase I hypersensitivity assay (La et al., 2004a).

The gene profiling study of Fontanière *et al.* (2006b) also showed an increase in the expression of various cyclins in *Men1*$^{-/-}$ insulinomas. This concurs with a recent study demonstrating the menin-mediated repression of *cyclin B2* (gene *Ccnb2*) expression, suggesting a role for menin in cell cycle regulation at the G2/M boundary (Wu et al., 2010). Menin binds directly to the promoter of *Ccnb2* and represses transcription, in this case, menin-associated repression corresponded with a reduction of H3ac at the *cyclin B2* locus. Menin's association at the *Ccnb2* promoter correlated with interference of CBP (histone acetyl transferase) and transcription factor NF-Y binding and increased recruitment of HDAC3 (Wu et al., 2010). *Men1*$^{-/-}$ MEF cell cultures show a higher number of M phase cells than those re-expressing *Men1* and this is linked to an increase in Cyclin B2 in the *Men1*$^{-/-}$ MEFs (Wu et al., 2010). Overall, the results demonstrate how menin regulation of gene expression contributes to cell cycle regulation at the G2/M transition and this complements the previous observation that menin regulates the cell cycle at the G1/S transition through regulation of the CDK inhibitors *p27* and *p18*, (Milne et al., 2005; Schnepp et al., 2006).

9.2 Menin represses the expression of hTERT

Menin was identified as a negative regulator of *hTERT* (human telomerase reverse transcriptase) expression. The *hTERT* gene encodes the protein portion of human telomerase, while *hTR* encodes the RNA template component (Lin and Elledge, 2003). Menin overexpression in HeLa cells results in decreased levels of *hTERT* transcript and protein; while siRNA-mediated down-regulation of *MEN1* in U2OS cells, that do not

normally express *hTERT*, leads to induction of its expression (Lin and Elledge, 2003). ChIP analyses revealed that menin binds to a region of the *hTERT* promoter with putative AP-1 and NF-κB binding sites, hinting at the possibility that menin could repress AP-1/NF-κB-mediated transcription through recruitment of mSin3A and HDAC complexes as demonstrated for the inhibition of JunD (Kim et al., 2003). Furthermore, depletion of *MEN1*, in conjunction with expression of an oncogene (*i.e. H-ras* or SV40 Large and Small T antigen), results in immortalization and transformation of human primary fibroblasts which is coupled with reactivation of *hTERT* expression and increased telomerase activity (Lin and Elledge, 2003). Overall, this work suggests that loss of *MEN1* could result in reactivation of *hTERT* expression, which could contribute to immortalization and tumourigenesis.

9.3 Menin activates the expression of caspase 8 and regulates apoptosis

Many tumour suppressors are important for regulating apoptosis and menin is no exception. Overexpression of *Men1* through an adenovirus in MEFs induces apoptosis; while loss of *Men1* impairs UV or TNF-α induced apoptosis (Schnepp et al., 2004b). This could be mediated by regulation of the expression of pro-apoptotic genes. Indeed, *caspase 8*, an important effector of the TNF-α and Fas pathways, was identified in a microarray for menin-regulated genes (La et al., 2007). Expression of c*aspase 8* was four-fold higher in *Men1* expressing versus *Men1*-null MEFs. *Men1*$^{-/-}$ MEFs had reduced caspase 8 enzymatic activity, observed by procaspase 3 cleavage in response to TNF-α, and this was restored when *Men1* was reintroduced (La et al., 2006; Schnepp et al., 2004b).

Further analysis of menin-regulated expression of *caspase 8* revealed that the NLS1, NLS2 and NLSa regions (see Section 3.1) are important; although a mutation in a single NLS does not impair nuclear localization, it greatly reduces *caspase 8* expression (La et al., 2006). Menin binds the 5' UTR of the *caspase 8* locus *in vivo* and can also activate the expression of a luciferase reporter carrying this sequence (La et al., 2007). Surprisingly, menin mediated expression of *caspase 8* is independent of its ability to recruit MLL complexes, as MLL and H3K4me3 are not significantly detected in the 5' UTR of the *caspase 8* locus. On the other hand, H3 and H4 acetylation in this region are high and are dramatically reduced in *Men1*$^{-/-}$ MEFs; however, treatment with vaproic acid, an HDAC inhibitor, did not significantly increase expression of caspase 8, suggesting that histone acetylation is not the most important feature for activation of expression (La et al., 2007).

The importance of *caspase 8* to menin's tumour suppressor function was investigated by analysing the effect *MEN1*-associated mutations (L22R, A242V) on *caspase 8* expression. *Men1*$^{-/-}$ MEFs reconstituted with MEN1 disease-associated missense mutants fail to induce *caspase 8* expression and these missense mutants are unable to bind to the *caspase 8* locus (La et al., 2007). Moreover, in insulinomas that develop in *Men1*$^{+/-}$ mice following a LOH, there is a marked decrease in expression of *caspase 8*. However, at earlier ages, before insulinoma development, the levels of *caspase 8* mRNA were comparable in *Men1*$^{+/-}$ and *Men1*$^{+/+}$ mice (La et al., 2007). This provides additional evidence for the importance of menin-mediated *caspase 8* expression for the suppression of tumourigenesis.

9.4 Examination of menin involvement in gene expression on a genome-wide scale

Menin binding to chromatin on the genome-wide scale (ChIP-Seq) was assessed and menin was found to occupy 1162 loci in HeLa cells (Agarwal et al., 2007). Of these occupied sites, 32 % were promoters, 21 % inside genes, 14 % at the 3'end of genes and the remaining sites were within regions where genes had not been identified. The categories most represented by the menin-bound genes were cellular metabolism, macromolecule metabolism and cell cycle (Agarwal et al., 2007). A similar study examined genome-wide menin binding in parallel with MLL1 and RBBP5 in HeLa, HepG2 and islet cells through ChIP-chip (Scacheri et al., 2006). These 3 proteins co-localized at the promoters of thousands of genes but menin also binds independently to additional sites. Interestingly, menin occupied a broad region throughout the *Hox* gene clusters but more specifically bound to the promoter regions and not within the coding region of other genes (Scacheri et al., 2006). Most sites occupied by menin were associated with high levels of gene expression; however, loss of menin did not result in altered gene expression for most of these loci (Scacheri et al., 2006). The results suggest that menin is a global regulator of transcription but a small subset of specific target genes are likely important for its tumour suppressor function.

In addition, the gene expression patterns of tumours from MEN1 patients have been examined to see which genes are affected. The global expression profile of neuroendocrine tumours revealed that of the 193 genes that were differentially expressed in comparison to control normal islet cells, 104 of these could be categorized as involved in cell growth, cell death or signal transduction. For example, 19 genes involved in apoptosis were significantly under-expressed in MEN1 patients (Dilley et al., 2005). Overall, these results suggest that menin regulates expression of many genes and

loss of menin function affects the expression of several genes which could contribute to increased proliferation and decreased apoptosis in tumour cells.

10. MENIN IS IMPORTANT FOR DNA DAMAGE RESPONSES, DNA REPAIR AND GENOME STABILITY

The interaction of menin with proteins involved in DNA repair, RPA2 and FANCD2, suggested that menin might be important for DNA repair which could be linked to its tumour suppressor role (see Section 7.3) (Jin et al., 2003; Sukhodolets et al., 2003). Furthermore, menin was shown to be phosphorylated at ATM/ATR consensus sites in response to UV or γ-IR suggesting that it is itself regulated by the DNA damage response pathway (see Section 6.2) (Francis et al., 2011; Matsuoka et al., 2007; Stokes et al., 2007).

An interaction was also established with Chk1, an essential kinase downstream of ATM/ATR, which is important for homology directed DNA repair of double-strand breaks (DSB) in the DNA damage response pathways (Gallo et al., 2010). Using a cell-based assay for DSB repair, based on reconstitution of GFP expression as a result of repair of a cleaved *I-SceI* site (DR-GFP/*I-SceI* system), the importance of menin in DSB repair in HeLa cells was demonstrated. Overexpression of menin results in increased DNA repair which is dependent on the ATM/ATR pathway as it is inhibited by caffeine treatment (Gallo et al., 2010). ChIP using primers for the *I-SceI* site in HeLa transfected cells, revealed that menin binds there along with Chk1. Furthermore, the two proteins co-immunoprecipitate in HEK 293 cells but surprisingly treatment with the DNA damaging agent etoposide does not enhance this association. In addition, menin overexpression

does not affect the phosphorylation and activation of Chk1 following etoposide or hydroxyurea treatment (Gallo et al., 2010). This work suggests that menin could be involved in DSB DNA repair but the importance of the Chk1 interaction has yet to be defined.

In addition to interacting with Chk1, menin has also been observed to interact with tp53, which functions downstream of Chk1 in the DNA damage response (Bazzi et al., 2008). In this study, menin overexpression in INS-1 insulinoma cells sensitizes them to apoptosis following γ-irradiation. This is accompanied by an increase in activation of the apoptotic effector caspase 3, as observed by the appearance of the cleaved form of the procaspase, and an increase in activated (acetyl K318) tp53 protein in menin overexpressing compared to control cells. In addition, *p21*, a transcriptional target of tp53, is also up-regulated more rapidly in menin overexpressing cells after γ-IR treatment (Bazzi et al., 2008). Interestingly, such observations correlated with menin overexpression are not observed when MEN1 missense mutants (A160T, H317Y, A541T) are overexpressed instead. This implies that menin's ability to elicit a DNA damage response and activate apoptosis could be important to its tumour suppressor function in endocrine cells (Bazzi et al., 2008).

Also in agreement with a role for menin in DNA damage responses, is the observation that *Men1*$^{-/-}$ MEFs are more sensitive to DNA damage resulting from exposure to DNA cross-linking agents (diepoxybutane and mitomycin C) as observed by decreased cell survival and increased chromosomal aberrations (Jin et al., 2003). Finally, menin has also been implicated in the maintenance of genome stability as MEN1 syndrome is associated with chromosome instability. Lymphocytes from MEN1 patients

have a significant increase in chromosome breakage, translocations, deletions and dicentric chromosomes and pancreatic tumours fail to maintain genomic integrity (Hessman et al., 2001; Scappaticci et al., 1991). In all, these studies propose a role for menin in the DNA damage response and the maintenance of genome stability; although, a direct and specific role has not yet been described.

11. A LINK BETWEEN MENIN, INSULIN REGULATION AND DIABETES MELLITUS

Due to the occurrence of insulinomas in about 10 % of MEN1 patients, studies have investigated a link between menin, insulin regulation and diabetes mellitus (Agarwal et al., 2004). As insulinomas are functional hormone secreting tumours they can have detrimental consequences as they can cause hypoglycemia due to the overproduction and secretion of insulin. On the other hand, several correlational studies compared MEN1 patients to controls and found an increased incidence of diabetes mellitus, impaired fasting glucose or insulin resistance in MEN1 patients (whose tumours did not include insulinomas) (McCallum et al., 2006; van Wijk et al., 2012; Wägner et al., 2005). Together this suggests that menin could be linked to fine tuning the balance between insulin production and the insulin response.

Loss of menin in the pancreas of mice is strongly correlated with uncontrolled β-cell proliferation which eventually results in the formation of insulinomas (see Section 5.3). This loss of menin function is generally associated with increased insulin levels and decreased blood glucose levels (Bertolino et al., 2003b; Bertolino et al., 2003c; Crabtree et al., 2001; Crabtree et al., 2003; Karnik et al., 2005). The high insulin levels associated with loss of *Men1* function in the pancreas could be the consequence of

hyperproliferation of the insulin producing cells or alternatively it could suggest that menin normally acts to inhibit insulin production. A role for menin in the regulation of insulin expression was proposed from studies with rat INS-1 insulinoma cells, where overexpression of *Men1* significantly reduced expression of a luciferase reporter under the control of the insulin promoter (Sayo et al., 2002). In addition, while control INS-1 cells have increased insulin secretion in response to glucose exposure, *Men1* overexpressing cells appear to be unable to adjust insulin secretion in response to increased glucose exposure (Sayo et al., 2002). However, menin has not yet been shown to bind to the endogenous promoter to repress expression. This work by Sayo *et al.* (2002) contradicts what was found by Karnik *et al.* (2007) who observed no change in *Ins1* and *Ins2* mRNA in pregnant mice overexpressing menin in pancreatic β-cells. Additionally, Yang *et al.* (2010a) show that glucose treatment of isolated *Men1*$^{-/-}$ mouse islet cells does not result in increased insulin secretion compared to controls, suggesting that secretion of insulin from individual cells is not affected. Thus, many studies have shown that menin negatively regulates pancreatic β-cell proliferation which can contribute to the disruption of normal insulin regulation; however, an unequivocal role for menin in direct regulation of insulin gene expression remains to be established.

Due to this observed negative regulation of β-cell proliferation by menin, researchers identified menin as potential target for diabetes patients since they have reduced β-cell mass or function. Deletion of *Men1* prevents hyperglycemia which can be induced by treatment with streptozotocin, a cytotoxic agent that preferentially damages β-cells (acts as a glucose analog that preferentially blocks GLUT2 localized in β-cells). In both an inducible model of *Men1* excision and a β-cell specific model of *Men1* ablation,

mice without *Men1* function become resistant to streptozotocin-induced hyperglycemia (Yang et al., 2010b).

In addition to preventing hyperglycemia, it was hypothesized that down-regulation of menin could be used to treat pre-existing hyperglycemia as this should result in the proliferation of β-cells and consequently insulin production (Yang et al., 2010a). Inducible excision of *Men1* after the development of hyperglycemia through streptozotocin treatment, results in decreased blood glucose levels, increased BrdU incorporation and an increase in the number of insulin-positive cells compared to controls retaining functional *Men1* (Yang et al., 2010a). Similar results were obtained with a type 2 diabetes mouse model that has a leptin receptor mutation (*db/db*) and with mice fed a high fat diet that induces type 2 diabetes. Inducible deletion of *Men1* in these mice reduces fasting glucose and improves the glucose intolerance and hyperglycemia that are initially observed (Yang et al., 2010a). Thus, deletion of *Men1* in mouse models of diabetes seems to improve glucose homeostasis and rescue hyperglycemia. There is controversy over the usefulness of this strategy for treating diabetes due to the fact that insulinomas often result with *Men1* inactivation in both mice and humans (Bertolino et al., 2003c; Crabtree et al., 2001; Marx, 2005; Schnepp et al., 2006).

Interestingly, menin inhibition of pancreatic β-cell proliferation is correlated with the development of gestational diabetes mellitus (Karnik et al., 2007). Adaptive proliferation of β-cells during pregnancy is required to meet the altered metabolic needs. Pancreatic islets isolated from normal pregnant mice reveal a decrease in *Men1* mRNA and menin protein, suggesting that *Men1* must be down-regulated to allow for

the necessary expansion of β-cells during pregnancy (Karnik et al., 2007). When, *Men1* is conditionally overexpressed in the β-cells of pregnant mice they developed hyperglycemia and have increased fasting glucose and impaired glucose tolerance as well as reduced insulin serum levels, all features that mimic gestational diabetes mellitus (Karnik et al., 2007). These results suggest that the presence of high menin levels impairs the β-cell expansion that is required during pregnancy and results in insufficient insulin production and gestational diabetes.

Overall, the results of these studies suggest that menin plays a crucial role in the pancreas to regulate proliferation and consequently insulin production. Menin is necessary for maintaining insulin homeostasis, where a loss of menin can result in insulinomas and hypoglycemia while too much menin can result in hyperglycemia and diabetes. An additional level of complexity is added to the scenario when one considers that insulin and glucose have been shown to repress *Men1* expression (Section 6.1) and that menin interacts with Akt and FOXO1 of the insulin signalling pathway (Section 7.7).

12. DROSOPHILA MENIN

12.1 Drosophila Mnn1 gene and protein

Mnn1, the *Drosophila melanogaster* orthologue of human *MEN1*, was identified and characterized by two autonomous groups in close succession (Guru et al., 2001; Maruyama et al., 2000). The *Drosophila Mnn1* gene spans 6.3 kb and is composed of 5 exons, with exons 2 to 5 encoding a 763 amino acid protein with a predicted molecular weight of 83 kDa (Guru et al., 2001; Maruyama et al., 2000). *Drosophila* menin is 46 % identical (56 % similar) to the human counterpart and more importantly, 69 % of

mutations (missense and in-frame deletions) documented in MEN1 patients occurred in residues that are identical in both species (Guru et al., 2001). This emphasizes the likely importance of these highly conserved regions and validates the use of the *Drosophila* model system to better understand menin function. Furthermore, NLS2 of human menin is conserved in *Drosophila*, suggesting that the protein is likely localized to the nucleus and this was also demonstrated by immunofluorescence (Cerrato et al., 2006; Guru et al., 2001). Since the identification and characterization of *Drosophila Mnn1* a few research groups have generated mutants to study menin function in this important genetic model system.

12.2 Generation of Mnn1 mutants to study menin function in Drosophila

Mnn1$^{-/-}$ flies established in three independent labs, including the Campos lab, are viable and fertile with no obvious phenotype (Busygina et al., 2004; Cerrato et al., 2006; Papaconstantinou et al., 2005). This contrasts to the scenario in mice, where loss of the *Men1* gene is embryonic lethal (see Section 5.1) (Bertolino et al., 2003a). This establishes that *Mnn1* is not an essential gene in *Drosophila* and is likely not involved in developmental processes. *Mnn1* mutants were shown to have a slightly reduced viability and lifespan by some groups (Busygina et al., 2004; Cerrato et al., 2006).

Two *Mnn1* deletion mutants were created in the Bédard/Campos lab by the imprecise excision of a P-element in exon 1 (GE11370, GenExcel Inc). *Mnn1*^{e30} has a 2096 bp deletion starting within exon 1 and ending in exon 4 while *Mnn1*^{e173} has a larger deletion of 4216 bp that begins upstream of exon 1 and ends in the fourth intron (Papaconstantinou et al., 2005). In addition to the deletion mutants, UAS-*Mnn1* and UAS-*Mnn1*-dsRNA (simplified *Mnn1-RNAi*) lines were generated for studying the effects

of overexpression and down-regulation of *Mnn1*, respectively (Papaconstantinou et al., 2005).

Brian Oliver's group also generated *Mnn1* deletion mutants from imprecise excision of a P-element in the 5' UTR of the *P{wHy}*^{30G01} line (Cerrato et al., 2006). They generated two *Mnn1* deletion mutants, *Mnn1*$^{\Delta 46}$ and *Mnn1*$^{\Delta 79}$, with *Mnn1*$^{\Delta 46}$ having a deletion that removes the entire P-element insertion as well as a small deletion of 70 bp downstream of start codon, while *Mnn1*$^{\Delta 79}$ has a 186 bp deletion downstream of the start codon but also retains part of the 5' sequence of the P-element (Cerrato et al., 2006). This group specifically screened for smaller deletions than those in *Mnn1*^{e30} and *Mnn1*^{e173} to ensure that genes proximal to the *Mnn1* locus would not also be disrupted. The gene *milton* (*milt*) is upstream of the *Mnn1* locus and the gene *CG31907* is nested in the antisense direction in intron 4 of *Mnn1*. The *Mnn1*^{e173} deletion approaches the 3' end of *milt*, and both *Mnn1*^{e30} and *Mnn1*^{e173} come near the 3' end of *CG31907*. Unlike Papaconstantinou *et al.* (2005) that did not observe any developmental defects with *Mnn1* overexpression, Cerrato *et al.* (2006) observed distinct defects in thoracic closure or an adult pharate lethality phenotype when *UAS-Mnn1* was overexpressed with certain drivers (*e.g. How24* (mesoderm), *elav*^{C155} (CNS), *daG32*^{UH1} (ubiquitous), *69B* (ectoderm), *OK6* (motor neurons), *pnr*^{MD237} (medial thorax)).

Allen Bale's group generated the *Mnn1*^{e200} deletion line which was also generated by P-element mobilization (from the P553 insertion line, Berkeley *Drosophila* genome project) (Busygina et al., 2004). The *Mnn1*^{e200} deletion extends to the middle of exon 4, deleting about 50 % of the coding region. As the *milt* gene was also affected by this deletion, a *milt* genomic rescue construct was maintained in this line (Busygina et

al., 2004). These various *Mnn1* deletion mutants were used to study menin function in *Drosophila* and this work suggested a role for menin in stress responses, DNA damage response and maintenance of genomic stability.

12.3 Drosophila menin regulates stress responses

Evidence for the importance of proper menin expression in the regulation of the *Drosophila* stress response was presented by Papaconstantinou *et al.* (2005). Deletion mutants, $Mnn1^{e30}$ and $Mnn1^{e173}$, and lines overexpressing (*UAS-Mnn1*) or down-regulating (*Mnn1*-RNAi) menin were found to be sensitive to various stresses, including, heat shock, hypoxia, hyperosmolarity and oxidative stress, as observed by increased lethality compared to control lines (Papaconstantinou et al., 2005). In addition, under conditions of heat stress, misexpression of menin disrupted the regulation of heat shock protein (*hsp*) gene expression. This was observed using an *hsp70-LacZ* reporter line and also by examining protein levels through immunoblotting. In *Mnn1* overexpressing lines there was an increase in HSP70 induction following heat stress, while in *Mnn1-RNAi* embryos and the *Mnn1* deletion mutants, the expression of HSP70 and HSP23 was significantly reduced. Furthermore, HSP70 protein levels were not properly down-regulated during recovery from heat stress when menin was overexpressed. ChIP analysis demonstrated that overexpressed menin is recruited to the *hsp70* promoter following heat shock. Furthermore, microarray analysis of $Mnn1^{e30}$ and *Mnn1-RNAi* embryos showed that menin was required for sustained expression of multiple *hsp* genes with a prolonged heat stress (1 hr) but was not required for the initiation of heat shock gene expression with a short heat shock (10 mins) (Papaconstantinou et al., 2010). Taken together, these results suggest that menin is a positive regulator *hsp* expression in

response to heat stress in *Drosophila* (please see Chapter 5 Introduction for more details) (Papaconstantinou et al., 2005).

12.4 Drosophila menin plays a role in DNA repair and the maintenance of genome integrity

The *Mnn1*^{e200} mutants are hypersensitive to both ionizing radiation and DNA damaging agents. γ-IR treatment of *Mnn1*^{e200} larvae results in reduced survival to adulthood compared to controls and this defect is rescued by reintroducing a *Mnn1* transgene (*UAS-Mnn1* with *hs-GAL4*) (Busygina et al., 2004) . It was later demonstrated that *Mnn1* mutants have a defect in the S phase checkpoint following exposure to γ-IR. Wild-type flies show a decrease in entry into S phase after γ-IR, as determined by reduced BrdU staining; however, *Mnn1* mutants fail to arrest at S phase and continue to incorporate BrdU during DNA synthesis (Busygina et al., 2006).

Similar to the sensitivity to γ-IR, Mnn1^{e200} flies are sensitive to treatment with the DNA cross-linking agents, nitrogen mustard and cisplatinum (Busygina et al., 2004). These results suggest a possible role for menin in DNA repair and additional experiments suggested a role in the maintenance of genome integrity. A loss of heterozygosity (LOH) assay based on the *lats* gene was used to assess frequency of mutations in *Mnn1*^{e200} flies. In this assay, heterozygous *lats*$^{+/-}$ flies are examined for ectopic tumour formation that occurs with loss of the wild-type *lats* allele. *Mnn1*^{e200} flies had 2-3 times more tumour foci than controls both under standard and γ-IR conditions, while with nitrogen mustard treatment they have seven fold more foci than controls (Busygina et al., 2004). This group attempted to further characterize the presumed defect in DNA repair but found no difference in DSB repair in *Mnn1* mutants compared to controls, which

contradicts the observation made by Gallo et al. (2010) showing that human menin expression stimulates homology directed repair of DSBs in HeLa cells (Busygina et al., 2004; Gallo et al., 2010). The authors suggested that *Mnn1* flies may have a defect in NER but this was not formally established (Busygina et al., 2004).

Moreover, similar to Busygina *et al.* (2004), loss of heterozygosity associated with *Mnn1* mutants was observed by Papaconstantinou *et al.* (2010). Loss of menin function was associated with increased genome instability when exposed to chronic sub-lethal heat stress during embryonic and larval development. This was observed through a LOH assay for the *multiple wing hair* (*mwh*) locus. *Mnn1* deletion mutants and *Mnn1-RNAi* flies in a heterozygous $mwh^{+/-}$ background, showed increased LOH with chronic heat stress or hypoxia compared to untreated flies of the same genotype (Papaconstantinou et al., 2010). Thus, menin is required for the maintenance of genome stability in response to stress. This function was not solely due to regulation of *hsp70* expression as *Mnn1* and *hsp70* double mutants showed higher frequency of LOH events compared to either single mutant (Papaconstantinou et al., 2010).

12.5 Mnn1 genetic interaction studies in Drosophila

Unlike human menin which binds JunD to repress its transcriptional activity, the *Drosophila* protein was not observed to interact directly with the single Jun family member (Guru et al., 2001); however, a genetic interaction between *Drosophila* menin and Jun was demonstrated. *Mnn1* functionally interacts with Jun/Fos in a complex manner and appears to either negatively or positively regulate Jun/Fos activity depending on the cellular context (*i.e.* thorax versus eye) (Cerrato et al., 2006).

Another genetic interaction was established between menin and the forkhead transcription factor *Ches1.* *Ches1* was identified in a genetic screen as a modifier of the thoracic cleft phenotype observed in *Mnn1* overexpressing flies (Busygina et al., 2006). Overexpression of *Ches1* in a *Mnn1* mutant background is able to restore the defect in S phase arrest as well as the viability of *Mnn1* mutants exposed to γ-IR (Busygina et al., 2006). These investigators also showed that human menin and CHES1 proteins interact by co-immunoprecipitation but this was not investigated for the *Drosophila* proteins (Busygina et al., 2006). Taken together, these results suggest that menin co-operates with this transcription factor in the DNA damage response, perhaps through interaction with histone modifying complexes as both menin and CHES1 have been shown to associate with histone deacetylases (Busygina et al., 2006).

As menin and FANCD2 were shown to interact in mammalian cells (Jin et al., 2003) this interaction was also investigated in *Drosophila.* Surprisingly, even though both *Mnn1* and *FANCD2* mutants are sensitive to cross-linking agents and have defects in S-phase arrest, they were not observed to interact genetically in the same pathway (Marek et al., 2008), nor have they been shown to interact physically in *Drosophila*. In fact, menin and FANCD2 appear to mediate DNA cross-link repair through distinct mechanisms. This was suggested based on the observation that mutants for each gene display a distinct spectra of mutations in response to DNA damaging agents; while *Mnn1* mutants show high levels of single base pair deletions as observed using a novel *supF* reporter assay specific for detection this type of mutation, *FANCD2-RNAi* flies do not. Both mutants displayed hypersensitivity in the *lats* LOH assay, which can detect small deletions in addition to larger ones, which seem to be predominant in *FANCD2-RNAi* flies

(Marek et al., 2008). Apart from these few genetic studies, *Drosophila Mnn1* has not been extensively studied. In addition, no menin protein-protein interactions have been documented so far in *Drosophila*. This led our lab to investigate menin function using the *Drosophila* model system to study protein-protein interactions.

13. THESIS OBJECTIVES

Although menin has been the focus of significant research since the *MEN1* gene was cloned in 1997, the mechanism of menin tumour suppression action is still not fully understood. For this reason, continued investigation into menin interacting proteins and the processes regulated by menin is important as it has potential clinical implications. Since the *Drosophila* model system is very genetically tractable, it is our system of choice for elucidating menin interactions and functions. In order to further investigate *Drosophila* menin function, a yeast two-hybrid screen was performed to isolate novel interacting proteins (Hybrigenics). One of the proteins indentified in this screen, Fas-associated death domain (FADD) became a primary focus of my research (see Chapter 3). In addition, another principal focus was the investigation of a potentially conserved interaction between *Drosophila* menin and Trithorax (Trx), the homologue of human MLL1 whose interaction with menin has been well documented (see Chapter 4). The initial objective of my research was to validate these two potential interactions in *Drosophila* S2 cells. This was followed by experiments designed to determine the functional significance of these interactions.

As previous work by Papaconstantinou *et al.* (2005, 2010) demonstrated a role for menin in the regulation of stress responses and the maintenance of genome stability,

determining the significance of these interactions for proper stress responses became the primary goal of my proposed research. The general hypothesis for this research was that menin controls cellular responses to a variety of stresses by regulating gene expression and ultimately functions in the maintenance of genomic integrity. I investigated this hypothesis by studying the importance of menin's interactions with Trithorax and dFADD for heat shock and pathogen stress responses and determined if these interactions were important for the maintenance of genomic stability.

More specifically, the working hypothesis for the menin-dFADD interaction was that menin plays a role in the pathogen stress response and interacts with dFADD in the nucleus to regulate gene expression after bacterial challenge. In order to investigate this, three specific aims were defined. The first of these was to determine the subcellular localization of the menin-FADD interaction to predict the potential functional significance of this interaction. The second was to characterize the role of menin in the *Drosophila* pathogen stress response and innate immune pathways. The third aim was to establish a genetic interaction between *Mnn1* and *dFADD* and determine its importance for pathogen and heat stress responses as well as the maintenance of genomic integrity. The key findings from this research are presented in Chapter 3.

The working hypothesis for the menin-Trithorax interaction was that menin interacts with Trithorax at chromatin to coordinate proper chromatin modifications required for transcription of heat shock proteins in response to heat stress. Two specific aims were defined for this area of research. The first was to examine a genetic interaction for *Mnn1* and *trx* and study its importance for the heat shock response and maintenance of genomic integrity. The second goal was to characterize the recruitment

of menin and Trithorax to chromatin for proper histone modification in response to heat stress. The principal results from this research are presented in Chapter 4.

Even though research with these two protein interactions seemed promising, regrettably problems were encountered with the *Drosophila Mnn1* stocks and previous findings regarding the heat stress response could not be reproduced. Thus, not all of the research goals outlined above could be completed. These issues and attempts to resolve them are summarized in Chapter 5. Finally, as a consequence of these difficulties, a new research goal was proposed; that is, investigating the potential role of menin in the *Drosophila* insulin signalling pathway. The reasons for embarking on this avenue of research include the following: menin was recently observed to interact with two proteins of the insulin signalling pathway in mammalian cells (Akt and FOXO1), menin is important in regulating pancreatic islet cell proliferation and consequently insulin production, menin regulates genes important for insulin signalling and insulinomas develop in MEN1 patients. The primary goal was to determine if *Mnn1* mutants display a similar phenotype as the well-studied *Drosophila* insulin signalling pathway mutants. This research is presented in Chapter 6.

CHAPTER 2. MATERIALS AND METHODS

1. BACTERIAL CULTURE

Bacterial cultures were used in order to amplify plasmid DNA. In most cases, the DH5α™ strain of *Escherichia coli* was used for transformation and plasmid amplification. Unless otherwise stated, cultures were grown in Luria-Bertani (LB) broth. LB is composed of 1 % w/v Bacto-Tryptone, 0.5 % w/v yeast extract, 1 % w/v sodium chloride. LB was sterilized by autoclaving and supplemented with suitable antibiotics before use for selection of antibiotic resistance genes present in plasmids. Cultures were grown at 37°C with shaking at 200 rpm. In most cases, 3 mL overnight cultures were prepared for mini-preps and plasmid DNA was isolated using the HiYield™ Plasmid DNA Kit and following the manufacturer guidelines (RBC Bioscience, YPD100). For larger DNA preps needed for cell transfection, 250 or 500 mL cultures were prepared and plasmid DNA was isolated using QIAGEN Plasmid Maxi Kit (QIAGEN, 12163) and following the guidelines provided by the manufacturer.

2. CELL CULTURE

2.1 Drosophila S2 cells

Drosophila Schneider 2 (S2) cells, initially generated from late stage embryos, were cultured in HyClone® SFX-Insect™ Cell Culture Medium (Thermo Scientific, SH30278.01) supplemented with Penicillin at a final concentration of 100 U/mL and Streptomycin at 100 µg/mL (Gibco®, 15140-122). Cells were maintained in 25 cm^2 vented flasks (Starstedt, 83.1810.002) in an incubator at room temperature.

2.2 293T cells

293T cells were cultured at 37°C with 5 % CO_2 in Dulbecco's Modified Eagle Medium (DMEM) (Gibco®, 11995073) supplemented with 10 % Fetal Bovine Serum (FBS) (Gibco®, 12483-020), 2 mM L-Glutamine (Gibco®, 25030-081) and 100 U/mL penicillin plus 100 µg/mL Streptomycin (Gibco®, 15140-122).

3. HEAT SHOCK TREATMENT OF S2 CELLS

For heat shock (HS) of S2 cells, plates were parafilmed tightly before being submerged in a water bath at 37°C. The length of HS varied depending on the experiment in question. Commonly the duration of the HS was 5, 15, 30, 45 or 60 mins. Immediately following HS, plates were removed from the water bath and placed on ice and the parafilm was removed. Cells were then scraped from the plates and collected for lysate preparation as described below (Section 5.1). For a treatment consisting of a heat shock with a recovery, once the HS was complete the parafilm was removed from the plate and the plate of cells was returned to the incubator at room temperature for the recovery period, which in most cases lasted 1 hr.

4. CELL TRANSFECTION

4.1 Calcium phosphate transfection method for 293T cells

The calcium phosphate transfection method was used for 293T cells. 293T cells were chosen since they are amenable to transfection and foreign proteins are readily expressed at high levels. The cell medium was changed to fresh DMEM about 4 hours before transfection. For 100 mm plates, this transfection method requires that 10 µg of

plasmid DNA be mixed with 20 µg of carrier DNA from salmon sperm and 0.25 M $CaCl_2$, in a total volume of 500 µL. This DNA and $CaCl_2$ mixture was added dropwise to an equal volume of 2 X HBSP (1.5 mM Na_2HPO_4, 10 mM KCl, 280 mM NaCl, 12 mM D-glucose, 50 mM Hepes, pH adjusted to 7.12 with NaOH) while mixing gently on a vortex set to minimum speed. The mixture was allowed to sit at room temperature for 30 mins to allow $Ca_3(PO_4)_2$-DNA precipitates to form. It was mixed by pipetting and then added dropwise to the plate of cells. Cells were left overnight at 37°C with the DNA and $Ca_3(PO_4)_2$. The following morning the transfection medium was removed and cells were rinsed gently 2 times with 1 X Phosphate Buffered Saline (PBS) (137 mM NaCl, 2.7 mM KCl, 10 mM Na_2HPO_4, 1.8 mM KH_2PO_4, pH adjusted to 7.4) before cells were returned to complete DMEM (supplemented with FBS, L-glutamine and Penicillin-Streptomycin as previously described) and placed back at 37°C.

This transfection method was used to transfect 293T cells with vectors for the expression of *Drosophila* menin and *Drosophila* FADD to see if these proteins interact. The experimental transfections were co-transfections of pIRES-GFP:menin with pIRES-GFP:HA-dFADD or pIRES-GFP:menin with pIRES-GFP:dFADD-HA (see Sections 9.1-9.4 for cloning of *dFADD*). For the co-transfections, 10 µg of each plasmid was used and the amount of carrier DNA was reduced to 10 µg. As a control, the empty vector (pIRES-GFP) was transfected into cells. Additional controls for the associated co-immunoprecipitation experiment (co-IP) experiments were the transfection of pIRES-GFP:menin alone, or pIRES-GFP:HA-dFADD or pIRES-GFP:dFADD-HA alone, without having the other *Drosophila* protein co-expressed. Cells were harvested 48 hours post-

transfection. The transfection of 293T cells was used for co-immunoprecipitation experiments to determine if menin and dFADD interact (see Section 7 below).

4.2 Cellfectin® transfection of S2 cells

Cellfectin® II reagent (Invitrogen™, 10362-100) was used to transfect S2 cells. The general guidelines of the manufacturer were followed. Throughout the transfection procedure, the HyClone® SFX-insect™ medium used was not supplement with serum or antibiotics. For a 60 mm plate of cells, 7.5 µg of DNA was used with 10 µL Cellfectin®. If cells were being co-transfected with two vectors, then the amount of Cellfectin® was increased to 15 µL per plate. Cells were incubated with the DNA and transfection reagent for 3-4 hours. The medium was then changed to fresh HyClone® medium supplemented with penicillin and streptomycin. Transfected S2 cell were harvested 48 hours post-transfection.

The pPACB:HA-dFADD and pPACB:dFADD-HA vectors were transfected into S2 cells and the vector alone was used as a control (see Sections 9.1-9.5 for *dFADD* cloning). These transfections were done in order to see if the HA-tagged dFADD protein interacted with endogenous menin in a more relevant physiological background (see Section 7 for co-IP experiments).

5. PREPARATION OF CELL LYSATES

5.1 Cell collection and lysis

Protein lysates for analysis by SDS-PAGE (sodium dodecyl sulfate polyacrylamide gel electrophoresis) and immunoblotting were prepared by lysis of cells in Sodium Dodecyl Sulfate Sample Buffer (SDS-SB, also referred to as Laemmli Buffer). This buffer consists

of 60 mM Tris-HCl (pH 6.8), 2 % SDS, 10 % glycerol and 5 % β-mercaptoethanol. Before use, this was supplemented with the phosphatase inhibitors sodium fluoride (1 mM) and sodium orthovanadate (1mM) and a protease inhibitor cocktail (cOmplete, Mini, EDTA-free Protease Inhibitor Cocktail Tablets, Roche Applied Science, 11836170001). In later experiments, the Roche protease inhibitor cocktail and the phosphatase inhibitors were replaced with HALT protease and phosphatase inhibitor cocktail (Thermo Fisher Scientific Inc., 78440). Note that for co-immunoprecipitation experiments, cells were not lysed in SDS-SB by an alternative buffer was used (see Section 7).

Generally, 100 mm plates of cells were grown for protein lysate preparation. Plates of cells were placed from the incubator onto ice and samples were kept on ice throughout the procedure unless otherwise stated. Weakly adherent cells, such as S2 and 293T, were collected in the medium to prevent cell loss. Cells were scraped from plates using plastic cell scrapers (Fisherbrand, 08-773-1) and cell suspensions were transferred to 15 mL Falcon tubes. To pellet cells, they were spun at 1000 rpm at 4°C for 5 mins in a table-top centrifuge (Beckman Coulter Allegra™ X-22R). The medium was aspirated from the cell pellet and cells were resuspended and washed with 4 mL of cold 1 X PBS. After cells were washed, they were resuspended in 1 mL of 1 X PBS and transferred to an Eppendorf tube. Cells were then spun at 6000 rpm for 3 min in a microcentrifuge at 4°C. The PBS was aspirated from the cells and SDS-SB added and cells were lysed by pipetting up and down. The amount of lysis buffer used was variable depending on the size of the cell pellet, generally between 300-600 µL for a 100 mm plate of cells. Samples were left on ice for 15-30 mins to ensure complete cell lysis. Samples were then vortexed and boiled for 3-5 minutes. Finally, they were spun at

maximum speed for 15 mins at 4°C and the supernatant was transferred to a new tube. At this point, protein lysates were ready for analysis by SDS-PAGE and immunoblotting (see Section 6).

5.2 Protein concentration determination using the Bradford assay

The protein concentration of lysates was determined using the Bradford assay. In brief, a series of bovine serum albumin (BSA; New England Biolabs, B9001S) standards from 0-10 µg/mL were prepared with Bradford Reagent (0.01 % w/v Coomassie Brilliant Blue G-250, 5 % v/v ethanol, 10 % v/v phosphoric acid). All samples being compared were prepared at the same time as the standards, using 2 µL of sample with 200 µL ddH_2O and 800 µL of Bradford Reagent. The absorbance at 595 nm was determined using a spectrophotometer (Biochrom Ultrospec 2100pro). The OD_{595} values for the standards of known protein concentration were used to generate a standard curve. From the equation of the line of best fit, the approximate concentration of each protein sample was determined based on their OD_{595} values.

6. SDS-PAGE AND IMMUNOBLOTTING

6.1 SDS-PAGE

Sodium dodecyl sulfate polyacrylamide gel electrophoresis (SDS-PAGE) was used to separate protein samples. The percentage of acrylamide used for a gel depended on the size of the proteins being examined by immunoblotting. The standard percentage used was 10 % acrylamide. To examine smaller proteins (*i.e.* less than 30 kDa) 12 % gels were used and to resolve larger proteins (*i.e.* greater than 150 kDa) 7 % gels were prepared. The recipe for a 10 % acrylamide separating gel is as follows: 8.8 mL of ddH_2O, 11.2 mL

of 4 X separating gel buffer (1.5 M Tris-HCl (pH 8.8), 0.4 % SDS), 15 mL of 30 % Acrylamide/Bis-Acrylamide Solution (29:1) (Bio-Rad, 161-0156), 70 µL of 10 % ammonium persulfate and 25 µL of TEMED (Invitrogen™, 15524-010). Once the separating gel was polymerized, a stacking gel was prepared by mixing 7.2 mL of ddH_2O, 3 mL of 4 X stacking gel buffer (0.5 M Tris-HCl (pH 6.8), 0.4 % SDS), 1.8 mL of 30 % Acrylamide/Bis-Acrylamide, 36 µL of 10 % ammonium persulfate and 12 µL TEMED.

Protein samples were prepared in SDS-SB as described above (Section 5.1). The amount of protein loaded for each sample was generally 50-100 µg, as determined by the Bradford assay (Section 5.2). Prior to loading samples into a gel for SDS-PAGE, they were boiled for 2 mins in order to denature proteins. Samples were loaded into wells using thin gel-loading tips. For the majority of gels, the Dual Color Precision Plus Protein™ Standard (Bio-Rad, 161-0374) was run alongside samples for protein size determination. Gels were run in 1 X SDS Running Buffer (25 mM Tris, 192 mM Glycine, 0.1 % SDS). Usually gels were run overnight at 60-90 V depending on the percentage of gel and the size of protein being studied. For 7 % gels, they were most often run at constant current, 20 mA for approximately 7 hours.

6.2 Protein transfer

Proteins were then transferred from the gel to a nitrocellulose membrane (Whatman® Protran, 09301108) using the Trans-Blot Cell (Bio-Rad, 170-3946). The transfer was done in 1 X Transfer buffer (25 mM Tris, 192 mM Glycine, 20 % methanol) at 60 V for 3-3.5 hrs at 4°C or at room temperature with a cooling coil and running cold water to prevent overheating. In some cases, when large proteins were of interest, gels were transferred at 80 V for 4 hrs or overnight at 40 V. To check that proteins transferred properly to the

membrane, the membrane was stained with Ponceau S (0.1 % Ponceau S (w/v) in 5 % acetic acid). The Ponceau S stain was rinsed off with ddH_2O before the membrane was blocked.

6.3 Membrane blocking and antibody incubation

Nitrocellulose membranes were blocked in order to decrease non-specific antibody binding. Membranes were blocked in 5 % skim milk powder (w/v) made in 1 X Tris buffered saline (TBS) for 1 hour at room temperature on an orbital shaker. The composition of 1 X TBS is 20 mM Tris and 140 mM NaCl with a final pH of 7.6. After the membrane was blocked, it was incubated in primary antibody solution. Primary antibodies were diluted in a solution of 5 % skim milk powder in 1 X TBS. The dilution used depended on the specific primary antibody (see Table 2.1 for a list of primary antibodies and dilutions used for immunoblotting).

Following incubation with primary antibody overnight at 4°C, membranes were washed several times with 1 X TBS or 1 X TBS-T (1 X TBS with 0.1 % Tween-20). Following washing, membranes were incubated in the appropriate secondary antibody solution. Secondary antibodies were diluted in 1 X TBS with 5 % skim milk powder. The secondary antibody dilution used was 1:5000 or 1:10000 and generally the length of incubation was 1 hr on an orbital shaker at room temperature. Secondary antibodies used included goat anti-rabbit IgG horseradish peroxidase (HRP)-linked antibody (Cell Signaling, #7074), horse anti-mouse IgG HRP-linked antibody (Cell Signaling, #7076) and donkey anti-goat IgG HRP-linked (Santa Cruz, sc-2020).

After secondary antibody incubation, membranes were washed several times in 1 X TBS and then treated for 2 mins with Pierce ECL (enhanced chemiluminescent)

Western Blotting Substrate (Thermo Fisher Scientific Inc., 32106). In some cases, a stronger ECL reagent, Immobilon Western Chemiluminescent HRP Substrate (Millipore, WBKLS0500), was used to improve the detection of less abundant proteins. Membranes were transferred into a plastic sheet inside a Hypercassette™ (8 x 10, Amersham Pharmacia Biotech, 12649). Immediately after, in a dark room, Amersham Hyperfilm ECL (GE HealthCare, 28-9068-39) was exposed to the ECL-treated membranes. The hyperfilm was developed using an SRX-101A Medical Film Processor (Konica Minolta Medical and Graphic Inc). Several different exposure times were used for each membrane, generally a 30 sec and 2 min exposure were obtained, although this depended on the strength of the antibodies being used.

6.4 Primary antibodies

The primary antibodies used for all experiments, including immunoblotting, co-immunoprecipitation, chromatin immunoprecipitation and immunofluorescence, are summarized in Table 2.1.

7. IMMUNOPRECIPITATION (IP) AND CO-IMMUNOPRECIPITATION (Co-IP)

7.1 Cell collection and lysis for IP experiments

Cells were collected as described above for cell lysate preparation for SDS-PAGE and immunoblotting (Section 5.1); however, for immunoprecipitation (IP) or co-immunoprecipitation (co-IP) experiments cells were not lysed in SDS-SB. Instead, a special lysis buffer, termed Bart's Modified TNE (BM-TNE), was used. This buffer has the following composition: 50 mM Tris-HCl (pH 7.6), 150 mM NaCl, 1 % Nonidet-P40, 2 mM EDTA, 1 mM EGTA, 10 mM NaF, 1 mM $NaVO_4$ and Roche protease inhibitor cocktail. The

amount of lysis buffer used was variable depending on the size of the cell pellet (generally between 300-600 µL for a 100 mm plate of cells). The cell lysates were transferred to Eppendorf tubes and left on ice for 15-30 mins to ensure complete lysis. Cell lysates were spun in a microcentrifuge at maximum speed at 4°C for 15 mins to pellet cellular debris. The supernatant, containing cytoplasmic and nuclear proteins, was then transferred to a new Eppendorf tube.

7.2 Co-Immunoprecipitation

For all co-IP experiments, lysates were used immediately and never frozen beforehand. After the protein concentrations of cell lysates were determined by Bradford assay (Section 5.2), aliquots of 500-750 µg of protein were used for each IP. The volume of each IP sample was adjusted to 1 mL with BM-TNE. An appropriate volume of antibody was then added to the lysates (see Table 2.1). An equal volume of the corresponding pre-immune serum was used as a negative control. Most IPs were carried out by incubating the antibody and lysate overnight at 4°C; however, in some cases, a 3 hr IP on ice was used.

Following incubation of the lysate with antibody, pre-washed Protein G Sepharose beads (GE Healthcare, 17-0618-01) were added to immunoprecipitate the beads. Before being added to lysate samples, beads were washed several times with BM-TNE and blocked with BSA (New England Biolabs, B9001S), used at 1 µg of BSA per µL of beads, for at least 1 hr on a rotator at 4°C. After blocking with BSA, beads were washed several more times and resuspended in two volumes of BM-TNE. Equal volumes of beads were aliquoted to each IP sample being compared; the volume of pelleted beads was approximately 25 µL.

Table 2.1. Antibodies used in IB, IF, IP and ChIP experiments.

Name	Antigen	Species	Source	Dilution/volume
5073*	*Drosophila* menin, C-terminal 15 a.a.	Rabbit	Sigma Genosys	IB =1:2500 IF = 1:200 IP = 2 µL ChIP = 5 µL
9561	Full-length *Drosophila* menin	Rabbit	Bédard Lab, McMaster	IB = 1:2500 IF = 1:200 IP = 2 µL ChIP = 5 µL
9562	Full-length *Drosophila* menin	Rabbit	Bédard Lab, McMaster	IB = 1:2500 IF = 1:200 IP = 2 µL ChIP = 5 µL
Rat menin	*Drosophila* Menin peptide (a.a. 628-624)	Rat	NEP	IF = 1:100
Menin BL342	Human menin peptide of C-term	Rabbit	Bethyl Lab Inc. A300-105A	IB = 1:2000 IP = 2.5 µL
N1	Trithorax, N-terminus Trx II	Rabbit	Mazo Lab	IB = 1:1000 IP = 2 µL ChIP = 5 µL
N6	Trithorax, C-terminus SET domain	Rabbit	Mazo Lab	IB = 1:1000 IP =2 µL
F3620	Trx peptide (a.a. 3164-3178)	Rabbit	NEP	Not specific
F3621	Trx peptide (a.a. 3164-3178)	Rabbit	NEP	Not specific
H3K4me2	Histone H3 Dimethyl Lysine 4 containing peptide	Rabbit	Millipore #05-790	ChIP = 1 µL
H3ac	Acetyl histone H3 (K9 & K14)	Rabbit	Millipore #06-599	IB = 1:1000 ChIP = 1 µL
HA-tag (6E2)	HA Epitope from influenza hemagglutinin	Mouse	Cell Signaling #2367	IB = 1:1000 IP = 2.5 µL
FADD polyclonal	Peptide Human FADD (a.a. 125-140)	Rabbit	Stressgen #AAP-210	IB = 1:250 IP = 3.5 µL
FADD monoclonal	Full-length human FADD-GST	Mouse	Stressgen #AAM-212	IB =1:500 IP = 3.5 µL
9678	Full-length dFADD-His	Rabbit	Bédard Lab, McMaster	IB = 1:2000 IF = 1:100 IP = 3 µL
9679	Full-length dFADD-His	Rabbit	Bédard Lab, McMaster	IB = 1:2000 IF = 1:100 IP = 3 µL
F3620	dFADD peptide (a.a. 102-117)	Rabbit	NEP	Not specific
F3621	dFADD peptide (a.a. 102-117)	Rabbit	NEP	Not specific
Hsp70 (dN-12)	*Drosophila* Hsp70, peptide of N-terminus	Goat	Santa Cruz SC-27028	IB = 1:1000
Hsp23	*Drosophila* Hsp23 SC 7B12	Mouse	Dr. Tanguay	IB = 1:2000
Hsp22	*Drosophila* Hsp22	Rabbit	Dr. Tanguay	IB =1:2000
Actin (clone C4)	Chicken actin (a.a. 50-70)	Mouse	Millipore MAB1501R	IB = 1:1000

The optimal dilution used for IB or IF or the volume of antibody used for a single IP or ChIP experiment are provided. "Not specific" indicates that the antibody did not recognize an appropriate sized protein. IB = immunoblotting, IP = immunoprecipitation, IF = immunofluorescence, ChIP = chromatin immunoprecipitation, a.a. = amino acid, * most frequently used *Drosophila* menin antibody.

The lysate-antibody samples were incubated with the Protein G Sepharose beads for 1 hr at 4°C on a nutator. Beads were pelleted by brief centrifugation and the unbound lysate was carefully removed. Beads were washed six times with BM-TNE to ensure all unbound protein was removed. After removal of the last wash, beads were resuspended in 60 µL of SDS-SB and 2 µL of 0.15 % bromophenol blue. Samples were then vortexed and boiled for 3-5 mins to release proteins from the beads. At this point samples were loaded into SDS-PAGE gels to determine whether or not proteins co-immunoprecipitated (see Section 6).

8. DNA GEL ELECTROPHORESIS

DNA was resolved by agarose gel electrophoresis. In most cases, 1 % agarose gels were used. For larger DNA fragments 0.8 % agarose gels were used, whereas smaller amplicons (< 200 bp) were resolved using 1.5 % agarose gels. All gels were made in 1 X TAE (40 mM Tris, 20 mM Acetic Acid, 1 mM EDTA) with ethidium bromide at a concentration of 0.5 µg/mL. Gels were run in 1 X TAE buffer at 100-140 V for 30 to 90 minutes. An appropriate DNA ladder was run alongside DNA samples on each gel. The ladder varied depending on availability and on the product size being examined. Those used included 1 kb DNA ladder (Invitrogen™, 15615-016), 100 bp DNA ladder (New England Biolabs, N3231) and KPlus DNA ladder RTU (GeneDirex®, DM011-R500). Gels were visualized and photographed using an Alpha Innotech MultiImager II and the associated AlphaImager 1.3.0.7 software.

Table 2.2. Primers used for cloning, ChIP and genotyping.

Name	Sequence	Use
Mnn1-ex2-F	5′-TCAATCTGTTCCGTCGCGCTCTAA-3′	*Mnn1* exon 2 amplification
Mnn1-ex2-R	5′-TGACTAATGTCACCTGCTGCGACT-3′	*Mnn1* exon 2 amplification
Mnn1-ex3-F	5′-ACAGCGTCCCGTTTCCAGTTGTTA-3′	*Mnn1* exon 3 amplification
Mnn1-ex3-R	5′-AGTTCCAGATCACATCCGACACCT-3′	*Mnn1* exon 3 amplification
Mnn1-ex5-F	5′-GGCCAAGCACAATCCCAAGTTCAA-3′	*Mnn1* exon 5 amplification
Mnn1-ex5-R	5′-AGAGATTGCAGTGATGGTGGCTGA-3′	*Mnn1* exon 5 amplification
E173-F	5′-CACAAAAGCTCGCAGTTAGC-3′	Diagnostic for $Mnn1^{e173}$
E30-F	5′-CAGCGAAGTAAACACAACGC-3′	Diagnostic for $Mnn1^{e30}$
E30-E173-R	5′-GAAAACAGGAGCAGTATATTGC-3′	Diagnostic for $Mnn1^{e173}$ and $Mnn1^{e30}$
Mnn1-ex2-A-5′	5′-GGCAATCAGAAGAACCC-3′	Diagnostic for *Mnn1* dsRNA
Mnn1-int2	5′-CAATTAGCAAAGGGTGAC-3′	Diagnostic for *Mnn1* dsRNA
hsp70-200F	5′-TGCCAGAAAGAAAACTCGAGAAA-3′	ChIP *hsp70* P1 forward
hsp70-108R	5′-GACAGAGTGAGAGAGCAATAGTACAGAGA-3′	ChIP *hsp70* P1 reverse
hsp70+4F	5′-CAATTCAAACAAGCAAAGTGAACAC-3′	ChIP *hsp70* P2 forward
hsp70+112R	5′-TGATTCACTTTAACTTGCACTTTA-3′	ChIP *hsp70* P2 reverse
hsp70+334F	5′-CACCACGCCGTCCTACGT-3′	ChIP *hsp70* P3 forward
hsp70+423R	5′-GGTTCATGGCCACCTGGTT-3′	ChIP *hsp70* P3 reverse
hsp70+358F	5′-ACGTGGCTTTCACAGATTCGGAAC-3′	ChIP *hsp70* P3b forward
hsp70+504R	5′-AGTGCTTCATGTCCTCTGCGATCT-3′	ChIP *hsp70* P3b reverse
hsp70+1649F	5′-GGGTGTGCCCCAGATAGAAG-3′	ChIP *hsp70* P4 forward
hsp70+1754R	5′-TGTCGTTCTTGATCGTGATGTTC-3′	ChIP *hsp70* P4 reverse
hsp70-upF	5′-CCCTTTGAGTTGTAACCATCCCA-3′	ChIP upstream negative control
hsp70-upR	5′-GTACTTGTACATTTGTAAGCGCGG-3′	ChIP upstream negative control
hsp70-downF	5′-TGTGGTGTGTGTCACCTCTTGCTA-3′	ChIP downstream negative control
hsp70-downR	5′-TTAAATGCCGGAACAAACGGTCGG-3′	ChIP downstream negative control
dFADD-5′	5′-CCGCTGAAAATACCGTCTCT-3′	Used for sequencing *dFADD*-HA
dFADD-3′	5′-GTGCGACATTATCTGCTCC-3′	Used for sequencing HA-*dFADD*
C-term-HA-dFADD-5′	5′-AAATCGATACCGCTGAAAATACCGTCTCT-3′	C-terminal HA-tag *dFADD*
C-term-HA-dFADD-3′	5′-AATCGATACTAGGCATAGTCAGGCACGTCATAAGGATAGTGCGACATTATCTGCTCC-3′	C-terminal HA-tag *dFADD*
N-term-HA-dFADD-5′	5′-AATCGATAATGTATCCTTATGACGTGCCTGACTATGCCCGTCTCTGTAAATTAGTCACA-3′	N-terminal HA-tag *dFADD*
N-term-HA-dFADD-3′	5′-AAATCGATACTAGTGCGACATTATCTGCTC-3′	N-terminal HA-tag *dFADD*
dFADD-F1b	5′-AAAAAAGGATCCAATGACTGCAGGCAGGCACTGG-3′	Cloning full *dFADD* in pET-29b
dFADD-R239b	5′-AAAAAACTCGAGGTGCGACATTATCTGCTCCACCCT-3′	Cloning full *dFADD* in pET-29b
dFADD-F1	5′-AAAAAGGATCCATGACTGCAGGCAGGCACTGG-3;	Cloning of *dFADD* DD (1-105) in pGEX-4T1
dFADD-R105	5′-AAAAAAGCGGCCGCCTAGGCCAATCGGAGTTCCTGG-3′	Cloning of *dFADD* DD (1-105) in pGEX-4T1
dFADD-F105	5′-AAAAAGGATCCGCCGAGGAACTTCGTCAGCAG-3′	Cloning of central *dFADD* (105-151) in pGEX-4T1
dFADD-R151	5′-AAAAAAGCGGCCGCCTATCGTTTGTGATCCGTAAAAGCAG-3′	Cloning of central *dFADD* (105-151) in pGEX-4T1
dFADD-F151	5′-AAAAAGGATCCCGAACGATGGTCTTTAAGAAAATATC-3′	Cloning of *dFADD* DED (151-239) in pGEX-4T1
dFADD-R239	5′-AAAAAAGCGGCCGCCTAGTGCGACATTATCTGCTCCAC-3′	Cloning of *dFADD* DED (151-239) in pGEX-4T1
fMCMV-3′end	5′-GGAAGTGAAAGGGCAGC-3′	Sequencing clones in pIRES-GFP

9. HA-TAGGING AND CLONING OF *dFADD*

9.1 PCR amplification of HA-tagged dFADD constructs

Since dFADD (*Drosophila* fas-associated death domain) antibodies were not available, the gene was amplified with primers that added an HA-tag (from Influenza Hemagglutinin) and cloned into an expression vector in order to investigate a potential interaction between menin and dFADD. Because *dFADD* is a small intronless gene (717 bp coding region) it was possible to amplify it by PCR using genomic Canton S DNA (previously isolated in the Bédard lab). Two different primer sets were used for amplification (see Table 2.2); one set was designed to incorporate an N-terminal HA-tag and the other a C-terminal HA-tag. The HA-tag generated has the protein sequence YPYDVPDYA. Both primer sets were designed with *Cla*I restriction enzyme sites to facilitate cloning into the pIRES-GFP vector. ProofStart DNA polymerase (QIAGEN, 202203), a high-fidelity polymerase with proofreading activity, was used for amplification of *dFADD*, following the reaction guidelines of the manufacturer. The program used for PCR consisted of an initial activation step at 95°C for 5 mins, followed by 40 cycles with 30 sec denaturation at 94°C, annealing at 56°C for 30 sec and extension at 72°C for 1 min. These amplification cycles were followed by a final extension at 72°C for 8 mins. PCR products for *HA-dFADD* (N-terminal HA-tagged dFADD) and *dFADD-HA* (C-terminal HA-tagged dFADD) were resolved by gel electrophoresis on 1 % agarose gels (see Section 8) and products were gel extracted and purified using QIAquick Gel Extraction Kit (QIAGEN, 28704) following manufacturer instructions. PCR amplified *dFADD-HA* and *HA-dFADD* were sequenced by Mobix Lab (McMaster University) using the dFADD-5' and dFADD-3' primers (Table 2.2).

9.2 Cloning of HA-tagged constructs into pCR®4-TOPO

Initial attempts to digest the ends of the PCR product with *Cla*I (New England Biolabs, R0197) and clone directly into *Cla*I-digested pIRES-GFP vector proved difficult, presumably due to inefficiency of restriction enzyme digestion at ends of PCR products. Alternatively, the PCR products were cloned first into the TOPO® TA cloning vector, pCR®4-TOPO® (Invitrogen™, K4575-J10). To clone into pCR®4-TOPO®, it was necessary to add 3'deoxyadenosine (A) overhangs to the PCR products. This was done by incubating the purified PCR products with 0.1 mM dATP (Invitrogen™, 55082) and *Taq* DNA Polymerase and its associated buffer (Invitrogen™, 18038-018) for 15 mins at 72°C. The PCR products with 3'A overhangs were then cloned into the pCR®4-TOPO® vector following manufacturer guidelines (Invitrogen™, K4575-J10).

The ligated products were used to transform One Shot® TOP10 chemically competent *E. coli* using reagents provided by the manufacturer and following guidelines of the manufacturer (Invitrogen™, K4575-J10). Transformation occurred by incubation on ice for 30 mins, followed by heat shock at 42°C for 30 sec. S.O.C. medium was added to the transformed TOP10 *E. coli* and the tube was shaken horizontally at 200 rpm for 1 hr at 37°C. Transformed bacteria were then plated on LB agar plates with 50 μg/mL ampicillin and incubated overnight at 37°C. Several colonies for both pCR®4-TOPO:HA-dFADD and pCR®4-TOPO:dFADD-HA were selected and grown in overnight LB cultures (Section 1) with 50 μg/mL ampicillin. Plasmid DNA was purified using HiYield™ Plasmid DNA Kit and following manufacturer guidelines (RBC Bioscience, YPD100).

9.3 Subcloning of HA-tagged dFADD constructs into pIRES-GFP expression vector

The pCR®4-TOPO cloned dFADD-HA and HA-dFADD were subcloned into the pIRES-GFP expression vector. pCR®4-TOPO:HA-dFADD, pCR®4-TOPO:dFADD-HA and pIRES-GFP were all digested with *Cla*I restriction enzyme for 5.5 hrs at 37°C, followed by heat inactivation of the enzyme at 65°C for 20 mins. To prevent recircularization of the plasmid during ligation, pIRES-GFP was first dephosphorylated by Calf Intestinal Phosphatase (CIP) (New England Biolabs, M02905). This was done by adding CIP to the *Cla*I-digested plasmid, using 1U CIP/1µg DNA in 1 X NEB Buffer 4 (B7004S) and incubating for 1 hr at 37°C. The *Cla*I digested pCR®4-TOPO:HA-dFADD and pCR®4-TOPO:dFADD-HA and the *Cla*I-digested and CIP-dephosphorylated pIRES-GFP were all run out on a 0.8 % agarose gel for extraction (Section 8). The approximate 800 bp *HA-dFADD* and *dFADD-HA* bands and the approximate 5.2 kb pIRES-GFP band were all gel extracted using the QIAquick Gel Extraction Kit (QIAGEN, 28704) following manufacturer instructions. Gel extracted products were ligated using 1 µL of T4 DNA ligase (400 U/µL) and its associated buffer (New England Biolabs, M02025) in a 10 µL reaction. The approximate ratio of plasmid:insert used for ligation was 1:5, determined based on molecular size and intensity of bands on the gel. Ligation was performed by incubating overnight at 16°C. To ensure complete ligation, an additional 0.5 µL T4 DNA ligase and 1 mM ATP (Invitrogen™, 18330-019) were added to the reaction and it was left at room temperature for 1 hr.

About 1/3 of the total ligation mixture was used to transform Subcloning Efficiency™ DH5α™ competent cells (Invitrogen™, 18265-017). The ligation mixture and DH5α™ were incubated together on ice for 30-60 min and then heat shocked at 42°C for

45 sec. This was transferred immediately to ice for 5 mins and then topped up with 4 volumes of LB medium (Section 1). Prior to plating, the transformed bacteria were transferred to a 15 mL conical tube and shook at 200 rpm for 1 hr at 37°C. The bacteria were spun down and most of the medium was removed (approximately 50 µL left) prior to resuspension. The transformed bacteria were then plated on LB-Agar with 50 µg/mL of ampicillin.

Several colonies were screened by preparing 3 mL overnight LB cultures with 50 µg/mL ampicillin. These were used for plasmid isolation with the HiYield™ Plasmid DNA Kit, following manufacturer guidelines (RBC Bioscience, YPD100). Plasmid DNA was digested with *Cla*I to ensure the presence of the *HA-dFADD* or *dFADD-HA* inserts. Those plasmids containing inserts were screened by diagnostic digest with the *Xmn*I restriction enzyme for 1.5 hrs at 37°C. *dFADD* contains a single *Xmn*I site 270bp from the transcription start site and the pIRES-GFP vector contains two *Xmn*I sites at 1257 bp and 3158 bp. Based on relative locations of the *Xmn*I sites and the *Cla*I site used for cloning it was calculated that if the *dFADD* construct was in the proper orientation then the size of fragments produced would be approximately 3160 bp, 2010 bp and 800 bp. Constructs were verified by sequencing by Mobix Lab (McMaster University) with a primer complementary to the vector promoter (fMCMV-3'end, Table 2.2).

9.4 Purification of pIRES-GFP:HA-dFADD and pIRES-GFP:dFADD-HA for transfection

After sequencing to ensure that *dFADD* was cloned in-frame along with the appropriate N-terminal or C-terminal HA-tag, large bacterial cultures were prepared for plasmid purification. Daytime 3 mL starter cultures in LB with 50 µg/mL ampicillin were prepared by inoculation from glycerol stocks and shook at 200 rpm at 37°C. These

starter cultures were grown during the day and used to inoculate 250 mL LB containing 50 µg/mL ampicillin for growth overnight at 37°C with shaking. Plasmid DNA was purified from bacterial cultures using the QIAGEN Plasmid Maxi Kit (QIAGEN, 12163) following the guidelines provided by the manufacturer.

9.5 Subcloning of HA-tagged dFADD constructs into pPACB expression vector

Due to the inefficient expression of HA-tagged dFADD constructs from the MCMV (murine cytomegalovirus) promoter of the pIRES-GFP vector in S2 cells, it was necessary to subclone the *HA-dFADD* and *dFADD-HA* constructs into a more suitable expression vector for *Drosophila* cells. The expression vector pPACB, containing a *Drosophila* actin promoter was obtained from Thomas Kusch (Rutgers University). Both HA-*dFADD* and *dFADD*-HA inserts were blunt-end ligated into this vector. The *Drosophila* menin cDNA was also cloned into the pPACB vector (completed by Wu, Y.).

10. FLY HUSBANDRY

10.1 Fly food

Drosophila melanogaster stocks were maintained on standard yeast-agar medium at room temperature. The recipe for 1 L of fly food is as follows: Solution A= 800 mL ddH_2O, 100 g sucrose, 16 g agar, 1 g potassium phosphate dibasic, 8 g sodium potassium tartrate tetrahydrate, 0.5 g sodium chloride, 0.5 g magnesium chloride hexahydrate, 0.5 g calcium chloride, 0.5 g ferric sulphate; Solution B = 200 mL ddH_2O, 50 g dry active yeast. Solutions A and B were autoclaved and then combined immediately after and stirred while cooling. Once the food cooled to below 60°C then 10 mL of acid mix (11:10:1 ddH_2O:propionic acid:o-phosphoric acid) and 7.5 mL of 10 % (w/v) Tegosept

(methyl 4-hydroxybenzoate) prepared in ethanol were added. Fly food was then poured into vials, tubes or plates before solidifying.

10.2 Fly stock maintenance and crosses

Stocks were maintained in vials (Applied Scientific *Drosophila* Products, AS-519) with about 10 mL of fly food per vial. Crosses were normally set up in smaller glass tubes (Fisherbrand, 14-961-29) containing standard yeast-agar food and supplemented with a few dry yeast pellets to promote egg laying. Virgin females were always selected for crosses so that the genotype of progeny would be known. Generally, crosses were established with more females than males (*e.g.* 15 females:10 males). Crosses were maintained in an incubator at 25°C to better control the developmental timing.

10.3 Fly houses

For experiments where many embryos or larvae at specific stages were required, fly "houses" were set up to facilitate collections. Large fly houses were made using 500 mL plastic beakers inverted over 100 mm plates (Fisherbrand, 0875712). Small fly houses were made using 150 mL beakers inverted over 60 mm plates (Corning®, 431066). Beakers had small holes poked in them to ensure air exchange. Fly houses were kept in the incubator at 25°C. For embryo collections, grape juice agar plates (3 % agar in 15 % pure grape juice) were used with a small amount of yeast paste (~50 % dry active yeast mixed in ddH_2O) to promote egg laying. In most other circumstances, standard food plates were used for collections. In general, adult flies were placed in the beakers and allowed to mate freely. One hour pre-clear collections were done to allow females to clear eggs for better staging. Collections were generally over 2 hour periods to allow

close control of developmental timing. In some cases, such as with the starvation and desiccation assays, overnight and daytime collections were used.

11. FLY STOCKS

Table 2.3, summarizes all the fly stocks used for experiments reported in this thesis. Some of the common lab stocks, such as wild-type stocks (OR, *yw*, w^{1118}) have been maintained in the Campos lab for many years so the original source of these stocks is unknown. Many fly stocks were obtained from central repositories such as the Bloomington Stock Centre (Indiana University) and the Vienna *Drosophila* RNAi Center (VDRC; Campus Vienna Biocenter). Other stocks were generated by previous members of the Campos lab; such as the *Mnn1* deletion mutants ($Mnn1^{e30}$ and $Mnn1^{e173}$) and the *UAS-Mnn1-RNAi* and *UAS-Mnn1* lines, that were previously characterized and described (Papaconstantinou et al., 2005). Important stocks (trx^{B11}, trx^{Z11}) for the study of menin and Trithorax interaction were received from our collaborator Dr. Alexander Mazo (Thomas Jefferson University, Philadelphia, USA). Stocks ($FADD^{f02804}$, $FADD^{f06954}$) for the study of dFADD and menin in immune response were obtained from Dr. Jean-Marc Reichhart (Université de Strasbourg & Institut Universitaire de France). Several new stocks were created by crossing and combining specific mutations to create double mutants. Also, the genetic background of several stocks was changed to facilitate comparisons between genotypes. General balancer stocks or various combinations of markers/balancers are not summarized in Table 2.3. Many other double mutants (*e.g. Mnn1*;*trx* mutants) were also generated, but are not included in the table.

Table 2.3. Fly Stocks.

Genotype	Source	Comments
$Oregon\ R\ (OR)$	Unknown	Wild-type
yw	Unknown	Wild-type
w^{1118}	Unknown	Wild-type
$\frac{Df(2L)spd^{j2}}{CyO}$	Bloomington #2414	Deficiency spanning *Mnn1* locus
$yw; \frac{Mnn1^{e30}}{CyO(y^+)}$	Campos	Original $Mnn1^{e30}$ deletion line
$yw; \frac{Mnn1^{e173}}{CyO(y^+)}$	Campos	Original $Mnn1^{e173}$ deletion line; extensive contamination
$yw; \frac{Mnn1^{e30}}{CyO}$	Pepper	Background changed with *yw*
$yw; \frac{Mnn1^{e173}}{CyO}$	Pepper	Rescued allele and background changed with *yw*; homozygous sterile
$w^{1118}; \frac{Mnn1^{e30}}{SM5}$	Pepper	Background changed to w^{1118}
$w^{1118}; \frac{Mnn1^{e173}}{SM5}$	Pepper	Background changed to w^{1118}; homozygous sterile
GE11370	GenExcel Inc.	P-element insertion in *Mnn1*
$yw; \frac{Mnn1^{+E314}}{SM5}$	Campos	Precise excision line
$yw; \frac{Mnn1^{+E323}}{SM5}$	Campos	Precise excision line
$w^{1118}; \frac{Mnn1^{+E314}}{SM5}$	Pepper	Background changed to w^{1118}
$w^{1118}; \frac{Mnn1^{+E323}}{SM5}$	Pepper	Background changed to w^{1118}
$H_1^6\ pUAST - DMnn1[2nd]$	Campos	Menin overexpression line
$H_{10}^2\ pUAST - DMnn1[3rd]$	Campos	Menin overexpression line
$H_{24}^1\ UAS - dsRNA - DMnn1[2nd]$	Campos	Menin RNAi line
$H_{16}^2\ UAS - dsRNA - DMnn1[3rd]$	Campos	Menin RNAi line
$w^-; +; \frac{FADD^{f02804}}{TM6B, Tb, Hu}$	Reichhart P2020	*dFADD* null; piggyBac insertion in coding region
$w^-; +; \frac{FADD^{f06954}}{TM6B, Tb, Hu}$	Reichhart P2021	*dFADD* hypomorph; piggyBac insertion in 5' UTR
$w^{1118};\ PBac\{PB\}key^{c02831}$	Bloomington #11044	*Kenny*; Imd pathway mutant; PBac insertion
$w^+; \frac{Mnn1^{e30}}{SM5}; \frac{FADD^{f02804}}{TM3}$	Pepper	Double mutant
$w^+; \frac{Mnn1^{e173}}{SM5}; \frac{FADD^{f02804}}{TM3}$	Pepper	Double mutant; $Mnn1^{e173}$ contaminated
$w^+; \frac{Mnn1^{e30}}{SM5}; \frac{FADD^{f06594}}{TM3}$	Pepper	Double mutant

Table 2.3 Continued. Fly Stocks.

Genotype	Source	Comments
$w^+; \frac{Mnn1^{e173}}{SM5}; \frac{FADD^{f06594}}{TM3}$	Pepper	Double mutant; *Mnn1*^{e173} contaminated
$\frac{trx^{Z11}}{TM3,GFP}$	Mazo	*trithorax* strong hypomorph, pupal lethal
$\frac{trx^{B11}}{TM3,GFP}$	Mazo	*trithorax* null, late embryonic lethal
trx^{RNAi}	VDRC CG8651	*trithorax* RNAi
$w^-; \frac{UAS-trx^{RNAi}}{T_S}; \frac{tub-GAL80^{ts}}{T_L}$	Papaconstantinou	*trithorax* RNAi with a temperature sensitive GAL80
$w^-; \frac{+}{T_S}; \frac{mwh}{T_L}$	Papaconstantinou	*multiple wing hair* mutation; for LOH assay
$w^-; \frac{tub-GAL4}{TM3,Sb}$	Unknown	*tubulin-GAL4* driver
$da-GAL4\ (III)$	Unknown	*daughterless-GAL4* driver
$yw;\ P\{GAL4-nos.NGT\}40$	Bloomington #4442	*nanos-GAL4* driver

12. INFECTION ASSAYS

The pricking method was used to infect adult flies with bacteria. This method has been used extensively to identify mutants of the Toll and Imd pathways (Naitza et al., 2002; Rutschmann et al., 2002). Before any experiments were conducted, several trials were carried out with OR flies to determine the optimal conditions for infection that would minimize death due to physical injury. Since it was more efficient to prick flies laterally, compared to dorsally, in the second thoracic segment, this was chosen as the infection site for all experiments. Furthermore, there was no significant difference between the survival of male and female flies in these preliminary trials, so both sexes were used in infection assays, keeping the ratio of male to female roughly equal for all genotypes.

12.1 Preparation of bacterial cultures for infection

The Gram-negative bacteria *Escherichia coli* (MG1655) (from Dr. Herb E. Schellhorn, McMaster University) or the Gram-positive bacteria *Micrococcus luteus* (Dr. Marie A. Elliot, McMaster University) were used for infection to look at the potential role of *Mnn1* mutants in the Imd or Toll pathways, respectively. To prepare cultures for infection, 5 mL of LB was inoculated with a single colony obtained from a previously prepared LB agar plate kept at 4°C. Cultures were grown overnight at 37°C with shaking at 200 rpm. The OD_{600} of a 10 X dilution was determined. Bacteria from 4 mL of culture were pelleted by centrifugation at 4500 rpm for 5 mins and then re-suspended in a small volume of LB, calculated based on the measured OD_{600} to produce cultures equivalent to an OD_{600}=200 for *E. coli* or OD_{600}=50 for *M. luteus.*

12.2 Pricking method for adult fly infection

For a typical infection assay, flies were collected for 2 days and aged for 3 days so that they were between 3-5 days at the time of infection. Thirty flies, both male and female, of each genotype and each infection type were used per trial and three independent trials were carried out. Flies were anesthetized and pricked laterally in the second thoracic segment. The site of infection was anterior to and in line with the site of wing emergence. Flies were pricked with the tip of a $30G^{1/2}$ needle dipped in sterile ddH_2O (negative control), *E. coli* (activates Imd pathway) or *M. luteus* (activates Toll pathway) cultures. Flies were kept in tubes with standard food and placed in the incubator at 25°C. Survival was checked 3 hours after infection and any lethality observed at this time was presumed to be due to injury from the needle and not the result of an acquired infection; thus, such flies were not included in calculations of percent lethality.

Survival was monitored daily for 10 days and flies were transferred to fresh food daily for the first four days and every other day thereafter. Average percent survival was graphed over a 10 day period, along with the standard error of the mean. For statistical analyses, the survival of individual flies was entered in order to generate survival curves for analysis using a log-rank (Mantel-Cox) test with GraphPad Prism version 5.00. Since 5 genotypes were being compared at a time, 10 possible pairwise comparisons could be made, so using the Bonferroni method to adjust for multiple comparisons, the significance level of $p<0.05$ was adjusted to $p<0.005$.

12.3 Feeding method for natural infection of larvae

Erwinia carotovora carotovora strain 15 (*Ecc15*) was isolated as a bacterial strain that is capable of inducing an immune response by natural/oral infection, characterized by the

production of antimicrobial peptides, without significantly affecting larval viability (Basset et al., 2000). *Ecc15* and *Ecc15* carrying a pOM-GFP construct (*Ecc15-GFP*) were obtained from Bruno Lemaitre (École polytechnique fédérale de Lausanne). Both strains are rifampicin resistant and *Ecc15-GFP* is also spectinomycin resistant. As ingestion of *Ecc15-GFP* could be visualized by fluorescence microscopy, this strain was used in place of the wild-type *Ecc15*. *Ecc15-GFP* was grown at 29°C in LB supplemented with rifampicin and spectinomycin, each at a concentration of 100 µg/mL. As rifampicin is light sensitive, cultures were covered in foil for growth. *Ecc15-GFP* was grown overnight and cultures were concentrated to an OD_{600}=200.

For larval collection, small fly houses (Section 10.3) were set up and adults were allowed to lay for 2 hr periods on standard food plates. After about 22 hrs, plates were cleared of any larvae that had already hatched to ensure those being used for the experiment were in the same developmental stage. First instar larvae that hatched in the hour following clearing of the plate were transferred, 100 per plate, to standard food plates that had been broken up with forceps to aid in feeding. Larvae developed on these plates and after 72 hrs from the collection period, larvae in the early third instar phase and were used in the natural feeding experiments.

Survival following *Ecc15-GFP* infection was assessed using the protocol of Basset et al. (2000) where *Ecc15-GFP* at an OD_{600}=200 was mixed with crushed banana (1:2) and fed to early 3^{rd} instar larvae for 1 hr following a 1 hr starvation period. Controls were fed LB medium mixed with crushed banana (1:2) (Basset et al., 2000). Larvae were starved by transferring them from food plates to empty plates with a ddH_2O soaked filter paper. After the starvation period was over, food with or without the *Ecc15*-GFP

was placed in the centre of the plate on the ddH_2O soaked filter paper and larvae were transferred with a fine paint brush into the food. Ingestion of *Ecc15*-GFP was also monitored by looking at GFP expression after feeding using a universal visualizing light source for fluorescent stereo microscopy (BLS, MAA-03) attached to the dissecting microscope. Larvae were rinsed with ddH_2O and transferred to food tubes after feeding and allowed to develop to adulthood at 29°C to check survival. They were also examined 24 hrs after feeding to see if any GFP expression remained.

12.4 Induction of HSP70 after natural Infection of larvae

It was reported that *hsp70* transcript levels were induced about 7-fold in the guts of adult flies 4 hours after infection (Buchon et al., 2009) so we wanted to see if this induction of *hsp70* due to bacterial infection could be reproduced. *Ecc15-GFP* at OD_{600}=200 was mixed with either yeast paste (1:1), or yeast paste alone was used as a control. Both second and third instar OR larvae were compared and they were starved for 2 hours prior to feeding for either 2 hrs or 4 hrs. About 10 larvae per condition were used. GFP expression was examined to ensure that *Ecc15-GFP* had been ingested by the larvae and only GFP positive larvae were used for lysate preparation. Protein lysates were prepared at the end of the feeding period by first rinsing larvae with ddH_2O and then flash freezing them in a dry ice/methanol bath and homogenizing them in SDS-SB (Section 5.1) using a micro pestle for 1.5 mL tubes (Kimble® Kontes, Sigma-Aldrich, Z359947). Samples were examined by SDS-PAGE and immunoblotting with HSP70 antibodies (Section 6, Table 2.1). This experiment was repeated mixing *Ecc15-GFP* with crushed standard fly food (1:1) instead of yeast paste. LB was mixed with crushed fly food for the controls (1:1).

12.5 Feeding method for adult natural infection

Induction of HSP70 expression was also examined in adults after natural infection with *Ecc15-GFP*. This more closely mimicked experimental conditions used by Buchon *et al.* (2009) in the microarray analysis that revealed *hsp70* induction in guts of adults following *Ecc15* infection. For natural infection of adults, filter paper was soaked with a 1:1 mixture of 5 % sucrose and *Ecc15-GFP* OD_{600}=200, or 5 % sucrose alone for controls. The filter paper was placed on top of standard fly food in vials and 2-3 day male flies were added to feeding vials after being starved for 2 hrs in empty vials. After 2 or 4 hours of feeding, flies were placed at -20°C for about 5 min to stun them so they could be collected in Eppendorf tubes. They were then homogenized with SDS-SB using a micro pestle and lysates were prepared and examined by SDS-PAGE and immunoblotting as previously described (Sections 5.1 and 6).

13. HEAT SHOCK EXPERIMENTS

13.1 Heat shock of embryos for protein expression studies

Most often, *Drosophila* embryos were exposed to heat shock (HS) at 3-5 hrs after egg laying (AEL) in order to compare to work done by Maria Papaconstantinou (Papaconstantinou et al., 2005). In some cases, older embryos (8-20 hrs AEL) were used. Embryos were collected for 2 hour periods (Section 10.3) and then aged accordingly. Once at the appropriate age, plates with embryos were parafilmed and submerged in a water bath at 37°C. Most commonly, 15, 30 and 60 min heat shocks were used. Immediately following the heat shock, plates were removed from the water bath and embryos were collected in a glass vial with a nitex sieve attached to the bottom by

rinsing the plate with ddH_2O to dislodge the embryos from the plate. Embryos were rinsed on the sieve with ddH_2O and then transferred from the nitex sieve into an Eppendorf tube with cold ddH_2O and placed on ice. After embryos settled to the bottom, the ddH_2O was removed and SDS-SB was added. Embryos were homogenized in the SDS-SB using a micro pestle. Lysates were then boiled and centrifuged as previously described (Section 5.1).

13.2 Heat shock of larvae for protein expression studies

Adult flies were allowed to mate and lay in houses with standard food plates. Plates were removed and embryos were left to develop in the food plates to the appropriate larval stage. Larvae of the desired stage were removed from the plates, using a paint brush, and rinsed with ddH_2O before being transferred into Eppendorf tubes. Larvae were heat shocked in the Eppendorf tubes, by submerging them in a water bath at 37°C. After heat shocking for the desired length of time larvae were removed and homogenized in SDS-SB and lysates were prepared as described (Section 5.1).

13.3 Heat shock of adults for protein expression studies

Adult males, age 1-3 d were used for heat shock experiments. In general, 10 males per genotype were used. Flies were anesthetized briefly and transferred to empty glass tubes. The cotton was placed about 1-2 cm from the bottom of the tube in order to restrict flies to this small area. Tubes were placed in a rack and heat shocked by placing it in a water bath at 37°C, ensuring that the water level was above the level of the cotton in the tubes. After the heat shock was complete, tubes were removed and placed at -20°C for 5 mins to slow flies so they could be transferred to Eppendorf tubes. Lysates were prepared as previously described (Section 5.1). The length of heat shock varied

from 15 min to 1 hr. In some cases, flies were left to recover from the 1 hr heat shock by transferring them to food tubes for a 3 hr period at 25°C prior to being collected for lysate preparation.

13.4 Heat shock of embryos for acute lethality experiments

Heat shock experiments were also carried out to examine the acute heat shock survival of embryos, similar to experiments conducted by Papaconstantinou et al. (2005). For such experiments, crosses were set up so that homozygous mutant progeny could be compared to heterozygous (over a balancer chromosome) sibling controls from the same cross. Mating adult flies were transferred to new food tubes and allowed to lay eggs for a 2 hour period before being transferred to another tube. Embryos were left to develop for 3 hours, and embryos age 3-5 hr AEL were heat shocked at 37°C for 1 hr by submerging tubes in a water bath. After the heat shock, tubes were removed and returned to 25°C and embryos were left to develop until adulthood. Adult flies were genotyped and a relative percent lethality was calculated based on the number of homozygous flies compared to sibling heterozygous flies. In general, three trials were conducted. For statistical analyses, Student's t-tests were used to compare the average relative lethality of two genotypes or to compare a single genotype under standard and acute heat shock conditions. If multiple genotypes were compared in the same study then Bonferroni's method was used to adjust for multiple comparisons.

14. LOSS OF HETEROZYGOSITY ASSAY

A loss of heterozygosity (LOH) assay was used to measure genomic instability. This assay was based on LOH at the *multiple wing hair* (*mwh*) locus. Experiments were conducted

as previously described (Papaconstantinou et al., 2010). In brief, crosses were set up in order to obtain mutant flies that were also heterozygous for a *mwh* mutation ($mwh^{-/+}$). A chronic heat shock was administered by repeating 20 min heat shocks 3 times during development - at 3-5 hr AEL, first instar stage and second instar stage. Wings from female flies that were exposed to a chronic HS, or left untreated, were removed and prepared for analysis. Wings were assessed blindly and the number of $mwh^{-/-}$ cells per wing was determined; cells where a LOH had occurred ($mwh^{-/-}$) had two or more wing hairs per cell while all other cells in a heterozygous background had only a single hair per wing cell. For most experiments, 30 wings were examined per genotype and condition and the average number of $mwh^{-/-}$ cells per wing was compared. ANOVAs were used to compare the LOH of multiple genotypes for a given condition followed by Bonferroni's post-hoc tests to determine which genotypes differed significantly.

15. CHROMATIN IMMUNOPRECIPITATION (ChIP)

15.1 Embryo collection and dechorionation

The chromatin immunoprecipitation (ChIP) technique was optimized in Dr. Alexander Mazo's lab (Thomas Jefferson University) and the presented experiments were performed there (Chapter 4). Embryos were collected in large houses on grape juice agar plates supplemented with yeast paste (Section 10.3) for a 10 hr period and aged for 3 hrs. Embryos were manually dechorionated, a process taking a maximum of 2 hrs, thus the age of embryos used in ChIP assays was between 3-15 hrs AEL. While manually dechorionating embryos, the light of the microscope was left off (or as low as possible), to avoid heat shocking the embryos due to the warmth from the light. For a single ChIP,

60 embryos of a given genotype were dechorionated. The embryos were gently transferred into an Eppendorf tube containing a small volume (~100 µL) of HyClone® cell culture medium. After enough embryos were dechorionated and transferred to an Eppendorf tube, they were fixed right away (Section 15.3).

15.2 Heat shock of embryos for ChIP

For the heat shock (HS) conditions used in ChIP experiments, 1 mL of medium was preheated in a water bath at 37°C. The dechorionated embryos were transferred directly to the Eppendorf tube with the preheated medium and then the tube was submerged in the 37°C water bath for a 5 min or 30 min HS. At the end of the HS treatment, embryos were fixed immediately.

15.3 Fixation of embryos for ChIP

Medium was carefully removed from the embryos (No HS or HS) and 600 µL of Fixing Solution (50 mM Hepes (pH 7.6), 100 mM NaCl, 0.1 mM EDTA, 0.5 mM EGTA) was added followed by 32.4 µL of 37 % formaldehyde and 600 µL of heptane. The tube was mixed vigorously and then put on a nutator at room temperature for 15 mins. During the 15 min fixation, the tube was removed every few mins and shook vigorously by hand. After the 15 mins of fixation, the tube was spun at 6000 rpm for 30 sec to pellet the embryos. The formaldehyde/heptane/fixing solution was carefully pipetted off the embryos. 1 mL of Stop Solution (0.01 % TritonX-100, 0.125 M Glycine in 1 X PBS; solution prepared fresh each time) was added and the tube was vigorously shaken and left on the nutator for 3 mins. Embryos were pelleted by centrifuging at 3000 rpm for ~ 15 sec. The Stop Solution was then removed and replaced with 1 mL of Embryo Wash Buffer (50 mM Tris (pH 7.6), 10 mM EDTA, 0.5 mM EGTA, 0.25 % TritonX-100). Embryos were washed on

the nutator for 3 mins and this wash step was repeated two more times with fresh Embryo Wash Buffer. After the final wash, the Embryo Wash buffer was removed.

15.4 Lysis and sonication

After washing fixed embryos, 25 µL of Lysis Buffer (0.4 % SDS, 10 mM EDTA, 50 mM Tris (pH 8.1), 1 X Protease inhibitors added fresh before use (Roche, 11836170001)) was added to the 60 embryos. Fixed embryos were frozen at -80°C until all embryos of different genotypes and heat shock conditions needed for a particular experiment were collected. After all embryos for a ChIP experiment were fixed and frozen, they were thawed in the Lysis Buffer. If there were several collections of embryos of the same genotype and treatment these were combined before sonication. Additional Lysis Buffer was added so that the total volume per tube was 150 µL. Sonication was performed in Eppendorf tubes using a small cup horn sonicator and 20 sec pulses. Sonication pulses were repeated 5 times, returning the tube to ice between each 20 sec sonication and mixing by pipetting up and down and then re-pulsing samples in a microcentrifuge before the next sonication. After sonication was complete, the lysate was spun at maximum speed at 4°C for 10 mins. Supernatant was transferred to a 2 mL tube for pre-clearing of lysate. The efficiency of sonication was checked by agarose gel electrophoresis (following Sections 15.7-15.9) to ensure that conditions were sufficient to shear DNA so that the smear of DNA was concentrated between 100-600 bp.

15.5 Immunoprecipitation

Sonicated samples were diluted with 9 volumes of ChIP Dilution Buffer (1.1 % TritonX-100, 1.2 mM EDTA, 16.7 mM Tris (pH 8.1), 167 mM NaCl, 1 X Protease inhibitors (Roche) added fresh before use). Lysates were pre-cleared by incubating with ~ 50 µL of Protein

A agarose beads pre-blocked with salmon sperm DNA and BSA (Millipore, 16-157) that were washed and resuspended in ChIP Dilution Buffer. To help reduce background signal, 3 µL of pre-immune serum (associated with one of the antibodies being used in the ChIP experiment) and 3 µL of rabbit IgG were added. Samples were pre-cleared on a nutator at 4°C for 1-2 hrs. While lysates were pre-clearing, all tubes for IPs were prepared and beads were pre-incubated with antibody. For this, 250 µL of 1 X PBS was added to ~ 25 µL of beads (washed and resuspended in 1 X PBS) and the appropriate antibody was added (see Table 2.1). A pre-immune IP (5 µL) was done as a negative control. The beads and antibodies were incubated together for 1 hr on a nutator at 4°C. After pre-clearing the lysate, the beads were pulsed down at 3000 rpm and 3 % of the diluted sample was removed as the Input for that sample and set aside at 4°C until the reverse cross-linking step (Section 15.7). For the antibody-incubated beads, the beads were pulsed down and the supernatant discarded. These antibody-bound beads were rinsed one time with ChIP Dilution Buffer (250 µL) and this wash was discarded. The pre-cleared lysate was then added to the antibody-bound beads. If embryos were combined for several IPs then the lysate was divided evenly among the IP tubes. The IPs were left on a nutator at 4°C for 8 hrs or overnight.

15.6 Washes and elution

After IPs were completed, unbound lysate was removed from the antibody/protein-bound beads and set aside. This unbound lysate was used to check the sonication efficiency by taking 500 µL and proceeding to the reverse cross-linking step (Section 15.7). Antibody/protein-bound beads were washed several times in different wash buffers to remove unbound protein. All wash buffers were pre-cooled on ice and

samples were placed on ice between washes. For all washes, tubes were placed on a nutator at room temperature for 4 mins and then the beads were pulsed down in a microcentrifuge at 3000 rpm. The buffer was removed from the beads and 1 mL of the next wash solution was added. The series of washes used was once in Low Salt Wash Buffer (0.1 % SDS, 1 % TritonX-100, 2 mM EDTA, 20 mM Tris-HCl (pH 8.1), 150 mM NaCl), once in High Salt Wash Buffer (same as previous but with 500 mM NaCl), once in LiCl Wash Buffer (0.25 M LiCl, 1 % NP40, 1 % sodium deoxycholate (w/v), 1 mM EDTA, 10 mM Tris-HCl (pH 8.1)) and twice in TE (10 mM Tris-HCl (pH 8), 1 mM EDTA (pH 8)). The final TE wash was removed from the beads and 250 µL of Elution Buffer (1 % SDS, 0.1 M $NaHCO_3$; made fresh and kept at room temperature) was added to each IP sample. Samples were vortexed briefly and then left on a nutator at room temperature for 15 mins. Beads were pulsed down and the eluate was transferred to a new Eppendorf tube. Another 250 µL of Elution Buffer was added to the beads and a second elution was performed in the same manner with the second eluate then being combined with the first. Input samples that had been set aside before the IPs were diluted up to a total volume of 500 µL with Elution Buffer.

15.7 Reverse cross-linking and Proteinase K treatment

To all IP samples, input samples, or unbound material (500 µL) being used to check sonication, 20 µL of 5 M NaCl was added. Samples were reverse cross-linked by incubating in a water bath at 65°C overnight (or for a minimum of 4 hrs). To reverse cross-linked samples the following were added: 10 µL of 0.5 M EDTA, 20 µL of 1 M Tris-HCl (pH 6.8), 2 µL of 10 mg/mL Proteinase K (Gibco BRL, 25530-015). Samples were then incubated at 45°C for 2 hrs.

15.8 Phenol/chloroform extraction and ethanol precipitation of DNA

To the Proteinase K treated samples, an equal volume (500 µL) of 1:1 phenol:chloroform was added. Samples were vortexed for 30 secs and then spun at maximum speed for 5 mins. The top aqueous phase was carefully transferred to a new tube, ensuring that there was no contamination from the bottom organic phase. To the extracted top phase, 500 µL of chloroform was added. This was vortexed and spun at maximum speed for 5 mins and the top phase was carefully transferred again to a new tube.

DNA was ethanol precipitated by adding 1 mL of cold 100 % ethanol and 10 µg of glycogen (Roche, 10901393001), which acts as a carrier to help precipitate small amounts of DNA, to each sample. Samples were left at -20°C overnight and then spun at maximum speed at 4°C for 15 mins to pellet DNA. The supernatant was carefully removed without disturbing the pellet. The DNA pellet was washed once with 500 µL of cold 70 % ethanol, which was then removed and the pellet was allowed to air dry before being resolved in 25 µL of sterile ddH_2O. DNA was stored at -20°C until use in real-time/quantitative PCR (qPCR).

15.9 RNase A treatment to check sonication

To check the efficiency of sonication of samples used in ChIP, the unbound material that was reverse cross-linked and precipitated was treated with RNase A. To each sample, 1 µL of 10 mg/mL RNase A (QIAGEN, 1031301) was added to the 25 µL of precipitated DNA sample. Samples were incubated at 37°C for 45 minutes and then run on agarose gels (Section 8). Ideally, a smear of DNA concentrated between 100-600 bp was observed. If sonication efficiency was being evaluated immediately (*i.e.* without performing a ChIP), then samples were reverse cross-linked and then treated with RNase A before the

Proteinase K treatment. This was followed by phenol/chloroform extraction and DNA precipitation. For ChIP samples that were evaluated by qPCR (and not standard PCR followed by gel electrophoresis), the RNase A treatment was not performed.

15.10 Real-time PCR for ChIP

Real-time PCR was done using a StepOne™ Real-Time PCR System (Applied Biosystems) and the associated software and SYBR®Green reagents and following the guidelines of the manufacturer. The locations of primer sets used to amplify the various regions of the *hsp70* gene were based off those used in Boehm *et al.* (2003) and are displayed schematically in Chapter 4, Figure 4.3. The sequences of all primers are provided in Table 2.2.

Input samples were diluted 50 X before use so they would be in a similar concentration range as the ChIP samples. Standards were made using genomic DNA prepared from OR embryos (*i.e.* sonicated, reverse cross-linked, Proteinase K treated, phenol/chloroform extracted, ethanol precipitated). Serial dilutions were done to generate standards with the following dilutions: S1=1:50, S2=1:500, S3=1:5000, S4=1:50000. These were assigned relative concentrations of 0.02, 0.002, 0.0002 and 0.00002 (with arbitrary units). Following completion of the qPCR run, a result summary was provided by the StepOne™ software, including the Ct (threshold cycle) and a relative quantity for each sample based on the standard curve generated from the standard DNA serial dilution. The qPCR was also followed by a melt curve analysis to ensure that only a single product was produced for each primer set.

The results were normalized based on ratios of input DNA. The input DNA should be equivalent for all ChIPs because an equal number of embryos were used; therefore,

the determined relative quantity of input DNA for all genotypes and treatment conditions should be the same. To account for differences, the highest input value was divided by the other input values to get input ratios that were then used to adjust the relative quantity determined for ChIP samples. For example if the OR No HS input had a relative quantity of 0.00245 and the OR 30 min HS input had a relative quantity of 0.00199 then the input ratio would be 0.00245/0.00199=1.23 and the ChIP results for OR 30 min HS would be multiplied by 1.23 to account for the discrepancy in the input values. A minimum of two qPCR replicates were performed with the same ChIP DNA and the determined normalized relative quantities were averaged. Results are displayed as bar graphs of the average relative quantity of DNA based on a standard curve, that was normalized based on input DNA ratios.

15.11 Summary of ChIP experiments conducted in Dr. Mazo's Lab

ChIPs with OR embryos (3-15 hrs) were completed for embryos under standard conditions, with a 5 min HS or with a 30 min HS and all *hsp70* primer sets (based on primers from Boehm et al., 2003) were used to compare binding of menin (9562) and Trx (N1). The control 2 (Cont2) primers were previously used in Dr. Mazo's lab and they correspond to an intergenic region where Trx is known not to bind. Two separate ChIP experiments were conducted with two qPCR replicates for each ChIP. Results are shown as the average relative quantity determined from a standard curve and normalized using input ratios.

Statistical analyses for ChIP experiments included one-way ANOVAs (analysis of variance) with Bonferroni's multiple comparisons post-hoc tests performed using GraphPad Prism version 5.00. Statistical analyses consisted of comparing the average

relative quantity of DNA for a given primer set and antibody under the three treatment conditions.

16. GENOTYPE VERIFICATION OF *Mnn1* STOCKS BY PCR

A simple method for checking the genotype of individual or small samples of flies by PCR was developed. This method was used to do a complete inspection of all the *Mnn1* stocks in the Campos lab, including all the balanced and double mutant combinations that were generated over the years by various graduate students (greater than 50 stocks).

16.1 Simple fly DNA preparations

A simple protocol for rapid and reliable DNA isolation for PCR was adapted from a previously published procedure (Gloor et al., 1993). Only male flies were used for these DNA preparations, as female flies could be carrying fertilized embryos and in the case of balanced or heterozygous stocks, this could appear as a contamination by a wild-type allele. Alternatively, virgin female flies could be used. The "squishing buffer" (SB) used for these DNA preps was composed of the following reagents : 10 mM Tris-HCl (pH 8.0), 1 mM EDTA (pH 8.0), 25 mM NaCl and 200 µg/mL Proteinase K (Gibco BRL, 25530-015) which was added immediately before use. Male flies were anesthetized and transferred to Eppendorf tubes. Flies were squished using the pipette tip containing the SB, first without dispensing liquid and further while slowly expelling the buffer from the tip. For a single fly, 50 µL of SB was used and the volume was increased according to the number of flies of a given genotype being tested. To test a stock, 5 males were used in order to

have a better sample of the population and to increase the chance of catching any contamination within the stock.

After flies were homogenized in the SB, tubes were vortexed briefly and then incubated in a water bath at 37°C for 30 minutes. The tubes were again vortexed briefly before incubating in a heat block at 95°C for 5 minutes. Samples were centrifuged at maximum speed for 8 minutes to precipitate any debris. DNA preparations were stored at 4°C for usage in PCR within 1-2 days or kept at -20°C for long-term storage.

16.2 Mnn1 exon specific primers

Primers were designed to assess whether or not the menin stocks (*Mnn1*^{e30} and *Mnn1*^{e173}) still contained the previously characterized deletions (Papaconstantinou et al., 2005). Since the deletions of both mutants span exon 2 and exon 3, primers were designed to amplify a 160 bp fragment and 150 bp fragment from each exon, respectively. Using these primers in standard PCR (Section 16.5), a pure *Mnn1*^{e30} or *Mnn1*^{e173} stock should not show any amplification; whereas a wild-type allele would show the appropriate size fragment for each primer set (see Chapter 5, Figure 5.1A for a schematic). Furthermore, a positive control primer set was designed for a fragment of exon 5 (294 bp) that is present in *Mnn1* mutants and wild-type. This ensured that a lack of amplification with exon 2 or 3 primers was not due to a problem with the DNA sample. The sequences for these primers can be found in the Table 2.2.

16.3 Diagnostic primers spanning Mnn1 deletions

The use of the primers described above could only tell whether or not there was a wild-type *Mnn1* allele present. They could not be used to distinguish between *Mnn1*^{e30} or *Mnn1*^{e173} deletions or to indicate if there were any deletion alleles still floating in a

contaminated stock. Diagnostic primers, designed by Niko Pretorius for the original characterization of the *Mnn1*^{e30} and *Mnn1*^{e173} deletions were used for this purpose (see Chapter 5, Figure 5.3A for a schematic). PCR with *Mnn1*^{e173} diagnostic primers should give rise to a 700 bp amplicon if the *Mnn1*^{e173} deletion is present, whereas the expected size of the amplicon from a wild-type allele is 4.9 kb (which is too large to be amplified with the PCR conditions used). For the *Mnn1*^{e30} diagnostic primers, the *Mnn1*^{e30} mutants should give rise to a 2.6 kb amplicon; whereas the wild-type allele would produce a 4.2 kb amplicon (not detectable with the PCR conditions used). Primer sequences are provided Table 2.2.

16.4 Primers for checking Mnn1-RNAi stocks

Due to the widespread contamination of *Mnn1* stocks, the *Mnn1-RNAi* stocks were also verified to see if they still contained the dsRNA sequence. The construct used to create these stocks consisted of exon 2 followed by intron 2 and exon 2 in reverse orientation (Papaconstantinou et al., 2005). Using a forward primer for intron 2 with a reverse primer for exon 2, a portion of the inserted fragment could be amplified, without amplifying the endogenous gene (see Chapter 5, Figure 5.4A for a schematic). Using such primers, the presence of the dsRNA sequence was confirmed by the amplification a 420 bp band.

16.5 Polymerase Chain Reaction (PCR)

GoTaq® Green Master Mix (2X) (Promega, M712) was used for PCR with fly DNA samples following guidelines of the manufacturer and using 3 µL DNA in 25 µL reactions. The PCR program used for *Mnn1-ex2, Mnn1-ex3* and *Mnn1-ex5* primer sets consisted of an initial 5 minute denaturation at 95°C, followed by 28 cycles composed of 30 sec

denaturation at 95°C, 30 sec annealing at 60°C and 30 sec elongation at 72°C. This was completed with a final elongation step at 72°C for 8 minutes. The PCR program used for *Mnn1*^{e173} and *Mnn1*^{e30} diagnostic primers had the same initial and final stages. Between these, were 15 cycles consisting of 30 sec denaturation at 95°C, 30 sec annealing at 50°C and 2 min 30 sec elongation at 72°C followed by an additional 25 cycles using the same denaturation and annealing conditions but with each consecutive cycle an additional 10 seconds was added to the elongation step. Agarose gel electrophoresis, as described previously in Section 8, was used for *Mnn1* stock verification. Only half of the total PCR products were run on the gel.

17. RESCUE OF THE *Mnn1*^{e173} ALLELE

After the wide-spread contamination of *Mnn1* stocks was discovered, all supposed *Mnn1*^{e173} stocks were screened using the *Mnn1*^{e173} diagnostic primers (Table 2.2) to attempt to find a stock that still contained a floating *Mnn1*^{e173} allele. A single stock was identified (*Mnn1*^{e173};*trx*^{Z11},*mwh*/*TM3 (Recombinant #10)*) and used to rescue the *Mnn1*^{e173} deletion allele and place it in the *yw* background. The genetic scheme for *Mnn1*^{e173} rescue is found in Figure 2.1B. Multiple crosses were set up and the presence/absence of the *Mnn1*^{e173} allele was determined by PCR after each step.

A **Background Change for Mnn1^{e30}**

$$\frac{yw^{*}}{yw^{*}};\frac{Mnn1^{e30}}{Mnn1^{e30}};\frac{+^{*}}{+^{*}} \quad \text{X} \quad \frac{w^{+}}{Y};\frac{Sp}{SM5};\frac{Ly}{TM3} \qquad \text{Several males and females}$$

↓

$$\frac{yw^{*}}{Y};\frac{Mnn1^{e30}}{SM5};\frac{+^{*}}{TM3} \ \text{X} \quad \frac{yw}{yw};\frac{Sco}{CyO};\frac{+}{+} \qquad \text{Pairs}$$

↓

$$\frac{yw}{Y};\frac{Mnn1^{e30}}{CyO};\frac{+}{TM3} \quad \text{X} \quad \frac{yw}{yw};\frac{Sco}{CyO};\frac{+}{+} \qquad \text{Pairs}$$

↓

$$\frac{yw}{yw};\frac{Mnn1^{e30}}{CyO};\frac{+}{+} \quad \text{X} \quad \frac{yw}{Y};\frac{Mnn1^{e30}}{CyO};\frac{+}{+}$$

Several to make stock

B **Recovery of Mnn1^{e173}**

$$\text{A)}\ \frac{?^{*}}{?^{*}};\frac{Mnn1^{e173}}{Mnn1^{e173}};\frac{trx^{Z11},mwh(10)^{*}}{TM3^{*}} \quad \text{X} \quad \frac{w^{+}}{Y};\frac{Sp}{SM5};\frac{Ly}{TM3} \qquad \text{Pairs}$$

↓

$$\text{B)}\ \frac{?^{*}}{Y};\frac{Mnn1^{e173}}{SM5};\frac{Ly}{TM3^{*}} \quad \text{X} \quad \frac{yw}{yw};\frac{Sco}{CyO};\frac{+}{+} \qquad \text{Pairs}$$

↓

$$\frac{yw}{Y};\frac{Mnn1^{e173}}{CyO};\frac{+}{Ly} \quad \text{X} \quad \frac{yw}{yw};\frac{Sco}{CyO};\frac{+}{+} \qquad \text{Pairs}$$

↓

$$\frac{yw}{yw};\frac{Mnn1^{e173}}{CyO};\frac{+}{+} \quad \text{X} \quad \frac{yw}{Y};\frac{Mnn1^{e173}}{CyO};\frac{+}{+}$$

Several to make stock

Figure 2.1. Genetic scheme for background change of *Mnn1^{e30}* and rescue of *Mnn1^{e173}*
Genetic crosses were carried out to change the background of *Mnn1^{e30}* to *yw* (A) and to rescue a floating *Mnn1^{e173}* allele while also changing to the *yw* background (B). * indicate chromosomes from the original stock that were changed.

18. EXPERIMENTS ATTEMPTING TO RE-ESTABLISH THE *Mnn1* PHENOTYPE

18.1 Changing genetic background of Mnn1^{e30}

Since Mnn1^{e30} mutants no longer showed the previously reported defect in HSP70 expression following a 1 hr heat shock (Papaconstantinou et al., 2005), in order to attempt to eliminate the effect of any potential background mutations, the genetic background of the *Mnn1^{e30}* flies was changed. Essentially all chromosomes, except the 2nd chromosome containing the *Mnn1^{e30}* deletion allele, were changed for a wild-type chromosome from the *yw* stock. The scheme followed for these crosses is found in Figure 2.1A. Multiple different "lines" were generated following this scheme and after amplification of these new lines, they were tested for HSP70 expression following HS, relative acute HS lethality and LOH (Sections 13 and 14).

18.2 Treatment for potential parasites

One possible factor that could have be contributing to the altered phenotype of *Mnn1* mutants was that there may have been an unidentified parasite/bacterial/viral infection that was being propagated from one generation to the next in fly cultures. In order to try and eliminate any potential parasite contamination we followed a treatment protocol received from Dr. Tim Westwood (University of Toronto, Mississauga Campus). Briefly, embryos were collected on grape juice agar plates and were rinsed off the plate and collected in a nitex sieve using 0.05 % Triton-X. Embryos were washed several times with 0.05 % Triton-X and then dechorionated with 50 % bleach for 2 mins. Dechorionated embryos were then washed thoroughly with 0.05 % Triton-X followed by 0.02 % Triton-X then ddH_2O. Dechorionated embryos were then transferred, using a fine paint brush, to drops of halocarbon oil placed on top of grape juice agar plates and left

until hatching. First instar larvae were transferred to pure food (see Section18.3) using 10-20 larvae per vial to re-establish treated stocks. This procedure was done for the following stocks: *OR, yw, Mnn1*^{e30}*/CyO* (background changed to *yw*) and *Mnn1*^{e173}*/CyO* (rescued and background changed to *yw*). This procedure was assumed to eliminate an infection that could be transferred from adult flies to the chorion of embryos and continually propagated in cultures.

18.3 Pure fly food

As some components of the fly food are purchased on a large scale (*e.g.* yeast (Fleischmann's Yeast) and agar (Moorhead and Company, Mooragar Inc.)) and we are unsure of the quality control involved in their preparation, it is possible that they could be contaminated with toxins. More expensive, and presumable more pure, molecular biology grade agar (BioShop, AGR003500) and dry active yeast (MP Biomedical, 101400) were used to make the so-called pure food. All other components of the food were the same as that previously described (Section 10.1). Flies that were treated for potential parasites (Section 18.2) were put on this pure food and maintained for many generations. The third generation of progeny that were treated and maintained on pure food were tested in the embryonic stage (3-5 hr AEL) with various heat shocks to examine HSP70 expression by immunoblotting (Section 6).

18.4 Trichostatin A (TSA) treatment

It was hypothesized that epigenetic changes were responsible for the altered *Mnn1* phenotypes. In an attempt to reset the epigenetic code of these flies, they were treated with the HDAC inhibitor, Trichostatin A (TSA) (Sigma-Aldrich, T8552). TSA food was prepared, using the pure agar and yeast, and adding TSA to a final concentration of 10

µM after the temperature cooled to below 55°C. This food was made without propionic acid as suggested by *Pile et al.* (2001); generally it is added as a fungal/bacterial inhibitor, but it has been shown to be a deacetylase inhibitor itself (Pile et al., 2001). DMSO (Sigma, D2650) control food was prepared in the same manner.

Flies were allowed to mate and lay eggs on this food (either TSA or DMSO) for 2 hr periods. Embryos were then allowed to develop normally on this food or were additionally exposed to a 1 hr acute HS at 3-5hr AEL or to a chronic HS regime throughout development (20 min HS at 3-5hr AEL, 1st instar and 2nd instar). Flies were then left to develop to eclosion. Three separate crosses for both OR and *Mnn1*^{e30} were used. For each food type and HS condition, 2-3 2hr collections were made. Survival of DMSO and TSA treated flies was assessed. The surviving flies from these TSA or DMSO treatments were mated and then adult progeny of the treated flies were examined for HSP70 expression with or without a 30 min HS. The idea was to see if any heritable changes could be observed in the regulation of HSP70 expression.

Another experiment was conducted using third instar larvae (OR and *Mnn1*^{e30}) and exposing them to a 6 hr treatment of either TSA or DMSO (as described in Zhao et al., 2006). Third instar larvae were collected from food plates and transferred to dishes with filter paper soaked in a physiological brine (130 mM NaCl, 4.7 mM KCl, 1.9 mM $CaCl_2$) containing 10 µM of TSA or DMSO and left for 6 hrs. Larvae were then rinsed and exposed to a 30 min HS at 37°C or lysed immediately in SDS-SB. SDS-PAGE and immunoblotting were used to examine HSP70 expression in OR and *Mnn1*^{e30} larvae exposed to TSA; immunoblotting with an anti-acetyl histone H3 antibody (Table 2.1) was

used as a control to show that the TSA treatment was sufficient to affect histone acetylation levels.

18.5 Propionic acid – free food

Food without propionic acid (PA) was found to have significant bacterial growth compared to food containing propionic acid. As bacterial growth interfered with development and was an additional factor in the experiments, antibiotics were added to the food to inhibit bacterial growth so that the effect of propionic acid could be examined. Penicillin/Streptomycin (Gibco®, 15140-122) was added to fly food at a concentration of 80 U/mL penicillin and 80 µg/mL streptomycin after food cooled below 60°C. Food containing antibiotics was made with and without propionic acid. OR and *Mnn1*^{e30} adults were added to food tubes and allowed to mate and lay eggs so that progeny would develop with or without propionic acid. Progeny were removed at the third instar stage and also when they had eclosed as adults (0-3 d). These progeny that developed with or without propionic acid were exposed to various heat shocks and lysates were prepared and examined by immunoblotting for differences in HSP70 expression.

18.6 Homologous recombination to clean-up the second chromosome

After rescuing the *Mnn1*^{e173} allele from the contaminated stock, the mutants were found to have a sterility problem associated with the second chromosome. Consequently, we attempted to clean-up the second chromosome by allowing homologous recombination to occur with a wild-type allele. Although it would not be possible to determine whether or not recombination was occurring, or where on the chromosome it had occurred, due to the high frequency of homologous recombination in *Drosophila*, it was

believed that if recombination was allowed to occur repeatedly by backcrossing to a wild-type stock it could be possible to remove deleterious background modifications by this method. In addition to *Mnn1*^{e173} flies, the *Mnn1*^{e30} line was also used in this recombination. Please see Figure 2.2 for the full scheme used for this recombination with the wild-type second chromosome from the *w*^{1118} stock. Recombination should occur in the oocytes of heterozygous females (*Mnn1*$^{-/+}$). After mating with the second chromosome balancer stock, individual male progeny that could have a recombined chromosome were tested by PCR with diagnostic primers (see Section 16.3) to identify those that still contained the *Mnn1* alleles. Those lines testing positive by PCR were then used for a second round of homologous recombination and this process was repeated. For each step, a minimum of 10-20 crosses were carried out for each genotype and for pairwise crosses where the presence of the *Mnn1* deletions could not confirmed until after mating and sacrificing the male, about 30-50 crosses were set up. A total of six rounds of homologous recombination were completed, which involved 15 steps of crosses. After this, crosses were set up to test whether homologous recombination was success at generating a *Mnn1*^{e173} line that was no longer sterile. About forty lines that were positive for the *Mnn1*^{e173} allele by PCR were used to attempt to create a homozygous stock.

1. ♀ $\frac{y\,w}{y\,w}; \frac{Mnn\,1^{e173}}{Mnn\,1^{e173}}; \frac{+}{+}$ X ♂ $\frac{w^{1118}}{Y}; \frac{+}{+}; \frac{+}{+}$

↓

2. ♀ $\frac{y\,w}{w^{1118}}; \frac{Mnn\,1^{e173}}{+}$ X ♂ $\frac{w^{1118}}{Y}; \frac{S\,p}{S\,M5}$ HR will occur in ♀ oocytes

↓

3. ♂ $\frac{w^{1118}}{Y}; \frac{?Mnn\,1^{e173}?}{S\,M5}$ X ♀ $\frac{w^{1118}}{w^{1118}}$ mate pairwise, then check ♂ by PCR

4-5. Repeat steps 2 and 3 for second HR event

6-7. Repeat steps 2 and 3 for third HR event

*Check for sterility by following steps 13-15 but simultaneously continue with step 8

8-9. Repeat steps 2 and 3 for fourth HR event

10-11. Repeat steps 2 and 3 for fifth HR event

12. Repeat step 2 for sixth HR event

13. ♂ $\frac{w^{1118}}{Y}; \frac{?Mnn\,1^{e173}?}{S\,M5}$ X ♀ $\frac{w^{1118}}{w^{1118}}; \frac{S\,p}{S\,M5}$ mate pairwise, then check ♂ by PCR

↓

14. ♂ X ♀ $w^{1118}; \frac{Mnn\,1^{e173}}{S\,M5}$ Mate sibling progeny

↓

15. ♂ X ♀ $w^{1118}; \frac{Mnn\,1^{e173}}{Mnn\,1^{e173}}$ *establish homozygous stock if possible

Figure 2.2. Genetic scheme using homologous recombination to attempt to clean-up the second chromosome background.
Mnn1^{e173} and *Mnn1*^{e30} (not shown) were both used in this series of crosses and numerous tubes were set up at each step. The females, where homologous recombination should occur in their oocytes, are highlighted in grey (step 2). Male progeny that could contain a recombined chromosome were tested by diagnostic PCR after mating to determine whether or not they contained the desired *Mnn1* allele. In total, six rounds of potential homologous recombination were allowed before attempting to create homozygous *Mnn1* stocks.

19. CHANGE TO w^{1118} GENETIC BACKGROUND

In order to decrease variability among genotypes due to differences in genetic background, all lines used for investigating a potential role of menin in insulin signalling were put into the w^{1118} background. The complete scheme for this can be found in Figure 2.3A. A w^{1118};*Sp*/SM5;+ stock was created so that the X and Y chromosomes as well as the wild-type third chromosomes all came from the w^{1118} stock. Since no markers/balancers are available for the fourth chromosome it was ignored and assumed that since it carries few genes it would not be a factor. This stock was used to place the *Mnn1* deletion alleles into the w^{1118} background starting with previously generated stocks with the third chromosome marked and balanced to ensure the introduction of the wild-type alleles (*i.e.* w^{+};*Mnn1*/SM5;*Ly*/TM3) (see Figure 2.3B for the scheme). As the precise excision lines ($Mnn1^{+E314}$, $Mnn1^{+E323}$) had never been used, I first had to generate a balanced stock with the third chromosome marked and balanced before I could trace the exchange to the wild-type alleles from the w^{1118} stock (see Figure 2.4 for the scheme). Once the deletion mutants and precise excisions were placed in the w^{1118} background, homozygous lines were generated for all except $Mnn1^{e173}$.

19.1 Sterility check for $Mnn1^{e173}$

After the $Mnn1^{e173}$ allele was recovered from the stock that it was found floating in and also after it was transferred to the w^{1118} background, the stocks were found to be homozygous sterile. To determine the source of the sterility issue, for each sex of $Mnn1^{e173}$, three separate crosses to w^{1118} of the opposite sex were carried out. To determine if this sterility was linked to the $Mnn1^{e173}$ allele the fertility of $Mnn1^{e173}/Mnn1^{e30}$ and $Mnn1^{e173}/Df(2L)spd^{j2}$ were also examined.

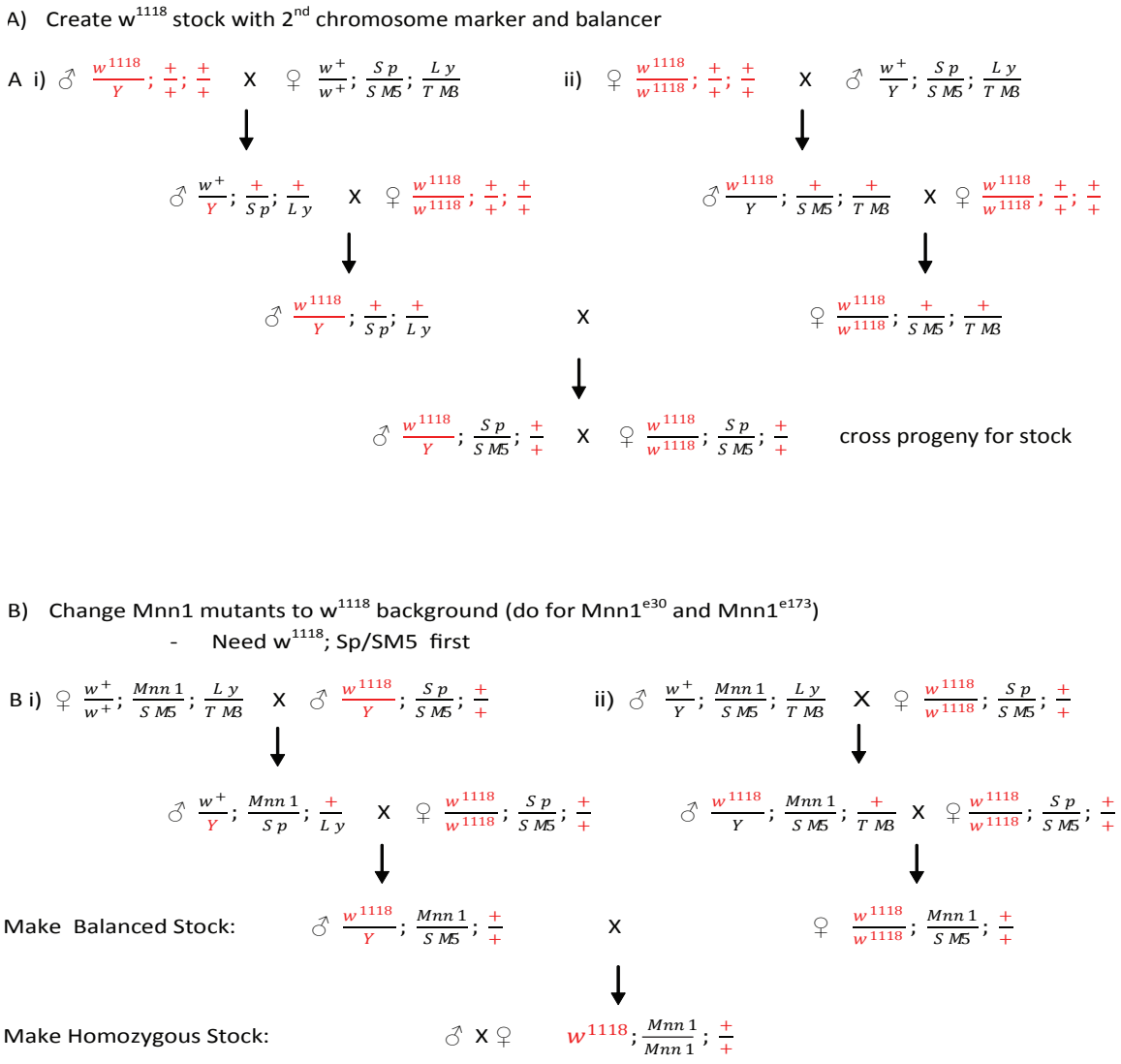

Figure 2.3. Genetic schemes used to change *Mnn1* mutants to the *w*^{1118} background.
A) A second chromosome marker/balancer was generated first. B) *Mnn1* deletions mutants (*Mnn1*^{e30} and *Mnn1*^{e173}) were then put into the *w*^{1118} background. All chromosomes coming from the *w*^{1118} stock are followed in red.

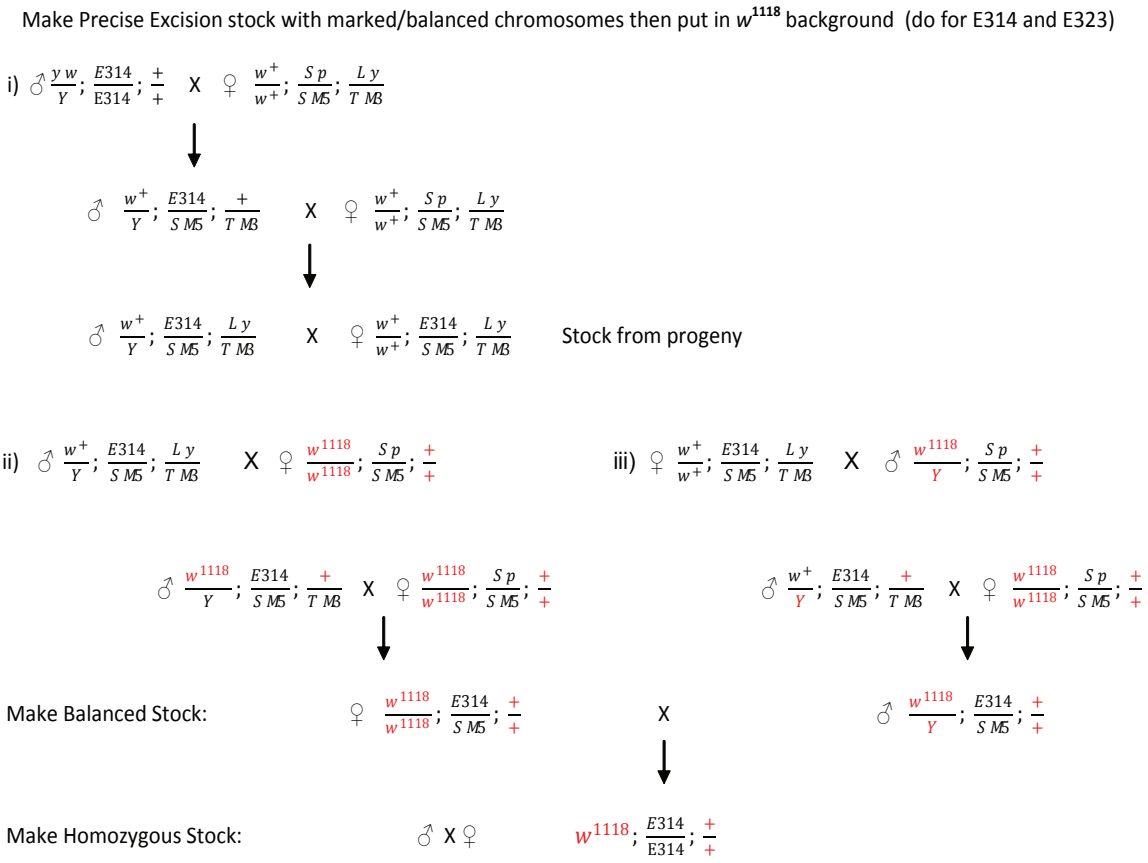

Figure 2.4. Genetic scheme used to change *Mnn1* precise excision lines to the *w*^{1118} background. Precise excision alleles *Mnn1*$^{+E314}$ (E314) and *Mnn1*$^{+E323}$ (not shown) were placed into a marked and balanced stock and then into the *w*^{1118} background using the scheme shown. All chromosomes coming from the *w*^{1118} stock are followed in red.

20. CONTROL FOR LARVAL DENSITY

Due to differences in the fecundity of different genotypes, some genotypes could experience overcrowding or reduced nutrient availability during larval development. In order to ensure that flies of all genotypes developed under similar conditions, equal numbers of larvae were placed in each vial. Small fly houses were created and flies were allowed to mate and lay for 12 hr periods. Collections were made both during the daytime and overnight. Embryos were aged until they hatched as first instar larvae. Using a fine paintbrush, first instar larvae were transferred, 100 per vial, to vials with standard fly food (about 10 mL of food per vial). In order to facilitate larval feeding, the food was cut up with forceps before transferring larvae. After counting and transferring first instar larvae they were allowed to develop until eclosion as adults. Eclosed flies were collected on a daily basis (age 0-1 day) in vials with standard fly food and allowed to mate freely while they aged for 4 to 5 days. At that time, the starvation or desiccation assays were set up using mated 4-6 day old flies (Section 21).

21. STARVATION AND DESICCATION ASSAYS

21.1 Starvation assay

Adult mated flies, age 4-6 days, were used in the starvation assay. Starvation vials contained 10 mL of a solidified 1 % agar solution. This ensured that flies had access to water but not to any nutrients. Anesthetized flies were separated by sex and counted 10 flies of a given sex and genotype per vial. Flies were maintained at room temperature and transferred to new vials every other day. Survival was examined every 24 hours until all flies had perished. Two separate parental houses were prepared to

generate each genotype tested. All eleven parental crosses were done simultaneously so all genotypes could be tested together. Multiple collections were made in order to get enough progeny of the desired genotype at the same developmental stage. Two to three trials, starting on different days, were done with progeny from each parental house, with the number of flies tested varying depending on availability. The second experiment was separated temporally from the first and consisted of eleven new parental crosses. Again, progeny were tested in 2-3 trials, with the number of individuals varying for each trial. Combining data from these two experiments, created a sample size of 180-350 flies for each sex and genotype.

21.2 Desiccation assay

Similar to the starvation assay, 4-6 day old mated flies were used in the desiccation assay. For this assay, flies were entirely deprived of food and water. Flies were anesthetized and separated by placing 10 flies of a given sex and genotype per empty glass tube. Survival was examined after 10 hours and then every 2 hours consecutively until all flies had perished. Similar to the starvation assay, two separate experiments, that were temporally separated, were conducted with all eleven parental crosses set up simultaneously for each experiment. Several trials from each parental house were conducted, with the number of flies tested varying depending on availability. Combining data from these two experiments, created a sample size of 150-350 flies for each sex and genotype.

21.3 Statistical analyses of survival curves

Starvation and desiccation data were analyzed using GraphPad Prism version 5.00. Survival curves were generated for each genotype and a log-rank (Mantel-Cox) test was

performed for the entire data set. Pairwise comparisons were made using the same log-rank (Mantel-Cox) tests to determine which pairs of curves were significantly different. It was necessary to adjust for multiple comparisons using the Bonferroni method. This was done by dividing the desired significance level (*i.e.* $p<0.05$) by the total number of comparisons being made. With the entire data set consisting of 11 genotypes, a total of 55 possible comparisons could be made; however, not all of these pairwise comparisons were meaningful. A total of 25 pairwise comparisons were determined to be meaningful, as they were comparisons made to control genotypes (*e.g.* w^{1118} and $Mnn1^{+E314}$) or the two genotypes being compared varied by a single allele (*e.g.* $Mnn1^{e30}$ versus $Mnn1^{e30}$/+). Thus, the corrected significance level used for the entire data set became $p<0.002$. In addition, further statistical analyses were done by choosing a single time point from each experiment and comparing survival of all genotypes using a one-way ANOVA, followed by Bonferroni's post-hoc test to determine which genotypes were significantly different.

CHAPTER 3. MENIN INTERACTS WITH DFADD

INTRODUCTION

Fas-associated death domain (FADD) was identified in a search for novel menin-interacting proteins. Due to the established role of *Drosophila* FADD (dFADD) in the innate immune response, this led to the investigation of a potential function for menin in the immune response. The key signalling pathways of *Drosophila* innate immunity, as well as a review of FADD functions in both *Drosophila* and mammalian cells, will be summarized in this introduction.

1. Drosophila innate immunity

Drosophila lacks adaptive immunity and thus relies solely on innate immunity for defense against invading pathogens. The innate immune response is composed of two branches, the cellular and humoral responses. The cellular response involves activation of plasmatocytes for phagocytosis of foreign organisms as well as activation of the phenoloxidase cascade that results in melanization at the site of injury. The humoral response is characterized by the induction of antimicrobial peptide (AMP) genes in the fat body and their release into the hemolymph (reviewed in Brennan and Anderson, 2004; Hultmark, 2003; Lemaitre and Hoffmann, 2007). Surface epithelial cells, such as in the intestines and respiratory tract, can also recognize and respond to the presence of pathogens (Tzou et al., 2000). Two signalling pathways, the Toll pathway and the immune deficiency (Imd) pathway, govern the *Drosophila* immune response. Each pathway is activated by the recognition of pathogen-associated molecular patterns (PAMPs) and culminates in the activation of specific members of the nuclear factor

kappa B (NF-κB)/Rel family of transcription factors which are required for the induction of AMP gene expression. The Toll pathway responds primarily to fungi and Gram-positive bacteria; whereas the Imd pathway is stimulated by Gram-negative bacteria (reviewed in Lemaitre and Hoffmann, 2007). A summary of the method of pathogen recognition for pathway activation, as well as a review of the antimicrobial peptides that are the key effectors of the immune response, will be provided first. This will be followed by a summary of the key components of the Toll and Imd signalling pathways, with emphasis on the Imd pathway due to the function of dFADD in this pathway.

1.1 Pathogen recognition

Pathogen recognition by *Drosophila* depends on recognition of specific components of the pathogen cell wall or other virulence factors that are unique to the pathogen and absent in the host (*i.e.* PAMPs) (reviewed in Aggarwal and Silverman, 2007). It was originally believed that lipopolysaccharide (LPS), which is an important component of the outer cell membrane of Gram-negative bacteria, was the distinguishing feature that specifically activated the Imd pathway (Werner et al., 2003). Peptidoglycan (PGN), which forms the multilayered outer cell wall of Gram-positive bacteria, was presumed to be important for specifically activating the Toll pathway (Michel et al., 2001). Surprisingly, the ability to discern between the different types of bacteria occurs through the recognition of specific types of PGNs found in both Gram-positive and Gram-negative bacteria and not LPS as initially reported (Kaneko et al., 2004; Leulier et al., 2003). Previous results suggesting that LPS activated the Imd pathway are believed to be due to contamination of commercial LPS with PGN (Kaneko et al., 2004). Bacterial PGN is a polymer of repeating N-acetylglucosamine and N-acetylmuramic acid with

polymers cross-linked by short peptides called stem peptides. The main distinction between PGNs is that Gram-positive bacteria have a lysine amino acid at the third position of the stem peptide (lysine-type PGN), while Gram-negative bacteria differ by having a diaminopimelic acid residue at this position (DAP-type PGN) (reviewed in Charroux et al., 2009).

The lysine-type PGN of Gram-positive bacteria is recognized by a circulating peptidoglycan recognition protein (PGRP-SA, encoded by *semmelweis (seml)* gene) and binding results in stimulation of the Toll pathway by activating cleavage of the endogenous ligand Spätzle (Michel et al., 2001). Mutations in *seml* render flies susceptible to Gram-positive infection (*e.g. Micrococcus luteus*) but not fungal infection (*e.g. Beauvaria bassiana*), suggesting that Gram-positive bacteria and fungi must activate the Toll pathway via different mechanisms (Michel et al., 2001). It was established that PGRP-SA is circulating and not membrane-imbedded like other PGRPs, as injection of wild-type hemolymph into *seml* mutants was sufficient to restore the ability to induce the expression of *Drosomycin*, the key Toll-regulated AMP, following *M. luteus* challenge (Michel et al., 2001).

In contrast, Gram-negative bacteria (and *Bacillus* species of Gram-positive bacteria) possess DAP-type PGN that is recognized by the transmembrane PGRP-LC and leads to activation of the Imd pathway (Gottar et al., 2002). Mutations in *PGRP-LC* result in severely reduced expression of *Diptericin*, *Cecropin* and *Attacin* following Gram-negative bacterial infection (*e.g. Escherichia coli*, *Agrobacterium tumefaciens*), without affecting induction of *Drosomycin* after infection by Gram-positive bacteria or fungi (*e.g. M. luteus, B. bassiana*) (Gottar et al., 2002). Three different isoforms of *PGRP-LC* are

generated through alternative splicing (*PGRP-LCa, PGRP-LCx, PGRP-LCy*) and they differ only in the C-terminal extracellular domain (Werner et al., 2003). The PGRP-LCa and PGRP-LCx protein isoforms are the most important for PGN recognition. They can form homotypic or heterotypic dimers through interaction of their cytoplasmic domains and this oligomerization is required for receptor activation (Choe et al., 2005).

PGRP-LC mutants are highly susceptible to Gram-negative infections (*e.g. A. tumefaciens, Erwinia carotovora carotovora* (*Ecc*), *Enterobacter cloacae*), while survival following Gram-positive or fungal infections is similar to that wild-type flies (Gottar et al., 2002). Although *PGRP-LC* mutants are susceptible to Gram-negative infection, the phenotype is not as severe as that of mutants of the downstream component *kenny*. This suggested to researchers that other PGRPs might be involved in Gram-negative bacteria recognition and Imd pathway activation.

Identification of PGRP-SA and PGRP-LC as important proteins for the recognition of pathogens and activation of the Toll and Imd pathways, respectively (Gottar et al., 2002; Michel et al., 2001), spawned a huge surge in research on the mechanisms of pathogen recognition and determination of the sequence of events upstream of Toll and Imd (reviewed in Aggarwal and Silverman, 2007; Charroux et al., 2009; Lemaitre and Hoffmann, 2007). In addition to the requirement of PGRP-SA, PGRP-SD and GNBP-1 (Gram-negative binding protein 1) are involved in recognition of Lysine-type PGNs in the hemolymph. They are required for activation of a serine protease cascade that cleaves and activates the ligand Spätzle, which subsequently activates the Toll receptor (Aggarwal and Silverman, 2007; Valanne et al., 2011). Fungi appear to activate the Toll pathway through the recognition of β-glucan from fungal cells by GNBP-3 which acts

upstream of the serine protease cascade that results in Spätzle activation (reviewed in Valanne et al., 2011). Activation of the Imd pathway by DAP-type PGNs also utilizes PGRP-LE, which is located in the cytosol, in addition to the transmembrane PGRP-LC. How signals are transmitted from these PGRPs to downstream components of the pathway is still not well understood (reviewed in Aggarwal and Silverman, 2007).

1.2 Antimicrobial peptide (AMP) genes

The antimicrobial peptide (AMP) genes are primarily expressed in the fat body, the equivalent to the mammalian liver. These genes have promoters which are activated by NF-κB transcription factors (*e.g.* Dif (Dorsal-related immunity factor), Dorsal, Relish). The peptides encoded by the AMP genes are cationic and very small, generally less than 10 kDa (Attacin is an exception at 25 kDa) (reviewed in Lemaitre and Hoffmann, 2007). Upon production in the fat body, they are released and circulated in the hemolymph where they function by inhibiting growth of the invading microorganisms. They are believed to act by disrupting bacterial cell membranes, although the exact mechanism is unknown.

Seven different AMP gene families have been identified in *Drosophila*. Those that are most effective against Gram-negative bacteria include the Attacin *(Att)*, Drosocin (*Dro*) and Diptericin (*Dpt*) gene families. Defensin (*Def*) is most active against Gram-positive bacteria while Drosomycin (*Drs*) has antifungal properties. Cecropins (*Cec*) are most active against bacteria but are also effective against some fungi and Metchnikowin (*Mtk*) is primarily antifungal but also has antibacterial properties (reviewed in Lemaitre and Hoffmann, 2007).

Pricking or injury results in a low but detectable level of expression of all AMPs; however, high expression levels or more sustained expression of certain AMPs occurs with some degree of specificity depending on the type of infecting microorganism (Lemaitre et al., 1997). Fungal infection (*e.g. B. bassiana*) results in strong expression of *Drs* which occurs through activation of the Toll pathway (Lemaitre et al., 1996; Lemaitre et al., 1997). *Drs* is moderately induced by Gram-positive *M. luteus* but not by Gram-negative *E. coli* infection. *Dpt*, *CecA*, *Att*, and *Def* are all most strongly induced by *E. coli* infection and moderately induced by fungal infection. *Dro* is also strongly induced by *E. coli* but only mildly induced by *M. luteus* and *B. Bassiana*. *Mtk* is strongly induced by *B. bassiana*, *M. luteus* and *E. coli* (Lemaitre et al., 1997). Overall, infection by different microorganisms is able to activate primarily the Imd or Toll pathway for the production of various AMPs that are specific to the type of invading pathogen.

1.3 Toll pathway overview

A simplified overview of the Toll pathway from the Toll receptor to activation of the NF-κB family transcription factors responsible for AMP gene expression will be described in this section. The complex mechanism of pathogen recognition and the protease cascade upstream of Spätzle that result in its activation will not be described (reviewed in Valanne et al., 2011).

The *Drosophila* Toll receptor (*Tl*) is activated by binding of the endogenous ligand Spätzle (*spz*). Upon activation, the cytoplasmic portion of Toll, which contains a TIR (Toll/Interleukin-1 receptor homology) domain, interacts with a homologous domain in the adaptor dMyD88 (*Drosophila* myeloid differentiation factor 88). dMyD88 also contains a death domain (DD) that interacts with the DD in the adaptor Tube which in

turn interacts with the kinase Pelle (*pll*; Interleukin-1 receptor associated kinase (IRAK) homologue) through DD interactions. Signalling results in the phosphorylation of Cactus (*cact*). Cactus is an IκB (inhibitor of kappa B) that binds to and inhibits the nuclear translocation of the NF-κB family members Dorsal (*Dl*) and Dif in the absence of signalling. The kinase responsible for Cactus phosphorylation remained elusive although recent evidence suggests that Pelle itself may phosphorylate Cactus instead of acting through another unidentified kinase as originally assumed. In a screen that targeted all known and predicted *Drosophila* kinases, Pelle was the only one implicated in Cactus phosphorylation (Huang et al., 2010). The phosphorylation of Cactus leads to its ubiquitination and proteasome-mediated degradation which is required for the release and nuclear translocation of Dif (or Dorsal in larvae). These NF-κB members are required for transcription of AMP genes, particularly the antifungal gene *Drs,* and *Mtk* to a lesser extent (the Toll pathway is reviewed in Lemaitre and Hoffmann, 2007; Valanne et al., 2011).

The Toll pathway was originally defined for its role in dorsal-ventral patterning during embryonic development (reviewed in Belvin and Anderson, 1996). The *Drosophila* Toll pathway bears some semblance to the vertebrate toll-like receptor (TLR) and interleukin-1 (IL-1) pathways which have defined roles in immunity and inflammation (reviewed in Hoffmann and Reichhart, 2002). A potential role for the Toll receptor, and corresponding pathway, in immunity was first established in the *Drosophila* mbn-2 blood cell line. Expression of a constitutive active form of Toll, Tl^{10b}, resulted in induction of the AMP gene *CecA1* (Rosetto et al., 1995). Shortly after, Lemaitre *et al.* (1996) demonstrated that the Spätzle-Toll-Cactus developmental

pathway controlled the antifungal response in *Drosophila*. Mutants of the Toll pathway (*i.e.* $Tl^{r632/l\text{-}RXA}$, $pll^{078/21}$, $tube^{238/3}$, $spz^{rm7/197}$) had severely reduced survival following fungal infection but survival following Gram-negative infection was similar to wild-type flies (Lemaitre et al., 1996). Expression of the antifungal gene *Drs* was significantly reduced in Toll pathway mutants following bacterial challenge; the induction of antibacterial genes *CecA*, *Def* and *Att* was mildly to moderately reduced in these mutants (Lemaitre et al., 1996). The proteolytic pathway upstream of Spätzle that results in Spätzle cleavage and activation that is required for dorsal-ventral patterning (*i.e. snake*, *easter*, *gastrulation defective* genes) was not required for survival following fungal infection or for *Drs* expression. This suggested that for the immune response, the pathway is activated in a different manner than the developmentally regulated pathway (Lemaitre et al., 1996). Surprisingly, *Dorsal* mutants did not have defects in expression of *Drs* following infection of adults (Lemaitre et al., 1996). It was later established that in adults *Dif*, another NF-κB family member, is required for the antifungal response and transcription of *Drs* (Rutschmann et al., 2000a).

Lemaitre *et al.* (1996) established that the core Spätzle-Toll-Tube-Pelle cascade was required for antifungal immunity. It was later established that the Toll pathway was also essential for Gram-positive bacteria survival (Rutschmann et al., 2002). *Dif* and *spz* mutants succumbed rapidly to infection by Gram-positive bacteria (*i.e*. *Enterococcus faecalis, Staphylococcus saprophyticus* or *Pediococcus acidolactici*) (Rutschmann et al., 2002). Thus, in *Drosophila*, the Toll pathway is required for survival following Gram-positive bacteria and fungi infections.

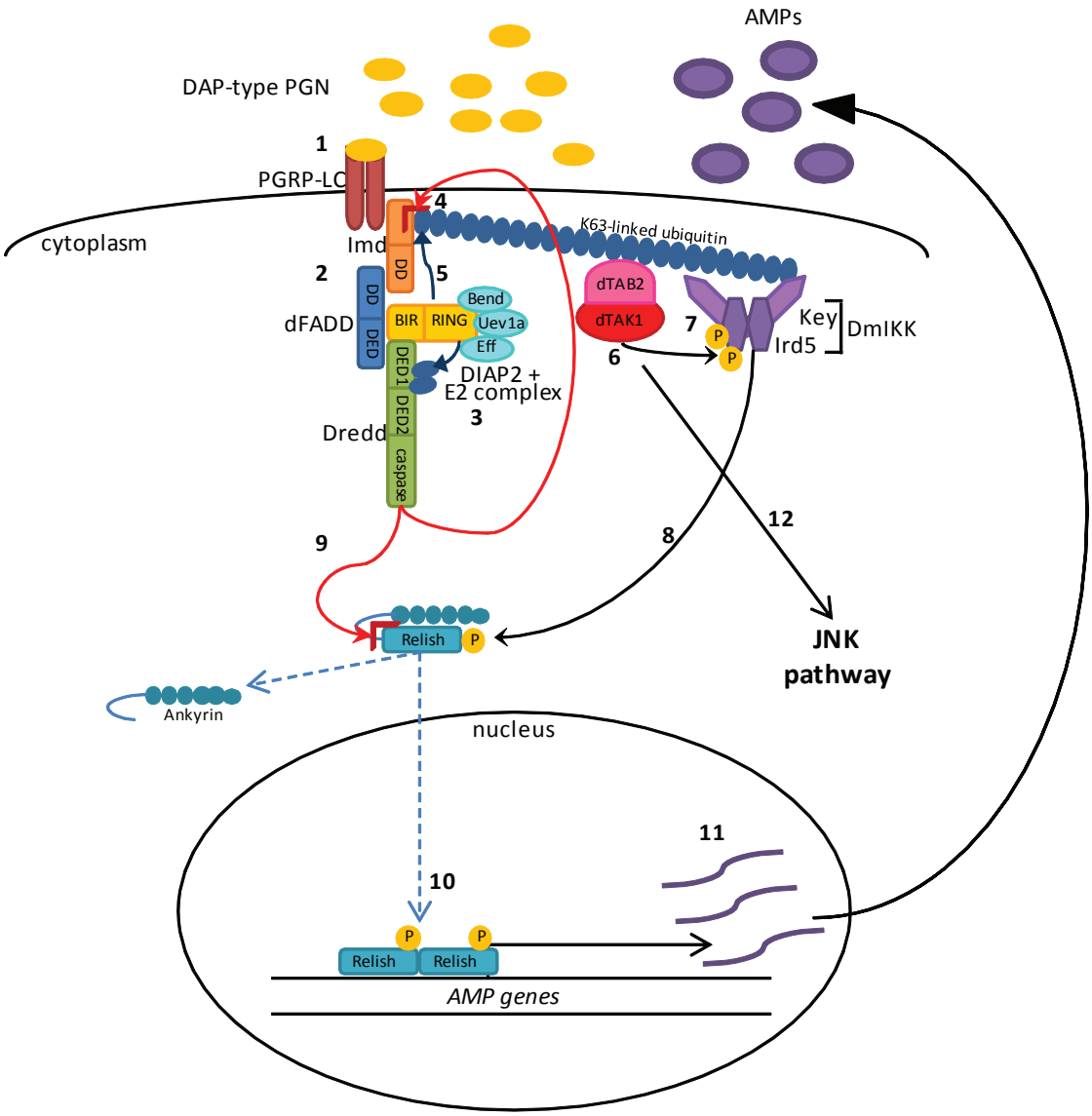

Figure 3.1. Overview of *Drosophila* immune deficiency (Imd) pathway.
The Imd pathway is activated by DAP-type PGN from Gram-negative bacteria that bind to the PGRP-LC receptors (1). This results in the recruitment of Imd, dFADD and Dredd that bind through DD and DED interactions (2). DIAP2 and the E2 complex consisting of Bendless, Uev1a and Effete are then recruited to dFADD/Dredd, which results in the DIAP2-mediated ubiquitination of Dredd (3). Activated Dredd then cleaves Imd (4), creating a site for DIAP2-mediated ubiquitination of Imd (5). The K63-linked polyubiquitin chain is believed to create a scaffold for recruitment of the kinase dTak1 and its adaptor dTab2 (6). dTak1 then phosphorylates and activates the DmIKK complex consisting of the kinase Ird5 and the adaptor Key (7). The activated DmIKK complex then phosphorylates Relish (NF-κB) which is required for activation of its transactivation potential (8). Dredd cleaves Relish (9) which results in the release of the inhibitory ankyrin repeats allowing for the translocation of Relish to the nucleus (10). Active Relish dimers transcribe AMP genes (11) which are important for the defense against bacterial infection. In addition, the JNK pathway is also activated downstream of dTak1 (12). Please refer to the text for additional details (Chapter 3 Introduction, Section 1).

1.4 Immune deficiency (Imd) pathway overview

The *Drosophila* Imd pathway shares similarities with the vertebrate tumour necrosis factor alpha (TNF-α) signalling pathway (reviewed in Hoffmann and Reichhart, 2002). Please refer to Figure 3.1 for a schematic of the *Drosophila* Imd pathway. The Imd pathway is activated primarily by Gram-negative bacteria, whose DAP-type PGN is recognized by PGRP-LC that is embedded in the plasma membrane (Gottar et al., 2002). Cytoplasmic PGRP-LE also plays a role in pathogen recognition although the mechanism of PGN detection and activation within the cytoplasm is not well understood. Binding of Gram-negative PGN to PGRPs results in receptor dimerization and Imd interacts with the cytoplasmic domain of PGRP-LC to transmit the signals from the receptor to the internal signalling cascade (Choe et al., 2005). Imd was the first identified component of the pathway and is similar to mammalian RIP (receptor-interacting protein) (Lemaitre et al., 1995). Imd has a C-terminal death domain (DD) through which it interacts with a homologous domain in the adaptor dFADD (Naitza et al., 2002). dFADD also contains a death effector domain (DED) and interacts with a similar domain in the caspase 8 homologue Dredd (Death related ced-3/Nedd2-like) (Hu and Yang, 2000).

It was recently shown that Dredd is activated by ubiquitination. This is mediated through the interaction of DED1 of Dredd with DIAP2 (*Drosophila* inhibitor of apoptosis 2) (Meinander et al., 2012). DIAP2 contains three BIR (Baculovirus IAP repeat) domains that bind N-terminal alanines generated by proteolytic cleavage and a RING (really interesting new gene) finger domain which confers E3 ubiquitin ligase activity and is used to interact with E2 ubiquitin-conjugating enzymes (Kleino et al., 2005). E2 ubiquitin-conjugating enzymes Bendless (Ubc13), dUev1a, and Effete (Ubc5) are all

required for ubiquitination and downstream signalling in the Imd pathway (Paquette et al., 2010; Zhou et al., 2005). This E2 complex associates with DIAP2 which results in ubiquitination and activation of Dredd (Meinander et al., 2012). Dredd caspase activity is believed to be required for substrate cleavage at two points in the Imd pathway – cleavage of Imd and cleavage of Relish (Paquette et al., 2010; Stöven et al., 2003). First Dredd is required for cleavage of Imd which exposes an IAP-binding motif through which a BIR domain of DIAP2 interacts. Binding of DIAP2 along with the E2 complex results in polyubiquitination of Imd (Paquette et al., 2010). The polyubiquitination of both Imd and Dredd occurs through K63-linked ubiquitin chains which are common when the ubiquitination plays a regulatory role, which contrasts to the K48-polyubiquitination that results in proteasome-mediated degradation (Paquette et al., 2010).

The generation of polyubiquitinated Dredd and Imd is believed to form important scaffolds for the recruitment of the downstream kinases (dTak1 and Ird5/DmIKKβ) and their corresponding structural proteins (Meinander et al., 2012). *Drosophila* Tak1 (transforming growth factor β activated kinase 1), a MAP kinase kinase kinase, functions at an important branching point of the Imd pathway as it is required for activation of downstream JNK (Jun N-terminal kinase) and NF-κB signalling (Silverman et al., 2003). dTak1 binds to dTab2 (*Drosophila* Tak1-binding protein 2), which contains a CUE (coupling of ubiquitin to ER degradation) domain believed to be important for recruitment of dTak1 to the K63-linked polyubiquitin scaffolds generated by DIAP2 (Kleino et al., 2005; Zhuang et al., 2006). dTak1 phosphorylates and activates the DmIKK (*Drosophila melanogaster* IκB kinase) complex, composed of the kinase Ird5/DmIKKβ and the structural component Kenny (Key/DmIKKγ) (Lu et al., 2001;

Rutschmann et al., 2000b; Silverman et al., 2000). The DmIKK complex is required for Relish activation. Relish is a bipartite NF-κB transcription factor (similar to vertebrate p105 and p100), composed of an N-terminal Rel homology domain and a C-terminal inhibitory IκB-like ankyrin repeat domain (Dushay et al., 1996). Relish is endoproteolytically cleaved by Dredd, which removes the ankyrin repeat domain and exposes the nuclear localization signal, allowing the nuclear translocation of the N-terminal Rel-homology domain (Stöven et al., 2000; Stöven et al., 2003). Activation of Relish also requires phosphorylation by the DmIKK complex that is necessary for full activation of the transactivation domain needed for proper recruitment of RNAP II and induction of AMP expression (Ertürk-Hasdemir et al., 2009). Once in the nucleus, Relish acts as the primary transcription factor for AMPs that are active against bacteria including *Dpt*, *Dro*, *Att* and *Cec*. These AMPs have conserved NF-κB binding sites in their promoters (Han and Ip, 1999).

2. Further examination of dFADD and Dredd function

2.1 dFADD is an important adaptor in the Imd pathway

Drosophila FADD (previously named BG4) was identified by Hu and Yang (2000) in a search for DD-containing proteins. dFADD contains a C-terminal DD that is 28 % identical to human FADD, with 49 % similarity. There is little similarity between the N-terminal region of the human and *Drosophila* proteins (Hu and Yang, 2000). The N-terminal region of dFADD was found to be similar to a region in the *Drosophila* caspase Dredd. The N-terminus of dFADD and a region of the prodomain of Dredd, which Hu and Yang (2000) named the death-inducing domain (DID), share 19 % identity and 39 % similarity. (Note: this domain is referred to as a death-effector domain (DED) by most

groups, even though the sequence differs significantly from the DED of mammalian FADD and caspases.)

dFADD and Dredd were shown to interact when tagged proteins were overexpressed in 293 cells. By generating expression constructs with various domains deleted, the DED of dFADD was shown to be both necessary and sufficient for interaction with the DED of Dredd (Hu and Yang, 2000). The authors also reported that dFADD and Dredd stabilize each other when co-transfected into HeLa cells. Similarly, processing of Dredd, resulting from self-oligomerization and auto-cleavage to produce the active caspase, was enhanced by the presence of dFADD in 293 cells (Hu and Yang, 2000). Furthermore, the authors hypothesized that a dFADD-mediated apoptotic pathway may also exist in *Drosophila* since Dredd-induced apoptosis of HeLa or 3T3 cells was enhanced by co-transfection with *dFADD* or the DED of *dFADD* (Hu and Yang, 2000). An upstream receptor for a pathway through which dFADD could translate extrinsic apoptotic signals to Dredd has not yet been identified. Importantly, overexpression of *Dredd* or *dFADD* in *Drosophila* cells does not induce apoptosis, therefore the role of dFADD in apoptosis is unclear (Hu and Yang, 2000).

The interaction between dFADD and Dredd, that was first demonstrated in 293 cells by Hu and Yang (2000), was later confirmed in S2 cells, a more physiologically relevant cell line (Guntermann and Foley, 2011). dFADD was also identified in a yeast two-hybrid screen for Imd-interacting proteins that specifically interact with its DD (Naitza et al., 2002). The DD of dFADD is essential for its interaction with the homologous domain of Imd. Epitope-tagged Imd and dFADD proteins co-immunoprecipitate when expressed in S2 cells (Naitza et al., 2002). In addition, dFADD

also co-immunoprecipitates with DIAP2 when the tagged proteins are expressed in S2 cells. DIAP2 immunoprecipitations result in the purification of roughly equal amounts of dFADD and Dredd. As there appeared to be no competition between dFADD and Dredd for binding to DIAP2, this suggests that these three proteins form a complex together (Guntermann and Foley, 2011). Thus, dFADD acts as an adaptor between Imd and Dredd-DIAP2 to activated downstream signalling.

Furthermore, dFADD interacts with dMyD88, an adaptor protein of the Toll pathway that contains an N-terminal DD and a C-terminal TIR domain (Horng and Medzhitov, 2001). Although this interaction was shown through co-immunoprecipitation of tagged proteins in S2 cells, the functional significance was never determined and a role for dFADD in the Toll pathway has not been established (Horng and Medzhitov, 2001). In fact, contrary to dMyD88, its overexpression does not result in induction of *Drs* expression (Horng and Medzhitov, 2001). Moreover, unlike Toll pathway components, dFADD is dispensable for survival following fungal or Gram-positive infection (Leulier et al., 2002; Naitza et al., 2002). A pathway composed of Toll-dMyD88-dFADD-Dredd was proposed as a potential apoptosis pathway that could link immune response and apoptosis (Horng and Medzhitov, 2001); however, to date, there is no substantial evidence in support of such a pathway in *Drosophila*.

The first described function for dFADD was its role in *Drosophila* innate immunity. The pricking assay was used to infect adult flies with a needle dipped in a concentrated suspension of the Gram-negative bacteria *Erwinia carotovora carotovora 15* (*Ecc15*). *UAS-dFADD-IR*, which produces a dsRNA hairpin structure due to the presence of an inverted repeat, was specifically expressed in the fat body of females

using the *yolk-GAL4* driver. This RNAi-mediated down-regulation of *dFADD* results in increased susceptibility to *Ecc15* infection, with the majority of flies perishing by 3 days post-infection (Leulier et al., 2002). Survival was similar to flies down-regulating *dTak1* (*yolk-GAL4; UAS-dTak1-IR*), another component of the Imd pathway. Following infection with a mixture of Gram-negative (*E. coli*) and Gram-positive (*M. luteus*) bacteria, *UAS-dFADD-IR* flies have reduced expression of antibacterial peptide genes (*Dpt* and *Att*) but the expression of the antifungal peptide gene *Drs* is not affected (Leulier et al., 2002).

Genetic epistasis experiments placed dFADD downstream of Imd but upstream of Dredd, between two proteins that dFADD was shown to directly interact with. The overexpression of *imd* (*UAS-imd*) or *Dredd* (*UAS-Dredd*) results in constitutive expression of *Dpt* in the absence of infection. Down-regulation of *dFADD* (*UAS-dFADD-IR*) in flies overexpressing *imd* results in a decrease in *Dpt* expression, suggesting that dFADD functions downstream of Imd. Conversely, the expression of *Diptericin-LacZ* induced through *Dredd* overexpression is not affected by down-regulation of *dFADD*, suggesting that dFADD is upstream of Dredd (Leulier et al., 2002). Expression of a gain-of-function *Toll* mutation (Tl^{10b}) results in expression of *Drs*; this expression is not affected by down-regulation of *dFADD* which indicates that dFADD does not function in the Toll pathway (Leulier et al., 2002).

The results of Leulier *et al.* (2002) were corroborated by Naitza *et al.* (2002) who also demonstrated through RNAi-mediated knock-down of *dFADD* that such flies are sensitive to Gram-negative (*E. coli*) infection but have normal resistance to Gram-positive (*Streptococcus faecalis*) infection. Similar results were obtained with $dFADD^{f02804}$ mutants that contain an insertion within the coding region. $dFADD^{f02804}$ is

considered a null allele since the PiggyBac insertion disrupts the gene so that no transcript is detected by northern blotting (Naitza et al., 2002). Heterozygous *dFADD*^{f02804} flies have normal levels of *Dpt* and *Att* induction following infection; while homozygous mutants do not have any detectable expression of these AMP genes (Naitza et al., 2002). *dFADD*^{f02804} mutants are highly susceptible to Gram-negative infection, with all flies perishing by 3 days after the infection. The survival curve for *E. coli* infected *dFADD*^{f02804} is very similar to that of *key*^{1} mutants, which were previously identified as Imd pathway mutants (Naitza et al., 2002). Thus, these results demonstrate that dFADD is an essential component of the Imd pathway.

2.2 Dredd, a Drosophila caspase, functions at multiple locations in the Imd pathway

Dredd is a homologue of mammalian caspase 8. It is composed of a prodomain containing two DED domains followed by the large (p15) and small (p10) caspase subunits (Chen et al., 1998). Dredd was identified in a screen for mutations on the X chromosome affecting infection-induced expression of *Diptericin* (Leulier et al., 2000). *Dredd* mutants are defective in the expression of all antibacterial peptide genes but the expression of the antifungal gene *Drs* is not altered in these mutants following infection with a mixture of *E. coli* and *M. luteus* (Leulier et al., 2000). Moreover, *Dredd* mutants are highly sensitive to Gram-negative infection but survive Gram-positive and fungal infections as well as wild-type flies (Leulier et al., 2000). Thus, *Dredd* mutants were shown to be phenotypically similar to *Imd* and *Relish* mutants, which were the only other Imd pathway components identified at the time.

As previously mentioned, Dredd interacts with dFADD through homotypic DED interaction (Hu and Yang, 2000). This interaction was also observed around the same

time by Horng and Medzhitov (2001). Dredd, as well as its adaptor dFADD, are required at two steps in the Imd pathway. Dredd functions upstream of dTak1 since it is required for activation of both the JNK and NF-κB branches of the Imd pathway. In addition, Dredd also functions downstream of dTak1 as *Dpt* expression induced by overexpression of *dTak1* is inhibited by down-regulation of *Dredd* or *dFADD* (Zhou et al., 2005). The function of Dredd downstream of dTak1 is the cleavage of Relish resulting in the removal of the inhibitory ankyrin repeats (Stöven et al., 2003). In agreement with Dredd playing dual roles in the Imd pathway, it was more recently implicated in Imd cleavage, which is required for interaction with and ubiquitination by DIAP2 (Paquette et al., 2010). Furthermore, Dredd itself interacts with DIAP2 through its DED1 domain and is also ubiquitinated and activated by DIAP2 (Meinander et al., 2012). The DIAP2-mediated ubiquitination of Dredd is essential for induction of AMP genes as a mutant of Dredd that cannot be ubiquitinated, $Dredd^{D44}$, is unable to induce expression of *Att* and *Dpt*, despite still being catalytically active and able to interact with dFADD and DIAP2. Moreover, $Dredd^{D44}$ flies are highly susceptible to *Ecc15* infection. Hence, the ubiquitination of Dredd is important for Imd signalling and is predicted to be important for scaffolding and recruitment of downstream kinase complexes (dTak1/dTab2 and DmIKK complex) (Meinander et al., 2012).

Although Dredd is implicated as an effector of Reaper, Grim and Hid (head involution defective) mediated apoptosis during embryonic development (Chen et al., 1998), overexpression of *Dredd* or *dFADD* is unable to induce apoptosis in S2 cells (Hu and Yang, 2000). To date, the link between the involvement of Dredd and dFADD in the

immune response pathway and a role for them in inducing apoptosis in *Drosophila* is not clear (see Chapter 7 for more details).

3. Mammalian FADD

Mammalian FADD (previously called MORT1) is a small adaptor molecule (approximately 25 kDa) that is required for death receptor-induced apoptosis (reviewed in Kim, 2002; Tourneur and Chiocchia, 2010). The gene is located on chromosome 11q13.3 in humans, and consists of two exons. The protein is 208 amino acids long and contains an N-terminal death effector domain (DED; amino acids 1-76) and a C-terminal death domain (DD; amino acids 111-180) (reviewed in Strasser and Newton, 1999). The gene is expressed ubiquitously in fetal and adult tissues (Chinnaiyan et al., 1995). Unlike in *Drosophila*, mammalian FADD is essential for embryonic development as knock-out mice die before embryonic day 12.5 and show cardiac failure and abdominal hemorrhages (Yeh et al., 1998; Zhang et al., 1998).

In order to mediate apoptosis, FADD interacts with a variety of death receptors and adaptors and links the activated receptor complex to initiator caspases of the apoptotic cascade (reviewed in Kim, 2002; Tourneur and Chiocchia, 2010). FADD interacts with the cytoplasmic tail of ligand-bound transmembrane death receptors via homotypic DD interactions. This occurs either directly, such as with Fas/CD95/APO-1 (Boldin et al., 1995; Chinnaiyan et al., 1995) or indirectly, such as with TNF-R1 (tumour necrosis factor receptor 1), where the interaction is mediated by another bridging adaptor TRADD (TNF-R1-associated death domain) that also interacts though DDs (Hsu et al., 1996). Signalling downstream of FADD occurs via homotypic DED interactions with apical procaspases (*e.g.* procaspase 8/FLICE or procaspase 10), which results in

their autocatalytic activation and initiates the apoptotic cascade leading to cell death (Medema et al., 1997). The ligand bound death receptor in association with adaptors, FADD and procaspases form a complex that initiates apoptosis and is referred to as the death-inducing signalling complex (DISC). Conversely, interaction of FADD with c-FLIP (cellular FLICE-inhibitory protein) blocks apoptosis and leads to cell survival because c-FLIP prevents binding of procaspases to the DED domain of FADD (Irmler et al., 1997). Thus, depending on its DED interactions FADD can either mediate apoptosis (procaspase 8/10) or survival (c-FLIP).

3.1 Role of mammalian FADD in immunity and apoptosis

Similar to FADD-mediated apoptosis that occurs by signalling through traditional death receptors (*e.g.* Fas, TNF-R1, TRAIL1/2) (reviewed in Tourneur and Chiocchia, 2010), FADD can also function downstream of innate immune receptors, such as the toll-like receptor (TLR) family, to initiate apoptosis (reviewed in Salaun et al., 2007). TLR pathways can respond to pathogen infection and activate NF-κB for host defense or can signal apoptosis through FADD. TLRs act as PAMP recognition receptors with different members responding to different microbial components such as lipopolysaccharides, peptidoglycans, flagellin and dsRNA. Unlike the traditional death receptors, TLRs lack DDs and therefore do not interact directly with FADD but require additional adaptor proteins. TLRs all contain TIR (toll/interleukin 1 receptor) domains in their cytoplasmic tails that are involved in interactions with these additional adaptor proteins (reviewed in Kawai and Akira, 2010).

TLR2 responds primarily to bacterial lipoproteins and peptidoglycans, and binding to the extracellular domain of the receptor results in recruitment of MyD88 to

the intracellular domain of TLR2 through homotypic TIR domain interaction. MyD88 acts at the junction of the decision for survival or apoptosis. It interacts through its DD with a homologous domain in IRAKs (interleukin-1 receptor-associated kinases; *e.g.* IRAK-1 and IRAK-4) to initiate a signalling cascade leading to NF-κB activation and expression of immune response genes (reviewed in Salaun et al., 2007). Alternatively, MyD88 can interact with FADD through homotypic DD interactions, and FADD can then interact with procaspase 8 via DED interactions thus initiating the apoptotic cascade downstream of an activated TLR2 (Aliprantis et al., 2000). Similarly, dFADD can be activated downstream of TLR3 which responds to viral dsRNA, or TLR4 that responds to LPS, with each receptor using different adaptors to recruit dFADD (Han et al., 2004; reviewed in Kawai and Akira, 2010; Zhande et al., 2007).

In addition to its role as an adaptor in the apoptotic cascade downstream of death receptors and TLRs, FADD also plays a non-apoptotic role in mammalian immunity, similar to its function in the *Drosophila* immune deficiency pathway (Balachandran et al., 2004). *FADD*$^{-/-}$ MEFs are significantly more sensitive to viral infection by vesicular stomatitis virus (VSV) and encephalomyocarditis virus (EMCV) than wild-type MEFs. Using a luciferase reporter for the interferon (IFN) β promoter, which is normally activated by viral infection, *FADD*$^{-/-}$ MEFs were shown to be defective in induction of IFN following viral infection. Microarray analysis also uncovered defects in expression of several IFN and IFN-inducible genes (*e.g. Ifna2, Ifna4, Ifna5, Irf7*) in the absence of FADD function (Balachandran et al., 2004). The requirement of FADD for the inhibition of viral replication is not dependent on caspase 8 as null MEFs or MEFs treated with caspase inhibitors do not have increased susceptibility to viral infection. This

suggests that a pathway different from that involved in apoptosis is required for FADD-mediated viral immunity (Balachandran et al., 2004). The pathway requires RIP-1 and is reminiscent of the *Drosophila* Imd signalling pathway that requires the action of Imd (RIP-1 homologue) upstream of dFADD (Balachandran et al., 2004).

Overall, in mammalian cells, FADD is an important adaptor for several signalling pathways involved in apoptosis and immunity and it exerts its function through multiple protein-protein interactions involving both its DD and DED domain. Another role for FADD related to immunity is a role in T cell and B cell development and proliferation, which is required for adaptive immunity. Chimeric mice, with *FADD*$^{-/-}$ lymphocytes have impaired T cell proliferation suggesting that in addition to its role in apoptotic signalling, FADD is also required for proliferation signalling in certain cell types (Zhang et al., 1998). Furthermore, *FADD*$^{-/-}$ B cells have impaired proliferation in response to TLR3 or TLR4 stimulation (Imtiyaz et al., 2006). The pathways involved in FADD-dependent T-cell and B-cell proliferation have not been fully elucidated.

3.2 Nuclear localization of FADD

FADD was initially believed to function only as a cytoplasmic adaptor protein and to function primarily near the plasma membrane. Surprisingly, FADD was later observed in the nucleus in several different cell lines, suggesting it has novel roles apart from signalling apoptosis through death receptors (Gomez-Angelats and Cidlowski, 2003; Screaton et al., 2003). FADD's cellular location was shown through both immunofluorescence with several different antibodies and through cell fractionation, with the majority of FADD protein found to be nuclear (Gomez-Angelats and Cidlowski, 2003; Screaton et al., 2003). In contrast, overexpression of FADD, like what was done in

earlier studies of FADD function, before specific antibodies were available, results in a predominantly cytoplasmic localization, suggesting this is an artefact of protein overexpression (Gomez-Angelats and Cidlowski, 2003). The nuclear localization of FADD is dictated by its phosphorylation state, with phosphorylation on serine 194 required for nuclear import and export. Phosphorylation of S194, or of the corresponding serine 191 residue in mice, is required for proper cell cycle progression, but mutation of this residue has no impact on apoptosis (Hua et al., 2003; Scaffidi et al., 2000). FADD S194A mutation in human cells inhibits nuclear translocation of FADD, as does elimination or mutation of the N-terminal DED (amino acids 1-80) (Screaton et al., 2003). More specifically, within the DED, a conserved basic KRK sequence acts as a NLS and is necessary for nuclear import while a leucine-rich motif (LTELKFLCL) acts as nuclear export signal (Gomez-Angelats and Cidlowski, 2003). Exportin-5, which also acts as an importin, prefers phosphorylated substrates and interacts with FADD, suggesting that it is important for FADD nuclear-cytoplasmic shuttling. Mutations that inhibit FADD nuclear localization (S194A, Δ1-80) also prevent interaction with exportin-5 (Screaton et al., 2003). Since FADD is localized to both the cytoplasm and the nucleus, it is possible that two separate pools of FADD exist – a cytoplasmic pool to mediate signalling through death receptors and TLRs and a nuclear pool with an unknown function. Another hypothesis is that since the majority of FADD seems to be located in the nucleus in unstimulated cells, FADD might be sequestered there until it is transported to the cytoplasm to mediate apoptosis through death receptors.

A yeast two-hybrid screen identified MBD4 (methyl-CpG binding domain protein 4) as a FADD interacting protein. MBD4 is a nuclear protein involved in mismatch repair;

it excises thymine (created from spontaneous deamination of methylcytosine) from GT mismatches. The interaction was confirmed through co-immunoprecipitation of endogenous proteins in MCF10a cells and mutational analysis identified the DED of FADD as essential for the interaction with MBD4 (Screaton et al., 2003). This interaction provides a potential link between genome surveillance, DNA repair and apoptosis and suggests a novel role for nuclear FADD.

3.3 FADD acts as a tumour suppressor

Evidence suggests that FADD acts as a tumour suppressor as loss of FADD leads to tumour progression in mice and humans (reviewed in Tourneur et al., 2005). Targeted expression of a dominant negative FADD lacking the DED in lymphocytes of *rag1*$^{-/-}$ mice (loss of *recombinase activating gene 1* prevents mature T cell development) results in the development of thymic lymphomas suggesting that loss of FADD function contributes to tumourigenesis (Newton et al., 2000). In a study using a mouse model for thyroid adenoma, very low FADD protein expression was observed in adenomas while non-pathological tissues expressed very high levels for FADD. This suggests that loss of FADD following oncogene activation contributes to tumourigenesis (Tourneur et al., 2003). In addition, low FADD expression is correlated with resistance to Fas and TNF-α-mediated apoptosis (Tourneur et al., 2003). In humans, a correlation was found between low expression of FADD in acute myelogenous leukemia (AML) cells and an increased resistance to chemotherapy as well as a poor survival outcome (Tourneur et al., 2004). Leukemic cells from two thirds of AML patients examined had very low or no FADD expression (Tourneur et al., 2004). Thus, FADD plays a role as a tumour suppressor, at least in some cell types.

4. Objectives and hypotheses

FADD was identified in a yeast two-hybrid screen as a potential menin interacting protein. The first objective was to confirm this interaction in *Drosophila* cells and then in flies. As dFADD had not been studied in our lab, and commercial reagents were not available, significant efforts were required for cloning and antibody generation before the interaction could be adequately studied.

The second objective was to determine the functional significance of this interaction in *Drosophila*. The hypothesis was that menin could interact with dFADD in the innate immune response to help regulate gene expression in response to bacterial infection. As menin was shown to be important for several stress responses (*e.g.* heat stress, oxidative stress, osmotic stress, and hypoxic stress) (Papaconstantinou et al., 2005), it was reasonable to predict that menin could also be important for survival when exposed to pathogen stress. An alternative hypothesis was that perhaps dFADD played a novel role in the heat shock response through its interaction with menin, providing a link between pathogen and heat stress responses. Finally, another hypothesis was that dFADD could interact with menin and function in the maintenance of genomic integrity. This was an attractive hypothesis due the role of menin in the maintenance of genomic stability (Papaconstantinou et al., 2010) and the interaction of mammalian FADD with MBD4, which is important for mismatch repair (Screaton et al., 2003).

RESULTS

1. Menin and dFADD proteins interact

1.1 Yeast two-hybrid identification of dFADD as a menin-binding protein

In order to identify novel menin-interacting proteins in *Drosophila*, a yeast two-hybrid (Y2H) screen was carried out by Hybrigenics (Paris, France) using a *Drosophila* embryo (0-24 hr) library. An initial Y2H screen was done with using LexA DNA-binding domain (DBD) fused to menin as the bait to screen the library. In this initial screen, only 9 positive prey clones were identified, and Fas-associated death domain (FADD) was among these potential menin-interacting proteins. Hybrigenics later performed a second, less stringent, Y2H screen using the GAL4-DBD fused to menin for the bait. After this screen was performed and the company provided the final results, it came to our attention that dFADD was no longer included in the list of potential menin-interacting proteins. After contacting the company, they informed us that human FADD, not *Drosophila* FADD, had contaminated the screen and was found to interact with *Drosophila* menin. Since there was a significant delay between receiving the results from the two Y2H screens, a great deal of work had already been invested into confirming the dFADD-menin interaction. Despite the unfortunate scenario, we continued to investigate the menin-dFADD interaction as often the most interesting discoveries in science happen by fluke. Hybrigenics never resolved where the error occurred or whether the *Drosophila* proteins actually interacted.

1.2 Drosophila menin and dFADD interact in 293T cells

As described in Chapter 2 Section 9, in order to confirm the menin and dFADD interaction, it was necessary to clone dFADD so that a tagged protein could be expressed

since antibodies were not available. Constructs for both N-terminal (HA-dFADD) and C-terminal (dFADD-HA) HA-tagged dFADD were generated and cloned into the pIRES-GFP expression vector. Transfection of *Drosophila* S2 cells with pIRES-GFP:HA-dFADD or pIRES-GFP:dFADD-HA did not result in detectable expression of the tagged protein as observed through examination of GFP and immunoblotting with an HA antibody (data not shown). It was assumed that the genes under control of the MCMV (murine cytomegalovirus) promoter could not be expressed in *Drosophila* cells.

The pIRES-GFP:HA-dFADD and pIRES-GFP:dFADD-HA vectors, along with a pIRES-GFP:menin vector, were co-transfected into 293T cells for the expression of the *Drosophila* proteins since this cell line is amenable to transfection and high levels of exogenous protein expression. The dFADD-HA protein was found to be expressed at higher levels than the HA-dFADD construct in 293T lysates (Figure 3.2A), possibly due to the fact that non-tagged dFADD could also be expressed from the original start codon with the HA-dFADD vector and would not be detected with an anti-HA antibody. In addition, the HA-dFADD construct migrates a little higher due to the presence of extra amino acids introduced by the primer used for adding the HA-tag (Figure 3.2A and C). Co-transfection of *Drosophila* menin and HA-tagged dFADD resulted in the co-immunoprecipitation of these proteins from 293T cells suggesting an interaction (Figure 3.2). Immunoprecipitation with the *Drosophila* menin 5073 antibody resulted in detection of dFADD-HA, and to a lesser extend HA-dFADD (Figure 3.2A). With the reciprocal anti-HA immunoprecipitation, menin was initially observed only in the HA immunoprecipitation from HA-dFADD transfected cells (Figure 3.2A), but it was later observed in anti-HA immunoprecipitations from cells transfected with either dFADD-HA

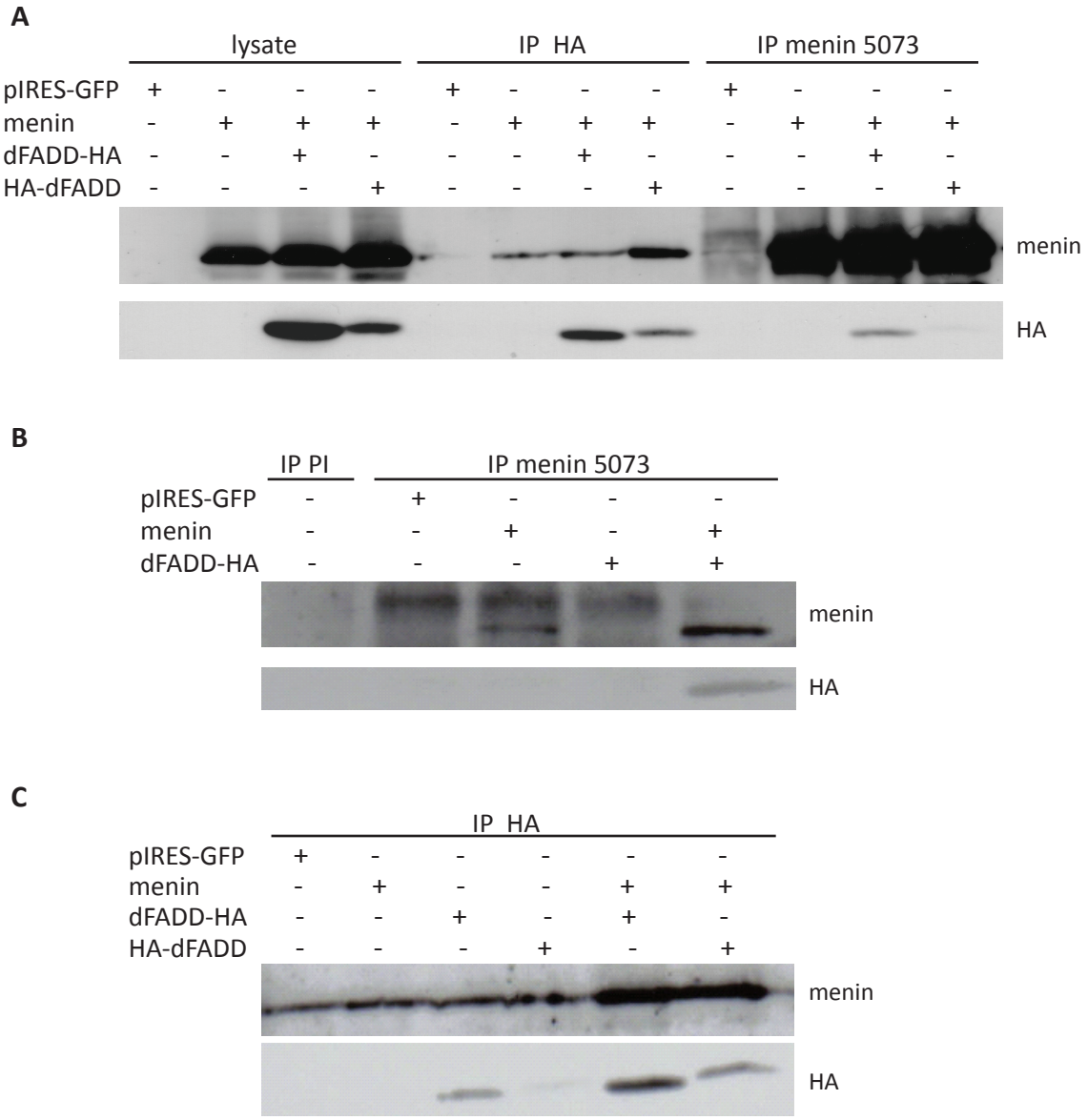

Figure 3.2. Co-immunoprecipitation of *Drosophila* menin and dFADD in 293T cells.
A) 293T cells were transfected with an empty vector (pIRES-GFP) or with the same vector expressing *Drosophila* menin, dFADD-HA or HA-dFADD. Transfections were done with menin alone or co-transfected with dFADD-HA or HA-dFADD. Menin was observed to co-IP with HA-dFADD using an anti-HA antibody. dFADD-HA, and to a lesser extent HA-dFADD, were observed in menin IPs with the 5073 antibody. The experiment was repeated several times with different combinations of vectors being co-transfected and IPs done with both the anti-menin 5073 antibody and pre-immune serum (B) and anti-HA antibody (C). *Drosophila* menin and dFADD expressed in 293T cells interact, as observed through reciprocal co-IPs.

or HA-dFADD (Figure 3.2C) (Note that there is also a contaminating band that migrates at the same level as menin in these immunoprecipitations). Pre-immune serum from the rabbit used to generate the 5073 antibody was used a negative control, and no bands were detected by the menin or HA antibody in this immunoprecipitation (Figure 3.2B). Also, transfection of an empty vector (pIRES-GFP) or single transfection of menin or dFADD did not result in any contaminating bands for immunoprecipitations with the 5073 antibody (Figure 3.2B). Therefore, when the *Drosophila* menin and FADD proteins were overexpressed in 293T cells they were found to interact in co-immunoprecipitation experiments.

1.3 Endogenous menin interacts with HA-dFADD in S2 cells

To study the menin-dFADD interaction in a more physiologically relevant background, the HA-dFADD and dFADD-HA constructs were cloned into the pPACB vector containing the *Drosophila* actin promoter for expression in S2 cells (received from Thomas Kusch, Rutgers University). Immunoprecipitation with the menin 5073 antibody showed a co-immunoprecipitation of HA-dFADD and a very weak band for dFADD-HA (Figure 3.3). Thus, the endogenous menin was shown to interact with HA-tagged dFADD in *Drosophila* S2 cells. When comparing the amount of HA-tagged dFADD protein present in the S2 cell lysates with the amount of dFADD in the menin immunoprecipitates, it appears that only a small fraction is interacting with menin (Figure 3.3). It should also be noted that on other occasions, HA-dFADD could not be detected in menin immunoprecipitates. This suggests that perhaps the interaction is tightly regulated or highly transient and thus only weakly detectable under standard cell growth conditions.

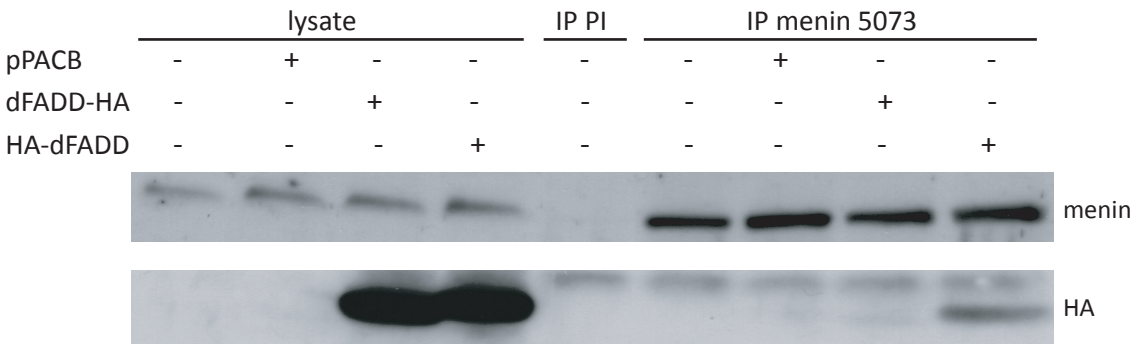

Figure 3.3. Co-immunoprecipitation of menin and dFADD in S2 cells.
Drosophila S2 cells were transfected with the empty vector pPACB or with the vector containing dFADD-HA or HA-dFADD constructs. Whole cell lysates were immunoprecipitated (IP) with pre-immune serum (PI) or with a menin antibody (5073). Lysates are shown along with the IPs and the blot was probed with the menin 5073 antibody as well as an HA antibody to detect the tagged FADD constructs that co-IP with menin. HA-dFADD interacts with endogenous menin; a very weak band can also be seen for dFADD-HA in the menin IP.

In order to further study the menin-dFADD interaction and to confirm that both endogenous proteins interact in S2 cells, as well as to investigate an interaction in *Drosophila*, an antibody capable of detecting and immunoprecipitating dFADD was essential. Please refer to Appendix A for a summary of the work done to generate and test dFADD polyclonal antibodies. The dFADD polyclonal antibodies, as well as menin antibodies, were also tested in immunofluorescence and these preliminary data are shown in Appendix B.

2. Menin is not required for the Drosophila immune response

2.1 Overview of pricking/infection assay for adult flies

In order to determine if menin played a role in the *Drosophila* immune response, *Mnn1* mutants were subjected to bacterial infection using the pricking assay that was used extensively to identify mutants of the Imd and Toll pathways (*e.g.* Naitza et al., 2002; Rutschmann et al., 2002). Imd pathway mutants were obtained as controls to compare to *Mnn1* mutants in infection assays. A *kenny*/*DmIKKγ* mutant, key^{c02831}, containing a PiggyBac insertion, was obtained from Bloomington's Stock Centre (#11044) and *dFADD* mutants were obtained from Dr. Jean-Marc Reichhart (Université de Strasbourg & Institut Universitaire de France). The $FADD^{f02804}$ line was previously characterized and contains a PiggyBac insertion within the coding region that results in a null mutant with no detectable mRNA produced (Naitza et al., 2002). The $FADD^{f06954}$ line had not been characterized by northern or western blots nor had it been described in bacterial infection assays. It contains a PiggyBac insertion in the 5' untranslated region (33 bp upstream of the start codon) (Flybase.org).

Pilot infection experiments were carried out with Oregon R (OR) flies to determine the optimal technique that would minimize death due to physical injury (see Chapter 2, Section 12). Since there was no significant difference between the survival of male and female flies in these initial trials (data not shown), both sexes were used in a roughly equal ratio in the infection assays. Flies were collected over a two day period and aged three days so they were 3-5 days old at the time of infection.

The Gram-negative bacteria *Escherichia coli MG1655* and the Gram-positive bacteria *Micrococcus luteus* were used for infection to look at the potential role of menin in the Imd or Toll pathway, respectively. Along with these bacterial infections, a mock infection was done using sterile ddH_2O to ensure that there was not significant lethality associated with the physical injury caused by pricking the flies with the needle. Bacterial cultures were grown in LB and concentrated before infection to an OD_{600}=200 for *E. coli* and OD_{600}=50 for *M. luteus*. Initially, an OD_{600}=200 was attempted for *M. luteus* but the lethality of all genotypes was higher than anticipated so this was reduced to OD_{600}=100 and finally to an OD_{600}=50. Because of this change in OD for the *M. luteus* infection, $Mnn1^{e30}$ flies only have one trial at the OD_{600}=50 that could be included in the final graph comparing survival of different genotypes (Figure 3.6). All three trials with the different bacterial concentrations are shown in Appendix C, Figure C.1; the overall trend was similar for each concentration of *M. luteus*.

Not all genotypes were tested together since they were not all initially available in the lab. However, for each experiment Oregon R was used as a negative control and key^{c02831} was use as a positive control since it is a known mutant of the Imd pathway. Because these genotypes were used as controls in several experiments and results were

consistent from one experiment to the next, the data were pooled creating a larger sample size. Graphs show the average percent survival each day over a ten day period along with the standard error of the mean for all trials conducted for a given genotype (Figures 3.4-3.6). Sample sizes are provided in Table 3.1. Data were also assessed by creating survival curves by entering the survival data for each individual fly. These were analyzed using GraphPad Prism 5.00 and performing log-rank (Mantel-Cox) statistical analyses. The statistical analyses are summarized in Appendix C, Tables C.1-C.3.

2.2 Mnn1 mutants survive bacterial infection as well as wild-type controls

As shown in Figure 3.4, the mock infection did not result in significant lethality for any of the genotypes tested. *key*^{c02831} flies did show some lethality, with an average of 78 % of flies surviving 10 days after infection, whereas all other genotypes had between 90-98 % survival 10 days after infection. It is possible that *key*^{c02831} flies were susceptible to secondary infections after they were wounded by the mock infection and thus some flies died a few days after the injury was inflicted. Statistical analyses using log-rank tests, showed that *key*^{c02831} survived significantly worse than all other genotypes (except *Mnn1-RNAi*, p=0.0244; Appendix C, Table C.1). The overall high survival with the mock infection showed that only negligible lethality resulted from physical injury or wounding that occurred following pricking with the needle.

Table 3.1. Sample size for infection assays (number of flies and trials)

Genotype	ddH_2O	*E. coli*	*M. luteus*
OR	226 (8)	193 (7)	244 (9)
yw	88 (3)	88 (3)	172 (6)
key^{c02831}	144 (5)	142 (5)	113 (4)
$FADD^{f02804}$	89 (3)	90 (3)	89 (3)
$FADD^{f06954}$	89 (3)	90 (3)	87 (3)
$FADD^{f02804}/FADD^{f06954}$	N/A	71 (3)	N/A
$Mnn1^{e30}$	84 (3)	73 (3)	26 (1)*
UAS-Mnn1	89 (3)	90 (3)	90 (3)
Mnn1-RNAi	90 (3)	90 (3)	90 (3)

Each trial began with 30 adults (3-5 d) being infected. The total number of flies that survived 3 hrs post-infection is given along with the number of separate trials in parentheses. Flies that perished by 3 hrs after infection were not included in survival calculations as the death was assumed to be due to physical injury from pricking with the needle and not from the infection. *UAS-Mnn1* and *Mnn1-RNAi* listed above are simplifications for the full genotypes *UAS-Mnn1/+;tub-GAL4/+* and *UAS-Mnn1-dsRNA/+;tub-GAL4/+*, respectively (+ chromosomes are from crosses to OR).
*Only a single trial for *M. luteus* is shown because the other trials were at higher OD_{600} (see Appendix C, Figure C.1).

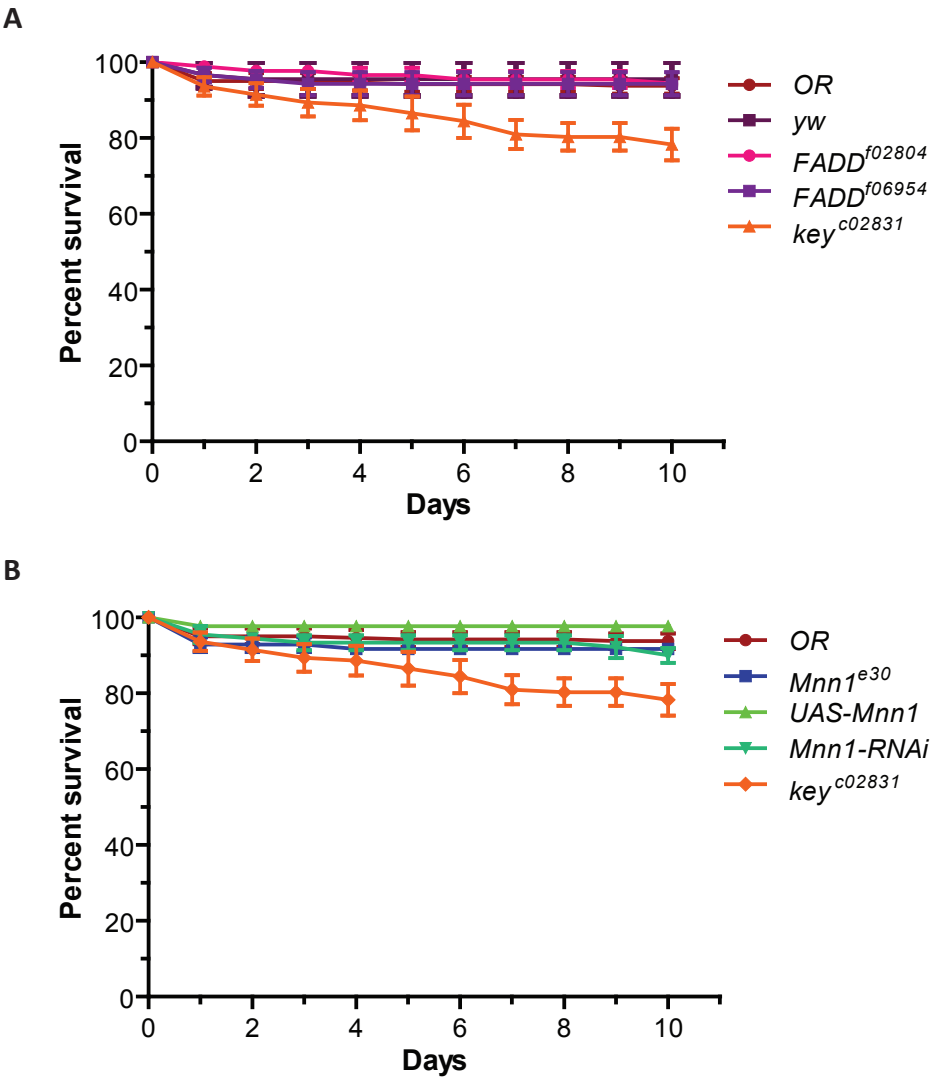

Figure 3.4. Survival of adult flies with mock ddH_2O infection.
Adult flies were mock infected using a needle dipped in sterile water and survival was assessed over a 10 day period. For each genotype, 30 flies were infected per trial and a minimum of 3 separate trials were conducted. The average percent survival for all trials of the same genotype and the standard error of the mean are shown. A) Control genotypes (*OR* and *yw*) and Imd mutants ($FADD^{f02804}$, $FADD^{f06954}$, key^{c02831}) are graphed together. B) $Mnn1^{e30}$ mutants as well as flies overexpressing *Mnn1* (*UAS-Mnn1*) or down-regulating *Mnn1* through RNAi (*Mnn1-RNAi*) using the *tubulin-GAL4* driver are shown with the wild-type control (*OR*) and the Imd pathway mutant key^{c02381}. Overall, very little lethality was observed for any genotypes with the mock infection, suggesting that there was minimal lethality due to physical injury. key^{c02381} flies survived worse than the other genotypes, suggesting that they may be susceptible to secondary infections following injury. Note, not all genotypes that are graphed together were infected at the same time.

Infection of *key*^{c02831} and *FADD*^{f02804} with *E. coli MG1655* resulted in nearly 100 % lethality by two days post-infection (Figure 3.5A). This result was expected since *FADD* and *key* have previously been shown to be essential components of the Imd pathway required for survival against Gram-negative bacteria (Naitza et al., 2002; Rutschmann et al., 2000b). The other *FADD* mutant, *FADD*^{f06954}, was more susceptible to Gram-negative infection than controls (*OR* and *yw*) but was not nearly as susceptible as *FADD*^{f02804} or *key*^{c02831} (Figure 3.5A). It is possible that this mutant is a hypomorph and only partial lethality is observed because these flies may still be able to produce functional dFADD protein, but perhaps at a lower level than wild-type. Heteroallelic mutants, *FADD*^{f02804}/*FADD*^{f06954} were created and infected with *E. coli*; these flies were more susceptible to Gram-negative infection than *FADD*^{06954} flies but did not perish as quickly as *FADD*^{f02804} or *key*^{c02831} flies (Figure 3.5A). Nearly all *FADD*^{f02804}/*FADD*^{f06954} flies had perished by 5 days post-infection. This result suggests that *FADD*^{f06954} is a hypomorphic allele. Log-rank tests indicated that OR and yw had similar survivals (p=0.3737) with *E. coli* infection, but *FADD*^{f02804}, *FADD*^{f06954}, *FADD*^{f02804}/*FADD*^{f06954}, *key*^{c02831} were all significantly different from the controls and also from each other (see Appendix C, Table C.2 for a summary of the statistics). Although the curves for *FADD*^{f02804} and *key*^{c02831} are quite similar, because *key*^{c02831} survived better in the first 24 hours post-infection these curves were found to be statistically different (Figure 3.5A).

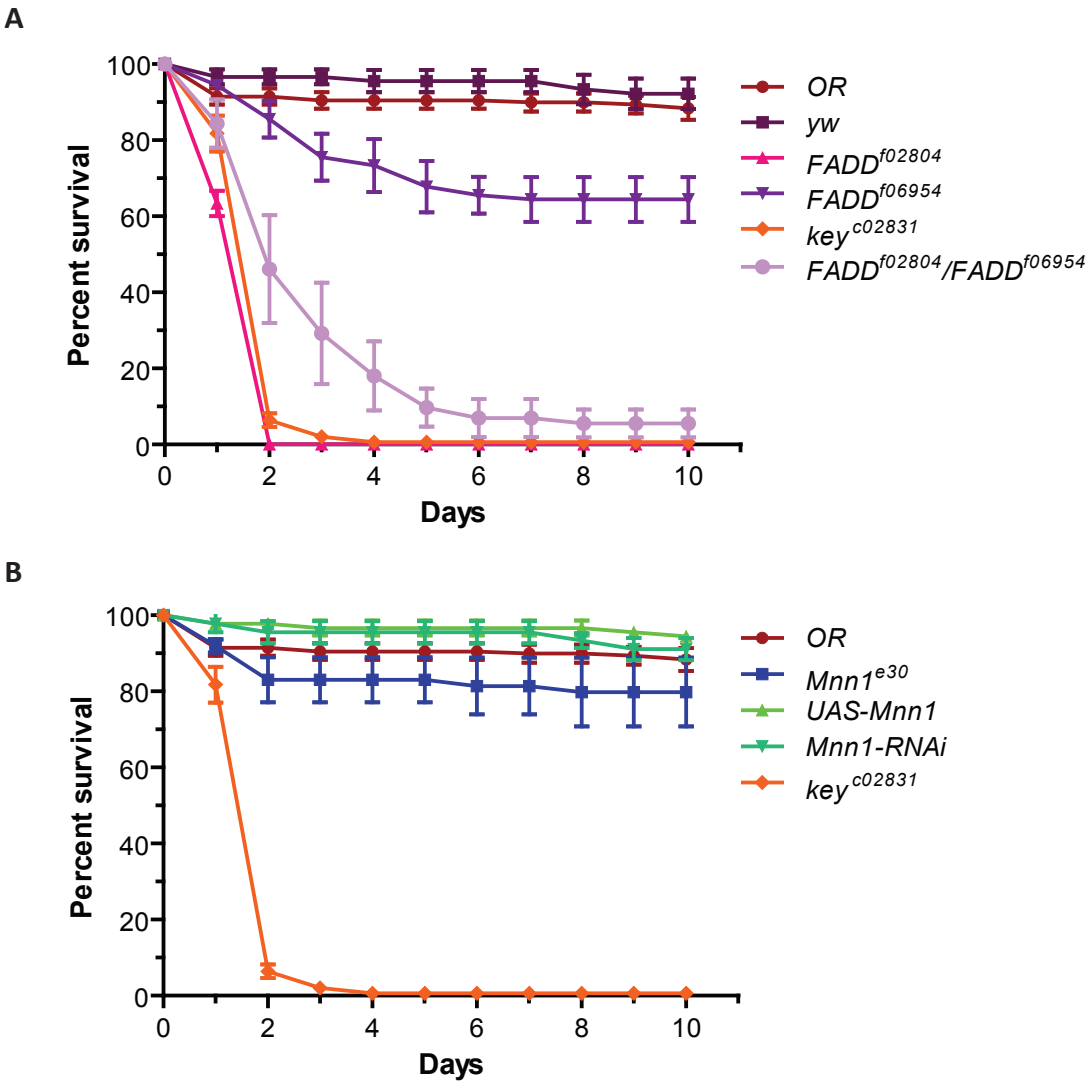

Figure 3.5. Survival of adult flies infected with *E. coli MG1655*.
Adult flies were infected using a needle dipped in a concentrated solution of *Escherichia coli MG1655* (OD_{600}=200) and survival was assessed over a 10 day period. For each genotype, 30 flies were infected per trial and a minimum of 3 separate trials were conducted. The average percent survival for all trials of the same genotype and the standard error of the mean are shown. A) Control genotypes (*OR* and *yw*) and Imd mutants ($FADD^{f02804}$, $FADD^{f06954}$, key^{c02831}) are graphed together. $FADD^{f02804}$ and key^{c02831} flies were highly susceptible to *E. coli* infection. $FADD^{f02804}/FADD^{f06954}$ heteroallelic flies were also susceptible. The $FADD^{f06954}$ allele appears to be a hypomorph. B) $Mnn1^{e30}$ mutants as well as flies overexpressing *Mnn1* (*UAS-Mnn1*) or down-regulating *Mnn1* through RNAi (*Mnn1-RNAi*) using the *tubulin-GAL4* driver have similar survival as the wild-type control (*OR*) and survive dramatically better than the Imd pathway mutant key^{c02381}. Note, not all genotypes that are graphed together were infected at the same time.

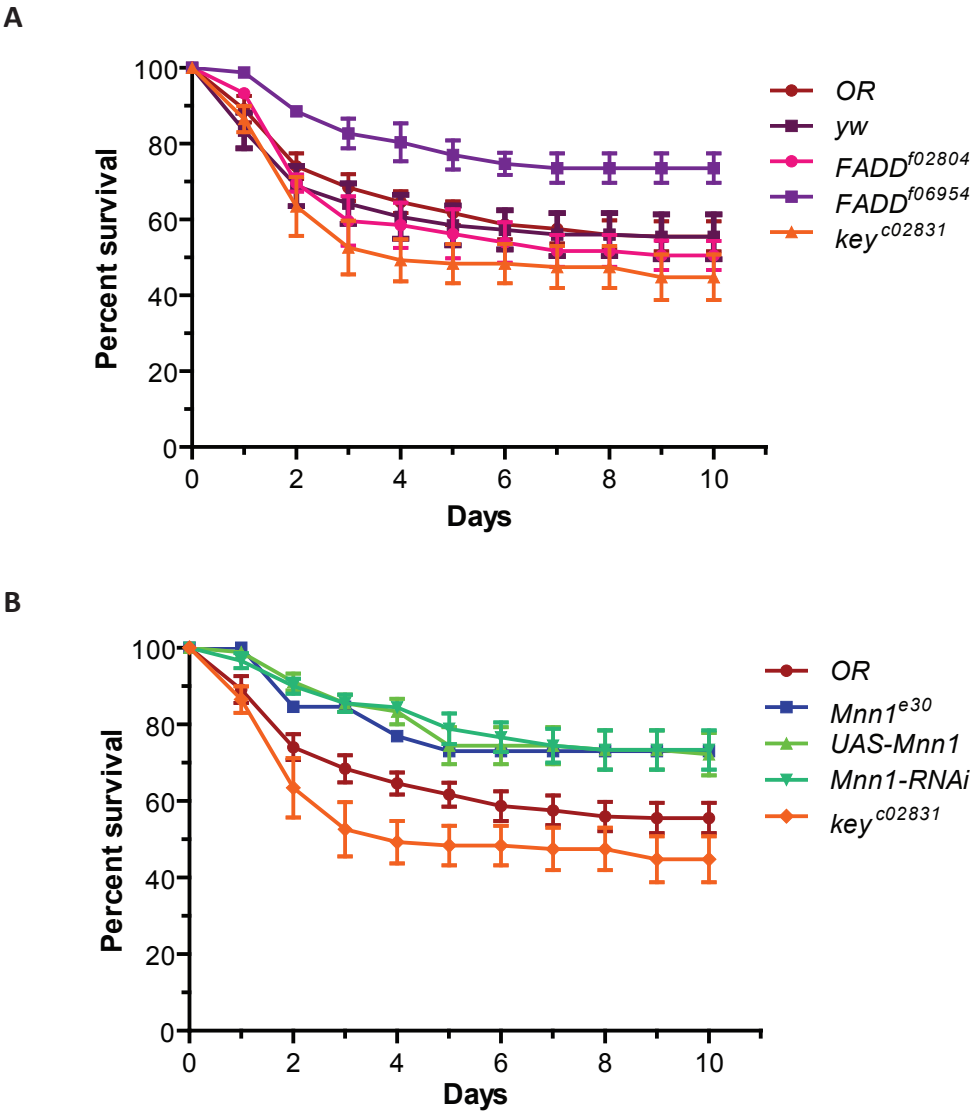

Figure 3.6. Survival of adult flies infected with *M. luteus*.
Adult flies were infected using a needle dipped in a concentrated solution of *Micrococcus luteus* (OD_{600}=50) and survival was assessed over a 10 day period. For each genotype, 30 flies were infected per trial and a minimum of 3 separate trials were conducted (except for $Mnn1^{e30}$, only 1 trial is shown since the other trials were with different ODs, see Appendix C, Figure C.1). The average percent survival for all trials of the same genotype and the standard error of the mean are shown. A) Control genotypes (*OR* and *yw*) and Imd mutants ($FADD^{f02804}$, $FADD^{f06954}$, key^{c02831}) are graphed together. All genotypes were moderately susceptible to *M. luteus* infection. B) $Mnn1^{e30}$ mutants as well as flies overexpressing *Mnn1* (*UAS-Mnn1*) or down-regulating *Mnn1* through RNAi (*Mnn1-RNAi*) using the *tubulin-GAL4* driver survived a bit better than the wild-type control (*OR*) and the Imd mutant key^{c02381}. Note, not all genotypes that are graphed together were infected at the same time.

Although the Imd mutants, *FADD*^{f02804} and *key*^{c02831}, were highly susceptible to Gram-negative infection, *Mnn1*^{e30} mutants were not (Figure 3.5B). In addition, overexpression of *Mnn1* (*UAS-Mnn1/+;tub-GAL4/+*) or down-regulation of *Mnn1* through RNAi (*Mnn1-RNAi/+; tub-GAL4/+*) did not alter survival following *E. coli* infection (Figure 3.5B). *Mnn1*^{e30}, *Mnn1-RNAi* and *UAS-Mnn1* flies all had similar survival as OR flies (no significant differences with log-rank tests, see Appendix C Table C.2). These genotypes all had between 80-90 % survival 10 days post-infection; this contrasts dramatically with the nearly complete lethality of *key*^{c02831} mutants 2 days after infection (Figure 3.5B). Overall, menin is not required for survival of *E. coli* infection and unlike dFADD, it is not an essential component of the Imd pathway.

Infection with the Gram-positive bacteria *M. luteus* resulted in more variable lethality than with the mock or *E. coli* infection. All genotypes tested were somewhat susceptible to *M. luteus* infection, especially at the higher concentrations initially tested (*i.e.* OD_{600}=200, OD_{600}=100, see Appendix C, Figure C.1). Using an OD_{600}=50, by 10 days post-infection, most genotypes had between 50 – 75 % survival (Figure 3.6). *FADD*^{f02804} and *key*^{c02831} survived *M. luteus* infection as well as *OR* and *yw* controls (Figure 3.6A). Surprisingly, *FADD*^{f06954} survived *M. luteus* infection significantly better than the other Imd mutants and controls (Figure 3.6A) (see Appendix C, Table C.3). *UAS-Mnn1* and *Mnn1-RNAi* flies survived *M. luteus* infection significantly better than *OR* and *key*^{c02831} (Figure 3.6B) (see Appendix C Table C.3).

Although no Toll mutants were available for testing in this assay, from the literature they have been shown to succumb to infection after only a few days (Rutschmann et al., 2002). The results from the *M. luteus* pricking assay showed that

menin is not required for survival against Gram-positive infection and is not an essential component of the Toll pathway. Since overexpression (*UAS-Mnn1*) and down-regulation of *Mnn1* (*Mnn1-RNAi*) both resulted in somewhat enhanced survival with *M. luteus* infection it is possible that there are other factors besides menin levels that could be contributing to infection survival. Even with an OD_{600}=50 there was still a much higher lethality associated with *M. luteus* infection compared to *E. coli* infection for wild-type flies (Figures 3.6A versus 3.5A). The lethality observed with this strain of *M. luteus* is higher than that reported in previous infection assays (Rutschmann et al., 2002).

2.3 Natural infection of Ecc15 does not induce larval lethality

As *Mnn1* mutants survived the bacterial infection induced through pricking as well as controls, it was concluded that menin is not required for survival following Gram-negative or Gram-positive infection. Natural infection, induced through ingestion of bacteria, generally does not trigger a systemic immune response; however, *Erwinia carotovora carotovora* strain 15 (*Ecc15*) was isolated as a strain that is capable of inducing an immune response through oral infection, which is characterized by the production of AMPs (Basset et al., 2000). Natural infection of larvae with *Ecc15* does not result in significant lethality (Basset et al., 2000), but has been shown to induce expression of stress response genes such as *hsp70* (Buchon et al., 2009). Due to the observed increase in *hsp70* expression following natural infection of wild-type bacteria with *Ecc15*, it was proposed that because *Mnn1* mutants had defects in *hsp70* expression with heat shock (Papaconstantinou et al., 2005) perhaps they would also have defects in *hsp70* expression following natural infection. Natural infection of *OR*, key^{c02831} and $Mnn1^{e173}$ third instar larvae with *Ecc15* was well tolerated by all genotypes

with no significant differences in survival observed (data not shown). This was not surprising given that Imd mutants (*Rel*^{E20}, *Dredd*^{B118}, *PGRP-LC*^{E12}), which are susceptible to Gram-negative infection through injection, were not susceptible to *Ecc15* infection through ingestion (Ha et al., 2005).

2.4 Natural infection of Ecc15 does not induce noticeable HSP70 protein expression

Wild-type larvae were examined to see if expression of HSP70 was induced after natural infection with *Ecc15*, as observed by Buchon *et al.* (2009) who reported a 7-fold increase in *hsp70* transcript level in the guts 4 hrs after *Ecc15* oral infection (Buchon et al., 2009). Immunoblot analysis of lysates taken from whole larvae after feeding for 2 hours on *Ecc15* mixed in yeast paste did not reveal any significant induction of HSP70 protein after *Ecc15* ingestion (Figure 3.7A). In fact, there was a low level of HSP70 expression in all control and *Ecc15* samples. This was not observed in untreated larvae, so it was speculated that the yeast itself could be inducing low levels of HSP70 expression. Second instar larvae also seemed to have slightly higher HSP70 protein levels compared to third instar larvae (Figure 3.7A). A similar experiment was conducted; however, instead of using yeast paste, crushed standard fly food was mixed with *Ecc15*-GFP at OD_{600}=200. Comparable results were obtained in immunoblots of lysates from whole larvae and no noticeable induction of HSP70 was observed for *Ecc15* infection. There was similar HSP70 expression for all second instar larvae samples (Figure 3.7B).

Adult male flies (2-3 d) were also examined for HSP70 expression after oral infection with *Ecc15,* as Buchon *et al.* (2009) used adults in their microarray analysis where the increased *hsp70* mRNA expression was detected. For this experiment, filter paper was soaked with a 1:1 mixture of 5 % sucrose and *Ecc15*-GFP OD_{600}=200, or 5 %

sucrose alone was used for controls. Lysates were prepared from whole flies and western blots did not show any HSP70 expression after *Ecc15* infection (Figure 3.7C). Therefore, at the protein level, no increase in HSP70 expression was observed following natural infection of *Ecc15* for either larvae or adults at the time points tested (2 or 4 hrs after infection). The microarray results showing increased *hsp70* transcript with *Ecc15* ingestion (Buchon et al., 2009) could not be reproduced in our system at the protein level, perhaps due to the fact that we were examining whole fly lysates and not just gut tissue.

2.5 E. coli or M. luteus infection do not induce HSP70 expression

Oral infection of larvae and adults with *Ecc15-GFP* did not result in an observable induction of HSP70 protein in lysates from whole organisms (Figure 3.7). The effect of *E. coli MG1655* or *M. luteus* infection of male adults on HSP70 expression was also examined 6 hrs post-infection through the pricking method used for infection survival assays. Lysates were prepared from OR and $Mnn1^{e30}$ males (3-5 d) that were left untreated or infected with ddH_2O (mock infection), *E. coli* or *M. luteus*. Six hours after infection there was only slight induction of HSP70 expression in infected OR and $Mnn1^{e30}$ males. No noticeable differences were observed between genotypes or between infection types (Figure 3.8). $Mnn1^{e173}$ and key^{c02831} flies were also examined and similar results were obtained (data not shown). Overall, only minimal HSP70 protein expression was observed following mock or bacterial infection, and $Mnn1^{e30}$ mutants did not have any obvious defects in HSP70 expression following infection. If anything, $Mnn1^{e30}$ flies had higher baseline levels of HSP70 (Figure 3.8). No additional work was done to examine HSP70 expression following infection since results did not seem promising.

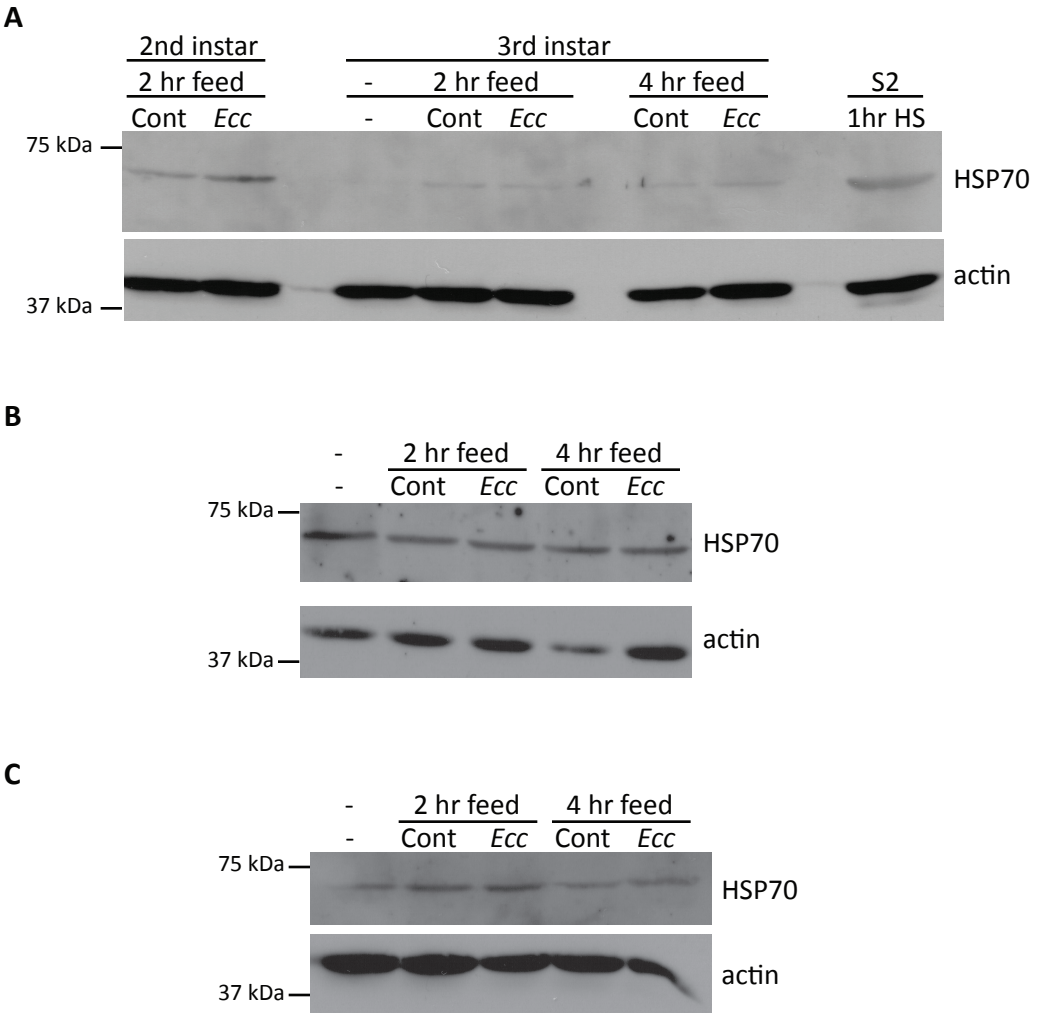

Figure 3.7. HSP70 induction in OR larvae or adults after natural infection with *Ecc15-GFP*. Larvae or adult *OR* were examined for HSP70 expression after natural infection of *Erwinia carotovora carotovora strain 15 (Ecc15-GFP)* through feeding after a 2 hr starvation period. Lysate from S2 cells exposed to a 1 hr HS is shown in A as a positive control for HSP70 expression. A) Lysates from 2nd or 3rd instar larvae that were left untreated (-), fed a control of yeast paste (Cont) or fed 1:1 *Ecc15-GFP*:yeast paste (*Ecc*) for 2 hr or 4 hr after a 2 hr starvation. B) Lysates from 2nd instar larvae that were left untreated (-), fed a control of 1:1 crushed fly food:LB media (Cont) or fed 1:1 *Ecc15-GFP*: crushed fly food (*Ecc*) for 2 hr or 4 hr after a 2 hr starvation. C) Lysates from 2-3 d adult males left untreated (-), fed a control of 5 % sucrose soaked on filter paper (Cont) or 1:1 *Ecc15-GFP*:5 % sucrose (*Ecc*) for 2 hr or 4 hr after a 2 hr starvation. Overall, there was not a significant induction of HSP70 expression following natural infection with *Ecc15-GFP* in larvae or adults. Actin is shown as a loading control.

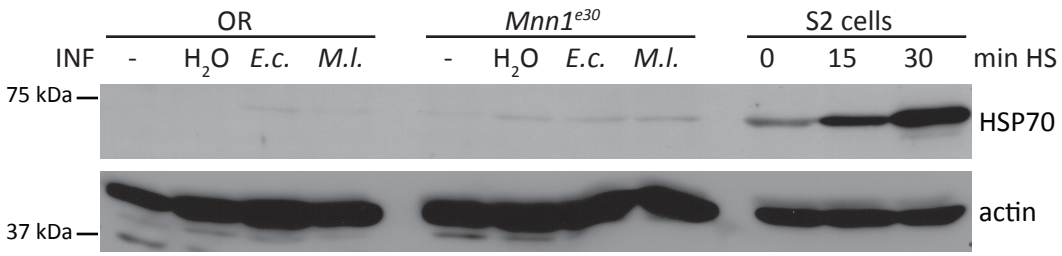

Figure 3.8 HSP70 expression after infection through the pricking method.
OR and *Mnn1*^{e30} adult males were left untreated (-), were mock infected with ddH_2O (H_2O) or were infected with *E. coli MG1655* OD_{600}=200 *(E.c.)* or *M. luteus* OD_{600}=50 *(M.l.)*. Lysates were prepared 6 hrs after infection. S2 cells that were left untreated (0 min) or exposed to 15 min or 30 min HS at 37°C are shown to compare HSP70 induction. Very low levels of HSP70 were detected with mock, *E.coli* or *M. luteus* infection. *Mnn1*^{e30} mutants had similar HSP70 levels, if not higher levels, than *OR* controls. Actin is shown as a loading control.

3. dFADD mutants are not sensitive to heat stress

Due to the role of menin in the regulation of HSP70 expression and heat shock (HS) survival (Papaconstantinou et al., 2005), *dFADD* mutants were tested for heat shock survival to see if they had a phenotype similar to that of *Mnn1* mutants which could suggest a novel role for dFADD in the regulation of the heat stress response. $FADD^{f02804}$ and $FADD^{f06954}$ embryos were exposed to a 1 hr acute heat stress at 3-5 hr AEL. Relative lethality of homozygous mutants compared to heterozygous sibling controls from the same cross was determined for embryos exposed to heat shock and for untreated controls (Figure 3.9A). There was no difference in relative lethality for standard and HS conditions for either $FADD^{f02804}$ (p=0.5304, Student's t-test) or $FADD^{f06954}$ (p=0.5734). This suggests that FADD is not required for heat shock survival.

$Mnn1^{-/-};FADD^{-/-}$ double mutants were created and under standard conditions there was approximately 20 % lethality for both $Mnn1^{e30};FADD^{f02804}$ and $Mnn1^{e30};FADD^{f06954}$ (Figure 3.9B); this is similar to the lethality observed for *dFADD* mutants alone (Figure 3.9A). $FADD^{f02804}$, $Mnn1^{e30}$ and $Mnn1^{e30};FADD^{f02804}$ mutants were compared under standard conditions (*i.e.* No HS) and with a 1 hr HS at 3-5 hr AEL (Note, this experiment was completed by Maria Papaconstantinou when I was working in Dr. Mazo's lab). The average relative percent lethality compared to heterozygous sibling controls for three trials is reported in Figure 3.9C. $Mnn1^{e30}$ embryos had a high relative lethality with an acute HS whereas $FADD^{f02804}$ embryos had no increased lethality with HS compared to standard conditions. $Mnn1^{e30};FADD^{f02804}$ embryos had a No HS lethality similar to that of $FADD^{f020804}$ mutants while the HS lethality was similar to that of $Mnn1^{e30}$ (Figure 3.9C). There was not a statistically significant difference with a one-way

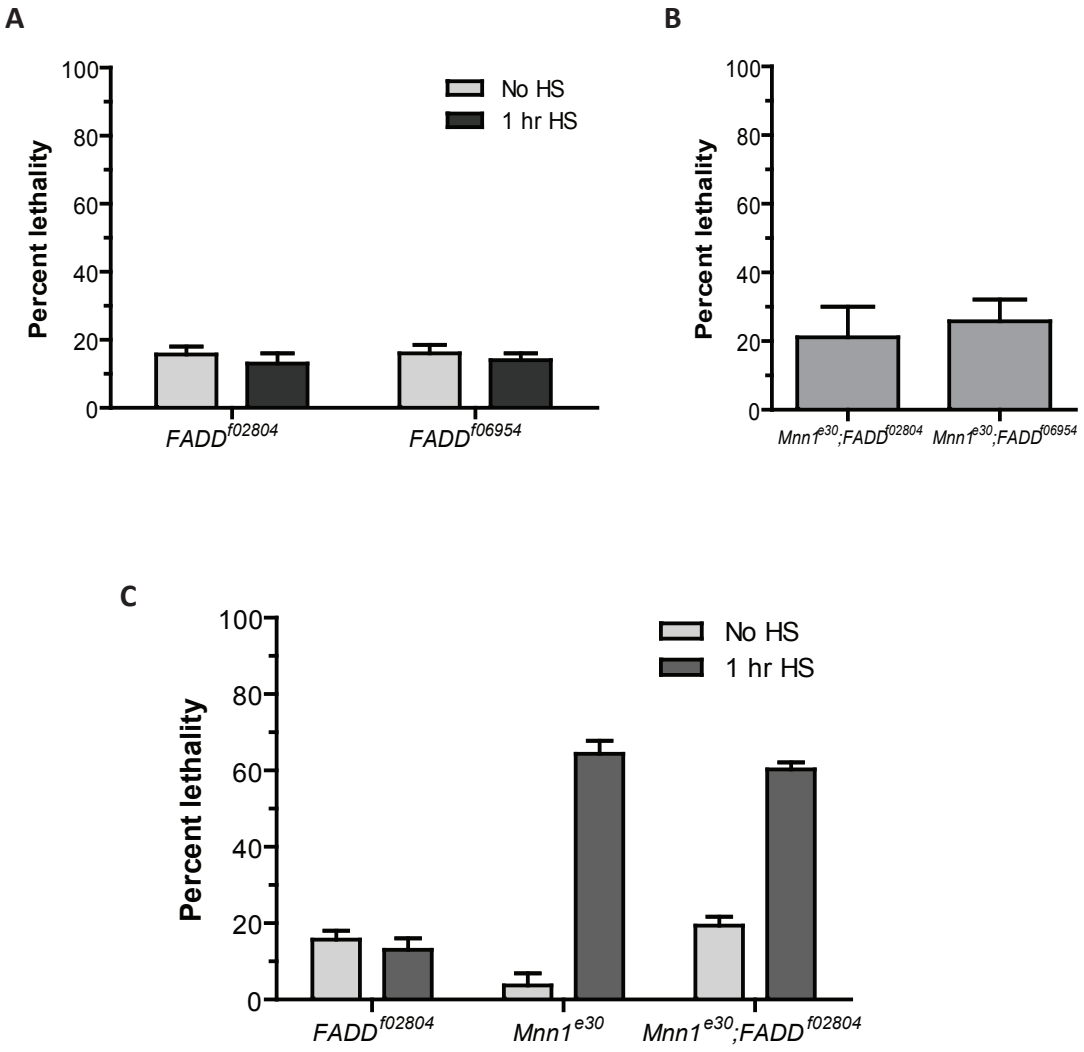

Figure 3.9. *dFADD* mutants do not have a HS lethality phenotype.
A) *FADD*^{f02804} and *FADD*^{f06954} embryos were exposed to a 1 hr HS 3-5 hrs after egg laying (AEL) or left untreated (No HS) and left to develop to eclosion. Average relative lethality of homozygous mutants compared to heterozygous sibling controls was calculated for three trials. No increase in lethality was observed when embryos were exposed to a 1 hr HS. B) *Mnn1*^{e30}*;FADD*^{f02804} or *Mnn1*^{e30}*; FADD*^{f06954} double mutants do not show significant relative lethality under standard conditions. C) *FADD*^{f02804} mutants do not have increased lethality with a 1 hr HS. *Mnn1*^{e30} mutants show increased in relative HS lethality compared to heterozygous sibling controls with a 1 hr HS 3-5 hr AEL compared to untreated controls (No HS). *Mnn1*^{e30}*;FADD*^{f02804} double mutants have a similar phenotype as *Mnn1*^{e30} with an acute HS.

ANOVA followed by Bonferroni's post-hoc tests for either of these comparisons. This suggests that the additional loss of *dFADD* in a *Mnn1*-null background had no additive effect on HS lethality. The overall conclusions are that *dFADD* mutants do not have a heat shock sensitivity phenotype and loss of *dFADD* in a *Mnn1*-null background has no additional influence on heat shock lethality.

4. Summary of menin-dFADD interaction studies

In summary, menin and dFADD proteins were shown to interact when both *Drosophila* proteins were overexpressed in 293T cells. In addition, endogenous menin from *Drosophila* S2 cells was shown to interact with overexpressed HA-dFADD. Confirmation of an interaction with both endogenous proteins and establishment of an interaction in flies were hindered by lack of a suitable antibody for dFADD detection. Additional work is required in this area. Investigation of a potential role for menin in *Drosophila* immune response showed that menin is not required for survival of Gram-negative or Gram-positive infection. Thus, there was no support for the hypothesis that the menin-dFADD interaction was important for the *Drosophila* immune response. The alternative hypothesis, that dFADD was required for the heat shock response was also not supported by experimental evidence since *dFADD* mutants did not have any lethality with an acute heat shock. Research into the expression of HSP70 following natural infection with *Ecc15*, or infection with *E. coli* or *M. luteus* using the pricking method, was also not fruitful. Despite significant investment of time and resources, the functional significance of the putative menin-dFADD interaction in *Drosophila* remains unknown.

DISCUSSION

1. Confirmation of the Menin and dFADD interaction

Drosophila FADD and menin proteins interact when both are expressed in 293T cells (Figure 3.2). Furthermore, endogenous menin and HA-tagged dFADD interact in S2 cells (Figure 3.3). It remains to be established if both endogenous proteins interact under standard cellular conditions and if menin and dFADD interact in fly lysates. When dFADD was first characterized and the interaction between dFADD and Dredd was demonstrated, this work was done using overexpressed proteins in HeLa or 293 cells (Hu and Yang, 2000). These authors suggested that the interaction between these proteins resulted in their mutual stabilization since GFP-dFADD co-transfected with untagged Dredd resulted in more prominent fluorescence in HeLa cells than GFP-dFADD alone and vice versa (Hu and Yang, 2000). Interestingly, a more prominent dFADD band was detected in immunoprecipitations with the anti-HA antibody when dFADD-HA or HA-dFADD were co-transfected with *Drosophila* menin in 293T cells than when either dFADD construct was transfected alone (Figure 3.2C). This could suggest that the interaction with menin contributes to dFADD protein stabilization.

Progress with studying the menin-dFADD interaction was severely hindered by lack of a suitable antibody for dFADD detection. Commercial antibodies generated against human FADD did not detect the *Drosophila* protein. Moreover, peptide antibodies raised against a *Drosophila* dFADD peptide, produced by New England Peptide (F3620, F3621), failed to detect endogenous or HA-tagged dFADD from S2 cell lysates (data not shown). Finally, I cloned full-length dFADD into a His-vector for purification and injection into rabbits to generate polyclonal antibodies (9678 and 9679

antibodies). The dFADD polyclonal antibodies were able to detect dFADD from S2 cells lysates but not from lysates from OR embryos or adults (Appendix A, Figure A.1). These antibodies were also tested in a single co-immunoprecipitation experiment; however, I failed to detect dFADD in menin immunoprecipitates and vice versa (Appendix A, Figure A.1C). Thus, there is still not a suitable antibody for studying the interaction in fly lysates. Recently, new chemiluminescent detection reagents, Luminata Crescendo and Forte (WBLUR0500, WBLUF0500, Millipore), have been used in the lab and have proven useful for detection of proteins that are expressed at low levels and could be helpful for these co-immunoprecipitation experiments and perhaps even for detection of dFADD in fly lysates, where the amount of protein in total organism lysates could be quite low.

It is possible that the interaction between menin and dFADD might not occur under standard cell culture conditions. It could be highly regulated by external factors or conditions, or it could occur only transiently under specific conditions and therefore would be difficult to detect between endogenous proteins, despite being observed in unstimulated cells when dFADD was overexpressed. Even though an interaction between endogenous proteins is the most convincing evidence for the authenticity of an interaction it is not always feasible to observe such interactions. In this regard, it is important to acknowledge that most of the cell-based analyses of the interactions between dFADD and other components of the Imd pathway were done in conditions where tagged proteins were overexpressed (see Introduction, Section 2.1).

Additional evidence suggests that the menin-dFADD interaction may represent an important and conserved interaction. Since studies of FADD's interaction with menin began due to the yeast two-hybrid results where human FADD mistakenly contaminated

the screen and was found to interact with *Drosophila* menin, we decided to also investigate this interaction in human cells to see if it was conserved (most of this work was completed by Jennifer Law, a former undergraduate thesis student in the Bédard lab). In HeLa cells grown under standard culture conditions, a faint menin band was observed in an immunoprecipitation with α-FADD; however, this result was not reproducible therefore various treatments were tested (Law, 2008). Since peptidoglycans activate dFADD through the Imd pathway in *Drosophila*, or can activate apoptosis through FADD via TLR2 signalling in mammalian cells (Aliprantis et al., 2000; Kaneko et al., 2004), we investigated if the FADD-menin interaction in HeLa cells could be observed with PGN treatment. Following treated of HeLa cells with PGN from *M. luteus* (Fluka, 53243), menin was found to co-immunoprecipitate with FADD. This result was reproducible; however, there was some discrepancy in the length of treatment required to observe the interaction (Law, 2008). The Toll-like receptor 2 (TLR2) is key to Gram-positive PGN recognition in mammalian cells and can initiate an innate immune response or can recruit FADD through MyD88 to activate apoptosis (Akira et al., 2006). From these preliminary results it was speculated that stimulation of the TLR2 pathway might lead to the interaction of FADD with menin.

2. Menin is not required for the Drosophila immune response

In an attempt to determine the functional significance of the menin-dFADD interaction, *Mnn1* mutants were tested for their ability to survive bacterial infection. This was investigated due to the well established role of dFADD in the Imd pathway which is required for Gram-negative resistance (see Introduction, Section 2.1). Control infections with sterile ddH_2O established that there was not significant lethality associated with

physical injury induced by pricking with a needle or due to acquired secondary infections after wounding (Figure 3.4). *Mnn1*^{e30} adults survived *E. coli MG1655* infection as well as control flies (*yw* or *OR*), while Imd mutants (*FADD*^{f02804} and *key*^{c02831}) were highly susceptible to Gram-negative infection, with all flies perishing by 3 days post-infection (Figure 3.5). Since the Imd mutants behaved as expected and previously described (Naitza et al., 2002; Rutschmann et al., 2000b) this demonstrated that the pricking assay was successful, and the lack of phenotype observed for *Mnn1* mutants was not due to unsuccessful bacterial infection.

Mnn1^{e30} mutants had similar *M. luteus* infection survival as controls. It appeared as though *Mnn1*^{e30} flies might survive infection slightly better than *OR* and *key*^{c02831} flies (Figure 3.6); however, this was not statistically significant, most likely due to the small sample size for *Mnn1*^{e30} with *M. luteus* infection at an OD_{600}=50. The idea that *Mnn1* mutants could survive infection better than controls was intriguing as it would suggest that menin could be a negative regulator of the immune response. In order to test this, flies overexpressing (*UAS-Mnn1*) and down-regulating (*Mnn1-RNAi*) menin were compared. Both these lines were found to survive *M. luteus* infection better than *OR* and *key*^{c02831} controls, suggesting that it was not differences in menin levels that were contributing to the increased survival, but that other factors were at play (Figure 3.6B).

In retrospect, a few criticisms regarding the infection experiments should be made. First of all, the different genotypes tested were not all in the same genetic background. Differences observed between genotypes could have been due not only to the specific alleles being tested but also due to unidentified background mutations or modifications. That being said, since the difference between susceptible and resistant

flies was quite dramatic (*e.g.* compare *FADD*^{f02804} to *OR* in *E. coli* infection, Figure 3.5), differences in genetic background probably did not affect any conclusions that were drawn. In addition, *OR* and *yw* controls were both tested to ensure that differences in genetic background did not have a noticeable effect on infection survival and these lines both behaved similarly for all infection types (Figures 3.4-3.6). However, it is possible that the slightly increased survival of the *Mnn1-RNAi* and *UAS-Mnn1* flies compared to controls could be the result of background effects.

Another criticism is that a Toll pathway mutant should have been obtained for a control for Gram-positive infection survival. For example, *Dif*^{1} or *seml* (PGRP-SA gene) would have been good candidates since they are homozygous viable, unlike most other Toll pathway mutants (Michel et al., 2001; Rutschmann et al., 2000a). In addition, only a single type of Gram-negative and Gram-positive bacteria was tested in the infection assays and fungal infection was not tested. *E. coli* and *M. luteus* were chosen as activators of the Imd and Toll pathway, respectively, due to their prolific use in the innate immune studies used to identify the key components of the signalling pathways. Since results with *E. coli* and *M. luteus* did not provide any indication that menin was functioning in the *Drosophila* immune response it did not seem necessary to test survival following infection with other types of bacteria or fungi.

Overall, results from infection assay studies indicated that menin is not required in either the Imd or the Toll pathway as *Mnn1* mutants were not more susceptible to infection than wild-type controls. Since all essential components of the immune response pathways have been characterized as having increased susceptibility to infection, this provides evidence that menin function is not essential for either immune

response. Although it does not seem likely, these results do not completely rule out the possibility that menin could interact with dFADD in order to somehow modulate the response, such as efficiency or duration, without being essential for survival. It seems more reasonable to predict that the functional significance of the menin-dFADD interaction lies outside the known role for dFADD in the immune response (see Chapter 7 for more details).

3. dFADD is not required for heat shock survival

Since *Mnn1* mutants did not show a similar *E. coli* sensitivity as *dFADD* mutants, the next logical step was to determine if *dFADD* mutants had a similar heat shock sensitivity phenotype as *Mnn1* mutants. $dFADD^{f02804}$ and $dFADD^{f06954}$ embryos had minimal lethality with an acute 1 hr heat shock (HS) compared to heterozygous sibling controls from the same cross, with about 15 % lethality observed for both mutants under standard and heat shock conditions (Figure 3.9A). In contrast $Mnn1^{e30}$ and $Mnn1^{e173}$ flies were shown to have about 60 % relative lethality following a 1 hr HS at 3-5 hr AEL (Papaconstantinou et al., 2005). This suggested that *dFADD* was not required for survival following acute heat shock. When the $Mnn1^{e30}$;$FADD^{f02804}$ double mutant was tested with a 1 hr acute HS, the relative survival was comparable to that of $Mnn1^{e30}$ and the additional loss of *dFADD* did not contribute to increased heat shock lethality (Figure 3.9C). Therefore, dFADD is not required for the heat shock response and the menin-dFADD interaction is likely not important for the heat stress response.

4. Future Directions

4.1 Establish interaction in Drosophila embryos/larvae

As previously mentioned, work on the menin-dFADD interaction was limited by the unavailability of a suitable antibody for detection and immunoprecipitation of dFADD in *Drosophila*. After no obvious functional significance could be assigned to the menin-dFADD interaction, this research came to a halt and emphasis was placed on the menin-Trx interaction studies (see Chapter 4). Future work on the menin-dFADD project first requires validation of this interaction in fly lysates. As this interaction may be tissue type specific it might not be detectable in whole organism samples. It might be necessary to dissect tissues, such as the fat body or guts, for co-immunoprecipitation experiments in order to confirm the interaction and to ensure that it was not an artefact of overexpression in S2 or 293T cells (Figures 3.2 and 3.3). As previously mentioned, it is possible that the menin-dFADD interaction could be regulated and therefore not detected under standard developmental conditions. Thus, exposing flies to different stimuli or stresses may be required before an interaction can be established. For example, it could be of interest to investigate the interaction following treatment with DNA damaging agents, UV or γ-IR. In mammalian cells, FADD was shown to interact with the DNA mismatch repair protein MBD4 in the nucleus which suggested a potential link between the genome surveillance function of MBD4 and the apoptosis-inducing function of FADD (Screaton et al., 2003).

Assuming that the interaction can be demonstrated in fly lysates, it will then be important to map the domains of interaction for each protein. To this end, constructs for the expression of GST-tagged dFADD domains (DD, DED and central domain) have

already been generated (data not shown). These could be used in *in vitro* pull-down assays with recombinant menin protein in order to determine which domain of dFADD interacted directly with menin. Similarly, different tagged menin peptides could be generated to map the domain of interaction with dFADD.

4.2 Study the role of the menin-FADD interaction in genome surveillance and apoptosis

I had planned to investigate the role of dFADD in the maintenance of genome stability since menin was shown to be important for this function when flies were exposed to chronic heat stress (Papaconstantinou et al., 2010). This could be investigated using the loss of heterozygosity (LOH) assay based on the *multiple wing hair* (*mwh*) locus that was used for *Mnn1* mutants (Papaconstantinou et al., 2010) (see also Chapter 2, Section 14). Examining the potential role of dFADD in the maintenance of genome stability could be promising, especially in light of the interaction observed between mammalian FADD and MBD4 (Screaton et al., 2003). Since MBD4 is involved in DNA repair through removal of GT mismatches, the discovery of this interaction evoked the idea that it could provide a link between genome surveillance and apoptosis (Screaton et al., 2003). Moreover, in mammalian cells, menin has been shown to interact with proteins involved in DNA repair, such as FANCD2 and RPA2 (Jin et al., 2003; Sukhodolets et al., 2003) and also plays a role in apoptosis (see Chapter 1, Sections 7.3 and 9.3). Therefore, an interaction between menin and dFADD could be important for recruiting other proteins needed for DNA repair; although, interactions with *Drosophila* menin or dFADD with DNA repair proteins have not been established.

Another possibility is that since menin is involved in the maintenance of genome integrity and FADD is involved in apoptosis, the menin-dFADD interaction could be

important for inducing apoptosis under conditions of extensive DNA damage so that mutations or chromosomal aberrations are not propagated. However, the role of dFADD in apoptosis has not been well studied in *Drosophila*. Although dFADD has not been shown to function in an extrinsic apoptotic cascade, similar to its primary function in mammalian cells, this does not rule out the possibility that dFADD and Dredd could somehow be involved in an intrinsic apoptotic signalling pathway in *Drosophila*, such as in response to extensive DNA damage. Dredd was found to be necessary for apoptosis induced through Reaper, Grim or Hid expression, showing that Dredd is an important effector of apoptosis in *Drosophila* (Chen et al., 1998). There is also preliminary evidence to suggest that menin may regulate apoptosis in *Drosophila*, at least in response to heat stress in embryos (Papaconstantinou et al., 2005). Thus, it will be interesting to investigate a potential role for dFADD in the maintenance of genomic stability and future studies could then evaluate whether the menin-dFADD interaction is important for DNA repair or apoptosis following DNA damage. Such studies could shed light on a novel function for dFADD in the nucleus and provide important links between genome surveillance and apoptosis. This idea will be revisited in the final discussion (Chapter 7).

5. Conclusions

Despite considerable work being done on this project, very few substantial results have been obtained to date. All that has been established is that the *Drosophila* menin and FADD proteins interact when overexpressed in 293T cells and HA-tagged dFADD interacts with endogenous menin in S2 cells. Investigation of the potential functional significance of this interaction yielded only negative results and provided no support for

the initial hypotheses. In summary, menin is not required for survival following Gram-negative or Gram-positive infection and therefore is not an essential component of the Imd or Toll immune pathways and dFADD is not essential for heat shock survival.

A pessimistic view for the lack of significant results is that the observed menin-dFADD interaction is actually an artefact due to protein overexpression. This would not be entirely surprising given the fact that the interaction was identified in a yeast two-hybrid screen with what turned out to be contaminating human FADD protein. The optimistic view for this project is that improved reagents (antibodies) and optimization of techniques (for co-immunoprecipitation and protein detection) may be able to confirm the interaction between endogenous proteins and also in fly lysates. Perhaps, the significance of the interaction, which has been elusive so far, can be uncovered by researching the roles of dFADD and menin in processes such as genome surveillance, DNA repair and apoptosis.

CHAPTER 4. MENIN INTERACTS WITH TRITHORAX

INTRODUCTION

In order to study menin function in *Drosophila*, in addition to trying to identify novel interacting proteins, such as dFADD (see Chapter 3), we also investigated if some of the menin interactions identified in mammalian cells represented conserved interactions that were also important in *Drosophila*. One of the best studied, and clinically most significant, of menin's protein-protein interactions is that with mixed lineage leukemia (MLL1), due to the importance of this interaction in development of acute leukemia associated with *MLL1* chromosomal translocations (reviewed in Thiel et al., 2012). We therefore wanted to know if this interaction was conserved and if *Drosophila* menin and the MLL1 homologue Trithorax (Trx) also interact. Conservation of this interaction from *Drosophila* to humans could suggest that this interaction is especially important for menin function and could perhaps shed light on the role of menin in tumourigenesis. In this introduction, the discovery of *MLL1* and a summary of its protein structure and important functional and interaction domains will be provided. The menin-MLL interaction will only be briefly summarized (see Chapter 1, Section 8 for more details) before reviewing Trithorax function in *Drosophila*.

1. Mixed Lineage Leukemia

1.1 MLL1 discovery

Human acute leukemias, including both childhood and adult forms, are frequently associated with chromosomal translocations involving 11q23 and one of several possible chromosomes (*e.g.* 1, 4, 6, 9, 10, 19). Analysis of 11q23 led to the identification of the

MLL1 gene (previously called *ALL1* (*acute lymphoid leukemia*) or *HRX* (*homologue of trithorax*)) at this locus. Characterization of the gene and its protein product showed that *MLL1* is a homologue of *Drosophila trithorax* (see Section 4 below for details) (Gu et al., 1992; Tkachuk et al., 1992). The *MLL1* gene is 89 kb long and consists of 37 exons (reviewed in Krivtsov and Armstrong, 2007). Initial characterization revealed that MLL (note, MLL1 will most often be referred to as just MLL unless distinguishing with MLL2, another Trx homologue) and Trx share three important regions of homology – the C-terminal 220 amino acids are 82 % similar and 61 % identical (later named the SET domain) and two cysteine-rich regions that are homologous to zinc finger domains (later called PHD 1-3 and PHD4, see Section 2.1 below). The presence of zinc finger-like domains predicted that MLL would be able to bind DNA and might act as a transcription factor (Gu et al., 1992; Tkachuk et al., 1992).

1.2 MLL1 translocations and fusion proteins

MLL1 translocations occur frequently in acute infant and adult leukemias including acute lymphoblastic leukemia (ALL), acute myelogenous leukemia (AML) or biphenotypic/ mixed lineage leukemia (MLL) and such translocations are associated with a poor prognosis (reviewed in Krivtsov and Armstrong, 2007). Translocations involving 11q23 result in the formation of fusion proteins that contain roughly the first 1300 amino acids of MLL in-frame with the C-terminus of another protein. More than 50 different fusion partners have been identified so far, with these fusion partners being quite variable in structure and function. Five translocations account for about 80 % of all MLL-associated leukemias – MLL-AF4 t(4:11), MLL-AF9 t(9:11), MLL-ENL t(11:19), MLL-AF10 t(10:11), MLL-AF6 t(6:11) (Krivtsov and Armstrong, 2007). *MLL1* translocations are present in

about 70 % of infant leukemias but are less frequent in adult leukemias, compromising about 10 % of cases (reviewed in Krivtsov and Armstrong, 2007).

Of the identified fusion partners, the most commonly occurring are nuclear proteins (*e.g.* AF4, AF9, AF10, ENL, ELL) with most of them being putative DNA-binding proteins and some containing transactivation domains (*e.g.* AF4, AF9, ENL) (reviewed in Krivtsov and Armstrong, 2007). These MLL-fusions likely function by recruiting other proteins/complexes important for transcription. In fact, AF4 and ENL were shown to form a complex with P-TEFb (positive transcription elongation factor b, composed of CDK9, and cyclin T1/2); this so called AEP (AF4, ENL, P-TEFb) interacts with wild-type MLL and is recruited to normal MLL targets for transcription. The MLL-AF4 and MLL-ENL fusions result in constitutively active MLL/AEP complexes (Yokoyama et al., 2010). Other fusion proteins are cytoplasmic proteins (*e.g.* AF6, GAS7, EEN, AF1p) which contain oligomerization domains that are important for leukemogenesis (Krivtsov and Armstrong, 2007).

How these variable MLL fusion proteins contribute to leukemogenesis became a topic of keen interest and is still not fully understood. Since the MLL fusion proteins lack the C-terminal SET domain, they lack their enzymatic histone methyltransferase (HMT) activity (see Section 1.4) and how they function to regulate gene expression has been a point of confusion and debate. Interestingly, several fusion partners (*e.g.* MLL-AF9, MLL-AF10) have been shown to interact with DOT1L (disruptor of telomeric silencing 1-like), a histone methyltransferase specific for H3K79, which is an epigenetic mark associated with actively transcribed genes (Nguyen et al., 2011; Okada et al., 2005). MLL-AF10 or artificially generated MLL-DOT1L fusions result in transformation in a DOT1L-dependent

manner that is associated with increased *Hoxa9* expression and H3K79 methylation at this locus (Okada et al., 2005). The interaction with DOT1L is necessary for both the initiation and maintenance of MLL-AF9 induced leukemia (Nguyen et al., 2011). Therefore, regardless of the translocation, an interaction of the MLL fusion protein with other positive regulators of transcription seems to be crucial for the altered gene expression associated with leukemogenesis.

1.3 MLL1 and Hox gene regulation in normal development and leukemogenesis

After the discovery that the *MLL1* gene was involved in chromosomal translocations that contribute to leukemogenesis, studying the normal function of MLL became an important focus. Since MLL1 was found to be a structural homologue of Trx, which was known to be important for the maintenance of *homeotic* gene expression and segment identity in *Drosophila*, it was predicted that MLL1 might also regulate *Homeobox* (*Hox*) gene expression and segment identity in mammals. *In situ* hybridization of embryonic mice at day 7 revealed that *Mll1* expression is widespread and this expression persists until adulthood (Yu et al., 1995). The strongest *Mll1* expression was observed in the nervous system and developing somites of embryonic mice.

Mll1$^{-/-}$ mice are embryonic lethal, similar to *Drosophila trx*$^{-/-}$ mutants, with lethality occurring around embryonic day 10.5 (E10.5) (Yu et al., 1995). Heterozygous *Mll1*$^{+/-}$ mice display segment abnormalities, haematopoietic abnormalities and small size, suggesting that *Mll1* is important for normal development of the haematopoietic system and for pattern formation (Yu et al., 1995). *Hoxa7* and *Hoxc9* expression could not be detected in whole mount staining of *Mll1*$^{-/-}$ mice examined at E10.5 and expression in *Mll1*$^{+/-}$ mice was disrupted, with the normal *Hox* gene expression

boundaries shifted posteriorly (Yu et al., 1995). Further analysis of the *Hox* expression defects in *Mll1*$^{-/-}$ mice revealed that the initial induction of *Hox* expression occurs normally in the absence of *Mll1* but the expression cannot be maintained (Yu et al., 1998). Normal *Hoxa7* expression begins between E7.5-8.5 and examination of *Mll1*$^{-/-}$ mice at E8.0 revealed that *Hoxa7* induction was normal at this stage; however, from E9.0 onward, *Hoxa7* expression could no longer be detected in the neural tube or somites by *in situ* hybridization (Yu et al., 1998). Other *Hox* genes, such as *Hoxc8*, were also initiated normally but expression was not maintained after E9.0 in *Mll1*$^{-/-}$ mice, suggesting that the MLL1 protein is required for the maintenance, but not the initiation, of *Hox* gene expression (Yu et al., 1998).

Generation of chimeric embryos demonstrated that *Mll1*$^{-/-}$ cells fail to contribute to the haematopoietic stem cell or progenitor cell populations. In chimeric adult mice, *Mll1*$^{-/-}$ cells fail to differentiate into T or B lymphocytes (Ernst et al., 2004a). Thus, MLL function is necessary for generation of haematopoietic stem cells in the embryo and also for differentiation of cell lineages in adults. This requirement for MLL stemmed from its role in maintaining expression of *Hox* genes which are important effectors for haematopoiesis (Ernst et al., 2004b). When embryonic stem cells are cultured *in vitro* they form embryoid bodies that progress through defined steps similar to cells *in vivo* and are thus useful for studying progression of haematopoiesis. *Mll1*$^{-/-}$ embryoid bodies form with the early steps occurring normally; however, they fail to produce haematopoietic colonies, due to defects in cell division and differentiation. *Mll1*$^{-/-}$ embryoid bodies have severely reduced expression of *Hoxa* (*Hoxa7, Hoxa9, Hoxa10*) and *Hoxb* (*Hoxb4, Hoxb5, Hoxb6, Hoxb8*) gene clusters, with *Hoxa9* expression most

dramatically reduced compared to *Mll1*$^{+/-}$ embryoid bodies (Ernst et al., 2004b). Re-expression of individual *Hox* genes (*Hoxa9*, *Hoxa10*, *Hoxb4*) was able to restore colony formation of *Mll1*$^{-/-}$ embryoid bodies, suggesting that the block in haematopoiesis observed in *Mll1*$^{-/-}$ embryoid bodies was due to the loss of *Hox* gene expression (Ernst et al., 2004b). In addition to being required for embryonic haematopoiesis, MLL is also required for the maintenance of haematopoietic stem cells and bone marrow progenitor cells in adults (Jude et al., 2007). Inducible Cre-mediated excision of *Mll1* specifically in the bone marrow led to failure of haematopoietic stem cells to self-renew and reduced proliferation of progenitor cells which resulted in death by about three weeks (Jude et al., 2007).

Since MLL functions to maintain *Hox* gene expression for normal development, it was speculated that if MLL fusion proteins overexpressed *Hox* genes, either resulting in spatial or temporal changes in *Hox* expression, this could contribute to leukemogenesis. Indeed, the overexpression of *Hox* genes is frequently observed in MLL-associated AML and ALL. For example, ALL caused by the most frequent translocation t(4:11) is associated with high levels of expression of *HOXA9* and *MEIS1* (myeloid ectropic viral integration site 1, an essential co-factor for *Hox* genes) (13/14 tumours examined), whereas ALL cases lacking 11q23 translocations do not have increased *HOXA9* or *MEIS1* expression. Similar analyses of AML tumours with MLL translocations (t(9:11), t(11:19), t(10:11)) also demonstrated increased *HOXA9* and *MEIS1* expression (8/8 tumours examined) (Rozovskaia et al., 2001). In addition, cell lines derived from MLL-associated human leukemias (MLL-ENL, MLL-AF4, MLL-AF6, MLL-AF9) show high expression of *HOXA9* (Ayton and Cleary, 2003).

Expression of MLL fusion proteins (*e.g.* MLL-ENL, MLL-AF6, MLL-CBP, MLL-ELL, MLL-AF10) in murine primary myeloid progenitor cell lines results in high levels of *Hoxa7*, *Hoxa9*, *Hoxa10* and *Hoxa11* expression and in cell immortalization. Expression of the *Hox* co-factor *Meis1* is also up-regulated (Ayton and Cleary, 2003). Using tamoxifen-inducible expression of MLL-ENL in primary bone marrow (BM) cells, the MLL fusion protein is necessary to initiate and sustain the clonogenic activity in immortalization assays and this corresponds with expression of *Hoxa7*, *Hoxa9*, *Hoxa10* (Ayton and Cleary, 2003). BM cells from *Hoxa9* or *Hoxa7* deficient mice transduced with MLL-ENL do not maintain clonogenic activity in immortalization assays, unlike wild-type BM cells transduced with MLL-ENL. Furthermore, transplantation of MLL-ENL transduced wild-type BM cells results in leukemia in mice after about 3 months; however, transplantation of MLL-ENL transduced *Hoxa9*$^{-/-}$ BM cells did not result in development of leukemia in the 12 months monitored. These results demonstrate the importance of *Hox* genes, especially *Hoxa9* expression, in MLL-associated immortalization of progenitor cells and in leukemia development *in vivo* (Ayton and Cleary, 2003).

1.4 MLL1 is a histone methyltransferase

After the discovery that MLL fusion proteins were the causative agent of many childhood and adult leukemias, the quest began to determine the normal function of MLL as well as how MLL fusions caused leukemogenesis. Two labs simultaneously identified the biochemical function of MLL as a histone methyltransferase (HMT) with specificity for lysine 4 of histone H3 (H3K4) (Milne et al., 2002; Nakamura et al., 2002). Nakamura *et al.* (2002) isolated a human MLL1 supercomplex of 29 proteins, including components of the SWI/SNF, NuRD, Sin3A and TFIID complexes involved in chromatin

remodelling, histone modification and transcription. This isolated supercomplex displayed histone methylation activity towards core histones and mononucleosomes (Nakamura et al., 2002). It was speculated that this activity could be attributed to the MLL1 SET domain, since the Set1 protein in yeast, with a homologous domain, was shown to display H3K4me activity (Roguev et al., 2001). A recombinant peptide containing the MLL1 SET domain was able to methylate histone H3 as well as combined core histones or nucleosomes. The methylation on H3 was mapped to lysine 4 (Nakamura et al., 2002). H3K4 methylation, as well as H3 and H4 acetylation, were examined through chromatin immunoprecipitation (ChIP) at *HOXA9* following RNAi-mediated knock-down of *MLL1.* Expression of *HOXA9* was reduced with knock-down of *MLL1* and this was associated with reduced H3K4 dimethylation (H3K4me2) and H3 acetylation at the promoter and 5' coding region (Nakamura et al., 2002).

Studying the *Hoxc8* locus Milne *et al.* (2002) also observed that acetylation and methylation of histones is MLL dependent and essential for expression of certain *Hox* genes. $Mll1^{-/-}$ MEFs re-expressing *Mll1* with the SET domain deleted ($Mll1^{\Delta SET}$) failed to re-establish *Hoxc8* expression unlike those re-expressing full-length *Mll1*, suggesting that the SET domain is essential for *Hox* expression (Milne et al., 2002). $Mll1^{-/-}$ MEFs have reduced H3K4 methylation in the 5'enhancer, promoter and intergenic regions compared to $Mll1^{+/+}$ MEFs. The methylation defect in the promoter of $Mll1^{-/-}$ cells could be partially restored by re-expression of *Mll1* but not by re-expression of $Mll1^{\Delta SET}$, suggesting that the SET domain is necessary for H3K4 methylation of target genes (Milne et al., 2002). In addition, $Mll1^{-/-}$ MEFs have significantly reduced H3 and H4 acetylation in the 5' enhancer, promoter and intergenic regions compared to wild-type MEFs. This

acetylation is restored in *Mll1*$^{-/-}$ MEFs by re-expressing full-length *Mll1*, suggesting that MLL also directs histone acetylation at target genes (Milne et al., 2002).

The MLL SET domain was shown to have intrinsic H3K4 methyltransferase activity using an *in vitro* methylation assay. Recombinant MLL SET was able to methylate histone H3, an unmodified H3 peptide as well as core histones. Furthermore, methylation of the H3 peptide was enhanced when it was previously acetylated on K9 or K14, suggesting that MLL SET may preferentially methylate acetylated H3, at least *in vitro* (Milne et al., 2002). The results of Milne *et al*. and Nakamura *et al.* (2002) clearly show that the SET domain of MLL conveys histone methyltransferase (HMT) activity and thus, these studies established a biochemical function to MLL despite previous researchers failing to identify this HMT activity (Rea et al., 2000). Although HMT activity partly explains how MLL regulates target gene expression, it does not describe the role of MLL in leukemogenesis since the SET domain is deleted in MLL fusions as the breakpoint cluster region occurs after about 1300 amino acids. Expression of the MLL-AF9 fusion in *Mll1*$^{-/-}$ MEFs results in increased *Hoxc8* expression; however, this is not accompanied by H3K4me at the locus. This indicates that fusion proteins activate target genes through novel mechanisms and not through H3K4 methylation (Milne et al., 2002).

2. MLL and Trithorax protein structure

2.1 Protein domains

MLL1 is a structural and functional homologue of *Drosophila* Trithorax (Trx), the founding member of the Trithorax group (TrxG) of epigenetic regulators of transcription. MLL1 and Trx are large proteins, consisting of 3969 and 3726 amino acids, respectively

(Kuzin et al., 1994; Tkachuk et al., 1992). The murine and human proteins are 90.8 % identical (Ma et al., 1993). These large proteins carry several functional and interaction domains allowing them to form large multi-protein structures (reviewed in Cosgrove and Patel, 2010; Thiel et al., 2012). The structure of mammalian MLL1 will be described since it has been better characterized than *Drosophila* Trithorax; though, many of the main domains are conserved (see also Appendix D, Figure D.1 for an alignment).

At the N-terminus of MLL is the menin binding domain (4-44), that consists of two menin-binding motifs, MBM1 (4-15) and MBM2 (23-40), that contact menin, with MBM1 being the high-affinity binding motif (Caslini et al., 2000; Grembecka et al., 2010). Within MBM1, amino acids RWRFP (6-10) were shown to be crucial as their deletion was sufficient to abrogate binding to menin (Yokoyama et al., 2005) (see Chapter 1, Section 8.2 for more detail). The LEDGF binding domain (amino acids 112-153) is located next to the MBM (Yokoyama and Cleary, 2008). Next, are three AT hook domains (169-180, 217-227, 301-309) which are important for binding to the minor groove of DNA. The AT hooks are not conserved in *Drosophila* Trx (Tkachuk et al., 1992).

The next important domain shares homology with a DNA methyltransferase (DNMT) domain and is also absent in *Drosophila* (Ma et al., 1993). This domain is cysteine-rich and is frequently referred to as the CXXC domain of MLL (residues 1146-1244). It has been shown to interact with unmethylated CpG sites of DNA (Birke et al., 2002). Furthermore, this domain is essential for interaction with the polymerase associated factor complex (PAFc), which interacts with RNAP II to regulate transcriptional elongation (Milne et al., 2010; Muntean et al., 2010). The interaction of MLL fusion proteins with the PAFc appears to be essential for leukemogenesis as

demonstrated by a deletion of MLL-AF9 that disrupts interaction with PAFc leading to prevention of MLL-AF9 induced immortalization (Muntean et al., 2010).

The chromosomal breakpoint cluster region occurs after the DNMT/CXXC domain, between exons 8 and 13 (Krivtsov and Armstrong, 2007). Thus, MLL fusion proteins consist of the first 1300-1400 amino acids of MLL and include the menin and LEDGF binding domains, the AT hooks and the DNMT/CXXC domain but lack all other domains (*i.e.* PHDs, Bromodomain, TAD, SET). The plant homeodomain (PHD) zinc finger motifs occur after the breakpoint cluster region. There are three PHDs which are followed by a single bromodomain and then a fourth PHD. The PHDs are cysteine-rich sequences that form zinc fingers which are important for protein-protein interactions. These are homologous to the cysteine-rich zinc figure domains identified in the original characterization of Trx (Mazo et al., 1990). PHDs have been demonstrated to bind to trimethylated H3K4 (H3K4me3) and PHD3 of MLL appears to be particularly important for this function which could be important for transcriptional maintenance by MLL (Chang et al., 2010). The bromodomain, which is found in many transcriptional co-activators that interact with histone acetyltransferases (HATs), also binds to modified histones; although, in this case the recognized histone mark is acetylated histone H4 lysine 16 (H4K16ac) (Dhalluin et al., 1999). The specific role of this domain in MLL function and leukemogenesis has not been well elucidated.

These important chromatin binding domains are followed by the FYRN domain (phenylalanine and tyrosine rich N-terminal region) and the Taspase1 endoprotease cleavage sites CS1 (D/GADD, 2666-26667) and CS2 (D/GVDD, 2718-2719). Cleavage at these sites results in the formation of the MLL^N and MLL^C fragments that remain

associated through interaction of the FYRN domain of MLL^N with a similar FYRC domain in MLL^C (see Section 2.2). The FYRC domain is located before the *Win* and SET domains (Hsieh et al., 2003a; Hsieh et al., 2003b).

The transactivation domain (TAD) is located after the Taspase1 cleavage sites. The TAD is responsible for recruitment of co-activators such as CBP (CREB (cAMP response element-binding) binding protein), an acetyltransferase that acetylates histones and transcription factors (Ernst et al., 2001). The HAT MOF (MYST family member) also interacts with the TAD of MLL and is responsible for H4K16 acetylation, another epigenetic mark associated with active transcription sites (Dou et al., 2005).

Although WDR5 (WD40 repeat containing protein 5) was initially believed to interact with the SET domain, its domain of interaction was localized to six highly conserved amino acids (GSARAE, 3762-3767) N-terminal to the SET domain, with the R3765 residue essential for the interaction (Patel et al., 2008; Song and Kingston, 2008). This domain was later named the *Win* (WDR5 interacting) domain and interaction of WDR5 with this domain is important for assembly of the other core complex proteins and for stimulation of MLL HMT activity (Patel et al., 2008).

The SET domain, named for its occurrence in *Drosophila* su(var)3-9, enhancer of zeste, trithorax (Tschiersch et al., 1994), conveys histone methyltransferase activity specific for lysine 4 of histone H3 (H3K4me) (Milne et al., 2002; Nakamura et al., 2002) (see Section 1.4). The SET domain is located at the C-terminus of MLL1 (3790-3969) and interacts with other core component proteins including RBBP5, ASH2L and DPY-30 (see Chapter 1, Section 8.1 for more details) (Hughes et al., 2004; Yokoyama et al., 2004). In

addition the SET domain has been shown to interact with INI1/SNF5, a component of the SWI/SNF chromatin remodelling complex (Rozenblatt-Rosen et al., 1998).

2.2 Cleavage by Taspase1

Evidence for proteolytic processing of MLL came from immunoblotting studies using antibodies raised against the N-terminus or C-terminus of MLL since neither antibody detected a band of the expected size of ~430 kDa. Instead, the anti-N-terminus antibody recognized a fragment of ~320 kDa, while anti-C-terminus recognized a ~180 kDa band (Hsieh et al., 2003b; Yokoyama et al., 2002). Two cleavage sites were identified in MLL1, CS1 (D/GADD) and CS2 (D/GVDD), located at residues 2666-2667 and 2718-2719, with CS2 being the preferred cleavage site (Hsieh et al., 2003b; Yokoyama et al., 2002). Mutation of both sites completely prevents cleavage of MLL and results in accumulation of the full-length protein. The CS2 (D/GVDD) cleavage site is conserved in MLL2 and *Drosophila* Trithorax (Hsieh et al., 2003b; Yokoyama et al., 2002).

The enzyme responsible for cleavage of MLL was found to be a novel protease since inhibitors of known proteases, including serine proteases, cysteine proteases, metalloproteases and acid proteases, all failed to prevent MLL cleavage (Hsieh et al., 2003a). The responsible enzyme was isolated and characterized and named Taspase1. Taspase1 is a threonine aspartase, which means that it cleaves its substrates after an aspartic acid residue using a threonine (Thr234) as the active site nucleophile (Hsieh et al., 2003a). A Taspase1 homologue exists in *Drosophila* and contains a conserved LDTVG motif surrounding the active site threonine. RNAi knockdown of *Taspase1* in HeLa cells results in reduced MLL cleavage, as observed by an accumulation of full-length MLL and a decrease in the 180 kDa MLL^{C} fragment. Uncleaved MLL1 has impaired, but not

completely eliminated, HMT activity, suggesting that cleavage is necessary for full activation of the SET domain function (Takeda et al., 2006). Moreover, MLL is not cleaved in *Taspase1*$^{-/-}$ MEFs and *Taspase1*-deficient mice display homeotic transformations, which provides additional evidence that Taspase1 function is crucial for MLL cleavage and consequently for proper *Hox* gene expression (Takeda et al., 2006).

Taspase1-mediated cleavage results in the generation of two MLL fragments, the 320 kDa MLL^{N} and 180 kDa MLL^{C}, that remain associated after cleavage. The association of the two fragments occurs through interaction of the FYRN domain of MLL^{N} with the FYRC and SET domains of MLL^{C} (Hsieh et al., 2003b). This cleavage and interaction between the two fragments is necessary for stabilization of the MLL^{N} fragment, which has a shorter half-life in the presence of a truncated MLL^{C} that lacks the FYRC and SET domains. Furthermore, truncation of MLL^{C}, which prevents interaction with MLL^{N}, also results in improper sub-nuclear localization of MLL^{C} as the normal punctuate staining pattern is no longer observed (Hsieh et al., 2003b).

The conservation of the CS2 cleavage site in Trx, as well as the FYRN and FYRC domains, and the existence of a *Drosophila* Taspase1 homologue suggested that Trx would be processed in the same manner as MLL1 (Hsieh et al., 2003a; Hsieh et al., 2003b; Yokoyama et al., 2002). Furthermore, the *trx*^{E3} mutant that contains a 271 amino acid internal deletion that results in loss of the Taspase1 cleavage site, accumulates full-length Trx protein and lacks the smaller fragments found in wild-type flies (Kuzin et al., 1994). Direct proof of Taspase1 cleavage of Trx was eventually provided as recombinant *Drosophila* Taspase1 cleaves wild-type Trx (QMDGVDD) but not a cleavage site mutant (QMAAVDD) in an *in vitro* cleavage assay (Capotosti et al., 2007).

3. Menin interacts with Mixed Lineage Leukemia (MLL)

The interaction between menin and wild-type MLL1 and MLL2 has been well documented, as well as the interaction of menin with MLL1 fusion proteins that result from chromosomal translocations and are associated with childhood and adult leukemias (Caslini et al., 2007; Hughes et al., 2004; Yokoyama et al., 2005; Yokoyama et al., 2004). The interaction of menin and MLL1 fusions is necessary for leukemogenesis and for up-regulation of key target genes (*e.g. HOXA9*, *MEIS1*) that results in increased proliferation and blockage of haematopoietic differentiation. Thus, menin was established as an essential oncogenic co-factor for MLL-associated leukemogenesis (Caslini et al., 2007; Yokoyama et al., 2005; Yokoyama et al., 2004). The function of menin in MLL complexes appears to be the recruitment of other essential interacting partners, such as LEDGF, and thus menin may be functioning as an adaptor for the large MLL transcriptional regulatory complexes (reviewed in Thiel et al., 2012). Please see Chapter 1, Section 8 for a full review of the menin-MLL interaction.

4. Drosophila Trithorax

4.1 Characterization of the Trx gene and protein

The *Drosophila trithorax* (*trx*) gene spans 25 kb on the third chromosome (3R, 88B) and consists of four exons (Mazo et al., 1990). Five different mRNA transcripts are generated by alternative splicing (between 11-14 kb) (Sedkov et al., 1994). These encode two different protein isoforms that differ at the N-terminus - Trx I which is 3358 amino acids and 368 kDa and Trx II which is 3726 amino acids and 404 kDa (Kuzin et al., 1994). The smaller Trx I isoform is more abundant during early embryogenesis, while the longer Trx II isoform does not become abundant until later in embryogenesis (11-15 hrs).

Immunohistochemistry using an antibody capable of detecting both isoforms reveals strong staining for Trx in imaginal discs, salivary glands and gut tissues, (Kuzin et al., 1994). Immunoblotting of lysates from embryo nuclear extracts demonstrated that the large full-length proteins are unstable and very difficult to detect. Instead, the large full-length isoforms appear to be cleaved to form two fragments, 240 and 200 kDa fragments for Trx I and 275 and 200 kDa for Trx II (Kuzin et al., 1994).

The first hint at the molecular function of Trx came from examination of the predicted protein sequence. Several putative zinc finger motifs were identified. These cysteine-rich sequences were anticipated to bind DNA. Also, two acidic regions were located, with consecutive aspartic and glutamic acid residues, which were speculated to act as a transactivation domain since they resembled domains in known transcription factors (Mazo et al., 1990). Initial characterization of Trx function found that it is in fact a chromatin binding protein and Trx was localized strongly to 16 distinct loci on polytene chromosomes of third instar larvae, with other weaker bands also observed (Kuzin et al., 1994).

4.2 Trithorax and Drosophila development

Trithorax (Trx) has long been known to be important in *Drosophila* development and in the maintenance of segment identity. It was identified as a gene that when mutated causes homeotic transformations, where segments take on the characteristics of those located more anteriorly. Through genetic studies, *trx* was identified as a positive regulator of the bithorax complex (BX-C) and Antennapedia complex (ANT-C), two gene clusters of the *homeotic* (*Hox*) genes that regulate body segment identity in *Drosophila* (Mazo et al., 1990; Sedkov et al., 1994). Trx is believed to be important for the

maintenance of expression but not for initiation of *Hox* gene expression (Sedkov et al., 1994). The Trithorax Group (TrxG) proteins, which were grouped based on phenotype, are positive regulators of these *Hox* gene clusters and they act by assembling large protein complexes that maintain an open chromatin state for active gene expression. The action of TrxG proteins opposes that of Polycomb group (PcG) proteins that act as gene repressors which maintain closed chromatin conformation to repress gene expression. The TrxG and PcG bind to specific DNA sequences known as TREs (Trithorax response elements) and PREs (Polycomb response elements), respectively and then recruit complexes to regulate gene expression through histone modification or chromatin remodelling (reviewed in Grimaud et al., 2006). In addition to the identification of Trx as a repressor of the polycomb phenotype, evidence for a role in *Hox* gene regulation came from studies of *trx* mutants. trx^{B11} mutant embryos show reduced *Ultrabithorax* (*Ubx*) staining, suggesting that Trx is required for expression of *Ubx*, which is part of the BX-C cluster (Mazo et al., 1990). Polytene chromosome staining localizes Trx to the ANT-C complex and also the *fork head* (*fkh*) locus, a *Hox* transcription factor that is not clustered within the BX-C or ANT-C. Mutants (trx^{B11}, trx^{E12}, trx^{B16}) have reduced *fkh* mRNA in all tissues examined by *in situ* hybridization compared to wild-type late embryos and larvae (Kuzin et al., 1994). It was initially thought that Trx acted as a co-activator for *Hox* gene expression, but work with double mutants of *trx* and PcG genes suggested that instead Trx functions by inhibiting PcG-mediated silencing of *Hox* genes (Klymenko and Muller, 2004).

4.3 Trithorax mutants

Many different *trx* alleles have been identified and most mutations result in late embryonic lethality, but a few mutants survive until third instar or early pupal stages and temperature sensitive alleles have also been created (Breen, 1999). The characteristics of a few important *trx* alleles will be summarized since some of these were used in my own research. The trx^{B11} allele has a small deletion that results in a frameshift which truncates the protein after amino acid 658 (Mazo et al., 1990). It is a null allele that is embryonic lethal (Breen, 1999). The trx^{E3} allele also has a small deletion, but this one is an in-frame deletion of 271 amino acids within the coding region (Mazo et al., 1990). This deletion eliminates the Taspase1 cleavage site and these mutants accumulate full-length Trx protein and lack the smaller fragments found in wild-type flies (Kuzin et al., 1994). Interestingly, both trx^{B11} and trx^{E3} are embryonic lethal; however, only trx^{B11} mutants show defects in expression of *Ubx* in embryos. This suggests that Trx is required for essential functions other than expression of *Hox* genes, and that different regions of this large protein could be required for diverse functions (Mazo et al., 1990). Another allele, trx^{Z11}, is considered a hypomorph and is pupal lethal. This mutant has a mutation (Gly3601Ser) in the SET domain (Breen, 1999). The trx^{B11} and trx^{Z11} alleles were kindly donated by Dr. Alexander Mazo for use in the characterization of the menin-Trx interaction in *Drosophila*.

4.4 Trithorax protein-protein interactions

The first protein-protein interaction identified for Trx was with SNR1 (SNF5-related 1), another TrxG protein that is a component of the SWI/SNF chromatin remodelling complex (Rozenblatt-Rosen et al., 1998). This interaction was discovered in a yeast two-

hybrid screen using the Trx SET domain to identify potential binding partners. The interaction was confirmed by co-immunoprecipitation experiments as well as *in vitro* binding assays to prove a direct interaction (Rozenblatt-Rosen et al., 1998). When SNR1 is overexpressed using a heat shock promoter it co-localizes to about half of Trx binding sites on larval polytene chromosomes, suggesting that SNR1 and the SWI/SNF complex interact with Trx to facilitate chromatin remodelling at some target gene loci, such as the *fkh* locus, to activate transcription. The human homologues of Trx and SNR1, MLL1 and INI1/hSNF5, respectively, also interact through the SET domain of MLL1 (Rozenblatt-Rosen et al., 1998).

Trx and Ash1, another TrxG protein, were shown to interact through co-immunoprecipitation experiments using embryo nuclear extracts. The protein-protein interaction is mediated through their conserved SET domains (Rozovskaia et al., 1999). Trx and Ash1 also co-localize on several sites on larval polytene chromosomes and bind to an inserted transgene containing the regulatory *bxd* region of the *Ubx* gene. Furthermore, placing a *bxd*-reporter construct, containing three TREs upstream of mini-white gene, in an *ash1* (*ash1*^{B1}, *ash1*^{12}, *ash1*^{22}) heterozygous background results in reduced eye colour compared to a wild-type background (Rozovskaia et al., 1999). Similar results were obtained with this reporter construct in *trx*^{B11} heterozygotes (Tillib et al., 1999). Together, these results suggest that Trx and Ash1 interact *in vivo* and are important for regulation of *homeotic* genes.

The physical interaction observed between Trx and Ash1 agrees with an earlier observation that larvae with the *ash1*^{vb234} temperature sensitive allele have dramatically reduced Trx binding to polytene chromosome loci (Kuzin et al., 1994). This suggests that

Ash1 could be required for Trx binding to chromatin as *ash1* mutants do not have decreased Trx mRNA or protein levels. In addition, immunostaining of salivary glands revealed that Trx was nuclear with a punctuate staining pattern; however, in the absence of Ash1, the nuclear distribution of Trx became diffuse, perhaps reflecting loss of chromatin association (Kuzin et al., 1994).

4.5 The TAC1 complex and the heat shock response

Dr. Alexander Mazo's group purified *Drosophila* Trx from embryos and found that it associates stably with two other proteins, dCBP (*Drosophila* CREB (cAMP response-element binding) binding protein) and Sbf1 (SET binding factor 1). dCBP is a histone acetyltransferase (HAT) and Sbf1 is an anti-phosphatase. This 1 MDa complex was named the Trithorax acetylation complex 1 (TAC1) and was shown to be capable of acetylating the four core histones (Petruk et al., 2001). This complex was later shown to also methylate histone H3 on lysine 4 (H3K4me) in a Trx-dependent, and more specifically a SET-dependent, manner (Smith et al., 2004). Trx, dCBP and Sbf1 co-localize on many sites on salivary gland polytene chromosomes. The TAC1 complex is required for expression of *Hox* genes, such as *Ubx*, as mutations in either *trx* (trx^{B11}) or *dCBP* (nej^{Q7}, nej^{S103}) result in reduced *Ubx* expression. Reduced expression of a *bxd-LacZ* reporter was also observed for these mutants, suggesting that Trx and dCBP may function through activation of gene expression at TREs (Petruk et al., 2001).

In addition to its function in the regulation of *Hox* genes, the TAC1 complex is also important for the regulation of heat shock (*hsp*) genes following heat stress (Smith et al., 2004). Heat shock of larvae results in significant recruitment of Trx to heat shock gene loci (*e.g.* 87A, 87C, 93D, 95D), which can be observed as puffs on polytene

chromosomes. The other members of the TAC1 complex, dCBP and Sbf1, show overlap at these loci with heat shock (Smith et al., 2004). Chromatin immunoprecipitation analyses in embryos also show that Trx, dCBP and Sbf1 are localized to *hsp70* after heat shock. Using primer sets for different regions of the gene, the TAC1 complex was shown to bind primarily within the 5' coding region and not in the upstream promoter region (Smith et al., 2004). Binding in the 5' coding region suggests that the TAC1 complex might interact with RNAP II phosphorylated on Ser 2 of the CTD, which is important for the elongation phase of transcription. This was confirmed by co-immunoprecipitation of RNAP II p-Ser2 with Trx (Smith et al., 2004). Loss of either Trx (trx^{B11}) or dCBP (nej^{Q7}) results in the lack of recruitment of the other components to *hsp70*, suggesting that the proteins may all be recruited together as a complex. Also, mutations in the SET domain of Trx (trx^{Z11}) reduce binding of dCBP and Sbf1 to *hsp70*, suggesting that the Trx SET domain is important for interactions with other proteins and for complex recruitment (Smith et al., 2004). Furthermore trx^{B11} and nej^{Q7} embryos have reduced expression of *hsp70*, *hsp68, hsp83* and *hsrω* mRNA compared to wild-type following a 30 min heat shock; however, there was still some induction of these *hsp* genes in the absence of Trx and dCBP. The SET mutant trx^{Z11}, along with the null trx^{B11}, were also shown to have reduced HSP70 protein following a 30 min heat shock of embryos. The reduced expression of *hsp70* in these mutants following heat shock is correlated with reduced histone methylation (H3K4me2) and acetylation (H3ac) in the 5' coding region of *hsp70.* (Smith et al., 2004). Overall, the results demonstrate that the TAC1 complex is important for the regulation of *hsp* gene expression, and the histone methylation

activity of Trx and histone acetylation activity of dCBP are important for full induction of *hsp70* expression.

5. Objectives and Hypotheses

The main objective for the research described in this chapter was to determine if the menin-MLL interaction was conserved, that is, if *Drosophila* menin and Trithorax also interact. We were especially interested in this interaction due the importance of Trx in the TAC1 complex which is necessary for *hsp* gene expression (Petruk et al., 2004; Smith et al., 2004). Since menin was also observed to be required for proper heat shock gene expression and heat shock survival (Papaconstantinou et al., 2005), we predicted that the proposed menin-Trx interaction was essential for gene expression in response to heat stress. More specifically, we hypothesized that menin interacts with Trx at chromatin to coordinate proper histone modification and chromatin remodelling required for transcription of heat shock proteins in response to heat stress. The first objective was to establish that menin and Trx interact through co-immunoprecipitation in S2 cells. Secondly, we wished to demonstrate this interaction in embryos and determine the importance of this interaction for the heat shock response and the maintenance of genome stability. The third objective was to characterize the recruitment of menin and Trx to chromatin for proper histone modification in response to heat stress. For this objective, we hypothesized that since menin is required for the recruitment of MLL to target genes (*e.g. p27, p18*) in mammalian cells (Milne et al., 2005), it would also be essential in *Drosophila* for the recruitment of Trx to *hsp* loci for activation of gene expression in response to heat stress.

RESULTS

1. Trx and MLL1 sequence alignment

Before investigating whether or not *Drosophila* menin and Trithorax interact, like the mammalian menin and MLL1 homologues, a protein sequence alignment for Trx II (GI 19550184) and human MLL1 (GI 56550039) was done using Clustal W 2.1 (European Bioinformatics Institute). The Trx II isoform contains extra N-terminal amino acids that are missing the Trx I isoform (Kuzin et al., 1994) so Trx II was used for the alignment since the menin-binding motif of MLL1 is located in the very N-terminus of the large protein (Yokoyama et al., 2005). Thus, only the Trx II isoform, which is predominant from late embryogenesis on, is expected to interact with menin (Kuzin et al., 1994). The protein alignment reveals that the high affinity menin binding motif (hMBM) RXRFP, identified by Yokoyama et al. (2005), consisting or residues 6-10 RWRFP in MLL1, is conserved in Trx as RSKFP (Appendix D, Figure D.1). The second arginine of the MLL1 sequence is instead a lysine in Trx, but since this is also a basic residue the charge is conserved. Other groups identified a larger domain of the N-terminus of MLL1 as important for menin interaction. Grembecka *et al.* (2010) demonstrated that two regions interact with menin, MBM1 (menin binding motif 1) and MBM2, with MBM1 having a much higher affinity. MBM1, which contains the hMBM identified by Yokoyama *et al.* (2005), but not MBM2, appear to be conserved in Trx. Determination of the crystal structure of menin in complex with MLL^N showed that three hydrophobic residues of the MBM1 of MLL1 contribute most to the interaction with menin – F9, P10, P13 (Grembecka et al., 2010) (see Chapter 1, Section 8.2). All three of these residues are conserved in Trx (F6, P7, P10) (Appendix D, Figure D.1). Thus, this analysis predicts that

menin can likely interact with Trx since the most important residues of MLL1 involved in menin binding are conserved. The conservation of other domains of Trx/MLL1 are also indicated on the alignment (Appendix D, Figure D.1).

2. Menin and Trithorax interact in S2 cells

Since the hMBM of MLL1 is conserved in Trx, we predicted that menin and Trx would also interact in *Drosophila*. Trithorax antibodies were kindly provided by Dr. Alexander Mazo (Thomas Jefferson University) (see Figure 4.1A and Chapter 2, Table 2.1). Co-immunoprecipitation experiments in *Drosophila* S2 cells showed that menin and Trx interact (Figure 4.1B and C). Immunoprecipitation with an anti-menin antibody (5073) and immunoblotting with an antibody against the N-terminal Trx fragment (Trx N1) showed that the proteins interact (Figure 4.1B). This N1 antibody recognizes the N-terminus of Trx that is only present in the larger Trx II isoform (Figure 4.1A) (Kuzin et al., 1994). The Trx N-terminal fragment (Trx^N) migrated above the 250 kDa protein marker which agrees with its expected size of 275 kDa (Kuzin et al., 1994). The reciprocal co-immunoprecipitation was also successful as menin was detected in Trx N1 immunoprecipitates (Figure 4.1B). Since the Trx protein is cleaved into the Trx^N and Trx^C fragments, and the Trx^C fragment contains the enzymatic SET domain, we wanted to see if this fragment also interacted with menin. When the immunoprecipitation was done with the menin antibody and immunoblotting with a Trx antibody specific to the SET domain located at the C-terminus (Trx N6), it was difficult to detect the Trx^C fragment (Figure 4.1B). However, reverse immunoprecipitations, using the Trx N6 antibody and immunoblotting with the menin antibody revealed small amounts of menin in Trx N6 immunoprecipitates (Figure 4.1B, bottom panel). The size of the fragment detected with

the Trx N6 antibody was about 200 kDa which agrees with previous reports (Kuzin et al., 1994). Immunoprecipitations with the Trx N6 antibody also clearly revealed the presence of the Trx^N fragment, and the reverse immunoprecipitation with N1, revealed the Trx^C fragment, although this was more difficult to detect (Figure 4.1B). Therefore, as expected, the Trx^C fragment remains associated with Trx^N. The amount of menin observed in immunoprecipitations with the N6 antibody is reduced compared to what is observed with the N1 antibody (Figure 4.1C). This observation supports the prediction that menin interacts directly with Trx^N because the interaction appears more prominent than with the indirect Trx^C interaction. The association of the Trx^C SET domain containing fragment with the Trx^N fragment and menin suggests that menin's interaction with Trx could be associated with HMT activity. Co-immunoprecipitation experiments in S2 cells were repeated several times and demonstrated that the interaction between menin and Trx is well conserved.

2.1 The menin-Trithorax interaction is regulated by heat stress

Since Trx is part of the TAC1 complex that is required for high *hsp* expression and since menin is also required for proper *hsp* expression (Papaconstantinou et al., 2005; Smith et al., 2004), we investigated the kinetics of this interaction when cells were exposed to various heat shock (HS) and recovery times. The hypothesis was that menin is involved in the recruitment of Trx to *hsp* gene loci, similar to the requirement of menin for MLL recruitment to target gene loci (Milne et al., 2005). Thus, it was expected that we would observe more Trx in menin immunoprecipitations when cells were exposed to HS. The co-immunoprecipitation experiments shown in Figure 4.1 revealed that with a 30 min HS, the interaction between menin and Trx was weakened, contrary to what was

expected. With different HS times, it can be seen that the proteins interact strongly under normal conditions; however, the amount of Trx protein (detected with N1 antibody) in menin immunoprecipitations decreases with increasing heat shock exposure (Figure 4.2A). The disruption of the interaction is evident with a HS of 15 min or greater. With a 1 hr HS Trx was usually not detected in menin immunoprecipitations (data not shown). Menin and Trx appear to re-associate following a 1 hr recovery at the normal temperature (Figure 4.2A).

To ensure that the low levels of Trx in the menin immunoprecipitation samples generated from heat shocked cells were due to loss of interaction and not protein degradation, the total level of Trx in S2 lysates were examined by immunoblotting. There was some loss of Trx, as detected with the N1 antibody, with prolonged HS (15 -60 mins), with the decrease being most evident after a 60 min HS (Figure 4.2B). Note that the lower band observed with the Trx N1 antibody in S2 cell lysates (just above 250 kDa) is a non-specific band and its intensity does not change with heat shock. It is possible that the decrease in Trx in menin immunoprecipitates reflects the decrease in total Trx protein levels; however, the decrease in protein lysates may not be large enough to fully explain the striking abolishment of the menin-Trx interaction following heat stress (Figure 4.2A). The co-immunoprecipitation experiment with various heat shock and recovery times were repeated several times and results consistently showed that the association of menin and Trx proteins was lost with prolonged heat shock exposures.

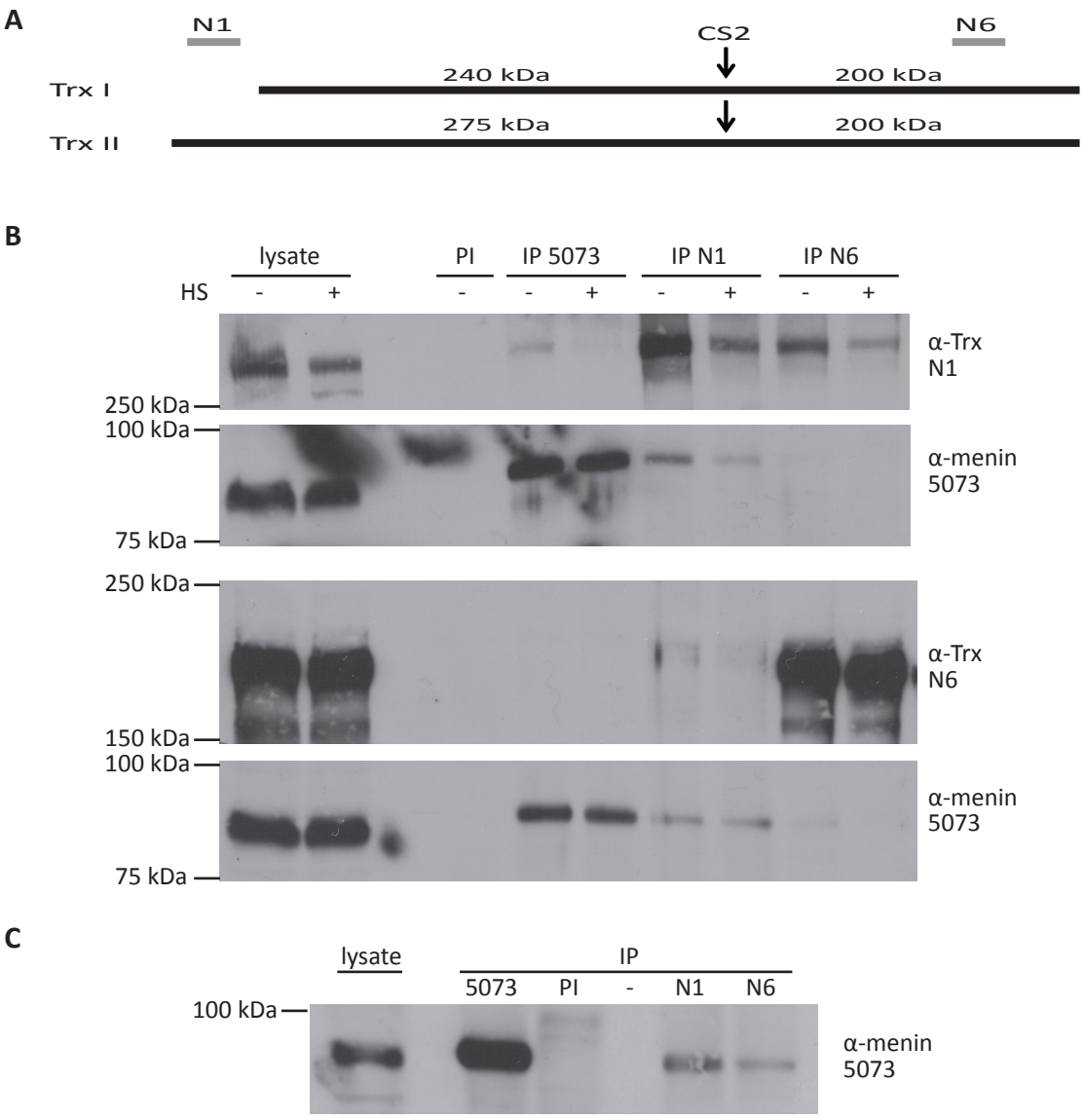

Figure 4.1. Menin and Trithorax interact in S2 cells.
A) Regions of Trithorax (Trx) protein recognized by the N1 and N6 antibodies. The N1 antibody recognizes the N-terminal Trx fragment (Trx^N) that is found only in the larger Trx II isoform. The N6 antibody recognizes the C-terminal Trx fragment (Trx^C) and was raised against a peptide containing the SET domain. The approximate location of the conserved Taspase1 cleavage site (CS2) is shown. B) S2 cells were untreated (-) or exposed to a 30 min heat shock (HS) at 37°C and immunoprecipitations(IP) were carried out with a pre-immune serum (PI), menin 5073, Trx N1 or Trx N6 antibodies and immunoblotted with Trx and menin antibodies as indicated. The top two panels are from the same gel as are the bottom two panels. Menin co-IPs with the Trx N1 antibody and weakly with the Trx N6 antibody. The Trx^N fragment associates with the Trx^C fragment, as seen most clearly in the top panel. C) IP with Trx N1 and Trx N6 antibodies showing that menin co-IPs with both antibodies, but more strongly with Trx N1.

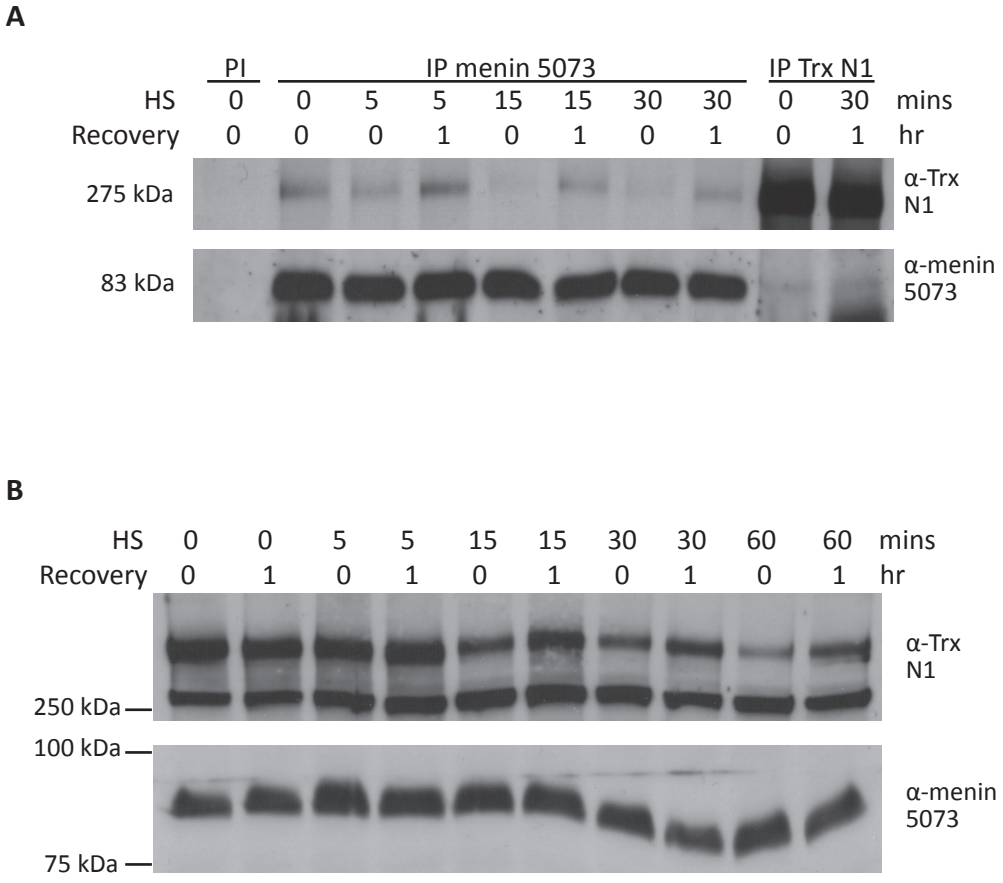

Figure 4.2 Regulation of the menin-Trithorax interaction with heat stress.
A) Immunoprecipitation (IP) of S2 cell lysates with the menin 5073 antibody resulted in co-IP of Trithorax (Trx). The interaction was strongest under normal conditions or with a short heat shock (HS). With longer HS (15, 30 mins) decreased Trx interacts with menin; however, with a 1 hr recovery from HS the interaction returns. Reciprocal IPs with the Trx N1 antibody reveal that menin co-IPs, although the interaction is harder to detect than in menin IPs. A pre-immune serum from 5073 was used as a negative control. B) Lysates from S2 cells exposed to various heat shock times with or without a 1 hr recovery from HS were immunoblotted with Trx N1 and menin 5073 antibodies. There is a decrease in the total amount of Trx protein with longer HS exposure (15 - 60 min) that worsens with the increase in the length of the HS. The bottom band in the top panel is a non-specific band that does not appear in IPs.

3. Examination of menin and Trx localization at the hsp70 gene

Since Trx and menin were independently shown to be important for proper regulation of heat shock gene (*e.g. hsp70*) expression (Papaconstantinou et al., 2005; Smith et al., 2004), we predicted that their interaction was important for this purpose. The prediction was that menin is required for the recruitment of Trx and the TAC1 complex to *hsp70* loci. This recruitment is needed for proper histone modification which is necessary to maintain gene expression during exposure to heat stress. The goal was to investigate this hypothesis using chromatin immunoprecipitation (ChIP) in order to study the recruitment of Trx to various regions of the *hsp70* gene in wild-type and *Mnn1* mutants under standard or HS conditions. In addition, the histone modifications (*i.e.* H3K4me2) at *hsp70* were also compared. It was postulated that menin mutants would have abnormal patterns of histone modifications if menin's interaction with Trx was crucial for this regulation.

After conducting preliminary ChIP experiments it was clear that the technique required improved sensitivity and specificity. For this reason, I worked in the lab of Dr. Alexander Mazo (Thomas Jefferson University) in order to optimize the conditions and then characterize menin and Trx localization at *hsp70* under standard and heat shock conditions. The goal was to compare the localization of Trx and histone modifications at *hsp70* in wild-type and *Mnn1* mutants in order to determine if menin was required for Trx recruitment. Unfortunately, experiments could only be conducted with OR embryos since there was a problem with the *Mnn1* mutant stocks that Dr. Mazo had received from Maria Papaconstantinou. I was unable to amplify *hsp70* from $Mnn1^{e30}$ or $Mnn1^{e173}$ genomic DNA using five different primer sets for different regions of the gene. This

suggested that the stocks they had received were *hsp70A*$^{-}$*B*$^{-}$ mutants that lacked all six copies of the *hsp70* gene (see Chapter 5 for more information). Consequently, I could not investigate the recruitment of Trx to *hsp70* in *Mnn1* mutants and was only able to characterize menin and Trx binding in OR embryos.

3.1 Characterization of menin and Trx localization at hsp70 in Oregon R embryos

The locations of all primer sets used for qPCR are shown schematically in Figure 4.3. Most of the primers used for real-time PCR for *hsp70* came from John Lis's paper (Figure 4.3B) (Boehm et al., 2003). Please note that the Cont2 primer set is not shown in Figure 4.3 but is used regularly in Dr. Mazo's lab as a negative control since the primers amplify an intergenic region where Trx is known not to bind. Similar background levels were also obtained with RP49 negative control primers (data not shown).

The results from two separate ChIP experiments followed by two qPCR replicates for each ChIP sample were averaged and are shown graphically in Figure 4.4. Results are shown as relative quantities that were determined from a standard curve and are normalized based on the ratios of input signal for a given primer set. Statistical analyses included one-way ANOVAs with Bonferroni's multiple comparisons post-hoc tests performed using GraphPad Prism version 5.00. Statistical analyses consisted of comparing the average relative quantity of DNA for a given primer set and antibody under the three treatment conditions (Appendix E, Table E.1). For example, menin signal with the *hsp70P3b* primers was compared for the No HS, 5 min HS and 30 min HS treatments, but statistical tests were not done to compare menin signal with the P1 versus P3 primers or to compare menin versus Trx binding at a specific location.

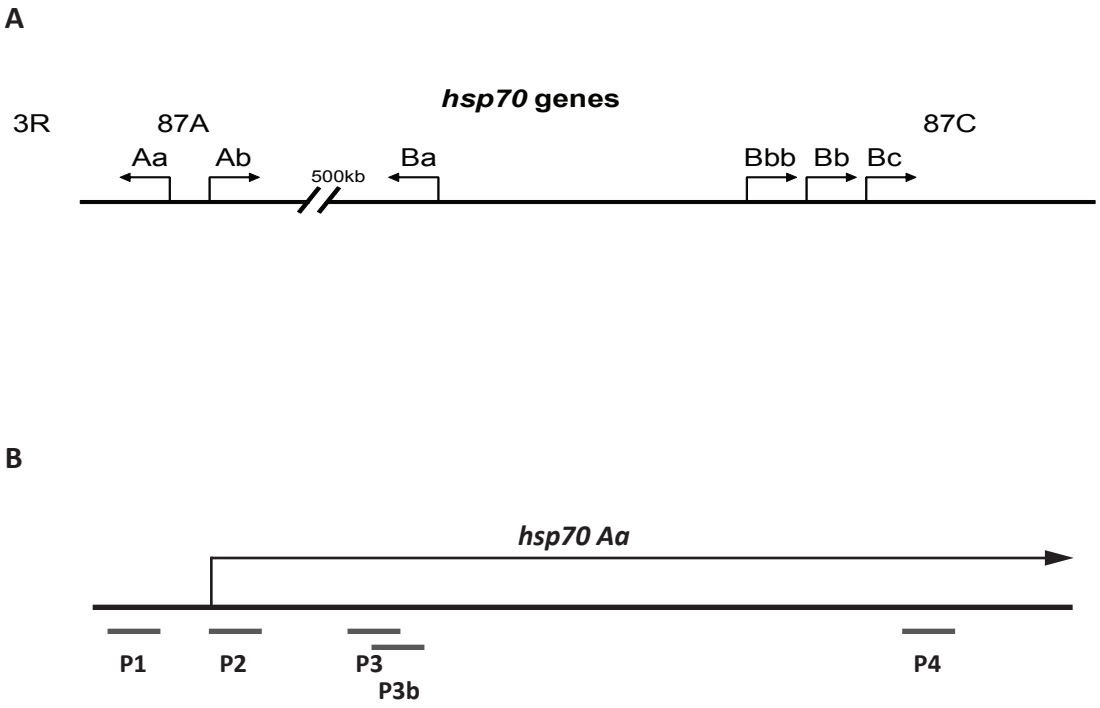

Figure 4.3. Schematic representation of the location of primers used for qPCR for ChIP.
A) Shows the approximate location of the 6 *hsp70* genes on chromosome arm 3R. B) Location of primer sets for the different regions of the *hsp70* gene. *hsp70P1* is in the promoter region where the heat shock elements (HSEs) are located. *hsp70P2* is located at the site of the stalled RNA polymerase II, just after the transcription start site. *hsp70P3* and *hsp70P3b* are in the 5' coding region, while *hsp70P4* is in the 3' coding region. Most primers for the various regions of *hsp70* are based off of those used by Boehm *et al.* (2003). Schematics are not drawn exactly to scale.

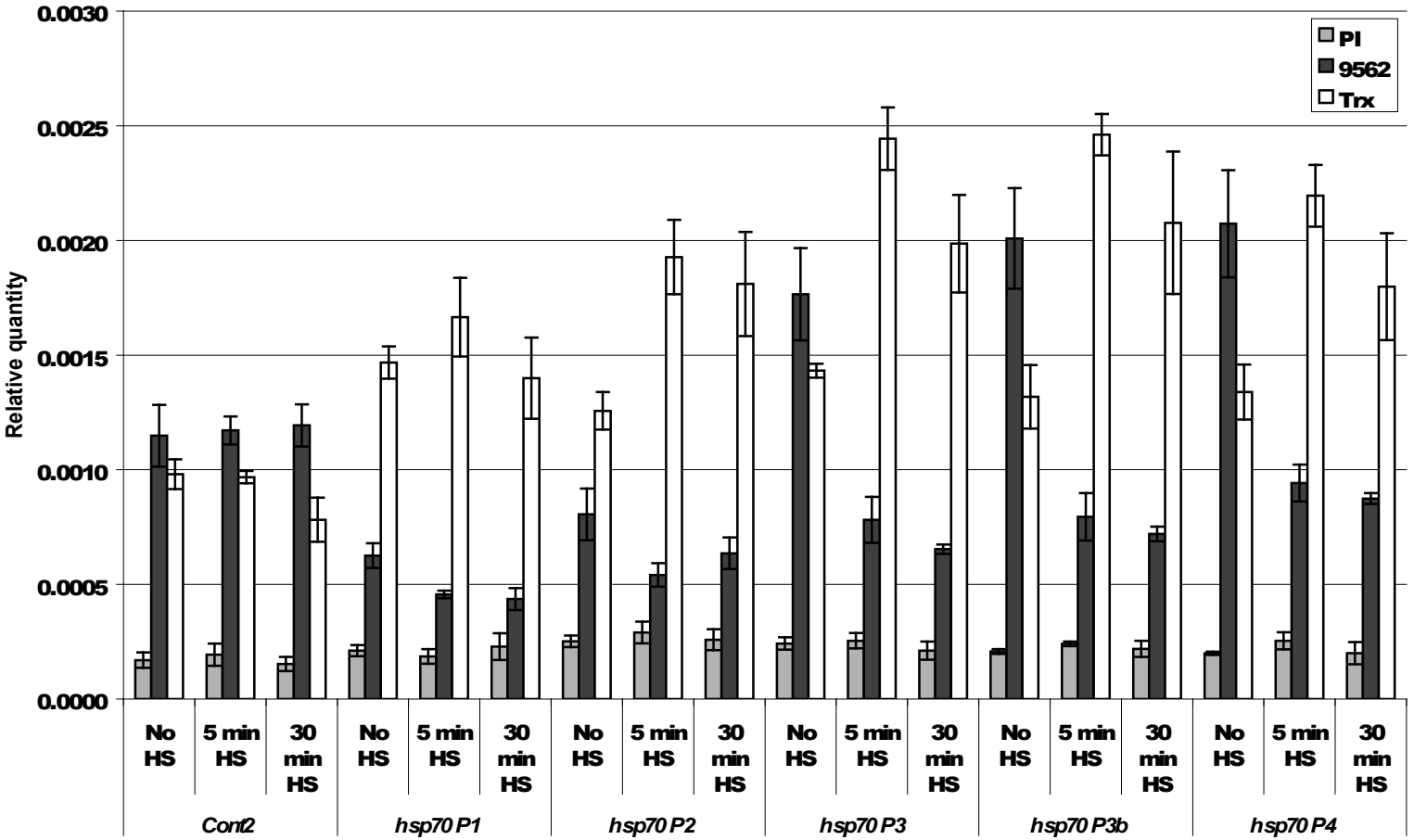

Figure 4.4. Chromatin Immunoprecipitation (ChIP) results from Oregon R embryos.
ChIP using pre-immune serum (PI), menin (9562) or Trithorax (Trx N1) antibodies. Embryos (3-15 hrs) were left untreated (No HS) or heat shocked (HS) for 5 or 30 mins. *Cont2* is a negative control primer set in an intergenic region. *hsp70 P1* and *P2* are in the promoter and site of stalled RNA Pol II, respectively. *hsp70 P3* and *P3b* are in the 5' coding region and *Hsp70 P4* is in the 3' coding region of the gene. Menin shows a decrease in binding to the coding region of *hsp70* with HS while Trx shows an increase in binding. Results are shown as relative quantity based on a standard curve. Results are normalized to input ratios and 2 separate ChIP experiments with 2 separate qPCRs for each were averaged and graphed.

ChIP experiments (see Chapter 2, Section 15 for details) consistently showed that both menin and Trx were localized to *hsp70* prior to heat shock (Figure 4.4). This was somewhat unexpected since we predicted that these proteins would not be present before heat shock but would be recruited, perhaps simultaneously and co-dependently, following heat shock. Menin binding occurred primarily in the coding region of the gene (5' and 3'). Trx binding was also most significant in the coding region; however, Trx also showed some degree of binding in the promoter region, whereas menin binding was negligible there (Figure 4.4). With a short HS (5 mins), a decrease in menin binding was observed and there was no further loss of menin at *hsp70* with a longer HS (30 mins). This decrease in menin binding in *the hsp70* P3, P3b and P4 regions with 5 min or 30 min heat shock was found to be statistically significant; that is, the signal for the No HS condition differed significantly from the 5 min HS and from the 30 min HS conditions; however, there was no significant difference between the 5 min and 30 min HS for menin using the P3, P3b or P4 primer sets (see Appendix E, Table E.1 for a summary of statistical analyses).

Trx binding followed the opposite pattern as that for menin, with an increase in binding with a short HS (Figure 4.4). This increase in Trx binding with heat shock was expected from previous work done in the Mazo lab (Smith et al., 2004). With a longer HS there was some decrease in Trx binding, possibly due to protein degradation occurring with prolonged HS (as observed in immunoblots, Figure 4.2B). The increase in Trx binding at *hsp70* regions spanning P3, P3b and P4 with a 5 min HS was statistically significant; however, there was not a statistically significant difference in the amount of Trx binding with a 30 min HS (see Appendix E, Table E.1). These results were not as

expected since we predicted that both proteins would show a similar pattern of recruitment and binding. The pre-immune control showed minimal binding for all regions of *hsp70*. The relative binding of Trx and menin was higher in the negative control (Cont2) region than the pre-immune serum, suggesting that there is some non-specific binding associated with these antibodies; however, the relative binding in the coding regions was higher than in the Cont2 region.

ChIP was also done using a histone H3 lysine 4 dimethyl (H3K4me2) antibody in OR embryo lysates (Figure 4.5). This experiment was conducted at the same time as that with menin and Trx antibodies (Figure 4.4) but it is displayed on a separate graph due to the differences in the magnitude of the signal with this antibody. H3K4me2 was most prominent in the 5' coding region of *hsp70.* Minimal signal was observed in the promoter region (P1), the region where stalled RNAP II is located near the transcriptional start site (P2) and the 3' coding region (P4) (Figure 4.5). For the 5' coding region, H3K4me2 signal was high under standard conditions but then dropped significantly following a 5 or 30 min heat shock (see Appendix E, Table E.1 for statistical analyses). There was also a decrease in the H3K4me2 at the P1 and P2 regions with a 30 min HS, although the initial level of H3K4me2 was less in these regions than in the 5' coding region (*hsp70* P3 and P3b) (Figure 4.5). The decrease in H3K4me2 that occurred with heat shock was highly reproducible but the result did not agree with what was previously observed in the Mazo Lab (see discussion for more details) (Smith et al., 2004).

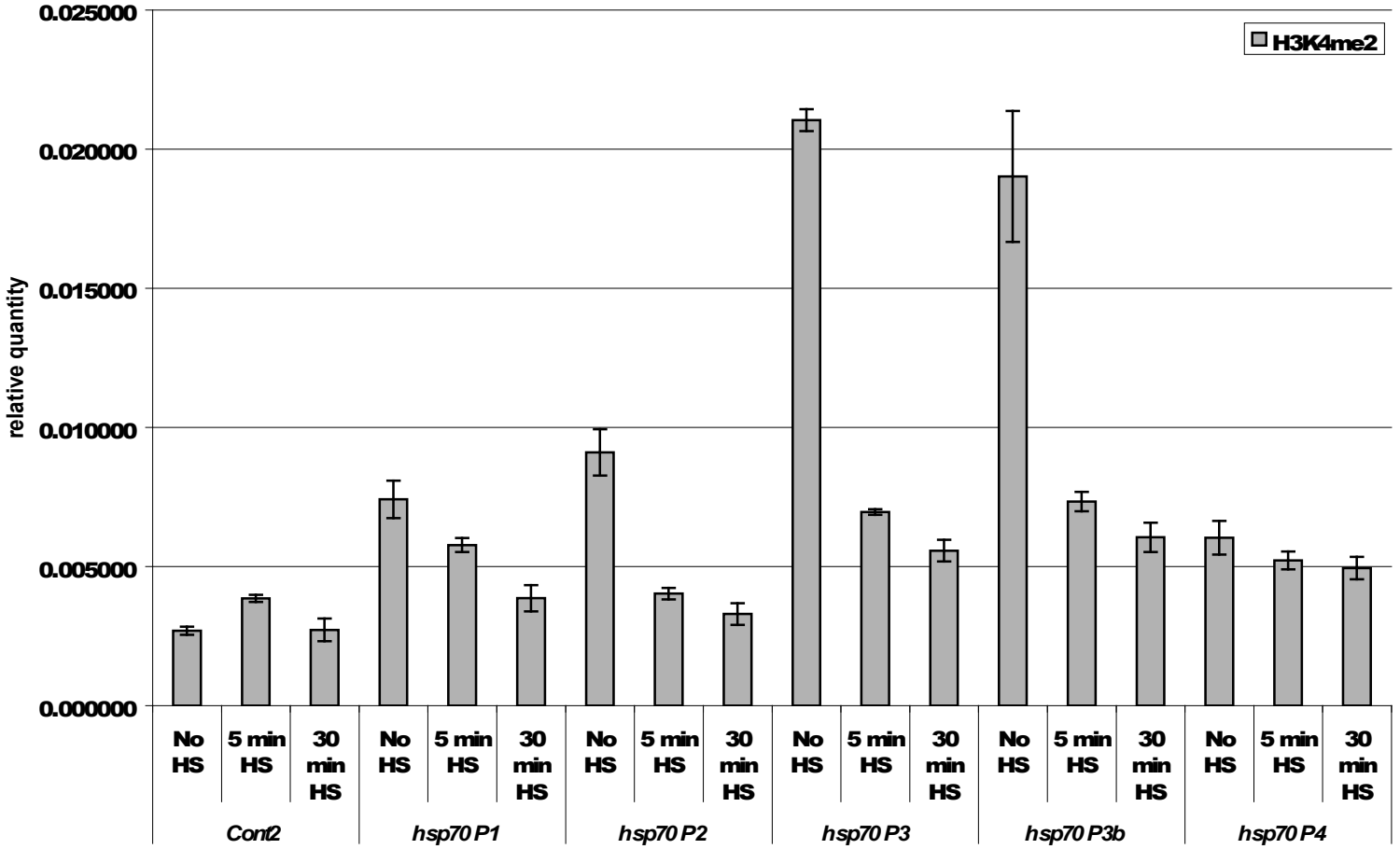

Figure 4.5. Chromatin Immunoprecipitation (ChIP) results from Oregon R embryos using an H3K4me2 antibody.
ChIP was performed with an antibody specific to dimethylated lysine 4 of histone H3 (H3K4me2). Embryos (3-15 hrs) were left untreated (No HS) or heat shocked (HS) for 5 or 30 mins. *Cont2* is a negative control primer set in an intergenic region. *hsp70 P1* and *P2* are in the promoter and location of stalled RNA Pol II, respectively. *hsp70 P3* and *P3b* are in the 5' coding region and *hsp70 P4* is in the 3' coding region of the gene. There is a decrease in H3K4me2 signal in the 5' coding region of *hsp70* with HS. Results are shown as relative quantity based on a standard curve. Results are normalized to input ratios and 2 separate ChIP experiments with 2 qPCRs replicates for each were averaged.

Overall, the results from chromatin immunoprecipitations in OR embryos suggest that menin and Trx are localized primarily to the coding region of *hsp70* before heat shock. Following a short heat shock exposure, menin no longer localizes at *hsp70*, while Trx binding is enhanced. As *Mnn1* mutants could not be examined for Trx binding, it is not possible to conclude whether or not menin is required for recruitment of Trx to *hsp70.*

4. Summary

Overall, results presented in this chapter demonstrate that menin and Trithorax interact in S2 cells through co-immunoprecipitation; thus, this represents a conserved interaction (Figure 4.1). This interaction was predominant under standard cellular conditions and the interaction was lost with exposure to longer heat shock (15 mins or more), with the degradation of Trx protein following heat shock accounting partly for loss of Trx in menin immunoprecipitates (Figure 4.2). An interaction between these proteins in *Drosophila* lysates has not yet been established by co-immunoprecipitation. ChIP studies revealed that in wild-type OR embryos, menin and Trx were bound in the 5' and 3' coding regions of *hsp70* prior to heat shock. While a loss of menin occurred with heat shock, Trx localization to *hsp70* increased (Figure 4.4). Co-localization of menin and Trx was also examined through immunostaining of polytene chromosomes and preliminary results suggest that these proteins overlap at several loci both in the absence and presence of heat shock, although the sites of co-localization could not be mapped (Appendix F, Figures F.1 and F.2).

Work on the menin-Trx interaction ended abruptly after the discovery that there was a problem with the *Mnn1* stocks and the mutants no longer displayed the heat

shock phenotype previously reported (see Chapter 5) (Papaconstantinou et al., 2005). Because the reason for this could not be resolved it was no longer meaningful to study the menin-Trx interaction since the entire project was based on the potential significance of this interaction to the regulation of the heat shock response in *Drosophila*.

It should be noted that work was done to examine a potential role for Trx in the maintenance of genome stability using a loss of heterozygosity assay for the *multiple wing hair* (*mwh*) locus. Most of these results are not valid due to the *Mnn1* stock issues, but trx^{B11} or trx^{Z11} heterozygous mutants did not appear to have any increase in LOH following a chronic heat shock treatment during development (data not shown). In addition, a system for transiently knocking-down *trx* without inducing organismal lethality was developed using a *UAS-*trx^{RNAi} construct and a temperature-sensitive GAL80 to regulate GAL4 function. This work is summarized in Appendix G as it could be useful for any future work on *trx* function in *Drosophila*.

DISCUSSION

1. Menin and Trithorax represent a conserved interaction

Since menin and Trx have independently been implicated in the regulation of *hsp70* expression and the heat shock (HS) response (Papaconstantinou et al., 2005; Smith et al., 2004) and since the interaction between the mammalian homologues has been well established (Hughes et al., 2004; Yokoyama et al., 2004), we hypothesized that the *Drosophila* proteins would interact to coordinate proper expression of *hsp* genes. It was expected that the proteins might not interact, or would interact minimally, under

normal cell culture conditions but that they would associate in response to heat stress. It was predicted that there would be an increase in Trx interaction with menin following heat shock. Furthermore, it was speculated that the proteins would remain associated for the duration of the HS treatment and then possibly dissociate during recovery from heat shock until basal levels of interaction were re-established.

The interaction between menin and Trx in S2 cells was highly reproducible as these co-immunoprecipitation experiments were repeated numerous times. The interaction was readily observed under standard cell culture conditions (Figure 4.1). There was consistently more menin observed in immunoprecipitations with the Trx N1 antibody than with the Trx N6 antibody (Figure 4.1C), which is similar to what was observed in mammals by Yokoyama *et al.* (2004) where more menin was recovered with an antibody against MLL^N than with one against MLL^C. This is likely due to the fact that menin directly interacts with the N-terminal fragment.

Surprisingly, there was a decrease in the amount of Trx protein in menin immunoprecipitations following exposure to heat shock, with the amount of interacting Trx decreasing as the length of heat shock increased (Figure 4.2A). This decrease in Trx binding to menin was partly a reflection of a decrease in the total Trx protein level (detected with the N1 antibody) observed with longer heat shock exposures (Figure 4.2B). Although some Trx protein was still detected after a 1 hr HS, the amount was less than half that observed prior to heat shock exposure (estimated from Figure 4.2B but not determined by band quantification). With a 1 hr HS, Trx protein could not be detected in menin immunoprecipitations (data not shown), suggesting that the remaining Trx protein observed in lysates was not involved in menin interactions. This

could suggest that only a fraction of the total Trx protein interacts with menin. Alternatively, this may suggest that heat shock exposure somehow results in a disruption or inhibition of the interaction. If this is the case then this would suggest that disruption of the menin-Trx interaction occurs as part of a normal heat shock response.

Although an increase in Trx and menin interaction was expected to occur following heat shock, perhaps it is not so surprising that the proteins interact under standard cell culture conditions since the mammalian counterparts also interact in the absence of additional stimuli; that is, they are found to associate under regular cell culture conditions (Hughes et al., 2004; Yokoyama et al., 2004). The mammalian proteins may also respond to developmental cues since their interaction is important for the maintenance of *Hox* gene expression (Chen et al., 2006; Hughes et al., 2004; Yokoyama et al., 2005; Yokoyama et al., 2004). Loss of *Men1* in mice results in embryonic lethality around E11.5, unlike *Mnn1* mutants that are homozygous viable. Thus, even though *trx* is developmentally required, *Mnn1* is not. So while the regulation of *homeotic* gene expression in *Drosophila* is *trx*-dependent, it is presumed to be *Mnn1*-independent as *Mnn1* homozygous mutants do not display any defects in pattern formation (Busygina et al., 2004; Cerrato et al., 2006; Papaconstantinou et al., 2005). Accordingly, only a subset of *trx*-regulated genes might be sensitive to *Mnn1* function in *Drosophila*.

The purification of Trx from embryos led to the isolation of the TAC1 complex, which also includes dCBP and Sbf1 proteins (Petruk et al., 2001). These three proteins form a stable complex involved in the regulation of *Hox* genes, such as *Ubx*, as well as heat shock genes, such as *hsp70* (Petruk et al., 2001; Smith et al., 2004). The purification of the TAC1 complex did not result in the identification of menin as an interacting

protein. This suggests that menin may only interact transiently with Trx and not stably like dCBP and Sbf1. Alternatively, menin may only interact with Trx when it is not in a complex with dCBP and Sbf1. Interestingly, in mammalian cells, initial purification of the MLL1 supercomplex did not reveal menin as an interacting component of this complex (Nakamura et al., 2002). It was only through purification of menin, that the interaction with MLL1 and the other components (RBBP5, WDR5, DPY-30, ASH2L) of the core MLL complex were identified (Hughes et al., 2004; Yokoyama et al., 2004).

It is not yet clear whether menin only interacts with Trx outside of the TAC1 complex or whether menin interacts with Trx when it is associated with dCBP and Sbf1. In an effort to answer this question, an immunoprecipitation with an anti-dCBP antibody (from Dr. Mazo) was attempted. Menin was not detected in this immunoprecipitation, nor was Trx^{N} (using Trx N1 antibody); however, the Trx^{C} fragment was very weakly detected (with Trx N6 antibody) (data not shown). Since Trx^{N} was not detected and Trx^{C} was only very weakly detected this suggests that dCBP interacts directly with the C-terminal fragment. This was also suggested by the fact that trx^{Z11} mutants with a SET mutation have reduced dCBP recruitment to *hsp70* (Smith et al., 2004) and in mammals CBP was shown to bind to TAD of MLL1 which is in the C-terminal fragment (Ernst et al., 2001). In addition, successful co-immunoprecipitations between menin and Trx were probed with the dCBP antibody; however, a band for dCBP was not detected in any of these immunoprecipitations (data not shown). This could suggest that menin interacts with Trx in the absence of dCBP, although it still must be ruled out that the lack of co-immunoprecipitation was not due to inadequate recognition by the dCBP antibody.

2. Comparison of menin and Trx ChIP results with previously published findings

Chromatin immunoprecipitation (ChIP) was used to study menin and Trx binding to various regions of the *hsp70* gene under standard and heat shock conditions. An initial study of menin binding at *hsp70* by Papaconstantinou *et al.* (2005) only investigated its potential localization to the promoter region, where heat shock factor (HSF) binds to the heat shock elements (HSEs). In conditions of overexpression (*nos-GAL4;UAS-Mnn1*), menin was shown to bind to the promoter of *hsp70* (-365 to +5) with heat shock exposure but not to an upstream control region (*hsp70* -998 to -572) (Papaconstantinou et al., 2005). Binding of menin within the coding region of *hsp70* was not examined in this study.

Results from my ChIP analyses of menin binding at *hsp70* in OR embryos cannot be directly compared to those of Papaconstantinou *et al.* (2005) as overexpressed menin may not have the same pattern of recruitment as endogenous menin. That being said, under conditions of menin overexpression their results suggested that there is a heat shock induced recruitment of menin to the *hsp70* promoter. These authors were unable to detect menin binding to the promoter in wild-type embryos with normal menin levels (Singh, N. and Bédard, A. personal communication), which agrees with my results demonstrating that menin binding to the promoter region (P1) was negligible under standard and HS conditions (Figure 4.4). Their observation that menin is recruited to the promoter following heat shock could reflect an artefact of overexpression. This contrasts with my observation that menin binding decreases in the coding region of the gene after heat shock exposure, a region not examined by Papaconstantinou *et al.* (2005).

Previous ChIP experiments examining Trx localization at *hsp70* compared binding in the promoter, 5' coding region and 3' coding region. Trx was primarily bound in the 5' coding region following a 30 min HS, while binding in the promoter and 3' coding region was negligible and no change in signal was observed in these regions with HS (Smith et al., 2004). It is worth mentioning that these early studies were conducted using semi-quantitative methods that are not as sensitive for detection of binding at various regions of *hsp70* as what was described in this chapter using quantitative PCR.

Results for my Trx ChIP experiments did not fully reflect what was previously observed by Smith *et al.* (2004). Similar to what was previously observed, Trx binding was highest in the 5' coding region of *hsp70* (P3 and P3b); however, unlike previous findings, I also observed Trx in the 3'coding region (P4) (Figure 4.4). This difference could reflect the fact that my 3' coding region primers (+1649 to +1754) were further upstream than those used by Smith *et al*. (2004) (+1751 to +2175). Therefore, it is possible that Trx may bind throughout most of the coding region but not at the most distal 3' end. With a short 5 min HS there was increased Trx signal within the coding region and this increase was statistically significant (Figure 4.4 and Appendix E, Table E.1). Surprisingly though, Trx binding did not seem to remain with a longer HS as the signal decreased with a 30 min HS. This differs from what was observed by Smith *et al.* (2004) that also used a 30 min HS and showed an increase in Trx binding to the 5' coding region compared to standard conditions. Since they did not examine a shorter heat shock time, it is possible that there could have been even more amplification with a shorter heat shock than what they observed with a 30 min HS. It is possible that the decrease in Trx observed with a 30 min HS is a reflection of a decrease in total protein

that I observed with longer heat shock exposures (Figure 4.2B). I also observed a small degree of Trx binding in the P1 and P2 regions, although these regions did not show a significant increase in signal with HS; however, the signal in these regions was still higher than with Cont2 primers (Figure 4.4).

Along with investigating menin and Trx binding at *hsp70*, histone modifications associated with the various regions of the gene were also examined using an antibody specific for dimethylated histone H3 lysine 4 (H3K4me2), a mark associated with active gene transcription. Since Trx is a histone methyltransferase, the location of H3K4me was expected to mimic that of Trx. In agreement with this notion, H3K4me2 was most prominent in the 5'coding region of *hsp70* (P3 and P3b), with comparatively low levels in the promoter and 3'coding region (Figure 4.5). The specific localization of H3K4me2 only to the 5' coding region, is similar to what was observed by Smith *et al.* (2004). For the 5' coding region, H3K4me2 signal was high without HS and then dropped significantly following 5 or 30 min HS. This result did not agree with that of Smith *et al.* (2004) and seems counterintuitive since an increase in H3K4 methylation would be expected with heat shock to accompany the dramatic increase in *hsp70* transcription. A possible explanation for this discrepancy is that with heat shock the gene may become predominantly trimethylated (Adelman et al., 2006; Ardehali et al., 2011). Thus, if the antibodies are in fact as specific as they claim and only recognized the dimethylated form, then with increasing heat shock you would observe a decrease with the dimethyl-specific antibody as these histones become trimethylated. This could perhaps explain the results of this experiment but does not explain why Smith *et al.* (2004) observed an increase in H3K4me2 with heat shock. Other researchers have mentioned that there can

be cross-reactivity with antibodies for specific histone modifications, for example some H3K4me3 antibodies also recognize H3K4me2 (Ardehali et al., 2011; Cosgrove and Patel, 2010; Kohlmaier et al., 2004). Although this is entirely speculation, perhaps a different H3K4me2 antibody was used by Smith *et al.* (2004) and it was not specifically recognizing only H3K4me2.

Another possible explanation for a decrease in H3K4me2, is that there may be a loss of nucleosomes at *hsp70* associated with the high levels of transcription required in response to heat stress. A study from John Lis' lab demonstrated that there is a rapid decrease in nucleosomes at *hsp70* after heat shock (Petesch and Lis, 2008). Although there is still detectable histone H3 bound to the gene, after a 2 min HS, the level is 3 times less than under no HS conditions. According to this observation, a decrease in H3K4me2 signal would not be surprising, although this observation also disagrees with that of Smith *et al.* (2004). Incorporating the use of a total histone H3 antibody as well as an antibody specific for H3K4me3 should help resolve the interpretation of the ChIP results for H3K4me2.

3. Control of the heat shock response by the menin-Trx interaction

Overall, the ChIP results in OR embryos suggest that both menin and Trx bind to the 5' coding region of *hsp70* under standard conditions and that following heat shock treatment there is a loss of menin but an increase in Trx. This indicates that the interaction is more complex and transient than initially predicted. The localization of menin and Trx to *hsp70* prior to heat shock suggests that these proteins may be there so that the gene is primed and ready for a rapid response. This idea is not surprising given the knowledge that RNAP II is also loaded and stalled on *hsp70* so that a rapid response

can be elicited (O'Brien and Lis, 1991). Perhaps menin plays a role in the recruitment of factors necessary for maintenance of active transcription and then must be lost before Trx or other unidentified factors can be fully loaded on the gene. It is also possible that the interaction between menin and Trx that was observed in co-immunoprecipitation experiments does not occur at the *hsp70* locus as we predicted. On the other hand, it is possible that the interaction of menin with Trx prevents Trx from interacting with other factors, perhaps dCBP and Sbf1, that are required to maintain high levels of *hsp70* expression during heat stress. This could also explain why menin was not observed in the stable TAC1 complex isolated by Petruk *et al.* (2001). Menin's interaction with Trx is likely just transient and could be important for regulation of the TAC1 complex or for recruiting additional factors to *hsp70*.

The observation of menin and Trx binding in the coding region of *hsp70*, but not in the promoter region, agrees well with the previously published localization of Trx (Smith et al., 2004). In addition, some work in mammalian cells showed that menin and MLL1 were localized to the 5'coding region of some of their target genes (*e.g.* $p27^{Kip1}$, $p18^{INK4c}$) (Milne et al., 2005). In contrast, others found that menin and the MLL complex associated with the promoter and 5'UTR but not the coding region of *Hoxa9* (Chen et al., 2006). In mammalian cells there is evidence that menin is required for MLL recruitment to target genes since $Men1^{-/-}$ MEFs have defects in MLL recruitment to *p27* and *p18* (Milne et al., 2005). So far, there is no evidence that the same holds true in *Drosophila* as the analysis of *Mnn1* mutants is necessary to answer such questions.

4. Discussion of the various Drosophila histone methyltransferase complexes

Recent studies identified dSet1 (CG4031) as the primary H3K4 histone methyltransferase (HMT) for di and trimethylation associated with global activation of transcription in *Drosophila* (Ardehali et al., 2011; Hallson et al., 2012; Mohan et al., 2011). dSet1 was found to be a component of a conserved COMPASS-like complex. Knock-down of *dSet1* with RNAi, but not knock-down of *trr* (*trithorax-related*) or *trx*, resulted in global loss of H3K4me2 and H3K4me3 marks. In addition, dSet1 co-localized with these marks of active gene transcription on polytene chromosomes (Ardehali et al., 2011). Similar conclusions were made by another group that observed that *dSet1* mutants had severely reduced H3K4me2 and H3K4me3 levels from late larval stages onward (Hallson et al., 2012). They also examined the other known *Drosophila* HMT mutants, *trx* (trx^{Z11}/ trx^{B11}), trr^{1} and *ash1* ($ash1^{B1}$/$ash1^{B7}$), and did not observe such widespread effects on H3K4me2 and H3K4me3 patterns. These results suggested that Trx, Trr and Ash1 likely have specific targets or could be more important for early developmental stages than dSet1 (Hallson et al., 2012).

Other prior studies support the notion that Trx (or Ash1, which was later found to be an H3K36 HMT) is not the primary HMT responsible for H3K4me3 *in vivo*. In this study trx^{1} temperature-sensitive mutants did not show any decrease in H3K4me2 or H3K4me3 on salivary gland polytene chromosomes at the restrictive temperature (Srinivasan et al., 2008). This suggests that because there was no global alteration in H3K4me levels in *trx* mutants, Trx targets may be limited to a specific group of genes, such as the *homeotic* genes.

A third study published around the same time as that of Ardehali *et al.* (2011) and Hallson *et al.* (2012) also biochemically characterized the dSet1 COMPASS-like complex as well as the *Drosophila* Trithorax COMPASS-like and Trithorax-related COMPASS-like complexes (Mohan et al., 2011). They did not isolate Trx in the TAC1 complex (Petruk et al., 2001) but instead found Trx in a COMPASS-like complex similar to those formed by MLL1 and MLL2 orthologues in mammals (Mohan et al., 2011). Similar to Ardehali *et al.* (2011) and Hallson *et al.* (2012) they found that dSet1 is the primary HMT for the establishment of H3K4me2 and H3K4me3; this was demonstrated by RNAi-mediated knock-down of *dSet1*, *trx* or *trr* in wing imaginal discs followed by immunostaining for H3K4me3 or H3K4me2 and also through polytene chromosome staining of RNAi flies (Mohan et al., 2011).

In this study of the *Drosophila* HMT complexes, they purified Ash2 from S2 cells in order to identify the proteins of the *Drosophila* complexes; Ash2 was used since the homologue Ash2L is a common component of all the mammalian COMPASS-like complexes. They successfully co-purified dSet1, Trx and Trr as well as several other proteins that were homologous to mammalian proteins that were either shared by these complexes or were unique to a single complex. Among these, menin was identified in the Ash2 immunoprecipitates that were subjected to protein identification analyses (Mohan et al., 2011). To further characterize each of the *Drosophila* HMT complexes, they also wanted to purify each complex individually using a unique protein from each of the homologous mammalian complexes- Wdr82 for the dSet1 complex, dUTX or dPA1 for the Trr complex, and menin for the Trx complex. Strangely, they report that they were not able to detect FLAG-HA-*Mnn1* expression so the Trx-specific components were

deduced to be the Ash2-associated proteins that were not found in the dSet1 and Trr isolated complexes (Mohan et al., 2011). In this paper, the authors present a schematic showing menin interacting with Trx in the Trx COMPASS-like complex although a direct interaction was not investigated and no experimental evidence was provided to support this in the study. But this may strengthen the validity or reliability of my observation that menin and Trx interact in S2 cells (Figure 4.1 and 4.2). Although the authors do not discuss this, there was a single menin peptide identified in the dSet1 purified complex. This may just be an artefact or it could suggest that menin may weakly or transiently associate with the dSet1 complex as well.

Since this study identified menin as a component of a Trx COMPASS-like complex in *Drosophila* (Mohan et al., 2011) but menin was not identified as a component of the TAC1 complex (Petruk et al., 2001), this could suggest that menin associates more strongly or stably with Trx when it is in the Trx COMPASS-like complex than when it is in the TAC1 complex. Also, since dCBP and Sbf1 were not identified along with menin and Trx in the Ash2 immunoprecipitate (Mohan et al., 2011), this lends some support to the prediction that perhaps menin only associates with Trx in the absence of dCBP and Sbf1.

The story of the *Drosophila* HMT complexes is further complicated by the observation by Ardehali *et al.* (2011) that dSet1 is important for the regulation of *hsp70*, *hsp26* and *hsp83*. Using live imagining of salivary gland cells, they showed that EGFP-dSet1 was rapidly recruited to *hsp70* loci following heat shock. They observed that the peak signal for dSet1 recruitment to heat shock puffs occurred within 6 mins of HS and then began to slowly decline between 8-15 mins to 50 % of its maximal intensity. Similarly, RNAP II signal reaches its maximum level around 8 mins of HS (Ardehali et al.,

2011). Using RNAi-mediated knock-down of *dSet1* in S2 cells, followed by RT-qPCR analysis of mRNA transcript levels, a reduction in *hsp70* and *hsp26* expression was observed. Interestingly, for the first 10 mins of HS, the expression pattern of the *hsp* genes was not affected by loss of dSet1. *dSet1* RNAi and *LacZ* RNAi controls had a similar expression pattern of *hsp70* mRNA for the first 10 minutes, which represented the initial activation phase where only low expression was observed; however, there was a dramatic increase in *hsp70* and *hsp26* mRNA between 10-20 mins of HS in control RNAi cells but *dSet1* RNAi cells displayed significantly reduced transcript accumulation during this phase (Ardehali et al., 2011). This is similar to the HSP70 protein profile observed for *Mnn1* mutants, where for the first 15 mins of HS a normal expression pattern was observed but with longer HS, protein expression was abolished (Papaconstantinou et al., 2005).

Moreover, H3K4me3 levels along *hsp* genes were low along the entire gene before heat shock, with a substantial increase in the region surrounding the transcriptional start site observed by 5 mins. Increased H3K4me3 was also observed in the first 1000 bp of the *hsp* coding regions by 5 mins; however, the level was not as high as that observed near the transcriptional start site and there was minimal signal at the 3' end. There was no major increase in H3K4me3 after 5 mins HS (Ardehali et al., 2011). The pattern of dSet binding at *hsp70* and *hsp26* mirrored that of the H3K4me3 levels with respect to both location within the gene and increase with heat shock. The level of H3K4me3 in *dSet1* RNAi cells was dramatically reduced, suggesting that dSet1 was responsible for the observed H3K4me3 at *hsp70*. In my ChIP experiments with H3K4me2, I observed lower signal in the promoter and transcriptional start regions than I did in the 5' coding region

and also observed minimal binding in the 3' end of *hsp70* (Figure 4.4). I observed a dramatic decrease in H3K4me2 with a 5 min HS that could correspond to the rapid increase in H3K4me3 that occurs at this time, assuming the antibodies were specific for the different methylation levels. The observation that H3K4me3 at *hsp70* is dependent on dSet1, contradicts the observations by Smith *et al.* (2004) that show that trx^{B11} mutants have reduced H3K4me2 with a 30 min HS, unless these two HMTs somehow function together to coordinate H3K4 methylation at *hsp70*.

If dSet1 is the primary histone methyltransferase in *Drosophila* and is responsible for the H3K4me3 at *hsp70* in response to heat stress then this could suggest that Trx is not essential for this function. This could explain why trx^{B11} mutants only showed reduced *hsp70* mRNA levels with a 30 min HS but that expression was not completely abolished in these mutants (Smith et al., 2004). It would be interesting to determine whether loss of *trx* results in a heat shock lethality phenotype, or if the presence of dSet1 is able to compensate for the loss of Trx. Examination of the *trx* HS lethality phenotype was planned for trx^{RNAi}*;tub-GAL80*^{ts}*/tub-GAL4* flies but not completed (Appendix G).

Perhaps, dSet1 and Trx functions at *hsp70* are redundant and the existence of two HMTs that function at *hsp70* serves as a safeguard due to the importance of *hsp70* for survival when exposed to heat stress. Although, since mutations in both genes are lethal, it is hard to imagine a scenario where one protein would need to compensate in the absence of the other (Breen, 1999; Hallson et al., 2012). Unless of course Trx function was needed to supplement that of dSet1 at *hsp70* due to its global action in histone methylation. Alternatively, the two proteins could localize and modify histones

at different regions of *hsp70* or different stages of transcription/elongation. This is proposed since dSet1 localized primarily at the transcriptional start site (Ardehali et al., 2011) while Trx localized mainly to the 5' coding region (Smith et al., 2004). Also, Trx was shown to co-immunoprecipitate with p-Ser2 RNAP II which is associated with the elongation phase of active transcription (Smith et al., 2004), while dSet1 was found to co-localize on polytene chromosomes with p-Ser5 and p-Ser2 RNAP II so it could associate with the promoter paused and elongating forms of RNAP II (Ardehali et al., 2011). Furthermore, *dSet1* knock-down in cells leads to a modest increase in RNAP II at the promoter and 5' end of *hsp70* and a reduction in downstream regions; thus, the authors predict that dSet1 might be important for the release of stalled RNAP II that allows for productive transcriptional elongation (Ardehali et al., 2011). Thus, due to its localization primarily within the coding region of the gene and its absence in the promoter region, Trx could function during the productive elongation phase in order to maintain an active transcriptional status (Smith et al., 2004).

Overall, these studies of the *Drosophila* histone methyltransferase complexes illustrate that most active genes are regulated by dSet1 HMT activity, especially from larval stages onward, while Trx/TAC1 and Trr complexes have specific targets during development such as the *homeotic* genes and hormone response genes, respectively (Petruk et al., 2001; Sedkov et al., 2003). The regulation of *hsp* genes by the different HMT complexes is unclear, as both the Trx/TAC1 complex and dSet1 COMPASS-like complex have been implicated in the regulation of these heat stress responsive genes. The role of the Trx COMPASS-like complex and its target genes have not been studied yet, but it is possible that this complex may regulate a distinct set of genes from the

Trx/TAC1 complex. Although, since the mammalian MLL1/2 complexes are homologous to the *Drosophila* Trx COMPASS-like complex, and not the Trx/TAC1 complex, this would suggest that the Trx COMPASS-like complex would be involved in the regulation of *homeotic* gene expression due to the function of MLL1/2 complexes in regulation of *Hox* gene expression. However, *homeotic* gene regulation has already been shown for the *Drosophila* TAC1 complex (Petruk et al., 2001). How exactly menin fits in with these two Trx complexes remains to be elucidated. Perhaps, menin functions to coordinate whether Trx functions within the TAC1 complex or within the Trx COMPASS-like complex. Or maybe the two complexes coordinate different stages of gene expression. For example, the Trx COMPASS-like complex may function more in the initial entry into active transcriptional elongation while TAC1 may function more to maintain this active chromatin structure for prolonged gene expression.

Other studies have suggested that the TAC1 complex may be more important for the histone acetylation function provided by dCBP than for the histone methylation function provided by Trx (Tie et al., 2009). The initial isolation and characterization of the TAC1 complex demonstrated that there was histone acetylation activity associated with this complex. *In vitro* acetylation was observed against the four core histones and also mononucleosomes and oligonucleosomes (Petruk et al., 2004). The specific residues acetylated by dCBP of the TAC1 complex were not determined in this study. When the TAC1 complex was demonstrated to be important for the regulation of heat shock genes an acetyl H3 antibody (residues not specified in the paper but assumed to be the commonly used H3ac(K9/K14) polyclonal antibody from Millipore) was used to demonstrate that trx^{B11} and nej^{Q7} (dCBP) have defects in histone H3 acetylation at *hsp70*

following heat shock. However, recent experiments suggest that histone H3K9/K14ac may not reflect TAC1-dependent acetylation. Acetylation of H3K27 in mice and humans was not identified until 2007 (Garcia et al., 2007) and was not demonstrated in *Drosophila* until 2009 (Tie et al., 2009). Interestingly, dCBP was identified as the HAT responsible for H3K27ac and Trx was required for dCBP-mediated H3K27ac of polycomb target genes associated with active transcription. This suggested that the inhibition of polycomb silencing by Trx occurred through H3K27 acetylation which precluded the H3K27 methylation that is associated with gene silencing (Tie et al., 2009). In addition to the acetylation of H3K27, these authors also demonstrated that dCBP is capable of acetylating H3K18, but was not shown to acetylate H3K9 or H3K14 (Tie et al., 2009). Thus, it would be interesting to examine H3K27ac at *hsp70* as a readout for the importance of dCBP in the regulation of *hsp70* expression.

5. Future Directions

An interaction between menin and Trx has not yet been demonstrated in fly lysates and this should be done to further validate the interaction. Preparation of nuclear extracts for immunoprecipitations, an approach used in Dr. Mazo's lab for studying Trx interactions, may improve chances of detecting this interaction in embryo lysates (Petruk et al., 2001). There were several experiments planned that were not conducted, such as the temperature-sensitive knock-down of *trx* via RNAi utilizing the GAL80/GAL4 system to study the genetic interaction between *Mnn1* and *trx* (Appendix G).

Additional work was also planned for the ChIP experiments, such as examining total H3, H3K4me3 and H3ac levels to answer some of the questions regarding the histone modifications at *hsp70* associated with heat shock. Furthermore, the intention

was to compare Trx binding and *Mnn1* mutants to determine if menin was required for Trx localization or histone modification at *hsp70*. Unfortunately, this project came to an abrupt end after the discovery of problems with the *Mnn1* mutants and loss of the heat shock phenotype (see Chapter 5), making it futile to study this interaction in the context of the heat shock response.

Due to the recent characterization of the *Drosophila* HMT complexes, it may be interesting to investigate the importance of menin in the Trx COMPASS-like complex and identify target genes for this complex. Furthermore, studies could determine whether menin interacts with Trx in the TAC1 complex or in the COMPSS-like complex, and whether the interaction of menin with Trx prevents the association of other complex components.

6. Conclusions

The main conclusion for the research outlined in this chapter is that menin interacts with Trithorax and this represents a conserved interaction in *Drosophila*. This interaction was most prominent under standard cell culture conditions and decreased with heat stress exposure. Analysis of menin and Trx binding in chromatin immunoprecipitations suggested that these two proteins are localized at *hsp70* prior to heat shock and are localized primarily to the coding region of the gene. Heat shock exposure resulted in a loss of menin binding at *hsp70* but an increase in Trx localization. Overall, no evidence has been provided to support the hypothesis that menin is required for the recruitment of Trx to *hsp70* in response to heat stress.

CHAPTER 5. ANALYSIS OF *MNN1* STOCKS AND ATTEMPTS TO REPRODUCE THE *MNN1* HEAT SHOCK PHENOTYPE

INTRODUCTION

1. Review of previously described Mnn1 phenotype

The *Drosophila Mnn1* mutant phenotypes that have been described in the literature will be reviewed here since most of the results described in this chapter involve a direct comparison to the previously reported phenotypes (please see Chapter 1, Section 12 for additional details on *Drosophila Mnn1* mutants). $Mnn1^{-/-}$ flies established in three independent labs, including the Campos lab, were all described as viable and fertile with no obvious phenotypes (Busygina et al., 2004; Cerrato et al., 2006; Papaconstantinou et al., 2005). *Drosophila* lines overexpressing menin (*UAS-Mnn1*) or down-regulating menin through RNA interference (RNAi) via expression of a dsRNA construct (*UAS-Mnn1-RNAi*), as well as deletion mutants, $Mnn1^{e30}$ and $Mnn1^{e173}$, were sensitive to various stresses. The disruption of normal *Mnn1* expression resulted in increased lethality compared to control lines when exposed to heat shock, hypoxia, hyperosmolarity and oxidative stress (Papaconstantinou et al., 2005). As both overexpression and down-regulation of *Mnn1* resulted in increased stress sensitivity, this suggested that proper menin expression was necessary for the regulation of the *Drosophila* stress responses.

The heat stress phenotype that resulted from menin misexpression was further characterized and was found to coincide with improper regulation of heat shock gene expression in embryos exposed to heat stress. *Mnn1* deletion mutants and *Mnn1-RNAi* embryos had normal expression of HSP70 with short heat shocks (HS) (*e.g.* 5 or 15 min HS) but no longer expressed the HSP70 protein with longer heat shocks (*e.g.* 30 min or 1

hr HS). HSP23 was expressed at the 15 min time point for *Mnn1*^{e30} mutants but was absent with longer heat shock exposures. While wild-type embryos had complete down-regulation of HSP70 and HSP23 expression after 3 hours of recovery from a 1 hour HS exposure, *UAS-Mnn1* embryos maintained high HSP70 protein levels for a longer time after recovery from HS, with protein still observed 5 hours after the HS was removed (Papaconstantinou et al., 2005). In addition, using a strain harbouring an *hsp70-LacZ* promoter construct, *UAS-Mnn1* embryos showed increased *hsp70* promoter activity while *Mnn1-RNAi* embryos had reduced promoter activation. A chromatin immunoprecipitation (ChIP) assay also showed that overexpressed menin localized to the promoter of *hsp70* following heat shock (Papaconstantinou et al., 2005). Taken together, these results suggest that menin is a positive regulator of heat shock protein (HSP) expression in response to heat stress.

Furthermore, microarray analysis of *Mnn1*^{e30} and *Mnn1-RNAi* embryos showed that menin was required for sustained expression of multiple heat shock genes with a prolonged heat stress (1 hr) but was not required for the initiation of heat shock gene expression with a short heat shock (10 mins) (Papaconstantinou et al., 2010). Moreover, loss of menin function was associated with increased genome instability when exposed to chronic sub-lethal stress during embryonic and larval development. This was observed through a loss of heterozygosity (LOH) assay for the *multiple wing hair* (*mwh*) locus. *Mnn1* deletion mutants and *Mnn1-RNAi* flies, that were also heterozygous for *mwh*, showed increased LOH with chronic heat stress or hypoxia compared to untreated flies of the same genotype (Papaconstantinou et al., 2010). Thus, menin is required for the maintenance of genome stability in response to stress. This was not solely due to its

role in regulation of *hsp70* expression as *Mnn1;hsp70A⁻B⁻* double mutants showed increased LOH compared to either single mutant (Papaconstantinou et al., 2010). In agreement with the LOH assay results, another group found that *Drosophila Mnn1* mutants are hypersensitive to both ionizing radiation and DNA cross-linking agents, as established by increased mutational rates; this suggests a potential defect in DNA repair and a role for menin in the maintenance of genomic integrity (Busygina et al., 2004).

2. Objectives

The work summarized in this chapter differs from that described in the previous chapters where menin interactions were investigated followed by *in vivo* experiments to investigate the functional significance of the interactions. Furthermore, the work described in this chapter does not reflect the typical hypothesis-based research. Instead, this work arose due to a suspicion with the *Mnn1* stocks and a personal need to appease any doubt before continuing with other planned research. The initial objective was to use PCR-based genotyping to confirm that *Mnn1* mutants contained the expected deletions. From there, new objectives arose and each step led systematically to the next. Unfortunately, what was anticipated to be a quick genotype confirmation, led to extensive genotyping of the entire *Mnn1* stock collection in the Campos lab. Following the discovery of wide-spread stock contamination, *Mnn1* deletion alleles were recovered from contaminated stocks. This was followed by a re-examination of the phenotypes previously described by Maria Papaconstantinou (Papaconstantinou et al., 2005). Finally, attempts were made to recapitulate the previously described phenotype and eliminate factors that could be contributing to the observed loss of phenotype. As this research developed progressively with each observation dictating how to proceed

with the next step, it will be described in this manner with the results and rationales for subsequent experiments presented together. Please see Chapter 2, Sections 16-18 for details of the experimental protocols.

RESULTS

1. PCR-based genotyping of Mnn1 stocks

1.1 PCR testing of the Mnn1 deletion stock collection

The *Mnn1* imprecise excision mutants were generated and the deletions were characterized in 2005. At the time, the mutated regions of the deletion alleles were mapped by PCR and sequencing; however, since their creation, the presence of the deletions in the stocks were never verified through sequencing or PCR-based techniques. As many years had passed since the genotype was verified, this seemed like an essential action before proceeding with planned experiments. In addition, I suspected that there may have been a problem with the mutants since I was observing a high level of background binding of the menin 9562 antibody in ChIP experiments with the *Mnn1* mutants (data not shown).

Primers were designed to assess whether or not the *Mnn1* stocks ($Mnn1^{e30}$ and $Mnn1^{e173}$) still contained the previously characterized deletions (Papaconstantinou et al., 2005). Since the deletions in both mutants span exon 2 and exon 3, primers were designed to amplify a 160 bp fragment and 150 bp fragment from each exon, respectively (see Table 2.2 for primer sequences). Using these primers in standard PCR, a pure $Mnn1^{e30}$ or $Mnn1^{e173}$ stock should not show any amplification; whereas a wild-type allele should show the appropriate size fragment for each primer set (see Figure

5.1A). Furthermore, a positive control primer set was designed for a 294 bp fragment of exon 5 that is present in both *Mnn1* mutants and wild-type. Use of this primer set would ensure that a lack of amplification with exon 2 or 3 primers was not due to a problem with the DNA sample.

As input DNA from ChIP experiments was available for immediate testing this was examined first. OR, $Mnn1^{e30}$ and $Mnn1^{e173}$ genomic DNA was tested with exon 3 primers followed by standard PCR. Results confirmed that $Mnn1^{e30}$ contained the exon 3 deletion, whereas $Mnn1^{e173}$ did not (Figure 5.1B). Simultaneously, ChIP input DNA from Flora Suen's stocks was tested and both $Mnn1^{e30}$ and $Mnn1^{e173}$ DNA had amplification of exon 3, indicating contamination of both stocks with a wild-type allele (Figure 5.1B). Following these disconcerting results, I decided to do a wide-scale screening of all stocks that were supposed to contain *Mnn1* deletions in order to assess the severity of the stock contamination. To do so, I used a simple and rapid DNA isolation method from whole flies (adapted from Gloor et al., 1993). For each stock, the DNA sample was prepared from 5 homozygous male flies pooled together. Approximately 50 different stocks expected to have either $Mnn1^{e30}$ or $Mnn1^{e173}$ deletion alleles were examined, including those from Flora Suen and Jennifer Erickson (Please see Table 5.1 for the genotypes and corresponding genotype ID numbers used in the Figures). Overall, the results were quite disturbing as contamination was widespread. Essentially, all $Mnn1^{e173}$ stocks were contaminated with a wild-type allele and all $Mnn1^{e30}$ stocks from the Suen and Erickson collections were contaminated as shown by amplification of both the exon 2 and exon 3 fragments (Figure 5.2). The only stocks that were still pure mutants were my $Mnn1^{e30}$ stock and all double mutants created from it.

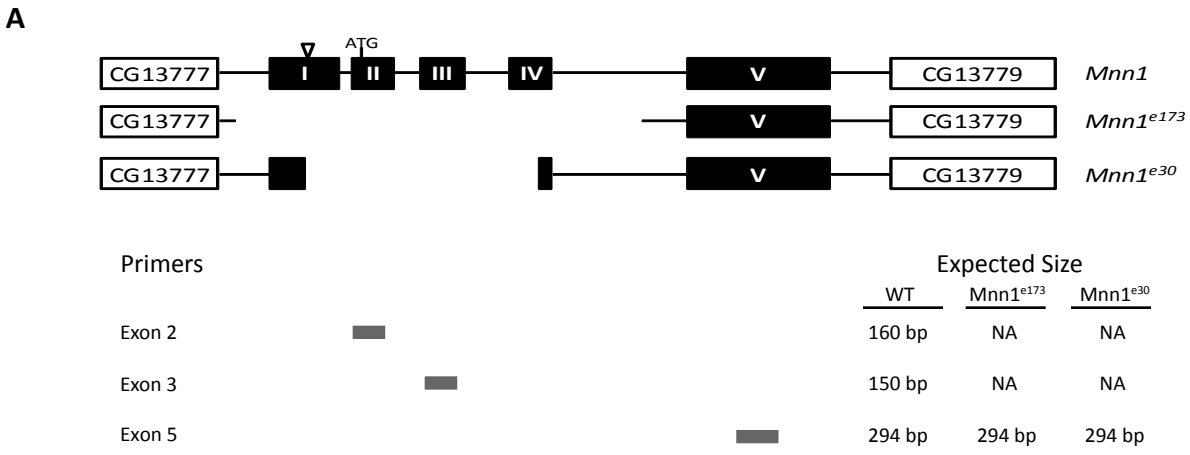

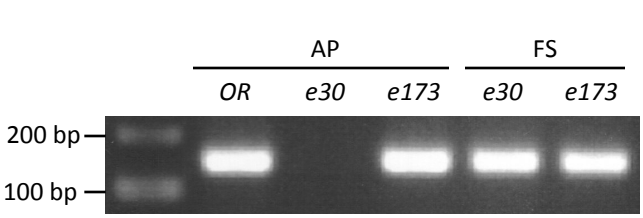

Figure 5.1. Screening of *Mnn1* mutants for expected deletions.
A) Schematic of the *Mnn1* gene and *Mnn1* deletion mutants (adapted from Papaconstantinou et al., 2005). The triangle shows the approximate location of the P-element in the insertion line. Below the schematic the approximate location of the primer sets and the expected size of the amplicon in WT and mutant backgrounds are shown. Note that the diagram is not drawn perfectly to scale. NA = No amplification expected. B) Screening of ChIP input DNA with exon 3 primers. *Mnn1*^{e30} from the AP sample did not show amplification and thus the deletion was still present. *Mnn1*^{e173} from both the AP and FS samples as well as *Mnn1*^{e30} from the FS sample no longer had the deletion and thus were contaminated stocks. AP=Alicia Pepper; FS=Flora Suen.

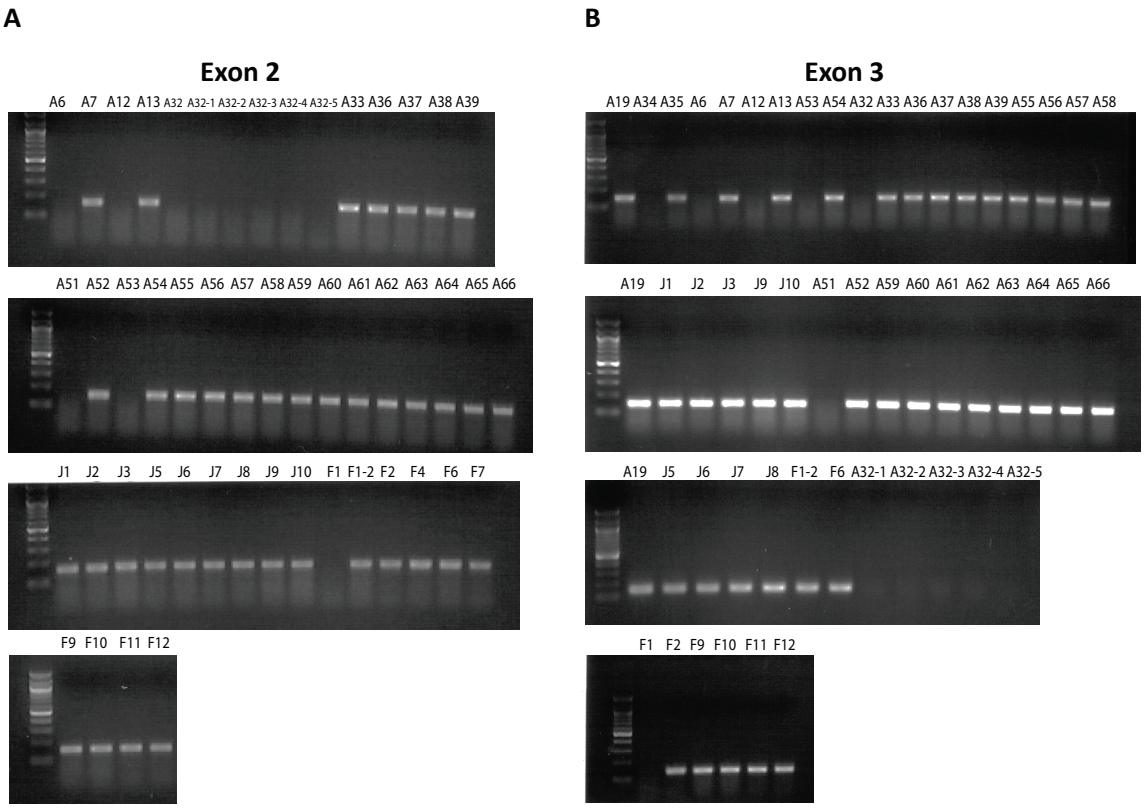

Figure 5.2. Screening of *Mnn1* stock collection for expected deletions.
Screening of multiple stocks that were supposed to be *Mnn1* deletion mutants using exon 2 (A) and exon 3 (B) primers. All stocks were expected to be mutant and not show amplification with the exon 2 or exon 3 primers except A19 (Oregon R). See Table 5.1 for a list of the genotypes associated with the given ID#. Note that the order of samples is not the same in A and B. Results for a given sample are consistent with both primer sets. Results for exon 5 primers are not shown, but amplification of the 294 bp fragment was observed for all lines as expected.

Table 5.1. Genotypes and corresponding ID# used for PCR screening of *Mnn1* stocks.

ID#	GENOTYPE	ID#	GENOTYPE
A6	$yw; Mnn1^{e30}$ $(lost\ T_S; T_L)$	A63	$Mnn1^{e173}; \frac{Trx^{Z11}, mwh}{TM3, Sb}$ $(Recomb\ \#10)(lost\ SM5)$
A7	$yw; Mnn1^{e173}$ $(lost\ T_S; T_L)$	A64	$Mnn1^{e173}; \frac{Trx^{Z11}, mwh}{TM3, Sb}$ $(Recomb\ \#15)(lost\ SM5)$
A12	$yw; Mnn1^{e30}; FADD^{f02804}$ $(T_S; T_L stock\ \#1)$	A65	$Mn1^{e30}; \frac{Trx^{Z11}, mwh}{TM3, Sb}$ $(Recomb\ \#10)(lost\ SM5)$
A13	$yw;\ Mnn1^{e173};\ FADD^{f02804}$ $(T_S; T_L stock\ \#1)$	A66	$Mnn1^{e30}; \frac{Trx^{Z11}, mwh}{TM3, Sb}$ $(Recomb\ \#15)(lost\ SM5)$
A19	*Oregon R*	F1	$yw;\ Mnn1^{e30}$ $(CyO(y^+)\ stock)$
A32	$yw;\ Mnn1^{e30}$ $(CyO(y^+)\ stock)$	F2	$yw;\ Mnn1^{e173}$ $(CyO(y^+)\ stock)$
A33	$yw;\ Mnn1^{e173}$ $(CyO(y^+)\ stock)$	F4	$yw;\ Mnn1^{e30};\ Hsp70A^-B^-, mwh\ (T_S; T_L stock)$
A34	$yw;\ Mnn1^{e30}$ $(homozygous\ stock\ , Oct\ 2009)$	F6	$yw;\ Mnn1^{e173};\ Hsp70A^-B^-, mwh\ (T_S; T_L stock)$
A35	$yw;\ Mnn1^{e173}$ $(homozygous\ stock\ , Oct\ 2009)$	F7	$yw;\ Mnn1^{e30};\ p53^1, mwh\ (T_S; T_L stock)$
A36	$w^+;\ Mnn1^{e30}; mwh\ (lost\ SM5\ \&\ TM3)$	F9	$yw;\ Mnn1^{e30};\ Hsp70A^-B^-$
A37	$w^+;\ Mnn1^{e173}; mwh\ (SM5\ stock; lost\ TM3)$	F10	$yw;\ Mnn1^{e173};\ Hsp70A^-B^-$
A38	$w^+;\ Mnn1^{e30};\ p53^1\ (SM5\ stock; lost\ TM3)$	F11	$Mnn1^{e173};\ p53^1$
A39	$w^+;\ Mnn1^{e173}; p53^1\ (SM5\ stock; lost\ TM3)$	F12	$Mnn1^{e30};\ p53^1$
A51	$yw; Mnn1^{e30};\ FADD^{f02804}$ $(T_S; T_L stock\ \#2)$	J1	$yw; Mnn1^{e173}; \frac{Ly}{TM3, Sb}$ $(lost\ SM5)$
A52	$yw;\ Mnn1^{e173};\ FADD^{f02804}$ $(T_S; T_L stock\ \#2)$	J2	$yw; Mnn1^{e30}; \frac{Ly}{TM3, Sb}$ $(lost\ SM5)$
A53	$yw; Mnn1^{e30};\ FADD^{f06954}$ $(T_S; T_L stock\ \#2)$	J3	$yw;\ Mnn1^{e173}$ $(CyO(y^+)\ stock)$
A54	$yw;\ Mnn1^{e173};\ FADD^{f06954}$ $(T_S; T_L stock\ \#2)$	J5	$Mnn1^{e30}; \frac{mwh}{TM3, Sb}(SM5\ stock)$
A55	$Mnn1^{e173}; \frac{Trx^{B11}}{TM3, Sb}$ $(lost\ SM5)$	J6	$Mnn1^{e173}; \frac{mwh}{TM3, Sb}(SM5\ stock)$
A56	$Mnn1^{e30}; \frac{Trx^{B11}}{TM3, Sb}$ $(lost\ SM5)$	J7	$yw; Mnn1^{e30}; \frac{P\{lacW\}Atu^{s1938}}{TM3, Sb}$ $(SM5\ stock)$
A57	$Mnn1^{e173}; \frac{Trx^{Z11}}{TM3, Sb}$ $(lost\ SM5)$	J8	$yw; Mnn1^{e173}; \frac{P\{lacW\}Atu^{s1938}}{TM3, Sb}$ $(SM5\ stock)$
A58	$Mnn1^{e30}; \frac{Trx^{Z11}}{TM3, Sb}$ $(lost\ SM5)$	J9	$yw; Mnn1^{e30}; \frac{P\{PZ\}atms^{rk509}ry^{506}}{TM3, Sb}$ $(SM5\ stock)$
A59	$Mnn1^{e173}; \frac{Trx^{B11}, mwh}{TM3, Sb}$ $(Recomb\ \#8)(lost\ SM5)$	J10	$yw; Mnn1^{e173}; \frac{P\{PZ\}atms^{rk509}ry^{506}}{TM3, Sb}$ $(SM5\ stock)$
A60	$Mnn1^{e173}; \frac{Trx^{B11}, mwh}{TM3, Sb}$ $(Recomb\ \#11)(lost\ SM5)$		
A61	$Mnn1^{e30}; \frac{Trx^{B11}, mwh}{TM3, Sb}$ $(Recomb\ \#8)(lost\ SM5)$		
A62	$Mnn1^{e30}; \frac{Trx^{B11}, mwh}{TM3, Sb}$ $(Recomb\ \#11)(lost\ SM5)$		

If flies were selected from a balanced stock, the balancers are stated in brackets. A = Alicia Pepper; F=Flora Suen; J=Jennifer Erickson

It should be noted that there were no obvious signs of contamination in these stocks, that is, there were no changes in eye colour or other markers/balancers.

PCR with the *Mnn1* exon 2 and exon 3 primers only showed whether or not a stock was contaminated with a wild-type allele. It did not, however, indicate if a deletion allele was still floating in the stock. Diagnostic primers that could specifically detect the presence of the $Mnn1^{e30}$ or $Mnn1^{e173}$ allele within a contaminated stock were required for this purpose. I used the same primer sets designed by Niko Pretorius for the original characterization of the $Mnn1^{e30}$ and $Mnn1^{e173}$ deletions (see Figure 5.3A for a schematic) (Papaconstantinou et al., 2005). As there was not a pure $Mnn1^{e173}$ stock remaining, it was important to be able to find the deletion allele and recover it from a contaminated stock. PCR with $Mnn1^{e173}$ diagnostic primers is expected to give rise to a 700 bp amplicon for $Mnn1^{e173}$ mutants, while the expected size of the amplicon from a wild-type allele is 4.9 kb, which is too large to be amplified with standard PCR. For the $Mnn1^{e30}$ diagnostic primers, the deletion allele should give rise to a 2.6 kb amplicon; whereas the wild-type allele should produce a 4.2 kb amplicon that would not be detected by standard PCR. Using the $Mnn1^{e173}$ diagnostic primers, a single stock containing the floating mutant allele was identified (Genotype ID A63, $Mnn1^{e173}$;Trx^{Z11}, *mwh*/*TM3 (Recombinant #10)*) (Figure 5.3B). The $Mnn1^{e30}$ diagnostic primers did not identify any additional stocks with the floating mutant allele, but reconfirmed the results from PCR with the exon 2 and exon 3 primers (Figure 5.3C).

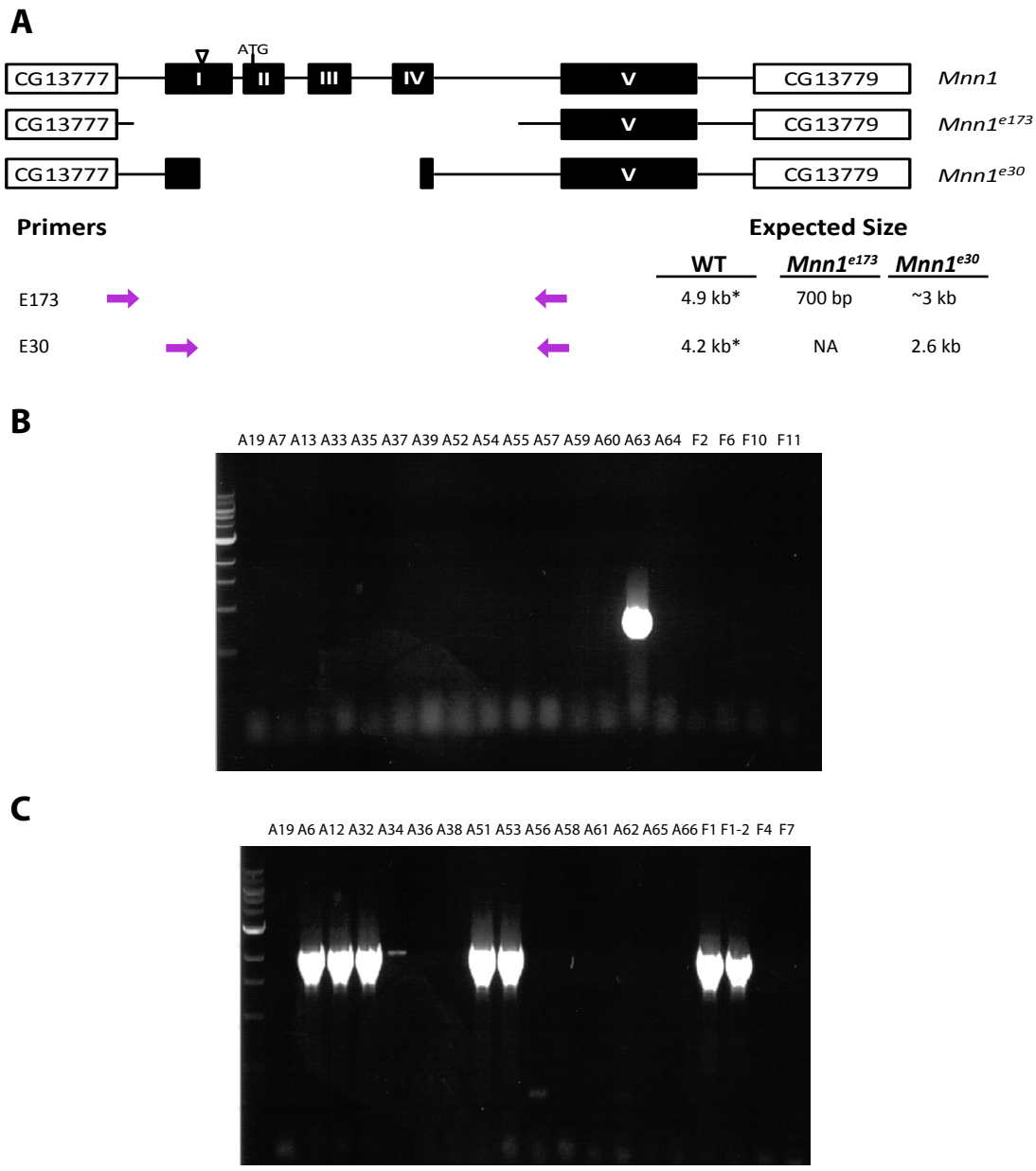

Figure 5.3. Screening of *Mnn1* stocks for the *e173* and *e30* alleles using diagnostic primers. A) Schematic showing the *Mnn1* mutant deletions. Below shows the approximate location of the *e173* and *e30* diagnostic primers along with the expected size of the amplicon. Note that the schematic is not perfectly to scale. NA= No amplification expected, * indicates that the fragment is too large to be observed with the PCR conditions used. B) Screening of lines with the *e173* diagnostic primers located the allele in only one stock. C) Screening of lines with the *e30* diagnostic primers found the allele only in lines that were found to be pure mutants with the *Mnn1* exon 2 and 3 primers (Figure 5.2). See Table 5.1 for a list of the genotypes associated with the ID#. Note that not all tested stocks are shown in this figure.

Mnn1 stocks were received from Dr. Tim Westwood (University of Toronto, Mississauga) for testing since he had received them from Papaconstantinou a few years prior. When screened as described above, both $Mnn1^{e30}$ and $Mnn1^{e173}$ from Dr. Tim Westwood were also found to be contaminated (data not shown).

1.2 Testing RNAi stocks for the presence of the dsRNA construct

Due to all the problems with the *Mnn1* deletion mutant stocks it was important to test the *Mnn1-RNAi* stocks to see if they still contained the dsRNA sequence. The construct used to create these stocks consisted of the UAS sequence followed by exon 2 then intron 2 and finally exon 2 again in the reverse orientation (construct named *Mnn1-RNAi* for short) (Papaconstantinou et al., 2005). Using a forward primer for intron 2 with a reverse primer for exon 2, a portion of the inserted fragment could be amplified, without amplifying the endogenous gene (Figure 5.4A). Using such primers, the presence of the dsRNA sequence was confirmed by the amplification a 420 bp band. Using this screening technique, all the *Mnn1-RNAi* stocks, with insertions on different chromosomes, were found to still contain the dsRNA sequence. Only the *nanos-GAL4;UAS-dsRNA-Mnn1* stocks appeared to have lost the dsRNA sequence but the *UAS-dsRNA-Mnn1/*T_S*; tub-GAL4/*T_L stock was still good (Figure 5.4B). Therefore, we can be relatively confident that *Mnn1-RNAi* stocks are not contaminated, although it is possible that they accumulated other mutations or modifications over time. The overexpression lines were not tested for the insertion of the *UAS-Mnn1* construct.

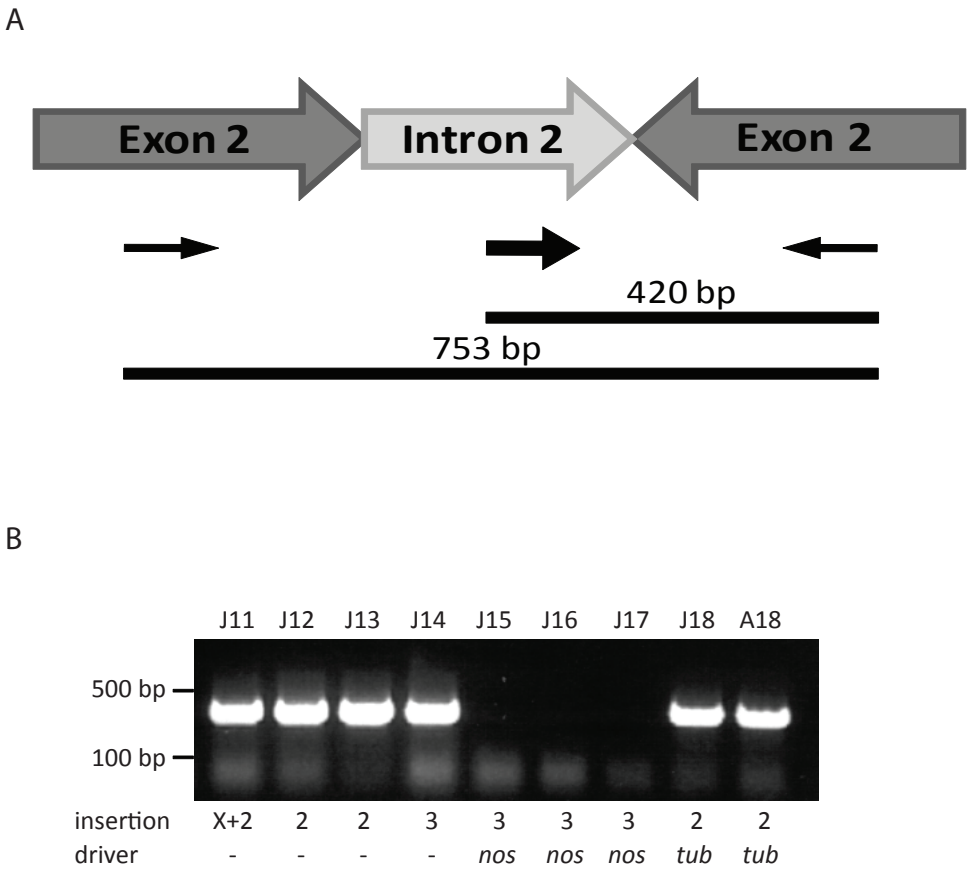

Figure 5.4. Screening of *Mnn1-RNAi* lines for the dsRNA construct.
A) Schematic of the dsRNA construct showing location of the intron 2 forward primer and exon 2 reverse primer used for screening along with the predicted 420 bp fragment size. Theoretically the exon 2 primers alone should be able to amplify a 753 bp product but this was not observed. B) PCR screening of *Mnn1-RNAi* stocks using the intron 2 and exon 2 primers showed most stocks still contained the dsRNA construct. Below the gel image, the chromosome where the dsRNA construct is inserted as well as the presence of any *GAL4* drivers in the same stock are indicated. Only the *nos-GAL4; UAS-dsRNA-Mnn1* stocks (J15, J16, J17) had lost the dsRNA construct. *nos=nanos-GAL4; tub=tubulin-GAL4.*

1.3 PCR testing for the hsp70 deletion

I also checked *Mnn1*$^{-/-}$;*hsp70A*$^{-}$*B*$^{-}$ double mutant stocks using the *Mnn1* primers described above and *hsp70* primers that had previously been used in ChIP experiments (*hsp70* qP3b primers, see Table 2.2). Using the screening methods described above, all these supposed double mutant lines were found to no longer be mutant for *Mnn1*, nor were they found to contain floating deletion alleles using the diagnostic primers (Genotypes F9 and F10 in Figures 5.2 and 5.3). Surprisingly, these lines were still defective for *hsp70*, as no amplification was observed in these lines using primers for the 5'coding region of *hsp70* (Figure 5.5). This suggests that these lines were falsely identified or the *Mnn1* lines used to generate these double mutants may have been contaminated, since random contamination would be expected to affect both the second chromosome and third chromosome simultaneously and not solely the second chromosome harbouring the *Mnn1* deletion.

In addition to all the contamination that was observed in the *Mnn1* stock collection in the Campos lab, it should be mentioned that the *Mnn1* stocks received by Dr. Alexander Mazo (Thomas Jefferson University) from Maria Papaconstantinou several years earlier were found to be lacking the *hsp70* genes. These stocks were supposed to be *Mnn1*^{e30} and *Mnn1*^{e173} deletion lines but when I analyzed them by quantitative PCR during my work period in Dr. Mazo's lab (summer of 2009), *hsp70* could not be amplified from these stocks. This lack of amplification was reproduced from several different samples and five different primer sets spanning various regions of the *hsp70* gene were tested (data not shown). As there are six copies of the *hsp70* gene in *Drosophila*, located in two different gene clusters, this would not represent a spontaneous mutation and a

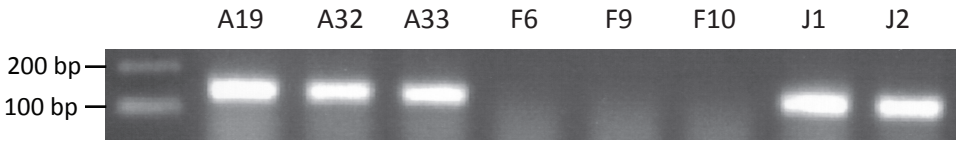

Figure 5.5. PCR with *hsp70* primers.
Double mutants of *Mnn1* and *hsp70* (F6, F9, F10) did not show amplification with the *hsp70* qP3b primers indicating they still contain the *hsp70* deletion. These lines all had amplification with *Mnn1* exon 2, exon 3 primers but not with the *Mnn1* diagnostic primers (Figures 5.2 and 5.3) indicating that they did not have the expected *Mnn1* deletions. *Mnn1* mutant stocks (A32, A33, J1, J2) were also examined to see if they had unexpected deletions of *hsp70*; however, amplification was observed with *hsp70* qP3B primers indicating that *hsp70* genes were still present. See Table 5.1 for the genotypes and corresponding ID#.

random stock contamination would not be expected to knock-out all copies of the gene. In addition, other *hsp70* mutant stocks were not present in Dr. Mazo's lab to have acted as a potential contamination source. Unfortunately, I did not have the foresight at the time to investigate whether or not these stocks actually contained the *Mnn1* deletions by performing PCR with *Mnn1* primers.

2. Re-examination of the heat shock phenotype of Mnn1 mutants

2.1 Mnn1 deletion mutants have normal expression of HSP70

After showing that the $Mnn1^{e30}$ stock was genetically pure, I wanted to reproduce the HSP70 expression phenotype observed by Papaconstantinou *et al.* (2005). *Mnn1* mutants were previously described as having defects in HSP70 expression following heat shock (HS). More specifically, *Mnn1* mutants expressed HSP70 normally for a short HS (up to 15 mins) but then had no detectable HSP70 protein with a longer HS (30-60 mins) (Papaconstantinou et al., 2005). When I tested the $Mnn1^{e30}$ embryos (homozygous stocks created from both a $CyO(y^{+})$ and $T_S;T_L$ balanced stocks) with a 1 hour HS, HSP70 expression was similar to that of Oregon R (OR) controls (Figure 5.6). Therefore, despite being genetically pure $Mnn1^{e30}$ flies, they no longer had the HSP70 expression defect described by Papaconstantinou *et al.* (2005). In order to ensure that the HSP70 antibody being used was specific, it was tested with OR and *hsp70* mutant lines ($Hsp70A^{-}B^{-}$ and $Hsp70A^{-}B^{-}(w^{+})$) that had been shown by PCR to be deletion mutants of *hsp70* (data not shown). Immunoblotting with the HSP70 antibody did not detect any heat shock inducible protein in the *hsp70* mutants suggesting that the antibody was specific (Figure 5.7).

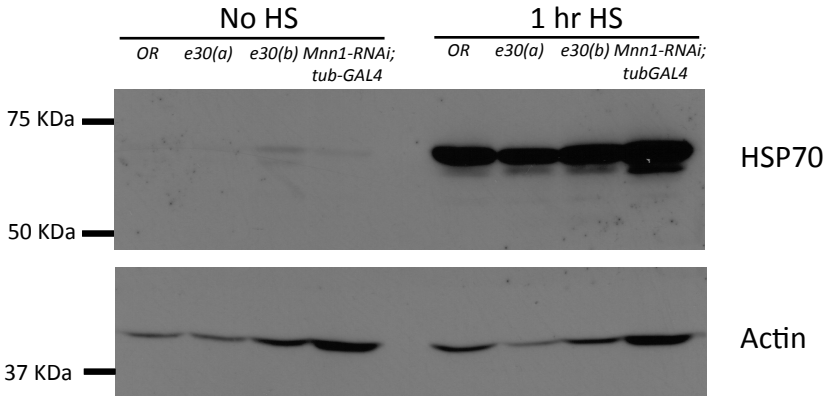

Figure 5.6. Expression of HSP70 in *Mnn1^{e30}* and *Mnn1-RNAi* embryos.
Mnn1^{e30} embryos, age 3-5 hr after egg laying, were collected under standard conditions or exposed to a 1 hr heat shock (HS); 20-22 hr embryos were used for *Mnn1-RNAi; tub-GAL4*. *e30(a)* embryos were *Mnn1^{e30}* homozygous from a *CyO(y^{+})* balanced stock (ID# A34 in Table 5.1) and *e30(b)* were *Mnn1^{e30}* homozygous embryos from a stock previously balanced with T_S;T_L (ID# A6 in Table 5.1). Immunoblotting with an HSP70 antibody showed that *Mnn1^{e30}* mutants and *Mnn1-RNAi; tub-GAL4* no longer had a defect in HSP70 expression with a 1 hr HS, as previously described by Papaconstantinou et al. (2005). Actin is shown as a loading control.

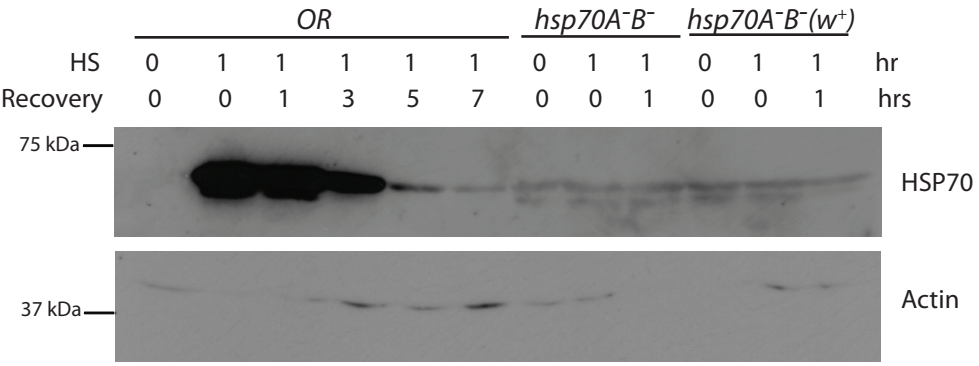

Figure 5.7. Testing of the HSP70 Antibody using *hsp70A⁻B⁻* mutants.
The HSP70 antibody was tested with *hsp70A⁻B⁻* mutants, that have deletions of all 6 copies of the *hsp70* gene, to ensure that it was specific to HSP70. This blot also confirms that *hsp70A⁻B⁻* mutants are still good, as was also shown by PCR using *hsp70* primers (data not shown). Actin is shown as a loading control (note the signal is weak due to re-use of the same antibody solution).

2.2 Mnn1-RNAi stocks have normal HSP70 expression

Knock-down of *Mnn1* using RNAi, was also previously shown to result in defects in HSP70 expression with prolonged HS (Papaconstantinou et al., 2005). After confirming by PCR that *Mnn1-RNAi* stocks still contained the dsRNA sequence, I wanted to see if knock-down of *Mnn1* by RNAi would still result in an HSP70 expression defect. The *Mnn1-RNAi/*T_S*; tub-GAL4/*T_L stock was tested at the same time as the $Mnn1^{e30}$ mutants described above. Embryos, age 20-22 hrs after egg laying (AEL) were used to ensure *tub-GAL4* was expressed. Like $Mnn1^{e30}$ embryos, they also appeared to have normal HSP70 expression with a 1 hr HS (Figure 5.6).

There was some concern that keeping the *Mnn1-RNAi* construct with the driver would lead to constant down-regulation of menin and over time could result in selection for flies that had accumulated some sort of survival advantage to compensate for loss of menin function. The second chromosome *Mnn1-RNAi* stock was crossed to the *daughterless-GAL4* (*da-GAL4*) driver. As this driver is homozygous viable, all progeny contained the driver and RNAi construct. The *UAS-Mnn1* overexpression line was also examined in parallel. Embryos overexpressing *Mnn1* were previously described as having prolonged HSP70 protein expression after recovery from HS compared to controls that rapidly down-regulate HSP70 levels after the HS is removed (Papaconstantinou et al., 2005). To ensure that the *da-GAL4* driver was being expressed, 6-8 hr embryos were examined. As shown in Figure 5.8A, there is essentially no difference in the level of HSP70 protein with a 1 hr HS between the *da-GAL4* controls and the *Mnn1-RNAi* or *UAS-Mnn1* embryos. Also, the control and *Mnn1-RNAi* and *UAS-Mnn1* embryos still show a high level of HSP70 with a 3 hr recovery, a phenotype that

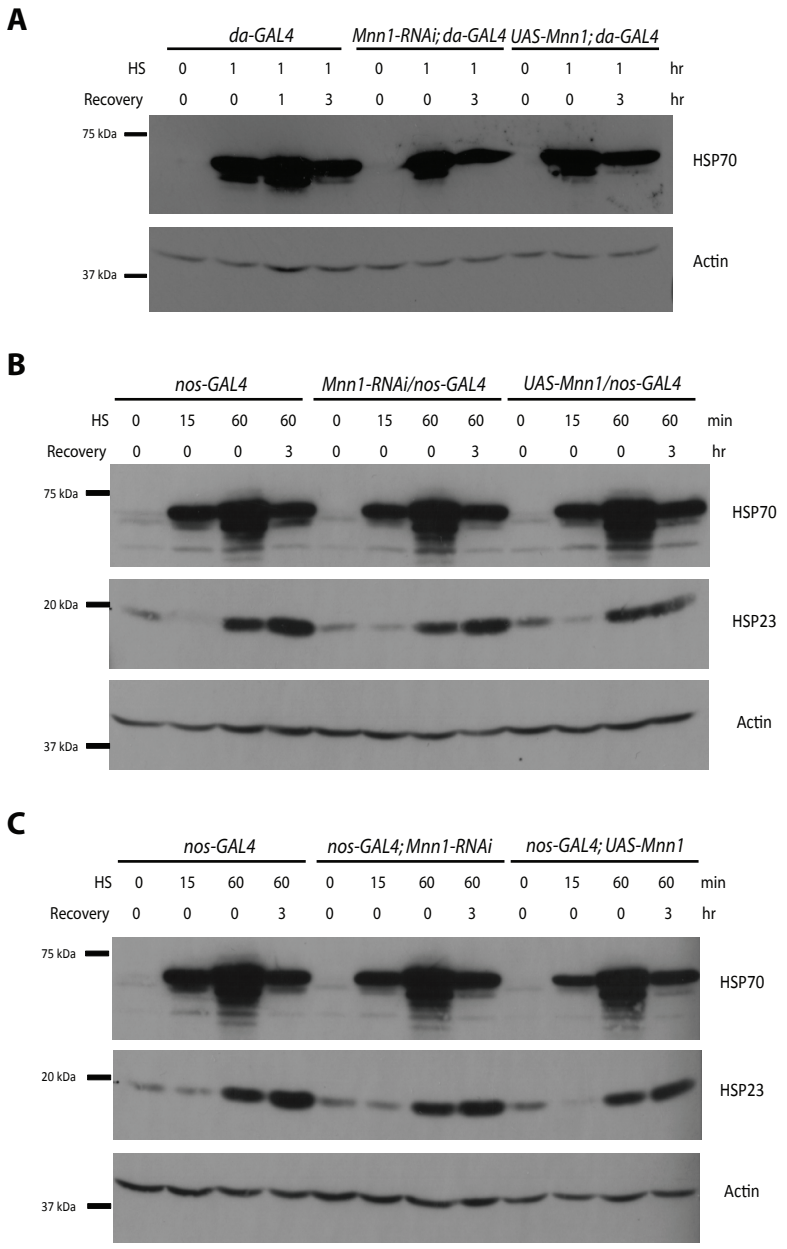

Figure 5.8. HSP70 and HSP23 expression in *Mnn1-RNAi* lines with different GAL4 drivers.
A) Second chromosome *Mnn1-RNAi* and *UAS-Mnn1* lines were crossed to the *daughterless-GAL4* (*da-GAL4*) driver and lysates were made from 6-8 hr embryos following 1 hr heat shock (HS) and recovery. HSP70 expression was the same in the menin down-regulating (*Mnn1-RNAi*) and menin overexpressing (*UAS-Mnn1*) lines as in the *da-GAL4* control. Second chromosome (B) and third chromosome (C) *Mnn1-RNAi* and *UAS-Mnn1* lines were crossed to the *nanos-GAL4* (*nos-GAL4*) driver and 3-5 hr embryos were examined for HSP70 and HSP23 expression following HS. Again, the same pattern was observed in these embryos as in the *nos-GAL4* controls. Actin is shown as a loading control.

was previously only described for the overexpression line (Papaconstantinou et al., 2005). Here, the *da-GAL4* embryos show higher levels of HSP70 protein with a 1 hr recovery from HS than they do immediately after the 1 hr HS and even after 3 hrs of recovery the level of HSP70 remains high (Figure 5.8A). This contrasts with what was previously observed, that is, that the HSP70 protein was essentially eliminated with a 3 hr recovery from HS; this suggested that the HSP70 expression pattern differed also in control lines and not just lines with altered *Mnn1* expression.

As most of the *Mnn1-RNAi* work of Papaconstantinou was done using 3-5 hr embryos and the *nanos-GAL4* (*nos-GAL4*) driver, this driver was ordered from Bloomington's Stock Center (Stock # 4442) so that experiments would be more comparable to the previous work. Crosses were done to generate *Mnn1-RNAi* or *UAS-Mnn1* flies with the *nos-GAL4* driver, using the second and third chromosome insertions. Embryos, age 3-5 hrs, were exposed to various HS times with and without recovery. Figure 5.8B shows the results for the second chromosome *Mnn1-RNAi* and *UAS-Mnn1* constructs and Figure 5.8C shows the results with the third chromosome insertions. As observed with the *da-GAL4* driver, there was no apparent difference in the HSP70 expression patterns of the *nos-GAL4* control compared to either *Mnn1-RNAi* or *UAS-Mnn1* lines with either the second or third chromosome insertions. In addition, HSP23 was examined because defects in HSP23 expression with prolonged HS were also previously reported (Papaconstantinou et al., 2005). As with HSP70 expression, the expression patterns for HSP23 were similar to controls (Figure 5.8B and 5.8C). HSP23 also showed prolonged expression with recovery from HS, for both control, *Mnn1-RNAi* and *UAS-Mnn1*. In fact, there was a slight increase in HSP23 in the 3 hr recovery

samples in this experiment. Therefore, the loss of phenotype occurred with multiple heat shock proteins (HSPs) and was not specific to HSP70.

In summary, the *Mnn1-RNAi* and *UAS-Mnn1* lines no longer showed the previously described defects in HSP expression. This suggests that the problems with the stocks expanded further than just the *Mnn1* deletion mutant lines. We therefore tried to think of more systemic factors that could be affecting the heat shock phenotype of the flies (see Results Section 5 below).

3. Genetic background change and rescue of the Mnn1^{e173} allele

As *Mnn1^{e30}* mutants no longer showed a defect in HSP70 expression following a 1 hr heat shock (Figure 5.6), it was proposed that perhaps they had accumulated modifiers that were rescuing the defect in HSP70 expression. These modifying mutations could have somehow allowed these mutants to adapt and properly express HSPs in the absence of menin. In order to attempt to eliminate the effect of any potential background mutations that could be contributing to the loss of the phenotype, the genetic background of the *Mnn1^{e30}* flies was changed. Essentially all chromosomes, except the second chromosome containing the *Mnn1^{e30}* deletion allele, were changed for a wild-type chromosome from a *yw* stock (the scheme followed for these crosses is explained in Chapter 2, Section 18.1 and shown in Figure 2.1A). Several crosses were followed for each step and thus multiple different lines were generated. After the background change was complete, the genotypes of the new lines were verified by PCR analysis using exon 2 and 3 primers as well as the diagnostic primers (data not shown).

A similar genetic scheme was followed in order to recover the *Mnn1^{e173}* allele that was floating in the single stock identified using the *Mnn1^{e173}* diagnostic primers

(Figure 5.3B, and see Figure 2.1B for the genetic scheme). Multiple crosses were set up and the presence/absence of the *Mnn1*^{e173} allele was determined by PCR after each step and also after the final stocks were generated (data not shown).

After the final cross for the background change of *Mnn1*^{e30} and the recovery of the *Mnn1*^{e173} allele, progeny were counted to compare survival of homozygous versus heterozygous siblings. Overall, the expected number of homozygous to heterozygous progeny was obtained for most new lines generated (data not shown). Surprisingly, *Mnn1*^{e30} lines generated from one of the initial crosses did not produce any homozygous flies, suggesting that they had accumulated a lethal mutation on the second chromosome along with the *Mnn1*^{e30} deletion. The expected ratios of *Mnn1*^{e173} homozygous to heterozygous flies were obtained from the final crosses. Unexpectedly, I was unable to generate a homozygous *Mnn1*^{e173} stock, suggesting that there was now some other factor affecting the fertility of these mutants (see Results Section 6 below).

4. Examination of HS and LOH phenotypes after background change

4.1 Mnn1 mutants have normal HSP expression after background change

After changing the genetic background and recreating several homozygous *Mnn1*^{e30} lines, two of them (*Mnn1*^{e30} B1 and B2) were tested for HSP70 expression in 3-5 hr embryos following HS (Figure 5.9A). Despite attempting to eliminate any contributions from the background, these *Mnn1*^{e30} lines still showed wild-type HSP70 expression and no longer showed the phenotype observed by Papaconstantinou *et al.* (2005). The HSP23 expression pattern was also similar in *Mnn1*^{e30} embryos and controls following HS (Figure 5.9A).

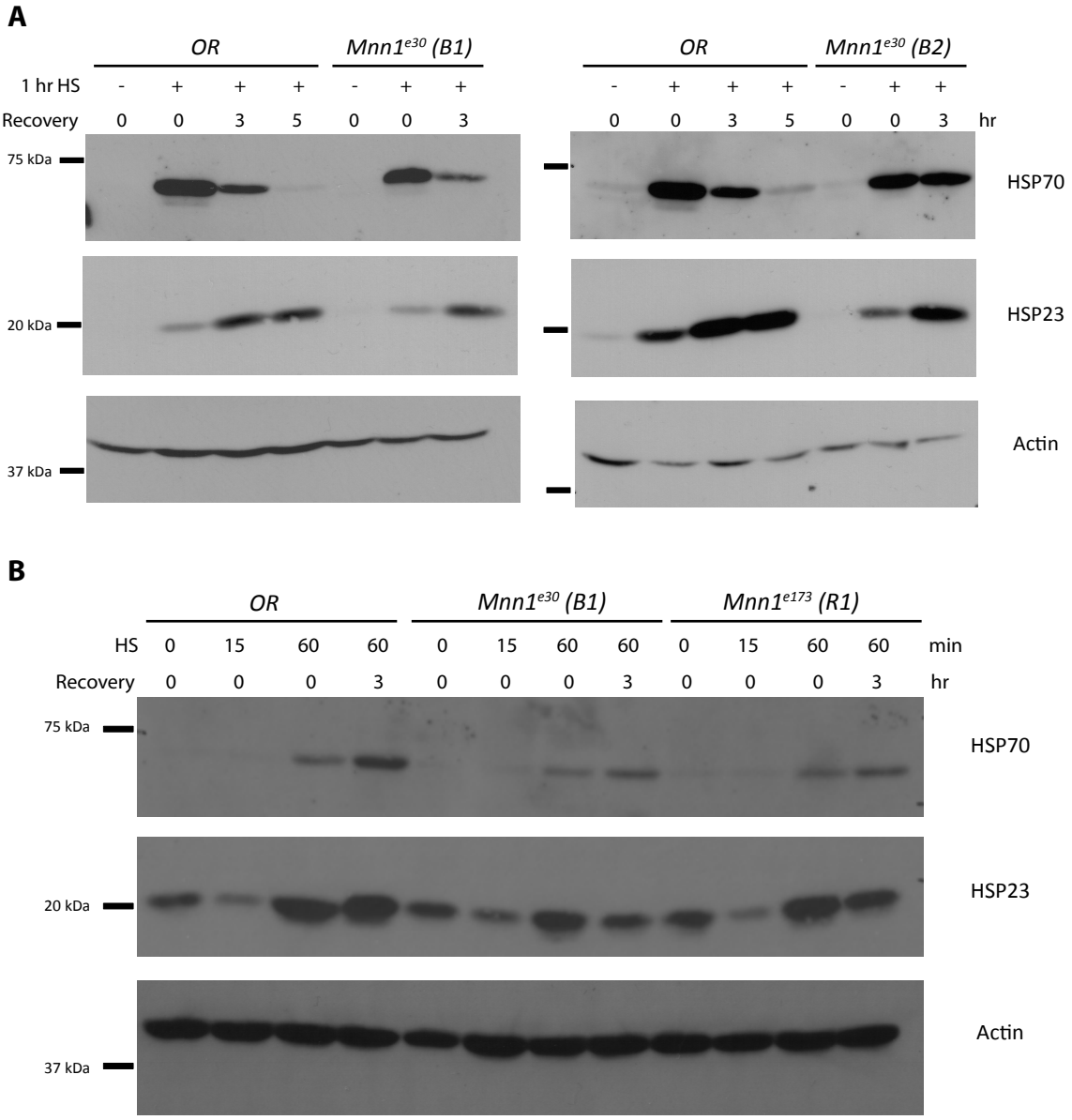

Figure 5.9. HSP70 and HSP23 expression in *Mnn1* mutants after background change/recovery. A) Expression of HSP70 and HSP23 after a 1 hr HS of 3-5 hr embryos from 2 different "lines" of *Mnn1*^{e30} generated by changing the background (B1 and B2). Both lines had an expression pattern similar to wild-type. B) 1-3 d adult males from *Mnn1*^{e30} (B1) and the recovered *Mnn1*^{e173} (R1) line were exposed to various HS and recovery and lysates were immunoblotted for HSP70 and HSP23. Again, *Mnn1* mutants showed the same expression patterns of HSP70 and HSP23 as OR. Actin is shown as a loading control.

As I was unable to create a new *Mnn1*^{e173} homozygous stock after recovering the deletion allele from a contaminated stock, I could not look at HSP70 expression in embryos. In order to check HSP70 expression in *Mnn1*^{e173} mutants, homozygous adult male flies (1-3 d after eclosion) were selected from crosses of balanced flies and exposed to HS of various durations. Immunoblotting with an HSP70 antibody showed that both *Mnn1*^{e30} and *Mnn1*^{e173} adult males overall had similar expression of HSP70 and HSP23 as Oregon R (Figure 5.9B). There appears to be slightly reduced levels of HSP70 and HSP23 in the *Mnn1*^{e30} and *Mnn1*^{e173} adults exposed to a 1 hr HS with a 3 hr recovery (Figure 5.9B), but this does not reflect the drastic absence of HSPs previously observed in *Mnn1* mutant embryos.

Therefore, changing the genetic background did not rescue the HSP expression defect phenotype that was previously observed. *Mnn1*^{e30} and *Mnn1*^{e173} flies, which were shown by PCR to contain deletions in the *Mnn1* gene, did not show any obvious defects in the expression of HSPs following HS. As the second chromosomes were not changed in these stocks, it remains possible that mutations or modifications on the second chromosome could be contributing to the change in the HS phenotype.

4.2 Mnn1^{e30} *mutants still show a mild heat shock lethality phenotype*

After repeatedly observing that *Mnn1* mutants no longer displayed defects in expression of HSPs I wanted to see if other phenotypes observed by Papaconstantinou *et al.* (2005) were also affected. Crosses were set up to examine the HS lethality phenotype with a 1 hr HS at 3-5 hr AEL. Previously, *Mnn1*^{e30} and *Mnn1*^{e173} showed approximately 60 % relative lethality with a 1 hr HS, compared to heterozygous sibling controls from the same cross (Papaconstantinou et al., 2005). As the aim of this experiment was just to

determine if they HS lethality phenotype was still observed, it was only carried out on a small scale and only with the *Mnn1*^{e30} mutants. This experiment was repeated with four separate crosses (*Mnn1*^{e30} X *Mnn1*^{e30}*/CyO* (B1)) and 2 hr collections were made for the No HS and HS conditions from each of the crosses. *Mnn1*^{e30} homozygous flies were still more sensitive to HS than heterozygous sibling controls; however, the phenotype was not as severe as that observed by Papaconstantinou *et al.* (2005). *Mnn1*^{e30} flies had a 40 % relative lethality with a 1 hr HS at 3-5 hr AEL, while under standard conditions there was a 17 % relative lethality (Figure 5.10A). The difference in survival of *Mnn1*^{e30} under standard versus acute HS conditions was statistically significant (p=0.037, Student's t-test). The lethality observed under standard conditions was higher than what was observed by Papaconstantinou, who previously observed less than 10 % lethality under standard conditions.

4.3 Mnn1 mutants show no increase in loss of heterozygosity with heat shock

Since the initial *Mnn1*^{e30}*;mwh* and *Mnn1*^{e173}*;mwh* stocks from Papaconstantinou were contaminated, these stocks were recreated using the background changed *Mnn1*^{e30} and *Mnn1*^{e173} stocks. PCR analysis was used to confirm the genotypes of the newly created stocks and wings were removed from homozygous flies to confirm the presence of the *mwh* mutation. Crosses were set up and 2 hr collections were used for both No HS and chronic HS conditions (2 x 20min HS at 3-5 hr AEL, first instar and second instar) to look at loss of heterozygosity (LOH) at the *mwh* locus. Female *Mnn1*^{e30}; *mwh*$^{-/+}$ and *Mnn1*^{e173}*; mwh*$^{-/+}$ flies were collected along with *mwh*$^{-/+}$ control flies. A single wing was prepared per fly as previously described (Papaconstantinou et al., 2010). Fifteen wings were counted per genotype (with the exception of *Mnn1*^{e173}*;mwh*$^{-/+}$ where only 14 and

11 wings were counted for the No HS and HS conditions, respectively). All wings were analyzed blindly and for each wing, the total number of *mwh* cells and clonal groups of cells were counted. Cells were considered as clones if they were located directly beside each other. Results graphed as the number of *mwh*$^{-/-}$ cells per wing are summarized in Figure 5.10B and the number of *mwh*$^{-/-}$ clones per wing are shown in Figure 5.10C. The number of *mwh*$^{-/-}$ cells per wing was slightly inflated, especially for *Mnn1*^{e173} due to the presence of some larger clusters of *mwh* cells. There was no statistically significant difference between the standard and HS conditions for any of the genotypes, suggesting that the *Mnn1* mutants no longer display an increase in LOH with a chronic HS. There was greater genome instability under standard conditions for both control and *Mnn1* mutants compared to previous findings (Papaconstantinou et al., 2010). This suggests that there could be some other factor affecting the flies. The additional heat stress does not seem to be adding significantly to the genome instability already experienced under standard conditions. One-way ANOVA was used to compare genotypes within a condition (either No HS or HS) and Dunnett's multiple comparison post-hoc test was used to compare genotypes to the control (*mwh*$^{-/+}$). The only significant difference observed was that for the No HS condition, *Mnn1*^{e173}*;mwh*$^{-/+}$ had a significantly higher LOH compared to the control. This was found with analysis of both the number of *mwh*$^{-/-}$ cells or the number of *mwh*$^{-/-}$ clones per wing (Figure 5.10B and C). Therefore, menin function no longer appears to be as crucial in the maintenance of genome stability with chronic stress, as previously described (Papaconstantinou et al., 2010).

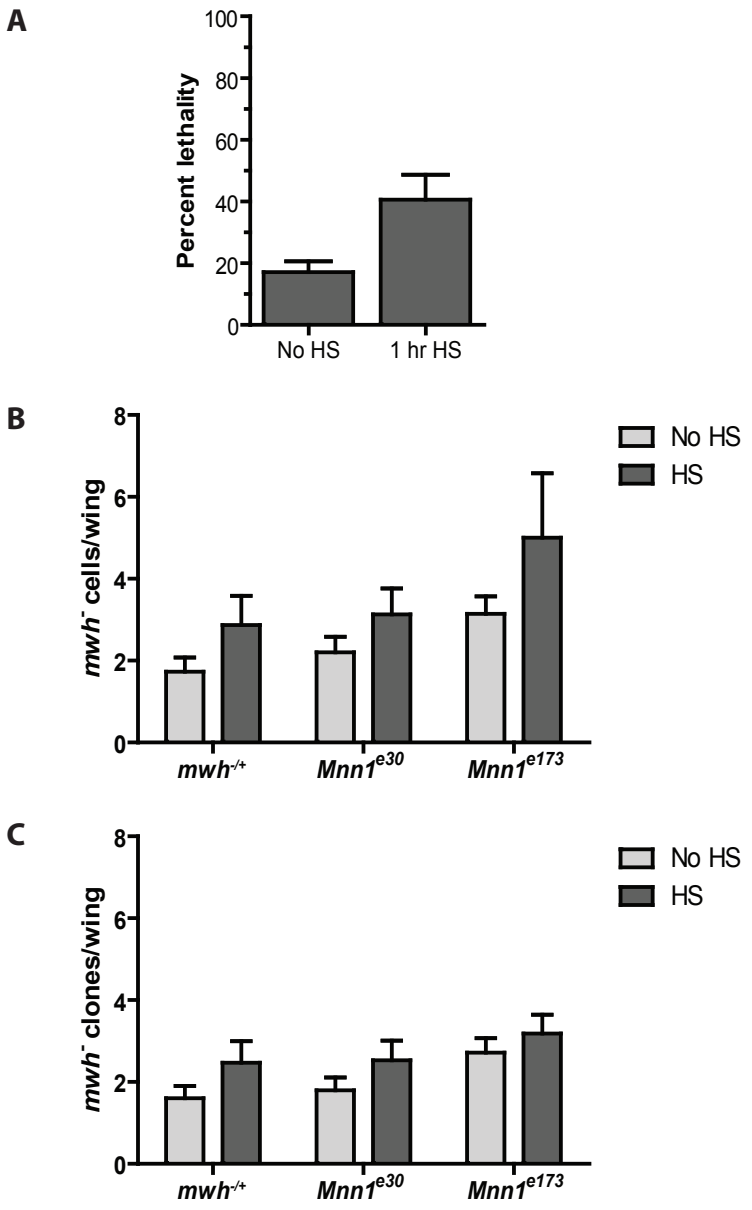

Figure 5.10.Repeat of HS lethality and LOH assays with *Mnn1* mutants after background change. A) Relative HS lethality of *Mnn1*^{e30} mutants compared to heterozygous sibling controls. There was still a HS lethality phenotype (p=0.037) although it was not as severe as previously observed (Papaconstantinou et al., 2005). *Mnn1*^{e173} was not tested in this assay. B-C) Loss of heterozygosity (LOH) assay for the *mwh* locus for *Mnn1*^{e30} and *Mnn1*^{e173} mutants after changing the genetic background. The graphs show the average number of *mwh*$^{-/-}$ cells per wing (B) or the average number of *mwh*$^{-/-}$ clones per wing (C) (n=15, except *Mnn1*^{e173} No HS n=14 and HS n=11). Controls had a higher LOH under standard and HS conditions than previously reported. *Mnn1* mutants also showed higher LOH under standard conditions so the difference between the No HS and HS conditions for each genotype was no longer statistically significant. The only statistically significant difference was between *Mnn1*^{e173} and *mwh*$^{-/+}$ for the No HS condition (one-way ANOVA with Dunnett's post-hoc test).

5. Testing variables that could be affecting the phenotype

The observed phenotype differences were not limited to the expression of HSPs in *Mnn1* deletion mutants, but extended to discrepancies in the phenotype of *Mnn1-RNAi* and *UAS-Mnn1* flies as well as to the LOH phenotype. This suggested that if there had been a change in the flies since the phenotypes were originally reported then the cause must be something more systemic. This train of thought led to the investigation of potential variables that might have contributed to the loss of phenotype. As a readout of the effectiveness of changing certain variables, the expression of HSPs after HS was examined.

5.1 Impurities in fly food as a source of toxin contamination

Because the problems with the flies appeared to be quite broad, affecting multiple stocks and phenotypes, it was proposed that something more widespread must be affecting them. The main commonality of all stocks is that they are maintained on the same fly food. It was hypothesized that there could be some sort of contaminant in the food that was affecting the flies. As some components of the fly food are purchased on a large scale (*e.g.* yeast (Fleischmann's Yeast) and agar (Moorhead and Company, Mooragar Inc.)) and we were unsure of the quality control involved in their preparation, it was possible that they could be contaminated with toxins. Mycotoxins, produced by fungus, are common contaminants of human food and were found to upregulate expression of *MLL1* and other components of MLL complex as well as several target genes (Ansari et al., 2009). It was hypothesized that if the fly food had mycotoxin contamination, then it was possible that flies could have an upregulation of Trx, the MLL

homologue, and associated targets genes and thus the requirement for the menin interaction with Trx for the regulation of stress responsive genes could be bypassed.

More expensive, and presumable more pure, laboratory grade agar (for microbiological applications) (BioShop, AGR003500) and dry active baker's yeast (MP Biomedical, 101400) were used to make more pure fly food (named pure food to distinguish it from the normal fly food). All other components of the food were the same as in the standard fly food recipe used in the Campos lab (see Chapter 2, Section 10.1 for the standard fly food recipe). After flies were treated for potential parasite contamination (see section 5.2) they were maintained on pure food for several generations before HSP70 expression was re-assessed.

5.2 Potential parasite infection

Another possibility, in addition to impurities in the food, was that there was some sort of parasite, bacterial or viral infection that was being passed from one generation to the next in fly cultures. According to Cold Spring Harbor Protocols, *Drosophila* C Virus commonly infects lab cultures and has been shown to block induction of transgenes under the control of the *hsp70* promoter (Ashburner and Roote, 2007). Therefore, if there were some sort of viral infection affecting the stocks it could have an effect on the expression of stress responsive genes, which is problematic when attempting to study the stress response.

In order to try and eliminate any potential parasite contamination we followed a treatment protocol received from Dr. Tim Westwood (see Chapter 2, Section 18.2 for the protocol). Treated first instar larvae were transferred to pure food (see Section 5.1 above), using 10-20 larvae per vial to re-establish treated stocks. This procedure was

done for OR, *yw, Mnn1^{e30}/CyO (B1)* and *Mnn1^{e173}/CyO (R1)* stocks. There is no way to know for certain if this method successfully eliminated any parasites, bacteria or virus infections, as the technique was quite simple and aimed to eliminate transfer of infection from the mother to offspring via the chorion.

The treated flies were kept on pure food for several generations and a homozygous *Mnn1^{e30}* stock was created. Third generation progeny were collected as embryos and exposed to HS of various durations before lysates were prepared for examination of HSP70 expression. No differences between OR, *yw* or *Mnn1^{e30}* were observed in HSP70 expression with a 1 hr HS (Figure 5.11). From this immunoblot, it appeared as though the treatment for parasites and maintenance on pure food did not result in any change in HSP70 expression as *Mnn1^{e30}* embryos responded to HS in the same manner as wild-type flies. Treated flies were maintained on pure food for many generations (approximately 8 months). Later generations were used in the TSA and propionic acid studies (see Sections 5.3 and 5.4 below) so after many generations on the pure food there was still no change in the HSP70 expression phenotype.

5.3 Trichostatin A treatment

After trying to rule out many factors that could be contributing to loss of the *Mnn1* heat stress phenotype, it was suggested that if the problem could not be explained genetically then maybe epigenetic factors were at play. There is emerging evidence for stress-induced epigenetic changes that are transmitted across generations. An example of this is the stress-induced phosphorylation of dATF-2 and consequent heterochromatin disruption that can be transmitted to future generations (Seong et al., 2011).

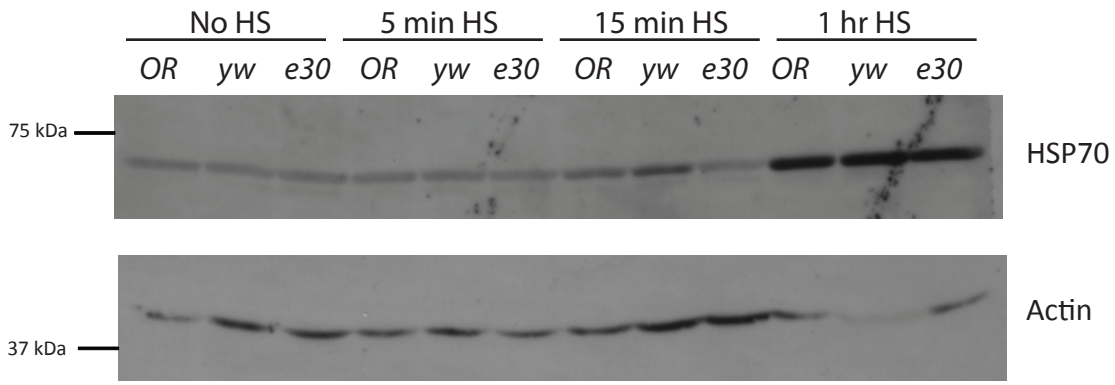

Figure 5.11. HSP70 expression in OR, *yw* and *Mnn1*^{e30} after treatment for potential parasites followed by maintenance on pure food.
After treatment for potential parasites, F3 generation embryos were exposed to various HS conditions and HSP70 levels were examined by immunoblotting. There was no difference in HSP70 protein levels in *Mnn1*^{e30} compared to OR and *yw* with a 1 hr HS. Actin is shown as a loading control. In this experiment, very little HSP70 was seen with a 15 min HS, but this could be due to the antibody being weaker after being reused several times, as expression after 1 hr also appeared weaker than normal.

Also, reduced HSP90 activity was shown to cause morphological changes resulting from altered chromatin states through an unknown interaction with Trithorax group (TrxG) proteins and these changes were epigenetically inherited (Sollars et al., 2003). In this study, treatment with the histone deacetylase inhibitor Trichostatin A (TSA) resulted in a decrease in the epigenetically inherited ectopic outgrowth phenotype (Sollars et al., 2003). Based on this observation, we speculated that if epigenetic changes were affecting *hsp70* expression, perhaps treatment of *Mnn1* mutants with TSA could restore the previously observed phenotype. The idea was to attempt to reset the epigenetic code through histone deacetylase inhibitor treatment. As histone acetylation at the *hsp70* gene is important in the regulation of its expression, we hoped that TSA treatment could restore proper acetylation levels (Chen et al., 2002; Zhao et al., 2006).

TSA food was prepared, using the more pure agar (BioShop, AGR003500) and yeast (MP Biomedical, 101400) and adding TSA to a final concentration of 10 μM. This food was made without propionic acid as suggested by Pile et al. (2001); generally it is added as a fungal/bacterial inhibitor, but it has been shown to be a deacetylase inhibitor itself (Pile et al., 2001). DMSO control food was prepared in the same manner. Flies were allowed to mate and lay eggs on this food (either TSA or DMSO) for 2 hr periods. Embryos were then allowed to develop normally on this food or were additionally exposed to a 1 hr acute HS at 3-5hr AEL or to a chronic HS regime throughout development (20 min HS at 3-5hr AEL, first instar and second instar). Two or three 2 hr collections were made for each genotype (OR and $Mnn1^{e30}$) and treatment. Flies were then left to develop to eclosion on the DMSO or TSA food. The number of $Mnn1^{e30}$ flies that survived was very low for all conditions for both DMSO and TSA. Since the adults

used for the collections seemed to be laying normally, there was probably a lot of lethality in both the DMSO and TSA collections. Perhaps, the change in pH due to removal of propionic acid was affecting the survival of the *Mnn1*^{e30} flies. No *Mnn1*^{e30} flies on TSA food that were exposed to an acute 1 hr HS survived to adulthood (data not shown).

The surviving flies from these TSA or DMSO treatments were mated and then adult progeny of the treated flies were examined for HSP70 expression with or without a 30 min HS. The idea was to see if any heritable changes could be observed in the regulation of HSP70 expression. Not all surviving treated flies mated enough to collect progeny for this analysis; therefore, not all conditions from the initial experiment were examined for changes in HSP70 expression. As seen in Figure 5.12A, for the TSA and DMSO alone conditions, *Mnn1*^{e30} progeny of treated flies had lower expression of HSP70 and HSP23 compared to OR when exposed to a 30 min HS. Since both DMSO and TSA showed this reduction, it may have been due to the absence of propionic acid in the food and not the TSA treatment per se. A confounding factor is that removal of propionic acid resulted in increased bacterial growth on this food, which may have also affected the survival and stress response of the flies. The observed reduction in HSP expression in *Mnn1*^{e30} was minimal compared to the complete loss of HSP70 expression observed by Papaconstantinou.

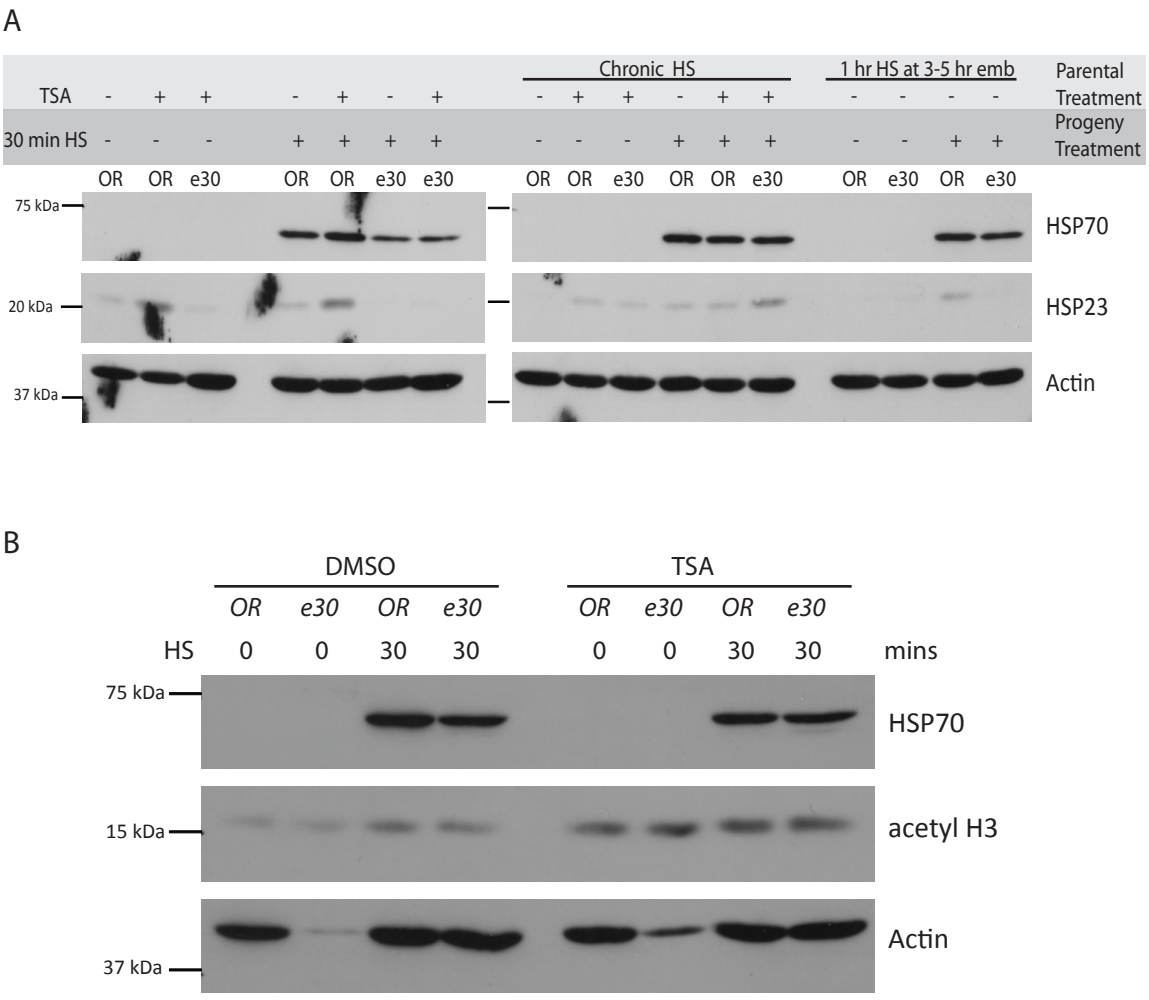

Figure 5.12. Treatment with the histone deacetylase inhibitor Trichostatin A (TSA).
A) Adult flies were allowed to mate and lay eggs on DMSO or TSA (10 uM) food and progeny were left to develop normally or were also exposed to an acute HS (1 hr at 3-5hr AEL) or chronic HS (3 x 20 min HS) during development. The surviving TSA or DMSO treated flies were allowed to mate and adult progeny of treated flies were exposed to 30 min HS (or left untreated) and examined for any changes in HSP70 or HSP23 expression. For the TSA or DMSO alone conditions, the progeny of *Mnn1*^{e30} flies seemed to have less HSP70 and HSP23 expression than OR for both the DMSO and TSA treatment (perhaps reflecting absence of propionic acid in food of both treatment conditions). B) Third instar larvae were treated with TSA (10 uM) or DMSO in physiological brine for 6 hr and then exposed to a 30 min HS or collected immediately. The TSA affected HDACs as there was an increase in acetyl histone H3. However, no effect on HSP70 expression was observed with the brief larval TSA treatment.

Another experiment was conducted using third instar larvae and exposing them to a 6 hr treatment of either TSA or DMSO (as described in Zhao et al., 2006). Third instar larvae were collected from food plates and transferred to dishes with filter paper soaked in a physiological brine containing 10 µM of TSA or DMSO and left for 6 hrs. Larvae were then lysed in SDS sample buffer directly or exposed to a 30 min HS prior to lysate preparation. Immunoblotting of lysates from these larvae showed no major difference in HSP70 expression between OR and *Mnn1*^{e30} (Figure 5.12B). However, an increase in acetyl histone H3 was observed suggesting that the TSA was having the appropriate effect on histone acetylation.

5.4 Removal of propionic acid from food

As *Mnn1*^{e30} progeny of flies that were maintained on TSA or DMSO food had reduced expression of HSP70 and HSP23 compared to OR when exposed to a 30 min HS (Figure 5.12A), it was proposed that the absence of propionic acid in this food could be contributing to the decreased HSP expression. In order to determine if the presence of propionic acid in the food influenced the regulation of HSP expression, food was made with (PA+) or without (PA-) propionic acid. This food was supplemented with antibiotics (penicillin/streptomycin), as increased bacteria growth was observed on food in the absence of PA. Adult flies mated and laid eggs on the PA+ and PA- food and progeny were allowed to develop on this food. Third instar larvae were removed and exposed to 30 min or 1 hr HS before lysates were prepared to examine HSP70 expression (Figure 5.13A). A few *Mnn1*^{e30} samples had slightly reduced HSP70 expression compared to OR; however, this was not consistent with the absence of propionic acid.

Male adults, 0-3 day after eclosion, that had developed on the PA+ or PA- food were exposed to various HS times and examined for HSP70 expression. Figure 5.13B shows only the 30 min and 1 hr HS samples and no differences were observed between the PA+ or PA- food for either OR or *Mnn1*^{e30}. No HS, 5 min HS and 15 min HS samples were also examined but are not shown as there was only a low level of HSP70 in the 15 min sample and no differences were observed between any samples (data not shown). As with larval lysates, *Mnn1*^{e30} adults had slightly reduced HSP70 expression compared to OR in both types of food; this was more obvious with the 30 min HS (note that bands were not quantified so this is only a qualitative observation). In addition, adult flies that had developed on PA+ or PA- food were mated and their progeny were examined during the embryonic stage (3-5 hr AEL) for HSP70 expression in response to heat stress (Figure 5.13C). No obvious differences in HSP70 expression were observed for embryo progeny of adults that developed with or without propionic acid. HSP23 expression was also examined for larvae, adults and embryo progeny but no differences were observed between genotypes or between PA+ or PA- food (data not shown).

In some cases, *Mnn1*^{e30} showed reduced HSP70 levels compared to OR; however, this was not consistent with removal of propionic acid, nor was the reduction anywhere near the previous phenotype where HSP70 expression was absent with a 30 min or longer HS. Thus, removal of propionic acid did not appear to significantly influence HSP70 expression in response to HS. Perhaps the differences observed in the TSA experiment (Figure 5.12) were due to a confounding factor, such as increased bacterial growth in the absence of propionic acid. Either way, this reduced HSP expression was in no way a restoration of the previous phenotype.

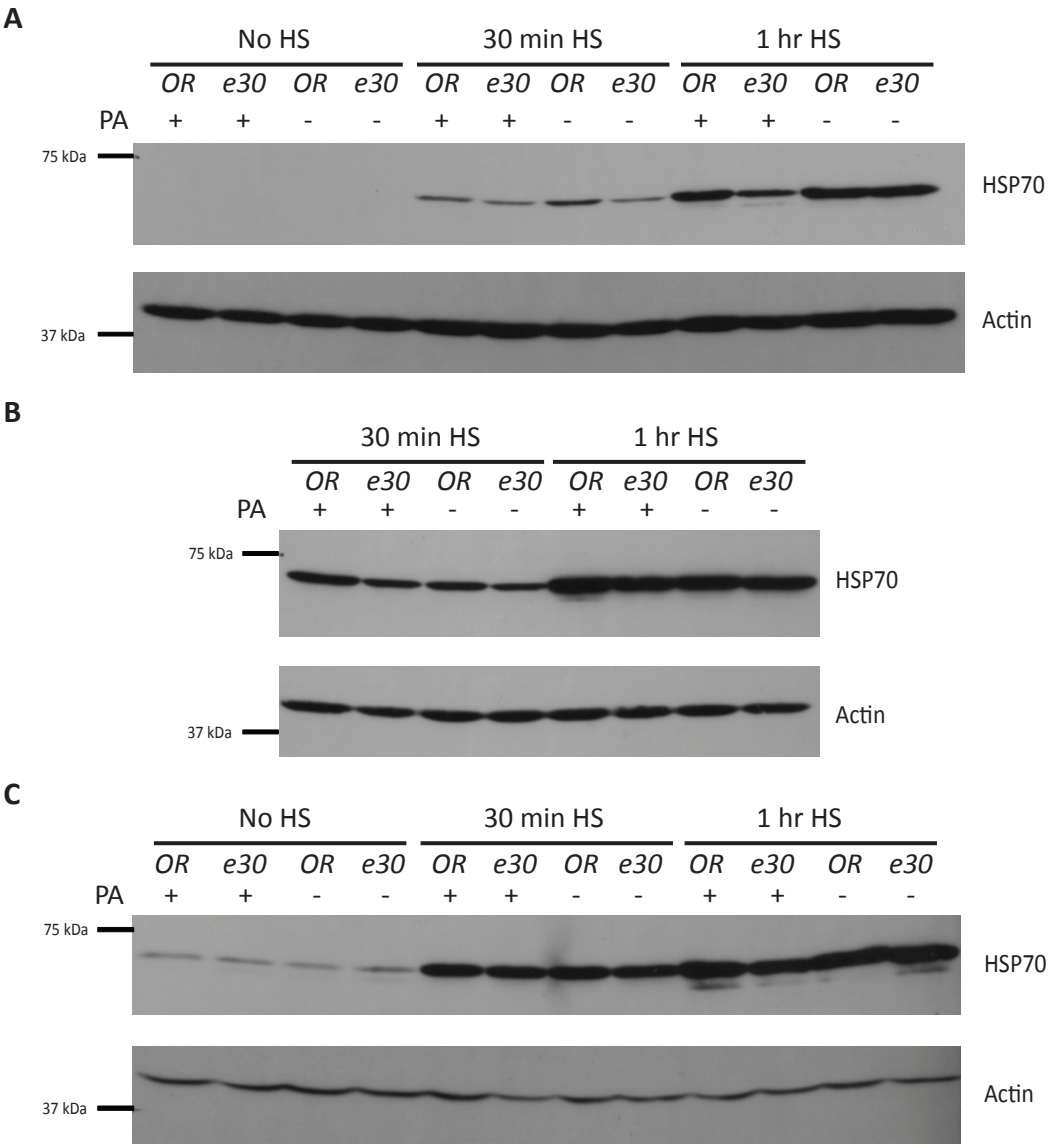

Figure 5.13. HSP70 expression in larvae, adults, and progeny of flies that developed with or without propionic acid.

A) Late 3rd instar larvae that developed with propionic acid (PA+) or without (PA-) were examined for HSP70 expression following 30 min or 1 hr HS exposure. B) Male adults, age 0-3d that developed with or without PA were examined for HSP70 expression. Note that No HS, 5 min and 15 min HS samples were run on a separate gel but are not shown since there was no HSP70 observed for No HS and 5 min samples and 15 min samples only showed weak expression with no differences between genotypes and treatment. C) Embryo progeny (3-5 hr AEL) of flies that developed with or without PA were examined for HSP70 expression after HS exposure. Overall, no differences in HSP70 expression were observed with removal of PA from food.

6. Homologous recombination of the second chromosome to eliminate sterility

6.1 Discovery of sterility in $Mnn1^{e173}$ stock

As mentioned above, after the $Mnn1^{e173}$ allele was recovered from the stock that it was found floating in, the newly generated stock in the *yw* background was homozygous sterile. When the genetic background of $Mnn1^{e173}$ was changed again into the w^{1118} background for the starvation and desiccation experiments (See Chapter 6, Results Section 1), it was again found to be homozygous sterile. This time the sterility issue was examined more in depth. For each sex of $Mnn1^{e173}$, three separate crosses to w^{1118} of the opposite sex were carried out. Both $Mnn1^{e173}$ males and females were sterile (Table 5.2). To determine if this sterility was linked to the $Mnn1^{e173}$ allele the fertility of $Mnn1^{e173}/Mnn1^{e30}$ and $Mnn1^{e173}/Df(2L)spd^{i2}$ were also examined. Both these genotypes were fertile when crossed to w^{1118} of the opposite sex (Table 5.2). This suggests that the sterility was not linked to *Mnn1*.

6.2 Homologous recombination of second chromosome

Since the second chromosome harbouring the $Mnn1^{e173}$ allele was the only chromosome not switched when the background was changed on two separate occasions, the sterility must be associated with this chromosome. As the initial $Mnn1^{e173}$ stock was not described as being sterile, it was assumed that a mutation was acquired at some point that caused the sterility. Also, the $Mnn1^{e173}$ allele did not behave as well as the $Mnn1^{e30}$ allele in starvation survival assays (see Chapter 6, Results Section 3), suggesting that in addition to what was assumed to be causing the sterility there could be other deleterious mutations carried on the second chromosome with the $Mnn1^{e173}$ deletion.

Table 5.2. Fertility Summary for *Mnn1*^{e173} flies.

Genotype	Female	Male
Mnn1^{e173}	Sterile	Sterile
Mnn1^{e173}/*Mnn1*^{e30}	Fertile	Fertile
Mnn1^{e173}/*Df(2L)spd*^{j2}	Fertile	Fertile *

All fertility was based on crosses to *w*^{1118} of the opposite sex. For *Mnn1*^{e173}, three separate crosses for each sex were used. For *Mnn1*^{e173}/*Mnn1*^{e30} and *Mnn1*^{e173}/*Df(2L)spd*^{j2}, six crosses were carried out for each sex and genotype. * Male *Mnn1*^{e173}/*Df(2L)spd*^{j2} had few progeny compared to the other crosses but were not sterile.

For these reasons, homologous recombination was used in order to attempt to clean-up the second chromosome and remove any deleterious mutations. The *Mnn1*^{e173}-containing chromosome was allowed to recombine with a wild-type allele from the *w*^{1118} background for six generations (see Chapter 2, Section 18.6 and Figure 2.2 for the genetic scheme). *Mnn1*^{e30} flies were also used in this recombination as a comparison and to keep these two mutants as similar as possible. Meiotic recombination should occur in the oocytes of heterozygous females (*Mnn1*$^{+/-}$) generated by crossing to *w*^{1118}. After each round of potential recombination, flies were crossed to a balancer stock and then mated again with the *w*^{1118} line. Individual male progeny that could have a recombined chromosome were tested by PCR with diagnostic primers to identify those that still contained the *Mnn1* deletion alleles (about 50% of progeny). Those lines testing positive by PCR were then used for a second round of homologous recombination and this process was repeated. For each step, a minimum of 10-20 crosses were carried for each genotype and for pairwise crosses where the presence of the *Mnn1* deletions could not confirmed until after mating and sacrificing the male, about 30-50 crosses were set up.

After six rounds of homologous recombination, a process that required 15 steps of crosses, *Mnn1*^{e173} homozygous flies were mated to determine if homologous recombination had successfully eliminated the sterility. Homozygous flies from 37 different "lines" that were all positive for the *Mnn1*^{e173} deletion allele were tested. Homozygous stocks could not be generated from any of these lines suggesting that homologous recombination of the second chromosome did not eliminate the sterility. Perhaps the mutation associated with the sterility was closely linked to the *Mnn1* locus

and therefore would be difficult to eliminate through homologous recombination. As the sterility was not eliminated, these lines were not tested for HSP70.

7. Summary of the current status of Mnn1 mutants

The *Mnn1* stocks have been shown to contain the appropriate deletions and were re-confirmed by PCR over a year after they were changed into a different genetic background. These mutants no longer have defects in the expression of HSP70, HSP23 or HSP22 following heat shock exposure. Relative to sibling controls, the $Mnn1^{e30}$ mutants were more sensitive to an acute HS at 3-5 hr AEL, although there was also relative lethality under standard conditions. This suggests that they still have a mild heat shock lethality phenotype albeit not as severe as previously reported. Lethality after acute HS was not tested with the $Mnn1^{e173}$ flies. The *Mnn1* mutants did not show an increase in loss of heterozygosity following chronic heat shock, but the level of LOH under standard conditions was higher than previously observed. Controls also had higher LOH under standard conditions.

Significant attempts were made to reproduce the phenotypes of the *Mnn1* mutants that were previously reported by Papaconstantinou *et al.* (2005). The genetic background was changed to try to eliminate mutations or modifications on other chromosomes that could have been influencing the heat shock phenotype. Later, attempts were made to clean-up the second chromosome containing the $Mnn1^{e173}$ allele, to try to eliminate the sterility associated with this stock after recovery of the floating deletion allele in a contaminated stock. Possible factors that could account for the change in heat shock sensitivity were assessed, such as potential parasite contamination and impurities in the food. Furthermore, flies were treated with the

histone deacetylase inhibitor, TSA, in order to attempt to reset their epigenetic code in case epigenetic modifications were affecting regulation of gene expression in response to heat stress. All attempts to re-create the phenotype reported by Papaconstantinou were in vain; after all these changes, the mutants still did not have a defect in expression of heat shock proteins.

DISCUSSION

The work described in this chapter began from a desire to confirm that the *Mnn1* mutants still contained the appropriate deletions and sadly culminated in an inability to reproduce the previously described *Mnn1* heat shock phenotype, despite consideration of numerous possible influencing factors and significant efforts to re-establish the phenotype. Due to the nature of the issues and results described in this chapter, one can never know for certain what happened to the stocks, when the contamination began or why the mutants no longer show the previously described phenotype. Consequently, a lot of the discussion that follows is purely speculation and can never really be tested. As the loss of a phenotype is not something that is frequently or openly discussed in the scientific community, it was difficult to find many comparative examples in the literature. This discussion will conclude with some potential explanations that could account for a change in phenotype.

1. Stock contamination issues

The original stocks that Papaconstantinou used for her experiments were not kept after she left the lab as three other students, myself included, had all independently received copies of the stocks from her. Since all three of us had contaminated *Mnn1*^{e173} stocks, it

is reasonable to speculate that the contamination probably occurred some time ago in the original stock before it was passed on to each of us (Figure 5.2). Furthermore, all the double mutants that I created from the original *Mnn1*^{e173} stock that I received were also contaminated. It seems very unlikely that so many individual contamination events could have occurred and is arguably much more realistic to assume that the original stock that I received was not a pure *Mnn1*^{e173} stock. The contamination of the *Mnn1*^{e30} stocks was probably more recent than that of *Mnn1*^{e173} stocks, as Jen Erickson and Flora Suen, who received their copies of the stocks from Papaconstantinou at a later time than myself, both had contamination; whereas my stock, that was received at least a year previous, was still pure as were all the double mutants that I derived from it (Figure 5.2). Due to the widespread contamination of the *Mnn1*^{e173} stocks, and the assumption that this probably occurred before I received the stock, I did not trust any previous work done with these mutants and thus this mutant was eliminated from the results described in the previous chapters.

In addition to the contamination of the *Mnn1* stocks with a wild-type *Mnn1* allele, there were also some alarming mix ups with *Mnn1* and *hsp70* mutants. Firstly, the *Mnn1* mutants sent by Papaconstantinou to Dr. Mazo, that were intended to be purely *Mnn1* deletion stocks, were actually mutant for *hsp70*. As mentioned in Results Section 1.3 above, this could not have been an unfortunate coincidence as *Drosophila* contains six copies of the *hsp70* gene that are present at two distinct genetic loci on the third chromosome. Since at the time, I did not have the foresight to test by PCR whether or not these stocks were in fact *Mnn1* mutants they may have either been *Mnn1;hsp70A*$^{-}$*B*$^{-}$ double mutants or simply *hsp70A*$^{-}$*B*$^{-}$ mutants that were falsely

identified only as *Mnn1* mutants. Either way, a serious mistake was made with the *Mnn1* and *hsp70* stocks and the repercussions are extreme considering that the heat shock phenotype was being studied and at the time I was attempting to study *Mnn1* regulation of *hsp70* expression. Secondly, when I examined stocks from the Campos collection identified as $Mnn1^{-/-};hsp70A^{-}B^{-}$ double mutants with both *Mnn1* and *hsp70* primers, they were found to still be mutant for *hsp70* but not for *Mnn1* (Figure 5.2 and Figure 5.5). This was true for both $Mnn1^{e173};hsp70A^{-}B^{-}$ and $Mnn1^{e30};hsp70A^{-}B^{-}$ double mutants. It is highly improbable that random contamination would occur in both these stocks and only affect the $Mnn1^{-/-}$-containing second chromosome without affecting the $hsp70A^{-}B^{-}$-containing third chromosome. A more plausible explanation is that there was also a mix up with these stocks and what was identified as a double mutant was in fact only mutant for *hsp70*. Alternatively, but equally as disturbing, is that the *Mnn1* stocks used to generate these double mutants were already contaminated at the time the stock was created and these flies were never in fact pure double mutant stocks as they were labelled. Regardless, the integrity of the *Mnn1* and $Mnn1^{-/-};hsp70A^{-}B^{-}$ stocks was compromised.

2. Mnn1 mutants no longer have a heat shock phenotype

Differences in the *Mnn1* mutant phenotypes observed over time could be explained in two possible ways: 1) other factors could have been influencing the previous flies that contributed to the defect in HSP expression and heat shock survival that were previously described or 2) other factors were influencing the more recent flies which compensated for the defects in HSP expression and allowed for their increased survival under heat stress conditions. It is possible that the previously described phenotype could have

been due to other unidentified factors working independently or in conjunction with loss of menin function; but, as the flies used in the past experiments were no longer available nor could the past conditions be reproduced exactly, all that could be done was to test how changing certain variables affected the heat shock response in the existing *Mnn1* stocks. I can however say with complete certainty, that the flies I was using for my experiments contained *Mnn1* deletions as they were tested throughout the course of all the experiments and were most recently tested in September 2012 and still contained the appropriate deletions (data not shown).

A change in the heat stress phenotype could potentially be explained by selection of flies that were more resistant to heat shock or were able to adapt and express HSPs in the absence of menin function. If this were due to the selection and accumulation of mutations that increased survival under heat stress conditions then one would expect that changing the genetic background with chromosomes from a wild-type stock, that presumably would not have been under the same selective pressures, should revert the flies back to the original heat shock sensitivity phenotype. After changing the $Mnn1^{e30}$ and $Mnn1^{e173}$ containing chromosomes into a *yw* background, the mutants still did not have the previously reported phenotype (Figure 5.9). This suggests that the accumulation of mutations on chromosomes other than those containing the *Mnn1* deletions could probably not account for the loss of the heat shock phenotype.

A similar loss of stress related phenotype was described by Broughton *et al.* (2008) for oxidative stress resistance. In one study they found that ablation of the median neurosecretory cells (NSCs) resulted in increased resistance of flies to both hydrogen peroxide and paraquat (Broughton et al., 2005); however, in a later study NSC-

ablated flies were no longer resistant to paraquat but were still resistant to H_2O_2 (Broughton et al., 2008). The researchers suggested that the loss of the paraquat resistance phenotype was due to a change in the fly food used. In addition, they also observed metabolic phenotype changes. They had previously observed increased lipid accumulation but no increase in hemolymph trehalose in NSC-ablated flies (Broughton et al., 2005). Later, these same flies no longer showed increased lipid content but had higher hemolymph trehalose levels than controls (Broughton et al., 2008). These researchers related these changes to alterations in the food sucrose content and type of yeast used, as these were changed for the second study in order to optimize for lifespan experiments (Bass et al., 2007).

To my knowledge, the yeast supplier was not changed from when Papaconstantinou did her experiments to when I did mine, but because the yeast was purchased in bulk, as well as the agar, there was concern that the quality control for these sources might not be as stringent and there could potentially be toxin contaminations. Mycotoxins are common food contaminants and exposure of human cells (H358 cells) to mycotoxins was found to induce the expression of *MLL1* as well as *WDR5* and *RBBP5*, other components of the MLL complex (Ansari et al., 2009). The increase in expression of *MLL1*, at both the transcript and protein level, corresponded with an increase in expression of *Hox* target genes (*e.g. HOXA7*, *HOXA2* and *HOXB1*) (Ansari et al., 2009). If the fly food was contaminated with mycotoxins then perhaps this stress would be associated with an increase in the expression of *trx*, the *Drosophila* homologue of *MLL1*. If *trx* was overexpressed, then it is possible that these flies would no longer require menin for proper expression of heat shock genes when exposed to

heat stress (see Chapter 4 for a discussion of menin and Trx interaction). We tried to address the possibility of food being contaminated with toxins by replacing the agar and yeast with more expensive, and presumably more quality controlled sources but this did not restore the previous phenotype. Since we did not test directly for mycotoxin or other toxin contaminations, we do not know for sure that the food was free of toxins.

3. Possible explanations for altered Mnn1 phenotype

3.1 Other factors that could have contributed to the altered phenotype

There are a few other factors worth discussing that may have contributed to the change in phenotype from Papaconstantinou's flies to the ones that I tested. Firstly, during the summer of 2007, there was a mite problem in the fly labs and stocks were treated with tedion (tetradifon, 4-chlorophenyl 2,4,5-trichlorophenyl sulfone); however, as Papaconstantinou was finishing experiments she did not treat her stocks with tedion. All of the stocks that I had, and those that the current *Mnn1* mutants are derived from, were treated with tedion. This treatment is known to be hard on stocks and although most can survive, it likely imposes a significant stress. When parental *Daphnia magna* were exposed to tedion, their progeny, although not having reduced survival, had reduced growth and reproduction compared to those from unexposed parents; this occurred even when the progeny developed in a toxin free environment (Villarroel et al., 2000). This suggests that tedion negatively affects growth and reproduction and can negatively impact several generations. Dietary intake of tedion by rats results in oxidative stress. Although no direct genotoxic effect was observed in bone marrow through chromosomal aberration analysis, it was suggested that exposure could lead to indirect genotoxic effects; however, conclusive evidence has not be shown (Badraoui et

al., 2007). Also in rats, tedion was shown to result in kidney damage and oxidative stress in erythrocytes, with a reduction in the activity of antioxidant enzymes (superoxide dismutase and glutathione peroxidase) observed in both renal tissues and erythrocytes (Badraoui et al., 2011; Badraoui et al., 2012). Furthermore, tedion exposure results in endocrine disruption and impairs ovarian follicle development in rats (Badraoui et al., 2010). These results suggest that tedion results in oxidative damage that can have negative effects on multiple organ systems.

There is no way to determine whether or not the tedion treatment led to lasting effects on the *Mnn1* flies but this is a factor that may have contributed to the altered phenotype, as well as the sterility observed in the current $Mnn1^{e173}$ flies, as the current stocks were derived from treated flies while Papaconstantinou's stocks were not treated. Since the *Mnn1* flies described by Papaconstantinou were shown to be susceptible to oxidative stress, perhaps tedion-induced oxidative stress was not as well tolerated in these *Mnn1* flies and resulted in non-lethal genotoxic effects that were transmitted in flies that survived the treatment.

Another factor that warrants mentioning in this discussion is that lead was found in the water of the McMaster Life Sciences Building in July 2010. As the fly food in the Campos lab was made with tap water, and not reverse osmosis filtered water, until the time I began investigating factors that could be contributing to the altered phenotype of *Mnn1* mutants, it is possible that flies were exposed to lead contamination in their food. How long flies were exposed to lead or how high the levels were are not known, all that is known is that the levels were higher than the Ministry of the Environment's guidelines for human consumption; so the impact on small organisms like

flies could have been substantial. Exposure of *Drosophila* larvae to lead nitrate, results in increased DNA damage in a dose-dependent manner, as observed with the comet assay using extracted larval haemocytes (Carmona et al., 2011). Lead is believed to be a mild mutagen because not all forms of lead (*e.g.* lead chloride) resulted in increased DNA damage, and genotoxic effects of lead were not observed with the less sensitive wing spot loss of heterozygosity assay (Carmona et al., 2011). There is also evidence that lead acts as an endocrine disruptor in *Drosophila;* development, longevity, willingness to mate, fecundity and locomotion were all influenced by lead exposure (reviewed in Hirsch et al., 2010). Furthermore, lead also causes oxidative stress by inducing the generation of reactive oxygen species and by depleting glutathione and thus depleting the antioxidant defense of cells (reviewed in Gurer and Ercal, 2000). It is plausible that if flies underwent chronic lead exposure it may have had unforeseen effects on the *Mnn1* stocks which could have contributed to an altered stress related phenotype.

3.2 Epigenetic changes could possibly explain the altered phenotype

Genetic changes did not seem to be contributing to the altered *Mnn1* HS phenotype, since changing the genetic background did not restore the original phenotype (Figure 5.9). It remains possible that genetic mutations on the second chromosomes that contain the *Mnn1* deletions could have been contributing to the phenotype since these chromosomes were not changed when the rest of the background was switched. As genetic changes did not seem to provide the answer to the altered phenotype, it was proposed that epigenetic changes could be contributing to the altered regulation of heat shock gene expression. Before discovering all the problems with the *Mnn1* mutants that

were described in this chapter, the working hypothesis was that menin helped regulate heat shock gene expression through an interaction with Trithorax and the TAC1 complex (see Chapter 4). Thus, it was proposed that menin helped regulate expression of heat shock genes through epigenetic regulation of the loci, particularly through interaction with histone modifying complexes to activate gene expression. The hypothesis was that loss of menin would result in decreased trithorax mediated histone methylation (H3K4me3), which is needed to maintain an open chromatin conformation for active gene transcription during prolonged stress. A possible explanation for the observation that loss of menin (in the current *Mnn1* mutants) no longer results in defects in HSP expression is that heritable epigenetic changes occurred so that menin was no longer needed to help maintain the open chromatin confirmation at heat shock gene loci under stress conditions.

There is emerging evidence for stress-induced heritable epigenetic changes. One example of this is that heat stress and osmotic stress were shown to cause disruption of heterochromatin. This occurred through p38-mediated phosphorylation of dATF-2 which resulted in loss of dATF-2 binding at heterochromatin as well as a decrease in H3K9me2 levels in these regions (Seong et al., 2011). When heat shocked flies were mated with unstressed flies, the disrupted heterochromatin state was observed in the next generation but not in successive generations. If the stress was continually applied then there was prolonged inheritance of the altered chromatin state; however, once the stress was removed the normal heterochromatin was eventually re-established (Seong et al., 2011).

In another study, an artificially induced stress that would not normally be environmentally encountered by *Drosophila*, also led to heritable epigenetic changes (Stern et al., 2012). In this study, flies carrying a neomycin resistance gene (*neo-GFP*) under the control of a developmentally regulated promoter (*e.g. hairy* or *drumstick*), were exposed to toxic levels of G418. As these developmentally regulated promoters should not normally be expressed in the midgut of larvae, expression of neo-GFP could only occur through derepression at these promoters. Challenge of larvae with G418 was found to result in expression of neo-GFP in the midgut and led to survival of a significant proportion of larvae. This occurred through inhibition of polycomb group (PcG) proteins that normally act to repress many developmentally regulated genes and are involved in maintenance of a repressed chromatin state. Thus, inhibition of PcG proteins led to an overall derepression and broadening of promoter activation (Stern et al., 2012). The epigenetic changes that occurred in G418 challenged flies were inherited by offspring that were never exposed to toxic challenge; the number of generations for which the changes persisted was variable, with an eventual reversion to the normal phenotype (Stern et al., 2012).

The heat shock protein HSP90 (encoded by *hsp83* in *Drosophila*) has been described as a capacitor for evolutionary change. Mutations in *hsp83* led to the emergence of morphological variants in many different structures of the adult fly (Rutherford and Lindquist, 1998). It is believed that normally HSP90 acts as a buffer to suppress genetic variation in the population, but when HSP90 is mutated or inhibited (*e.g.* by geldanamycin treatment), phenotypic variation emerges. The altered morphological phenotypes could be passed from one generation to the next and later

generations no longer required inhibition of HSP90 for the maintenance of the newly emerged trait (Rutherford and Lindquist, 1998). It is assumed that under normal conditions HSP90 interacts with unstable proteins involved in developmental pathways; however, when exposed to stress, HSP90 becomes overwhelmed by other denatured proteins and thus no longer regulates the developmental pathways. This allows for the emergence of morphological variants that are otherwise suppressed, and these new variants could then be selected for if they provided a survival advantage (Rutherford and Lindquist, 1998). This model of evolutionary change is based on the presence of pre-existing genetic variation; however, later studies suggest that HSP90 may be involved in more rapid epigenetic mechanisms of evolutionary change. Sollars *et al.* (2003) identified *hsp83*, as well as mutations in nine different genes of the Trithorax group (TrxG) (*e.g. trithorax-like* (*trl*), *verthandi* (*vtd*)), in a genetic screen for ectopic eye outgrowths when combined with a Krüppel ($Kr^{Jf\text{-}1}$) allele that causes ectopic expression in eye imaginal discs. Maternal loss of the TrxG gene *vtd* or inhibition of HSP90 with geldanamycin resulted in ectopic outgrowths. Selective breeding of flies with ectopic outgrowths resulted in increased frequency of outgrowths in successive generations; this occurred even though only the initial flies were exposed to geldanamycin and the *vdt* mutation was not maintained in flies with outgrowths (Sollars et al., 2003). Although, the epigenetic inheritance was not stably maintained as the ectopic phenotypes disappeared after a few generations without selection. The ectopic outgrowth phenotype was suppressed by treatment with the histone deacetylase inhibitor trichostatin A (TSA), suggesting that hypoacetylation of histones due to TrxG mutation contributed to the altered phenotype (Sollars et al., 2003). In this study, they

also showed that mutation of *hsp83* or *vdt* resulted in the ectopic expression of a *wingless-LacZ* construct which could also be suppressed by HDAC inhibitors (Sollars et al., 2003).

One possibility is that perhaps the original *Mnn1* flies that displayed the defects in HSP expression were at the time being exposed to an unknown stress which prevented the maintenance of an active chromatin state at heat shock loci and if this was epigenetically determined and inherited it could have later been lost after the stress was removed (*i.e.* in the *Mnn1* mutants tested more recently that showed wild-type HSP expression). Treatment of the existing *Mnn1* mutants with TSA did not restore the previously observed defect in HSP expression (Figure 5.12). The idea was to attempt to reset the epigenetic code, as perhaps the chromatin states of heat shock genes or regulators of the heat shock response had been altered over time and were contributing to the observed changes in HSP expression. The fact that a phenotype characterized by defects in expression of HSP was not re-established with TSA treatment is not surprising since treatment with HDAC inhibitors would result in increased levels of histone acetylation, which are associated with an active chromatin conformation. In fact, both the basal and inducible levels of *hsp70* mRNA were shown to be increased with TSA treatment; this corresponded with hyperacetylation of histone H3 (Chen et al., 2002; Zhao et al., 2006). Although this is impossible to test, it would have been more reasonable to have tested Papaconstantinou's *Mnn1* mutants that had defects in HSP expression with HDAC inhibitors to see if this could restore HSP expression with prolonged HS to that of wild-type flies.

Alternatively, if *Mnn1* mutants were unintentionally exposed to stress, for example due to poor maintenance of the stock, prolonged temperature changes, poor nutrition or bacterial/toxin contamination, then changes at the chromatin level could have allowed flies to alter their chromatin state to allow the necessary changes in gene expression to adapt to the imposed stress. If these epigenetic changes were passed from one generation to the next this would ensure that the next generation was already prepped to survive the stress. Perhaps, if epigenetic changes that maintained the heat shock gene loci in an open chromatin conformation were passed in *Mnn1* mutants from one generation to the next, this would allow for efficient and prolonged heat shock protein expression. In this case, menin would not be required to interact with Trx or other regulators of heat shock gene expression. If an epigenetic model were at play, then once the stress was removed, then the normal epigenetic chromatin signature would be expected to eventually be re-established and the original phenotype be restored. However, if the same stress was present across many generations allowing enough time for genetic variation to occur and be selected for, this could have led to a more stable and persistent genetic change. From an evolutionary perspective, defects in expression of HSPs would provide a survival disadvantage, so selection for an adaptation that could restore the normal heat shock gene regulation would be beneficial. Although this is entirely speculation, it represents a plausible mechanism for the inheritance of an altered stress resistance phenotype in the *Mnn1* mutants.

Ruden *et al.* (2008) have proposed the EDGE (Epigenetically Directed Genetic Errors) hypothesis to describe how heritable epigenetic changes can result in permanent DNA mutations that can lead to the stabilization of an environmentally induced

phenotype. They hypothesized that epigenetic changes, such as DNA methylation or histone modifications, occur with exposure to environmental stresses, possibly through HSP90 inactivation during stress and altered interaction with chromatin modifying proteins. The epigenetic changes tend to target DNA regions that code for repeat-containing proteins and are associated with increased mutational rates (*e.g.* increase or decrease in the number of repeats) which can result in a new phenotype that is adaptive for the imposed environmental stress. If the epigenetic change resulted in a genetic change in germ line cells then it would be perpetuated and maintained even if the stress was removed (Ruden et al., 2008). Furthermore, they illustrate that repeat-containing proteins can be grouped into several distinct classes, such as regulators of splicing, regulators of transcription and regulators of synaptogenesis, which would all be important for evolution of new adaptive phenotypes (Ruden et al., 2008). Although this hypothesis is in a way a modern take on Lamarckian-type inheritance, where the environment can alter the phenotype of parents which results in acquired adaptations in the offspring, it was met with some criticism but is becoming more popular as epigenetics have become the focus of intense research efforts in the last few years.

4. Conclusions

An invaluable lesson that can be learned from the turmoil with the *Mnn1* mutants is that *Drosophila* genetics labs should implement regular screening of essential stocks to ensure that the appropriate deletions, insertions or mutations are present. This should be done using molecular techniques, such as diagnostic PCR or sequencing, to ensure that contamination has not occurred. This is especially crucial for homozygous viable mutants as contamination is more likely to go undetected in these stocks. PCR-based

testing is also extremely important when mutants do not have an obvious morphological defect or easily testable phenotype that yields indisputable results (*i.e.* not based on a percent survival that can be influenced by many factors). Regular PCR-based genotype confirmation could have ensured that any contamination was contained and thus would have saved substantial time and effort that were lost using unreliable stocks.

Admittedly, the work described in this chapter in no way furthers our understanding of menin function in *Drosophila*, if anything it casts doubt on the previously described function of menin as an essential regulator of the heat shock response. As there were no longer defects in HSP expression, the planned experiments investigating the menin-Trithorax interaction and its importance in the regulation of the heat shock response were abandoned (Chapter 4) and I began a completely new area of research to investigate a potential role of menin in the insulin signalling pathway in *Drosophila* (Chapter 6).

CHAPTER 6. INVESTIGATING A POTENTIAL ROLE FOR MENIN IN INSULIN SIGNALLING

INTRODUCTION

1. Menin regulation of pancreatic beta cells and insulin in humans and mouse models

1.1 Insulinomas in MEN1 syndrome and mouse models

Multiple endocrine neoplasia type 1 (MEN1) is characterized by tumours in multiple endocrine organs, including the pancreas. Within the endocrine pancreas, hormone secreting tumours are often observed, such as glucagonomas that arise from the glucagon-producing alpha (α) islet cells and insulinomas that arise from the insulin-producing beta (β) islet cells. Although insulinomas are present in only about 10 % of MEN1 patients, they are the most common type of functional (hormone secreting) pancreatic tumour in these patients (Agarwal et al., 2004). In addition, 17 % of sporadic insulinomas have somatic *MEN1* mutations (Agarwal et al., 2004; Marx et al., 1999). Heterozygous *Men1*$^{+/-}$ mice, and mice with pancreatic specific knock-out of *Men1,* develop insulinomas with high frequency (Bertolino et al., 2003b; Bertolino et al., 2003c; Crabtree et al., 2001; Crabtree et al., 2003). Refer to the Chapter 1, Section 5 for a complete review of *Men1* mouse models.

Insulinomas arising from deletion of *Men1* are also found to have up-regulation of cell cycle regulators (*e.g. cyclins A2, B2* and *D2*) as well as components of the insulin-like growth factor (IGF) signalling pathway (*e.g. Igf2*, *Igfbp3, Igfbp2*) (Fontanière et al., 2006b; La et al., 2004a). Menin negatively regulates pancreatic β-cell proliferation as loss of *Men1* leads to hyperproliferation while overexpression of *Men1* in mouse cells reduces their proliferative capacity (Karnik et al., 2005; Schnepp et al., 2006). This

regulation of β-cell proliferation occurs in part through menin regulation of histone H3, lysine 4 trimethylation (H3K4me3), to promote expression of the cyclin-dependent kinase inhibitors $p27^{Kip1}$ and $p18^{INK4c}$ (Fontanière et al., 2006a; Karnik et al., 2005; Schnepp et al., 2006). Refer to Chapter 1, Sections 8.4 and 9.1 for more details.

1.2 Regulation of insulin and menin's interaction with insulin signalling proteins

A link between menin and diabetes has been established with mouse models. Although most studies suggest that menin regulates insulin levels by blocking proliferation of insulin-producing β-cells and not through altering insulin production in individual cells (Karnik et al., 2007; Yang et al., 2010a), one study suggests that menin might inhibit insulin expression (Sayo et al., 2002). Refer to Chapter 1, Section 11 for more details.

Menin's ability to regulate insulin levels and glucose homeostasis may be closely regulated by the insulin/insulin-like growth factor signalling (IIS) pathway as part of an important feedback mechanism. Both insulin and glucose treatment of cells have been shown to down-regulate expression of *Men1* (Wuescher et al., 2011; Zhang et al., 2012). Furthermore, the key transcription factor downstream in the IIS pathway, FOXO1, is a direct regulator of *Men1* expression (Zhang et al., 2012). Thus, inhibition of FOXO1 by Akt-dependent phosphorylation could account for the observed decrease in *Men1* expression with glucose or insulin exposure (see Chapter 1, Section 6.1 for more details).

More recent research suggests a direct role for menin in the IIS pathway through interactions with Akt/PKB (protein kinase B) and FOXO1 (forkhead box class O, protein 1), although some conflicting results have been observed. Menin directly interacts with Akt and negatively regulates its kinase activity, in part by sequestering Akt in the cytoplasm away from the plasma membrane where it is activated (Wang et al., 2011).

Furthermore, menin interacts with the transcription factor FOXO1 and causes its sequestration in the cytoplasm (Wuescher et al., 2011). See Chapter 1, Section 7.7 for a detailed review of each of these studies.

Elucidating how menin regulates proliferation of β-cells and insulin production, as well as any feedback mechanisms that might exist to regulate insulin signalling and glucose metabolism, are active areas of research. This is important not only to understanding MEN1-related tumourigenesis, particularly that occurring in the pancreas, but it may also contribute to our understanding of diabetes development and treatment.

2. Insulin signalling in Drosophila

2.1 Conservation of the insulin signalling pathway

The IIS pathway is well conserved from *Caenorhabditis elegans*, to *Drosophila* to humans (reviewed in Piper et al., 2005). It is important to note that a lot of the discoveries for the insulin-PI3K-Akt and TOR pathways were initially made in *Drosophila*. The *Drosophila* model system is ideal for studying these pathways due to its simplicity compared to mammalian cells. For example, *Drosophila* contains a single FOXO, 4E-BP and S6K member whereas mammalian cells have four FOXOs, three 4E-BPs and two S6Ks. The main IIS pathway will be discussed for *Drosophila* using the *Drosophila* specific nomenclature for the components of the pathway; however, not every interacting protein or pathway will be discussed (please refer to Teleman, 2009 for a review).

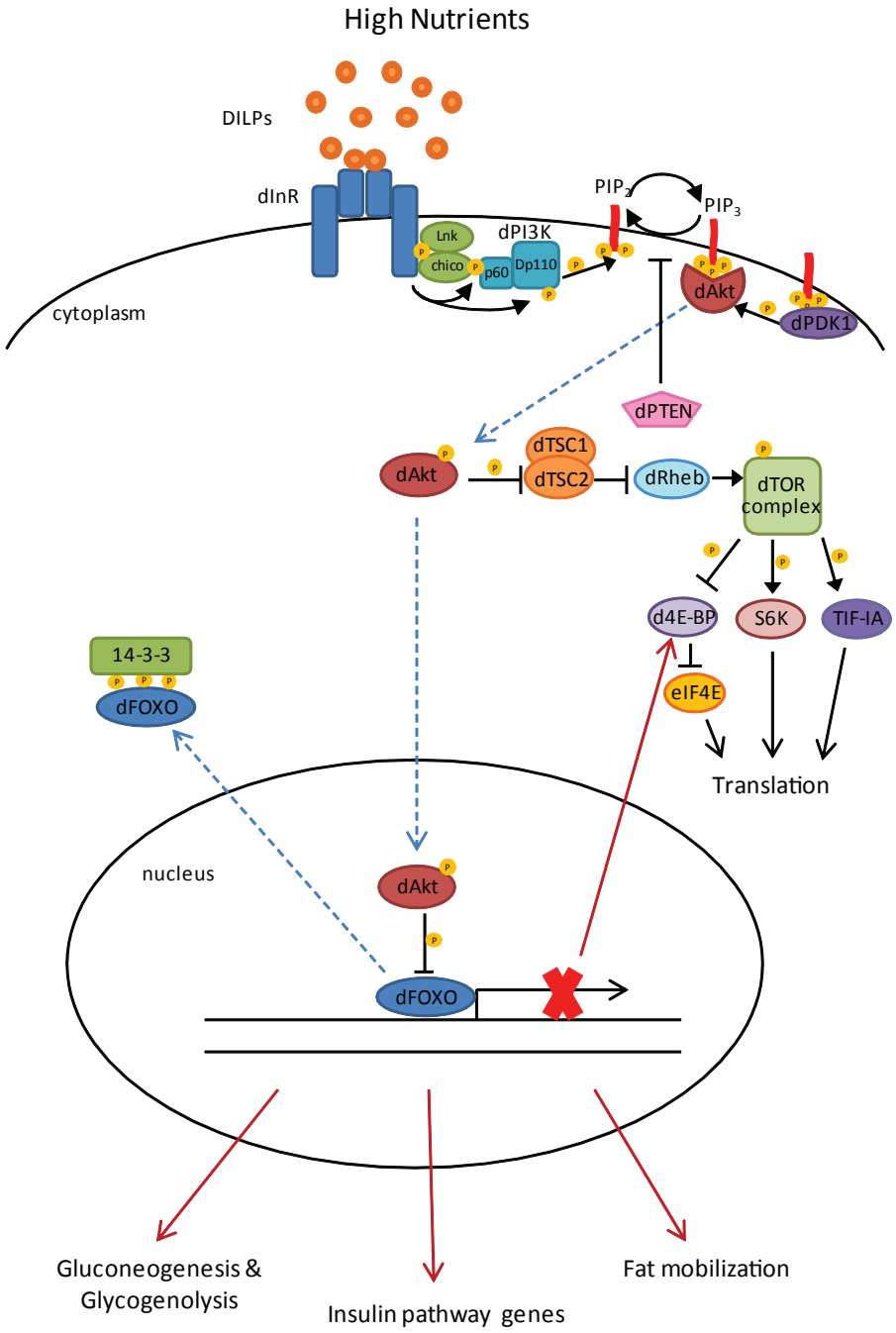

Figure 6.1. Overview of the *Drosophila* insulin signalling pathway.
Insulin signalling through dInR-dPI3K-dAkt results in activation of the dTOR complex resulting in increased protein translation. In addition dFOXO transcriptional activity is repressed, as are the processes regulated by its target genes (indicated with red arrows). Note that this pathway is simplified as many other proteins/pathways interact. Please refer to the text for additional details (Chapter 6 Introduction, Section 2.2).

2.2 Overview of insulin signalling pathway in Drosophila

Please refer to Figure 6.1 for a simplified schematic of the *Drosophila* insulin signalling pathway. The *Drosophila* insulin receptor (dInR) is a receptor tyrosine kinase composed of two alpha (α) and two beta (β) subunits, with the α subunits functioning as extracellular ligand-binding domains and the β subunits containing the cytoplasmic kinase domains (Fernandez et al., 1995). The receptor is activated by binding of insulin-like peptides (DILPs) to the extracellular domain. *Drosophila* has seven DILPs (1-7) that are homologues of mammalian insulin and insulin-like growth factors (IGFs) (Brogiolo et al., 2001). *DILP* genes are expressed in specific locations, such as the median neurosecretory cells (NSCs) (also called insulin-producing cells or IPCs), imaginal discs, salivary glands and midgut, with some DILPs being expressed in more than one type of tissue. *DILP2* is the most closely related to mammalian insulin (Brogiolo et al., 2001; Ikeya et al., 2002; Rulifson et al., 2002).

Upon DILP binding to the extracellular domains, dInR autophosphorylates on the cytoplasmic domains and this generates binding sites for the adaptor protein Chico, the homologue of the insulin receptor substrates (IRS1-4) (Böhni et al., 1999). In addition, Lnk (also called dSH2B), a src homology 2 domain-containing homologue, can act as an adaptor in this pathway (Werz et al., 2009). dInR phosphorylates the adaptor protein which can then serve as a docking site for *Drosophila* phosphoinositide 3-kinase (dPI3K). Alternatively, dPI3K can bind directly to an activated dInR in the absence of Chico or Lnk (Yenush et al., 1996). *Drosophila* PI3K is composed of Dp110, the catalytic kinase subunit and p60 the regulatory subunit (homologous to mammalian p85 subunit) (Weinkove et al., 1999). Upon binding of p60 to the adaptor or dInR, dPI3K is

phosphorylated which activates its own kinase domain. Activated Dp110 then phosphorylates inositol-containing phospholipids in the plasma membrane. That is, phosphatidylinositol 4,5-bisphosphate (PIP_2) is phosphorylated by dPI3K at the third carbon position to generate phosphatidylinositol 3,4,5-triphosphate (PIP_3) (Leevers et al., 1996).

Proteins containing a pleckstrin homology (PH) domain are recruited to the membrane via binding to PIP_3. *Drosophila* Akt/PKB (dAkt), contains a PH domain and is recruited to the plasma membrane in this manner following generation of PIP_3 by dPI3K (Verdu et al., 1999). At the plasma membrane dAkt is phosphorylated and activated by dPDK1 (phosphoinositide-dependent kinase 1), another PH domain containing kinase that is recruited to the membrane through PIP_3 (Rintelen et al., 2001). An important method of negative regulation occurs at this level in the pathway. The phosphatase dPTEN (phosphatase and tensin homology) counteracts the action of dPI3K by removing the phosphate from the third position of PIP_3 to regenerate PIP_2, thus inhibiting recruitment of dAkt to the plasma membrane and downstream signalling (Goberdhan et al., 1999).

Activated dAkt has several targets, both in the cytoplasm and nucleus, with the main target for insulin signalling being the transcription factor dFOXO. dAkt moves into the nucleus and phosphorylates dFOXO on several residues. This results in binding of 14-3-3 proteins which leads to the transportation of dFOXO out of the nucleus and its sequestration in the cytoplasm. Thus, dFOXO phosphorylation by dAkt leads to inhibition of dFOXO and down-regulation dFOXO target genes (reviewed in Van Der Heide et al., 2004). Therefore, dFOXO targets are transcribed under conditions of low

nutrients and reduced insulin signalling and repressed when there is high nutrient availability and signalling through the insulin receptor.

The transcription factor dFOXO has many target genes, most of which are regulated in a tissue-specific manner. One of the most important targets of dFOXO is the gene for the translational repressor *d4E-BP* (eIF4E-binding protein) (Junger et al., 2003; Puig et al., 2003). *Drosophila* 4E-BP binds to and inhibits the eukaryotic translation initial factor 4E (eIF4E) which is required for 5' mRNA cap recognition and initiation of cap-dependent translation (Miron et al., 2001). Binding of d4E-BP prevents binding of eIF4G to eIF4E, as both compete for the same binding site on eIF4E; this prevents recruitment of the rest of the initiation complex including the 40S ribosomal subunit (reviewed in Gingras et al., 1999). Thus, during nutrient deprivation, when insulin signalling is reduced, translation is inhibited through transcriptional up-regulation of the repressor *d4E-BP* (Note that d4E-BP is also regulated post-translationally via the TOR pathway which will be discussed below). This ensures that energy is not wasted on translation of proteins that are not essential for survival under adverse conditions. Another important target gene regulated by dFOXO is the insulin receptor gene, thus creating an important feedback mechanism for the insulin signalling pathway. This allows for sensitization of cells to DILP signalling because *dInR* transcription gets up-regulated during starvation and receptors will accumulate in the membrane making the cell more sensitive to signalling when nutrients become available again (Puig and Tjian, 2005).

In addition to dAkt phosphorylation of dFOXO, another key target of dAkt is the tuberous sclerosis complex (dTSC1/dTSC2), thus dAkt is important for regulation of

protein synthesis via the TOR (target of rapamycin) pathway (Schleich and Teleman, 2009). Phosphorylation by dAkt inhibits dTSC2. dTSC2 normally functions as an inhibitor of the small GTPase dRheb by acting as a GTPase-activating protein (GAP) for dRheb (Garami et al., 2003). Therefore, phosphorylation of dTSC by dAkt allows dRheb to remain active so that it can activate dTOR. dTOR phosphorylates many targets that are important for translation and ribosome biosynthesis and controls overall protein synthesis (reviewed in Grewal, 2009). Thus, signalling through insulin-dAkt-dTOR promotes protein synthesis by increasing translation and ribosome synthesis.

A key target of dTOR is d4E-BP; phosphorylation of the inhibitor d4E-BP prevents its binding to eIF4E, thus freeing eIF4E to interact with eIF4G and allowing the translation initiation complex to assemble (Miron et al., 2003). Phosphorylation of dS6K (ribosome S6 kinase) by dTOR activates it so dS6K can then phosphorylate and activate the ribosomal protein S6, a component of the 40S ribosomal subunit (Miron et al., 2003). dS6K can also be activated in a dPI3K-dAkt-dTOR independent manner through direct phosphorylation by dPDK1 (Radimerski et al., 2002). In addition, dTOR phosphorylates and activates the transcription factor TIF-IA (transcriptional intermediary factor-IA) that is important for expression of ribosomal RNAs through RNA Polymerase I (Grewal et al., 2007).

2.3 Role of insulin signalling components in development, cell growth and proliferation

The IIS pathway is essential for development and mutations in most genes of this pathway lead to lethality. Despite this lethality, the function of this signalling pathway and its various components can be studied by targeted loss-of-function or

overexpression. In *Drosophila*, extensive work has been done to assess the role of insulin signalling components in the regulation of cell size, cell number and organ size.

The overall phenotypes of insulin signalling pathway mutants are summarized in Table 6.1. Mutations in *dInR, dPI3K, dPTEN, dAkt, dTSC1/dTSC2,* and *dTOR* results in lethality during embryonic to larval stages while mutations in *Chico, Lnk, dFOXO, dS6K,* and *d4E-BP* are viable. The targeted overexpression of positive regulators of the pathway, for example in the eyes or wings, results in an increased size phenotype, with both the cell size and cell number increased with *dInR* and *dPI3K*, but only the cell size increased with *dAkt* overexpression. On the other hand, down-regulation (*e.g.* hypomorphs or targeted loss-of-function) of *dInR*, *Chico*, *Lnk* and *dPI3K* all display reduced cell size and cell number. Loss of *dAkt*, *dTOR* or *dS6K* results only in reduced cell size (see Table 6.1). Negative regulators of the pathway display the opposite phenotypes. That is, overexpression of *dPTEN* results in reduced cell size and cell number while overexpression of *dFOXO* results in reduced cell number and that of *dTSC1*/*dTSC2* results in reduced cell size. Mutations in *dFOXO* and its transcriptional target *4E-BP* do not result in obvious size phenotypes (see Table 6.1). Overall, the results suggest that the insulin signalling pathway is important for the regulation of cell proliferation, cell growth and organ size.

2.4 Insulin signalling mutants have altered longevity and stress survival phenotypes

Mutants of the IIS pathway show developmental delays, small size and reduced fertility, characteristics that resemble those of starved flies. In *C. elegans*, starvation or genetic mutations in insulin signalling components causes entry into the dauer stage, where development is arrested to allow the organism to survive harsh environmental

conditions. These observations led investigators to examine the role of homologous IIS pathway components in starvation survival in *Drosophila*. Research in *C. elegans* also prompted the examination of lifespan extension and oxidative stress survival in *Drosophila* as mutations in homologues of insulin signalling genes in *C. elegans* lead to increased longevity and survival under unfavorable conditions such as starvation and oxidative stress (reviewed in Guarente and Kenyon, 2000).

Table 6.1 summarizes the longevity, starvation and oxidative stress survival phenotypes of the key components of the insulin signalling pathway. In summary, IIS mutants frequently show increased lifespan and increased starvation and oxidative stress resistance. Mutations in the negative regulators of this pathway result in the opposite phenotypes, with shorter lifespan and increased stress sensitivities observed. Thus, down-regulation of the IIS pathway is important for survival under adverse conditions as it results in inhibition of protein synthesis and allows for conservation of energy during difficult times. In addition, many IIS mutants also accumulate triglycerides and/or glycogen, such as *dInR*, *Chico* and *Lnk* (Böhni et al., 1999; Slack et al., 2010; Tatar et al., 2001; Werz et al., 2009).

In addition to the insulin signalling mutants described in the Table 6.1, alteration of DILP levels results in lifespan and stress resistance phenotypes. Ablation of the NSCs, cells in the adult brain that produce DILP2, 3 and 5, generates a phenotype that mimics starvation, with flies showing developmental delays and reduced size (Ikeya et al., 2002; Rulifson et al., 2002). NSC-ablated flies have increased lifespan for males and females (Broughton et al., 2005). These flies show increased resistance to oxidative stress (20 mM paraquat) and complete starvation (1 % agar) compared to controls.

Table 6.1. Summary of insulin signalling mutant phenotypes.

Gene	Lethality	Fertility	Size Phenotypes		Longevity	Starvation	Oxidative Stress	References
			Overexpression	Down-regulation				
Positive factors in the insulin signalling pathway								
dInR	Embryo, early larval	♀sterile (hypomorph)	Increased – cell size and number	Reduced – cell size and number	Increased - heteroallelic	Increased survival - RNAi in renal tubules	N.D.	(Brogiolo et al., 2001; Chen et al., 1996; Fernandez et al., 1995; Söderberg et al., 2011; Tatar et al., 2001)
Chico	Viable	♀sterile	N.D.	Reduced – cell size and number	Increased	Increased survival (♀)	No increased resistance	(Böhni et al., 1999; Clancy et al., 2001)
Lnk	Viable	♀almost sterile	N.D.	Reduced – cell size and number	Increased	Increased survival	Increased survival	(Slack et al., 2010; Werz et al., 2009)
dPI3K (p60/Dp110)	Larval	N.A.	Increased - cell size and number	Reduced – cell size and number	N.D.	Overexp. →decreased survival	N.D.	(Britton et al., 2002; Leevers et al., 1996; Weinkove et al., 1999)
dAkt	Larval	N.A.	Increased – cell size	Reduced – cell size	N.D.	N.D.	N.D	(Staveley et al., 1998; Verdu et al., 1999)
dTOR	Larval	N.A.	N.D.	Reduced – cell size	Increased – dom. neg. mutant	Increased survival – with rapamycin	Increased survival – with rapamycin	(Bjedov et al., 2010; Oldham et al., 2000; Zhang et al., 2000)
dS6K	Viable	Fertile	N.D.	Reduced – cell size	Increase – dom. neg. mutant	N.D.	N.D.	(Kapahi et al., 2004; Montagne et al., 1999)

Table 6.1 continued. Summary of insulin signalling mutant phenotypes.

Gene	Lethality	Fertility	Size Phenotypes		Longevity	Starvation	Oxidative Stress	References
			Overexpression	**Down-regulation**				
Negative factors in the insulin signalling pathway								
dPTEN	Embryo, early larval	N.A.	Reduced – cell size and number	Increased – cell size and number	N.D.	Decreased - heteroallelic hypomorph	N.D.	(Gao et al., 2000; Goberdhan et al., 1999; Huang et al., 1999; Oldham et al., 2002)
dFOXO	Viable	Fertile	Reduced – cell number*	No obvious size phenotype	Overexp.→ increased lifespan	Decreased survival	Decreased survival	(Giannakou et al., 2004; Junger et al., 2003; Kramer et al., 2003; Kramer et al., 2008; Puig et al., 2003)
dTSC1/dTSC2 (gigas)	Embryo, early larval (*dTSC1*); Late larval (*dTSC2*)	N.A.	Reduced – cell size (when co-express *TSC1*/ *TSC2*)	Increased – cell size	Overexp. → increased lifespan	N.D.	N.D.	(Gao and Pan, 2001; Ito and Rubin, 1999; Kapahi et al., 2004; Potter et al., 2001)
d4E-BP (Thor)	Viable	Fertile	No size phenotype^	No obvious size phenotype	Reduced	Decreased survival	Decreased survival	(Bernal and Kimbrell, 2000; Miron et al., 2001; Teleman et al., 2005; Tettweiler et al., 2005)

For the cell size phenotypes, overexpression was usually localized to the wings or eyes. Down-regulation refers to targeted loss of function in the wings or eyes, or the phenotype of viable mutants (*e.g.* heteroallelic, hypomorphs). N.A. = not applicable (*i.e.* because mutants not viable and no hypomorphs). N.D. = not determined. * conflicting results over whether cell size is also affected. ^overexpression of a mutated form that more efficiently binds eIF4E results in mild decrease in wing size. Overexp. = overexpression. Dom. neg. = dominant negative mutation.

Despite showing increased oxidative stress and starvation survival, these flies are more sensitive to heat shock at 38.5°C and do not recover as quickly from cold stress at 0°C for 4 hours (Broughton et al., 2005). The expression of *DILP3* and *DILP5* in the median NSCs is regulated by starvation; there is a reduction in transcript levels following larval starvation (Ikeya et al., 2002). Examination of whole body extracts show that NSC-ablated adults have increased energy stores, with higher levels of trehalose, glycogen and lipids compared to controls (Broughton et al., 2005). Taken together, this indicates that DILPs produced by the NSCs are important for insulin signalling and the regulation of circulating sugar levels and stored energy reserves which contribute to overall energy metabolism.

2.5 Examination of the mutant phenotype of dFOXO and its target d4E-BP

Due to the interaction between menin and FOXO1 identified in mammalian cells (Wuescher et al., 2011), a closer examination of the *dFOXO* mutant phenotype will be provided so that comparisons can be made to *Mnn1* mutants to help determine if menin may regulate dFOXO in the *Drosophila* insulin signalling pathway. Even though an interaction was also described for menin and Akt in mammalian cells (Wang et al., 2011), due to the lethality associated with loss of *dAkt*, the metabolic phenotypes of *dAkt* mutants have not been well studied and additional details will not be provided.

In contrast to most other mutants of the IIS pathway, homozygous *dFOXO* mutants (*dFOXO*^{21} and *dFOXO*^{25}) are viable with no obvious size phenotype. Overexpression of *dFOXO* in adults, using an inducible fat body specific driver (RU486/mifepristone $S_1$106 driver), leads to an increase in lifespan and reduced fecundity of female flies with no effect on male lifespan (Giannakou et al., 2004). This

observation contrasts with work done by Hwangbo *et al.* (2004) that used the same S_1106 inducible driver but did not observe a significant increase in lifespan with the overexpression of *dFOXO* in the abdominal/thoracic fat body; however, using an inducible S_1132 driver that expresses specifically in the head fat body an increased lifespan with overexpression of *dFOXO* was observed (Hwangbo et al., 2004). This increased longevity was not accompanied by decreased fecundity in females (Hwangbo et al., 2004).

In addition, flies overexpressing a mutated dFOXO protein (*dFOXO-TM*), that cannot be phosphorylated or inactivated by dAkt, in the head fat body tissue have increased oxidative stress resistance compared to those with wild-type levels of dFOXO (Hwangbo et al., 2004). No comment was made as to whether or not the overexpression of a wild-type form of *dFOXO* also results in increased oxidative stress resistance. Increased survival with *dFOXO* overexpression agrees with previous work that showed *dFOXO* loss-of-function mutants have increased sensitivity to oxidative stress (Junger et al., 2003). It was shown later that resistance to oxidative stress is mediated through *d4E-BP* as expression of *d4E-BP* in *dFOXO*-null flies restores the oxidative stress resistance to the level of control flies (Tettweiler et al., 2005). When Junger *et al.* (2003) first reported this oxidative stress sensitivity, they did not observe any sensitivity to bacterial infection, heat shock, heavy metal exposure or complete starvation; although, the data were not shown to support such claims. In another study, *dFOXO*-null larvae and adults ($dFOXO^{21/25}$) had reduced survival in response to amino acid starvation compared to heterozygous or wild-type controls (Kramer et al., 2008).

The increased sensitivity of *dFOXO* nulls makes sense as *dFOXO* is negatively regulated by the IIS pathway, and other IIS mutants have increased starvation resistance.

Despite not playing a role in regulating normal tissue growth, d4E-BP regulates *Drosophila* lifespan, as nulls show significantly reduced longevity (~ 25 %) compared to controls from the same genetic background (Tettweiler et al., 2005). In addition, d4E-BP plays a role in regulating growth and survival in response to oxidative stress or starvation (Tettweiler et al., 2005). Transcription of *d4E-BP* increases in response to oxidative stress (*i.e.* hydrogen peroxide) or amino acid starvation in a dFOXO-dependent manner (Teleman et al., 2005). Like *dFOXO* mutants ($dFOXO^{21}/dFOXO^{25}$), *d4E-BP*-null flies are more sensitive to oxidative stress (Tettweiler et al., 2005) and more susceptible to starvation than controls. Systemic overexpression of *d4E-BP* leads to increased triglyceride accumulation as does the inhibition of dTOR with rapamycin, which results in loss of d4E-BP negative regulation. The latter also corresponds with increased survival under starvation conditions (Teleman et al., 2005). Thus, although d4E-BP does not influence normal development or growth, it affects fat metabolism and starvation survival. Similar to the starvation sensitivity observed for adult *d4E-BP* mutants, null larvae or those with a mutation that inhibits eIF4E binding (*d4E-BP(Y54A,M59A)*) also show a similar decreased starvation survival compared to controls (Tettweiler et al., 2005). Other research suggests that d4E-BP may be important in response to other stresses, as loss of *d4E-BP* is also associated with compromised immunity. Mutants of *d4E-BP* are more susceptible to gram-positive bacterial infections (*Staphylococcus epidermidis*, *Micrococcus roseus*) but show similar resistance to gram-negative

(*Escherichia coli*, *Enterobacter cloacae* B_{12}) infections as controls (Bernal and Kimbrell, 2000).

3. Objectives and predictions

As the insulin signalling pathway is well conserved between *Drosophila* and mammals (Piper et al., 2005), investigating a role for menin in insulin signalling in *Drosophila* seemed like an interesting and promising venture. In my previous studies, I first established a molecular interaction between menin and other proteins (*e.g.* Trx and dFADD) and then tried to determine the functional significance of these interactions with *in vivo* studies. This time, due to the well established phenotypes of IIS mutants, it seemed more important to first determine if *Drosophila Mnn1* mutants had a similar phenotype before investing time into molecular studies to determine if the interactions with Akt and FOXO1 were conserved. To do so, the *Mnn1* mutants were tested in starvation and desiccation survival assays to compare their phenotypes to those of other IIS mutants.

Since *Mnn1* mutants do not have an obvious severe size phenotype and are homozygous viable, it was hypothesized that if menin is involved in the insulin signalling pathway it would most likely be playing an auxiliary role and acting as an adaptor to fine tune the regulation of this pathway. The interactions described in mammalian cells for menin and components of the insulin signalling pathway, Akt and FOXO1, suggest opposing roles for menin. If menin acts as an inhibitor of dAkt then it would be negatively regulating the pathway. If this interaction is conserved in *Drosophila* then *Mnn1* mutants should have a phenotype similar to that of negative regulators of the pathway (such as *dPTEN* and *dFOXO*) and thus would have reduced starvation and

desiccation survivals. On the other hand, if menin acts as an inhibitor of dFOXO then it would be positively regulating the pathway and *Mnn1* mutants should have a phenotype similar to other mutants of the pathway (*e.g. DILPs*, *dInR*, *Chico*, *Lnk*, *dPI3K*) and have increased starvation and desiccation survivals.

Thus, the main objective of the research described in this chapter was to characterize the starvation and desiccation phenotypes of *Mnn1* deletion mutants in order to predict if menin could be playing a role in this pathway and to suggest whether menin might be positively or negatively regulating this pathway. This would provide the necessary preliminary phenotypic data to suggest whether or not investigating a potential role for menin in *Drosophila* insulin signalling is a justifiable avenue of research. All the experimental protocols and statistically analyses used in this Chapter are provided in Chapter 2, Sections 19-21.

RESULTS

1. Concerns from preliminary desiccation and starvation experiments

In order to determine if *Mnn1* mutants have a similar survival phenotype as previously characterized IIS mutants, preliminary desiccation and starvation experiments were conducted with OR, *yw*, *yw*;*Mnn1*^{e30} and *yw*;*Mnn1*^{e173} (see Appendix H). As results from the initial experiments were promising, the starvation and desiccation survival of *Mnn1* mutants were further investigated. Two major concerns from the initial experiments were addressed before experimentation was continued. The first major concern was that differences in genetic background could be influencing the results and causing the observed differences. The second concern was that the different genotypes have

observable differences in fecundity which lead to differences in larval density during development which in turn could affect survival in the starvation and desiccation assays. The concern was that wild-type stocks tend to produce more progeny and such stocks often become overcrowded during larval development. This overcrowding can lead to nutrient deprivation or reduced adult size which in turn could influence the fitness of such flies, especially under conditions of starvation and desiccation (Borash and Ho, 2001; Kolss et al., 2009).

To address the concern regarding the influence of genetic background on starvation and desiccation survival, all lines were crossed into the w^{1118} genetic background (Refer to Figures 2.3 and 2.4 for the genetic schemes). This was carried out in such a way that all the chromosomes were switched to those from w^{1118}, with the exception of the second chromosome carrying the desired *Mnn1* allele. The deletion mutants, $Mnn1^{e30}$ and $Mnn1^{e173}$, as well as the precise excision lines, $Mnn1^{+E314}$ and $Mnn1^{+E323}$, were all crossed into the w^{1118} background. Because both precise excision lines were found to have similar survivals in the starvation and desiccation experiments (data not shown), only $Mnn1^{+E314}$ was used in the final experiments described below. All desiccation and starvation assays, described from here on, were done using flies in the w^{1118} background. For simplicity, w^{1118};$Mnn1^{e30}$ will only be written as $Mnn1^{e30}$, and the same applies for the other genotypes.

Attempts were made to cross the $Df(2L)spd^{j2}$ (referred to as *Df(2L)*) line into the same w^{1118} background to minimize differences arising from first or third chromosomes; however, the intermediary stock with a balanced and marked third chromosome along with the deficiency and balancer second chromosomes could not be generated. This is

presumed to be due to the disruption of *wingless* in the *Df(2L)spd*^{j2} deletion which is further influenced by the *lyra* (*Ly*) or *dichaete* (*D*) markers of the third chromosome (Nolo et al., 2001). Consequently, all stocks used in the following experiments, except those containing *Df(2L)spd*^{j2}, are all in the same w^{1118} background. It is important to note that for all genotypes, the second chromosomes could still be a source of genetic variation, as they were not changed due to the presence of the desired *Mnn1* alleles, thus, there could still be differences among the various stocks.

The issue of different genotypes having different larval densities during development was addressed by transferring 100 first instar larvae per food vial for development (see Chapter 2, Section 20). All desiccation and starvation experiments described henceforth were done using this method to control for larval density to eliminate crowding or nutrient deprivation during development.

2. Desiccation survival of Mnn1 mutants

2.1 Male desiccation survival analysis

After addressing the issues of variation in genetic backgrounds and potential effects of different larval densities, desiccation experiments were repeated with 4-6 day males. Although several experiments were carried out and all gave rise to similar overall results, due to the inherent variability in these assays, only the final two experiments were grouped together for analysis as all genotypes were tested simultaneously for these experiments. Combining data from these two temporally separated experiments generated a sample size of 150-350 males for each genotype (see Table 6.2 for sample sizes). Note that for each experiment, 2-3 trials were carried out for each genotype but the number of flies used in each trial was variable.

Table 6.2. Median survival* and sample size for desiccation assay.

Genotype	Males		Females	
	Median Survival (hrs)	n	Median Survival (hrs)	n
w^{1118}	16	330	20	290
$Mnn1^{+E314}$	14	230	18	250
$Mnn1^{e30}$	22	320	26	330
$Mnn1^{e173}$	20	150	24	170
$Mnn1^{e30}/Mnn1^{e173}$	18	220	24	260
$Mnn1^{e30}/+$	18	350	22	310
$Mnn1^{e173}/+$	16	210	20	200
+/Df(2L)	22	170	32	260
$Mnn1^{+E314}/Df(2L)$	20	210	32	210
$Mnn1^{e30}/Df(2L)$	24	190	28	210
$Mnn1^{e173}/Df(2L)$	24	150	30	150

*Median survival is defined as the time when 50 % of the population had perished.

The desiccation survival curves for all eleven genotypes were graphed together and are shown in Appendix I, Figure I.1. Due to the large number of curves on this graph it is difficult to make comparisons among genotypes. For this reasons, genotypes were grouped together in several graphs to simplify comparisons among certain genotypes. A summary of the statistical analyses for this data set is provided in Appendix I, Table I.1. Survival curves were compared using GraphPad Prism and performing a log-rank (Mantel-Cox) test. The series of curves was found to be statistically different ($p<0.0001$) and pairs of curves were then compared to determine which genotypes were statistically different. A Bonferroni corrected significance level of $p<0.002$ was used to correct for multiple comparisons (see Chapter 2, Section 21.3 for more details).

The survival of *Mnn1* mutants ($Mnn1^{e30}$ and $Mnn1^{e173}$) was compared to that of the wild-type control w^{1118} as well as the precise excision line $Mnn1^{+E314}$ (Figure 6.2A). $Mnn1^{+E314}$ was presumed to be a better control for the second chromosome as it was derived from the same P-element insertion line (GE11370, GenExcel Inc.) as the deletion mutants. Both homozygous *Mnn1* mutants survived better than the two control lines (Figure 6.2A), with $Mnn1^{e30}$ males surviving better than $Mnn1^{e173}$. The median survival, that is, the time point when 50 % of the population had perished, of $Mnn1^{e30}$ and $Mnn1^{e173}$ were 22 hr and 20 hrs, respectively (Table 6.2). This contrasts with w^{1118} and $Mnn1^{+E314}$ that had median desiccation survivals of 16 and 14 hrs, respectively. Surprisingly, the heteroallelic mutant, $Mnn1^{e30}/Mnn1^{e173}$, did not survive as well as either homozygous mutant; it did not survive as well as the weaker $Mnn1^{e173}$ allele as was expected. Despite this, the heteroallelic mutants still survived better than controls (Figure 6.2A).

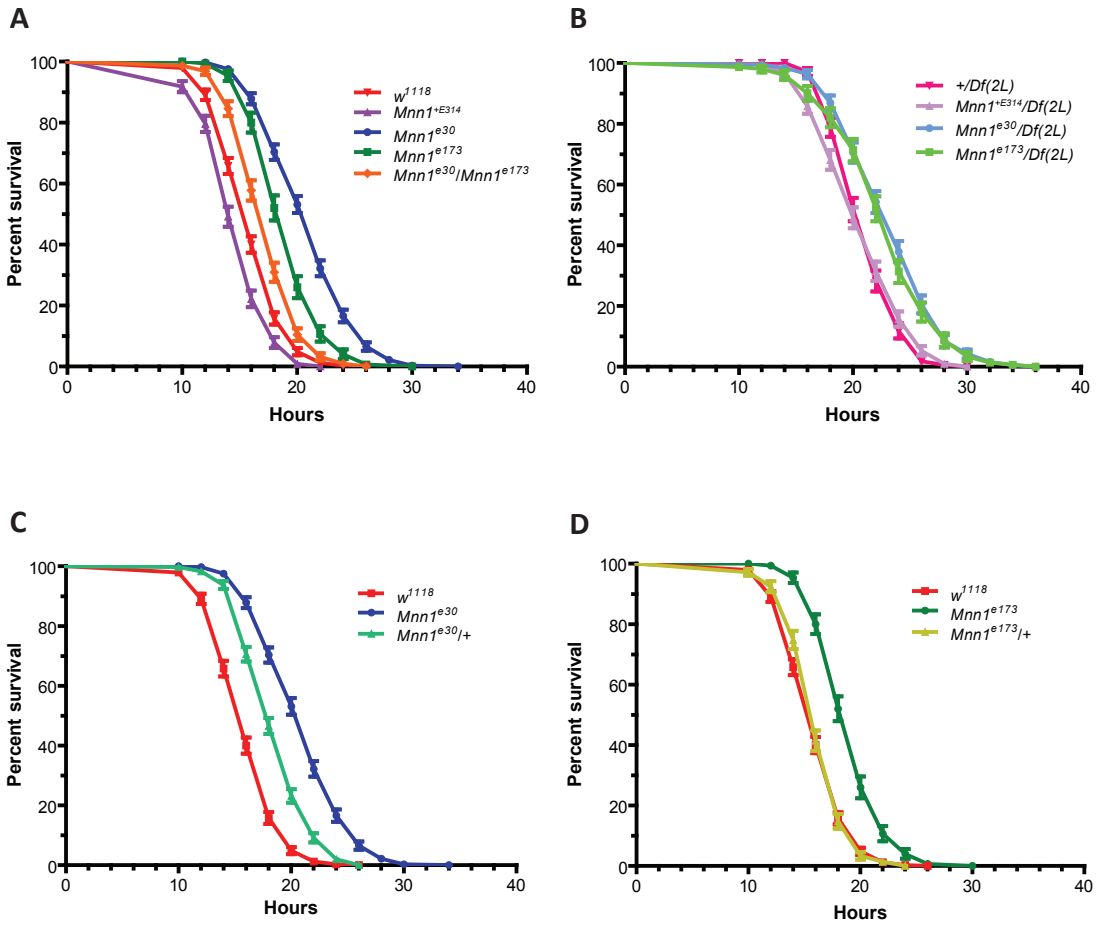

Figure 6.2. Desiccation survival of male flies.
The survival curves for 4-6 day males are grouped in order to ease comparison between specific genotypes. Larval density was controlled during development and males were allowed to mate freely prior to commencing the experiment. Desiccating conditions were created by transferring flies, ten per tube, to empty glass tubes. Survival was examined after 10 hrs and then every 2 hrs thereafter until all flies had perished. Two separate experimental crosses were used to generate flies for each genotype and 2-3 trials were carried out from each cross, with the number of individuals variable in each trial. All genotypes were tested simultaneously. A total of 150 - 350 flies were tested for each genotype. Survival curves were generated using GraphPad Prism and significance was determined using a log-rank (Mantel-Cox) test, followed by multiple pairwise tests (See Appendix I, Table I.1 for a summary of statistics for this experiment). A) *Mnn1* mutants ($Mnn1^{e30}$ and $Mnn1^{e173}$) and the heteroallelic combination ($Mnn1^{e30}/Mnn1^{e173}$) survive better than the wild-type control (w^{1118}) and precise excision control $Mnn1^{+E314}$. B) All alleles over the deficiency ($Df(2L)spd^{l2}$) survive well. *Mnn1* mutations over the deficiency ($Mnn1^{e30}/Df(2L)$ and $Mnn1^{e173}/Df(2L)$) survive better than controls over the deficiency ($+/Df(2L)$, $Mnn1^{+E314}/Df(2L)$). C) There is a trend that reducing the functional copy number of *Mnn1* with the $Mnn1^{e30}$ allele leads to increased desiccation survival. D) Two copies of the $Mnn1^{e173}$ allele are required for increased survival.

The presence of *Df(2L)* significantly enhanced survival of flies compared to most other genotypes (Figure 6.2B). Controls combined with the *Df(2L)* chromosome (*+/Df(2L)* and $Mnn1^{+E314}/Df(2L)$) had similar survivals (p=0.25) but survived dramatically better than homozygous controls (w^{1118}, $Mnn1^{+E314}$) (Appendix I, Figure I.1). This suggests that the presence of this deficiency chromosome on its own leads to a survival advantage that is independent of loss of menin function, as the controls over *Df(2L)* would retain a functional *Mnn1* allele. Haploinsufficiency of *Mnn1* cannot account for the increased survival of *+/Df(2L)* and $Mnn1^{+E314}/Df(2L)$, since heterozygous mutants ($Mnn1^{e30/+}$ and $Mnn1^{e173/+}$) do not have a similar increased survival (Appendix I, Figure I.1). Although $Mnn1^{e30/+}$ does survive better than w^{1118} (Figure 6.2C), $Mnn1^{e173/+}$ does not (Figure 6.2D). So reducing the functional copy number of *Mnn1* in half does not account for an increased survival. Combining a *Mnn1* deletion with *Df(2L)* further enhanced male desiccation survival, as $Mnn1^{e30}/Df(2L)$ and $Mnn1^{e173}/Df(2L)$ survived better than *+/Df(2L)* and $Mnn1^{+E314}/Df(2L)$ (Figure 6.2B). The survival of each $Mnn1^{e30}/Df(2L)$ and $Mnn1^{e173}/Df(2L)$ were similar (p=0.0078). Thus, the desiccation survival of males harbouring *Df(2L)* is further enhanced by complete loss of *Mnn1*, suggesting an additive effect.

Figure 6.2C and D show trends for each of the *Mnn1* deletion alleles comparing the wild-type (w^{1118}), that has two functional *Mnn1* genes, to heterozygous ($Mnn1^{-/+}$) and homozygous ($Mnn1^{-/-}$) flies. For $Mnn1^{e30}$, there is a trend that reducing the functional copy number of *Mnn1* leads to increased survival. The $Mnn1^{e173}$ allele does not show the trend to the same extent as $Mnn1^{e30}$ since the heterozygous mutants ($Mnn1^{e173/+}$) do not survive better than w^{1118} controls (p=0.6037). Only loss of both

copies of *Mnn1*^{e173} leads to increased survival (Figure 6.2D). The overall conclusion from these experiments is that a loss of menin function enhances survival of males exposed to desiccation stress.

2.2 Female desiccation survival analysis

Female desiccation survival was assessed in the same manner as that described for males. The final data set was compiled from two separate experiments with a total of 150-330 flies per genotype (see Table 6.2 for sample sizes). Survival curves for all 11 genotypes are graphed together in Appendix I, Figure I.2 and simplified curve comparisons are shown in Figure 6.3. A summary of the statistical analyses is provided in Appendix I, Table I.2. Table 6.2 also provides the median survivals for female flies in the desiccation experiment.

Most conclusions that can be drawn for male desiccation survival can also be made for female desiccation survival. As Figure 6.3A shows, female *Mnn1* deletion mutants survived better than controls (w^{1118} and *Mnn1*$^{+E314}$). Like males, female *Mnn1*^{e30} survived better than *Mnn1*^{e173}; however, unlike males, heteroallelic females had a similar survival as *Mnn1*^{e173}. This is the expected result as the heteroallelic combination should survive at least as well as the weaker of the two alleles. Another major difference between males and females is that with females, combining a *Mnn1* deletion allele with the *Df(2L)* chromosome did not enhance survival (Figure 6.3B). In fact, *Mnn1*^{e30}*/Df(2L)* survived significantly worse than *+/Df(2L)* and *Mnn1*$^{+E314}$*/Df(2L)*. Thus, in females, the *Df(2L)* enhanced survival is independent of loss of menin and appears to contribute more to the phenotype than loss of menin, as loss of the other *Mnn1* allele in *Df(2L)* females did not further enhance survival.

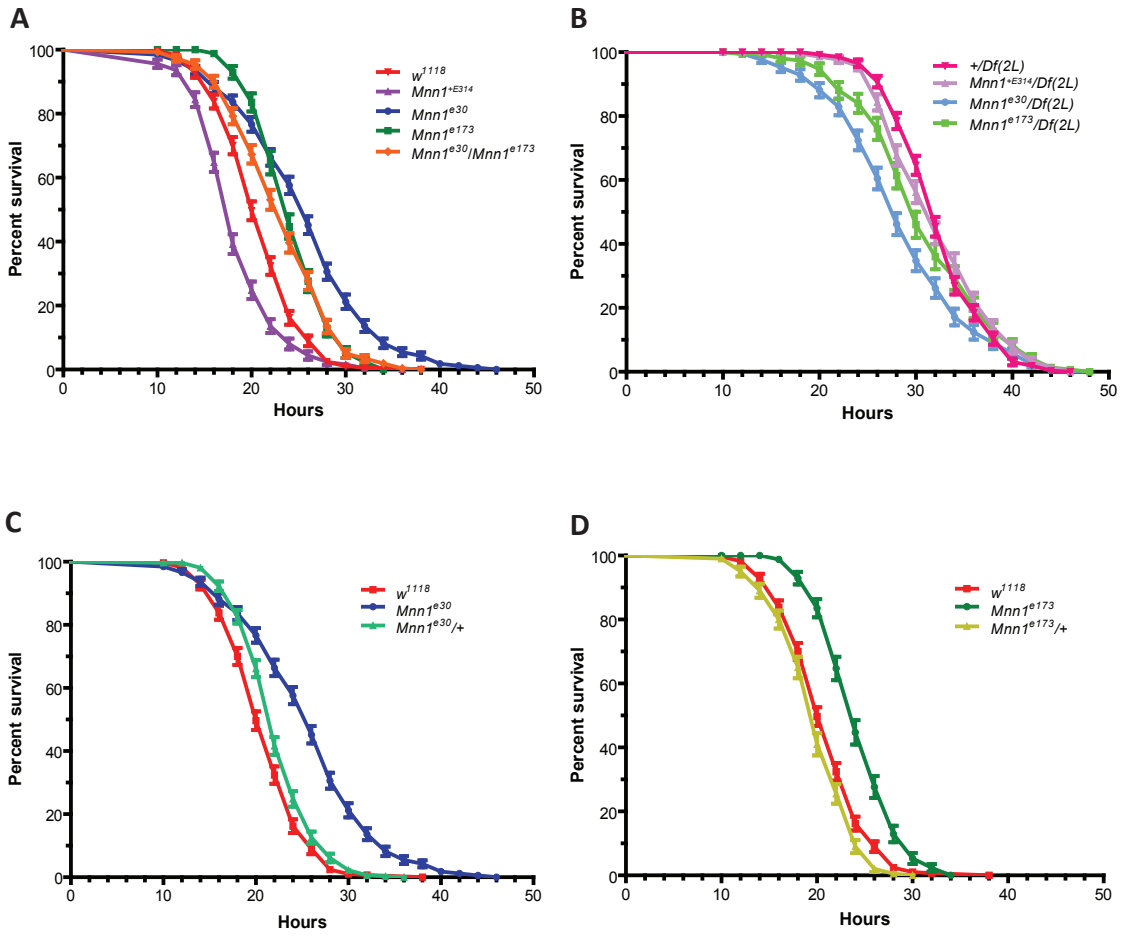

Figure 6.3. Desiccation survival of female flies.
The survival curves for 4-6 day females are grouped in order to ease comparison between specific genotypes. Larval density was controlled during development and females were allowed to mate freely prior to commencing the experiment. Desiccating conditions were created by transferring flies, ten per tube, to empty glass tubes. Survival was examined after 10 hrs and then every 2 hrs thereafter until all flies had perished. Two separate experimental crosses were used to generate flies for each genotype and 3 trials were carried out from each cross, with the number of individuals variable in each trial. All genotypes were tested simultaneously. A total of 150 - 330 flies were tested for each genotype. Survival curves were generated using GraphPad Prism and significance was determined using a log-rank (Mantel-Cox) test, followed by multiple pairwise tests (see Appendix I, Table I.2 for a summary of the statistics for this experiment). A) *Mnn1* mutants ($Mnn1^{e30}$ and $Mnn1^{e173}$) and the heteroallelic combination ($Mnn1^{e30}/Mnn1^{e173}$) survive better than the wild-type control (w^{1118}) and precise excision control ($Mnn1^{+E314}$). B) All alleles over the deficiency ($Df(2L)spd^{J2}$) survive well. *Mnn1* deletions over the deficiency ($Mnn1^{e30}/Df(2L)$, $Mnn1^{e173}/Df(2L)$) do not have any increased survival compared to controls ($+/Df(2L)$, $Mnn1^{+E314}/Df(2L)$). C) There is a slight increase in survival with a single $Mnn1^{e30}$ allele that is further enhanced in homozygous $Mnn1^{e30}$ mutants . D) A single $Mnn1^{e173}$ allele is not sufficient to cause an increase in survival. Only homozygous $Mnn1^{e173}$ mutants have increased survival.

The trends described for male *Mnn1* mutants (Figure 6.2C and D), where progressive loss of functional *Mnn1* alleles led to increased survival, are not as strong for females (Figures 6.3C and D). In females, $Mnn1^{e30/+}$ survived better than w^{1118} (p=0.0005) (Figure 6.3C); although, this difference was more obvious in males (Figure 6.2C). Heterozygous $Mnn1^{e173}$ females had similar survival curves as w^{1118} (p=0.0042); two copies of the $Mnn1^{e173}$ allele were required to provide any significant survival advantage (Figure 6.3D). As with males, the overall conclusion for females is that loss of menin function increases desiccation survival.

3. Starvation survival of Mnn1 mutants

3.1 Male starvation survival analysis

The results for male starvation survival are difficult to interpret due to the short window of time when most flies succumb to starvation. Most males survived after 24 hours; however, by 48 hours the majority had perished (see Appendix J, Figure J.1 for all genotypes graphed together). Although there does not appear to be much resolution, the survival curves for many genotypes were still found to differ significantly, probably due to the large sample size used for these studies (See Appendix J, Table J.1 for statistical analyses). Curves that appear very similar except for on a single day were often found to be statistically different using the log-rank (Mantel-Cox) test and the Bonferroni corrected significance level ($p<0.002$). In this analysis, results from two experiments, with different parental houses, were combined and the sample size varied from 190-350 flies per genotype (see Table 6.3 for sample sizes). The median survival of most genotypes was 2 days, with only $Mnn1^{e30}$, $Mnn1^{e30}/Df(2L)$ and $Mnn1^{+E314}/Df(2L)$ having median survivals of 3 days (Table 6.3).

Table 6.3. Median survival* and sample size for the starvation assay.

Genotype	Males		Females	
	Median Survival (days)	n	Median Survival (days)	n
w^{1118}	2	350	2	340
$Mnn1^{+E314}$	2	190	2	180
$Mnn1^{e30}$	3	310	3	350
$Mnn1^{e173}$	2	250	2	230
$Mnn1^{e30}/Mnn1^{e173}$	2	310	3	330
$Mnn1^{e30}/+$	2	270	2	270
$Mnn1^{e173}/+$	2	300	2	280
+/Df(2L)	2	240	4	290
$Mnn1^{+E314}/Df(2L)$	3	210	4	300
$Mnn1^{e30}/Df(2L)$	3	300	4	280
$Mnn1^{e173}/Df(2L)$	2	200	3	250

*Median survival is defined as the time when 50 % of the population had perished.

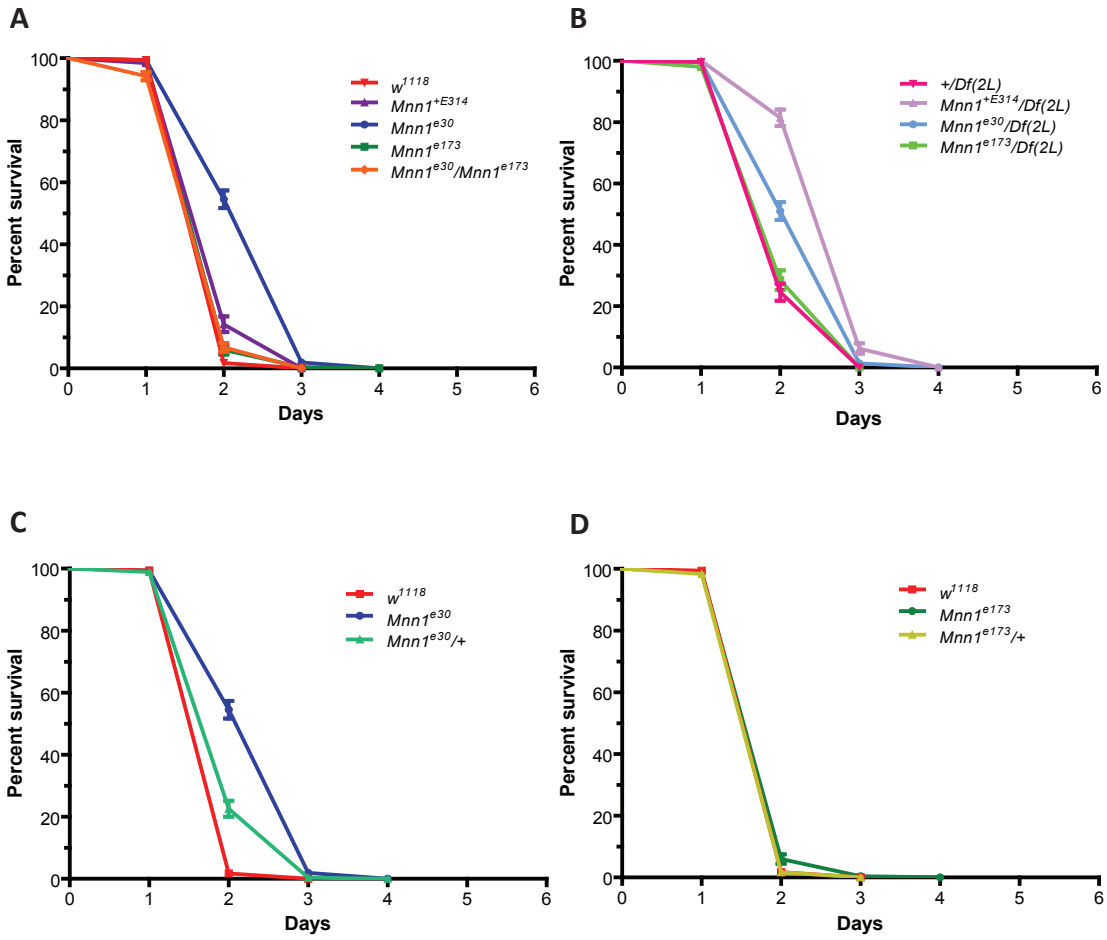

Figure 6.4. Starvation survival of male flies.
The survival curves for 4-6 d males are grouped in order to ease comparison between specific genotypes. Larval density was controlled during development and males were allowed to mate freely prior to commencing the experiment. Flies were starved by transferring to 1 % agar, with ten flies per vial. Survival was examined every 24 hrs until all flies had perished. Two separate experimental crosses were used to generate flies for each genotype and 2-4 trials were carried out from each cross, with the number of individuals variable in each trial. All genotypes were tested simultaneously and a total of 190 - 350 flies were tested for each genotype. Survival curves were generated using GraphPad Prism and significance was determined using a log-rank (Mantel-Cox) test, followed by multiple pairwise comparisons (see Appendix J, Table J.1 for a summary of the statistics for this experiment). Most males died within 24-48 hrs of starvation, making it difficult to identify differences between genotypes during this short time span. A) Only $Mnn1^{e30}$ mutants survived starvation significantly better than controls; $Mnn1^{e173}$ and $Mnn1^{e30}/Mnn1^{e173}$ did not have increased starvation survival. B) The deficiency $Df(2L)spd^{i2}$ led to increased survival; however, this was not dependent on complete loss of *Mnn1*. C) Heterozygous $Mnn1^{e30}/+$ survived starvation slightly better than wild-type. Homozygous $Mnn1^{e30}$ survived better than heterozygous flies and controls. D) Neither heterozygous ($Mnn1^{e173}/+$) nor homozygous $Mnn1^{e173}$ survived starvation better than wild-type.

The results of the starvation experiments are difficult to interpret since flies with the different *Mnn1* alleles, did not have similar survivals; unlike in the desiccation assay where, for the most part, both deletion mutants behaved similarly. In the starvation assay, $Mnn1^{e30}$ males survived significantly better than both the wild-type control (w^{1118}) and the precise excision control ($Mnn1^{+E314}$) (Figure 6.4A). $Mnn1^{e173}$ males did not survive better than either control (p=0.0248 and p=0.0180) (Figure 6.4A). The heteroallelic males ($Mnn1^{e30}/Mnn1^{e173}$) had a similar survival as $Mnn1^{e173}$ (p=0.1387).

The presence of the deficiency allele led to an increase in male starvation survival. The deficiency genotypes survived better than all other genotypes tested, except $Mnn1^{e30}$ (see Appendix J, Figure J.1). $Mnn1^{e30}/Df(2L)$ did not differ significantly from $Mnn1^{e30}$ (p=0.3579), suggesting in this case that the presence of the deficiency did not offer any additional survival advantage that was not associated with loss of menin. Surprisingly, $Mnn1^{+E314}/Df(2L)$ had the best starvation resistance (Figure 6.4B), which contradicts the train of thought that complete loss of menin function was necessary for increased starvation survival, since these flies retain a functional *Mnn1* allele. $Mnn1^{e173}/Df(2L)$ and $+/Df(2L)$ males had similar starvation survivals (Figure 6.4B, p=0.5247), thus the additional presence of the $Mnn1^{e173}$ deletion allele did not lead to any increased survival.

For male starvation survival, there was no overall trend that was consistent between the *Mnn1* alleles. For $Mnn1^{e30}$, it appears that loss of a single functional copy of *Mnn1* ($Mnn1^{e30/+}$) is sufficient to cause a moderate survival advantage, which is further enhanced in a homozygous mutant (Figure 6.4C). The same cannot be said for the $Mnn1^{e173}$ allele, as heterozygous and homozygous mutants both had survivals

comparable to w^{1118} (Figure 6.4D). The differences in the behaviour of the *Mnn1* deletion alleles in this assay, makes it difficult to draw any conclusions for the overall role of menin in starvation survival in males.

3.2 Female starvation survival analysis

As with males, females used in the starvation assay came from two separate parental crosses and 180-350 flies were tested per genotype (see Table 6.3 for the sample sizes and Appendix J, Table J.2 for a summary of the statistics). Overall, females resisted starvation much better than males (compare Figure 6.5 with Figure 6.4). Most females survived the first 24 hours of starvation and succumbed to starvation between days 2 and 5 (see Appendix J, Figure J.2 for all genotypes graphed together). Since females did not perish as rapidly as males, it was easier to distinguish between the starvation sensitivities of different genotypes. The median survivals for controls (w^{1118}, $Mnn1^{+E314}$), heterozygous mutants and homozygous $Mnn1^{e173}$ were all 2 days and the rest of the genotypes had 3 or 4 day median survivals (Table 6.3).

Figure 6.5A shows that like males, $Mnn1^{e30}$ females survived starvation significantly better than both controls. $Mnn1^{e173}$ females did not survive nearly as well as $Mnn1^{e30}$ mutants; they did survive better than w^{1118} but not better than the precise excision controls $Mnn1^{+E314}$. In this assay, $Mnn1^{+E314}$ mutants survived better than w^{1118}, suggesting that something else in the second chromosome background of these flies could be providing a starvation survival advantage. Thus, the increased survival of $Mnn1^{e173}$ females compared to w^{1118} is not likely due to loss of menin function as the survival of $Mnn1^{e173}$ females was no different than $Mnn1^{+E314}$. The survival curve of the transheterozygotes ($Mnn1^{e30}/Mnn1^{e173}$) fell in between that of $Mnn1^{e30}$ and $Mnn1^{e173}$,

but was closer to *Mnn1*^{e173}. In this case, the positive survival advantage afforded by the *Mnn1*^{e30} allele was mostly negated by the presence of the weaker *Mnn1*^{e173} allele. As the two *Mnn1* deletion alleles did not have similar phenotypes, there must be additional factors at play here, either contributing positively to the survival advantage of *Mnn1*^{e30} or negatively towards the survival disadvantage of *Mnn1*^{e173}.

As with males, the presence of *Df(2L)spd*^{j2} in females, regardless of what was on the other second chromosome, increased the starvation survival compared to all genotypes except *Mnn1*^{e30} (see Appendix J, Figure J.2). Combining a *Mnn1* deletion allele with the deficiency chromosome did not enhance survival (Figure 6.5B). In fact, *Mnn1*$^{+E314}$*/Df(2L)* and *+/Df(2L)* survived significantly better than *Mnn1*^{e30}*/Df(2L)* and *Mnn1*^{e173}*/Df(2L)*. This is not what you would expect to see if the enhanced survival phenotype was due to loss of menin function.

Meaningful trends correlating the functional copy number of *Mnn1* alleles with female starvation survival were not observed for both mutants. Similar to males, the presence of a single copy of the *Mnn1*^{e30} deletion allele (*Mnn1*$^{e30/+}$) led to enhanced survival compared to *w*^{1118} (Figure 6.5C). It should be noted that the heterozygous flies did not survive better than *Mnn1*$^{+E314}$ so this is probably not meaningful. Homozygous *Mnn1*^{e30} survived significantly better than heterozygous and *w*^{1118} flies. A single copy of the *Mnn1*^{e173} allele did not provide any survival enhancement (Figure 6.5D). Although *Mnn1*^{e173} survived better than *w*^{1118} and heterozygous *Mnn1*$^{e173/+}$, this enhanced survival is not meaningful since *Mnn1*^{e173} did not survive better than *Mnn1*$^{+E314}$ (Figure 6.5A).

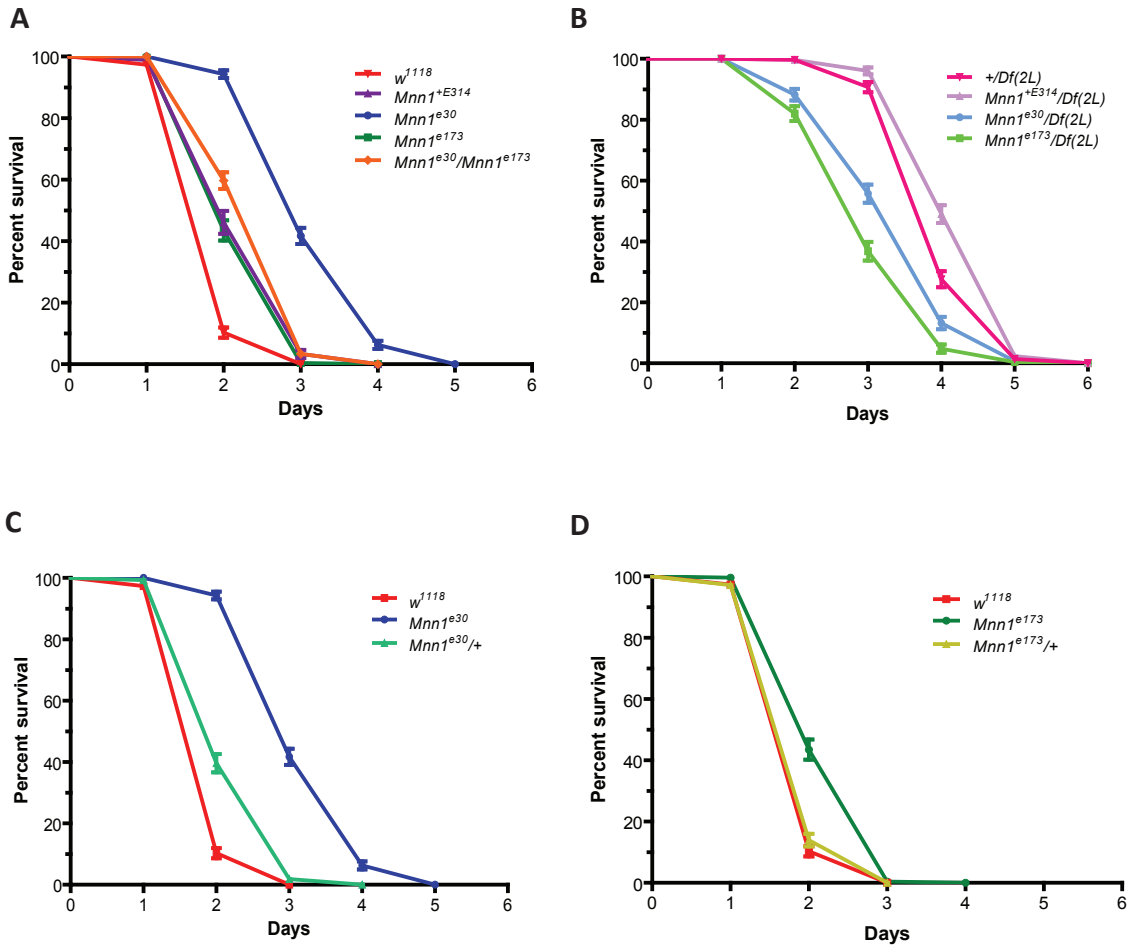

Figure 6.5. Starvation survival of female flies.
The survival curves for 4-6 d females are grouped in order to ease comparison between specific genotypes. Larval density was controlled during development and females were allowed to mate freely prior to commencing the experiment. Flies were starved by transferring to 1 % agar, with ten flies per vial. Survival was examined every 24 hrs until all flies had perished. Two separate experimental crosses were used to generate flies for each genotype and 2-4 trials were carried out from each cross, with the number of individuals variable in each trial. All genotypes were tested simultaneously. A total of 180 - 350 flies were tested for each genotype. Survival curves were generated using GraphPad Prism and significance was determined using a log-rank (Mantel-Cox) test, followed by multiple pairwise comparisons (see Appendix J, Table J.2 for a summary of the statistics for this experiment). A) *Mnn1*^{e30} and the heteroallelic *Mnn1*^{e30}/*Mnn1*^{e173} mutants survived better than both the wild-type (*w*^{1118}) and precise excision control (*Mnn1*$^{+E314}$). *Mnn1*^{e173} flies survived better than *w*^{1118} but not the precise excision control. B) The presence of *Df(2L)spd*^{j2} increased survival, with *Mnn1* deletions over *Df(2L)* not surviving as well as controls over the deficiency. C) Heterozygous *Mnn1*^{e30}/+ survived better than wild-type, with addition of the second *Mnn1*^{e30} allele further enhancing survival. D) Heterozygous *Mnn1*^{e173}/+ did not survive starvation better than wild-type but homozygous *Mnn1*^{e173} had increased starvation survival compared to *w*^{1118}.

Overall, it is difficult to conclude anything with certainty from the female starvation survival results as the two *Mnn1* deletion mutants did not behave similarly and only *Mnn1*^{e30} survived better than controls. Please note that the genotypes of the *Mnn1* mutants used in these assays were re-confirmed by PCR to ensure that no contamination had occurred (see Appendix K, Figure K.1).

DISCUSSION

The results described above suggest that loss of menin function contributes to an increased desiccation, and possibly starvation, resistance. Although these results are still preliminary and other lines need to be tested before reliable conclusions can be drawn, the hypothesis that menin is functioning in *Drosophila* insulin signalling warrants further investigation. Definitive proof that menin is a component of the pathway or that it regulates insulin signalling remains to be obtained. However, since *Mnn1* mutants have a similar phenotype to other insulin signalling mutants, it suggests menin plays a role in this pathway. More specifically, loss of menin function enhances survival under desiccation and starvation stress, just as loss of genes that positively regulate the pathway. Although it remains to be determined whether or not menin acts directly to positively regulate insulin signalling.

1. The Mnn1 mutant phenotype

1.1 Mnn1 mutant desiccation phenotype

When studying insulin signalling mutants, most researchers look at starvation survival phenotypes, with fewer also examining desiccation survival phenotypes. Perhaps because of the rapid death, it is more difficult to identify differences between genotypes

in this shorter time frame so researchers preferentially examine starvation survival. Overall, my results show that loss of menin function results in increased desiccation survival for both males and females (Figures 6.2 and 6.3). In general, complete loss of menin was required to provide a pronounced increase in desiccation survival as heterozygotes did not consistently survive better than controls for both *Mnn1* alleles and sexes. My results are consistent with those from other studies. For example, in a study by Söderberg *et al.* (2011), when 4-8 d males were subjected to desiccation, w^{1118} controls had all perished by 24 hrs with the median survival being about 17 hrs, while *DILP5* mutants had prolonged desiccation survival but were all dead by 28 hours with the median survival being about 19 hrs. In my male desiccation experiments, w^{1118} had a median survival of 16 hrs and $Mnn1^{e30}$ and $Mnn1^{e173}$ had median survivals of 22 hrs and 20 hrs, respectively (Table 6.2). So the increase in desiccation survival with *Mnn1* deletion is similar to that observed for the *DILP5* mutant (Söderberg et al., 2011). As this group only tested male flies, female flies cannot be compared.

There were some differences in the survival of the two *Mnn1* alleles in the desiccation assay; $Mnn1^{e30}$ flies consistently survived better than $Mnn1^{e173}$ flies (Figures 6.2A and 6.3A). Although both these deletion mutants are considered null, because mRNA and protein are not detected from these flies (Papaconstantinou et al., 2005), it is not uncommon for different alleles of the same gene to differ in these types of survival assays. For example, two *Lnk* mutants (Lnk^{Del29} and Lnk^{d07478}) differ in their longevity and starvation survival and for this reason different alleles were graphed separately, each with their corresponding controls (Slack et al., 2010). Unexpectedly, for males, the $Mnn1^{e30}/Mnn1^{e173}$ transheterozygotes did not survive as well as either homozygous

mutant (Figure 6.2A) but for females the transheterozygotes survived as well as *Mnn1*^{e173} flies which are the weaker stock (Figure 6.3A). The reason for this observation in males is unclear, but regardless, the male transheterozygotes still survived better than the *w*^{1118} and *Mnn1*$^{+E314}$ controls.

Surprisingly, the presence of the *Df(2L)spd*^{j2} chromosome dramatically increased survival under desiccation conditions (Appendix I, Figures I.1 and I.2). Normally, deficiency chromosomes are expected to have a survival disadvantage due to the loss of multiple genes from the deleted region. As mentioned, this chromosome could not be switched into the *w*^{1118} background like all the other alleles studied due to the inability to create an intermediary stock with *Df(2L)spd*^{j2} that was completely balanced and marked on the second and third chromosomes. Thus, compared to all the other genotypes tested, the *Df(2L)* flies had a different genetic background. This difference in genetic background could explain the increased survival, as there is great variability in these assays resulting from differences in genetic background. In addition, loss of some other gene in the deleted region of the *Df(2L)spd*^{j2} chromosome could provide a survival advantage (see Section 4.2 below). Because of this, examining the *Df(2L)spd*^{j2} phenotype does not add much to our understanding of the effects of loss of *Mnn1* on desiccation survival.

Despite the few inconsistencies described above, it is reasonable to conclude that *Mnn1* mutants have increased desiccation resistance and this phenotype is observed for both males and females. The physiological reason for this increased survival has not been well-studied. Wild populations of *D. melanogaster* that are desiccation resistant have higher total water and hemolymph content as well as

increased carbohydrate stores (Parkash et al., 2012). Also, loss of insulin signalling in the renal tubules may be important for promoting desiccation survival, as this organ is important for regulating water and ion homeostasis. Down-regulation of *DILP5* or *dInR* in principal cells of the renal tubules, mediated through RNAi, results in increased desiccation survival (Söderberg et al., 2011). Thus, perhaps *Mnn1* mutants are able to conserve water better than controls, or have increased glycogen stores that help them survive longer under desiccating conditions.

1.2 Mnn1 mutant starvation phenotype

The starvation phenotype of *Mnn1* flies is not as easy to interpret as the desiccation phenotype because in this assay, the two *Mnn1* mutants did not behave in the same manner (Figures 6.4 and 6.5). It was particularly difficult to interpret the starvation data from males because of the small time frame within which most of the flies perished. One flaw in my experimental design was to only check survival every 24 hours, as opposed to every 6 or 12 hours. Recording survival more frequently may have allowed for a greater resolution between the genotypes, especially for males where most flies succumbed to starvation between 24 and 48 hours. Despite this flaw, both male and female $Mnn1^{e30}$ flies survived starvation better than the wild-type and precise excision controls; however, $Mnn1^{e173}$ flies have a similar survival as the $Mnn1^{+E314}$ controls (Figures 6.4 and 6.5). This means that the observed phenotypes are not solely due to loss of menin as both alleles are considered null; therefore, additional factors are influencing the survival of *Mnn1* mutants in this assay.

These results could be interpreted in two ways. First, you could assume that the $Mnn1^{e30}$ mutants show the true phenotype for loss of menin function and that the

Mnn1^{e173} mutants carry some other deleterious mutation on their second chromosome that masks the survival advantage imparted by loss of menin. In this case, if *Mnn1*^{e30} is assumed to be the true phenotype, then it appears as though loss of menin results in increased starvation survival, similar to what was observed for desiccation survival. Also the phenotype of *Mnn1*^{e30} resembles that of other positive regulators of insulin signalling. This potential interpretation is logical because the chromosome carrying the *Mnn1*^{e173} deletion is also associated with sterility (see Chapter 5, Section 6); therefore, it would not be hard to imagine that other deleterious mutations or modifications also exist on the *Mnn1*^{e173} chromosome. An alternative interpretation for the discrepancy between the two *Mnn1* alleles is that the *Mnn1*^{e173} allele represents the true phenotype and the *Mnn1*^{e30} mutants carry additional modifications or mutations on the second chromosome that are enhancing survival under starvation conditions. If this is the case, then loss of *Mnn1* function would lead to no change in starvation survival, suggesting that menin does not share the starvation resistance phenotype that other insulin signalling mutants possess. This second interpretation would not agree as well with the *Mnn1* desiccation data. Although, starvation and desiccation phenotypes do not necessarily need to co-exist; populations can be selected for starvation or desiccation resistance and the basis for each resistance is physiologically different as increased lipids are found in the former and increased carbohydrates in the latter (Parkash et al., 2012). So the *Mnn1* mutants may not necessarily show resistance to both stresses and it is possible that they do not have a starvation phenotype if the *Mnn1*^{e173} results represent the true phenotype. In order to resolve this discrepancy, additional *Mnn1* alleles need to be tested to indisputably determine the *Mnn1* starvation phenotype (see Section 4.1).

As with the desiccation survival assay, the presence of the *Df(2L)* chromosome significantly increased the starvation survival of both males and females (Appendix J, Figures J.1 and J.2). There was no additional survival advantage when the *Df(2L)* chromosome was combined with $Mnn1^{e30}$ as controls over *Df(2L)* generally survived better than the *Mnn1* deletions over the deficiency. As explained before, this *Df(2L)* is in a different genetic background and may not be useful for comparison to the other genotypes. Alternatively, other genes could be deleted that when reduced in copy number increase survival under starvation conditions. Other deficiency 2L chromosomes, that can be switched into the w^{1118} genetic background, should be tested in order to determine if the increased survival observed in these assays is actually meaningful (see Section 4.2).

For the sake of interpretation and discussion I will assume that the $Mnn1^{e30}$, and not the $Mnn1^{e173}$, mutants represent the true phenotype associated with loss of *Mnn1*, even though as described above this remains to be proven. In general, my flies did not seem to survive starvation quite as long as what was observed by other experimenters (Bjedov et al., 2010; Broughton et al., 2005; Oldham et al., 2002). One study by Teleman *et al.* (2005) looked at survival of w^{1118} males and found that most perished between 24-48 hrs, with only about 20% surviving past 48 hrs, which is quite similar to what I observed. Differences between my study and others could be due to external factors that were not controlled during these experiments such as humidity, variable light/dark cycles and temperature fluctuations; these factors could differ significantly from one place to another and from one season to another. Not to mention that different genetic backgrounds were used in other experiments; therefore, they may not be directly

comparable. It should be noted that in some of my previous starvation experiments (data not shown), flies survived longer than what was observed in the final experiments described in this chapter; however, the overall trends between genotypes were similar.

As mentioned above, the starvation survival of *Mnn1* mutants cannot be compared directly to other studies; however, some commonalities can be identified. Firstly, in my assays males survived much worse than females and this has been observed by many other groups (*e.g.* Slack et al., 2010). Secondly, different alleles of the same gene often result in significantly different survival curves even though the overall phenotype is comparable (Slack et al., 2010). So the fact that the *Mnn1* alleles had different survival curves is not unheard of; however, in the case of the starvation assays, only $Mnn1^{e30}$ differed significantly from the controls which makes the results difficult to interpret.

Assuming that $Mnn1^{e30}$ flies represent the true phenotype for loss of menin function under starvation conditions, this would suggest that menin could be functioning as a positive regulator of insulin signalling since the phenotype resembles that of other components of the signalling pathway. Starvation resistance in wild *D. melanogaster* populations is linked with increased lipids (Parkash et al., 2012) and many insulin signalling mutants, such as *Chico* and *Lnk*, have been shown to have increased accumulation of lipids (Böhni et al., 1999; Slack et al., 2010). Although this has not been empirically determined for $Mnn1^{e30}$ flies, they may have higher lipid levels than controls as lysate preparations from $Mnn1^{e30}$ flies have been casually observed on numerous occasions to have seemingly more lipids than control flies. Since $Mnn1^{e30}$ flies survive

starvation longer than controls they may have elevated lipid stores that supply them with energy for a longer duration of time.

2. Important variables in desiccation and starvation survival analyses

Several variables greatly impact survival studies and there are some inconsistencies in the way experiments are conducted in the field making it difficult to directly compare one study to the next. I have attempted to address these factors in my studies to ensure that results obtained were due to loss of *Mnn1* function and not confounding variables. The first influential factor is the genetic background, which should be carefully controlled to ensure there are no other modifications or mutations that could be influencing survival. The second factor that can affect starvation and desiccation survival is the conditions of larval development. Flies should be reared with a controlled larval density since low nutrients during larval development, which can result from overcrowding of cultures, results in reduced adult size and altered fitness (Borash and Ho, 2001; Kolss et al., 2009). A third aspect to control is that male and female flies should always be examined separately in such studies since sex specific phenotypes may exist and there is quite a discrepancy in the survival of the sexes. In addition, the age of flies, as well as the mating status, can greatly influence survival. It has been demonstrated that mated females survive starvation better than virgins at all ages tested from 4 to 45 days (Rush et al., 2007). Finally, it should be mentioned that when comparing results of different starvation experiments some researchers examine amino acid starvation and flies still have access to sugar, while other researchers examine complete starvation conditions. The conditions used in my study were the more stringent complete starvation conditions with flies being deprived of all nutrients and

only having access to water to prevent the effects of dehydration. Thus, it is important to consider these variables when designing survival experiments and also when comparing results to other studies.

3. Discussion of the Mnn1 phenotype and potential role for menin in insulin signalling

3.1 Role for menin in Drosophila insulin signalling

The results of the starvation and desiccation experiments suggest that menin could play a role in the regulation of insulin signalling. As complete loss of function of many components of the insulin signalling pathway results in lethality or severe size phenotypes, which are not observed in *Mnn1* mutants, it is proposed that menin plays an auxiliary role in this pathway and is involved in regulation and fine-tuning of the insulin response but is not an essential component of the pathway, at least not during development. Interactions were observed in mammalian cells showing menin to associate with and inhibit both FOXO1 (Wuescher et al., 2011) and Akt (Wang et al., 2011) which seem to be contradictory observations (see Section 3.3 for more discussion). If menin was acting as an inhibitor of dAkt in *Drosophila* insulin signalling, then *Mnn1* mutants would be expected to have a phenotype similar to *dPTEN* mutants, as dPTEN counteracts the effects of dPI3K activity, leading to reduced dAkt activation. As *dPTEN* hypomorphs have decreased (Oldham et al., 2002) and $Mnn1^{e30}$ has increased starvation survival, it does not seem as though menin is acting as an inhibitor of dAkt. On the other hand, if menin is acting as an inhibitor of dFOXO, then loss of menin function should have the opposite phenotype as loss of dFOXO function. Since *dFOXO* nulls have reduced starvation survival (Kramer et al., 2008), the phenotype of $Mnn1^{e30}$

mutants in the starvation assay is in agreement with menin acting as an inhibitor of dFOXO.

3.2 dFOXO-mediated transcription and enhanced starvation survival

If menin is functioning as a dFOXO inhibitor, the loss of menin would result in increased dFOXO transcriptional activity which could result in increased starvation survival through activation of several target genes. A well-studied target of dFOXO-mediated transcription is d4E-BP, a suppressor of translation initiation (Junger et al., 2003; Puig et al., 2003). By blocking the initiation of translation of non-essential products, the cell can divert its energy resources specifically to processes that will promote survival under adverse conditions.

In mammalian cells, two key targets of FOXO1 that are important for starvation resistance are *PEPCK* (phosphoenolpyruvate carboxykinase) and *G6Pase* (Glucose-6-phosphatase) key enzymes in gluconeogenesis and glycogenolysis (Puigserver et al., 2003). Under starvation conditions, being able to release energy from glycogen stores is essential for prolonging survival when external nutrients are not available. The role for dFOXO regulation of PEPCK and gluconeogenesis in *Drosophila* is unclear (Gershman et al., 2007). Also, in mammalian cells, FOXO1 induces expression of the cyclin-dependent kinase inhibitor $p27^{Kip1}$ leading to cell cycle arrest (Medema et al., 2000) which would be important for limiting proliferation under poor nutrient conditions; however, to my knowledge, a similar mechanism of cell cycle regulation through the *Drosophila* p27 orthologue, *dacapo*, has not been demonstrated.

Various microarray and genome-wide target analyses have found that dFOXO regulates many genes and the targets also vary from larvae to adults. Gene ontology

analysis suggests that dFOXO is a key regulator of macromolecule and nucleic acid metabolism, signal transduction, cell growth/maintenance and organogenesis (Gershman et al., 2007). dFOXO-mediated fuel metabolism includes up-regulation of lipid oxidation and down-regulation of glucose oxidation. dFOXO regulates many genes involved in the insulin and TOR pathways (*dInR*, *Chico*, *Lnk*, *dAkt*, *dPDK1*, *dTOR*, *dS6K*) perhaps in an effort to sensitize the cells to insulin signalling if nutrients become available again (Alic et al., 2011; Gershman et al., 2007; Puig and Tjian, 2005). Overall, dFOXO is a key target that is repressed by insulin signalling and activated under low nutrient conditions. It is important for starvation survival and acts through regulation of targets involved in diverse functions such as translation inhibition, energy metabolism, nutrient sensing and proliferation.

3.3 Further discussion of results in relation to menin's interactions with Akt and FOXO1

As the investigation of a potential role for menin in insulin signalling was largely inspired by the identification of menin's interaction with Akt and FOXO1 (Wang et al., 2011; Wuescher et al., 2011), two key components of the insulin signalling pathway in mammals, it is important to discuss the current findings in *Drosophila* in the context of these two potential interactions. As previously mentioned, menin was shown to interact with both Akt and FOXO1 within the cytoplasmic compartment and was shown to inhibit both proteins. These results are somewhat contradictory, as Akt normally functions to inhibit FOXO1 through phosphorylation which results in its cytoplasmic sequestration. Consequently, inhibition of Akt by menin as suggested by Wang et al. (2011) would result in loss of FOXO1 inhibition, meaning FOXO1 would remain in the nucleus and continue to transcribe its target genes. Therefore, in this case menin function leads to

increased FOXO1 activity. However, Wuescher et al. (2011) show that menin inhibits FOXO1 by sequestering it in the cytoplasm, thus menin would be functioning in parallel to Akt here to inhibit FOXO1-mediated transcription.

One possible way to reconcile these seemingly contradictory interactions would be if there was cell specificity with each of these menin interactions. Interestingly, the interaction between menin and Akt was identified in primary pancreatic cells (Wuescher et al., 2011). Importantly, these are endocrine cells where menin has been shown to play a tumour suppressor function, as loss of menin in pancreatic cells results in hyperproliferation and tumourigenesis (Bertolino et al., 2003c; Crabtree et al., 2003; Karnik et al., 2005; Schnepp et al., 2006). The authors claim this interaction occurs in both endocrine and non-endocrine cells but the non-endocrine cells examined were immortalized HEK 293 cells, with overexpression of tagged proteins so this may not represent a physiologically relevant interaction (Wang et al., 2011). On the other hand, the interaction between menin and FOXO1 was identified in primary hepatocyte cells (Wuescher et al., 2011), a tissue type where menin has not been shown to play a tumour suppressor function (Scacheri et al., 2004). But liver, along with muscle tissue, are responsive to insulin signalling and play an important role under starvation conditions to regulate gluconeogenesis and glycogenolysis. Therefore it is possible that in endocrine cells, such as pancreatic cells, menin plays a tumour suppressor role through its interaction with Akt but in non-endocrine cells, such as the liver, menin is involved in regulation of the insulin signalling pathway through interaction with FOXO1. As menin is ubiquitously expressed, if there was a cell-type specific variation in its interacting

partners then this would have to be mediated by proteins that have more cell-type specific expression or activation.

This proposed cell-specific model for protein interactions suggests that in endocrine cells (*e.g*. pancreatic cells), menin interacts with and inhibits Akt. When a loss of menin function occurs then there is loss of Akt inhibition and the increased Akt activity could affect several targets that would contribute to increased proliferation. Firstly, increased Akt activity would result in increased phosphorylation and inhibition of FOXO1 and therefore increased translation as the translational repressor 4E-BP is no longer transcribed. Secondly, there would be increased phosphorylation and inhibition of the TSC1/2 complex resulting in increased TOR activation and increased protein synthesis (through 4E-BP inactivation and S6K activation). Thirdly, increased Akt activity would result in increased inhibition of apoptosis, through phosphorylation activating mdm2 or NF-κB, or inhibiting Bad (for a review of Akt signalling see De Luca et al., 2012). Thus, in endocrine cells, menin may inhibit Akt and consequently inhibit protein synthesis, proliferation and metabolism while activating apoptosis if needed.

According to this cell-specificity model of menin interactions, in non-endocrine tissues, particularly those responsive to insulin signalling, menin interacts with and inhibits FOXO1. As menin does not function as a tumour suppressor in these cells, loss of menin in these tissues does not result in tumourigenesis but could be important for the regulation of insulin signalling. Thus, loss of menin in these tissues would result in increased FOXO1 activity and consequently increased transcription of FOXO1 target genes. Targets of FOXO1 such as 4E-BP are important for inhibition of protein translation, while other targets include limiting enzymes in gluconeogenesis and

glycogenolysis pathways (*PEPCK*, *G6Pase*) that are important for use of energy stores under low nutrient conditions (for a review of FOXO in metabolism please see Gross et al., 2009; Kousteni, 2012). Thus, in non-endocrine cells menin may function to inhibit FOXO1 and this may be particularly important during increased insulin signalling, when there is plenty of energy for the cell to invest in protein synthesis and the use of energy stores (*e.g.* glycogen) is not required. In agreement with this notion, the interaction of menin with FOXO1 was enhanced following insulin stimulation of hepatocyte cells (Wuescher et al., 2011). So in these cells, loss of menin would be beneficial for surviving starvation conditions as FOXO1 would not be inhibited.

Different types of mammalian primary cells could be investigated to see if there is really this proposed cell specificity with menin's interactions with Akt and FOXO1. If these interactions are found to overlap in the same cell types then this would suggest that there must be some way to carefully coordinate when each interaction takes place so as not to counteract each other. As menin interacts with many different proteins that have varied functions (see Figure 1.1 and Table 1.1), perhaps this cell-specificity of menin interactions model could also help explain why so many different interactions have been found. If this situation is true it would imply that only those interactions occurring in endocrine tissues would be important for menin's role in tumour suppression, while interactions in other tissues may be more important for development or survival when exposed to various stressors. In order to investigate this, the previously identified interactions could be examined in multiple primary cell types, both endocrine and non-endocrine, in order to determine if they are ubiquitous or cell-type specific interactions.

Another alternative hypothesis to explain the seemingly opposing interactions of menin with both Akt and FOXO1 is that menin interacts with both proteins in all cell types but which interaction is predominant depends on other signalling cues. A possible scenario would be that insulin signalling itself regulates whether menin interacts with Akt or FOXO1. A feasible prediction is that in the absence of insulin signalling, menin functions to inhibit Akt, thus to keep Akt activity low when there is low insulin signifying low blood glucose and reduced nutrient availability. Evidence for this comes from the fact that the interaction between menin and Akt was observed in mouse pancreatic cells without the addition of extra insulin or glucose (apart from what was present in the standard medium) (Wang et al., 2011). Thus, under these conditions menin inhibition of Akt would allow for FOXO1 to remain activated and continue to transcribe target genes important for release of energy stores when blood glucose levels are low. In addition, other targets of FOXO1 such as 4E-BP would inhibit protein translation, allowing the cell to conserve energy until conditions become more favorable. Conversely, under conditions of high insulin signalling, meaning that blood glucose levels are high and there are plenty of nutrients available for growth, there could be a switch in menin interacting partners and in this case menin could interact with and inhibit FOXO1. This is in agreement with the interaction between menin and FOXO1 being enhanced with insulin exposure (Wuescher et al., 2011). Thus, the tumour suppressor function of menin falls more in line with it acting as an inhibitor of Akt but the observed role of *Drosophila* menin in starvation and desiccation survival falls more in line with menin being an inhibitor of FOXO1.

Neither of these interactions has been investigated in *Drosophila* to see if they are conserved or not. Although this is purely speculation, it could be that only one of these interactions is conserved from *Drosophila* to mammal while the other evolved later on as an adaptation to the increased complexity of the mammalian insulin signalling pathway and was required to provide an additional level of regulation. It is also interesting that in mammalian cells, menin itself was found to be a transcriptional target of FOXO1 (Zhang et al., 2012). This also agrees with the observed decrease in menin levels with insulin or glucose treatment, as in both cases this was dependent on PI3K-Akt activity which would result in decreased FOXO1 activity (Wuescher et al., 2011; Zhang et al., 2012). It is possible that FOXO1-mediated expression of menin forms a negative feedback loop to prevent prolonged FOXO1 activation. It would be interesting to determine if FOXO1 mediates menin expression in a cell-type specific manner and whether or not this is conserved in *Drosophila*.

4. Future directions

First of all, it must be acknowledged that these results, although repeated several times, are still preliminary as additional alleles and deficiencies should be tested before reliable conclusions can be drawn for the role of menin in desiccation and starvation resistance. If the increased desiccation or starvation survival observed were solely due to loss of menin function, then homozygous mutants, the transheterozygotes and the *Mnn1* deletions over the deficiency should all show similar survival curves. This is clearly not the case so other factors must be at play. The first thing that should be done to resolve the discrepancies in the results is to test other *Mnn1* alleles and other deficiency chromosomes, in parallel with the ones used in this study, to determine definitively

whether or not *Mnn1* mutants have enhanced starvation and desiccation stress resistance.

4.1 Testing of other Mnn1 alleles is necessary

Since the two deletion alleles did not always yield the same results, other *Mnn1* alleles need to be tested to ensure that the observed phenotypes are in fact due to loss of menin function and not other unidentified factors. At the time of these experiments, no other *Mnn1* alleles were available in the Campos lab. Other available *Mnn1* mutants should be obtained and tested in the starvation and desiccation assays (*e.g.* $Mnn1^{e200}$, $Mnn1^{\Delta 46}$ and $Mnn1^{\Delta 79}$) (Busygina et al., 2004; Cerrato et al., 2006). Due to the time commitment that would have been involved, new deletion mutants were not generated, although this is likely the best option for future experimentation. Generating new *Mnn1* deletion mutants from a P-element insertion line (*e.g.* GE11370; GenExcel Inc.) is suggested as these mutants would not have been exposed to potential selective pressures that could occur in the absence of *Mnn1* that might affect the phenotype (see Chapter 5).

4.2 Testing of other Df(2L) lines is required

The results for survival of flies with the $Df(2L)spd^{j2}$ chromosome were quite surprising. As deficiency lines contain large deletions, they are usually homozygous lethal, as essential genes are often lost as part of the deletions. Most deficiency lines are considered weaker stocks because they carry such large deletions, so it was surprising when flies bearing the $Df(2L)spd^{j2}$ chromosome consistently showed increased survival in both desiccation and starvation assays for both males and females (Figures 6.2-6.5). As mentioned, the $Df(2L)spd^{j2}$ chromosome could not be switched into the w^{1118}

background as all other stocks used for theses assays were. Thus, half the chromosomes in genotypes containing *Df(2L)* came from a different genetic background. It is possible that there were other mutations or modifications on one of these other chromosomes and the increased survival observed for all flies carrying *Df(2L)* was due to differences in genetic background. Another possibility is that deletion of a single copy of another gene found within the span of the deficiency is sufficient to cause increased survival. That is, haploinsufficiency in a gene other than *Mnn1* contributes to starvation and desiccation resistance.

The *Df(2L)spd*^{j2} chromosome has a deletion spanning regions 27B2-27F2 which is an approximately 550 kb region. Some potential genes of interest localized to this region include several proteins in the Wnt signalling pathway (*e.g. wg, Wnt4, Wnt6, Wnt10).* This is intriguing given that disregulation of Wnt signalling is linked to metabolic diseases (reviewed in Schinner, 2009). *Wnts* expressed from adipocytes lead to increased β-cell proliferation and insulin secretion (Schinner et al., 2008). Also, Wnt signalling has been shown to repress gluconeogenesis (Ip et al., 2012). Although this is based on research in mammalian cells, an interesting hypothesis is that down-regulation of Wnts (perhaps secreted from the fat body in *Drosophila*) could lead to reduced insulin secretion (DILPs in *Drosophila*), which would result in down-regulation of the insulin signalling pathway. Or down-regulation of Wnts could result in increased gluconeogenesis which would be useful under starvation conditions. Thus, deletion of *Wnt* genes in *Df(2L)spd*^{j2} could mimic what is observed with insulin signalling down-regulation and offer a starvation survival advantage. Other genes within the *Df(2L)spd*^{j2} deletion that may be of interest include several different ion transporters or proposed

ion binding proteins (*e.g. nrv2, Nha1, Ndae1, CG4495, CG4496*) that could have an effect on ion balance during starvation and desiccation.

Future investigation of the putative role of menin in insulin signalling requires that other *Df(2L)* lines with deletions spanning the *Mnn1* locus be tested. Deficiencies spanning smaller regions would be preferred to help narrow the phenotype down to *Mnn1*. A potential *Df(2L)* line that might be useful is *Df(2L)ED441* (Bloomington Stock #24652 or 21426) that spans 27A1;27E1 and has an approximately 375 kb deletion and would not have any of the *Wnt* genes deleted as these are located between 27E7;27F3.

4.3 Investigate if menin's interactions with Akt and FOXO1 are conserved

Given that menin was shown to interact with both Akt and FOXO1 in different mammalian cell types it will be important to determine if either or both of these interactions are conserved. As discussed already, if only one of these interactions exists in *Drosophila* it could suggest that the other interaction may have evolved later on in response to a more complex signalling mechanism for regulating energy homeostasis and responding to changing environmental conditions. These interactions could be examined by co-immunoprecipitation from S2 cells or *Drosophila* lysates. Since there could be tissue specificity with the interactions, they could also be investigated from lysates made from dissected tissues such as larval fat bodies or lysates from *Drosophila* heads, which would enrich for head fat body tissue and brain cells that are important in insulin signalling.

4.4 Additional approaches for investigating the role of menin in insulin signalling

After the *Mnn1* starvation and desiccation resistance phenotypes are confirmed with other *Mnn1* mutants and deficiency lines then work can be done to determine how

menin is involved in the insulin signalling pathway. Since insulin signalling mutants that are resistant to starvation usually have increased lipid levels and some have increased sugar levels, it would be interesting to measure these levels in *Mnn1* mutants (Broughton et al., 2005). Triglyceride content of *Mnn1* mutants could be estimated using the buoyancy based approach for larvae or determined using a commercially available kit (Harbison and Sehgal, 2009; Reis et al., 2010).

In vivo genetic epistasis experiments should be done to determine where in the insulin signalling pathway menin is functioning. *Mnn1* mutations could be combined with other mutations or with overexpression of other pathway genes to determine the combined effect on starvation or desiccation survival. For example, if menin is a negative regulator of dFOXO activity, then combining a *dFOXO* mutation in a *Mnn1*-null background should negate the increased survival observed with a *Mnn1* mutation alone. In addition, it would be important to create transgenic flies that re-express *Mnn1* in a null background to ensure that the phenotype observed in *Mnn1* mutants was due to loss of *Mnn1* and can be reversed with the rescue construct.

As mentioned above, the interactions that were identified in mammalian cells could be investigated by co-immunoprecipitation in *Drosophila* S2 cells or fly lysates. Additionally, *Drosophila* S2 cell culture could be used to better dissect the function of menin in the pathway. This may be useful as confounding effects of genetic background differences on survival would not be a factor in cell culture. S2 cells could be stimulated with insulin or glucose or starved of nutrients and overexpression or RNAi-based approaches could be used to up-regulate or down-regulate *Mnn1* or other components of the pathway (Verdu et al., 1999). The phosphorylation status of down-stream targets

could be used as readouts for pathway activation or transcript levels of key dFOXO targets could be monitored.

Some preliminary experiments were conducted to examine the level of phosphorylation of dAkt in *Mnn1*^{e30} mutants compared to controls under fed and desiccation conditions. However, no noticeable differences were detected for phospho-Akt levels in the *Mnn1* mutants (data not shown). If menin acts as an inhibitor of dAkt in *Drosophila*, as suggested by Wang et al. (2011), then deletion of menin should result in increased Akt activation and phosphorylation. As described above, menin acting as a dFOXO inhibitor falls more in line with the observation that *Mnn1* mutants have enhanced survival like other components of the IIS pathway and since this interaction would occur downstream of Akt, no noticeable change in Akt activation would be expected. Although, as these interactions may be localized to specific organs in the fly that are important for insulin signalling, it may be important to examine phospho-Akt levels in adult heads, as there would be an enrichment of the head fat body tissue. Alternatively, larval fat body could be isolated from fed and starved larvae to compare phospho-Akt levels.

5. Concluding Remarks

In summary, the results presented in this chapter suggest that menin could play a role as a positive regulator of insulin signalling. Both male and female *Mnn1*^{e30} and *Mnn1*^{e173} flies showed increased desiccation resistance and *Mnn1*^{e30} flies also showed increased starvation resistance. The enhanced starvation and desiccation resistance is comparable to that of known mutants in the insulin signalling pathway suggesting a shared function of menin in this pathway. As menin was shown to interact with FOXO1 in mammalian

cells, and the phenotype of menin loss-of-function is similar to that of dFOXO overexpression, it is proposed that menin may also be a negative regulator of dFOXO function in *Drosophila*. These preliminary results have set the stage for future endeavours that should aim to reconfirm the phenotype of $Mnn1^{e30}$ using other *Mnn1* alleles and then to show through genetic epistasis experiments that *Mnn1* is acting in the insulin signalling pathway. These results could be important to understanding menin's role in tumourigenesis and also in metabolic disorders such as diabetes mellitus. It should be mentioned that the cross-talk between insulin signalling through the PI3K-Akt-FOXO1 and the Ras-MAPK pathway were not discussed in this chapter as emphasis was made on the PI3K-Akt-FOXO1 branch due to the observed Akt-menin and FOXO1-menin interactions in mammalian cells. In addition, there are links between insulin signalling and innate immunity as well as JNK signalling that may be relevant to menin function that were not explored as they did not directly relate to the described experiments.

CHAPTER 7: DISCUSSION

1. Overview of key findings

The primary goal of this thesis was to identify menin protein interactions in the *Drosophila melanogaster* model system and assess the functional significance of these interactions. The general hypothesis for this research was that menin controls cellular responses to a variety of stresses by regulating gene expression and ultimately functions in the maintenance of genomic integrity. This hypothesis and the experimental design were established in relation to previous findings demonstrating that menin regulates stress responses and genome stability in *Drosophila* (Papaconstantinou et al., 2010; Papaconstantinou et al., 2005). In order to study the role of menin in stress responses and the maintenance of genome stability, I focused on two interactions – a novel interaction with *Drosophila* fas-associated death domain (dFADD) and a conserved interaction with Trithorax (Trx). After establishing these interactions using cell-based approaches, I attempted to elucidate the functional significance of these interactions.

FADD was identified as a potential menin-interacting protein in a yeast two-hybrid screen and this interaction was confirmed in 293T and S2 cells (Figures 3.2 and 3.3). Due to the crucial role of dFADD in the *Drosophila* innate immune response (see Chapter 3), it was predicted that menin could be important for the regulation of gene expression in response to pathogen stress. Infection assays demonstrated that menin is not required for resistance to Gram-negative or Gram-positive bacteria and consequently not an essential component of the Imd or Toll immune pathways (Figures 3.5 and 3.6). Next, I attempted to determine if dFADD played a role in the heat stress

response; however, *dFADD* mutants did not display a heat shock lethality phenotype like that reported for *Mnn1* mutants (Figure 3.9) (Papaconstantinou et al., 2005). Therefore, although the interaction between menin and dFADD was demonstrated in S2 cells, the functional significance of this interaction remains to be determined.

Since menin and MLL interact in mammalian cells and this interaction is important for chromatin modification and regulation of gene expression, we predicted that the *Drosophila* homologue Trx would also interact with menin (Chapter 4). Given that Trx is a component of the TAC1 complex that regulates the expression of *hsp* genes (Smith et al., 2004), the hypothesis was that menin interacts with Trx to coordinate proper chromatin modifications required for the transcriptional activation of heat shock genes in response to heat stress. This interaction was established in S2 cells and surprisingly the interaction occurred under standard conditions but was then lost with prolonged heat shock exposure (Figures 4.1 and 4.2). Likewise, both menin and Trx localized to *hsp70* and were found primarily in the coding region of the gene (Figure 4.4). Both proteins were localized there before heat shock and with a short heat shock menin was lost from *hsp70* but Trx localization to the coding region increased, suggesting that this interaction is dynamic and does not involve a simple menin-mediated recruitment of Trx, which was predicted from observations in mammalian cells (Milne et al., 2005).

As described in Chapter 5, many of the planned experiments could not be conducted and furthermore, many of the results from completed experiments were discarded due to problems with the *Mnn1* stocks and difficulties recapitulating previous results (Papaconstantinou et al., 2005). Consequently I began a new avenue of research to investigate the potential role of menin in the *Drosophila* insulin signalling pathway

(Chapter 6). This idea was based largely on the observation that in mammalian cells menin interacts with both Akt and FOXO1, two key proteins in this response pathway (Wang et al., 2011; Wuescher et al., 2011). Instead of first investigating whether these interactions were conserved in *Drosophila*, I began by determining if *Mnn1* mutants display a similar starvation and desiccation resistance as that described for insulin signalling pathway mutants (See Chapter 6 Introduction) (reviewed in Garofalo, 2002; Teleman, 2009). Similar to insulin signalling mutants, *Mnn1* mutants were more resistant to starvation and desiccation than controls, suggesting that menin may positively regulate this pathway (Figures 6.2-6.5).

Since I have already discussed the results for each chapter separately, this final discussion will attempt to synthesize all the findings of this thesis, provide a potential model for menin interactions and function, and emphasize the significance of this research.

2. Menin protein interactions in Drosophila

Investigating new interactions in *Drosophila* is an important undertaking since very little work has been done in this area. Although a vast number of menin-interacting proteins have been identified in humans and mice (see Table 1.1 and Figure 1.1), to my knowledge, menin protein interactions have not been published for *Drosophila*, apart from the putative dTip60 and dLeo1/Atu interactions presented by Master's thesis students in the Bédard/Campos labs (Erickson, 2011; Suen, 2010). Even though a few genetic interactions have been described for *Drosophila* menin, attempts to demonstrate conserved menin protein interactions in *Drosophila* have failed. Notably, a physical interaction between menin and Jun, the first interacting partner identified in

mammalian cells, could not be established despite the observation of a complex genetic interaction (Cerrato et al., 2006). Similarly, a physical association between menin and FANCD2 was not observed in *Drosophila* and in addition this study suggested that the proteins likely mediate distinct DNA repair pathways (Marek et al., 2008). A final example is that a genetic interaction was established for *Mnn1* and *Ches1*; however, the association of the proteins was only demonstrated for the human counterparts (note that the authors do not report whether or not they attempted to co-immunoprecipitate the *Drosophila* proteins) (Busygina et al., 2006). For this reason, if a menin interaction is found to be conserved from *Drosophila* to human, such as the case with Trx/MLL, this could emphasize the particular importance of this interaction for menin function.

2.1 Menin associates with Trx in a conserved interaction

I have demonstrated that menin and Trx interact in S2 cells under standard cellular conditions (Figures 4.1 and 4.2). This represents an important conserved interaction since menin has been well studied as a MLL-interacting partner and essential co-factor for normal MLL function and also for MLL-associated leukemogenesis. The interaction of menin with Trx, a histone methyltransferase, suggests that an important function of menin in *Drosophila* is likely also the regulation of gene expression at the chromatin level. In mammalian cells, menin interacts with numerous different transcription factors (see Table 1.1) and the regulation of gene expression is determined based on whether these interactions result in further recruitment of other complexes such as HDACs for gene silencing or HMTs for gene activation (see Chapter 1, Sections 7-9).

What has not yet been determined is whether menin interacts with Trx when it is part of the TAC1 complex or whether it interacts with Trx in the absence of dCBP and

Sbf1 (Smith et al., 2004). Preliminary evidence suggests that menin and Trx interact in the absence of dCBP, as dCBP was not detected in samples where Trx co-immunoprecipitated with menin, although this requires additional analysis. Recent characterization of *Drosophila* HMT complexes demonstrated that Trx also exists in a COMPASS-like complex with Ash2 and menin (Mohan et al., 2011). In this study immunoprecipitation of Ash2, which is common to the dSet1, Trr and Trx COMPASS-like complexes, resulted in the co-immunoprecipitation of menin. After separate isolation of the dSet1 and Trr complexes using unique proteins to each complex, the Trx COMPASS-like complex was deduced based on the remaining proteins in Ash2 immunoprecipitates and by comparison to the MLL1/2 complex. Thus, this work suggests that menin and Trx are part of a conserved COMPASS-like complex, but a more direct interaction between menin and Trx was not established (Mohan et al., 2011). Interestingly, dCBP and Sbf1 were not identified in this study as components of a Trx complex. Thus, this could suggest that Trx is primarily found in a COMPASS-like complex and the TAC1 complex could play a minor or more specialized role in gene expression. Accordingly, it would be interesting to determine if menin can be found in both Trx TAC1 and Trx COMPASS-like complexes and whether it preferentially associates with a particular type of Trx complex depending on cellular conditions (*e.g.* heat shock).

2.2 A novel interaction between menin and dFADD

An interaction between menin and dFADD was established in S2 cells where overexpressed HA-tagged dFADD interacted with endogenous menin (Figure 3.3). A preliminary co-immunoprecipitation experiment with newly generated dFADD antibodies did not reveal an interaction between both endogenous proteins; however,

this was not sufficiently investigated and enhanced detection methods will likely improve the chances of observing this interaction. It is possible that this interaction is transient or highly regulated by certain cellular responses, making it difficult to detect an interaction between endogenous proteins under standard cell culture conditions.

Although the analysis of the menin-dFADD interaction did not progress much past the initial observation of this interaction in 293T and S2 cells, this work represents a novel menin interaction which could someday be shown to be significant to menin function. It was demonstrated that *Mnn1* mutants are not sensitive to bacterial infection, suggesting that menin is not required for *Drosophila* immunity (Figures 3.5 and 3.6). Although this is considered a negative result, it still contributes to our understanding of menin function since it rules out a potential role that originally seemed probable and worthy of investigation. Consequently, this suggests that this interaction likely plays a novel role that has not yet been investigated. An intriguing idea is that perhaps further investigation of this interaction will reveal a role for dFADD in the nucleus, an idea that has been proposed but not adequately investigated (Screaton et al., 2003). dFADD's role in the innate immune response pathways has been well documented (Leulier et al., 2002; Naitza et al., 2002) but its role in apoptosis in *Drosophila* has not been fully examined, despite the well understood role of mammalian FADD in apoptosis (reviewed in Tourneur and Chiocchia, 2010). With this idea in mind, a proposed model for the menin-dFADD interaction will be described.

3. A potential link between dFADD, menin and Trx for the regulation of apoptosis

A role for dFADD in an extrinsic apoptotic pathway, similar to the one its mammalian homologue functions in, has not been described (see Chapter 3, Introduction). Although

Eiger, the *Drosophila* homologue of TNF, functions in apoptosis it does so independent of Dredd and dFADD, whose homologues both function in the mammalian TNF-α pathway. Eiger-induced apoptosis was however dependent on JNK signalling (Moreno et al., 2002). On the other hand, there was some preliminary evidence suggesting that dFADD and Dredd could induce apoptosis. This came from overexpression of the *Drosophila* proteins in HeLa or NIH 3T3 cells, which revealed that combining dFADD with Dredd resulted in an increase in Dredd-induced apoptosis (Hu and Yang, 2000). The significance of this experiment was questioned as it did not represent a physiologically relevant condition and there are known disparities between the apoptosis pathways of *Drosophila* and mammals. More recently, dFADD and Dredd were implicated in an intrinsic apoptotic pathway in *Drosophila* which was induced by the overexpression of dRYBP (*Drosophila* Ring1 and YY1 binding protein) (González and Busturia, 2009).

dRYBP is the homologue of human DEDAF (Death effector domain associated factor; first called RYBP in mouse but proteins were found to be homologous) (Zheng et al., 2001). dRYBP was previously shown to interact genetically with both Polycomb (PcG) and Trithorax group (TrxG) repressor and activator complexes, respectively (Bejarano et al., 2005; González et al., 2008). In addition, DEDAF/RYBP was identified in a yeast two-hybrid screen for proteins that interact with the death effector domain (DED) of procaspase 8 or procaspase 10. This interaction was confirmed by co-immunoprecipitation and in addition DEDAF/RYBP was shown to interact with FADD, another DED-containing protein (Zheng et al., 2001). DEDAF/RYBP interacts with Fas-FADD-caspase 8/10 complexes to enhance Fas-induced apoptosis. Furthermore, DEDAF/RYBP interacts in the nucleus with the death effector domain-containing DNA-

binding protein (DEDD) (Zheng et al., 2001). Therefore, DEDAF/RYBP interacts with DED-containing proteins both in the nucleus and in the cytosol.

As mentioned, dRYBP was shown to induce apoptosis and cause a reduced wing phenotype when overexpressed in *Drosophila* imaginal discs, even though dRYBP is not required for normal developmental apoptosis (González and Busturia, 2009). This dRYBP-induced apoptosis is dependent on dFADD and Dredd but not on the JNK signalling pathway, which is the reverse of what was observed for Eiger-induced apoptosis (González and Busturia, 2009; Moreno et al., 2002). In addition, dRYBP-mediated apoptosis relied on Reaper, Hid and Grim function and was inhibited by overexpression of DIAP1 (*Drosophila* inhibitor of apoptosis 1) or p35 (Baculovirus caspase inhibitor), which is consistent with Reaper/Hid/Grim being upregulated in order to inhibit the anti-apoptotic DIAP1 to allow apoptosis to proceed (González and Busturia, 2009). In addition, Dredd was previously shown to be an important effector in Reaper/Grim/Hid induced apoptosis in *Drosophila* (Chen et al., 1998).

Perhaps what is most intriguing about this study by González and Busturia was the observation that Trithorax is also required for dRYBP-induced apoptosis. Overexpression of Trx also increased apoptosis and resulted in a small wing phenotype. Furthermore, using a *reaper-LacZ* reporter, overexpression of either dRYBP or Trx resulted in expression of this reporter construct, suggesting that these proteins could regulate the expression of *reaper*. Additionally, ChIP analysis demonstrated that dRYBP associates directly with the *reaper* locus; although Trx binding was not tested in the ChIP assay it is reasonable to predict that it also binds to the reaper locus and together these proteins regulate expression of pro-apoptotic genes such as *reaper* (González and

Busturia, 2009). The authors proposed that since dRYBP and dFADD are not required developmentally, this apoptosis pathway likely responds to cellular stress signals; however, they have not yet identified which stresses may induce an increase in dRYBP and the associated apoptosis, nor has the mechanism for sensing the stress and activating the pathway been elucidated.

This work provides a link between the epigenetic regulation of gene expression by Trx and dRYBP and apoptosis involving dFADD and Dredd. As I have shown that menin interacts with both dFADD and Trx (Figures 3.2, 3.3, 4.1, 4.2), it is enticing, and also conceivable, to predict that menin is capable of bridging the gap between these two proteins in order to coordinate the epigenetic modifications required for the expression of pro-apoptotic genes. Based on the experiments and model proposed by González and Busturia (2009) I have taken the model further by suggesting a novel role for dFADD in the nucleus and the involvement of menin in bridging the cytoplasmic signal coming from dFADD with the regulation of gene expression by Trx (please see Figure 7.1 for a schematic). I propose a model where dRYBP interacts with dFADD in the cytoplasm to activate the caspase activity of Dredd which leads to activation of the downstream apoptotic caspase cascade. In addition to functioning in the cytoplasm, I propose that dFADD is translocated to the nucleus along with dRYBP. There, dFADD could then interact with menin which acts as a bridge to Trx. Thus, dFADD could bring dRYBP to menin, which results in the association between dRYBP and Trx. This dFADD-menin-Trx-dRYBP complex could then activate the expression of pro-apoptotic genes (*e.g. reaper, hid, grim*). The expression of these pro-apoptotic genes would result in the accumulation of their corresponding proteins in the cytoplasm, where they would inhibit

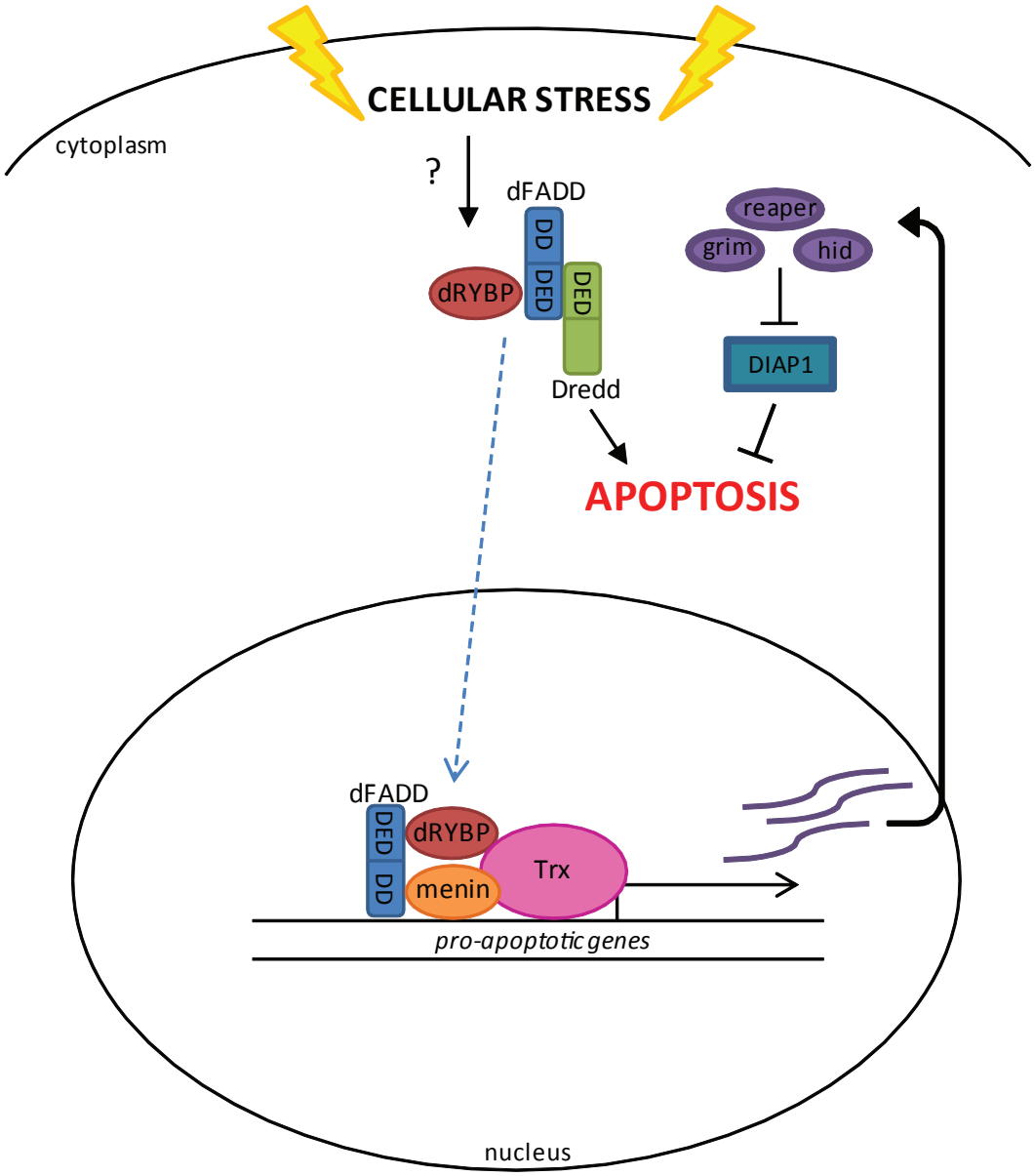

Figure 7.1. Proposed model for dFADD-menin-Trx interaction in stress-induced apoptosis. Proposed model to link dFADD-menin-Trx interactions in *Drosophila*. Note that much of this model has not been demonstrated experimentally. dFADD and Trx were shown to be necessary for dRYBP- induced apoptosis, which also requires the pro-apoptotic proteins reaper, grim and hid. dRYBP localizes to *reaper* in ChIP assay and Trx is predicted to be localized there due to the observation that both proteins can activate *reaper-LacZ* when overexpressed (González and Busturia, 2009). In mammals DEDAF/RYBP interacts with FADD in the cytoplasm (Zheng et al., 2001). Menin was shown to interact with both dFADD and Trx (this thesis) but whether all three proteins are found in a complex together has not been tested. This apoptotic pathway was proposed to be activated by cellular stress but the mechanism has not been defined (González and Busturia, 2009).

the anti-apoptotic DIAPs (*e.g.* DIAP1) to allow for activation of apoptosis. In this model, it is likely that menin, and maybe Trx, are already localized to the pro-apoptotic gene loci, similar to my observation that menin is found at the *hsp70* locus prior to heat shock exposure (Figure 4.4).

Unfortunately, I did not perform experiments that could provide credibility to this model, other than demonstrating independently that menin interacts with dFADD and Trx (Figures 3.2, 3.3, 4.1, 4.2). However, several additional lines of evidence support the plausibility of this model:

1. FADD has been localized to the nucleus but the functional significance of this localization has not been demonstrated. An interaction with MBD4, a CpG binding protein involved in mismatch DNA repair, has been demonstrated and it was proposed that FADD might link DNA repair and apoptosis (Screaton et al., 2003).
2. DEDAF/RYBP regulates both cytoplasmic and nuclear apoptotic events through interactions with FADD/caspase8 and the DNA binding protein DEDD, respectively (Zheng et al., 2001). It is possible that dFADD could move with dRYBP into the nucleus.
3. dRYBP interacts genetically with both PcG and TrxG proteins, and a physical interaction has been demonstrated for SCE and PHO (sex combs extra, pleiohomeotic; PcG proteins) but has not yet been tested for Trx (González et al., 2008). In mammalian cells menin also interacts with both PcG and TrxG proteins and could possibly form complexes with RYBP (Gao et al., 2009; Hughes et al., 2004; Xu et al., 2011; Yokoyama et al., 2004).

4. Overexpression of *Men1* (using adenovirus) in MEFs induces apoptosis. On the other hand, loss of *Men1* impairs UV or TNF-α induced apoptosis (see Chapter 1, Section 9.3) (Schnepp et al., 2004b). Thus, menin has been implicated in regulating apoptosis.
5. Menin positively regulates the expression of *caspase 8* and binds directly to the 5'UTR of *caspase 8* in MEF cells (see Chapter 1, section 9.3) (La et al., 2006; La et al., 2007; Schnepp et al., 2004b). Therefore, menin has been implicated in the activation of the expression of pro-apoptotic genes.
6. Gene expression profiling of neuroendocrine tumours from MEN1 patients revealed that 19 genes with a role in apoptosis were under-expressed, suggesting menin is important for activation of these apoptotic genes (Dilley et al., 2005).
7. Overexpression of *Mnn1* in *Drosophila* embryos (*nos-GAL4;UAS-Mnn1*) exposed to a 1 hr HS corresponded with increased apoptosis as observed through acridine orange staining (Papaconstantinou et al., 2005). Since *Mnn1-RNAi* embryos had a similar phenotype this suggests that proper menin levels may be necessary to regulate apoptosis, at least under heat stress conditions.
8. Menin has been shown to regulate several stress responses in *Drosophila*; therefore, it would be reasonable to predict that is involved in a stress-responsive apoptotic pathway (Busygina et al., 2004; Papaconstantinou et al., 2005).

Overall, this model proposes an interesting way in which menin's interaction with dFADD and Trx could be coordinated in order to regulate apoptosis, a process that menin has already been implicated in and which bears significance to its role as a tumour suppressor.

4. Potential role for menin in the insulin signalling pathway

Analysis of *Mnn1* mutants in starvation and desiccation assays suggests that menin may be involved in the positive regulation of the insulin signalling pathway. *Mnn1*^{e30} and *Mnn1*^{e173} mutants showed increased desiccation survival, while *Mnn1*^{e30} also showed increased starvation survival compared to controls (Figures 6.2-6.5). These results suggest that menin is likely acting to negatively regulate dFOXO function, since the opposite phenotype is observed for *Mnn1* mutants than for *dFOXO* mutants (see Chapter 6, Introduction) (Kramer et al., 2008). Interestingly, *dFOXO* nulls are viable and fertile with no obvious size phenotypes (Junger et al., 2003), similar to *Mnn1* mutants; whereas other components upstream in the insulin signalling pathway are required for viability or show severe size and/or fertility defects (see Table 6.1). This suggests that menin could be acting at the level of dFOXO and that this branch of the insulin signalling pathway could play a more important role in the regulation of metabolism in response to nutritional demands, without being required for development. The phenotype of *Mnn1* mutants also agrees with the observation that menin interacts with and inhibits FOXO1 in mammalian cells, contributing to its cytoplasmic sequestration and the down-regulation of target genes (Wuescher et al., 2011). Furthermore, menin's interaction with FOXO1 is not surprising given the fact that menin interacts with so many different transcription factors to help regulate gene expression (see Table 1.1).

4.1 Proposed interaction between menin and dFOXO in response to insulin signalling

Insulin exposure of HepG2 cells results in enhanced interaction between menin and FOXO1 and a translocation from the nuclear to cytoplasmic fraction. In addition, 14-3-3 also co-immunoprecipitates with menin-FOXO1, contributing to the sequestration and

inhibition of FOXO1 (Wuescher et al., 2011). Menin and FOXO1 were also shown to co-immunoprecipitate in nuclear fractions in the absence of insulin signalling; however, the precise role for menin in the regulation of FOXO1 target genes in the absence of insulin was not examined (Wuescher et al., 2011). This scenario is reminiscent of that described for menin's interaction with β-catenin. Menin down-regulates β-catenin transcriptional activity through its nuclear export and transport to adhesions junctions where it also interacts with IQGAP1 to promote β-catenin and E-cadherin association and cell adhesion (Cao et al., 2009; Yan et al., 2008). On the other hand, others have described a positive role for menin in the regulation of Wnt/β-catenin signalling, suggesting that menin recruits MLL complexes for H3K4me3 and activation of gene expression (Chen et al., 2008). It is possible that menin could play a regulatory role in β-catenin signalling where it switches from an activator to repressor depending on other signalling or environmental cues which results in an exchange of menin interacting proteins and changes in subcellular localization. A similar situation could be true for the menin-FOXO1 interaction although this has not been examined.

I propose that in *Drosophila*, menin could function in the nuclear export and down-regulation of dFOXO transcriptional activity in response to insulin signalling. Similar to what occurs in mammalian cells, menin could contribute to the cytoplasmic sequestration of dFOXO following phosphorylation by activated dAkt (see Figure 7.2 for a schematic). This would imply that in the absence of *Mnn1* function, dFOXO may be retained in the nucleus for prolonged expression of target genes which would result in inhibition of translation and proliferation, altered fat metabolism, increased gluconeogenesis and glycogenolysis. Under conditions of low nutrient availability such a

scenario would enhance survival. How dFOXO regulates fat metabolism is *Drosophila* is still unclear and conflicting results have been observed as on one hand IIS mutants (*e.g. dInR*, *Chico*, *Lnk*) have increased accumulation of triglycerides (Böhni et al., 1999; Slack et al., 2010; Tatar et al., 2001) and on the other hand overexpression of an activated dInR (*dInR*^{A1325D}) has also been shown to increase triglyceride storage (DiAngelo and Birnbaum, 2009), suggesting that secondary factors are likely involved. An active dFOXO that cannot be inhibited by Akt (dFOXO^{TM}), inhibits the insulin pathway induced triglyceride storage, suggesting that dFOXO functions more in fat mobilization (DiAngelo and Birnbaum, 2009). Either way, regulation of dFOXO activity is important for fat metabolism and survival under starvation conditions and menin may be important for its regulation.

Since dFOXO function is highly regulated by several different proteins and modifications, menin is potentially only one of several proteins acting in the insulin-induced down-regulation of dFOXO (reviewed in Daitoku et al., 2011) . Thus, the described model is an over simplification of dFOXO regulation and represents only one potential aspect of a much more complex signalling network. For example, in mammals, FOXO1 is regulated by phosphorylation and acetylation through a series of complex interactions involving kinases (*e.g.* Akt, JNK), phosphatases (*e.g.* PP2A), acetylases (*e.g.* CBP) and deacetylases (*e.g.* Sirtuins) (Daitoku et al., 2011; Mattila et al., 2008). Such a complex regulatory network is required for such an important transcription factor with functions far beyond the scope that has been discussed in this thesis that focused only on its role in insulin signalling and metabolism (reviewed in Puig and Mattila, 2011).

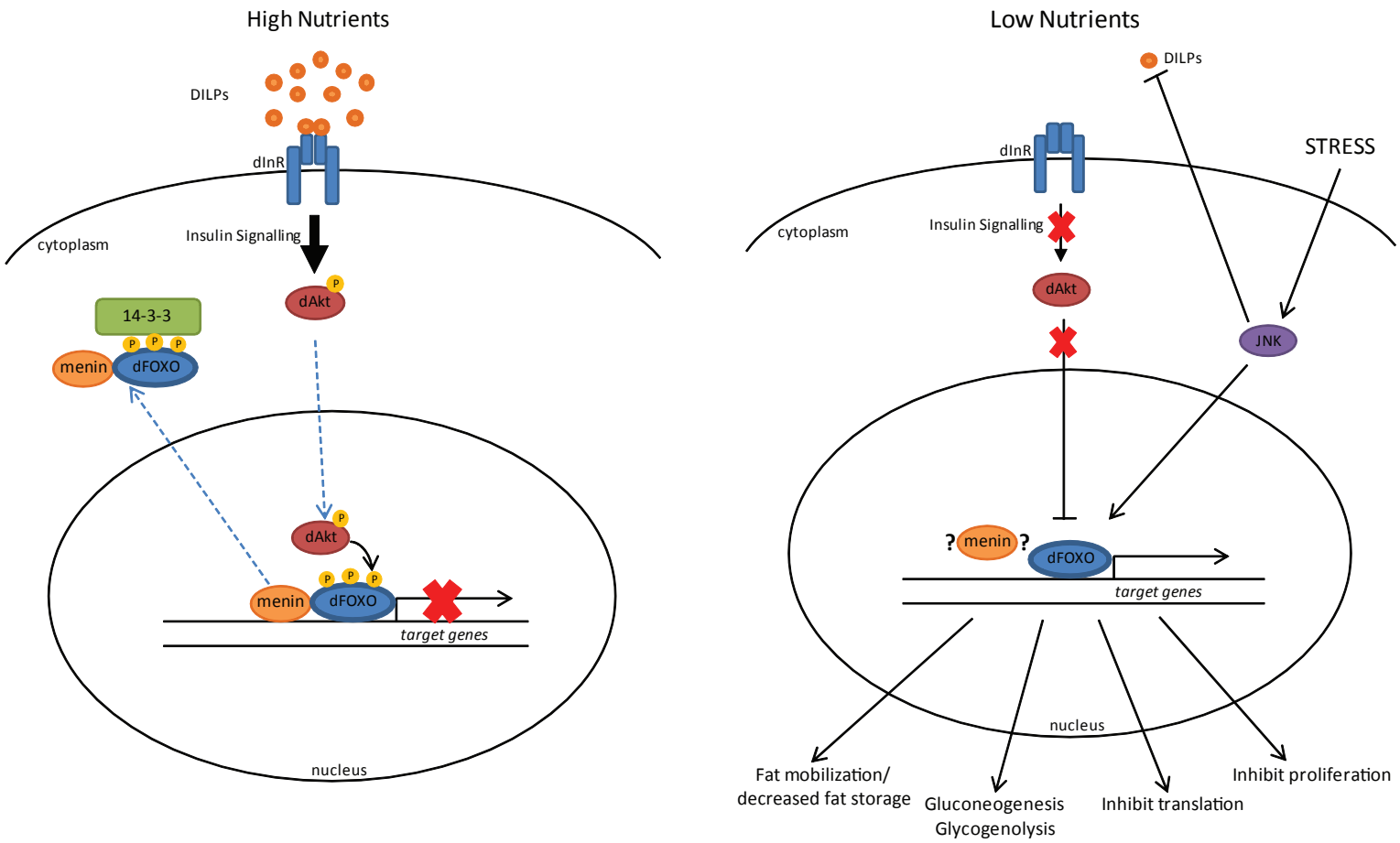

Figure 7.2 Schematic for proposed interaction between menin and dFOXO for the regulation of insulin signalling in *Drosophila*.
Mnn1 mutants have increased resistance to starvation/desiccation similar to other insulin signalling mutants suggesting that menin positively regulates insulin signalling. An interaction was demonstrate for menin and FOXO1 in mammalian cells showing that with insulin stimulation there is increased interaction of menin and FOXO1 in the cytoplasm and down-regulation of FOXO1 target genes. Thus, it is proposed that menin inhibits dFOXO by functioning in its nuclear export following insulin signalling in *Drosophila*.

4.2. Prediction that menin may be important for integrating immune and insulin signalling pathways

We hypothesized that the menin-dFADD interaction would be important in the *Drosophila* immune response due to the well established role of dFADD in the Imd pathway; however, *Mnn1* mutants displayed normal resistance to bacterial infection, suggesting that menin is not essential for signalling in the Toll or Imd pathways. Since there is a great deal of interplay between stress signalling pathways it is possible that menin and dFADD, or alternatively menin and dFOXO, could interact in order to coordinate these various response pathways.

Immune responses have been shown to result in inhibition of insulin signalling to inhibit growth and nutrient storage (DiAngelo et al., 2009). Although this was demonstrated for the Toll pathway, it is enticing to speculate that somehow the trio of menin-dFADD-dFOXO could be involved in coordinating such communication between pathways. Furthermore, the stress-induced JNK pathway is also important for both insulin signalling and immunity and the two pathways seem to be connected through JNK and dFOXO. JNK is activated downstream of dTAK1 in the Imd pathway (Silverman et al., 2003), while JNK is able to activate dFOXO and inhibit DILP secretion, thus inhibit insulin signalling during immune challenge (Wang et al., 2005). It is possible that menin could be important for the integration of these pathways through JNK and dFOXO.

Interestingly, when dFOXO is activated, such as under starvation or through down regulation of insulin signalling, it induces the expression of antimicrobial peptide genes (AMPs), even in the absence of immune challenge. This activation of AMPs by dFOXO is independent of the Toll and Imd pathways as it is still observed in mutants

from these pathways (Becker et al., 2010). This suggests that under starvation conditions dFOXO also induces a low level immune response which serves a protective function under adverse conditions. Furthermore, other stresses, such as oxidative stress and salt stress, also result in expression of AMPs and other immune response genes (reviewed in Davies et al., 2012). So it is possible that even if menin is not required to activate expression of AMPs in response to bacterial challenge, it could be involved in the regulation of such genes that occurs in response to other cellular stress. This would agree with the previously described sensitivity of *Mnn1* mutants to a variety of stresses (Papaconstantinou et al., 2005). It is enticing to speculate that the proposed dFADD-menin-dFOXO interactions somehow coordinate the cross-talk between immunity and insulin signalling but this remains to be established.

5. Menin acts as a scaffold to coordinate gene expression

The primary function of menin established in mammalian systems is that of a transcriptional regulator which controls the association of numerous different transcription factors with chromatin modifying complexes (see Chapter 1, Sections 7-9). In this manner, menin can either function to repress or activate transcription depending on the complement of factors that it bridges together at a particular gene locus. The emerging understanding of menin's primary function is that it is likely acting as a molecular scaffold in order to coordinate interactions between multiple proteins of the same pathway or maybe even for the convergence or cross-talk between different pathways. Such a role would agree with the observation that menin interacts with so many different proteins yet has no apparent enzymatic function (apart from the putative GTPase function that is not well understood (Yaguchi et al., 2002)).

A scaffolding role for menin makes sense when one considers the large number of interacting proteins that have been identified (see Figure 1.1). Moreover, the domains of menin required for these interactions are spread across the entire protein (Table 1.1), suggesting that multiple surfaces of the protein are likely to interact simultaneously with different proteins. The crystal structure of menin supports this idea as well. A deep pocket exists in menin that appears to be important for the interaction with the N-terminus of MLL1 and also with the menin-binding motif of JunD; however, a different surface of menin (the N-terminal domain) interacts with LEDGF in a manner that facilitates the concomitant interaction between MLL and LEDGF (Huang et al., 2012). The fact that MLL1 and JunD bind in the same pocket suggests that there can be competition for menin binding and also explains how some interactions with menin are mutually exclusive. This would also agree with experimental evidence showing that that interaction with JunD results in transcription repression while that with MLL results in activation of target gene expression (Agarwal et al., 1999; Kim et al., 2003; Milne et al., 2005; Yokoyama et al., 2005).

Furthermore, analysis of *MEN1* disease-associated mutations reveals that there is no mutational hotspot but that the mutations are spread across the entire gene (Tsukada et al., 2009). This agrees with the notion that menin is a scaffold protein that uses multiple protein domains to facilitate numerous simultaneous interactions, as opposed to menin possessing a single important interaction or enzymatic domain. Many *MEN1* mutations, such as frameshift and nonsense mutations, predict that a truncated protein is produced, while missense mutations throughout the gene are predicted to affect different menin protein-protein interactions. If multiple interaction domains are

present then some of these missense mutations might disrupt one interaction without affecting another region of the protein and the interactions taking place there. As an example *MEN1* disease-associated mutations P12L and L22R retain the ability to bind to MLL1 but the interaction with LEDGF is disrupted (Yokoyama and Cleary, 2008).

It is also possible that menin acts as a scaffold in both the nucleus and the cytoplasm, providing platforms for interactions of different proteins in each cellular compartment. Moreover, the existence of nuclear localization signals (NLS) and nuclear export signals (NES) suggest that menin could move back and forth from the cytoplasm and nucleus. The role of menin in the nuclear export of β-catenin supports the idea that menin could act also as a cytoplasmic scaffold (Cao et al., 2009). Several research groups have proposed that menin functions as a molecular scaffold protein and this idea is currently well accepted in the field (*e.g.* Balogh et al., 2010; Huang et al., 2012; Murai et al., 2011; Thiel et al., 2012; Yokoyama and Cleary, 2008).

6. Future Directions

Since future directions have already been outlined for each chapter they will not be discussed extensively here but attention will be drawn to a few important points. The first issue that must be addressed before any additional work is done with the *Drosophila* menin project is that of generating or acquiring new mutant strains. Generating new deletion mutants is preferable in order to ensure that the new *Mnn1* mutants have not accumulated any background modifications or been exposed to selective pressures that could have altered their phenotype. Furthermore, the appropriate controls in the same genetic background, such as precise excision lines should also be generated and used in conjunction with the deletion mutants. Screening

of homozygous viable mutants at regularly scheduled intervals using a quick PCR-based method will also be vital to ensuring the integrity of stocks that may be prone to contamination.

After new *Mnn1* mutants are available then the insulin signalling phenotype should be re-examined using additional *Df(2L)* lines (described in Chapter 6). Assuming confirmation of the enhanced starvation/desiccation resistance phenotype then additional work should address if menin negatively regulates dFOXO and functions at the level of dFOXO in the insulin signalling pathway. Also, determining if the *Drosophila* proteins interact also warrants examination.

The menin-dFADD project could likely progress using S2 cells to further analyze the interaction using the newly made dFADD antibodies. Cell fractionation could be used to determine if dFADD interacts with menin in the nucleus and also establish whether or not Trx can be found in the same complexes. Furthermore, a role for menin-dFADD-Trx in the regulation of pro-apoptotic gene expression or an interaction with dRYBP could be examined (as suggested in the model presented in Figure 7.1).

The menin-Trx interaction could also be further examined in S2 cells in order to establish whether or not menin interacts with Trx when it is in the TAC1 complex or the more recently described Trx COMPASS-like complex (Mohan et al., 2011). Furthermore, determining if menin interacts with the histone methyltransferase dSet1, which was shown to be a global regulator of H3K4me3 and is also implicated in the regulation of *hsp70* expression (Ardehali et al., 2011), would be an interesting endeavor.

7. Contributions, significance and concluding remarks

Regrettably, due to circumstances with the *Mnn1* mutants, this research did not progress as expected and the contributions to the field were not as great as anticipated. I did however successfully demonstrate two menin protein interactions in *Drosophila* S2 cells – a novel interaction with dFADD and a conserved interaction with Trx. This is an important contribution to the knowledge of *Drosophila* menin interacting proteins even though the functional significance of these interactions remains to be determined. In addition, I have demonstrated that menin potentially plays a role in positively regulating the *Drosophila* insulin signalling pathway. This suggests that menin may be important for regulating energy metabolism and homeostasis in *Drosophila*.

As previously stated, the goal of this research was to investigate menin protein-protein interactions in hopes of further elucidating menin function and its role as a tumour suppressor. This work successfully established two menin protein interactions but as is often the case with scientific research, these findings seem to have generated more questions than they have provided answers for. The work described in this thesis demonstrates a novel interaction with dFADD and a conserved interaction with Trx yet these interactions are shrouded with questions regarding their regulation and their significance to processes such as gene regulation, apoptosis and metabolism. That being said, this should not detract from the fact that this work has laid the foundation for future investigations and the proposed models of menin interactions and functions warrant further consideration. Thus, these findings may prove to someday contribute to our understanding of menin function and its role as a tumour suppressor.

REFERENCES

Adelman, K., Wei, W., Ardehali, M.B., Werner, J., Zhu, B., Reinberg, D., and Lis, J.T. (2006). Drosophila Paf1 modulates chromatin structure at actively transcribed genes. Mol Cell Biol *26*, 250-260.

Agarwal, S.K., Guru, S.C., Heppner, C., Erdos, M.R., Collins, R.M., Park, S.Y., Saggar, S., Chandrasekharappa, S.C., Collins, F.S., Spiegel, A.M.*, et al.* (1999). Menin interacts with the AP1 transcription factor JunD and represses JunD-activated transcription. Cell *96*, 143-152.

Agarwal, S.K., Impey, S., McWeeney, S., Scacheri, P.C., Collins, F.S., Goodman, R.H., Spiegel, A.M., and Marx, S.J. (2007). Distribution of menin-occupied regions in chromatin specifies a broad role of menin in transcriptional regulation. Neoplasia *9*, 101-107.

Agarwal, S.K., Kennedy, P.A., Scacheri, P.C., Novotny, E.A., Hickman, A.B., Cerrato, A., Rice, T.S., Moore, J.B., Rao, S., Ji, Y.*, et al.* (2005). Menin molecular interactions: insights into normal functions and tumorigenesis. Horm Metab Res *37*, 369-374.

Agarwal, S.K., Lee Burns, A., Sukhodolets, K.E., Kennedy, P.A., Obungu, V.H., Hickman, A.B., Mullendore, M.E., Whitten, I., Skarulis, M.C., Simonds, W.F.*, et al.* (2004). Molecular pathology of the MEN1 gene. Ann N Y Acad Sci *1014*, 189-198.

Aggarwal, K., and Silverman, N. (2007). Peptidoglycan recognition in Drosophila. Biochem Soc Trans *35*, 1496-1500.

Akira, S., Uematsu, S., and Takeuchi, O. (2006). Pathogen recognition and innate immunity. Cell *124*, 783-801.

Alic, N., Andrews, T.D., Giannakou, M.E., Papatheodorou, I., Slack, C., Hoddinott, M.P., Cocheme, H.M., Schuster, E.F., Thornton, J.M., and Partridge, L. (2011). Genome-wide dFOXO targets and topology of the transcriptomic response to stress and insulin signalling. Mol Syst Biol *7*.

Aliprantis, A.O., Yang, R.-B., Weiss, D.S., Godowski, P., and Zychlinsky, A. (2000). The apoptotic signaling pathway activated by Toll-like receptor-2. Embo J *19*, 3325-3336.

Ansari, K.I., Hussain, I., Das, H.K., and Mandal, S.S. (2009). Overexpression of human histone methylase MLL1 upon exposure to a food contaminant mycotoxin, deoxynivalenol. Febs J *276*, 3299-3307.

Ansari, K.I., Mishra, B.P., and Mandal, S.S. (2008). Human CpG binding protein interacts with MLL1, MLL2 and hSet1 and regulates Hox gene expression. Biochimica et Biophysica Acta (BBA) - Gene Regulatory Mechanisms *1779*, 66-73.

Ardehali, M.B., Mei, A., Zobeck, K.L., Caron, M., Lis, J.T., and Kusch, T. (2011). Drosophila Set1 is the major histone H3 lysine 4 trimethyltransferase with role in transcription. Embo J *30*, 2817-2828.

Ashburner, and Roote (2007). Maintenance of a Drosophila Laboratory: General Procedures Cold Springs Harbor Protocols *doi:10.1101/pdb.ip35*.

Ayton, P.M., and Cleary, M.L. (2003). Transformation of myeloid progenitors by MLL oncoproteins is dependent on Hoxa7 and Hoxa9. Genes & Development *17*, 2298-2307.

Badraoui, R., Abdelmoula, N.B., Feki, N., Nasr, H.B., and Rebai, T. (2010). Endocrine disruption and ovarian morphometric responses in rats following exposure to tetradifon. General and Comparative Endocrinology *166*, 268-272.

Badraoui, R., Abdelmoula, N.B., and Rebai, T. (2011). Erythrocytes oxidative damage and hematological effects of 2,4,4′,5-tetrachlorodiphenyl sulfone in rats. Experimental and Toxicologic Pathology *63*, 479-482.

Badraoui, R., Nasr, H.B., Louati, R., Ellouze, F., and Rebai, T. (2012). Nephrotoxic effect of tetradifon in rats: A biochemical and histomorphometric study. Experimental and Toxicologic Pathology *64*, 645-650.

Badraoui, R., Sahnoun, Z., Abdelmoula, N.B., Hakim, A., Fki, M., and Rebai, T. (2007). May antioxidants status depletion by Tetradifon induce secondary genotoxicity in female Wistar rats via oxidative stress? Pesticide Biochemistry and Physiology *88*, 149-155.

Balachandran, S., Thomas, E., and Barber, G.N. (2004). A FADD-dependent innate immune mechanism in mammalian cells. Nature *432*, 401-405.

Balogh, K., Patocs, A., Hunyady, L., and Racz, K. (2010). Menin dynamics and functional insight: take your partners. Mol Cell Endocrinol *326*, 80-84.

Balogh, K., Racz, K., Patocs, A., and Hunyady, L. (2006). Menin and its interacting proteins: elucidation of menin function. Trends Endocrinol Metab *17*, 357-364.

Bass, T.M., Grandison, R.C., Wong, R., Martinez, P., Partridge, L., and Piper, M.D. (2007). Optimization of dietary restriction protocols in Drosophila. J Gerontol A Biol Sci Med Sci *62*, 1071-1081.

Basset, A., Khush, R.S., Braun, A., Gardan, L., Boccard, F., Hoffmann, J.A., and Lemaitre, B. (2000). The phytopathogenic bacteria Erwinia carotovora infects Drosophila and activates an immune response. Proc Natl Acad Sci U S A *97*, 3376-3381.

Bazzi, W., Renon, M., Vercherat, C., Hamze, Z., Lacheretz–Bernigaud, A., Wang, H., Blanc, M., Roche, C., Calender, A., Chayvialle, J.A*., et al.* (2008). MEN1 Missense Mutations Impair

Sensitization to Apoptosis Induced by Wild-Type Menin in Endocrine Pancreatic Tumor Cells. Gastroenterology *135*, 1698-1709.e1692.

Becker, T., Loch, G., Beyer, M., Zinke, I., Aschenbrenner, A.C., Carrera, P., Inhester, T., Schultze, J.L., and Hoch, M. (2010). FOXO-dependent regulation of innate immune homeostasis. Nature *463*, 369-373.

Bejarano, F., González, I., Vidal, M., and Busturia, A. (2005). The Drosophila RYBP gene functions as a Polycomb-dependent transcriptional repressor. Mechanisms of Development *122*, 1118-1129.

Belvin, M.P., and Anderson, K.V. (1996). A CONSERVED SIGNALING PATHWAY: The Drosophila Toll-Dorsal Pathway. Annual Review of Cell and Developmental Biology *12*, 393-416.

Bernal, A., and Kimbrell, D.A. (2000). Drosophila Thor participates in host immune defense and connects a translational regulator with innate immunity. Proceedings of the National Academy of Sciences *97*, 6019-6024.

Bertolino, P., Radovanovic, I., Casse, H., Aguzzi, A., Wang, Z.Q., and Zhang, C.X. (2003a). Genetic ablation of the tumor suppressor menin causes lethality at mid-gestation with defects in multiple organs. Mech Dev *120*, 549-560.

Bertolino, P., Tong, W.M., Galendo, D., Wang, Z.Q., and Zhang, C.X. (2003b). Heterozygous Men1 mutant mice develop a range of endocrine tumors mimicking multiple endocrine neoplasia type 1. Mol Endocrinol *17*, 1880-1892.

Bertolino, P., Tong, W.M., Herrera, P.L., Casse, H., Zhang, C.X., and Wang, Z.Q. (2003c). Pancreatic beta-cell-specific ablation of the multiple endocrine neoplasia type 1 (MEN1) gene causes full penetrance of insulinoma development in mice. Cancer Res *63*, 4836-4841.

Birke, M., Schreiner, S., García-Cuéllar, M.-P., Mahr, K., Titgemeyer, F., and Slany, R.K. (2002). The MT domain of the proto-oncoprotein MLL binds to CpG-containing DNA and discriminates against methylation. Nucleic Acids Research *30*, 958-965.

Bjedov, I., Toivonen, J.M., Kerr, F., Slack, C., Jacobson, J., Foley, A., and Partridge, L. (2010). Mechanisms of Life Span Extension by Rapamycin in the Fruit Fly Drosophila melanogaster. Cell Metabolism *11*, 35-46.

Boehm, A.K., Saunders, A., Werner, J., and Lis, J.T. (2003). Transcription factor and polymerase recruitment, modification, and movement on dhsp70 in vivo in the minutes following heat shock. Mol Cell Biol *23*, 7628-7637.

Böhni, R., Riesgo-Escovar, J., Oldham, S., Brogiolo, W., Stocker, H., Andruss, B.F., Beckingham, K., and Hafen, E. (1999). Autonomous Control of Cell and Organ Size by CHICO, a Drosophila Homolog of Vertebrate IRS1–4. Cell *97*, 865-875.

Boldin, M.P., Varfolomeev, E.E., Pancer, Z., Mett, I.L., Camonis, J.H., and Wallach, D. (1995). A Novel Protein That Interacts with the Death Domain of Fas/APO1 Contains a Sequence Motif Related to the Death Domain. Journal of Biological Chemistry *270*, 7795-7798.

Borash, D.J., and Ho, G.T. (2001). Patterns of selection: stress resistance and energy storage in density-dependent populations of Drosophila melanogaster. Journal of Insect Physiology *47*, 1349-1356.

Breen, T.R. (1999). Mutant alleles of the Drosophila trithorax gene produce common and unusual homeotic and other developmental phenotypes. Genetics *152*, 319-344.

Brennan, C.A., and Anderson, K.V. (2004). Drosophila: the genetics of innate immune recognition and response. Annu Rev Immunol *22*, 457-483.

Brès, V., Yoshida, T., Pickle, L., and Jones, K.A. (2009). SKIP Interacts with c-Myc and Menin to Promote HIV-1 Tat Transactivation. Molecular Cell *36*, 75-87.

Britton, J.S., Lockwood, W.K., Li, L., Cohen, S.M., and Edgar, B.A. (2002). Drosophila's insulin/PI3-kinase pathway coordinates cellular metabolism with nutritional conditions. Dev Cell *2*, 239-249.

Brogiolo, W., Stocker, H., Ikeya, T., Rintelen, F., Fernandez, R., and Hafen, E. (2001). An evolutionarily conserved function of the Drosophila insulin receptor and insulin-like peptides in growth control. Current Biology *11*, 213-221.

Broughton, S., Alic, N., Slack, C., Bass, T., Ikeya, T., Vinti, G., Tommasi, A.M., Driege, Y., Hafen, E., and Partridge, L. (2008). Reduction of DILP2 in Drosophila triages a metabolic phenotype from lifespan revealing redundancy and compensation among DILPs. PLoS ONE *3*, e3721.

Broughton, S.J., Piper, M.D., Ikeya, T., Bass, T.M., Jacobson, J., Driege, Y., Martinez, P., Hafen, E., Withers, D.J., Leevers, S.J.*, et al.* (2005). Longer lifespan, altered metabolism, and stress resistance in Drosophila from ablation of cells making insulin-like ligands. Proc Natl Acad Sci U S A *102*, 3105-3110.

Buchon, N., Broderick, N.A., Poidevin, M., Pradervand, S., and Lemaitre, B. (2009). Drosophila intestinal response to bacterial infection: activation of host defense and stem cell proliferation. Cell Host Microbe *5*, 200-211.

Busygina, V., Kottemann, M.C., Scott, K.L., Plon, S.E., and Bale, A.E. (2006). Multiple endocrine neoplasia type 1 interacts with forkhead transcription factor CHES1 in DNA damage response. Cancer Res *66*, 8397-8403.

Busygina, V., Suphapeetiporn, K., Marek, L.R., Stowers, R.S., Xu, T., and Bale, A.E. (2004). Hypermutability in a Drosophila model for multiple endocrine neoplasia type 1. Hum Mol Genet *13*, 2399-2408.

Cao, Y., Liu, R., Jiang, X., Lu, J., Jiang, J., Zhang, C., Li, X., and Ning, G. (2009). Nuclear-Cytoplasmic Shuttling of Menin Regulates Nuclear Translocation of β-Catenin. Molecular and Cellular Biology *29*, 5477-5487.

Capotosti, F., Hsieh, J.J., and Herr, W. (2007). Species selectivity of mixed-lineage leukemia/trithorax and HCF proteolytic maturation pathways. Mol Cell Biol *27*, 7063-7072.

Carmona, E.R., Creus, A., and Marcos, R. (2011). Genotoxicity testing of two lead-compounds in somatic cells of Drosophila melanogaster. Mutation Research/Genetic Toxicology and Environmental Mutagenesis *724*, 35-40.

Caslini, C., Shilatifard, A., Yang, L., and Hess, J.L. (2000). The amino terminus of the mixed lineage leukemia protein (MLL) promotes cell cycle arrest and monocytic differentiation. Proc Natl Acad Sci U S A *97*, 2797-2802.

Caslini, C., Yang, Z., El-Osta, M., Milne, T.A., Slany, R.K., and Hess, J.L. (2007). Interaction of MLL amino terminal sequences with menin is required for transformation. Cancer Res *67*, 7275-7283.

Cerrato, A., Parisi, M., Santa Anna, S., Missirlis, F., Guru, S., Agarwal, S., Sturgill, D., Talbot, T., Spiegel, A., Collins, F*., et al.* (2006). Genetic interactions between Drosophila melanogaster menin and Jun/Fos. Dev Biol *298*, 59-70.

Chandrasekharappa, S.C., Guru, S.C., Manickam, P., Olufemi, S.E., Collins, F.S., Emmert-Buck, M.R., Debelenko, L.V., Zhuang, Z., Lubensky, I.A., Liotta, L.A*., et al.* (1997). Positional cloning of the gene for multiple endocrine neoplasia-type 1. Science *276*, 404-407.

Chandrasekharappa, S.C., and Teh, B.T. (2003). Functional studies of the MEN1 gene. J Intern Med *253*, 606-615.

Chang, P.-Y., Hom, R.A., Musselman, C.A., Zhu, L., Kuo, A., Gozani, O., Kutateladze, T.G., and Cleary, M.L. (2010). Binding of the MLL PHD3 Finger to Histone H3K4me3 Is Required for MLL-Dependent Gene Transcription. Journal of Molecular Biology *400*, 137-144.

Charroux, B., Rival, T., Narbonne-Reveau, K., and Royet, J. (2009). Bacterial detection by Drosophila peptidoglycan recognition proteins. Microbes and Infection *11*, 631-636.

Chen, C., Jack, J., and Garofalo, R.S. (1996). The Drosophila insulin receptor is required for normal growth. Endocrinology *137*, 846-856.

Chen, G., A, J., Wang, M., Farley, S., Lee, L.-Y., Lee, L.-C., and Sawicki, M.P. (2008). Menin Promotes the Wnt Signaling Pathway in Pancreatic Endocrine Cells. Molecular Cancer Research *6*, 1894-1907.

Chen, P., Rodriguez, A., Erskine, R., Thach, T., and Abrams, J.M. (1998). Dredd,a Novel Effector of the Apoptosis Activators Reaper, Grim,and Hid in Drosophila. Developmental Biology *201*, 202-216.

Chen, T., Sun, H., Lu, J., Zhao, Y., Tao, D., Li, X., and Huang, B. (2002). Histone acetylation is involved in hsp70 gene transcription regulation in Drosophila melanogaster. Arch Biochem Biophys *408*, 171-176.

Chen, Y.X., Yan, J., Keeshan, K., Tubbs, A.T., Wang, H., Silva, A., Brown, E.J., Hess, J.L., Pear, W.S., and Hua, X. (2006). The tumor suppressor menin regulates hematopoiesis and myeloid transformation by influencing Hox gene expression. Proc Natl Acad Sci U S A *103*, 1018-1023.

Chinnaiyan, A.M., O'Rourke, K., Tewari, M., and Dixit, V.M. (1995). FADD, a novel death domain-containing protein, interacts with the death domain of Fas and initiates apoptosis. Cell *81*, 505-512.

Choe, K.M., Lee, H., and Anderson, K.V. (2005). Drosophila peptidoglycan recognition protein LC (PGRP-LC) acts as a signal-transducing innate immune receptor. Proc Natl Acad Sci U S A *102*, 1122-1126.

Clancy, D.J., Gems, D., Harshman, L.G., Oldham, S., Stocker, H., Hafen, E., Leevers, S.J., and Partridge, L. (2001). Extension of life-span by loss of CHICO, a Drosophila insulin receptor substrate protein. Science *292*, 104-106.

Cosgrove, M.S., and Patel, A. (2010). Mixed lineage leukemia: a structure–function perspective of the MLL1 protein. FEBS Journal *277*, 1832-1842.

Crabtree, J.S., Scacheri, P.C., Ward, J.M., Garrett-Beal, L., Emmert-Buck, M.R., Edgemon, K.A., Lorang, D., Libutti, S.K., Chandrasekharappa, S.C., Marx, S.J.*, et al.* (2001). A mouse model of multiple endocrine neoplasia, type 1, develops multiple endocrine tumors. Proc Natl Acad Sci U S A *98*, 1118-1123.

Crabtree, J.S., Scacheri, P.C., Ward, J.M., McNally, S.R., Swain, G.P., Montagna, C., Hager, J.H., Hanahan, D., Edlund, H., Magnuson, M.A.*, et al.* (2003). Of mice and MEN1: Insulinomas in a conditional mouse knockout. Mol Cell Biol *23*, 6075-6085.

Daitoku, H., Sakamaki, J.-i., and Fukamizu, A. (2011). Regulation of FoxO transcription factors by acetylation and protein–protein interactions. Biochimica et Biophysica Acta (BBA) - Molecular Cell Research *1813*, 1954-1960.

Davies, S.-A., Overend, G., Sebastian, S., Cundall, M., Cabrero, P., Dow, J.A.T., and Terhzaz, S. (2012). Immune and stress response 'cross-talk' in the Drosophila Malpighian tubule. Journal of Insect Physiology *58*, 488-497.

De Luca, A., Maiello, M.R., D'Alessio, A., Pergameno, M., and Normanno, N. (2012). The RAS/RAF/MEK/ERK and the PI3K/AKT signalling pathways: role in cancer pathogenesis and implications for therapeutic approaches. Expert Opinion on Therapeutic Targets *16*, S17-S27.

Dhalluin, C., Carlson, J.E., Zeng, L., He, C., Aggarwal, A.K., and Zhou, M.-M. (1999). Structure and ligand of a histone acetyltransferase bromodomain. Nature *399*, 491-496.

DiAngelo, J.R., and Birnbaum, M.J. (2009). Regulation of fat cell mass by insulin in Drosophila melanogaster. Mol Cell Biol *29*, 6341-6352.

DiAngelo, J.R., Bland, M.L., Bambina, S., Cherry, S., and Birnbaum, M.J. (2009). The immune response attenuates growth and nutrient storage in Drosophila by reducing insulin signaling. Proc Natl Acad Sci U S A *106*, 20853-20858.

Dilley, W.G., Kalyanaraman, S., Verma, S., Cobb, J.P., Laramie, J.M., and Lairmore, T.C. (2005). Global gene expression in neuroendocrine tumors from patients with the MEN1 syndrome. Mol Cancer *4*, 9.

Dou, Y., Milne, T.A., Tackett, A.J., Smith, E.R., Fukuda, A., Wysocka, J., Allis, C.D., Chait, B.T., Hess, J.L., and Roeder, R.G. (2005). Physical association and coordinate function of the H3 K4 methyltransferase MLL1 and the H4 K16 acetyltransferase MOF. Cell *121*, 873-885.

Dreijerink, K.M., Mulder, K.W., Winkler, G.S., Hoppener, J.W., Lips, C.J., and Timmers, H.T. (2006). Menin links estrogen receptor activation to histone H3K4 trimethylation. Cancer Res *66*, 4929-4935.

Dreijerink, K.M.A., Varier, R.A., van Beekum, O., Jeninga, E.H., Höppener, J.W.M., Lips, C.J.M., Kummer, J.A., Kalkhoven, E., and Timmers, H.T.M. (2009a). The Multiple Endocrine Neoplasia Type 1 (MEN1) Tumor Suppressor Regulates Peroxisome Proliferator-Activated Receptor γ-Dependent Adipocyte Differentiation. Molecular and Cellular Biology *29*, 5060-5069.

Dreijerink, K.M.A., Varier, R.A., van Nuland, R., Broekhuizen, R., Valk, G.D., van der Wal, J.E., Lips, C.J.M., Kummer, J.A., and Timmers, H.T.M. (2009b). Regulation of vitamin D receptor function in MEN1-related parathyroid adenomas. Molecular and Cellular Endocrinology *313*, 1-8.

Dushay, M.S., Asling, B., and Hultmark, D. (1996). Origins of immunity: Relish, a compound Rel-like gene in the antibacterial defense of Drosophila. Proceedings of the National Academy of Sciences *93*, 10343-10347.

Erickson, J. (2011). Identification of a novel interaction between menin and the PAF complex. In Biology (Hamilton, McMaster University), pp. 145.

Ernst, P., Fisher, J.K., Avery, W., Wade, S., Foy, D., and Korsmeyer, S.J. (2004a). Definitive Hematopoiesis Requires the Mixed-Lineage Leukemia Gene. Developmental Cell *6*, 437-443.

Ernst, P., Mabon, M., Davidson, A.J., Zon, L.I., and Korsmeyer, S.J. (2004b). An Mll-Dependent Hox Program Drives Hematopoietic Progenitor Expansion. Current Biology *14*, 2063-2069.

Ernst, P., Wang, J., Huang, M., Goodman, R.H., and Korsmeyer, S.J. (2001). MLL and CREB Bind Cooperatively to the Nuclear Coactivator CREB-Binding Protein. Molecular and Cellular Biology *21*, 2249-2258.

Ertürk-Hasdemir, D., Broemer, M., Leulier, F., Lane, W.S., Paquette, N., Hwang, D., Kim, C.-H., Stöven, S., Meier, P., and Silverman, N. (2009). Two roles for the Drosophila IKK complex in the activation of Relish and the induction of antimicrobial peptide genes. Proceedings of the National Academy of Sciences *106*, 9779-9784.

Feng, Z.J., Gurung, B., Jin, G.H., Yang, X.L., and Hua, X.X. (2013). SUMO modification of menin. Am J Cancer Res *3*, 96-106.

Fernandez, R., Tabarini, D., Azpiazu, N., Frasch, M., and Schlessinger, J. (1995). The Drosophila insulin receptor homolog: a gene essential for embryonic development encodes two receptor isoforms with different signaling potential. Embo J *14*, 3373-3384.

Fontanière, S., Casse, H., Bertolino, P., and Zhang, C.X. (2006a). Analysis of p27(Kip1) expression in insulinomas developed in pancreatic beta-cell specific Men1 mutant mice. Fam Cancer *5*, 49-54.

Fontanière, S., Tost, J., Wierinckx, A., Lachuer, J., Lu, J., Hussein, N., Busato, F., Gut, I., Wang, Z.Q., and Zhang, C.X. (2006b). Gene expression profiling in insulinomas of Men1 beta-cell mutant mice reveals early genetic and epigenetic events involved in pancreatic beta-cell tumorigenesis. Endocr Relat Cancer *13*, 1223-1236.

Francis, J., Lin, W., Rozenblatt-Rosen, O., and Meyerson, M. (2011). The menin tumor suppressor protein is phosphorylated in response to DNA damage. PLoS ONE *6*, e16119.

Fromaget, M., Vercherat, C., Zhang, C.X., Zablewska, B., Gaudray, P., Chayvialle, J.A., Calender, A., and Cordier-Bussat, M. (2003). Functional characterization of a promoter region in the human MEN1 tumor suppressor gene. J Mol Biol *333*, 87-102.

Gallo, A., Agnese, S., Esposito, I., Galgani, M., and Avvedimento, V.E. (2010). Menin stimulates homology-directed DNA repair. FEBS Lett *584*, 4531-4536.

Gao, S.B., Feng, Z.J., Xu, B., Wu, Y., Yin, P., Yang, Y., Hua, X., and Jin, G.H. (2009). Suppression of lung adenocarcinoma through menin and polycomb gene-mediated repression of growth factor pleiotrophin. Oncogene *28*, 4095-4104.

Gao, X., Neufeld, T.P., and Pan, D. (2000). Drosophila PTEN Regulates Cell Growth and Proliferation through PI3K-Dependent and -Independent Pathways. Developmental Biology *221*, 404-418.

Gao, X., and Pan, D. (2001). TSC1 and TSC2 tumor suppressors antagonize insulin signaling in cell growth. Genes & Development *15*, 1383-1392.

Garami, A., Zwartkruis, F.J.T., Nobukuni, T., Joaquin, M., Roccio, M., Stocker, H., Kozma, S.C., Hafen, E., Bos, J.L., and Thomas, G. (2003). Insulin Activation of Rheb, a Mediator of mTOR/S6K/4E-BP Signaling, Is Inhibited by TSC1 and 2. Molecular Cell *11*, 1457-1466.

Garcia, B.A., Hake, S.B., Diaz, R.L., Kauer, M., Morris, S.A., Recht, J., Shabanowitz, J., Mishra, N., Strahl, B.D., Allis, C.D.*, et al.* (2007). Organismal Differences in Post-translational Modifications in Histones H3 and H4. Journal of Biological Chemistry *282*, 7641-7655.

Garofalo, R.S. (2002). Genetic analysis of insulin signaling in Drosophila. Trends Endocrinol Metab *13*, 156-162.

Gershman, B., Puig, O., Hang, L., Peitzsch, R.M., Tatar, M., and Garofalo, R.S. (2007). High-resolution dynamics of the transcriptional response to nutrition in Drosophila: a key role for dFOXO. Physiological Genomics *29*, 24-34.

Giannakou, M.E., Goss, M., Jünger, M.A., Hafen, E., Leevers, S.J., and Partridge, L. (2004). Long-Lived Drosophila with Overexpressed dFOXO in Adult Fat Body. Science *305*, 361.

Gingras, A.C., Raught, B., and Sonenberg, N. (1999). eIF4 initiation factors: effectors of mRNA recruitment to ribosomes and regulators of translation. Annu Rev Biochem *68*, 913-963.

Gloor, G.B., Preston, C.R., Johnson-Schlitz, D.M., Nassif, N.A., Phillis, R.W., Benz, W.K., Robertson, H.M., and Engels, W.R. (1993). Type I repressors of P element mobility. Genetics *135*, 81-95.

Goberdhan, D.C.I., Paricio, N., Goodman, E.C., Mlodzik, M., and Wilson, C. (1999). Drosophila tumor suppressor PTEN controls cell size and number by antagonizing the Chico/PI3-kinase signaling pathway. Genes & Development *13*, 3244-3258.

Gobl, A.E., Berg, M., Lopez-Egido, J.R., Oberg, K., Skogseid, B., and Westin, G. (1999). Menin represses JunD-activated transcription by a histone deacetylase-dependent mechanism. Biochim Biophys Acta *1447*, 51-56.

Gomez-Angelats, M., and Cidlowski, J.A. (2003). Molecular evidence for the nuclear localization of FADD. Cell Death Differ *10*, 791-797.

González, I., Aparicio, R., and Busturia, A. (2008). Functional Characterization of the dRYBP Gene in Drosophila. Genetics *179*, 1373-1388.

González, I., and Busturia, A. (2009). High levels of dRYBP induce apoptosis in Drosophila imaginal cells through the activation of reaper and the requirement of trithorax, dredd and dFADD. Cell Res *19*, 747-757.

Gottar, M., Gobert, V., Michel, T., Belvin, M., Duyk, G., Hoffmann, J.A., Ferrandon, D., and Royet, J. (2002). The Drosophila immune response against Gram-negative bacteria is mediated by a peptidoglycan recognition protein. Nature *416*, 640-644.

Grembecka, J., Belcher, A.M., Hartley, T., and Cierpicki, T. (2010). Molecular basis of the mixed lineage leukemia-menin interaction: implications for targeting mixed lineage leukemias. J Biol Chem *285*, 40690-40698.

Grembecka, J., He, S., Shi, A., Purohit, T., Muntean, A.G., Sorenson, R.J., Showalter, H.D., Murai, M.J., Belcher, A.M., Hartley, T.*, et al.* (2012). Menin-MLL inhibitors reverse oncogenic activity of MLL fusion proteins in leukemia. Nat Chem Biol *8*, 277-284.

Grewal, S.S. (2009). Insulin/TOR signaling in growth and homeostasis: A view from the fly world. The International Journal of Biochemistry & Cell Biology *41*, 1006-1010.

Grewal, S.S., Evans, J.R., and Edgar, B.A. (2007). Drosophila TIF-IA is required for ribosome synthesis and cell growth and is regulated by the TOR pathway. J Cell Biol *179*, 1105-1113.

Grimaud, C., Negre, N., and Cavalli, G. (2006). From genetics to epigenetics: the tale of Polycomb group and trithorax group genes. Chromosome Res *14*, 363-375.

Gross, D., Wan, M., and Birnbaum, M. (2009). The role of FOXO in the regulation of metabolism. Current Diabetes Reports *9*, 208-214.

Gu, Y., Nakamura, T., Alder, H., Prasad, R., Canaani, O., Cimino, G., Croce, C.M., and Canaani, E. (1992). The t(4;11) chromosome translocation of human acute leukemias fuses the ALL-1 gene, related to Drosophila trithorax, to the AF-4 gene. Cell *71*, 701-708.

Guarente, L., and Kenyon, C. (2000). Genetic pathways that regulate ageing in model organisms. Nature *408*, 255-262.

Guntermann, S., and Foley, E. (2011). The Protein Dredd Is an Essential Component of the c-Jun N-terminal Kinase Pathway in the Drosophila Immune Response. Journal of Biological Chemistry *286*, 30284-30294.

Gurer, H., and Ercal, N. (2000). Can antioxidants be beneficial in the treatment of lead poisoning? Free Radical Biology and Medicine *29*, 927-945.

Guru, S.C., Crabtree, J.S., Brown, K.D., Dunn, K.J., Manickam, P., Prasad, N.B., Wangsa, D., Burns, A.L., Spiegel, A.M., Marx, S.J.*, et al.* (1999). Isolation, genomic organization, and expression analysis of Men1, the murine homolog of the MEN1 gene. Mamm Genome *10*, 592-596.

Guru, S.C., Goldsmith, P.K., Burns, A.L., Marx, S.J., Spiegel, A.M., Collins, F.S., and Chandrasekharappa, S.C. (1998). Menin, the product of the MEN1 gene, is a nuclear protein. Proc Natl Acad Sci U S A *95*, 1630-1634.

Guru, S.C., Prasad, N.B., Shin, E.J., Hemavathy, K., Lu, J., Ip, Y.T., Agarwal, S.K., Marx, S.J., Spiegel, A.M., Collins, F.S.*, et al.* (2001). Characterization of a MEN1 ortholog from Drosophila melanogaster. Gene *263*, 31-38.

Ha, E.M., Oh, C.T., Ryu, J.H., Bae, Y.S., Kang, S.W., Jang, I.H., Brey, P.T., and Lee, W.J. (2005). An antioxidant system required for host protection against gut infection in Drosophila. Dev Cell *8*, 125-132.

Hallson, G., Hollebakken, R.E., Li, T., Syrzycka, M., Kim, I., Cotsworth, S., Fitzpatrick, K.A., Sinclair, D.A.R., and Honda, B.M. (2012). dSet1 Is the Main H3K4 Di- and Tri-Methyltransferase Throughout Drosophila Development. Genetics *190*, 91-100.

Han, K.J., Su, X., Xu, L.G., Bin, L.H., Zhang, J., and Shu, H.B. (2004). Mechanisms of the TRIF-induced interferon-stimulated response element and NF-kappaB activation and apoptosis pathways. J Biol Chem *279*, 15652-15661.

Han, Z.S., and Ip, Y.T. (1999). Interaction and Specificity of Rel-related Proteins in Regulating Drosophila Immunity Gene Expression. Journal of Biological Chemistry *274*, 21355-21361.

Harbison, S.T., and Sehgal, A. (2009). Energy Stores Are Not Altered by Long-Term Partial Sleep Deprivation in <italic>Drosophila melanogaster</italic>. PLoS ONE *4*, e6211.

Heppner, C., Bilimoria, K.Y., Agarwal, S.K., Kester, M., Whitty, L.J., Guru, S.C., Chandrasekharappa, S.C., Collins, F.S., Spiegel, A.M., Marx, S.J.*, et al.* (2001). The tumor suppressor protein menin interacts with NF-kappaB proteins and inhibits NF-kappaB-mediated transactivation. Oncogene *20*, 4917-4925.

Hessman, O., Skogseid, B., Westin, G., and Åkerström, G. (2001). Multiple Allelic Deletions and Intratumoral Genetic Heterogeneity in MEN1 Pancreatic Tumors. Journal of Clinical Endocrinology & Metabolism *86*, 1355-1361.

Hirsch, H.V.B., Possidente, D., and Possidente, B. (2010). Pb2+: An endocrine disruptor in Drosophila? Physiology & Behavior *99*, 254-259.

Hoffmann, J.A., and Reichhart, J.-M. (2002). Drosophila innate immunity: an evolutionary perspective. Nat Immunol *3*, 121-126.

Horng, T., and Medzhitov, R. (2001). Drosophila MyD88 is an adapter in the Toll signaling pathway. Proc Natl Acad Sci U S A *98*, 12654-12658.

Hsieh, J.J., Cheng, E.H., and Korsmeyer, S.J. (2003a). Taspase1: a threonine aspartase required for cleavage of MLL and proper HOX gene expression. Cell *115*, 293-303.

Hsieh, J.J., Ernst, P., Erdjument-Bromage, H., Tempst, P., and Korsmeyer, S.J. (2003b). Proteolytic cleavage of MLL generates a complex of N- and C-terminal fragments that confers protein stability and subnuclear localization. Mol Cell Biol *23*, 186-194.

Hsu, H., Shu, H.-B., Pan, M.-G., and Goeddel, D.V. (1996). TRADD–TRAF2 and TRADD–FADD Interactions Define Two Distinct TNF Receptor 1 Signal Transduction Pathways. Cell *84*, 299-308.

Hu, S., and Yang, X. (2000). dFADD, a novel death domain-containing adapter protein for the Drosophila caspase DREDD. J Biol Chem *275*, 30761-30764.

Hua, Z.C., Sohn, S.J., Kang, C., Cado, D., and Winoto, A. (2003). A Function of Fas-Associated Death Domain Protein in Cell Cycle Progression Localized to a Single Amino Acid at Its C-Terminal Region. Immunity *18*, 513-521.

Huang, H.-R., Chen, Z.J., Kunes, S., Chang, G.-D., and Maniatis, T. (2010). Endocytic pathway is required for Drosophila Toll innate immune signaling. Proceedings of the National Academy of Sciences *107*, 8322-8327.

Huang, H., Potter, C.J., Tao, W., Li, D.M., Brogiolo, W., Hafen, E., Sun, H., and Xu, T. (1999). PTEN affects cell size, cell proliferation and apoptosis during Drosophila eye development. Development *126*, 5365-5372.

Huang, J., Gurung, B., Wan, B., Matkar, S., Veniaminova, N.A., Wan, K., Merchant, J.L., Hua, X., and Lei, M. (2012). The same pocket in menin binds both MLL and JUND but has opposite effects on transcription. Nature *482*, 542-546.

Hughes, C.M., Rozenblatt-Rosen, O., Milne, T.A., Copeland, T.D., Levine, S.S., Lee, J.C., Hayes, D.N., Shanmugam, K.S., Bhattacharjee, A., Biondi, C.A*., et al.* (2004). Menin associates with a trithorax family histone methyltransferase complex and with the hoxc8 locus. Mol Cell *13*, 587-597.

Hultmark, D. (2003). Drosophila immunity: paths and patterns. Curr Opin Immunol *15*, 12-19.

Hwangbo, D.S., Gersham, B., Tu, M.-P., Palmer, M., and Tatar, M. (2004). Drosophila dFOXO controls lifespan and regulates insulin signalling in brain and fat body. Nature *429*, 562-566.

Ikeya, T., Galic, M., Belawat, P., Nairz, K., and Hafen, E. (2002). Nutrient-Dependent Expression of Insulin-like Peptides from Neuroendocrine Cells in the CNS Contributes to Growth Regulation in Drosophila. Current Biology *12*, 1293-1300.

Imtiyaz, H.Z., Rosenberg, S., Zhang, Y., Rahman, Z.S., Hou, Y.J., Manser, T., and Zhang, J. (2006). The Fas-associated death domain protein is required in apoptosis and TLR-induced proliferative responses in B cells. J Immunol *176*, 6852-6861.

Inoue, Y., Hendy, G.N., Canaff, L., Seino, S., and Kaji, H. (2011). Menin Interacts with β-Catenin in Osteoblast Differentiation. Horm Metab Res *43*, 183-187.

Ip, W., Shao, W., Chiang, Y.-t.A., and Jin, T. (2012). The Wnt signaling pathway effector TCF7L2 is upregulated by insulin and represses hepatic gluconeogenesis. American Journal of Physiology - Endocrinology And Metabolism *303*, E1166-E1176.

Irmler, M., Thome, M., Hahne, M., Schneider, P., Hofmann, K., Steiner, V., Bodmer, J.-L., Schroter, M., Burns, K., Mattmann, C*., et al.* (1997). Inhibition of death receptor signals by cellular FLIP. Nature *388*, 190-195.

Ito, N., and Rubin, G.M. (1999). gigas, a Drosophila Homolog of Tuberous Sclerosis Gene Product-2, Regulates the Cell Cycle. Cell *96*, 529-539.

Jin, S., Mao, H., Schnepp, R.W., Sykes, S.M., Silva, A.C., D'Andrea, A.D., and Hua, X. (2003). Menin associates with FANCD2, a protein involved in repair of DNA damage. Cancer Res *63*, 4204-4210.

Jin, S., Zhao, H., Yi, Y., Nakata, Y., Kalota, A., and Gewirtz, A.M. (2010). c-Myb binds MLL through menin in human leukemia cells and is an important driver of MLL-associated leukemogenesis. The Journal of Clinical Investigation *120*, 593-606.

Jude, C.D., Climer, L., Xu, D., Artinger, E., Fisher, J.K., and Ernst, P. (2007). Unique and Independent Roles for MLL in Adult Hematopoietic Stem Cells and Progenitors. Cell Stem Cell *1*, 324-337.

Junger, M., Rintelen, F., Stocker, H., Wasserman, J., Vegh, M., Radimerski, T., Greenberg, M., and Hafen, E. (2003). The Drosophila Forkhead transcription factor FOXO mediates the reduction in cell number associated with reduced insulin signaling. Journal of Biology *2*, 20.

Kaji, H., Canaff, L., Lebrun, J.J., Goltzman, D., and Hendy, G.N. (2001). Inactivation of menin, a Smad3-interacting protein, blocks transforming growth factor type beta signaling. Proc Natl Acad Sci U S A *98*, 3837-3842.

Kaneko, T., Goldman, W.E., Mellroth, P., Steiner, H., Fukase, K., Kusumoto, S., Harley, W., Fox, A., Golenbock, D., and Silverman, N. (2004). Monomeric and polymeric gram-negative peptidoglycan but not purified LPS stimulate the Drosophila IMD pathway. Immunity *20*, 637-649.

Kapahi, P., Zid, B.M., Harper, T., Koslover, D., Sapin, V., and Benzer, S. (2004). Regulation of Lifespan in Drosophila by Modulation of Genes in the TOR Signaling Pathway. Current Biology *14*, 885-890.

Karnik, S.K., Chen, H., McLean, G.W., Heit, J.J., Gu, X., Zhang, A.Y., Fontaine, M., Yen, M.H., and Kim, S.K. (2007). Menin controls growth of pancreatic beta-cells in pregnant mice and promotes gestational diabetes mellitus. Science *318*, 806-809.

Karnik, S.K., Hughes, C.M., Gu, X., Rozenblatt-Rosen, O., McLean, G.W., Xiong, Y., Meyerson, M., and Kim, S.K. (2005). Menin regulates pancreatic islet growth by promoting histone methylation and expression of genes encoding p27Kip1 and p18INK4c. Proc Natl Acad Sci U S A *102*, 14659-14664.

Kawai, T., and Akira, S. (2010). The role of pattern-recognition receptors in innate immunity: update on Toll-like receptors. Nat Immunol *11*, 373-384.

Kim, H., Lee, J.E., Cho, E.J., Liu, J.O., and Youn, H.D. (2003). Menin, a tumor suppressor, represses JunD-mediated transcriptional activity by association with an mSin3A-histone deacetylase complex. Cancer Res *63*, 6135-6139.

Kim, K.S. (2002). Multifunctional role of Fas-associated death domain protein in apoptosis. J Biochem Mol Biol *35*, 1-6.

Kim, Y.S., Burns, A.L., Goldsmith, P.K., Heppner, C., Park, S.Y., Chandrasekharappa, S.C., Collins, F.S., Spiegel, A.M., and Marx, S.J. (1999). Stable overexpression of MEN1 suppresses tumorigenicity of RAS. Oncogene *18*, 5936-5942.

Kleino, A., Valanne, S., Ulvila, J., Kallio, J., Myllymaki, H., Enwald, H., Stoven, S., Poidevin, M., Ueda, R., Hultmark, D*., et al.* (2005). Inhibitor of apoptosis 2 and TAK1-binding protein are components of the Drosophila Imd pathway. Embo J *24*, 3423-3434.

Klymenko, T., and Muller, J. (2004). The histone methyltransferases Trithorax and Ash1 prevent transcriptional silencing by Polycomb group proteins. EMBO Rep *5*, 373-377.

Knudson, A.G., Jr. (1971). Mutation and cancer: statistical study of retinoblastoma. Proc Natl Acad Sci U S A *68*, 820-823.

Kohlmaier, A., Savarese, F., Lachner, M., Martens, J., Jenuwein, T., and Wutz, A. (2004). A Chromosomal Memory Triggered by <italic>Xist</italic> Regulates Histone Methylation in X Inactivation. PLoS Biol *2*, e171.

Kolss, M., Vijendravarma, R.K., Schwaller, G., and Kawecki, T.J. (2009). Life-history consequences of adaptation to larval nutritional stress in Drosophila. Evolution *63*, 2389-2401.

Kousteni, S. (2012). FoxO1, the transcriptional chief of staff of energy metabolism. Bone *50*, 437-443.

Kozuka, T., Sugita, M., Shetzline, S., Gewirtz, A.M., and Nakata, Y. (2011). c-Myb and GATA-3 Cooperatively Regulate IL-13 Expression via Conserved GATA-3 Response Element and Recruit Mixed Lineage Leukemia (MLL) for Histone Modification of the IL-13 Locus. The Journal of Immunology *187*, 5974-5982.

Kramer, J.M., Davidge, J.T., Lockyer, J.M., and Staveley, B.E. (2003). Expression of Drosophila FOXO regulates growth and can phenocopy starvation. BMC Dev Biol *3*, 5.

Kramer, J.M., Slade, J.D., and Staveley, B.E. (2008). foxo is required for resistance to amino acid starvation in Drosophila. Genome *51*, 668-672.

Krivtsov, A.V., and Armstrong, S.A. (2007). MLL translocations, histone modifications and leukaemia stem-cell development. Nat Rev Cancer *7*, 823-833.

Kuzin, B., Tillib, S., Sedkov, Y., Mizrokhi, L., and Mazo, A. (1994). The Drosophila trithorax gene encodes a chromosomal protein and directly regulates the region-specific homeotic gene fork head. Genes Dev *8*, 2478-2490.

La, P., Desmond, A., Hou, Z., Silva, A.C., Schnepp, R.W., and Hua, X. (2006). Tumor suppressor menin: the essential role of nuclear localization signal domains in coordinating gene expression. Oncogene *25*, 3537-3546.

La, P., Schnepp, R.W., C, D.P., A, C.S., and Hua, X. (2004a). Tumor suppressor menin regulates expression of insulin-like growth factor binding protein 2. Endocrinology *145*, 3443-3450.

La, P., Silva, A.C., Hou, Z., Wang, H., Schnepp, R.W., Yan, N., Shi, Y., and Hua, X. (2004b). Direct binding of DNA by tumor suppressor menin. J Biol Chem *279*, 49045-49054.

La, P., Yang, Y., Karnik, S.K., Silva, A.C., Schnepp, R.W., Kim, S.K., and Hua, X. (2007). Menin-mediated caspase 8 expression in suppressing multiple endocrine neoplasia type 1. J Biol Chem *282*, 31332-31340.

Larsson, C., Skogseid, B., Oberg, K., Nakamura, Y., and Nordenskjold, M. (1988). Multiple endocrine neoplasia type 1 gene maps to chromosome 11 and is lost in insulinoma. Nature *332*, 85-87.

Law, J. (2008). Identification of a novel protein interaction between FADD and menin in response to activation of the Toll-like receptor signaling pathway. In Biology (Hamilton, McMaster University).

Leevers, S.J., Weinkove, D., MacDougall, L.K., Hafen, E., and Waterfield, M.D. (1996). The Drosophila phosphoinositide 3-kinase Dp110 promotes cell growth. Embo J *15*, 6584-6594.

Lemaitre, B., and Hoffmann, J. (2007). The host defense of Drosophila melanogaster. Annu Rev Immunol *25*, 697-743.

Lemaitre, B., Kromer-Metzger, E., Michaut, L., Nicolas, E., Meister, M., Georgel, P., Reichhart, J.M., and Hoffmann, J.A. (1995). A recessive mutation, immune deficiency (imd), defines two distinct control pathways in the Drosophila host defense. Proc Natl Acad Sci U S A *92*, 9465-9469.

Lemaitre, B., Nicolas, E., Michaut, L., Reichhart, J.M., and Hoffmann, J.A. (1996). The dorsoventral regulatory gene cassette spatzle/Toll/cactus controls the potent antifungal response in Drosophila adults. Cell *86*, 973-983.

Lemaitre, B., Reichhart, J.M., and Hoffmann, J.A. (1997). Drosophila host defense: differential induction of antimicrobial peptide genes after infection by various classes of microorganisms. Proc Natl Acad Sci U S A *94*, 14614-14619.

Lemmens, I.H., Forsberg, L., Pannett, A.A., Meyen, E., Piehl, F., Turner, J.J., Van de Ven, W.J., Thakker, R.V., Larsson, C., and Kas, K. (2001). Menin interacts directly with the homeobox-containing protein Pem. Biochem Biophys Res Commun *286*, 426-431.

Lemos, M.C., and Thakker, R.V. (2008). Multiple endocrine neoplasia type 1 (MEN1): analysis of 1336 mutations reported in the first decade following identification of the gene. Hum Mutat *29*, 22-32.

Leulier, F., Parquet, C., Pili-Floury, S., Ryu, J.H., Caroff, M., Lee, W.J., Mengin-Lecreulx, D., and Lemaitre, B. (2003). The Drosophila immune system detects bacteria through specific peptidoglycan recognition. Nat Immunol *4*, 478-484.

Leulier, F., Rodriguez, A., Khush, R.S., Abrams, J.M., and Lemaitre, B. (2000). The Drosophila caspase Dredd is required to resist Gram-negative bacterial infection. EMBO Rep *1*, 353-358.

Leulier, F., Vidal, S., Saigo, K., Ueda, R., and Lemaitre, B. (2002). Inducible expression of double-stranded RNA reveals a role for dFADD in the regulation of the antibacterial response in Drosophila adults. Curr Biol *12*, 996-1000.

Libutti, S.K., Crabtree, J.S., Lorang, D., Burns, A.L., Mazzanti, C., Hewitt, S.M., O'Connor, S., Ward, J.M., Emmert-Buck, M.R., Remaley, A.*, et al.* (2003). Parathyroid gland-specific deletion of the mouse Men1 gene results in parathyroid neoplasia and hypercalcemic hyperparathyroidism. Cancer Res *63*, 8022-8028.

Lin, S.Y., and Elledge, S.J. (2003). Multiple tumor suppressor pathways negatively regulate telomerase. Cell *113*, 881-889.

Lopez-Egido, J., Cunningham, J., Berg, M., Oberg, K., Bongcam-Rudloff, E., and Gobl, A. (2002). Menin's interaction with glial fibrillary acidic protein and vimentin suggests a role for the intermediate filament network in regulating menin activity. Exp Cell Res *278*, 175-183.

Lu, J., Herrera, P.L., Carreira, C., Bonnavion, R., Seigne, C., Calender, A., Bertolino, P., and Zhang, C.X. (2010). α Cell–Specific Men1 Ablation Triggers the Transdifferentiation of Glucagon-Expressing Cells and Insulinoma Development. Gastroenterology *138*, 1954-1965.e1958.

Lu, Y., Wu, L.P., and Anderson, K.V. (2001). The antibacterial arm of the Drosophila innate immune response requires an IκB kinase. Genes & Development *15*, 104-110.

Ma, Q., Alder, H., Nelson, K.K., Chatterjee, D., Gu, Y., Nakamura, T., Canaani, E., Croce, C.M., Siracusa, L.D., and Buchberg, A.M. (1993). Analysis of the murine All-1 gene reveals conserved domains with human ALL-1 and identifies a motif shared with DNA methyltransferases. Proceedings of the National Academy of Sciences *90*, 6350-6354.

MacConaill, L.E., Hughes, C.M., Rozenblatt-Rosen, O., Nannepaga, S., and Meyerson, M. (2006). Phosphorylation of the menin tumor suppressor protein on serine 543 and serine 583. Mol Cancer Res *4*, 793-801.

Manickam, P., Vogel, A.M., Agarwal, S.K., Oda, T., Spiegel, A.M., Marx, S.J., Collins, F.S., Weinstein, B.M., and Chandrasekharappa, S.C. (2000). Isolation, characterization, expression and functional analysis of the zebrafish ortholog of MEN1. Mamm Genome *11*, 448-454.

Marek, L.R., Kottemann, M.C., Glazer, P.M., and Bale, A.E. (2008). MEN1 and FANCD2 mediate distinct mechanisms of DNA crosslink repair. DNA Repair (Amst) *7*, 476-486.

Maruyama, K., Tsukada, T., Honda, M., Nara-Ashizawa, N., Noguchi, K., Cheng, J., Ohkura, N., Sasaki, K., and Yamaguchi, K. (2000). Complementary DNA structure and genomic organization of Drosophila menin. Mol Cell Endocrinol *168*, 135-140.

Marx, S.J. (2005). Molecular genetics of multiple endocrine neoplasia types 1 and 2. Nat Rev Cancer *5*, 367-375.

Marx, S.J., Agarwal, S.K., Heppner, C., Kim, Y.S., Kester, M.B., Goldsmith, P.K., Skarulis, M.C., Spiegel, A.M., Burns, A.L., Debelenko, L.V.*, et al.* (1999). The gene for multiple endocrine neoplasia type 1: recent findings. Bone *25*, 119-122.

Matsuoka, S., Ballif, B.A., Smogorzewska, A., McDonald, E.R., Hurov, K.E., Luo, J., Bakalarski, C.E., Zhao, Z., Solimini, N., Lerenthal, Y.*, et al.* (2007). ATM and ATR Substrate Analysis Reveals Extensive Protein Networks Responsive to DNA Damage. Science *316*, 1160-1166.

Mattila, J., Kallijärvi, J., and Puig, O. (2008). RNAi screening for kinases and phosphatases identifies FoxO regulators. Proceedings of the National Academy of Sciences *105*, 14873-14878.

Mazo, A.M., Huang, D.H., Mozer, B.A., and Dawid, I.B. (1990). The trithorax gene, a trans-acting regulator of the bithorax complex in Drosophila, encodes a protein with zinc-binding domains. Proc Natl Acad Sci U S A *87*, 2112-2116.

McCallum, R.W., Parameswaran, V., and Burgess, J.R. (2006). Multiple endocrine neoplasia type 1 (MEN 1) is associated with an increased prevalence of diabetes mellitus and impaired fasting glucose. Clinical Endocrinology *65*, 163-168.

Medema, J.P., Scaffidi, C., Kischkel, F.C., Shevchenko, A., Mann, M., Krammer, P.H., and Peter, M.E. (1997). FLICE is activated by association with the CD95 death-inducing signaling complex (DISC). Embo J *16*, 2794-2804.

Medema, R.H., Kops, G.J.P.L., Bos, J.L., and Burgering, B.M.T. (2000). AFX-like Forkhead transcription factors mediate cell-cycle regulation by Ras and PKB through p27kip1. Nature *404*, 782-787.

Meinander, A., Runchel, C., Tenev, T., Chen, L., Kim, C.-H., Ribeiro, P.S., Broemer, M., Leulier, F., Zvelebil, M., Silverman, N.*, et al.* (2012). Ubiquitylation of the initiator caspase DREDD is required for innate immune signalling. Embo J *31*, 2770-2783.

Michel, T., Reichhart, J.M., Hoffmann, J.A., and Royet, J. (2001). Drosophila Toll is activated by Gram-positive bacteria through a circulating peptidoglycan recognition protein. Nature *414*, 756-759.

Milne, T.A., Briggs, S.D., Brock, H.W., Martin, M.E., Gibbs, D., Allis, C.D., and Hess, J.L. (2002). MLL targets SET domain methyltransferase activity to Hox gene promoters. Mol Cell *10*, 1107-1117.

Milne, T.A., Hughes, C.M., Lloyd, R., Yang, Z., Rozenblatt-Rosen, O., Dou, Y., Schnepp, R.W., Krankel, C., Livolsi, V.A., Gibbs, D*., et al.* (2005). Menin and MLL cooperatively regulate expression of cyclin-dependent kinase inhibitors. Proc Natl Acad Sci U S A *102*, 749-754.

Milne, T.A., Kim, J., Wang, G.G., Stadler, S.C., Basrur, V., Whitcomb, S.J., Wang, Z., Ruthenburg, A.J., Elenitoba-Johnson, K.S.J., Roeder, R.G*., et al.* (2010). Multiple Interactions Recruit MLL1 and MLL1 Fusion Proteins to the HOXA9 Locus in Leukemogenesis. Molecular Cell *38*, 853-863.

Miron, M., Lasko, P., and Sonenberg, N. (2003). Signaling from Akt to FRAP/TOR Targets both 4E-BP and S6K in Drosophila melanogaster. Molecular and Cellular Biology *23*, 9117-9126.

Miron, M., Verdu, J., Lachance, P.E.D., Birnbaum, M.J., Lasko, P.F., and Sonenberg, N. (2001). The translational inhibitor 4E-BP is an effector of PI(3)K/Akt signalling and cell growth in Drosophila. Nat Cell Biol *3*, 596-601.

Mohan, M., Herz, H.-M., Smith, E.R., Zhang, Y., Jackson, J., Washburn, M.P., Florens, L., Eissenberg, J.C., and Shilatifard, A. (2011). The COMPASS Family of H3K4 Methylases in Drosophila. Molecular and Cellular Biology *31*, 4310-4318.

Montagne, J., Stewart, M.J., Stocker, H., Hafen, E., Kozma, S.C., and Thomas, G. (1999). Drosophila S6 Kinase: A Regulator of Cell Size. Science *285*, 2126-2129.

Moreno, E., Yan, M., and Basler, K. (2002). Evolution of TNF Signaling Mechanisms: JNK-Dependent Apoptosis Triggered by Eiger, the Drosophila Homolog of the TNF Superfamily. Current Biology *12*, 1263-1268.

Muntean, A.G., Tan, J., Sitwala, K., Huang, Y., Bronstein, J., Connelly, J.A., Basrur, V., Elenitoba-Johnson, K.S., and Hess, J.L. (2010). The PAF complex synergizes with MLL fusion proteins at HOX loci to promote leukemogenesis. Cancer Cell *17*, 609-621.

Murai, M.J., Chruszcz, M., Reddy, G., Grembecka, J., and Cierpicki, T. (2011). Crystal structure of menin reveals binding site for mixed lineage leukemia (MLL) protein. J Biol Chem *286*, 31742-31748.

Naitza, S., Rosse, C., Kappler, C., Georgel, P., Belvin, M., Gubb, D., Camonis, J., Hoffmann, J.A., and Reichhart, J.M. (2002). The Drosophila immune defense against gram-negative infection requires the death protein dFADD. Immunity *17*, 575-581.

Nakamura, T., Mori, T., Tada, S., Krajewski, W., Rozovskaia, T., Wassell, R., Dubois, G., Mazo, A., Croce, C.M., and Canaani, E. (2002). ALL-1 is a histone methyltransferase that assembles a supercomplex of proteins involved in transcriptional regulation. Mol Cell *10*, 1119-1128.

Nakata, Y., Brignier, A.C., Jin, S., Shen, Y., Rudnick, S.I., Sugita, M., and Gewirtz, A.M. (2010). c-Myb, Menin, GATA-3, and MLL form a dynamic transcription complex that plays a pivotal role in human T helper type 2 cell development. Blood *116*, 1280-1290.

Newton, K., Harris, A.W., and Strasser, A. (2000). FADD/MORT1 regulates the pre-TCR checkpoint and can function as a tumour suppressor. Embo J *19*, 931-941.

Nguyen, A.T., Taranova, O., He, J., and Zhang, Y. (2011). DOT1L, the H3K79 methyltransferase, is required for MLL-AF9–mediated leukemogenesis. Blood *117*, 6912-6922.

Nolo, R., Abbott, L.A., and Bellen, H.J. (2001). Drosophila Lyra mutations are gain-of-function mutations of senseless. Genetics *157*, 307-315.

O'Brien, T., and Lis, J.T. (1991). RNA polymerase II pauses at the 5' end of the transcriptionally induced Drosophila hsp70 gene. Molecular and Cellular Biology *11*, 5285-5290.

Obungu, V.H., Lee Burns, A., Agarwal, S.K., Chandrasekharapa, S.C., Adelstein, R.S., and Marx, S.J. (2003). Menin, a tumor suppressor, associates with nonmuscle myosin II-A heavy chain. Oncogene *22*, 6347-6358.

Okada, Y., Feng, Q., Lin, Y., Jiang, Q., Li, Y., Coffield, V.M., Su, L., Xu, G., and Zhang, Y. (2005). hDOT1L Links Histone Methylation to Leukemogenesis. Cell *121*, 167-178.

Oldham, S., Montagne, J., Radimerski, T., Thomas, G., and Hafen, E. (2000). Genetic and biochemical characterization of dTOR, the Drosophila homolog of the target of rapamycin. Genes & Development *14*, 2689-2694.

Oldham, S., Stocker, H., Laffargue, M., Wittwer, F., Wymann, M., and Hafen, E. (2002). The Drosophila insulin/IGF receptor controls growth and size by modulating PtdInsP3 levels. Development *129*, 4103-4109.

Papaconstantinou, M., Maslikowski, B.M., Pepper, A.N., and Bedard, P.A. (2009). Menin: the protein behind the MEN1 syndrome. Adv Exp Med Biol *668*, 27-36.

Papaconstantinou, M., Pepper, A.N., Wu, Y., Kasimer, D., Westwood, T., Campos, A.R., and Bedard, P.A. (2010). Menin links the stress response to genome stability in Drosophila melanogaster. PLoS ONE *5*, e14049.

Papaconstantinou, M., Wu, Y., Pretorius, H.N., Singh, N., Gianfelice, G., Tanguay, R.M., Campos, A.R., and Bedard, P.A. (2005). Menin is a regulator of the stress response in Drosophila melanogaster. Mol Cell Biol *25*, 9960-9972.

Paquette, N., Broemer, M., Aggarwal, K., Chen, L., Husson, M., Ertürk-Hasdemir, D., Reichhart, J.-M., Meier, P., and Silverman, N. (2010). Caspase-Mediated Cleavage, IAP Binding, and Ubiquitination: Linking Three Mechanisms Crucial for Drosophila NF-κB Signaling. Molecular Cell *37*, 172-182.

Parkash, R., Aggarwal, D., Ranga, P., and Singh, D. (2012). Divergence of larval resource acquisition for water conservation and starvation resistance in <i>Drosophila melanogaster</i&gt. Journal of Comparative Physiology B: Biochemical, Systemic, and Environmental Physiology *182*, 625-640.

Patel, A., Vought, V.E., Dharmarajan, V., and Cosgrove, M.S. (2008). A Conserved Arginine-containing Motif Crucial for the Assembly and Enzymatic Activity of the Mixed Lineage Leukemia Protein-1 Core Complex. Journal of Biological Chemistry *283*, 32162-32175.

Petesch, S.J., and Lis, J.T. (2008). Rapid, transcription-independent loss of nucleosomes over a large chromatin domain at Hsp70 loci. Cell *134*, 74-84.

Petruk, S., Sedkov, Y., Smith, S., Tillib, S., Kraevski, V., Nakamura, T., Canaani, E., Croce, C.M., and Mazo, A. (2001). Trithorax and dCBP acting in a complex to maintain expression of a homeotic gene. Science *294*, 1331-1334.

Petruk, S., Sedkov, Y., Smith, S.T., Krajewski, W., Nakamura, T., Canaani, E., Croce, C.M., and Mazo, A. (2004). Purification and biochemical properties of the Drosophila TAC1 complex. Methods Enzymol *377*, 255-266.

Pile, L.A., Lee, F.W., and Wassarman, D.A. (2001). The histone deacetylase inhibitor trichostatin A influences the development of Drosophila melanogaster. Cell Mol Life Sci *58*, 1715-1718.

Piper, M.D.W., Selman, C., McElwee, J.J., and Partridge, L. (2005). Models of insulin signalling and longevity. Drug Discovery Today: Disease Models *2*, 249-256.

Potter, C.J., Huang, H., and Xu, T. (2001). Drosophila Tsc1 Functions with Tsc2 to Antagonize Insulin Signaling in Regulating Cell Growth, Cell Proliferation, and Organ Size. Cell *105*, 357-368.

Pradeepa, M.M., Sutherland, H.G., Ule, J., Grimes, G.R., and Bickmore, W.A. (2012). Psip1/Ledgf p52 Binds Methylated Histone H3K36 and Splicing Factors and Contributes to the Regulation of Alternative Splicing. PLoS Genet *8*, e1002717.

Puig, O., Marr, M.T., Ruhf, M.L., and Tjian, R. (2003). Control of cell number by Drosophila FOXO: downstream and feedback regulation of the insulin receptor pathway. Genes & Development *17*, 2006-2020.

Puig, O., and Mattila, J. (2011). Understanding Forkhead box class O function: lessons from Drosophila melanogaster. Antioxid Redox Signal *14*, 635-647.

Puig, O., and Tjian, R. (2005). Transcriptional feedback control of insulin receptor by dFOXO/FOXO1. Genes & Development *19*, 2435-2446.

Puigserver, P., Rhee, J., Donovan, J., Walkey, C.J., Yoon, J.C., Oriente, F., Kitamura, Y., Altomonte, J., Dong, H., Accili, D.*, et al.* (2003). Insulin-regulated hepatic gluconeogenesis through FOXO1-PGC-1[alpha] interaction. Nature *423*, 550-555.

Radimerski, T., Montagne, J., Rintelen, F., Stocker, H., van der Kaay, J., Downes, C.P., Hafen, E., and Thomas, G. (2002). dS6K-regulated cell growth is dPKB/dPI(3)K-independent, but requires dPDK1. Nat Cell Biol *4*, 251-255.

Rea, S., Eisenhaber, F., O'Carroll, D., Strahl, B.D., Sun, Z.W., Schmid, M., Opravil, S., Mechtler, K., Ponting, C.P., Allis, C.D*., et al.* (2000). Regulation of chromatin structure by site-specific histone H3 methyltransferases. Nature *406*, 593-599.

Reis, T., Van Gilst, M.R., and Hariharan, I.K. (2010). A Buoyancy-Based Screen of Drosophila Larvae for Fat-Storage Mutants Reveals a Role for <italic>Sir2</italic> in Coupling Fat Storage to Nutrient Availability. PLoS Genet *6*, e1001206.

Rintelen, F., Stocker, H., Thomas, G., and Hafen, E. (2001). PDK1 regulates growth through Akt and S6K in Drosophila. Proceedings of the National Academy of Sciences *98*, 15020-15025.

Roguev, A., Schaft, D., Shevchenko, A., Pijnappel, W.W.M.P., Wilm, M., Aasland, R., and Stewart, A.F. (2001). The Saccharomyces cerevisiae Set1 complex includes an Ash2 homologue and methylates histone 3 lysine 4. Embo J *20*, 7137-7148.

Rosetto, M., Engstrom, Y., Baldari, C.T., Telford, J.L., and Hultmark, D. (1995). Signals from the IL-1 Receptor Homolog, Toll, Can Activate an Immune Response in a Drosophila Hemocyte Cell Line. Biochemical and Biophysical Research Communications *209*, 111-116.

Rozenblatt-Rosen, O., Rozovskaia, T., Burakov, D., Sedkov, Y., Tillib, S., Blechman, J., Nakamura, T., Croce, C.M., Mazo, A., and Canaani, E. (1998). The C-terminal SET domains of ALL-1 and TRITHORAX interact with the INI1 and SNR1 proteins, components of the SWI/SNF complex. Proc Natl Acad Sci U S A *95*, 4152-4157.

Rozovskaia, T., Feinstein, E., Mor, O., Foa, R., Blechman, J., Nakamura, T., Croce, C.M., Cimino, G., and Canaani, E. (2001). Upregulation of Meis1 and HoxA9 in acute lymphocytic leukemias with the t(4 : 11) abnormality. Oncogene *20*, 874-878.

Rozovskaia, T., Tillib, S., Smith, S., Sedkov, Y., Rozenblatt-Rosen, O., Petruk, S., Yano, T., Nakamura, T., Ben-Simchon, L., Gildea, J*., et al.* (1999). Trithorax and ASH1 interact directly and associate with the trithorax group-responsive bxd region of the Ultrabithorax promoter. Mol Cell Biol *19*, 6441-6447.

Ruden, D.M., Jamison, D.C., Zeeberg, B.R., Garfinkel, M.D., Weinstein, J.N., Rasouli, P., and Lu, X. (2008). The EDGE hypothesis: Epigenetically directed genetic errors in repeat-containing proteins (RCPs) involved in evolution, neuroendocrine signaling, and cancer. Frontiers in Neuroendocrinology *29*, 428-444.

Rulifson, E.J., Kim, S.K., and Nusse, R. (2002). Ablation of Insulin-Producing Neurons in Flies: Growth and Diabetic Phenotypes. Science *296*, 1118-1120.

Rush, B., Sandver, S., Bruer, J., Roche, R., Wells, M., and Giebultowicz, J. (2007). Mating increases starvation resistance and decreases oxidative stress resistance in Drosophila melanogaster females. Aging Cell *6*, 723-726.

Rutherford, S.L., and Lindquist, S. (1998). Hsp90 as a capacitor for morphological evolution. Nature *396*, 336-342.

Rutschmann, S., Jung, A.C., Hetru, C., Reichhart, J.-M., Hoffmann, J.A., and Ferrandon, D. (2000a). The Rel Protein DIF Mediates the Antifungal but Not the Antibacterial Host Defense in Drosophila. Immunity *12*, 569-580.

Rutschmann, S., Jung, A.C., Zhou, R., Silverman, N., Hoffmann, J.A., and Ferrandon, D. (2000b). Role of Drosophila IKK gamma in a toll-independent antibacterial immune response. Nat Immunol *1*, 342-347.

Rutschmann, S., Kilinc, A., and Ferrandon, D. (2002). Cutting edge: the toll pathway is required for resistance to gram-positive bacterial infections in Drosophila. J Immunol *168*, 1542-1546.

Salaun, B., Romero, P., and Lebecque, S. (2007). Toll-like receptors' two-edged sword: when immunity meets apoptosis. European Journal of Immunology *37*, 3311-3318.

Sayo, Y., Murao, K., Imachi, H., Cao, W.M., Sato, M., Dobashi, H., Wong, N.C., and Ishida, T. (2002). The multiple endocrine neoplasia type 1 gene product, menin, inhibits insulin production in rat insulinoma cells. Endocrinology *143*, 2437-2440.

Scacheri, P.C., Crabtree, J.S., Kennedy, A.L., Swain, G.P., Ward, J.M., Marx, S.J., Spiegel, A.M., and Collins, F.S. (2004). Homozygous loss of menin is well tolerated in liver, a tissue not affected in MEN1. Mamm Genome *15*, 872-877.

Scacheri, P.C., Davis, S., Odom, D.T., Crawford, G.E., Perkins, S., Halawi, M.J., Agarwal, S.K., Marx, S.J., Spiegel, A.M., Meltzer, P.S*., et al.* (2006). Genome-wide analysis of menin binding provides insights into MEN1 tumorigenesis. PLoS Genet *2*, e51.

Scaffidi, C., Volkland, J., Blomberg, I., Hoffmann, I., Krammer, P.H., and Peter, M.E. (2000). Phosphorylation of FADD/ MORT1 at Serine 194 and Association with a 70-kDa Cell Cycle-Regulated Protein Kinase. The Journal of Immunology *164*, 1236-1242.

Scappaticci, S., Maraschio, P., del Ciotto, N., Fossati, G.S., Zonta, A., and Fraccaro, M. (1991). Chromosome abnormalities in lymphocytes and fibroblasts of subjects with multiple endocrine neoplasia type 1. Cancer Genet Cytogenet *52*, 85-92.

Schinner, S. (2009). Wnt-signalling and the metabolic syndrome. Horm Metab Res *41*, 159-163.

Schinner, S., Ülgen, F., Papewalis, C., Schott, M., Woelk, A., Vidal-Puig, A., and Scherbaum, W. (2008). Regulation of insulin secretion, glucokinase gene transcription and beta cell proliferation by adipocyte-derived Wnt signalling molecules. Diabetologia *51*, 147-154.

Schleich, S., and Teleman, A.A. (2009). Akt Phosphorylates Both Tsc1 and Tsc2 in Drosophila, but Neither Phosphorylation Is Required for Normal Animal Growth. PLoS ONE *4*, e6305.

Schnepp, R.W., Chen, Y.X., Wang, H., Cash, T., Silva, A., Diehl, J.A., Brown, E., and Hua, X. (2006). Mutation of tumor suppressor gene Men1 acutely enhances proliferation of pancreatic islet cells. Cancer Res *66*, 5707-5715.

Schnepp, R.W., Hou, Z., Wang, H., Petersen, C., Silva, A., Masai, H., and Hua, X. (2004a). Functional interaction between tumor suppressor menin and activator of S-phase kinase. Cancer Res *64*, 6791-6796.

Schnepp, R.W., Mao, H., Sykes, S.M., Zong, W.X., Silva, A., La, P., and Hua, X. (2004b). Menin induces apoptosis in murine embryonic fibroblasts. J Biol Chem *279*, 10685-10691.

Screaton, R.A., Kiessling, S., Sansom, O.J., Millar, C.B., Maddison, K., Bird, A., Clarke, A.R., and Frisch, S.M. (2003). Fas-associated death domain protein interacts with methyl-CpG binding domain protein 4: a potential link between genome surveillance and apoptosis. Proc Natl Acad Sci U S A *100*, 5211-5216.

Sedkov, Y., Cho, E., Petruk, S., Cherbas, L., Smith, S.T., Jones, R.S., Cherbas, P., Canaani, E., Jaynes, J.B., and Mazo, A. (2003). Methylation at lysine 4 of histone H3 in ecdysone-dependent development of Drosophila. Nature *426*, 78-83.

Sedkov, Y., Tillib, S., Mizrokhi, L., and Mazo, A. (1994). The bithorax complex is regulated by trithorax earlier during Drosophila embryogenesis than is the Antennapedia complex, correlating with a bithorax-like expression pattern of distinct early trithorax transcripts. Development *120*, 1907-1917.

Seong, K.H., Li, D., Shimizu, H., Nakamura, R., and Ishii, S. (2011). Inheritance of stress-induced, ATF-2-dependent epigenetic change. Cell *145*, 1049-1061.

Shen, H.-C.J., He, M., Powell, A., Adem, A., Lorang, D., Heller, C., Grover, A.C., Ylaya, K., Hewitt, S.M., Marx, S.J.*, et al.* (2009). Recapitulation of Pancreatic Neuroendocrine Tumors in Human Multiple Endocrine Neoplasia Type I Syndrome via Pdx1-Directed Inactivation of Men1. Cancer Research *69*, 1858-1866.

Shen, H.-C.J., Ylaya, K., Pechhold, K., Wilson, A., Adem, A., Hewitt, S.M., and Libutti, S.K. (2010). Multiple Endocrine Neoplasia Type 1 Deletion in Pancreatic α-Cells Leads to Development of Insulinomas in Mice. Endocrinology *151*, 4024-4030.

Shi, A., Murai, M.J., He, S., Lund, G., Hartley, T., Purohit, T., Reddy, G., Chruszcz, M., Grembecka, J., and Cierpicki, T. (2012). Structural insights into inhibition of the bivalent menin-MLL interaction by small molecules in leukemia. Blood *120*, 4461-4469.

Silverman, N., Zhou, R., Erlich, R.L., Hunter, M., Bernstein, E., Schneider, D., and Maniatis, T. (2003). Immune activation of NF-kappaB and JNK requires Drosophila TAK1. J Biol Chem *278*, 48928-48934.

Silverman, N., Zhou, R., Stoven, S., Pandey, N., Hultmark, D., and Maniatis, T. (2000). A Drosophila IkappaB kinase complex required for Relish cleavage and antibacterial immunity. Genes Dev *14*, 2461-2471.

Slack, C., Werz, C., Wieser, D., Alic, N., Foley, A., Stocker, H., Withers, D.J., Thornton, J.M., Hafen, E., and Partridge, L. (2010). Regulation of lifespan, metabolism, and stress responses by the Drosophila SH2B protein, Lnk. PLoS Genet *6*, e1000881.

Smith, S.T., Petruk, S., Sedkov, Y., Cho, E., Tillib, S., Canaani, E., and Mazo, A. (2004). Modulation of heat shock gene expression by the TAC1 chromatin-modifying complex. Nat Cell Biol *6*, 162-167.

Söderberg, J.A.E., Birse, R.T., and Nässel, D.R. (2011). Insulin Production and Signaling in Renal Tubules of <italic>Drosophila</italic> Is under Control of Tachykinin-Related Peptide and Regulates Stress Resistance. PLoS ONE *6*, e19866.

Sollars, V., Lu, X., Xiao, L., Wang, X., Garfinkel, M.D., and Ruden, D.M. (2003). Evidence for an epigenetic mechanism by which Hsp90 acts as a capacitor for morphological evolution. Nat Genet *33*, 70-74.

Song, J.-J., and Kingston, R.E. (2008). WDR5 Interacts with Mixed Lineage Leukemia (MLL) Protein via the Histone H3-binding Pocket. Journal of Biological Chemistry *283*, 35258-35264.

Sowa, H., Kaji, H., Canaff, L., Hendy, G.N., Tsukamoto, T., Yamaguchi, T., Miyazono, K., Sugimoto, T., and Chihara, K. (2003). Inactivation of menin, the product of the multiple endocrine neoplasia type 1 gene, inhibits the commitment of multipotential mesenchymal stem cells into the osteoblast lineage. J Biol Chem *278*, 21058-21069.

Sowa, H., Kaji, H., Hendy, G.N., Canaff, L., Komori, T., Sugimoto, T., and Chihara, K. (2004). Menin is required for bone morphogenetic protein 2- and transforming growth factor beta-regulated osteoblastic differentiation through interaction with Smads and Runx2. J Biol Chem *279*, 40267-40275.

Srinivasan, S., Dorighi, K.M., and Tamkun, J.W. (2008). <italic>Drosophila</italic> Kismet Regulates Histone H3 Lysine 27 Methylation and Early Elongation by RNA Polymerase II. PLoS Genet *4*, e1000217.

Staveley, B.E., Ruel, L., Jin, J., Stambolic, V., Mastronardi, F.G., Heitzler, P., Woodgett, J.R., and Manoukian, A.S. (1998). Genetic analysis of protein kinase B (AKT) in Drosophila. Current Biology *8*, 599-603.

Stern, S., Fridmann-Sirkis, Y., Braun, E., and Soen, Y. (2012). Epigenetically Heritable Alteration of Fly Development in Response to Toxic Challenge. Cell Reports *1*, 528-542.

Stokes, M.P., Rush, J., MacNeill, J., Ren, J.M., Sprott, K., Nardone, J., Yang, V., Beausoleil, S.A., Gygi, S.P., Livingstone, M.*, et al.* (2007). Profiling of UV-induced ATM/ATR signaling pathways. Proceedings of the National Academy of Sciences *104*, 19855-19860.

Stöven, S., Ando, I., Kadalayil, L., Engstrom, Y., and Hultmark, D. (2000). Activation of the Drosophila NF-kappaB factor Relish by rapid endoproteolytic cleavage. EMBO Rep *1*, 347-352.

Stöven, S., Silverman, N., Junell, A., Hedengren-Olcott, M., Erturk, D., Engstrom, Y., Maniatis, T., and Hultmark, D. (2003). Caspase-mediated processing of the Drosophila NF-kappaB factor Relish. Proc Natl Acad Sci U S A *100*, 5991-5996.

Strasser, A., and Newton, K. (1999). FADD/MORT1, a signal transducer that can promote cell death or cell growth. The International Journal of Biochemistry & Cell Biology *31*, 533-537.

Suen, F. (2010). Characterization of the menin and Tip60 interaction in Drosophila melanogaster. In Biology (Hamilton, McMaster Univeristy), pp. 103.

Sukhodolets, K.E., Hickman, A.B., Agarwal, S.K., Sukhodolets, M.V., Obungu, V.H., Novotny, E.A., Crabtree, J.S., Chandrasekharappa, S.C., Collins, F.S., Spiegel, A.M.*, et al.* (2003). The 32-kilodalton subunit of replication protein A interacts with menin, the product of the MEN1 tumor suppressor gene. Mol Cell Biol *23*, 493-509.

Takeda, S., Chen, D.Y., Westergard, T.D., Fisher, J.K., Rubens, J.A., Sasagawa, S., Kan, J.T., Korsmeyer, S.J., Cheng, E.H., and Hsieh, J.J. (2006). Proteolysis of MLL family proteins is essential for taspase1-orchestrated cell cycle progression. Genes Dev *20*, 2397-2409.

Tatar, M., Kopelman, A., Epstein, D., Tu, M.-P., Yin, C.-M., and Garofalo, R.S. (2001). A Mutant Drosophila Insulin Receptor Homolog That Extends Life-Span and Impairs Neuroendocrine Function. Science *292*, 107-110.

Teleman, A.A. (2009). Molecular mechanisms of metabolic regulation by insulin in Drosophila. Biochemical Journal *425*, 13-26.

Teleman, A.A., Chen, Y.-W., and Cohen, S.M. (2005). 4E-BP functions as a metabolic brake used under stress conditions but not during normal growth. Genes & Development *19*, 1844-1848.

Tettweiler, G., Miron, M., Jenkins, M., Sonenberg, N., and Lasko, P.F. (2005). Starvation and oxidative stress resistance in Drosophila are mediated through the eIF4E-binding protein, d4E-BP. Genes & Development *19*, 1840-1843.

Thakker, R.V. (2010). Multiple endocrine neoplasia type 1 (MEN1). Best Practice & Research Clinical Endocrinology & Metabolism *24*, 355-370.

Thiel, A.T., Huang, J., Lei, M., and Hua, X. (2012). Menin as a hub controlling mixed lineage leukemia. BioEssays *34*, 771-780.

Tie, F., Banerjee, R., Stratton, C.A., Prasad-Sinha, J., Stepanik, V., Zlobin, A., Diaz, M.O., Scacheri, P.C., and Harte, P.J. (2009). CBP-mediated acetylation of histone H3 lysine 27 antagonizes Drosophila Polycomb silencing. Development *136*, 3131-3141.

Tillib, S., Petruk, S., Sedkov, Y., Kuzin, A., Fujioka, M., Goto, T., and Mazo, A. (1999). Trithorax- and Polycomb-group response elements within an Ultrabithorax transcription maintenance unit consist of closely situated but separable sequences. Mol Cell Biol *19*, 5189-5202.

Tkachuk, D.C., Kohler, S., and Cleary, M.L. (1992). Involvement of a homolog of Drosophila trithorax by 11q23 chromosomal translocations in acute leukemias. Cell *71*, 691-700.

Tourneur, L., Buzyn, A., and Chiocchia, G. (2005). FADD adaptor in cancer. Med Immunol *4*, 1.

Tourneur, L., and Chiocchia, G. (2010). FADD: a regulator of life and death. Trends in Immunology *31*, 260-269.

Tourneur, L., Delluc, S., Levy, V., Valensi, F., Radford-Weiss, I., Legrand, O., Vargaftig, J., Boix, C., Macintyre, E.A., Varet, B.*, et al.* (2004). Absence or low expression of fas-associated protein with death domain in acute myeloid leukemia cells predicts resistance to chemotherapy and poor outcome. Cancer Res *64*, 8101-8108.

Tourneur, L., Mistou, S., Michiels, F.M., Devauchelle, V., Renia, L., Feunteun, J., and Chiocchia, G. (2003). Loss of FADD protein expression results in a biased Fas-signaling pathway and correlates with the development of tumoral status in thyroid follicular cells. Oncogene *22*, 2795-2804.

Tschiersch, B., Hofmann, A., Krauss, V., Dorn, R., Korge, G., and Reuter, G. (1994). The protein encoded by the Drosophila position-effect variegation suppressor gene Su(var)3-9 combines domains of antagonistic regulators of homeotic gene complexes. Embo J *13*, 3822-3831.

Tsukada, T., Nagamura, Y., and Ohkura, N. (2009). MEN1 gene and its mutations: Basic and clinical implications. Cancer Science *100*, 209-215.

Tzou, P., Ohresser, S., Ferrandon, D., Capovilla, M., Reichhart, J.M., Lemaitre, B., Hoffmann, J.A., and Imler, J.L. (2000). Tissue-specific inducible expression of antimicrobial peptide genes in Drosophila surface epithelia. Immunity *13*, 737-748.

Valanne, S., Wang, J.-H., and Rämet, M. (2011). The Drosophila Toll Signaling Pathway. The Journal of Immunology *186*, 649-656.

Van Der Heide, L.P., Hoekman, M.F., and Smidt, M.P. (2004). The ins and outs of FoxO shuttling: mechanisms of FoxO translocation and transcriptional regulation. Biochem J *380*, 297-309.

van Wijk, J.P.H., Dreijerink, K.M.A., Pieterman, C.R.C., Lips, C.J.M., Zelissen, P.M.J., and Valk, G.D. (2012). Increased prevalence of impaired fasting glucose in MEN1 gene mutation carriers. Clinical Endocrinology *76*, 67-71.

Verdu, J., Buratovich, M.A., Wilder, E.L., and Birnbaum, M.J. (1999). Cell-autonomous regulation of cell and organ growth in Drosophila by Akt/PKB. Nat Cell Biol *1*, 500-506.

Villarroel, M.J., Ferrando, M.D., Sancho, E., and Andreu, E. (2000). Population dynamics in Daphnia Magna as modified by chronic tetradifon stress. Journal of Environmental Science and Health, Part B *35*, 211-227.

Wägner, A.M., Martín-Campos, J.M., Mayoral, C., de Leiva, A., and Blanco-Vaca, F. (2005). Patients with MEN-1 are more insulin-resistant than their non-affected relatives. European Journal of Internal Medicine *16*, 507-509.

Wang, M.C., Bohmann, D., and Jasper, H. (2005). JNK Extends Life Span and Limits Growth by Antagonizing Cellular and Organism-Wide Responses to Insulin Signaling. Cell *121*, 115-125.

Wang, Y., Ozawa, A., Zaman, S., Prasad, N.B., Chandrasekharappa, S.C., Agarwal, S.K., and Marx, S.J. (2011). The Tumor Suppressor Protein Menin Inhibits AKT Activation by Regulating Its Cellular Localization. Cancer Research *71*, 371-382.

Wautot, V., Khodaei, S., Frappart, L., Buisson, N., Baro, E., Lenoir, G.M., Calender, A., Zhang, C.X., and Weber, G. (2000). Expression analysis of endogenous menin, the product of the multiple endocrine neoplasia type 1 gene, in cell lines and human tissues. Int J Cancer *85*, 877-881.

Weinkove, D., Neufeld, T.P., Twardzik, T., Waterfield, M.D., and Leevers, S.J. (1999). Regulation of imaginal disc cell size, cell number and organ size by Drosophila class IA phosphoinositide 3-kinase and its adaptor. Current Biology *9*, 1019-1029.

Werner, T., Borge-Renberg, K., Mellroth, P., Steiner, H., and Hultmark, D. (2003). Functional Diversity of the Drosophila PGRP-LC Gene Cluster in the Response to Lipopolysaccharide and Peptidoglycan. Journal of Biological Chemistry *278*, 26319-26322.

Werz, C., Kohler, K., Hafen, E., and Stocker, H. (2009). The Drosophila SH2B family adaptor Lnk acts in parallel to chico in the insulin signaling pathway. PLoS Genet *5*, e1000596.

Wu, T., Zhang, X., Huang, X., Yang, Y., and Hua, X. (2010). Regulation of cyclin B2 expression and cell cycle G2/m transition by menin. J Biol Chem *285*, 18291-18300.

Wuescher, L., Angevine, K., Hinds, T., Ramakrishnan, S., Najjar, S.M., and Mensah-Osman, E.J. (2011). Insulin regulates menin expression, cytoplasmic localization, and interaction with FOXO1. American Journal of Physiology - Endocrinology And Metabolism *301*, E474-E483.

Xu, B., Zeng, D.Q., Wu, Y., Zheng, R., Gu, L., Lin, X., Hua, X., and Jin, G.H. (2011). Tumor suppressor menin represses paired box gene 2 expression via Wilms tumor suppressor protein-polycomb group complex. J Biol Chem *286*, 13937-13944.

Yaguchi, H., Ohkura, N., Takahashi, M., Nagamura, Y., Kitabayashi, I., and Tsukada, T. (2004). Menin missense mutants associated with multiple endocrine neoplasia type 1 are rapidly degraded via the ubiquitin-proteasome pathway. Mol Cell Biol *24*, 6569-6580.

Yaguchi, H., Ohkura, N., Tsukada, T., and Yamaguchi, K. (2002). Menin, the multiple endocrine neoplasia type 1 gene product, exhibits GTP-hydrolyzing activity in the presence of the tumor metastasis suppressor nm23. J Biol Chem *277*, 38197-38204.

Yan, J., Yang, Y., Zhang, H., King, C., Kan, H.M., Cai, Y., Yuan, C.X., Bloom, G.S., and Hua, X. (2008). Menin interacts with IQGAP1 to enhance intercellular adhesion of [beta]-cells. Oncogene *28*, 973-982.

Yang, Y., Gurung, B., Wu, T., Wang, H., Stoffers, D.A., and Hua, X. (2010a). Reversal of preexisting hyperglycemia in diabetic mice by acute deletion of the Men1 gene. Proceedings of the National Academy of Sciences *107*, 20358-20363.

Yang, Y., and Hua, X. (2007). In search of tumor suppressing functions of menin. Mol Cell Endocrinol *265-266*, 34-41.

Yang, Y., Wang, H., and Hua, X. (2010b). Deletion of the Men1 gene prevents streptozotocin-induced hyperglycemia in mice. Exp Diabetes Res *2010*, 876701.

Yeh, W.-C., Pompa, J.L.d.l., McCurrach, M.E., Shu, H.-B., Elia, A.J., Shahinian, A., Ng, M., Wakeham, A., Khoo, W., Mitchell, K.*, et al.* (1998). FADD: Essential for Embryo Development and Signaling from Some, But Not All, Inducers of Apoptosis. Science *279*, 1954-1958.

Yenush, L., Fernandez, R., Myers, M.G., Jr., Grammer, T.C., Sun, X.J., Blenis, J., Pierce, J.H., Schlessinger, J., and White, M.F. (1996). The Drosophila insulin receptor activates multiple signaling pathways but requires insulin receptor substrate proteins for DNA synthesis. Mol Cell Biol *16*, 2509-2517.

Yokoyama, A., and Cleary, M.L. (2008). Menin Critically Links MLL Proteins with LEDGF on Cancer-Associated Target Genes. Cancer Cell *14*, 36-46.

Yokoyama, A., Kitabayashi, I., Ayton, P.M., Cleary, M.L., and Ohki, M. (2002). Leukemia proto-oncoprotein MLL is proteolytically processed into 2 fragments with opposite transcriptional properties. Blood *100*, 3710-3718.

Yokoyama, A., Lin, M., Naresh, A., Kitabayashi, I., and Cleary, M.L. (2010). A Higher-Order Complex Containing AF4 and ENL Family Proteins with P-TEFb Facilitates Oncogenic and Physiologic MLL-Dependent Transcription. Cancer Cell *17*, 198-212.

Yokoyama, A., Somervaille, T.C., Smith, K.S., Rozenblatt-Rosen, O., Meyerson, M., and Cleary, M.L. (2005). The menin tumor suppressor protein is an essential oncogenic cofactor for MLL-associated leukemogenesis. Cell *123*, 207-218.

Yokoyama, A., Wang, Z., Wysocka, J., Sanyal, M., Aufiero, D.J., Kitabayashi, I., Herr, W., and Cleary, M.L. (2004). Leukemia proto-oncoprotein MLL forms a SET1-like histone methyltransferase complex with menin to regulate Hox gene expression. Mol Cell Biol *24*, 5639-5649.

Yu, B.D., Hanson, R.D., Hess, J.L., Horning, S.E., and Korsmeyer, S.J. (1998). MLL, a mammalian trithorax-group gene, functions as a transcriptional maintenance factor in morphogenesis. Proc Natl Acad Sci U S A *95*, 10632-10636.

Yu, B.D., Hess, J.L., Horning, S.E., Brown, G.A., and Korsmeyer, S.J. (1995). Altered Hox expression and segmental identity in Mll-mutant mice. Nature *378*, 505-508.

Zablewska, B., Bylund, L., Mandic, S.A., Fromaget, M., Gaudray, P., and Weber, G. (2003). Transcription regulation of the multiple endocrine neoplasia type 1 gene in human and mouse. J Clin Endocrinol Metab *88*, 3845-3851.

Zhande, R., Dauphinee, S.M., Thomas, J.A., Yamamoto, M., Akira, S., and Karsan, A. (2007). FADD negatively regulates lipopolysaccharide signaling by impairing interleukin-1 receptor-associated kinase 1-MyD88 interaction. Mol Cell Biol *27*, 7394-7404.

Zhang, H., Li, W., Wang, Q., Wang, X., Li, F., Zhang, C., Wu, L., Long, H., Liu, Y., Li, X.*, et al.* (2012). Glucose-Mediated Repression of Menin Promotes Pancreatic β-Cell Proliferation. Endocrinology *153*, 602-611.

Zhang, H., Stallock, J.P., Ng, J.C., Reinhard, C., and Neufeld, T.P. (2000). Regulation of cellular growth by the Drosophila target of rapamycin dTOR. Genes & Development *14*, 2712-2724.

Zhang, J., Cado, D., Chen, A., Kabra, N.H., and Winoto, A. (1998). Fas-mediated apoptosis and activation-induced T-cell proliferation are defective in mice lacking FADD/Mort1. Nature *392*, 296-300.

Zhao, Y.M., Chen, X., Sun, H., Yuan, Z.G., Ren, G.L., Li, X.X., Lu, J., and Huang, B.Q. (2006). Effects of histone deacetylase inhibitors on transcriptional regulation of the hsp70 gene in Drosophila. Cell Res *16*, 566-576.

Zheng, L., Schickling, O., Peter, M.E., and Lenardo, M.J. (2001). The Death Effector Domain-associated Factor Plays Distinct Regulatory Roles in the Nucleus and Cytoplasm. Journal of Biological Chemistry *276*, 31945-31952.

Zhou, R., Silverman, N., Hong, M., Liao, D.S., Chung, Y., Chen, Z.J., and Maniatis, T. (2005). The role of ubiquitination in Drosophila innate immunity. J Biol Chem *280*, 34048-34055.

Zhuang, Z.-H., Sun, L., Kong, L., Hu, J.-H., Yu, M.-C., Reinach, P., Zang, J.-W., and Ge, B.-X. (2006). Drosophila TAB2 is required for the immune activation of JNK and NF-kappaB. Cellular Signalling *18*, 964-970.

APPENDIX A: Generation and preliminary testing of dFADD polyclonal antibodies

In order to further study the menin-dFADD interaction and to confirm that both endogenous proteins interact in S2 cells, as well as to investigate an interaction in *Drosophila*, an antibody capable of detecting and immunoprecipitating dFADD was essential. A commercially available human FADD antibody (Stressgen® Bioreagents (now Enzo Life Sciences), AAP-210C) claiming to also detect the *Drosophila* protein failed to do so (data not shown). New England Peptide™ (NEP) was contracted to design peptide antibodies for dFADD but after extensive testing, these antibodies failed to detect endogenous or HA-tagged dFADD from S2 cells. Consequently, I cloned dFADD into a His-tag vector for protein expression and purification in order to inject into rabbits to generate a polyclonal antibodies (9678 and 9679) through the McMaster Central Animal Facility.

The second bleed of 9678 was able to detect both endogenous dFADD from S2 lysates as well as overexpressed HA-dFADD and dFADD-HA (Figure A.1A). The second bleed of 9679 was not as strong as 9678 but was also able to detect endogenous dFADD and very weakly dFADD-HA and HA-dFADD (Figure A.1B). The 9679 antibody also had a very strong contaminating band that migrated above the dFADD band at about 30 kDa. Both antibodies were able to immunoprecipitate dFADD, with 9678 pulling down more protein than 9679 (Figure A.1C). The corresponding pre-immune serums did not have any contaminating bands (Figure A.1C). No co-immunoprecipitation with menin was observed from S2 cells with this attempt. dFADD appears as a doublet in S2 cells, with the higher band being much more prominent (Figure A.1A and C); however, only the

lower band was immunoprecipitated with both 9678 and 9679 antibodies. Neither antibody was able to detect dFADD in lysates from OR embryos (8-20 hrs) or adult males (3-5 d) (Figure A.1C); suggesting that the protein may be rare in flies and difficult to detect in whole organism lysates. Thus, a functional polyclonal antibody capable of detecting dFADD in S2 cells was produced, with the 9678 antibody being stronger and more specific than the 9679 antibody; however, detection in *Drosophila* lysates was still not achieved with these antibodies under standard conditions.

Reciprocal immunoprecipitations, using the menin 5073 antibody and immunoblotting for dFADD, also proved difficult due to the presence of a prominent contaminating band, which was observed with all antibodies tested, just above where the dFADD band migrates (Figure A.1C). This was initially assumed to be the light chain of IgG, but this seems to come from the protein G sepharose beads used for the immunoprecipitation since it was also observed in control immunoprecipitations that only had beads combined with lysate but did not have any BSA used for blocking or any antibody added (data not shown). For future immunoprecipitation experiments with dFADD, a different type of beads, such as Protein A agarose, should be used to see if this contamination that obscures detection of dFADD can be eliminated.

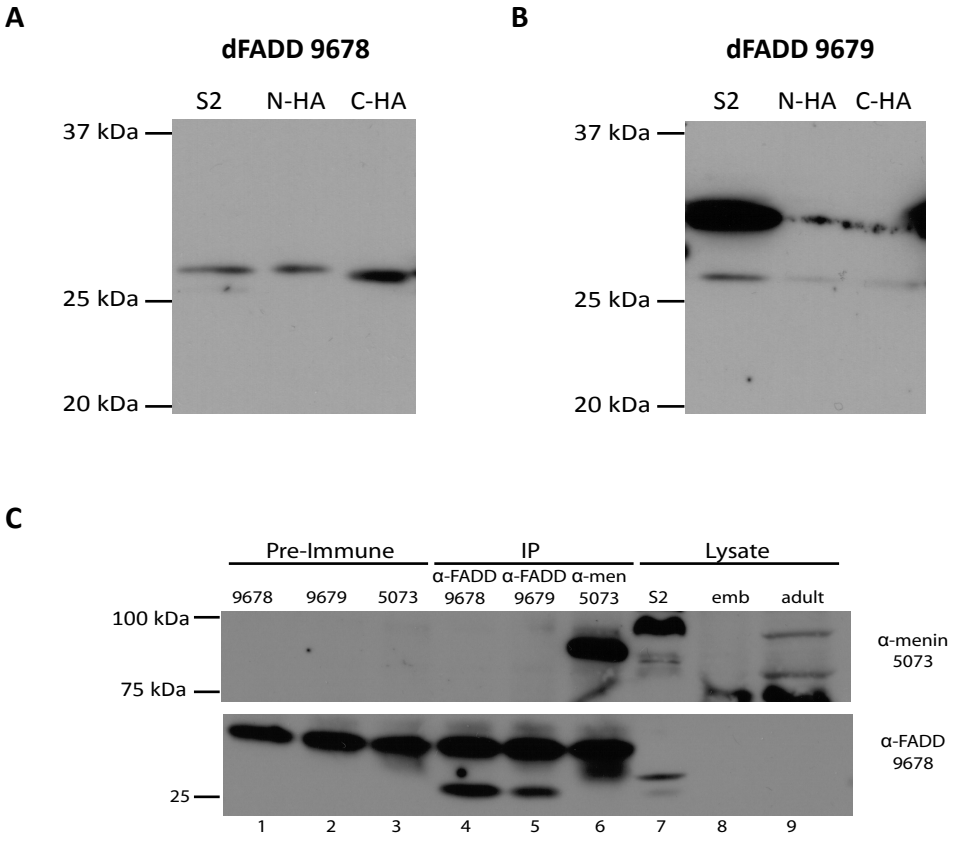

Figure A.1. Testing of full-length dFADD polyclonal antibodies.
The second bleeds of 9678 (A) and 9679 (B) polyclonal antibodies raised against full-length dFADD were tested using S2 cell lysates (150 µg) and lysates from cells overexpressing HA-dFADD (N-HA) and dFADD-HA (C-HA) (50 µg each). A) dFADD was detected with the 9678 antibody and migrated just above 25 kDa; HA-dFADD and dFADD-HA constructs were also detected with this antibody. B) dFADD was weakly detected in S2 cells but a prominent contaminating band was observed around 30 kDa with the 9679 antibody. HA-dFADD and dFADD-HA constructs were barely detected with the 9679 antibody. Both 9678 (A) and 9679 (B) were tested at a dilution of 1:2000, with the secondary anti-rabbit antibody used at 1:5000; immunoblots shown were incubated in the stronger Millipore ECL with A and B exposed for the same time. C) Immunoprecipitations were done using the dFADD antibodies (lanes 4, 5), menin 5073 antibody (lane 6) and the corresponding pre-immune serums (lanes 1-3). Lysates (150 µg) from S2 cells (lane 7), OR embryos (8-20 hrs) (lane 8) and OR adult males (3-5d) (lane 9) are also shown. Immunoblotting with anti-menin 5073 (1:2500) for the top part of the membrane was done using the standard Pierce ECL reagent but immunoblotting with dFADD 9678 antibody for the lower portion was done with the stronger Millipore ECL reagent. Both 9678 and 9679 antibodies immunoprecipitated dFADD, but no co-IP with menin was observed. The 9678 antibody also detected dFADD from S2 cell lysates but not from OR embryos or adults.

APPENDIX B: Immunofluorescence to detect menin and dFADD localization

We were interested in determining the subcellular localization of the menin-FADD interaction since menin is predominantly nuclear but the roles described for dFADD involve cytoplasmic localization.

MATERIALS AND METHODS

S2 cells were prepared for immunofluorescence using a methanol:acetic acid fixation method. Glass coverslips, dipped in ethanol, were flamed to sterilize them and placed 1 per well into 6-well plates (BD Falcon, 353046). S2 cells were seeded onto the coverslips and allowed to grow for 24 hours, or longer if an appropriate cell density had not been reached. Cells were rinsed twice with cold 1 X PBS and then permeabilized and fixed with 95 % methanol: 5 % acetic acid for 1 hr at -20°C. Cells were then rinsed 3 times with cold 1 X PBS. At this time, the coverslips were transferred to new 6-well plates for blocking. Blocking was done with 10 % FBS in 1 X PBS for 30 mins at room temperature. Primary antibody solutions were prepared in 10 % FBS in 1 X PBS. Table 2.1 shows the concentrations of primary menin and dFADD antibodies used for immunofluorescence. Incubation with antibody was carried out in a "humidifying chamber" constructed by placing wet paper towels on the bottom of sealable plastic container and covering this with parafilm. The antibody solution was placed as a drop (40 µL) on top of the parafilm and a coverslip was placed cell side down onto the antibody solution and incubated for 1 hr at room temperature. After incubation with primary antibody, coverslips were transferred back into the 6-well plate (cell side up) and washed 5 times for 5 mins each, with gentle shaking, in 1 X PBS.

Work with secondary antibodies was completed in the dark due to the light sensitivity of the fluorophores of secondary antibodies. Secondary antibody solutions were prepared in 10 % FBS in 1 X PBS with 1 µg/mL DAPI (4′,6-Diamidino-2-phenylindole dihydrochloride). The secondary antibodies and concentrations used are as follows: Alexa Fluor® 488 goat anti-rabbit (1:400) (Invitrogen™, A-11008) which provides green fluorescence, Alexa Fluor® 594 goat anti-mouse (1:400) (Invitrogen™, A-11005) which provides red fluorescence and Cy3 goat anti-rat (1:200) (from Campos Lab, original source unknown) which provides red fluorescence. A "humidifying chamber" was prepared in the same manner as for the primary antibody incubation and coverslips were placed on 40 µL of secondary antibody solution. The container was covered and placed in a dark place and cells were incubated with the secondary antibody solution for 45 mins. Coverslips were then washed 5 times with 1 X PBS as described above and dipped in ddH_2O before being mounted on glass slides using Aqua-Poly/Mount (Polysciences Inc., 18606-20). Slides were examined using a Zeiss Axioskop fluorescence microscope at 40 X magnification. Images were taken with the attached SPOT Diagnostic Instruments apparatus and software and fluorescence and DAPI merges were done using Adobe Photoshop CS3.

RESULTS

The results for the menin 9561 and 5073 antibodies are shown in Figure B.1. With anti-menin 9561, what appears to be localized subnuclear staining as well as a ring of more concentrated staining corresponding to the nuclear outline was consistently observed. However, it is hard to conclude definitively that this staining is within the nucleus and not on the surface of the nucleus. With the menin 5073 antibody, staining looks

predominantly cytoplasmic. The purified and unpurified forms of the rat menin antibody were also tested and staining was observed throughout the cell but was slightly more concentrated to the cytoplasm (Figure B.2). Since the different menin antibodies produced different patterns of staining, it is difficult to conclude the exact nature of menin localization, but it is expected to be mainly nuclear based on previous knowledge of menin function. Thus, it is speculated that the most distinct pattern of staining observed with the anti-menin 9561 antibody is likely the most accurate depiction of menin localization (Figure B.1).

Localization of endogenous dFADD has not been reported. In the initial characterization of dFADD, GFP-tagged dFADD was overexpressed in HeLa cells and found to localize to the cytoplasm (Hu and Yang, 2000), but localization in *Drosophila* cells was not examined. It is also known that overexpression of FADD in mammalian cells results in cytoplasmic localization even though endogenous proteins are predominantly found in the nucleus (Gomez-Angelats and Cidlowski, 2003; Screaton et al., 2003). Both dFADD antibodies, 9678 and 9679, localized dFADD primarily to the cytoplasm; however, it does not appear to be completely excluded from the nucleus (Figure B.3). Co-localization experiments using menin and dFADD antibodies simultaneously were not really feasible since the dFADD and best menin antibody (9561) were both made in rabbit and secondary antibodies would detect both antibodies. Cell fractionation could be used facilitate determination of the subcellular localization of the interaction since immunofluorescence is difficult with the available antibodies.

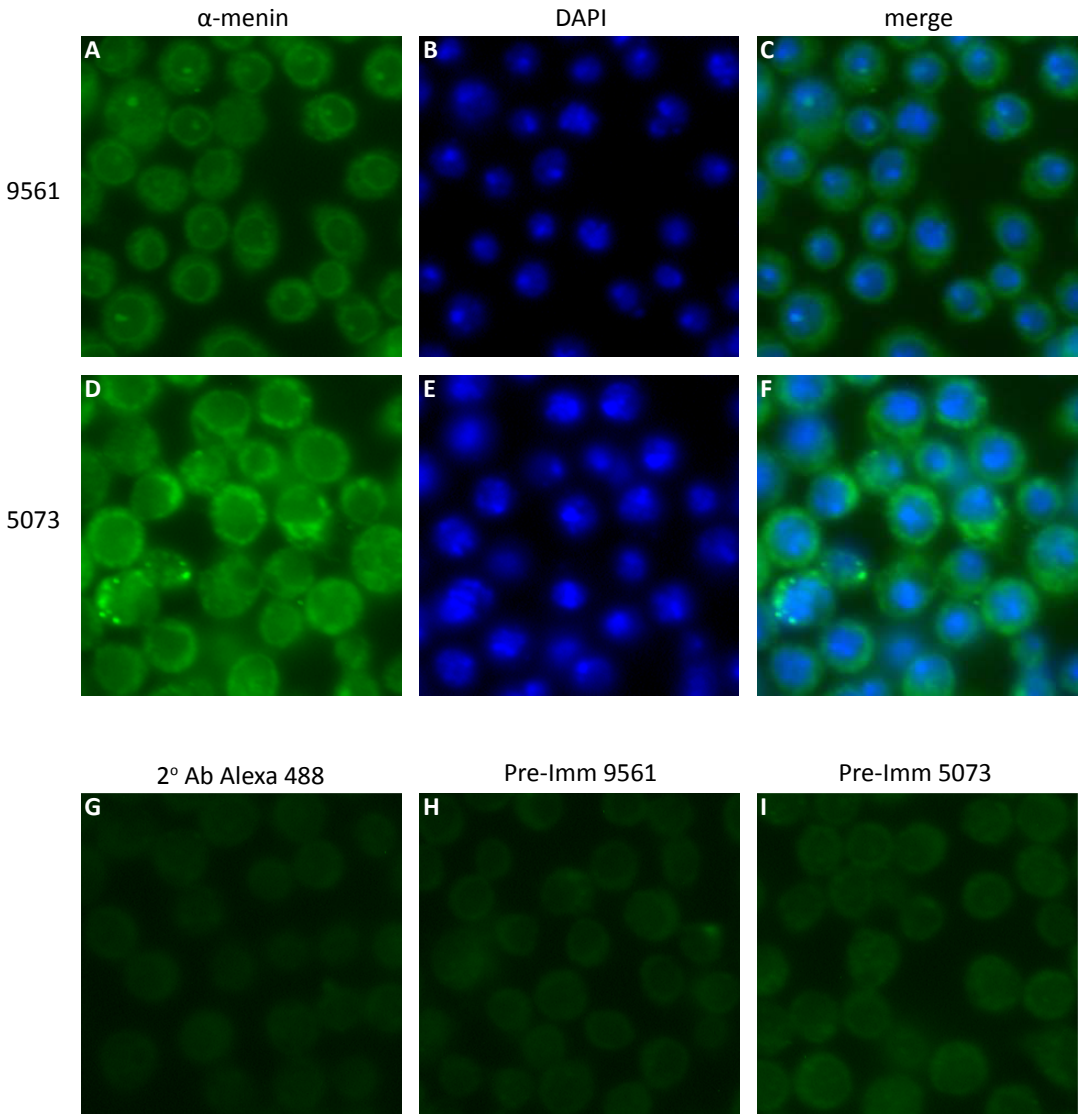

Figure B.1. Immunofluorescence with menin 9561 and 5073 antibodies in S2 cells.
S2 cells were fixed and permeabilized with 95 % methanol:5 % acetic acid. Rabbit α-menin antibodies 9561 (A,C) and 5073 (D,F) were used at a 1:200 dilution with the secondary α-rabbit Alexa 488 antibody used at 1:400. Immunostaining with menin antibody are shown (A,D) along with DAPI nuclear staining (B,E) and merged menin and DAPI (C,F). Control IF images are shown below and include the secondary Alexa 488 antibody alone (G) and pre-immune serums for 9561 (H) and 5073 (I).

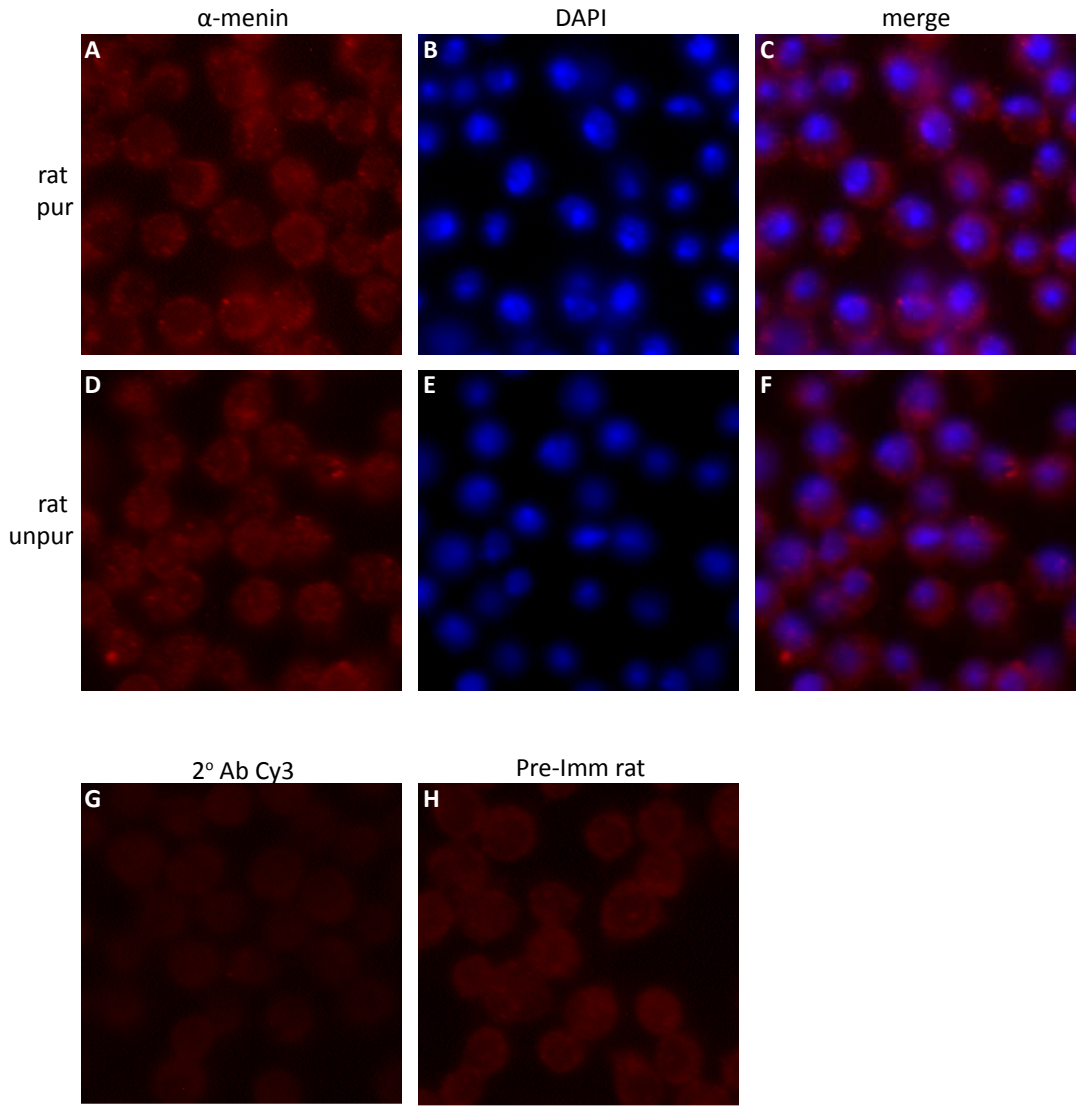

Figure B.2. Immunofluorescence with rat α-menin antibodies in S2 cells.
S2 cells were fixed and permeabilized with 95 % methanol:5 % acetic acid. Rat α-menin purified antibody (A,C) and unpurified antibody (D,F) were used at a 1:100 dilution, with the secondary α-rat Cy3 antibody used at 1:400. Immunostaining with menin antibody are shown (A,D) along with DAPI nuclear staining (B,E) and merged menin and DAPI (C,F). Control images are shown below with the secondary Cy3 antibody alone (G) and pre-immune rat serum (H).

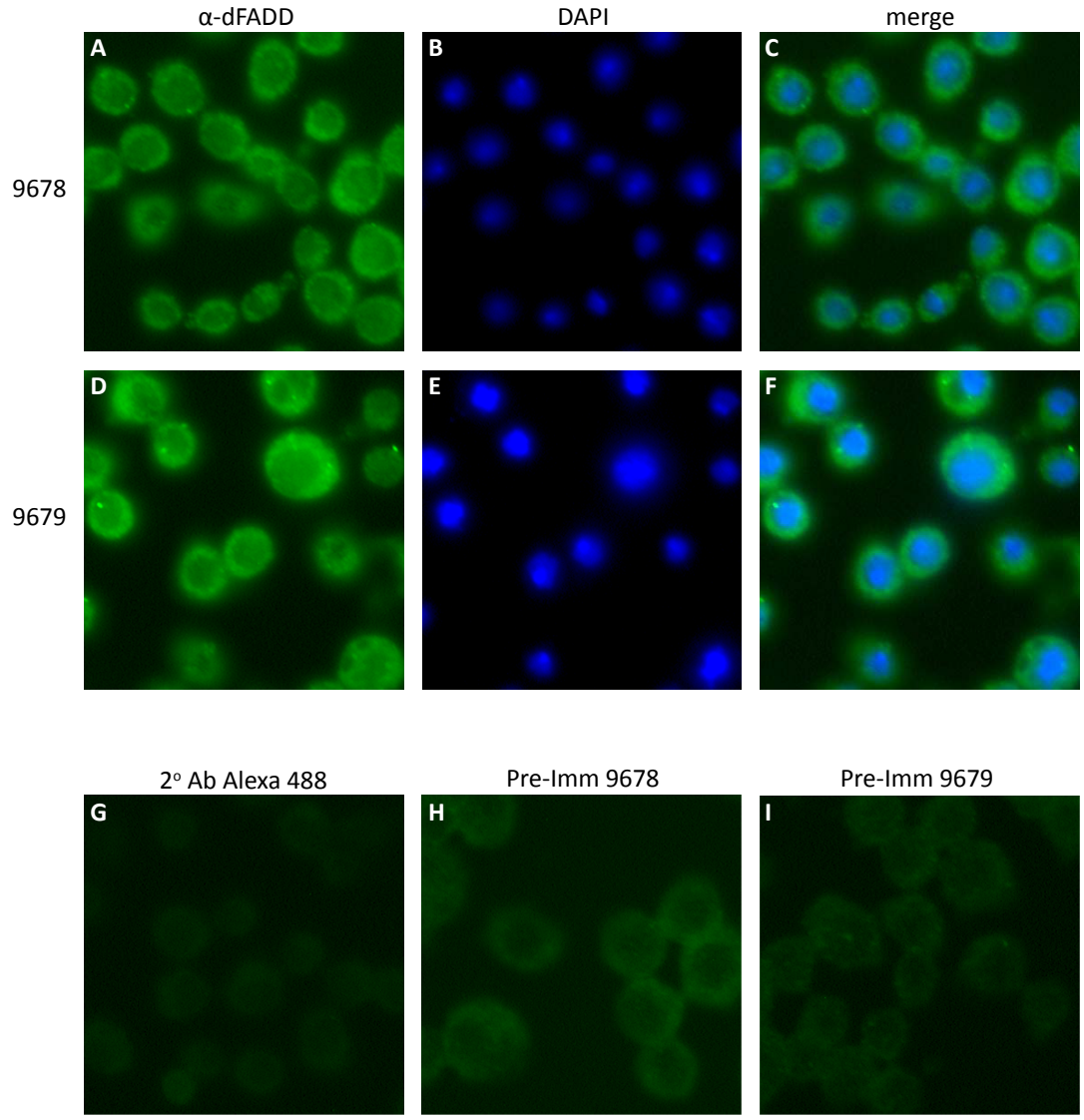

Figure B.3. Immunofluorescence with dFADD antibodies in S2 cells.
S2 cells were fixed and permeabilized with 95 % methanol:5 % acetic acid. Rabbit α-dFADD antibodies 9678 (A,C) and 9679 (D,F) were used at a 1:100 dilution with the secondary α-rabbit Alexa 488 antibody used at 1:400. Immunostaining with dFADD antibodies are shown (A,D) along with DAPI nuclear staining (B,E) and merged dFADD and DAPI (C,F). Control staining is shown below with the secondary Alexa 488 antibody alone (G) and pre-immune serums for 9678 (H) and 9679 (I).

APPENDIX C: Additional data and statistical analyses for infection assays

Additional data for *M. luteus* infections at different concentrations are provided in Figure C.1. Summary tables for the statistical analyses for infection with ddH_2O (Table C.1), *E. coli* (Table C.2) and *M. luteus* (Table C.3) are also provided.

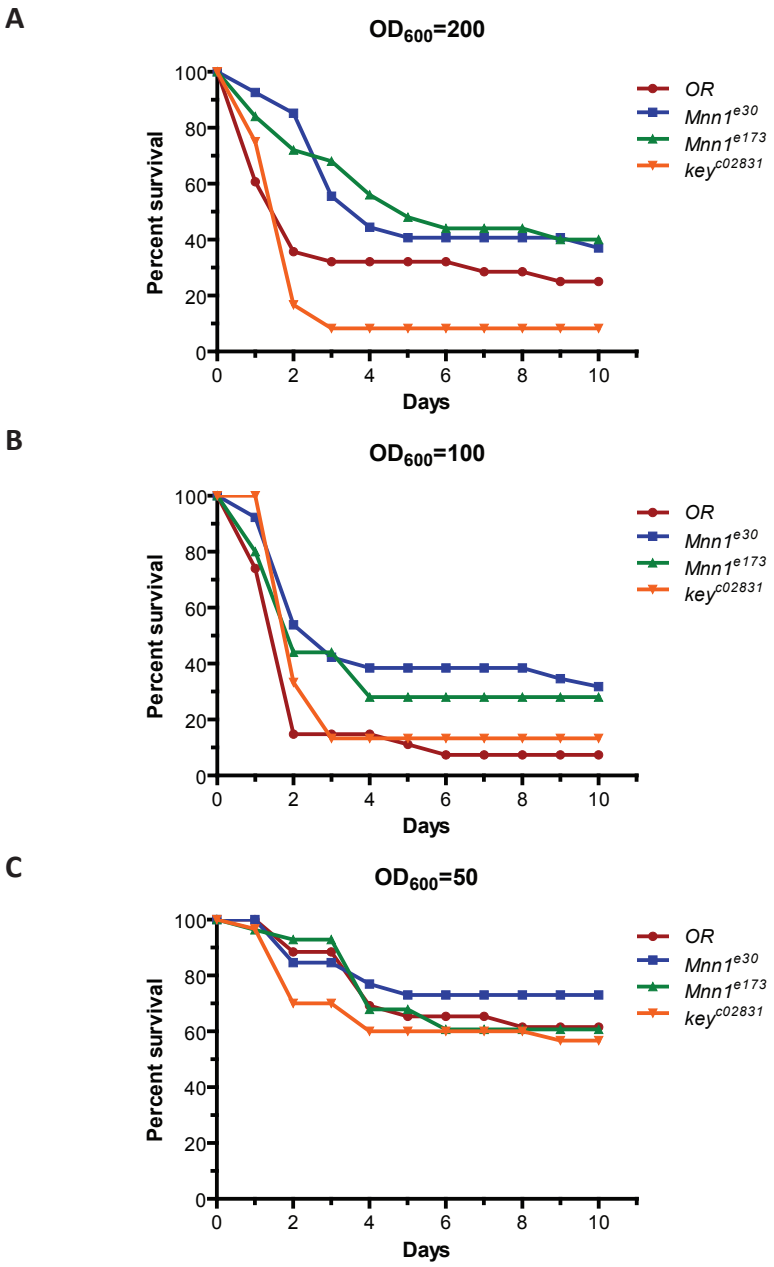

Figure C.1. Survival of adult flies infected with different concentrations *M. luteus*.
Micrococcus luteus was tested at different concentrations to determine the best conditions for infection using the pricking method. A needle was dipped in a concentrated solution of *M. luteus* at OD_{600}=200 (A), OD_{600}=100 (B) or OD_{600}=50 (C). Each graph shows the percent survival for a single trial, with 30 adults tested per genotype. Any flies that died during the first 3 hours post-infection were not included in the calculations of percent survival as the death was assumed to be due to physical injury and not infection. High lethality was observed for all genotypes with OD_{600}=200 or OD_{600}=100. For all other infections with *M. luteus* OD_{600}=50 was used.

Table C.1. Statistical summary for ddH_2O infection survival curves.

Comparison	Chi square	p value	Significant p<0.005
OR vs yw	0.3150	0.5746	No
OR vs FADD^{f02804}	0.04292	0.8359	No
OR vs FADD^{f06954}	0.03670	0.8481	No
OR vs key^{c02831}	18.97	<0.0001	Yes
yw vs FADD^{f02804}	0.09234	0.7612	No
yw vs FADD^{f06954}	0.1020	0.7494	No
yw vs key^{c02831}	11.71	0.0006	Yes
FADD^{f02804} vs FADD^{f06954}	0.0004917	0.9823	No
FADD^{f02804} vs key^{c02831}	10.44	0.0012	Yes
FADD^{f06954} vs key^{c02831}	10.11	0.0015	Yes
OR vs Mnn1^{e30}	0.4470	0.5038	No
OR vs UAS-Mnn1	2.048	0.1524	No
OR vs Mnn1-RNAi	1.342	0.2467	No
Mnn1^{e30} vs UAS-Mnn1	3.224	0.0725	No
Mnn1^{e30} vs Mnn1-RNAi	0.1283	0.7202	No
Mnn1^{e30} vs key^{c02831}	6.156	0.0131	No
UAS-Mnn1 vs Mnn1-RNAi	4.593	0.0321	No
UAS-Mnn1 vs key^{c02831}	16.23	<0.0001	Yes
Mnn1-RNAi vs key^{c02831}	5.069	0.0244	No

Survival curves were compared using a log-rank (Mantel-Cox) test. Pairwise comparisons were made and the Bonferroni method was used to account for multiple comparisons (10 comparisons per graph in Figure 3.4). The adjusted significance level used was p<0.005. *UAS-Mnn1* and *Mnn1-RNAi* are simplifications for the full genotypes *UAS-Mnn1/+;tub-GAL4/+* and *UAS-Mnn1-dsRNA/+;tub-GAL4/+*, respectively (+ chromosomes are from crosses to OR).

Table C.2. Statistical summary for *E. coli* infection survival curves.

Comparison	Chi square	p value	Significant p<0.005
OR vs yw	0.7915	0.3737	No
OR vs FADD^{f02804}	218.1	<0.0001	Yes
OR vs FADD^{f06954}	22.65	<0.0001	Yes
OR vs FADD^{f02804}/ FADD^{f06954}	195.9	<0.0001	Yes
OR vs key^{c02831}	251.4	<0.0001	Yes
yw vs FADD^{f02804}	154.6	<0.0001	Yes
yw vs FADD^{f06954}	19.95	<0.0001	Yes
yw vs FADD^{f02804}/ FADD^{f069540}	143.4	<0.0001	Yes
yw vs key^{c02831}	194.4	<0.0001	Yes
FADD^{f02804} vs FADD^{f06954}	125.5	<0.0001	Yes
FADD^{f02804} vs FADD^{f02804}/ FADD^{f06954}	43.11	<0.0001	Yes
FADD^{f02804} vs key^{c02831}	13.81	0.0002	Yes
FADD^{f06954} vs FADD^{f02804}/ FADD^{f06954}	69.31	<0.0001	Yes
FADD^{f06954} vs key^{c02831}	145.3	<0.0001	Yes
FADD^{f02804}/ FADD^{f06954} vs key^{c02831}	28.53	<0.0001	Yes
OR vs Mnn1^{e30}	2.712	0.0996	No
OR vs UAS-Mnn1	2.442	0.1181	No
OR vs Mnn1-RNAi	0.4340	0.5100	No
Mnn1^{e30} vs UAS-Mnn1	7.390	0.0066	No
Mnn1^{e30} vs Mnn1-RNAi	3.865	0.0493	No
Mnn1^{e30} vs key^{c02831}	132.1	<0.0001	Yes
UAS-Mnn1 vs Mnn1-RNAi	0.7463	0.3877	No
UAS-Mnn1 vs key^{c02831}	203.6	<0.0001	Yes
Mnn1-RNAi vs key^{c02831}	197.3	<0.0001	Yes

Survival curves were compared using a log-rank (Mantel-Cox) test. Pairwise comparisons were made and the Bonferroni method was used to account for multiple comparisons (10 comparisons per graph in Figure 3.5). The adjusted significance level used was p<0.005. Note that the extra comparisons to *FADD^{f02804}/FADD^{f06954}* were specific only to the *E. coli* infections and these extra comparisons were not included as part of the total number of comparisons used to determine the Bonferroni method in order to keep the corrected significance value consistent. All comparisons to *FADD^{f02804}/FADD^{f06954}* were highly significant (p<0.0001) and would also be significant at a corrected value of p<0.0033 for 15 comparisons. *UAS-Mnn1* and *Mnn1-RNAi* are simplifications for the full genotypes *UAS-Mnn1/+;tubGAL-4/+* and *UAS-Mnn1-dsRNA/+;tub-GAL4/+*, respectively (+ chromosomes are from crosses to OR).

Table C.3. Statistical summary for *M. luteus* infection survival curves.

Comparison	Chi square	p value	Significant p<0.005
OR vs yw	0.1347	0.7136	No
OR vs FADD^{f02804}	0.7208	0.3959	No
OR vs FADD^{f06954}	8.510	0.0035	Yes
OR vs key^{c02831}	4.455	0.0348	No
yw vs FADD^{f02804}	0.2124	0.6449	No
yw vs FADD^{f06954}	8.995	0.0027	Yes
yw vs key^{c02831}	2.460	0.1168	No
FADD^{f02804} vs FADD^{f06954}	10.82	0.0010	Yes
FADD^{f02804} vs key^{c02831}	0.9249	0.3362	No
FADD^{f06954} vs key^{c02831}	18.19	<0.0001	Yes
OR vs Mnn1^{e30}	3.019	0.0823	No
OR vs UAS-Mnn1	8.036	0.0046	Yes
OR vs Mnn1-RNAi	8.706	0.0032	Yes
Mnn1^{e30} vs UAS-Mnn1	0.00001912	0.9989	No
Mnn1^{e30} vs Mnn1-RNAi	0.00643	0.9361	No
Mnn1^{e30} vs key^{c02831}	6.535	0.0106	No
UAS-Mnn1 vs Mnn1-RNAi	0.02027	0.8868	No
UAS-Mnn1 vs key^{c02831}	18.18	<0.0001	Yes
Mnn1-RNAi vs key^{c02831}	18.45	<0.0001	Yes

Survival curves were compared using a log-rank (Mantel-Cox) test. Pairwise comparisons were made and the Bonferroni method was used to account for multiple comparisons (10 comparisons per graph in Figure 3.6). The adjusted significance level used was p<0.005. *UAS-Mnn1* and *Mnn1-RNAi* are simplifications for the full genotypes *UAS-Mnn1/+;tub-GAL4/+* and *UAS-Mnn1-dsRNA/+;tub-GAL4/+*, respectively (+ chromosomes are from crosses to OR).

APPENDIX D: Sequence alignment for Trx and MLL1

Figure D.1. Sequence Alignment for Trx and MLL1

```
Trx             ---MGRSKFPGKPSKSINRKRISVLQLEDDAAN--PAEPQQPAPESQQPSGSGSGSSAAR 55
MLL1            MAHSCRWRFPARPGTTGGGGGGGRRGLGGAPRQRVPALLLPPGPPVGGGGPGAPPSPPAV 60
                     * :**.:*..: .    .   * . . :  **    *.*     . ... *..*
                     hMBM
Trx             EKGNNCDNDEDDNAPGGASISGNTASSSAGSGNSGNGSSS-------------------- 95
MLL1            AAAAAAAGSSGAGVPGGAAAASAASSSSASSSSSSSSSASSGPALLRVGPGFDAALQVSA 120
                  .  . .... ..****: :. ::****.*..*...*:*

Trx             ------------GSSTGSGSSGS-------GSTNGGSVNGGTHHKSAANLDKEAVTKDQ 135
MLL1            AIGTNLRRFRAVFGESGGGGGSGEDEQFLGFGSDEEVRVRSPTRSPSVKTSPRKPRGRPR 180
                             *.* *.*.**.       ** :   *.. *:  *. .  ::.  : :
                             LBD                                  AT hook 1
Trx             NGDGDK----------TRGNVSSAPSGKLSAAASGKALSKS---SRTFSASTSVTSSGRS 182
MLL1            SGSDRNSAILSDPSVFSPLNKSETKSGDKIKKKDSKSIEKKRGRPPTFPGVKIKITHGKD 240
                .*.. :          :  * *.: **.     ..*::.*.   . **.. .   : *:.
                                                 AT hook 2
Trx             SGSSPDGNSGASSDGASSG-------------ISCGKSTAKSTEASSGKLAKTTGAGTCS 229
MLL1            ISELPKGNKEDSLKKIKRTPSATFQQATKIKKLRAGKLSPLKSKFKTGKLQIGRKGVQIV 300
                 .. *.**.  * .  .               : .** :. .:: .:***     .

Trx             SAKSSKASSG-----------------------------TTSEATTSGLSGACLKALFV 259
MLL1            RRRGRPPSTERIKTPSGLLINSELEKPQKVRKDKEGTPPLTKEDKTVVRQSPRRIKPVRI 360
                  :.  .*:                                *..: *.   *   :*.: :
                AT hook 3
Trx             ATPATSTGLACALVSPGGSSQGGTFPISAALLRAR-KNSNKKFKNLNLARGEVMLPSTSK 318
MLL1            IPSSKRTDATIAKQLLQRAKKGAQKKIEKEAAQLQGRKVKTQVKNIRQFIMPVVSAISSR 420
                 ..:. *. : *      :.:*.   *.    : : :: :.:.**:.     *: . :*:

Trx             LKQLNSPVVDNPSPSPPIASGSTPSVEGG-IGVGGVVSPGEDAALKRVLTEMPNEVARDP 377
MLL1            IIKTPRRFIEDEDYDPPIKIARLESTPNSRFSAPSCGSSEKSSAASQHSSQMSSDSSRSS 480
                : :    .::: . .***  .   *. .. :.. .  *. :.:* .:  ::*..: :*..

Trx             SPSSCTAAANGAASGKGSASNG-----------PPAMASSGDGSSPKSGADTGPSTSSTT 426
MLL1            SPSVDTSTDSQASEEIQVLPEERSDTPEVHPPLPISQSPENESNDRRSRRYSVSERSFGS 540
                ***  *:: . *:.     .:            * : :...:... :*   : .. *  :

Trx             AKQKKTVTFRNVLETSDDKSVVKRFYNPDIRIPIVSIMKKDSLNRPLNYSRGGECIVRPS 486
MLL1            RTTKKLSTLQSAPQQQTSSSPPPPLLTPPPPLQPASSIS-DHTPWLMPPTIPLASPFLPA 599
                 . **  *::.. : . ..*    : .*   :  .* :. *     :  :    . . *:

Trx             ILSKILNKNSNIDKLNSLKFRSAGASSSSSNQESGSSSNVFGLSR-----AFGAPMDEDD 541
MLL1            STAPMQGKRKSILREPTFRWTSLKHSRSEPQYFSSAKYAKEGLIRKPIFDNFRPPPLTPE 659
                  : : .*...* :  :::: *   * *..:  *.:.    ** *      * .*    :

Trx             EGGVTFRRNDSPEDQ--------NNAEDDEMDDDDDDEEAEEDDENEDDNDEAVSEKSAE 593
MLL1            DVGFASGFSASGTAASARLFSPLHSGTRFDMHKRSPLLRAPRFTPSEAHSRIFESVTLPS 719
                : *.:   . *            :..   :*.. .   .* .   .* ..    * . ..

Trx             TEKSAGADERDPDEKQLVMDSHFVLPKRSTRSSRIIKPNKRLLEEGAISTKKPLSLGDSK 653
MLL1            NRTSAGTSSSGVSNRKRKRKVFSPIRSEPRSPSHSMRTRSGRLSSSELSPLTPPSSVSSS 779
                ...***:.. . .:::   . .  : ...  .*: ::...  *... :*. .* *  .*.

Trx             GKNVFGTSSSSAGSTASTFSASTNLKLGKETFFNFGTLKPNSSAAGNFVLRQPRLQFQAD 713
MLL1            LSISVSPLATSALNPTFTFPSHSLTQSGESAEKNQRPRKQTSAPAEPFSSSSPTPLFPWF 839
                 .  ... ::** ..: **.: :  : *:.:  *  . * .*:.*  *   .*   *

Trx             NQQATFTAPKACPTSPSAIPKPANSLATSSFGSLASTNSSTVTPTPSACSICSAVVSSKE 773
MLL1            TPGSQTERGRNKDKAPEELSKDRDADKSVEKDKSRERDRREKEKNKRESRKEKRKKGSEI 899
                .  :     :   .:*. :.*  ::  : . ..  . : .  . .   .   .   .*:
```

Figure D.1 (page 2 of 5)

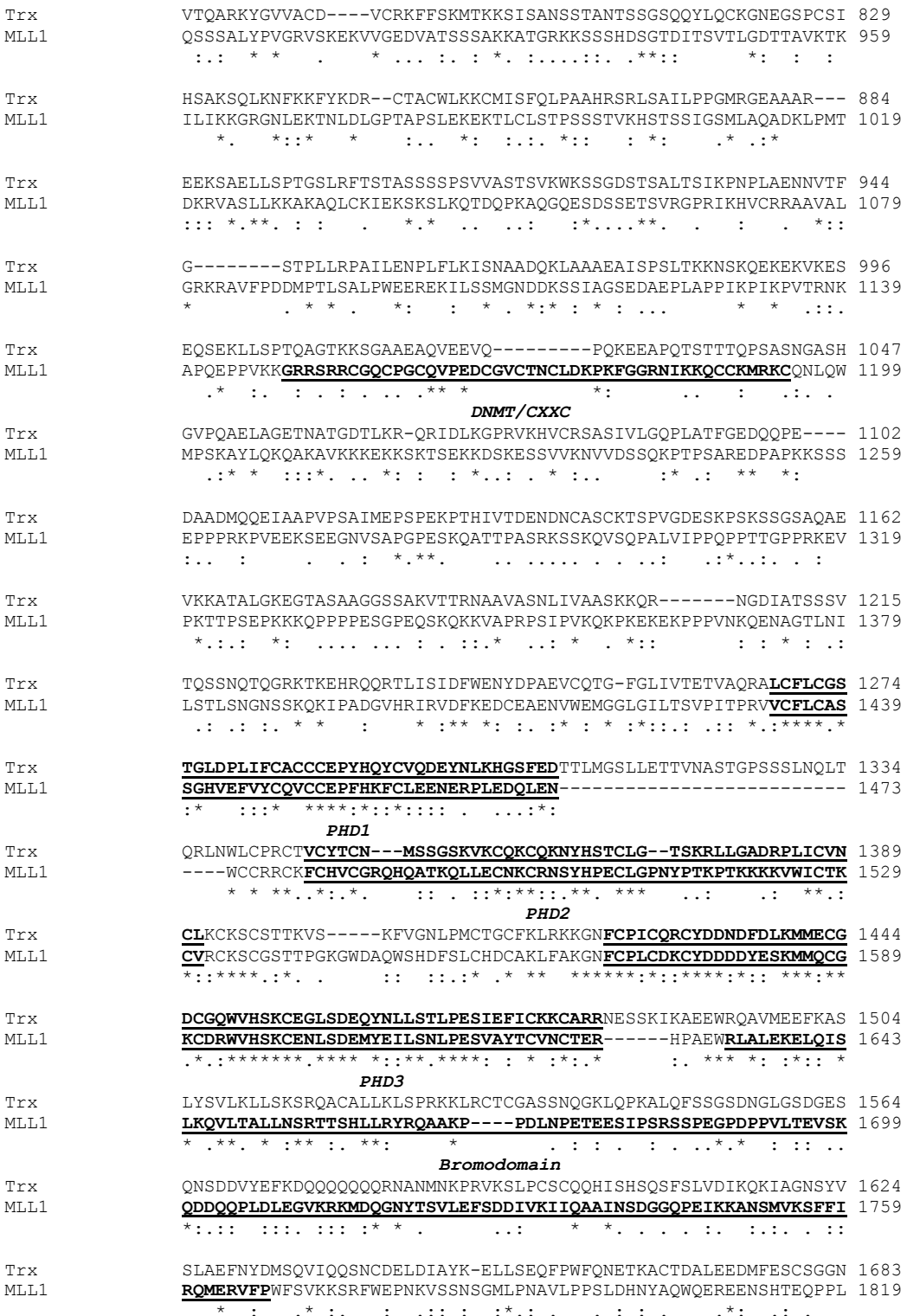

Figure D.1 (page 3 of 5)

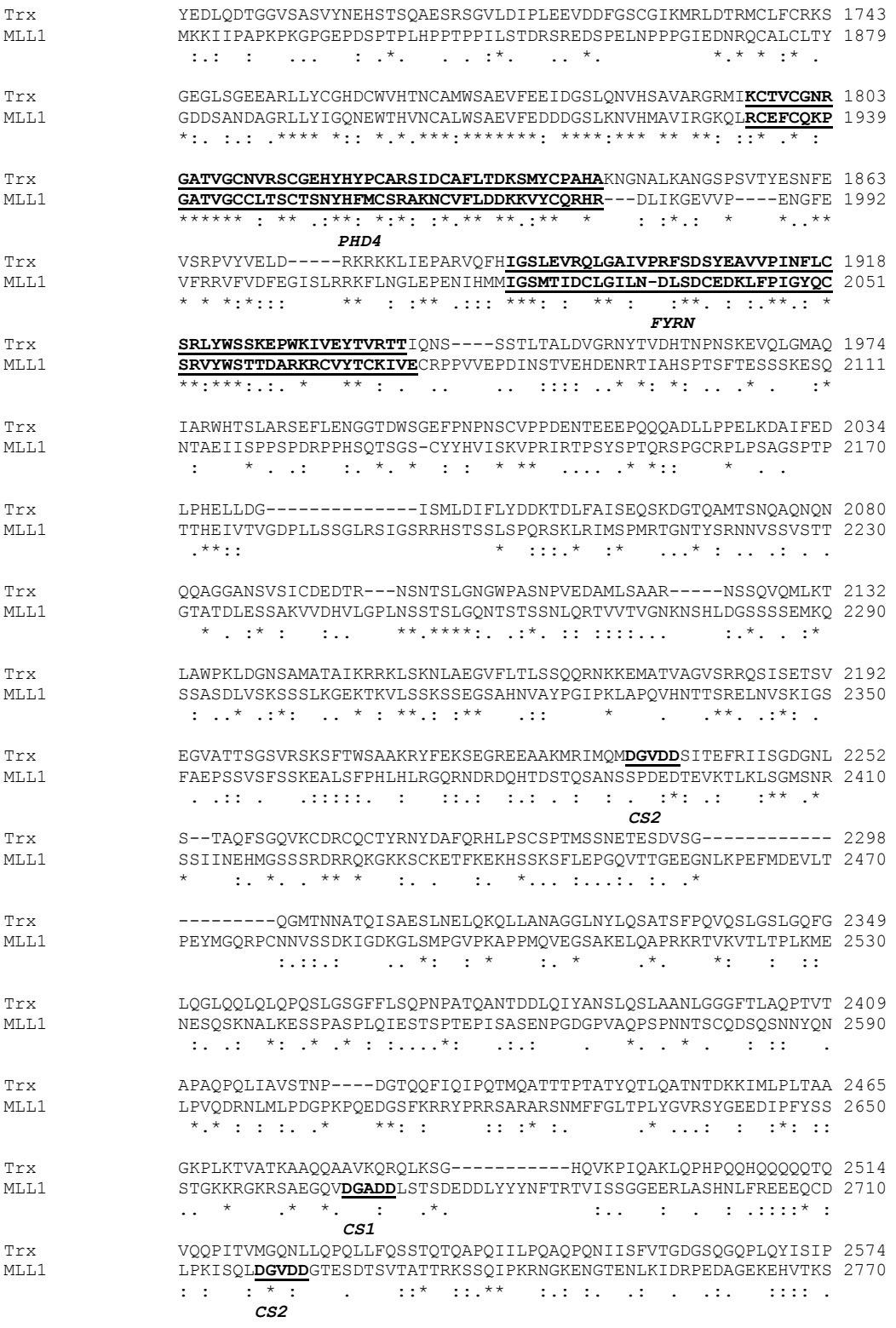

Figure D.1 (page 4 of 5)

```
Trx             TAGEYKPQPQPTATPTFLTTAPGAG--ATYLQTDASGNLVLTTTPSNS------GLQMLT 2626
MLL1            SVGHKNEPKMDNCHSVSRVKTQGQDSLEAQLSSLESSRRVHTSTPSDKNLLDTYNTELLK 2830
                :.*. :     .. ..  ..: * .   : *.:  *.. * *:***:.      . ::*.

Trx             AQSLQAQPQVIGTLIQPQTIQLGGG------ADGNQPGSNQQPLILGGTGGGS-SGLEFA 2679
MLL1            SDSDNNNSDDCGNILPSDIMDFVLKNTPSMQALGESPESSSSELLNLGEGLGLDSNREKD 2890
                ::* : :.:  *.:: .: :::         * *:.* *... *:  * * *  *. *

Trx             TTSPQVILATQPMYYGLETIVQNTVMSSQQFVSTAMPGMLSQNASFSATTTQVFQASKIE 2739
MLL1            MGLFEVFSQQLPTTEPVDSSVSSSISAEEQFELPLELPSDLSVLTTRSPTVPSQNPSRLA 2950
                    :*:    *    ::: *..:: :.:**  .       .  :  :.*.   :.*::

Trx             PIVDLPAGYVVLNNTGDASSAGTFLNAASVLQQQTQDDTTTQILQNANFQFQSVPTS--- 2796
MLL1            VISDSGEKRVTITEKSVASSESDPALLSPGVDPTPEGHMTPDHFIQGHMDADHISSPPCG 3010
                 * *     *.:.:.. *** .     :. ::  .:.. *.: : :.::: : :.:.

Trx             ---SGASTSMDYTSPVMVTAKIPPVTQIKRTNAQAKAAGISGVGKVPPQPQVVNKVLPTS 2853
MLL1            SVEQGHGNNQDLTRNSSTPGLQVPVSPTVPIQNQKYVPNSTDSPGPSQISNAAVQTTPPH 3070
                   .* ... * *    ...   **:     : *  ... :.    .  .:.. :. *.

Trx             IVTQQSQVQVKNSNLKQSQVKGKAASGTGTTCGAPPSIASKP--LQKKTNMIRPIH---- 2907
MLL1            LKPATEKLIVVNQNMQPLYVLQTLPNGVTQKIQLTSSVSSTPSVMETNTSVLGPMGGGLT 3130
                : .  .:: * *.*::   *  . ..*.  .   ..*::*.*  ::.:*.:: *:

Trx             -KLEVKPKVMKPTPKVQNQNHSLLQQQQQQQPQ-----LQQQIPAVVVNQVPKVTISQQR 2961
MLL1            LTTGLNPSLPTSQSLFPSASKGLLPMSHHQHLHSFPAATQSSFPPNISNPPSGLLIGVQP 3190
                 .  ::*.: .. . . . .:.**  .::*: :      *..:*. : *  . : *. *

Trx             IP-------------------------AQTQQQQLQQAQMIHIPQQQQPLQQQQVQVQP 2995
MLL1            PPDPQLLVSESSQRTDLSTTVATPSSGLKKRPISRLQTRKNKKLAPSSTPSNIAPSDVVS 3250
                 *                          :   .:**  :  ::. .. * :    :* .

Trx             SMPIITLAEAPVVQSQFVMEPQALEQ--QELANRVQHFSTSSSSSSSNCSLPTNVVNPMQ 3053
MLL1            NMTLINFTPSQLPNHPSLLDLGSLNTSSHRTVPNIIKRSKSSIMYFEPAPLLPQSVGGTA 3310
                .*.:*.:: : : :   ::: .:*:   :. . .: : *.**    . ..* .: *.

Trx             QQAPSTTSSSTTRPTNRVLPMQQRQEPAPLSNECPVVSSPTPPKPVEQP---------II 3104
MLL1            ATAAGTSTISQDTSHLTSGSVSGLASSSSVLNVVSMQTTTTPTSSASVPGHVTLTNPRLL 3370
                  *..*:: *   .     .:.   ..:.: *  .: ::.**..... *         ::

Trx             HQMTSASVSKCYAQKSTLPSPVYEAELKVSS-------VLESIVPDVTMDAILEEQPVTE 3157
MLL1            GTPDIGSISNLLIKASQQSLGIQDQPVALPPSSGMFPQLGTSQTPSTAAITAASSICVLP 3430
                     .*:*:   : *  .  : :  : :..       :  * .*..:  :  ..  *

Trx             SIYTEGLYEKNSPGESKTEQLLLQQQQREQLNQQLVNNGYLLDKHT-FQVEPMDTDVYRE 3216
MLL1            STQTTGITAASPSGEADEHYQLQHVNQLLASKTGIHSSQRDLDSASGPQVSNFTQTVDAP 3490
                *  * *:   ...**:. .  * : :*    :  : ..   **. :  **. :   *

Trx             EDLEEEEDEDDDFSLKMATS---------ACNDHEMSDSEEPAVKDKISKILDNLTNDDC 3267
MLL1            NSMGLEQNKALSSAVQASPTSPGGSPSSPSSGQRSASPSVPGPTKPKPKTKRFQLPLDKG 3550
                :.:  *:::  . ::: :.:         :..::. * *   ..* * ..   :*. *.

Trx             ADSIATATTMEVDASAGYQQMVEDVLATTAAQSAPTEEFEGALETAAVEAAATYINEMAD 3327
MLL1            NGKKHKVSHLRTSSSEAHIPDQETTSLTSGTGTPGAEAEQ--QDTASVEQSSQKECGQPA 3608
                 ..  ..: :...:* .:    * .  *:.: :. :*  :   :**:** ::      .

Trx             AHVLDLKQLQNGVELELRRRKEEQRTVSQEQEQSKAAIVPTAAAPEPPQPIQEPKKMTGP 3387
MLL1            GQVAVLPEVQVTQNPANEQESAEPKTVEEEESNFSSPLMLWLQQEQKRKESITEKKPK-K 3667
                .:*  * ::*   :   .:.. * :**.:*:.: .:.::      :  :     ** .

Trx             HLLYEIQSEDGFTYKSSSITEIWEKVFEAVQVARRAHGLTPLPEGPLADMGGIQMIGLKT 3447
MLL1            GLVFEISSDDGFQICAESIEDAWKSLTDKVQEARSNARLKQLS---FAGVNGLRMLGILH 3724
                 *::**.*:***   :.** : *:.: : ** **    *. *.   :*.:.*::*:*:
                                    FYRC
```

```
Trx             NALKYLIEQLPGVEKCSKYTPKYHKRNGNVSTAANGAHGGNLGGSSASAALSVSGGDSHG 3507
MLL1            DAVVFLIEQLSGAKHCRNYKFRFHKPE-------------------------------- 3751
                :*: :*****.*.::* :*. ::** :

Trx             LLDYGSDQDELEENAYDCARCEPYSNRSEYDMFSWLASRHRKQPIQVFVQPSDNELVPR- 3566
MLL1            ------EANEPPLNPHGSARAEVHLRKSAFDMFNFLASKHRQPPEYNPNDEEEEEVQLKS 3805
                      : :*   *.:..**.* : .:* :***.:***:**: *     : .::*:  :
                           Win
Trx             --RGTGSNLPMAMKYRTLKETYKDYVGVFRSHIHGRGLYCTKDIEAGEMVIEYAGELIRS 3624
MLL1            ARRATSMDLPMPMRFRHLKKTSKEAVGVYRSPIHGRGLFCKRNIDAGEMVIEYAGNVIRS 3865
                  *.*. :***.*::* **:* *: ***:** ******:*.::*:**********::***

Trx             TLTDKRERYYDSRGIGCYMFKIDDNLVVDATMRGNAARFINHCCEPNCYSKVVDILGHKH 3684
MLL1            IQTDKREKYYDSKGIGCYMFRIDDSEVVDATMHGNAARFINHSCEPNCYSRVINIDGQKH 3925
                  *****:****:*******:***. ******:*********.*******:*::* *:**
                                     SET
Trx             IIIFALRRIVQGEELTYDYKFPFEDE--KIPCSCGSKRCRKYLN 3726
MLL1            IVIFAMRKIYRGEELTYDYKFPIEDASNKLPCNCGAKKCRKFLN 3969
                *:***:*:* :***********:**   *:**.**:*:***:**
```

Figure D.1 (page 5 of 5). Sequence alignment for Trx and MLL1.
Protein sequences of *Drosophila* Trithorax (Trx Isoform II) (GI 19550184) and human MLL1 (GI 56550039) were aligned using Clustal W 2.1 (European Bioinformatics Institute). Some important protein domains are identified below the sequence alignment: hMBM = high affinity menin binding motif (Yokoyama et al., 2005); LBD = LEDGF binding domain (not conserved in Trx); AT hook 1-3 = potential DNA binding motifs (not conserved in Trx); DNMT/CXXC = DNA methyltransferase like domain, also called CXXC domain (not conserved in Trx); PHD1-4 = plant homeodomain zinc finger domains; Bromodomain (not conserved in Trx) ; FYRN = phenylalanine and tyrosine rich N-terminal region; CS1 = Taspase1 cleavage site 1 (not conserved in Trx); CS2 = Taspase1 cleavage site 2 (conserved in Trx, but not aligned together); FYRC = phenylalanine and tyrosine rich C-terminal region; *Win* = WDR5 interacting domain; SET = su(var)3-9, enhancer of zeste, trithorax histone methyltransferase domain. The two regions highlighted in gray are the menin binding motifs MBM1 and MBM2 identified by Grembecka *et al.* 2010. The alignment symbols used have the following meanings ***** = identical residue; **:** = highly similar residue; **.** = weakly similar residue.

APPENDIX E: Statistical analyses for ChIP assays

Table E.1. Statistical summary for ChIPs in OR embryos.

Antibody	Primer Set	ANOVA		Post- hoc tests (Bonferroni)	
		p value	Sig ? (p<0.05)	Comparison	Sig ? (t value)
PI	Cont2	0.7642	No	N/A	
	hsp70 P1	0	No	N/A	
	hsp70 P2	0.7824	No	N/A	
	hsp70 P3	0.6505	No	N/A	
	hsp70 P3b	0.5709	No	N/A	
	hsp70 P4	0.4925	No	N/A	
Menin (9562)	Cont2	0.9515	No	N/A	
	hsp70 P1	0.0212	Yes	No HS vs 5 min HS	No (t=2.842)
				No HS vs 30 min HS	Yes (t=3.176)
				5 min HS vs 30 min HS	No (t=0.3343)
	hsp70 P2	0.1233	No	N/A	
	hsp70 P3	0.0004	Yes	No HS vs 5 min HS	Yes (t=5.347)
				No HS vs 30 min HS	Yes (t=6.042)
				5 min HS vs 30 min HS	No (t=0.6955)
	hsp70 P3b	0.0002	Yes	No HS vs 5 min HS	Yes (t=6.091)
				No HS vs 30 min HS	Yes (t=6.467)
				5 min HS vs 30 min HS	No (t=0.3763)
	hsp70 P4	0.0003	Yes	No HS vs 5 min HS	Yes (t=5.589)
				No HS vs 30 min HS	Yes (t=5.925)
				5 min HS vs 30 min HS	No (t=0.3360)
Trx (N1)	Cont2	0.1265	No	N/A	
	hsp70 P1	0.4514	No	N/A	
	hsp70 P2	0.0432*	No*	N/A	
	hsp70 P3	0.0030	Yes	No HS vs 5 min HS	Yes (t=4.870)
				No HS vs 30 min HS	No (t=2.666)
				5 min HS vs 30 min HS	No (t=2.204)
	hsp70 P3b	0.0094	Yes	No HS vs 5 min HS	Yes (t=3.981)
				No HS vs 30 min HS	No (t=2.641)
				5 min HS vs 30 min HS	No (t= 1.340)
	hsp70 P4	0.0190	Yes	No HS vs 5 min HS	Yes (t=3.561)
				No HS vs 30 min HS	No (t=1.909)
				5 min HS vs 30 min HS	No (t=1.652)
H3K4me2	Cont2	0.0174	Yes	No HS vs 5 min HS	Yes (t=3.182)
				No HS vs 30 min HS	No (t=0.08453)
				5 min HS vs 30 min HS	Yes (t=3.098)
	hsp70 P1	0.0023	Yes	No HS vs 5 min HS	No (t=2.336)
				No HS vs 30 min HS	Yes (t= 5.060)
				5 min HS vs 30 min HS	No (t=2.725)
	hsp70 P2	<0.0001	Yes	No HS vs 5 min HS	Yes (t=6.606)
				No HS vs 30 min HS	Yes (t=7.559)
				5 min HS vs 30 min HS	No (t=0.9535)
	Hsp70 P3		Yes	No HS vs 5 min HS	Yes (t=30.65)
		<0.0001		No HS vs 30 min HS	Yes (t=33.68)
				5 min HS vs 30 min HS	Yes (t=3.030)
	hsp70 P3B		Yes	No HS vs 5 min HS	Yes (t=5.878)
		0.0002		No HS vs 30 min HS	Yes (t=6.523)
				5 min HS vs 30 min HS	No (t=0.6449)
	hsp70 P4	0.2689	No	N/A	

One-way ANOVAs were performed to compare relative quantity of DNA recovered in ChIP experiments for a given antibody and primer set. If the one-way ANOVA indicated a significant difference between the treatment conditions (No HS, 5 min HS, 30 min HS) then Bonferroni's multiple comparisons post-hoc tests were performed to compare the different treatment conditions to determine which ones differed significantly. N/A is indicated if the post-hoc tests were not applicable because the ANOVA was not significant. Sig = significance; * = although the p value for the ANOVA was significant, the Bonferroni multiple comparisons post-hoc tests were all not significant (after the multiple comparisons correction) so the overall the result is considered to be not statistically significant.

APPENDIX F: Preliminary results for immunostaining of polytene chromosomes

MATERIALS AND METHODS

The technique of immunostaining of polytene chromosomes from salivary glands of third instar larvae was completed in Dr. Mazo's lab following a protocol similar to that previously described (Rozenblatt-Rosen et al., 1998; Rozovskaia et al., 1999). Menin binding was examined using rabbit anti-menin 9562 antibody (1:80) with anti-rabbit texas red (1:75); while Trx binding was examined with rat anti-Trx (N1 region) antibody (1:25) with anti-rat FITC (1:75). Immunostained polytene spreads were mounted with Vectashield mounting medium containing DAPI and examined by fluorescence microscopy for the co-localization of menin and Trx under standard and 20 min HS conditions.

RESULTS

Preliminary results showed that menin and Trx co-localized on polytene chromosomes of Oregon R larvae at numerous loci in the absence of stress (Figure F.1). There was still overlap of menin and Trx binding with a 20 minute heat shock (Figure F.2). Some potential heat shock puffs are indicated with an asterisk and both proteins appear to be bound there, although these chromosomes have not been mapped so these may not be true HS puffs.

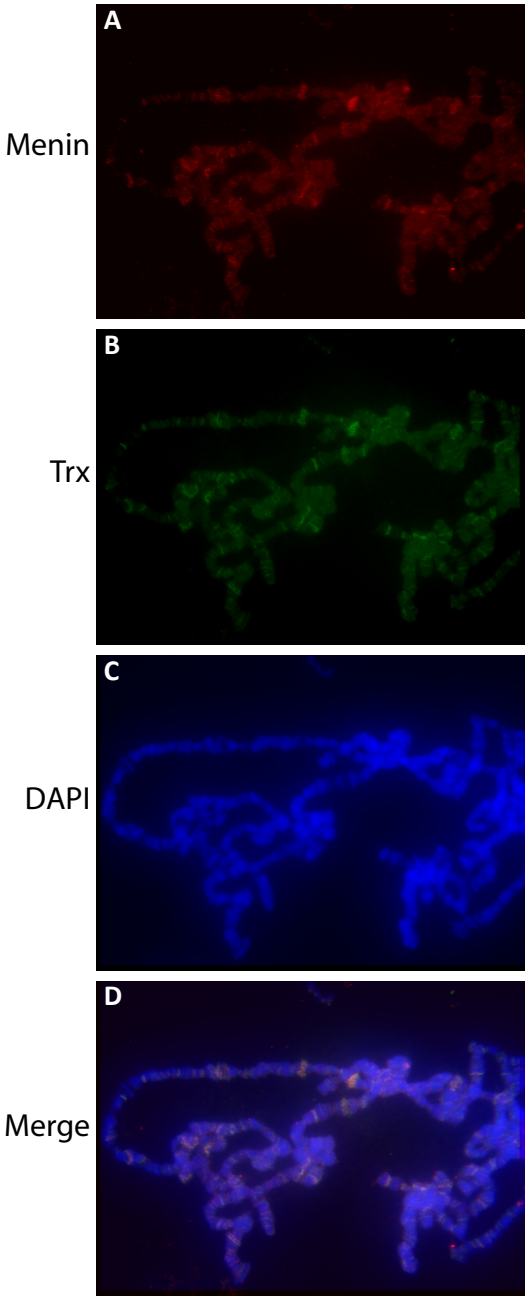

Figure F.1. Immunostaining of polytene chromosomes from OR larvae.
Polytene chromosomes from third instar larvae were immunostained with rabbit anti-menin 9562 (1:80) with anti-rabbit texas red (1:75) secondary antibody (A) and rat anti-trithorax (1:25) with anti-rat FITC (1:75) secondary antibody (B) and mounted with Vectashield mounting medium with DAPI (C). The merged images are shown D. Overlap of menin and trithorax binding can be seen for several loci in the absence of heat stress.

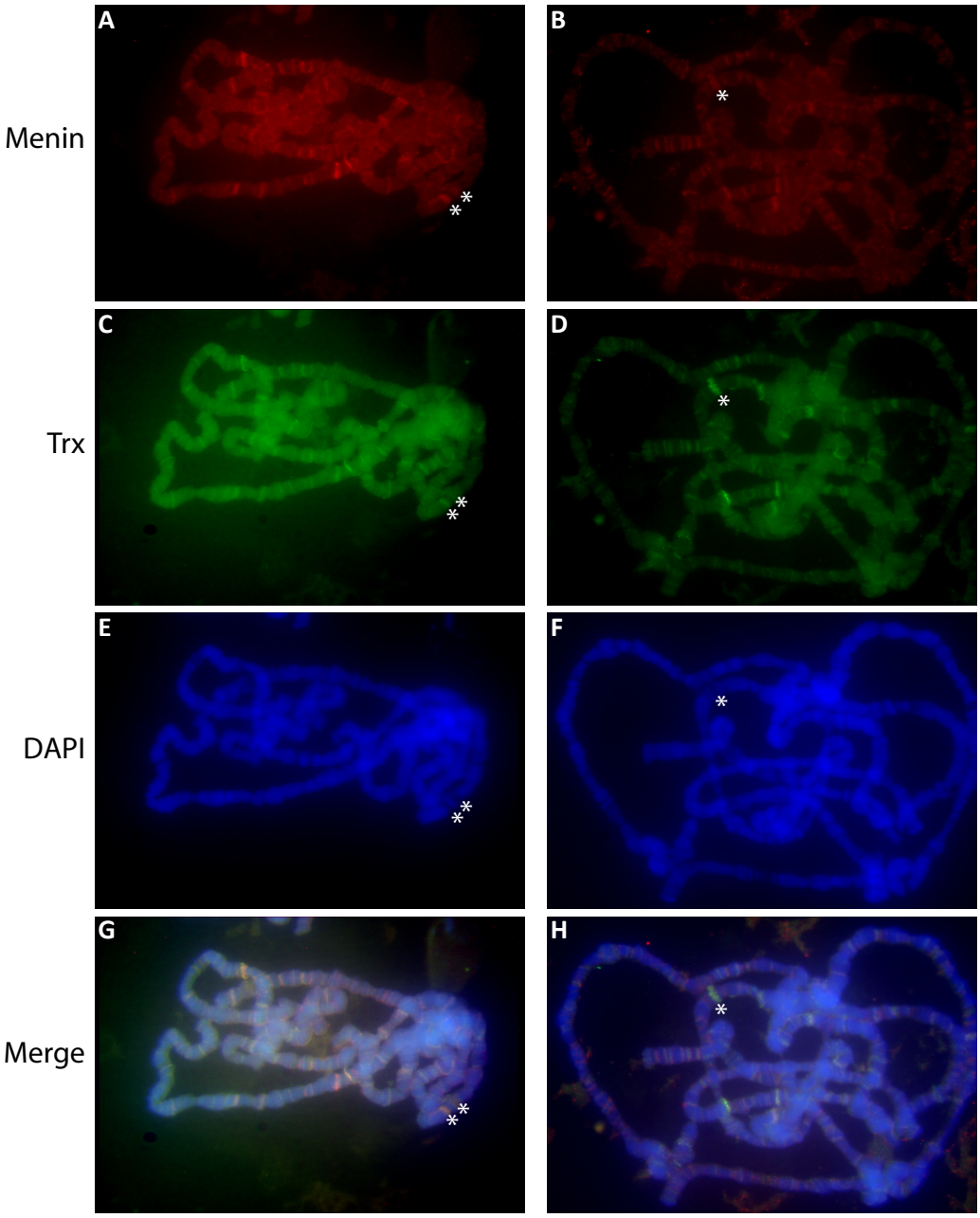

Figure F.2. Immunostaining of polytene chromosomes from heat shocked OR larvae.
Menin and Trithorax binding were examined in polytene chromosomes of third instar larvae exposed to a 20 min HS. Polytene chromosomes were immunostained with rabbit anti-menin 9562 (1:80) with anti-rabbit texas red (1:75) secondary antibody (A, B), rat anti-trithorax (1:25) with anti-rat FITC (1:75) secondary antibody (C,D) and mounted with Vectashield mounting medium with DAPI (E,F). The merged images are shown in the bottom row (G,H). Overlap of menin and trithorax binding can be seen for several loci. Potential heat shock puffs are indicated with asterisks. Two different chromosome spreads are shown, one per column.

APPENDIX G: Development of tools for studying *trx* function in *Drosophila*

Since both trx^{B11} and trx^{Z11} alleles are homozygous lethal during embryonic and pupal stages, respectively, experiments are limited to using only heterozygous mutants (Breen, 1999). However, reducing the level of functional *trx* by half may not necessarily produce an observable phenotype as the wild-type protein expressed from the non-mutated allele could compensate. In order to study the effects of loss of Trx function, a system where *trx* could be transiently knocked-down without inducing organismal lethality is needed. For this reason, I investigated the use of a temperature-sensitive GAL80 to regulate GAL4 function, which in turn controls expression of a *UAS-*trx^{RNAi} construct (Vienna *Drosophila* RNAi Centre, ID 37715) (see Figure G.1 for a schematic). In this system $GAL80^{ts}$ is active and capable of inhibiting GAL4 at lower temperatures (18-25°C) but is inactive at higher temperatures (29°C); therefore, GAL4 is only capable of transcribing UAS-target genes at the elevated temperature (Figure G.1C and D).

Since the trx^{RNAi} construct had not been tested, I compared its activity when combined with *tub-GAL4* at 18°C, 25°C and 29°C. If the trx^{RNAi} construct is capable of sufficiently down-regulating *trx*, then it should result in lethality as *trx* is required for proper development. When *UAS-*trx^{RNAi} flies were crossed to *tub-GAL4/TM3* there was complete lethality of *UAS-*trx^{RNAi}*/+;tub-GAL4/+* progeny at all three temperatures tested (Figure G.1B). *UAS-*trx^{RNAi}*;tub-*$GAL80^{ts}$ flies were generated (by Maria Papaconstantinou) and crossed to *tub-GAL4/TM3* flies and maintained at 18°C, 25°C or 29°C. As expected, there was no lethality of *UAS-*trx^{RNAi}*;tub-*$GAL80^{ts}$*/tub-GAL4* in crosses at 18°C or 25°C but 100 % lethality was observed in crosses at 29°C (Figure G.1B).

Next, conditions capable of knocking-down *trx* without causing lethality were determined. First of all, I assessed at what stage in development temperature shifts to 29°C could be tolerated. Embryos were laid at 25°C and then shifted to 29°C beginning at different times for the remainder of their development. Temperature shifts beginning during embryogenesis, 1st or 2nd larval instar stages resulted in lethality of *trx^{RNAi};tub-GAL80^{ts}/tub-GAL4*, while those commencing during the third instar or early pupal stage led to partial lethality (Table G.1). If the temperature shift to 29°C did not begin until the late pupal stage then the expected number of *trx^{RNAi};tub-GAL80^{ts}/tub-GAL4* progeny emerged (Table G.1), suggesting that knock-down of *trx* could be tolerated from late pupal stage onward.

Since survival of *trx^{RNAi};tub-GAL80^{ts}/tub-GAL4* flies shifted to 29°C before the late pupal stage was not tolerated, temporary temperature shifts, for 3-72 hrs, were tested and the results are summarized in Table G.2. In general, temperature shifts lasting less than 24 hrs were well tolerated during embryogenesis to late 3rd instar. A critical period for *trx* function occurred from late 3rd instar to early pupal stage as temperature shifts lasting 12-48 hrs resulted in partial lethality of *trx^{RNAi};tub-GAL80^{ts}/tub-GAL4* flies (Table G.2). Overall, temperature shifts lasting up to 48 hrs were well tolerated and did not result in significant lethality. The efficiency of *trx* knock-down during these shorter temperature shifts needs to be evaluated by reverse transcriptase PCR to look at mRNA levels or immunoblotting to look at protein levels. The system appears to be functioning as expected and could prove useful for future genetic studies of the *trx* and *Mnn1* interaction in *Drosophila*.

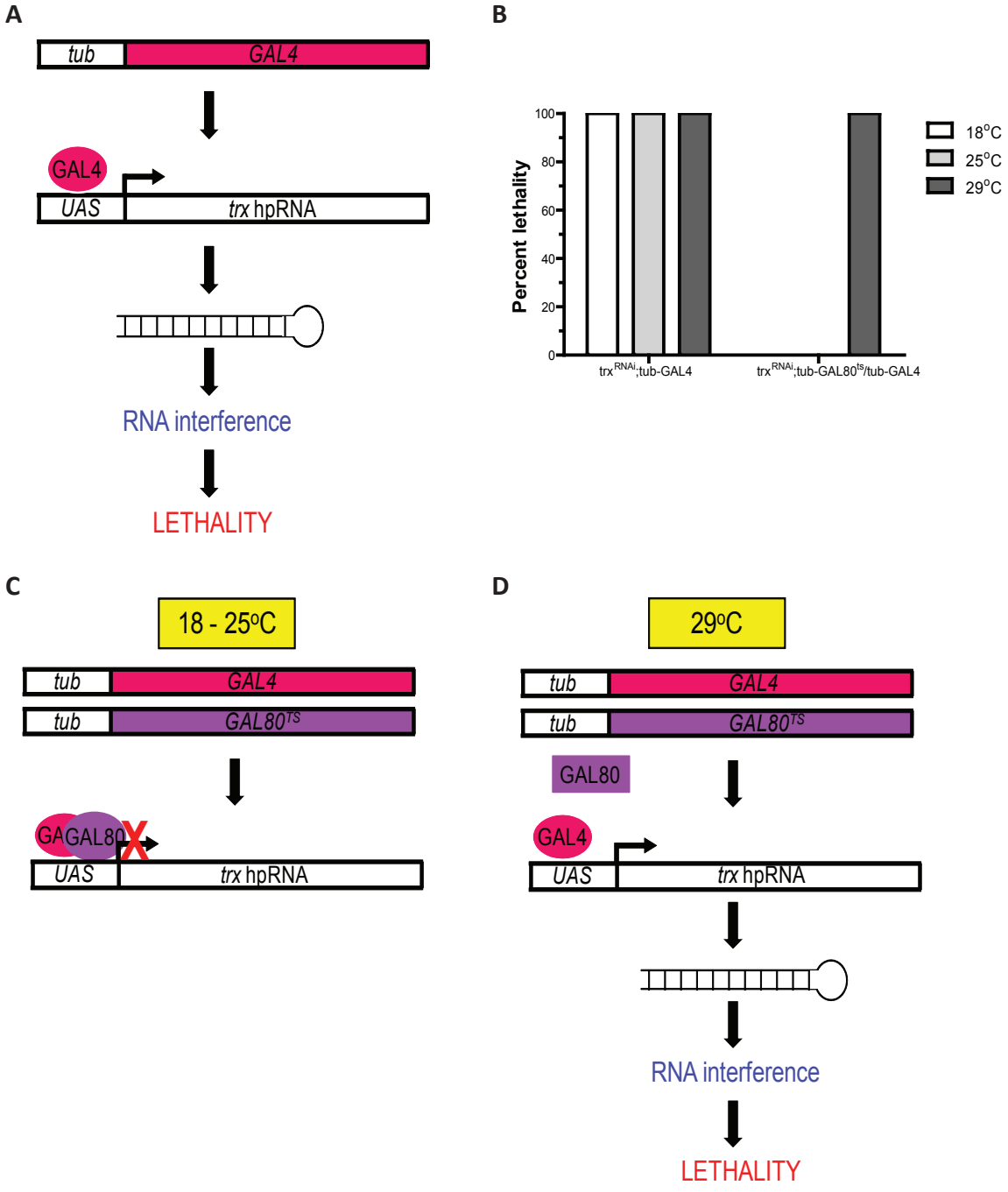

Figure G.1. Temperature sensitive knock-down using trx^{RNAi};*tub-GAL80^{ts}/tub-GAL4*.
When *UAS-trx^{RNAi}* expression is driven by *tub-GAL4* (A) there is 100 % lethality at 18°C, 25°C and 29°C (B). When this is combined with the temperature sensitive GAL80 (*trx^{RNAi};tub-GAL80^{ts}/ tub-GAL4*), there is no lethality when flies develop at 18°C or 25°C (B) because GAL80 inhibits GAL4-mediate transcription of *UAS-trx^{RNAi}* (C). In contrast, at 29°C there is 100% lethality of *trx^{RNAi};tub-GAL80^{ts}/tub-GAL4* (B) because a conformation change in the temperature sensitive GAL80 prevents the inhibition of GAL4 so the *trx^{RNAi}* construct is expressed (D).

Table G.1. Survival of *trx^{RNAi};tub-GAL80^{ts}/GAL4* following temperature shifts beginning at different developmental stages

Stage	Survival
Embryo 3-5 hr AEL	No
Embryo 20-22 hr AEL	No
Early 1st instar	No
Late 1st instar	No
Early 2nd instar	No
Late 2nd instar	No
Early 3rd instar	Partial
Late 3rd instar	Partial
Early pupal	Partial
Late pupal	Yes

Crosses between *trx^{RNAi};tub-GAL80^{ts}* and *tub-GAL4/TM3* flies were carried out at 25°C and shifted to 29°C at the various stages indicated for the remainder of development. The survival of *trx^{RNAi};tub-GAL80^{ts}/tub-GAL4* progeny was determined. Partial survival indicates that less than the expected ratio of trx^{RNAi};tub-GAL80^{ts}/tub-GAL4 to trx^{RNAi};tub-GAL80^{ts}/TM3 flies emerged.

Table G.2. Survival of *trx^{RNAi};tub-GAL80^{ts}/tub-GAL4* following temporary temperature shifts during different developmental stages

Stage	Temp Shift	Survival
Embryo 3-5 hr AEL	3 hr	Yes
Embryo 20-22 hr AEL	6 hr	Yes
	24 hr	Yes
Late 1st instar	3 hr	Yes
	6 hr	Yes
Late 2nd instar	24 hr	Yes
Early 3rd instar	24 hr	Yes
Late 3rd instar-early pupal	3 hr	Yes
	12 hr	Partial
	24 hr	Partial
	48 hr	Partial
Early-mid pupal	3 hr	Yes
	6 hr	Yes
	24 hr	Yes
	48 hr	Yes
	72 hr	Yes
Mid pupal	3 hr	Yes
	6 hr	Yes
	12 hr	Yes
	24 hr	Yes
	48 hr	Partial
Late pupal	3 hr	Yes
	6 hr	Partial
	24 hr	Yes

Crosses between *trx^{RNAi};tub-GAL80^{ts}* and *tub-GAL4/TM3* flies were carried out at 25°C and shifted temporarily to 29°C at various stages for the length of time indicated. The survival of *trx^{RNAi};tub-GAL80^{ts}/tub-GAL4* progeny was determined. Partial survival indicates that less than the expected ratio of trx^{RNAi};tub-GAL80^{ts}/tub-GAL4 to *trx^{RNAi};tub-GAL80^{ts}/TM3* flies emerged.

APPENDIX H: Preliminary starvation and desiccation experiments

1. Initial desiccation and starvation experiments

In order to determine if *Mnn1* mutants have a similar survival phenotype as previously characterized IIS mutants, preliminary desiccation and starvation experiments were conducted with OR, *yw*, *yw*;*Mnn1*^{e30} and *yw*;*Mnn1*^{e173}. These experiments were carried out using adult flies, age 4-6 days, from vials of amplified stocks.

1.1 Initial desiccation experiment

In the initial desiccation experiment, three trials were performed, with a total of 30 tubes of flies for all genotypes except *Mnn1*^{e173}, which only had 18 tubes of flies. Percent survival per tube of ten flies was determined and the average and standard error of the mean were calculated and graphed (Figure H.1). In this preliminary experiment both males and females showed very similar trends, with the males dying faster than the females. For both males and females, the two control lines, *yw* and OR, showed different desiccation survivals, with OR surviving better than *yw* (Figure H.1). This suggested that the genetic background was probably very influential in this experiment. As *Mnn1*^{e30} and *Mnn1*^{e173} used for this experiment were in the *yw* background, it was more logical to compare their survival to *yw* than OR. The two deletion mutants did not have similar survivals, as *Mnn1*^{e30} survived better than *yw* and *Mnn1*^{e173} survived worse. Perhaps differences between these two lines, that are independent of *Mnn1*, affected survival under desiccating conditions or other factors were influencing survival. Because the second chromosome bearing the *Mnn1*^{e173} allele

was also associated with sterility, it was suspected that this chromosome contained other deleterious mutations/modifications that were hindering survival in this assay.

1.2 Initial starvation experiment

In the initial starvation experiment OR, *yw*, *yw;Mnn1*^{e30} and *yw;Mnn1*^{e173} were tested. Three trials were performed with 21-26 vials, of 10 flies each, per sex and genotype. The percent survival was determined per vial on each day and the average and standard error were graphed (Figure H.2A & B). Both males and females showed similar behaviours. *Mnn1*^{e30} survived better than both *yw* and OR controls but *Mnn1*^{e173} survived worse (Figure H.2A & B). In this assay, the two controls had similar survivals for males. For females, they differed only on day 3 but were similar on all other days. This result differs from what was observed in the preliminary desiccation experiment where OR survived much better than *yw*.

Since the *Mnn1* mutants did not show similar behaviours in this assay, another experiment was carried out using the heteroallelic combination of *Mnn1*^{e30}/*Mnn1*^{e173} and both deletion mutants over *Df(2L)spd*^{j2} (referred to simply as *Df(2L)*) to see if the phenotype was linked to loss of *Mnn1*. For this experiment, crosses were set up to generate the appropriate genotypes (a cross with *yw* was used to generate *+/Df(2L)*). Since this experiment was carried out independently of the previous one, the results are graphed separately in Figure H.2C & D. For males, *Mnn1*^{e30}/*Mnn1*^{e173}, *Mnn1*^{e30}*/Df(2L)* and *Mnn1*^{e173}*/Df(2L)*, all had similar survivals. If these curves (Figure H.2C) were superimposed on the curves from Figure H.2A, then these three genotypes would cluster with *Mnn1*^{e30}. This suggested that the increased survival observed was probably due to the loss of *Mnn1* function. Surprisingly, *+/Df(2L)* survived better than the other

genotypes, the reason for this was not clear but it suggested that other factors, in addition to loss of *Mnn1* from the deletion region, were contributing to increased survival. The results for females (Figure H.2D) are a bit more difficult to interpret because the curves do not cluster together as closely as with males. In this experiment, $Mnn1^{e30}/Mnn1^{e173}$ survived well and if the graph was superimposed with that of Figure H.2B this curve would follow nicely with that of $Mnn1^{e30}$. This suggested that the survival advantage observed for $Mnn1^{e30}$ was most likely due to loss of *Mnn1* function, and the poor survival of $Mnn1^{e173}$ was likely due to other factors in the background of the second chromosome, as this negative effect was not observed in the heteroallelic combination. These interpretations are made cautiously, however, as these experiments were conducted at different times and other factors could have been contributing to survival.

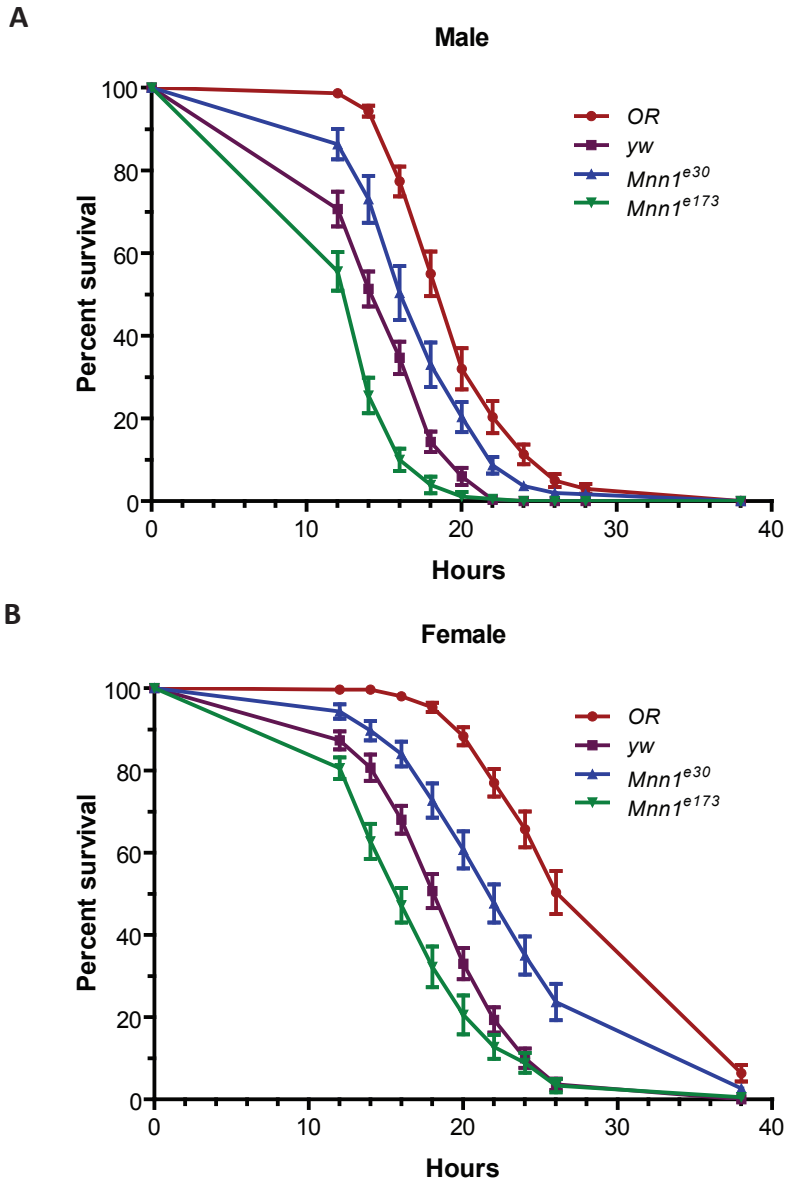

Figure H.1. Desiccation survival of male and female flies in initial experiments.
Flies, age 4-6 d, were tested in the desiccation assay by transferring them, 10 per tube, to empty glass tubes. Survival was determined after 12 hrs and then every 2 hrs thereafter (note that not all time points were determined from 26-38 hrs). For all genotypes, except Mnn1^{e173}, 30 tubes, from 3 separate trials were used; only 18 tubes were used for Mnn1^{e173}. The percent survival per tube of flies was determined for each time point and the average and standard error of the mean were calculated. The survival curves for both males (A) and females (B) look similar, with OR surviving best and with Mnn1^{e30} surviving better than yw and Mnn1^{e173} surviving worse.

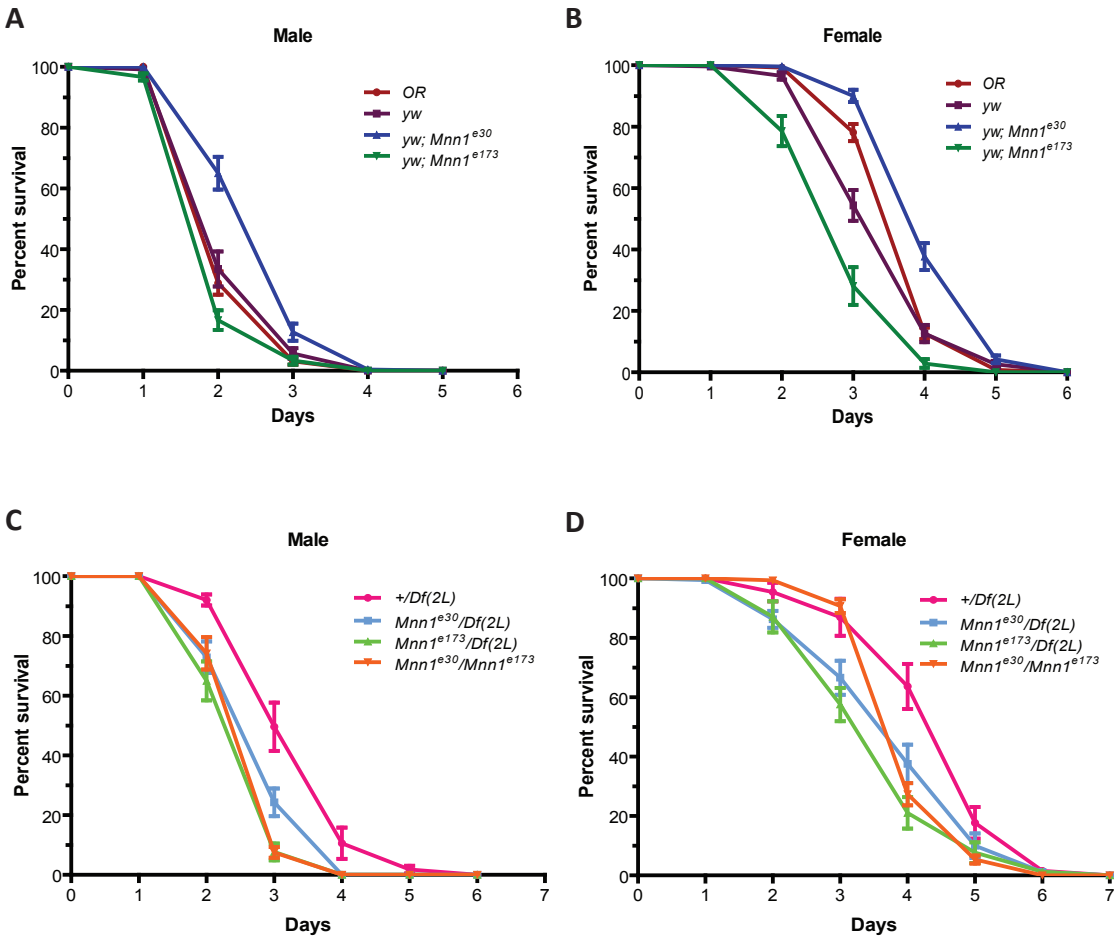

Figure H.2. Starvation survival of male and female flies in initial experiments.
The survival curves for 4-6 d males (A & C) and females (B & D) are each shown on two separate graphs because not all genotypes were tested simultaneously. Flies were starved by transferring to 1 % agar, with ten flies per vial. Survival was examined every 24 hrs until all flies had perished. The percent survival was determined each day for each vial of ten flies and then the average and standard error of the mean were calculated. For A & B, 21-26 vials of 10 flies each, coming from 3 separate trials, were used; for C & D, 13-17 vials were used, with 3 trials, all coming from one set of parental crosses. All genotypes A & B were tested simultaneously and all genotypes in C & D were tested simultaneously. *Mnn1*^{e30} males (A) and females (B) survived better than OR and *yw* controls; whereas, *Mnn1*^{e173} survived worse. C & D) Heteroallelic *Mnn1*^{e30}/*Mnn1*^{e173} as well as the three deficiency (*Df(2L)spd*^{j2}) genotypes all survived starvation well (when compared to genotypes shown in A & B). Surprisingly, *+/Df(2L)* survived best for both males (C) and females (D). Note that *+/Df(2L)* is from a cross to *yw*.

APPENDIX I: Additional data and statistical analyses for desiccation assays

All of the genotypes tested in the desiccation assays are graphed together in Figure I.1 for males and Figure I.2 for females. The genotypes were divided into separate graphs to simplify comparisons made in the Chapter 6 results section (Figure 6.2 and 6.3). Summaries of the statistical analyses are provided in Table I.1 and Table I.2.

The same data set was also analyzed in another manner; specific time points were chosen and the percent survival and standard error were plotted as bar graphs. For males, 18 hrs and 20 hrs of desiccation were chosen, as these time points showed the greatest divergence among genotypes. For each time point, a one-way ANOVA was performed followed by Bonferroni's multiple comparison tests to determine which pairs were significantly different (see Table I.3 for a summary of statistics). The significance level chosen for such comparisons was $p<0.001$. As expected, analyzing data in this manner leads to similar conclusions as comparing overall survival curves, although it is sometimes easier to compare differences between genotypes when visualizing with the aid of bar graphs (Figure I.3).

After 18 hrs of desiccation, the *Mnn1* deletion mutants both survived significantly better than controls (w^{1118} and $Mnn1^{+E314}$), with $Mnn1^{e30}$ surviving better than $Mnn1^{e173}$ (Figure I.3A). As mentioned for the survival curves, the heteroallelic combination does not survive as well as either homozygous mutant. In fact, $Mnn1^{e30}$/+ had a greater percent survival than $Mnn1^{e30}/Mnn1^{e173}$ after 18 hrs of desiccation, a result that was quite surprising. This contrasts with $Mnn1^{e173}$/+ that had a similar survival as wild-type w^{1118}. From the bar graph the increased survival of all *Df(2L)*

genotypes is apparent, with only *Mnn1*^{e30} having a percent survival similar to any of these *Df(2L)* lines (Figure I.3A). For the 18 hr time point there is not much difference between any of the *Df(2L)* lines.

After 20 hrs desiccation, the overall trend is similar to what was observed after 18 hrs (Figure I.3B). By this time point, most of the genotypes that did not have a complete loss of *Mnn1* function have almost completely perished, with the exception of *Mnn1*$^{e30/+}$ and the control deficiency genotypes (*+/Df(2L)* and *Mnn1*$^{+E314}$*/Df(2L)*). Also, at this time point, the transheterozygotes (*Mnn1*^{e30}*/Mnn1*^{e173}) do not have a significant survival advantage compared to heterozygous *Mnn1* mutants or controls. A key difference between 18 hrs and 20 hrs, was that at the latter time point there was a statistically significant difference between the control deficiency lines (*+/Df(2L)* and *Mnn1*$^{+E314}$*/Df(2L)*) and the *Mnn1* deletions over the deficiency (*Mnn1*^{e30}*/Df(2L)* and *Mnn1*^{e173}*/Df(2L)*) (Figure I.3A & B). Thus, with prolonged desiccation, the complete loss of *Mnn1* function leads to a more prominent survival advantage in the deficiency background. The overall conclusion from these experiments is that a loss of menin function enhances survival of males exposed to desiccation stress.

Percent survival and standard error for females after 22 hrs and 26 hrs of desiccation were compared for all genotypes by one-way ANOVA with Bonferroni's multiple comparisons test (see Table I.4 for the statistical summary). These results are shown as bar graphs to simplify comparisons between genotypes and the overall trend is quite similar to that observed for males with a few exceptions. After 22 hrs of desiccation *Mnn1*^{e30} and *Mnn1*^{e173} had similar survivals, with the heteroallelic combination having a slightly reduced survival (Figure I.3C). At this time point,

deficiency controls survived better than *Mnn1* deletions combined with the deficiency. The greater percent survival of controls over the deficiency was still maintained after 26 hrs of desiccation (Figure I.3D). At the later time point $Mnn1^{e30}$ survived better than $Mnn1^{e173}$ and $Mnn1^{e30}/Mnn1^{e173}$; the latter two genotypes showed similar percent survivals after 26 hrs. As with males, the overall conclusion for females is that loss of menin function increases desiccation survival.

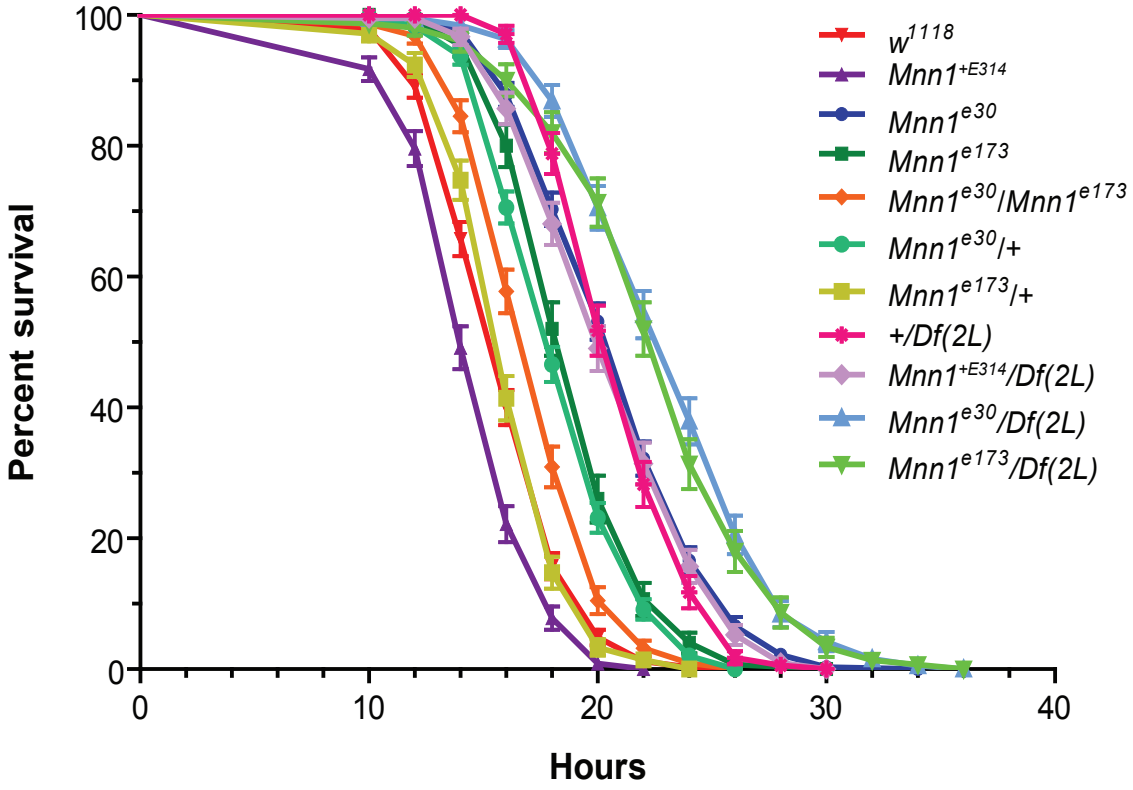

Figure I.1. Male desiccation survival for all genotypes.
The survival curves for 4-6 d males from all genotypes tested are plotted together. Larval density was controlled during development and males were allowed to mate freely prior to commencing the experiment. Desiccating conditions were created by transferring flies, ten per tube, to empty glass tubes. Survival was examined after 10 hrs and then every 2 hrs thereafter until all flies had perished. Two separate experimental crosses were used to generate flies for each genotype and 2-3 trials were carried out from each cross, with the number of individuals variable in each trial. All genotypes were tested simultaneously. A total of 150 - 350 flies were tested for each genotype. Survival curves were generated using GraphPad Prism and significance was determined using a log-rank (Mantel-Cox) test, followed by multiple pairwise tests (see Appendix I, Table I.1 for a summary of statistics for this experiment).

Table I.1. Statistical summary for male desiccation survival curves.

Comparison	Chi square	p value	Significant p<0.002
Mnn1^{e30} vs *Mnn1*^{e173}	36.56	<0.0001	Yes
Mnn1^{e30} vs *w*^{1118}	284.1	<0.0001	Yes
Mnn1^{e30} vs *Mnn1*$^{+E314}$	360.6	<0.0001	Yes
Mnn1^{e30} vs *Mnn1*^{e30}/*Mnn1*^{e173}	144.8	<0.0001	Yes
Mnn1^{e30} vs *Mnn1*^{e30}/+	89.72	<0.0001	Yes
Mnn1^{e30} vs *Mnn1*^{e30}/*Df(2L)*	37.05	<0.0001	Yes
Mnn1^{e173} vs *w*^{1118}	87.38	<0.0001	Yes
Mnn1^{e173} vs *Mnn1*$^{+E314}$	148.8	<0.0001	Yes
Mnn1^{e173} vs *Mnn1*^{e30}/*Mnn1*^{e173}	26.72	<0.0001	Yes
Mnn1^{e173} vs *Mnn1*^{e173}/+	77.41	<0.0001	Yes
Mnn1^{e173} vs *Mnn1*^{e173}/*Df(2L)*	74.06	<0.0001	Yes
w^{1118} vs *Mnn1*$^{+E314}$	26.33	<0.0001	Yes
Mnn1^{e30}/*Mnn1*^{e173} vs Mnn1^{e30}/+	22.11	<0.0001	Yes
Mnn1^{e30}/*Mnn1*^{e173} vs *Mnn1*^{e173}/+	19.69	<0.0001	Yes
Mnn1^{e30}/*Mnn1*^{e173} vs *w*^{1118}	25.97	<0.0001	Yes
Mnn1^{e30}/*Mnn1*^{e173} vs *Mnn1*$^{+E314}$	85.50	<0.0001	Yes
Mnn1^{e30}/+ vs *Mnn1*^{e173}/+	86.40	<0.0001	Yes
Mnn1^{e30}/+ vs *w*^{1118}	110.5	<0.0001	Yes
Mnn1^{e173}/+ vs *w*^{1118}	0.2695	0.6037	No
Mnn1^{e30}/*Df(2L)* vs *Mnn1*^{e173}/*Df(2L)*	0.5729	0.4491	No
Mnn1^{e30}/*Df(2L)* vs +/*Df(2L)*	41.54	<0.0001	Yes
Mnn1^{e30}/*Df(2L)* vs *Mnn1*$^{+E314}$/*Df(2L)*	39.97	<0.0001	Yes
Mnn1^{e173}/*Df(2L)* vs +/*Df(2L)*	27.06	<0.0001	Yes
Mnn1^{e173}/*Df(2L)* vs *Mnn1*$^{+E314}$/*Df(2L)*	25.23	<0.0001	Yes
+/*Df(2L)* vs *Mnn1*$^{+E314}$/*Df(2L)*	0.009150	0.9238	No

Survival curves were compared using a log-rank (Mantel-Cox) test. Pairwise comparisons were made and the Bonferroni method was used to account for multiple comparisons. The adjusted significance level used was p<0.002.

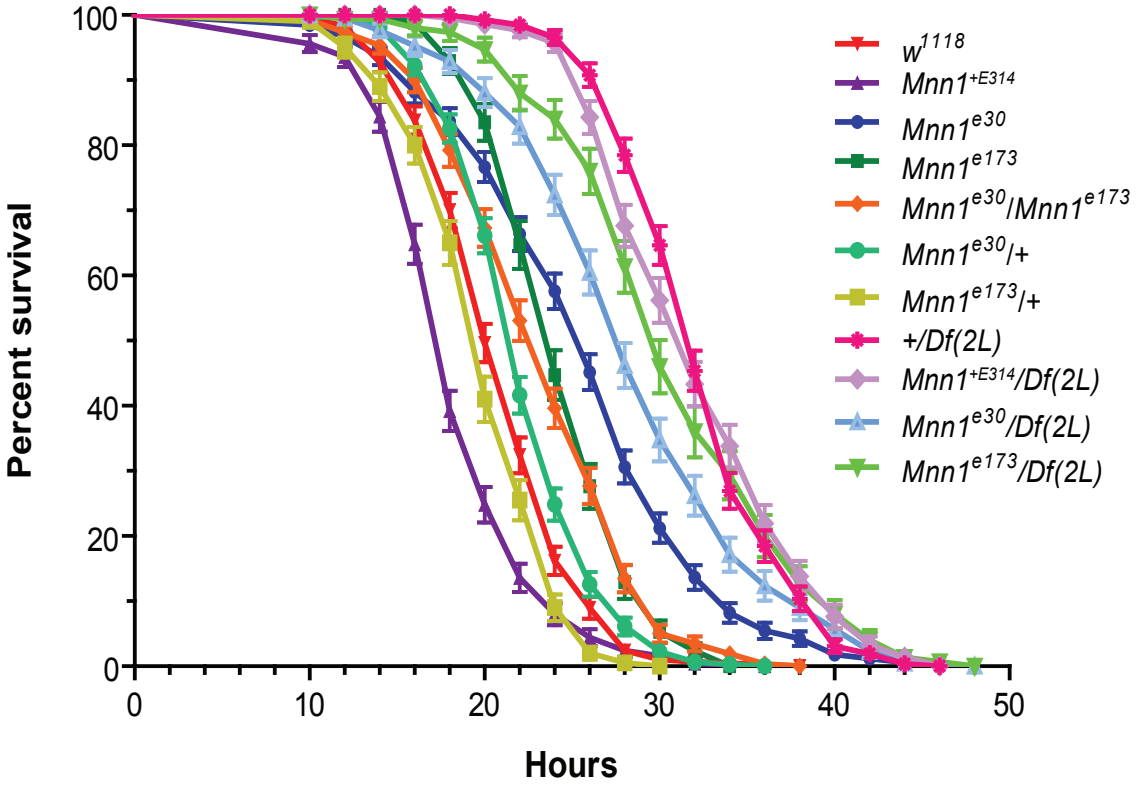

Figure I.2. Female desiccation survival for all genotypes.
The survival curves for 4-6 d females from all genotypes tested are plotted together. Larval density was controlled during development and females were allowed to mate freely prior to commencing the experiment. Desiccating conditions were created by transferring flies, ten per tube, to empty glass tubes. Survival was examined after 10 hrs and then every 2 hrs thereafter until all flies had perished. Two separate experimental crosses were used to generate flies for each genotype and 3 trials were carried out from each cross, with the number of individuals variable in each trial. All genotypes were tested simultaneously. A total of 150 - 330 flies were tested for each genotype. Survival curves were generated using GraphPad Prism and significance was determined using a log-rank (Mantel-Cox) test, followed by multiple pairwise tests (see Appendix I, Table I.2 for a summary of statistics for this experiment).

Table I.2. Statistical summary for female desiccation survival curves.

Comparison	Chi square	p value	Significant p<0.002
Mnn1^{e30} vs *Mnn1*^{e173}	18.68	<0.0001	Yes
Mnn1^{e30} vs *w*^{1118}	128.5	<0.0001	Yes
Mnn1^{e30} vs *Mnn1*$^{+E314}$	207.4	<0.0001	Yes
Mnn1^{e30} vs *Mnn1*^{e30}*/Mnn1*^{e173}	33.77	<0.0001	Yes
Mnn1^{e30} vs *Mnn1*^{e30}*/+*	87.55	<0.0001	Yes
Mnn1^{e30} vs *Mnn1*^{e30}*/Df(2L)*	18.83	<0.0001	Yes
Mnn1^{e173} vs *w*^{1118}	56.24	<0.0001	Yes
Mnn1^{e173} vs *Mnn1*$^{+E314}$	126.3	<0.0001	Yes
Mnn1^{e173} vs *Mnn1*^{e30}*/Mnn1*^{e173}	1.044	0.3070	No
Mnn1^{e173} vs *Mnn1*^{e173}*/+*	100.3	<0.0001	Yes
Mnn1^{e173} vs *Mnn1*^{e173}*/Df(2L)*	112.9	<0.0001	Yes
w^{1118} vs *Mnn1*$^{+E314}$	36.62	<0.0001	Yes
Mnn1^{e30}*/Mnn1*^{e173} vs Mnn1^{e30}*/+*	13.15	0.0003	Yes
Mnn1^{e30}*/Mnn1*^{e173} vs *Mnn1*^{e173}*/+*	70.81	<0.0001	Yes
Mnn1^{e30}*/Mnn1*^{e173} vs *w*^{1118}	38.29	<0.0001	Yes
Mnn1^{e30}*/Mnn1*^{e173} vs *Mnn1*$^{+E314}$	109.1	<0.0001	Yes
Mnn1^{e30}*/+* vs *Mnn1*^{e173}*/+*	41.07	<0.0001	Yes
Mnn1^{e30}*/+* vs *w*^{1118}	12.11	0.0005	Yes
Mnn1^{e173}*/+* vs *w*^{1118}	8.206	0.0042	No
Mnn1^{e30}*/Df(2L)* vs *Mnn1*^{e173}*/Df(2L)*	7.075	0.0078	No
Mnn1^{e30}*/Df(2L)* vs *+/Df(2L)*	21.08	<0.0001	Yes
Mnn1^{e30}*/Df(2L)* vs *Mnn1*$^{+E314}$*/Df(2L)*	18.93	<0.0001	Yes
Mnn1^{e173}*/Df(2L)* vs *+/Df(2L)*	0.7938	0.3730	No
Mnn1^{e173}*/Df(2L)* vs *Mnn1*$^{+E314}$*/Df(2L)*	1.172	0.2790	No
+/Df(2L) vs *Mnn1*$^{+E314}$*/Df(2L)*	0.2509	0.6164	No

Survival curves were compared using a log-rank (Mantel-Cox) test. Pairwise comparisons were made and the Bonferroni method was used to account for multiple comparisons. The adjusted significance level used was p<0.002.

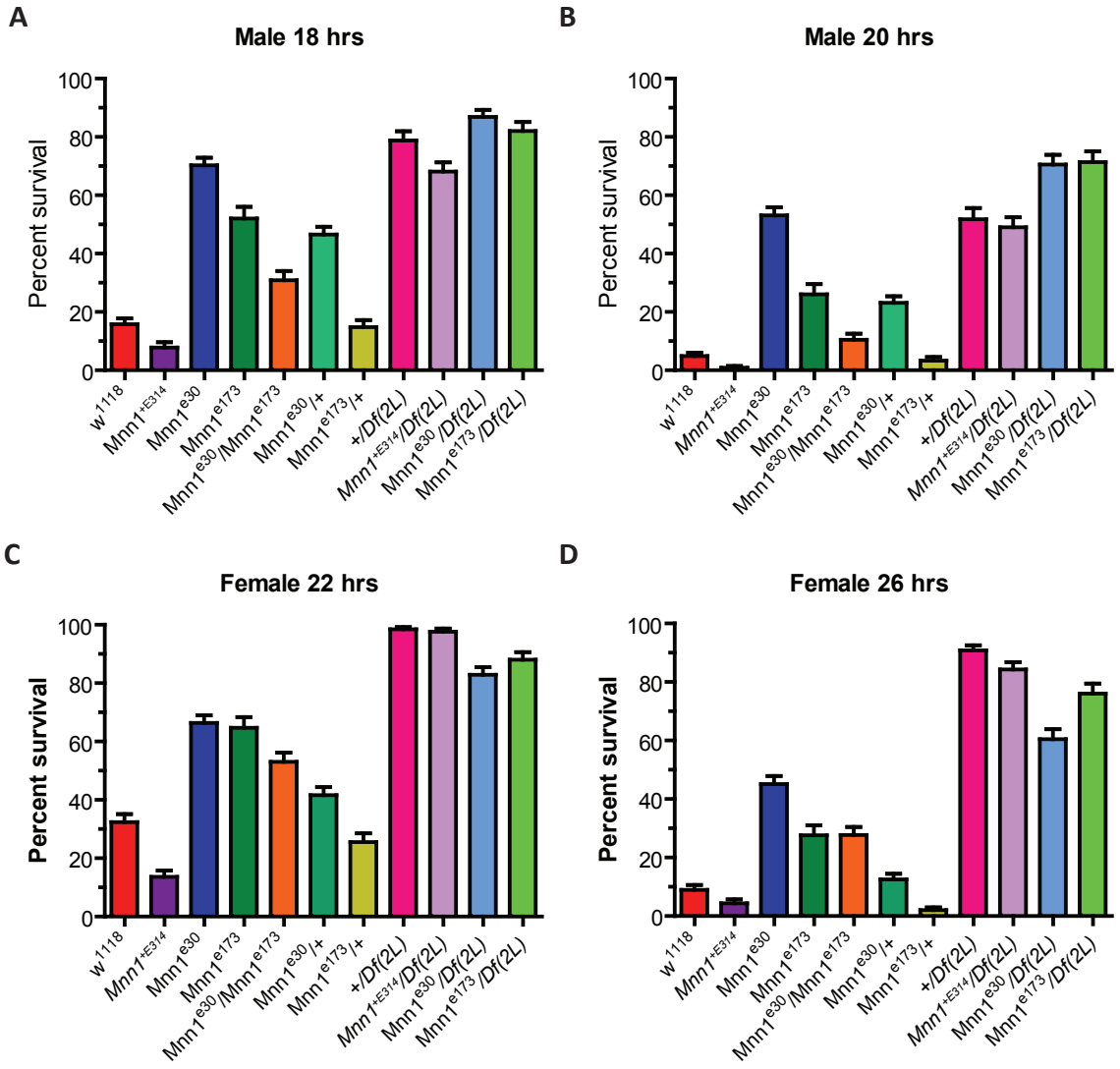

Figure I.3. Desiccation survival of male and female flies at various time points .

The percent survival of 4-6 d males (A & B) and females (C & D) after desiccation are shown for two separate time points taken from the survival curves (Appendix A, Figure 3 & 4) for better visual comparison between genotypes. For males, percent survival after 18 hrs (A) and 20 hrs (B) of desiccation are shown as bar graphs; for females, 22 hrs (C) and 26 hrs (D) were chosen. Each data set was analyzed using a one-way ANOVA with Bonferroni's multiple comparisons post-hoc test (See Appendix I, Table I.3 & I.4 for a summary of the statistics for these analyses). A-B) For males, *Mnn1* mutants (*Mnn1*^{e30} and *Mnn1*^{e173}) survive desiccation better than controls (*w*^{1118} and *Mnn1*$^{+E314}$). The presence of *Df(2L)spd*^{j2} significantly increases survival, with a *Mnn1* deletion over the deficiency having an obvious additive effect only at the later time point of 20 hrs (B). C-D) Overall, similar trends were observed for females, with *Mnn1* mutants surviving better than controls. Females differ from males in that the *Mnn1* deletions over the deficiency survive worse than controls over the deficiency.

Table I.3. Statistical summary for male desiccation survival at 18 hrs and 20 hrs.

Comparison	18 hrs		20 hrs	
	t	Significant p < 0.001	t	Significant p < 0.001
Mnn1^{e30} vs *Mnn1*^{e173}	4.423	Yes	7.069	Yes
Mnn1^{e30} vs *Mnn1*$^{+E314}$	17.27	Yes	15.59	Yes
Mnn1^{e30} vs *w*^{1118}	16.62	Yes	15.87	Yes
Mnn1^{e30} vs *Mnn1*^{e30}*/Mnn1*^{e173}	10.75	Yes	12.56	Yes
Mnn1^{e30} vs *Mnn1*^{e30}*/+*	7.336	Yes	9.997	Yes
Mnn1^{e30} vs *Mnn1*^{e30}*/Df(2L)*	4.314	Yes	4.901	Yes
Mnn1^{e173} vs *Mnn1*$^{+E314}$	10.06	Yes	6.175	Yes
Mnn1^{e173} vs *w*^{1118}	8.796	Yes	5.539	Yes
Mnn1^{e173} vs *Mnn1*^{e30}*/Mnn1*^{e173}	4.76	Yes	3.786	No
Mnn1^{e173} vs *Mnn1*^{e173}*/+*	8.325	Yes	5.468	Yes
Mnn1^{e173} vs *Mnn1*^{e173}*/Df(2L)*	6.211	Yes	10.13	Yes
Mnn1^{+E314} vs *w*^{1118}	2.207	No	1.195	No
w^{1118} vs *Mnn1*^{e30}*/+*	9.597	Yes	6.149	Yes
w^{1118} vs *Mnn1*^{e173}*/+*	0.2696	No	0.4427	No
Mnn1^{e30}*/Mnn1*^{e173} vs *Mnn1*^{e30}*/+*	4.35	Yes	3.803	No
Mnn1^{e30}*/Mnn1*^{e173} vs *Mnn1*^{e173}*/+*	4	No	1.904	No
Mnn1^{e30}*/Mnn1*^{e173} vs *w*^{1118}	4.160	No	1.661	No
Mnn1^{e30}/Mnn1^{e173} vs *Mnn1*$^{+E314}$	5.850	Yes	2.621	No
Mnn1^{e30}*/+* vs *Mnn1*^{e173}*/+*	8.709	Yes	5.853	Yes
Mnn1^{e30}*/Df(2L)* vs *Mnn1*^{e173}*/Df(2L)*	1.058	No	0.1924	No
Mnn1^{e30}*/Df(2L)* vs *Mnn1*$^{+E314}$*/Df(2L)*	4.475	Yes	5.533	Yes
Mnn1^{e30}*/Df(2L)* vs *+/Df(2L)*	1.816	No	4.584	Yes
Mnn1^{e173}*/Df(2L)* vs *Mnn1*$^{+E314}$*/Df(2L)*	3.111	No	5.378	Yes
Mnn1^{e173}*/Df(2L)* vs *+/Df(2L)*	0.68	No	4.507	Yes
Mnn1^{+E314}*/Df(2L)* vs *+/Df(2L)*	2.485	No	0.6789	No

Percent survival was compared using a one-way ANOVA ($p<0.001$) followed by Bonferroni's multiple comparisons post-hoc test. The results for the post-hoc pairwise comparisons are shown for biologically meaningful comparisons only.

Table I.4. Statistical summary for female desiccation survival at 22 hrs and 26 hrs.

Comparison	22 hrs		26 hrs	
	t	Significant P < 0.001	t	Significant P < 0.001
Mnn1^{e30} vs *Mnn1*^{e173}	0.4311	No	4.972	Yes
Mnn1^{e30} vs *Mnn1*$^{+E314}$	15.45	Yes	13.03	Yes
Mnn1^{e30} vs *w*^{1118}	10.36	Yes	12.06	Yes
Mnn1^{e30} vs *Mnn1*^{e30}/*Mnn1*^{e173}	3.934	No	5.646	Yes
Mnn1^{e30} vs *Mnn1*^{e30}/+	7.682	Yes	11.04	Yes
Mnn1^{e30} vs *Mnn1*^{e30}/*Df(2L)*	4.587	Yes	4.655	Yes
Mnn1^{e173} vs *Mnn1*$^{+E314}$	12.62	Yes	6.271	Yes
Mnn1^{e173} vs *w*^{1118}	8.207	Yes	5.186	Yes
Mnn1^{e173} vs *Mnn1*^{e30}/*Mnn1*^{e173}	2.895	No	0.0123	No
Mnn1^{e173} vs *Mnn1*^{e173}/+	9.227	Yes	6.593	Yes
Mnn1^{e173} vs *Mnn1*^{e173}/*Df(2L)*	5.106	Yes	11.58	Yes
Mnn1^{+E314} vs *w*^{1118}	5.352	Yes	1.419	No
w^{1118} vs *Mnn1*^{e30}/+	2.765	No	1.187	No
w^{1118} vs *Mnn1*^{e173}/+	1.847	No	2.032	No
Mnn1^{e30}/*Mnn1*^{e173} vs *Mnn1*^{e30}/+	3.347	No	4.819	Yes
Mnn1^{e30}/Mnn1^{e173} vs *Mnn1*^{e173}/+	7.198	Yes	7.325	Yes
Mnn1^{e30}/*Mnn1*^{e173} vs *w*^{1118}	5.940	Yes	5.880	Yes
Mnn1^{e30}/Mnn1^{e173} vs *Mnn1*$^{+E314}$	10.94	Yes	7.051	Yes
Mnn1^{e30}/+ vs *Mnn1*^{e173}/+	4.362	Yes	3.128	No
Mnn1^{e30}/*Df(2L)* vs *Mnn1*^{e173}/*Df(2L)*	1.182	No	3.895	No
Mnn1^{e30}/*Df(2L)* vs *Mnn1*$^{+E314}$/*Df(2L)*	3.714	No	6.542	Yes
Mnn1^{e30}/*Df(2L)* vs +/*Df(2L)*	4.129	No	8.756	Yes
Mnn1^{e173}/*Df(2L)* vs *Mnn1*$^{+E314}$/*Df(2L)*	2.208	No	2.078	No
Mnn1^{e173}/*Df(2L)* vs +/*Df(2L)*	2.504	No	3.862	No
Mnn1^{+E314}/*Df(2L)* vs +/*Df(2L)*	0.2229	No	1.874	No

Percent survival was compared using a one-way ANOVA ($p<0.001$) followed by Bonferroni's multiple comparisons post-hoc test. The results for the post-hoc pairwise comparisons are shown for biologically meaningful comparisons only.

APPENDIX J: Additional data and statistical analyses for starvation assays

All of the genotypes tested in the starvation assays are graphed together in Figure J.1 for males and Figure J.1 for females. The genotypes were divided into separate graphs to simplify comparisons made in the Chapter 6 results section (Figure 6.4 and 6.5). Summaries of the statistical analyses are provided in Table J.1 and Table J.2.

The same data were also analyzed by performing a one-way ANOVA using the percent survival of each genotype after two days of starvation (see Table J.3 for the statistics). From the bar graph, the dramatic difference between *Mnn1*^{e30} and *Mnn1*^{e173} survival is apparent (Figure J.3A). *Mnn1*^{e173} was not significantly different from *w*^{1118} or *Mnn1*$^{+E314}$. Heteroallelic *Mnnn1*^{e30}/*Mnn1*^{e173} had a similar survival to these three lines; this suggests that the negative effects of the *Mnn1*^{e173} were dominant to the survival promoting effects of *Mnn1*^{e30}.

The same data set for females was analyzed with a one-way ANOVA for day two survival because there was a great deal of variation among genotypes at this time point (see Table J.3 for a summary of statistics). Comparing the resulting bar graphs for females to those of males on the same day, the overall trend appears quite similar but females clearly resist starvation longer than males (Figure J.3A vs B). For females, the only genotypes with dramatically enhanced survival are *Mnn1*^{e30} and the four genotypes with the *Df(2L)* chromosome (Figure J.3B). Overall, it is difficult to conclude anything with certainty from the male or female starvation survival results as the two *Mnn1* deletion mutants do not behave similarly and only *Mnn1*^{e30} survives better than controls.

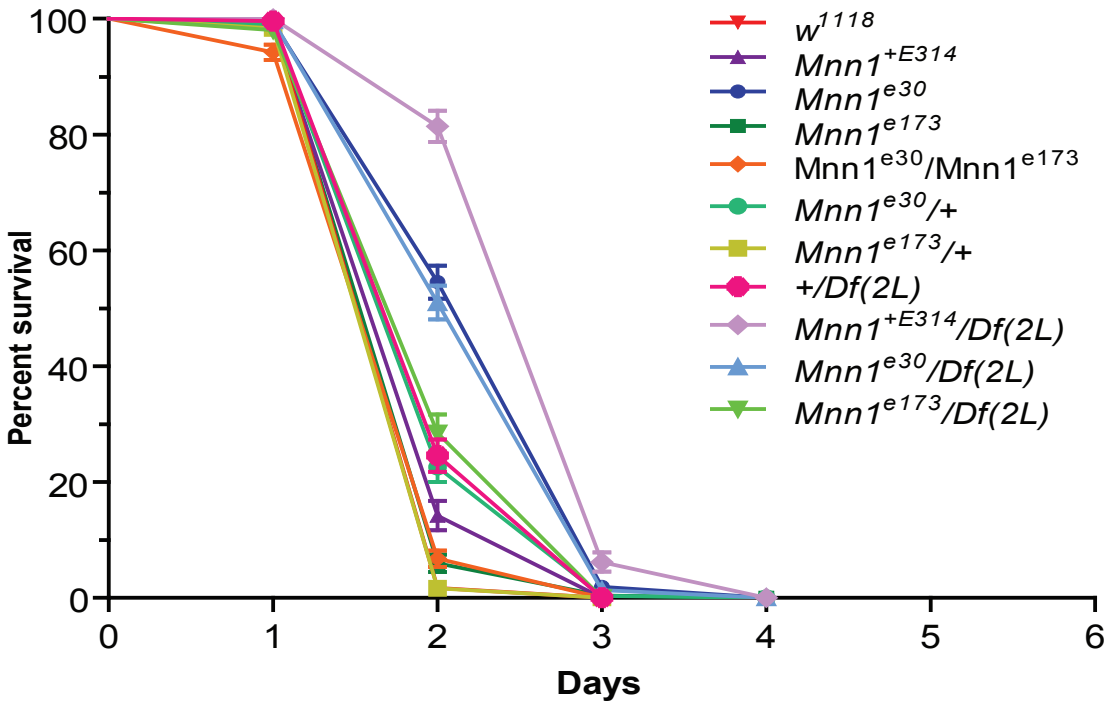

Figure J.1. Male starvation survival for all genotypes.
The survival curves for 4-6 d males from all genotypes tested are plotted together. Larval density was controlled during development and flies were allowed to mate freely prior to commencing the experiment. Flies were starved by transferring to 1 % agar, with ten flies per vial. Survival was examined every 24 hrs until all flies had perished. Two separate experimental crosses were used to generate flies for each genotype and 2-4 trials were carried out from each cross, with the number of individuals variable in each trial. All genotypes were tested simultaneously. A total of 190 - 350 flies were tested for each genotype. Survival curves were generated using GraphPad Prism and significance was determined using a log-rank (Mantel-Cox) test, followed by multiple pairwise tests (see Appendix J, Table J.1 for a summary of the statistics for this experiment). The *Mnn1*^{e30} deletion mutants showed incresed survival, but not the *Mnn1*^{e173} deletion mutants. Note, the curve for *w*^{1118} is obscured by that for *Mnn1*^{e173}/+.

Table J.1. Statistical summary for male starvation survival curves.

Comparison	Chi square	p value	Significant p<0.002
Mnn1^{e30} vs Mnn1^{e173}	140.5	<0.0001	Yes
Mnn1^{e30} vs w^{1118}	227.6	<0.0002	Yes
Mnn1^{e30} vs Mnn1^{+E314}	80.61	<0.0003	Yes
Mnn1^{e30} vs Mnn1^{e30}/Mnn1^{e173}	169.4	<0.0004	Yes
Mnn1^{e30} vs Mnn1^{e30}/+	60.63	<0.0005	Yes
Mnn1^{e30} vs Mnn1^{e30}/Df(2L)	0.8454	0.3579	No
Mnn1^{e173} vs w^{1118}	5.039	0.0248	No
Mnn1^{e173} vs Mnn1^{+E314}	5.599	0.0180	No
Mnn1^{e173} vs Mnn1^{e30}/Mnn1^{e173}	2.192	0.1387	No
Mnn1^{e173} vs Mnn1^{e173}/+	6.615	0.0101	No
Mnn1^{e173} vs Mnn1^{e173}/Df(2L)	32.81	<0.0001	Yes
w^{1118} vs Mnn1^{+E314}	24.72	<0.0001	Yes
Mnn1^{e30}/Mnn1^{e173} vs Mnn1^{e30}/+	36.67	<0.0001	Yes
Mnn1^{e30}/Mnn1^{e173} vs Mnn1^{e173}/+	0.2618	0.6089	No
Mnn1^{e30}/Mnn1^{e173} vs w^{1118}	0.0005019	0.981	No
Mnn1^{e30}/Mnn1^{e173} vs Mnn1^{+E314}	11.65	0.0006	Yes
Mnn1^{e30}/+ vs Mnn1^{e173}/+	56.10	<0.0001	Yes
Mnn1^{e30}/+ vs w^{1118}	60.79	<0.0001	Yes
Mnn1^{e173}/+ vs w^{1118}	0.7473	0.3873	No
Mnn1^{e30}/Df(2L) vs Mnn1^{e173}/Df(2L)	27.62	<0.0001	Yes
Mnn1^{e30}/Df(2L) vs +/Df(2L)	40.08	<0.0001	Yes
Mnn1^{e30}/Df(2L) vs Mnn1^{+E314}/Df(2L)	53.08	<0.0001	Yes
Mnn1^{e173}/Df(2L) vs +/Df(2L)	0.4046	0.5247	No
Mnn1^{e173}/Df(2L) vs Mnn1^{+E314}/Df(2L)	120.3	<0.0001	Yes
+/Df(2L) vs Mnn1^{+E314}/Df(2L)	147.8	<0.0001	Yes

Survival curves were compared using a log-rank (Mantel-Cox) test. Pairwise comparisons were made and the Bonferroni method was used to account for multiple comparisons. The adjusted significance level used was p<0.002.

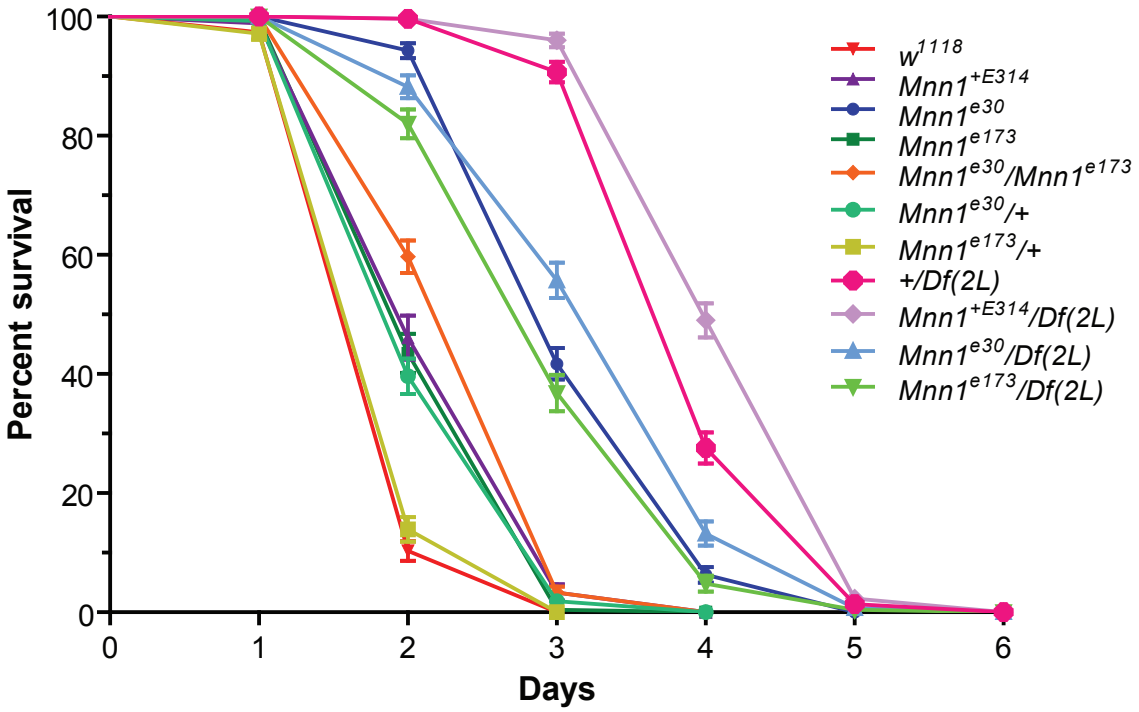

Figure J.2. Female starvation survival for all genotypes.
The survival curves for 4-6 d females from all genotypes tested are plotted together. Larval density was controlled during development and females were allowed to mate freely prior to commencing the experiment. Flies were starved by transferring to 1 % agar, with ten flies per vial. Survival was examined every 24 hrs until all flies had perished. Two separate experimental crosses were used to generate flies for each genotype and 2-4 trials were carried out from each cross, with the number of individuals variable in each trial. All genotypes were tested simultaneously. A total of 180 - 350 flies were tested for each genotype. Survival curves were generated using GraphPad Prism and significance was determined using a log-rank (Mantel-Cox) test, followed by multiple pairwise comparisons (see Appendix J, Table J.2 for a summary of the statistics for this experiment). *Mnn1*^{e30} mutants showed increased starvation survival compared to controls; *Mnn1*^{e173} mutants did not survive better than the precise excision control *Mnn1*$^{+E314}$.

Table J.2. Statistical summary for female starvation survival curves.

Comparison	Chi square	p value	Significant p<0.002
Mnn1^{e30} vs Mnn1^{e173}	244.9	<0.0001	Yes
Mnn1^{e30} vs w^{1118}	496.4	<0.0001	Yes
Mnn1^{e30} vs Mnn1^{+E314}	187.2	<0.0001	Yes
Mnn1^{e30} vs Mnn1^{e30}/Mnn1^{e173}	205.4	<0.0001	Yes
Mnn1^{e30} vs Mnn1^{e30}/+	265.9	<0.0001	Yes
Mnn1^{e30} vs Mnn1^{e30}/Df(2L)	10.10	0.0015	Yes
Mnn1^{e173} vs w^{1118}	84.49	<0.0001	Yes
Mnn1^{e173} vs Mnn1^{+E314}	0.9571	0.3279	No
Mnn1^{e173} vs Mnn1^{e30}/Mnn1^{e173}	17.51	<0.0001	Yes
Mnn1^{e173} vs Mnn1^{e173}/+	57.89	<0.0001	Yes
Mnn1^{e173} vs Mnn1^{e173}/Df(2L)	136.2	<0.0001	Yes
w^{1118} vs Mnn1^{+E314}	84.55	<0.0001	Yes
Mnn1^{e30}/Mnn1^{e173} vs Mnn1^{e30}/+	23.41	<0.0001	Yes
Mnn1^{e30}/Mnn1^{e173} vs Mnn1^{e173}/+	139.5	<0.0001	Yes
Mnn1^{e30}/Mnn1^{e173} vs w^{1118}	184.6	<0.0001	Yes
Mnn1^{e30}/Mnn1^{e173} vs Mnn1^{+E314}	7.394	0.0067	No
Mnn1^{e30}/+ vs Mnn1^{e173}/+	49.99	<0.0001	Yes
Mnn1^{e30}/+ vs w^{1118}	74.43	<0.0001	Yes
Mnn1^{e173}/+ vs w^{1118}	1.389	0.2385	No
Mnn1^{e30}/Df(2L) vs Mnn1^{e173}/Df(2L)	22.10	<0.0001	Yes
Mnn1^{e30}/Df(2L) vs +/Df(2L)	69.17	<0.0001	Yes
Mnn1^{e30}/Df(2L) vs Mnn1^{+E314}/Df(2L)	144.8	<0.0001	Yes
Mnn1^{e173}/Df(2L) vs +/Df(2L)	169.1	<0.0001	Yes
Mnn1^{e173}/Df(2L) vs Mnn1^{+E314}/Df(2L)	251.1	<0.0001	Yes
+/Df(2L) vs Mnn1^{+E314}/Df(2L)	28.93	<0.0001	Yes

Survival curves were compared using a log-rank (Mantel-Cox) test. Pairwise comparisons were made and the Bonferroni method was used to account for multiple comparisons. The adjusted significance level used was p<0.002.

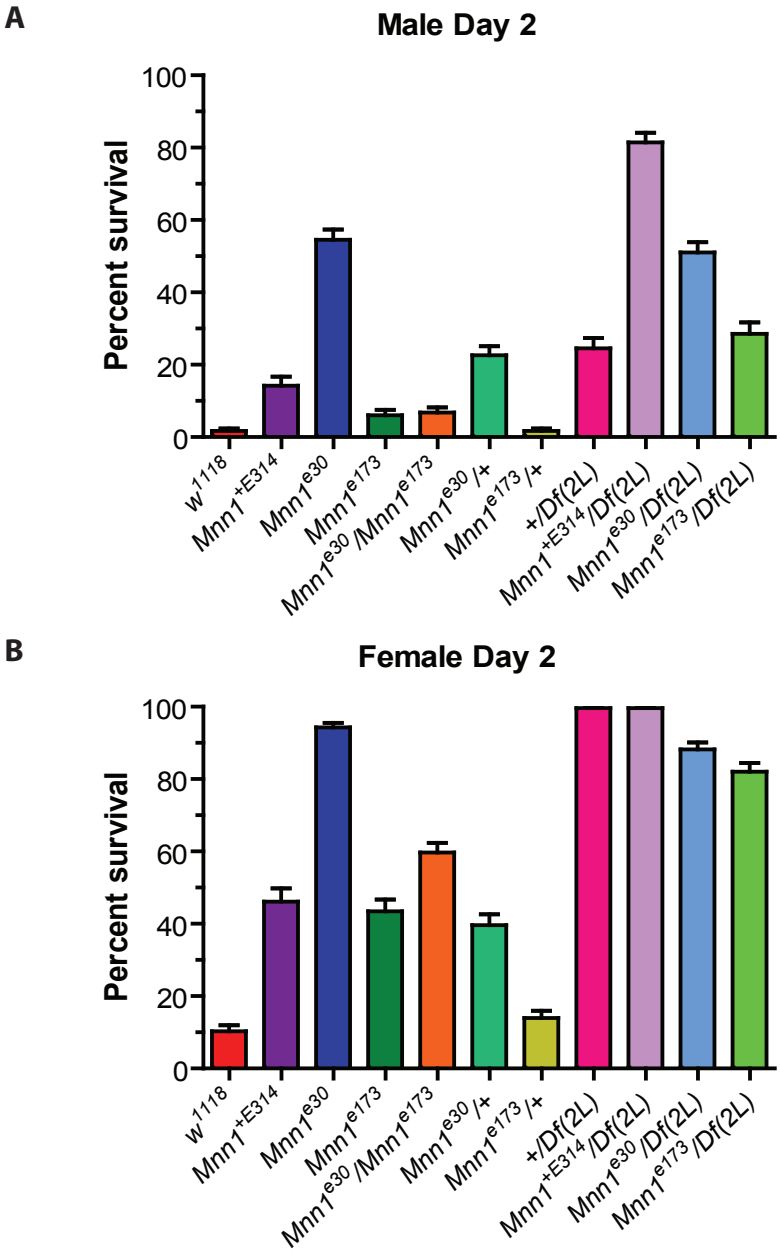

Figure J.3. Male and female starvation survival after 2 days.
The percent survival of 4-6 day males (A) and females (B) after 2 days of starvation are shown as bar graphs for better visual comparison (See Appendix A, Figures 5 & 6 for survival curves). Each data set was analyzed using a one-way ANOVA with Bonferroni's multiple comparisons post-hoc test (see Appendix J, Table J.3 for a summary of the statistics). A) For males *Mnn1*^{e30}, but not *Mnn1*^{e173}, survived starvation better than controls. The presence of *Df(2L)spd*^{j2} also increased survival. B) Females survived starvation longer than males. After 2 days, *Mnn1*^{e30} mutants and *Df(2L)* genotypes showed enhanced survival.

Table J.3. Statistical summary for male and female starvation survival after 2 days.

Comparison	Male		Female	
	t	Significant p < 0.001	t	Significant p < 0.001
Mnn1^{e30} vs Mnn1^{e173}	15.77	Yes	16.73	Yes
Mnn1^{e30} vs Mnn1^{+E314}	12.09	Yes	14.68	Yes
Mnn1^{e30} vs w^{1118}	18.71	Yes	30.82	Yes
Mnn1^{e30} vs Mnn1^{e30}/Mnn1^{e173}	16.43	Yes	12.6	Yes
Mnn1^{e30} vs Mnn1^{e30}/+	10.6	Yes	18.86	Yes
Mnn1^{e30} vs Mnn1^{e30}/Df(2L)	1.2	No	2.116	No
Mnn1^{e173} vs Mnn1^{+E314}	2.357	No	0.7393	No
Mnn1^{e173} vs w^{1118}	1.43	No	10.86	Yes
Mnn1^{e173} vs Mnn1^{e30}/Mnn1^{e173}	0.2517	No	5.276	Yes
Mnn1^{e173} vs Mnn1^{e173}/+	1.398	No	9.279	Yes
Mnn1^{e173} vs Mnn1^{e173}/Df(2L)	6.554	Yes	11.78	Yes
Mnn1^{+E314} vs w^{1118}	3.832	No	10.86	Yes
Mnn1^{+E314} vs Mnn1^{e30}/Mnn1^{e173}	2.23	No	4.097	No
w^{1118} vs Mnn1^{e30}/Mnn1^{e173}	1.793	No	17.87	Yes
w^{1118} vs Mnn1^{e30}/+	7.123	Yes	10.06	Yes
w^{1118} vs Mnn1^{e173}/+	0.01673	No	1.259	No
Mnn1^{e30}/Mnn1^{e173} vs Mnn1^{e30}/+	5.251	Yes	6.834	Yes
Mnn1^{e30}/Mnn1^{e173} vs Mnn1^{e173}/+	1.743	No	15.74	Yes
Mnn1^{e30}/+ vs Mnn1^{e173}/+	6.894	Yes	8.42	Yes
Mnn1^{e30}/Df(2L) vs Mnn1^{e173}/Df(2L)	6.811	Yes	1.996	No
Mnn1^{e30}/Df(2L) vs Mnn1^{+E314}/Df(2L)	9.346	Yes	3.851	No
Mnn1^{e30}/Df(2L) vs +/Df(2L)	8.429	Yes	3.816	No
Mnn1^{e173}/Df(2L) vs Mnn1^{+E314}/Df(2L)	14.8	Yes	5.765	Yes
Mnn1^{e173}/Df(2L) vs +/Df(2L)	1.13	No	5.717	Yes
Mnn1^{+E314}/Df(2L) vs +/Df(2L)	16.62	Yes	0.003899	No

Percent survival was compared using a one-way ANOVA ($p<0.001$) followed by Bonferroni's multiple comparisons post-hoc test. The results for the post-hoc pairwise comparisons are shown for biologically meaningful comparisons only.

APPENDIX K: Final genotype verification of flies used in starvation and desiccation assays

To rule out the possibility of stock contamination as an explanation for some of the results observed in the starvation and desiccation assays, the amplified stocks were checked by PCR to ensure that they were still the proper genotypes. *Mnn1*^{e30}, *Mnn1*^{e173}, *Mnn1*^{e30}*/Df* and *Mnn1*^{e173}*/Df* did not show amplification of *Mnn1* exon 2 or 3, indicating that the deletion of *Mnn1* was still present in these stocks (Figure K.1). Both controls, *w*^{1118} and *Mnn1*$^{+E314}$, had amplification of *Mnn1* exon 2 and 3, indicating that they did not harbour a deletion in the *Mnn1* locus. Thus, after extensive amplification of these stocks for use in these assays, stock contamination was not observed and genotypes were as expected.

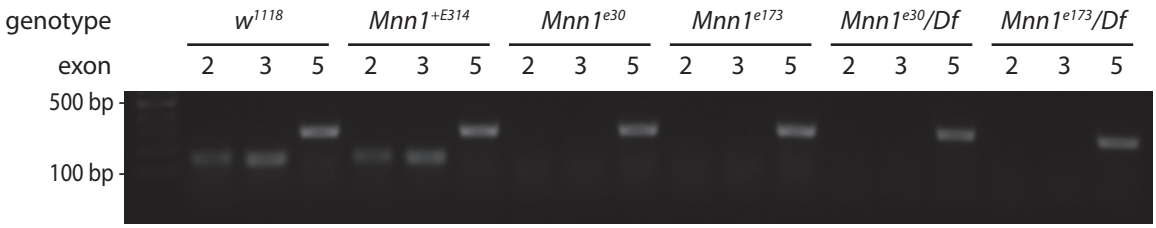

Figure K.1. Final genotype verification by PCR.
To verify that the mutants used in the starvation and desiccation assays were still the correct genotypes, 5 male flies from each were selected and DNA was analyzed by PCR. Primers were used to amplify exon 2, exon 3 and exon 5 of the *Mnn1* gene. $Mnn1^{e30}$ and $Mnn1^{e173}$ mutants are missing exons 2 and 3 but retain exon 5; therefore, amplification should only be seen for these mutants with exon 5 primers. Control lines, w^{1118} and the precise excision line $Mnn1^{+E314}$ have no deletions in the *Mnn1* gene and show amplification with all primer sets. Combination of $Mnn1^{e30}$ or $Mnn1^{e173}$ with the deficiency $Df(2L)spd^{j2}$ (simplified as *Df* above) results in no amplification of exon 2 or 3 as expected.